Melting

Detlef Lohse

Physics of Fluids Group, Max-Planck Center Twente, University of Twente, The Netherlands &
Max-Planck Inst. for Dynamics & Self Organization, Göttingen, Germany

Ice melting in water

Detlef Lohse

Physics of Fluids Group, Max-Planck Center Twente, University of Twente, The Netherlands &
Max-Planck Inst. for Dynamics & Self Organization, Göttingen, Germany

Ice melting in water

Physics of Fluids

UNIVERSITY OF TWENTE.

Coworkers

Rui
Yang

Chris
Howland

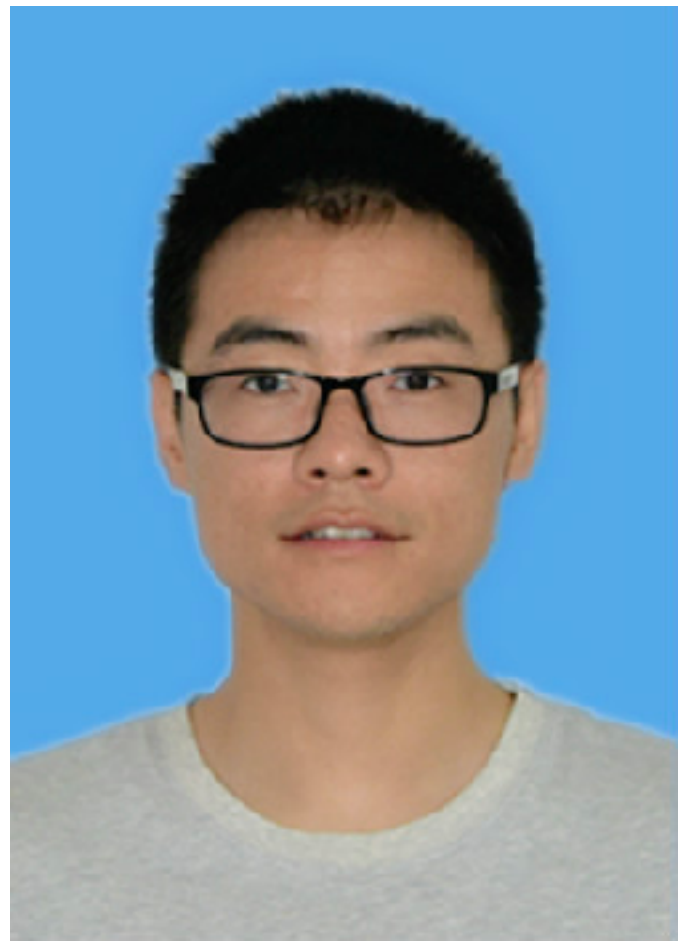

Hao-Ran
Liu

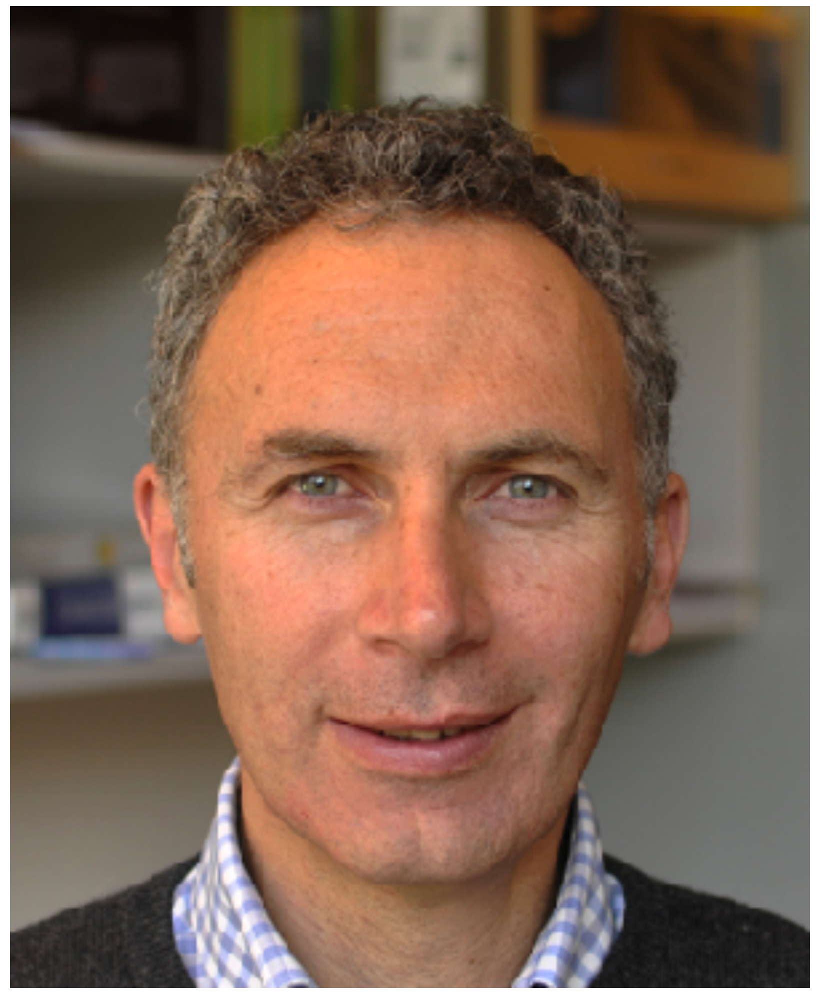

Roberto
Verzicco

erc

Melting as huge problem

Grand challenge in environmental fluid dynamics

What is the melt rate of icebergs & glaciers?

How does it depend on the parameters like salinity, temperature, size, …?

Current models are off by an order of magnitude!


Grand challenge in environmental fluid dynamics
What is the melt rate of icebergs & glaciers?
How does it depend on the parameters like salinity, temperature, size, …?
Current models are off by an order of magnitude!
How do these iceberg structures emerge?
Copyright Phillip Colla


Grand challenge in environmental fluid dynamics
What is the melt rate of icebergs & glaciers?
How does it depend on the parameters like salinity, temperature, size, …?
Current models are off by an order of magnitude!
How do these iceberg structures emerge?
Upscaling?
Copyright Phillip Colla


Grand challenge in environmental fluid dynamics
What is the melt
icebergs &
How does it
parameters
like sal
e, size, …?
Current mo
n order of magnitude!
Ho
erg structures emerge?
Lack of understanding is on a fundamental level
Copyright Phillip Colla

Ice melting as complex, multi-scale, multi-physics phenomenon

- **Multiphase, multicomponent** (salt, water) flow with **phase transition**
- **Multi-way coupling** and memory effects
- Mathematically: "**Stefan problem**":
  What is the evolution of the boundary between two phases during phase transition?

Josef Stefan
(1835-93)

g

4°C 5.6°C 8°C

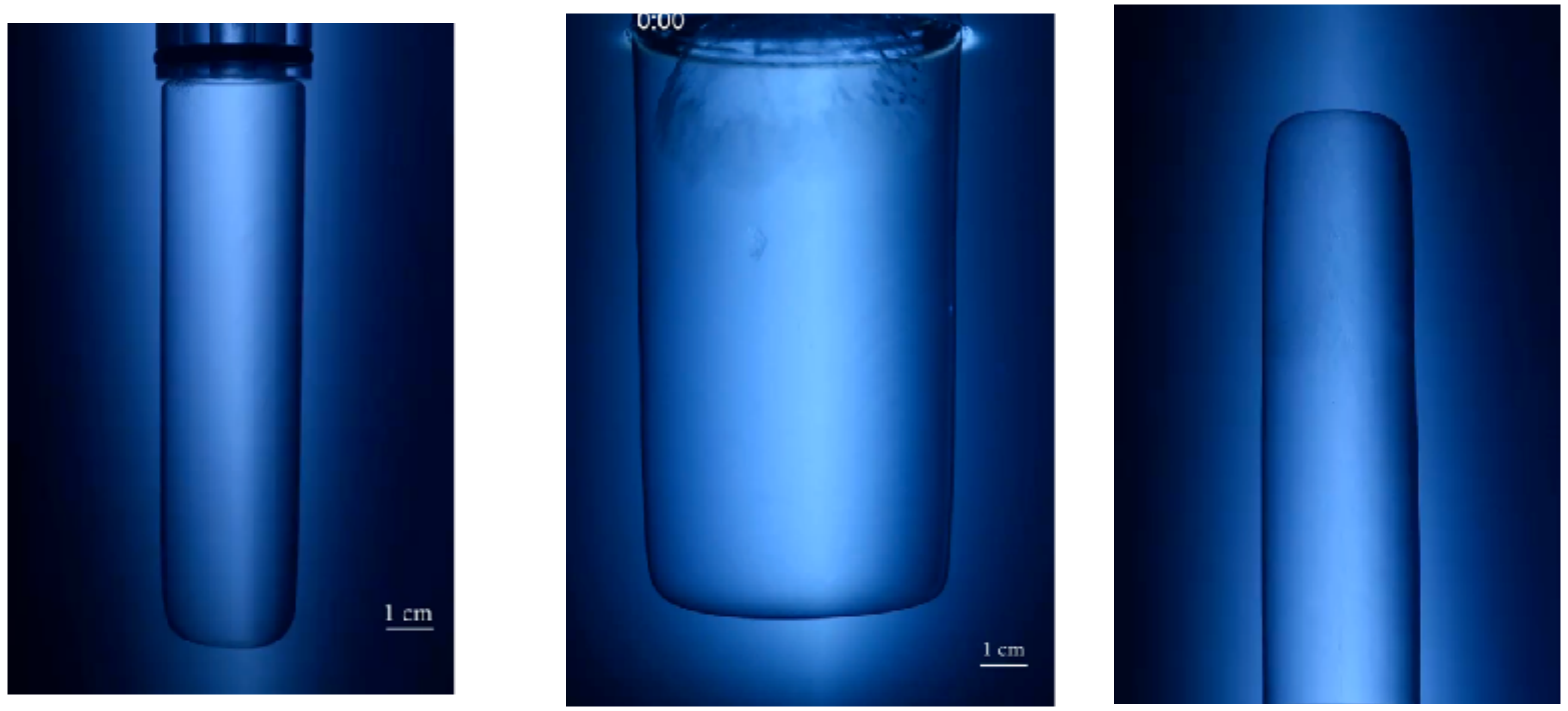

Weady et al. PRL 128, 044502 (2022)

$$\rho(T, S)$$

T = temperature
S = salinity

Ice melting as complex, multi-scale, multi-physics phenomenon

- **Multiphase, multicomponent** (salt, water) flow with **phase transition**
- **Multi-way coupling** and memory effects
- Mathematically: "**Stefan problem**":
  What is the evolution of the boundary between two phases during phase transition?

4°C 5.6°C 8°C

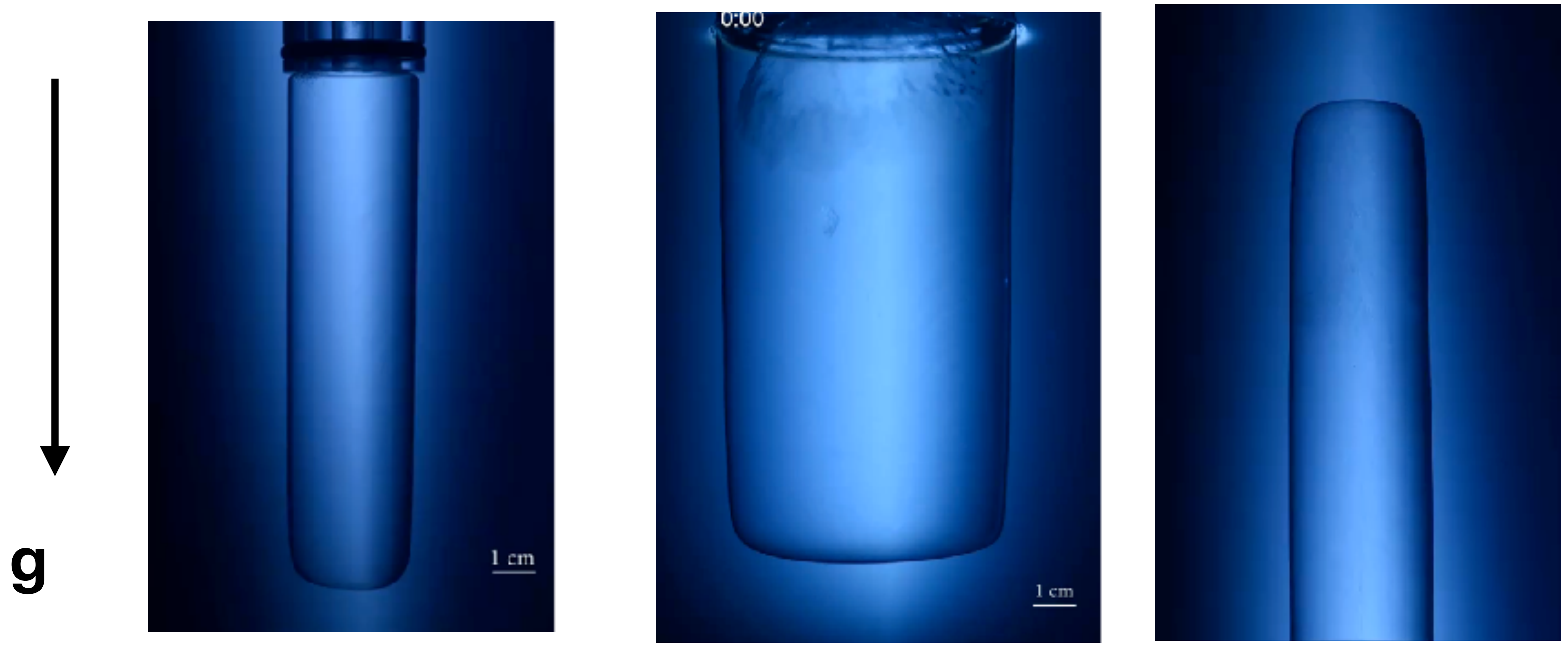

Weady et al. PRL 128, 044502 (2022)

$$\rho(T, S)$$

T = temperature
S = salinity

Josef Stefan
(1835-93)


Multiscale

Multiscale

Relevance of Stefan problem on large scales: buoyancy driven flow

Melting in geophysical context

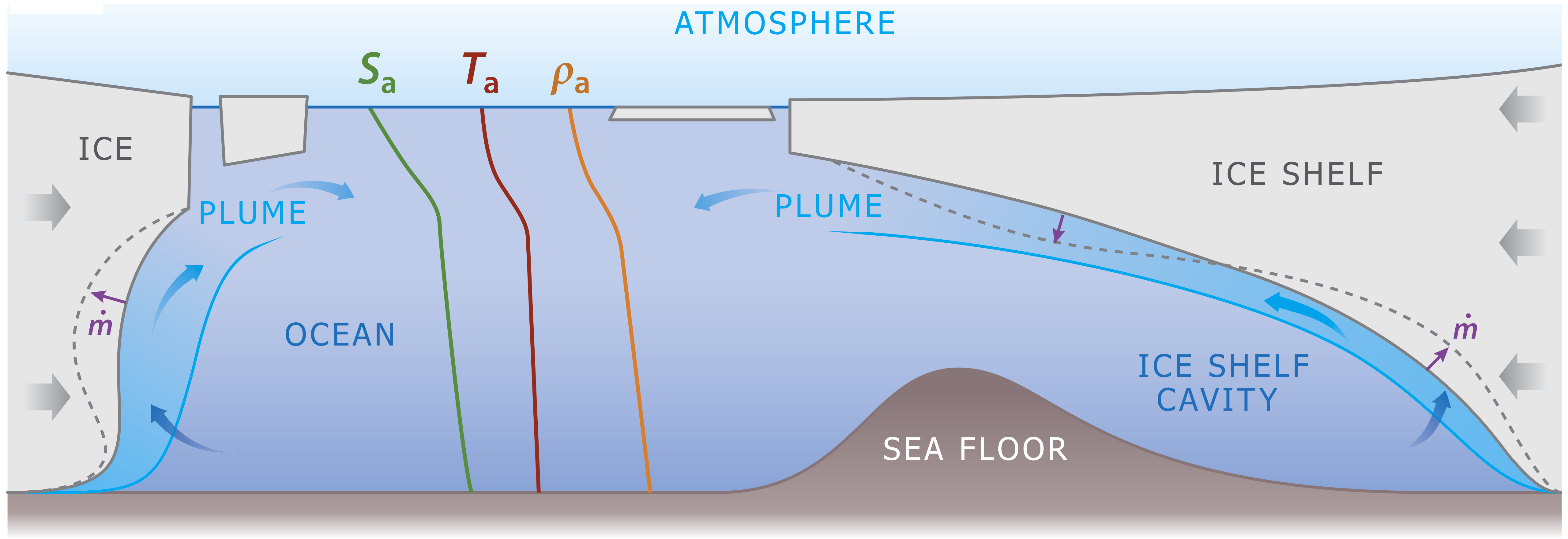

adapted from I. J. Hewitt, Subglacial plumes, Annu. Rev. Fluid Mech. 52, 145 (2020).

Subglacial plumes majorly contribute to basal glacier melting

Antarctic sea ice

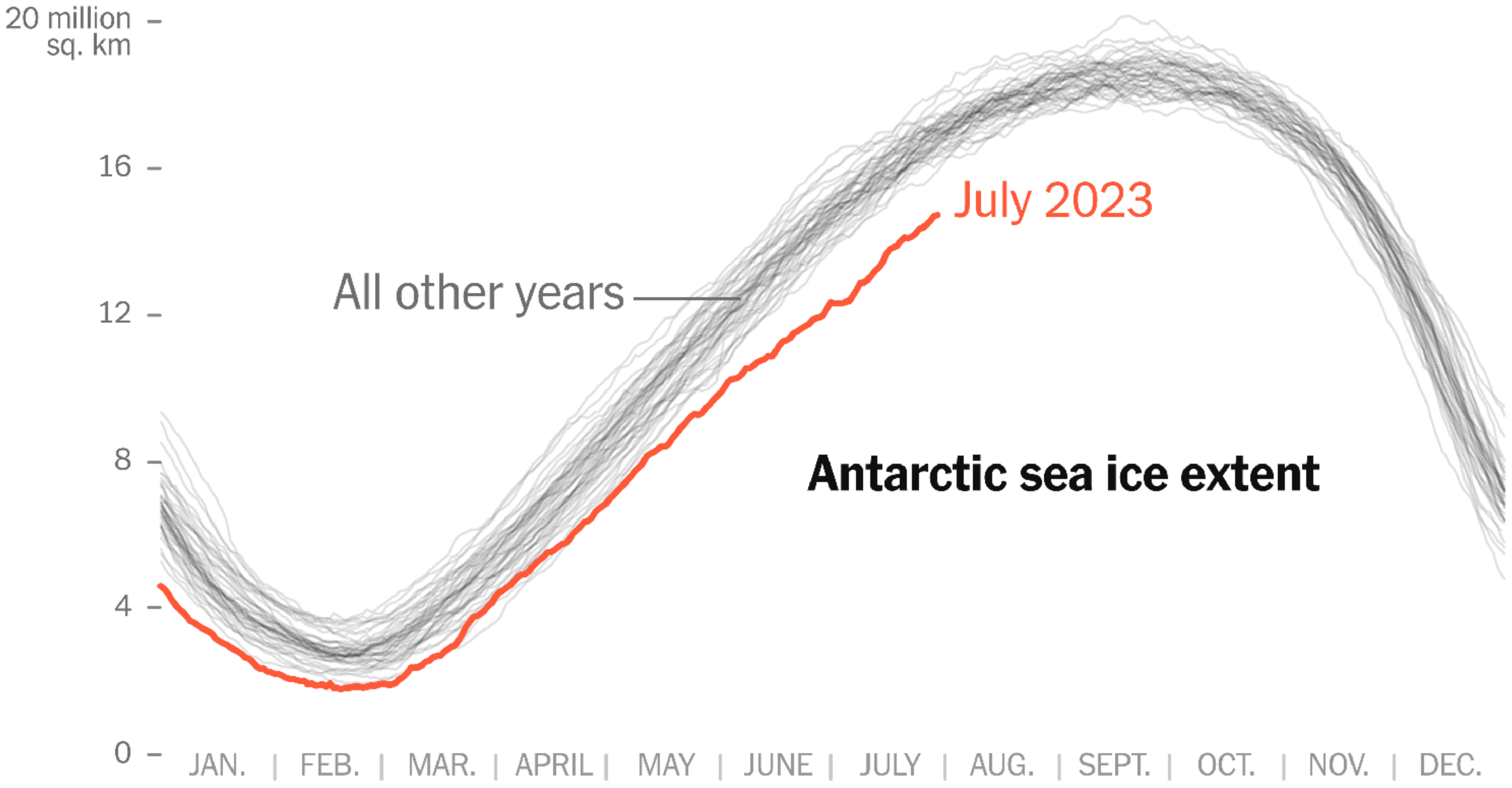

Antarctic sea ice

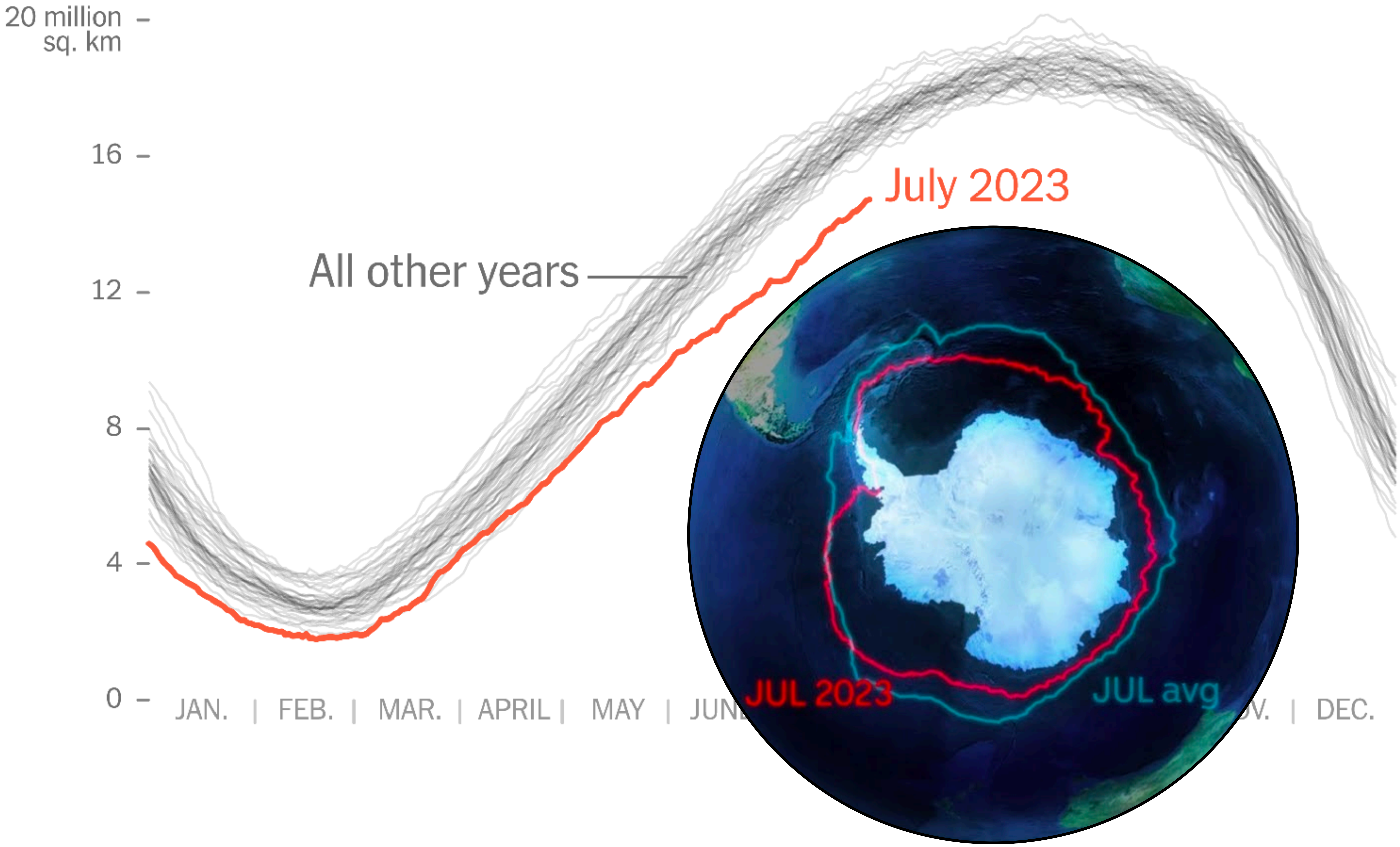

Antarctic sea ice

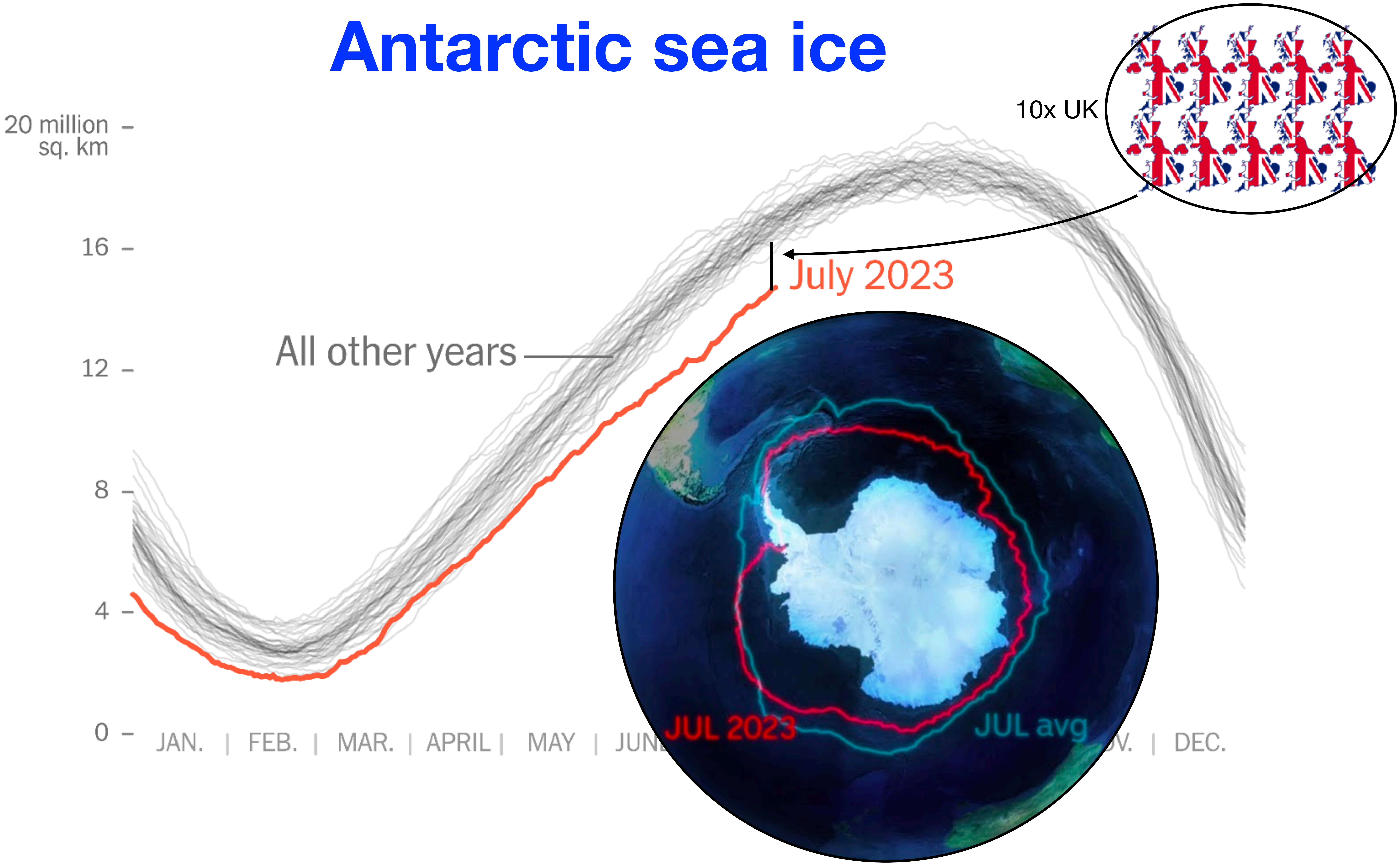

Abyssal ocean overturning slowdown and warming driven by Antarctic meltwater

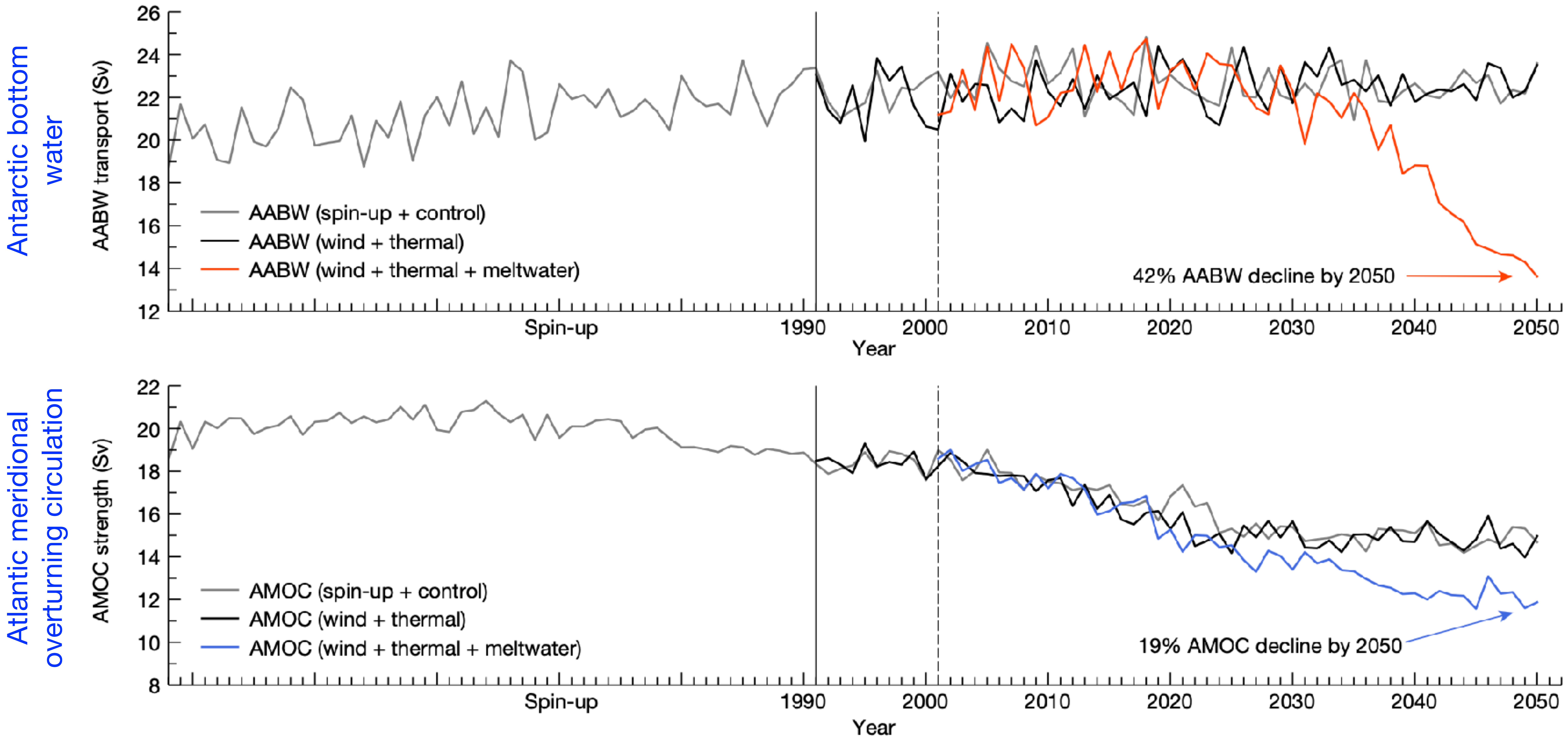

Li, England, Hogg, Rintoul, Morrison, Nature 615, 841 (2023)

Melting on smaller scale: Melt ponds:
Essential for radiative heat balance of earth (lowers albedo)

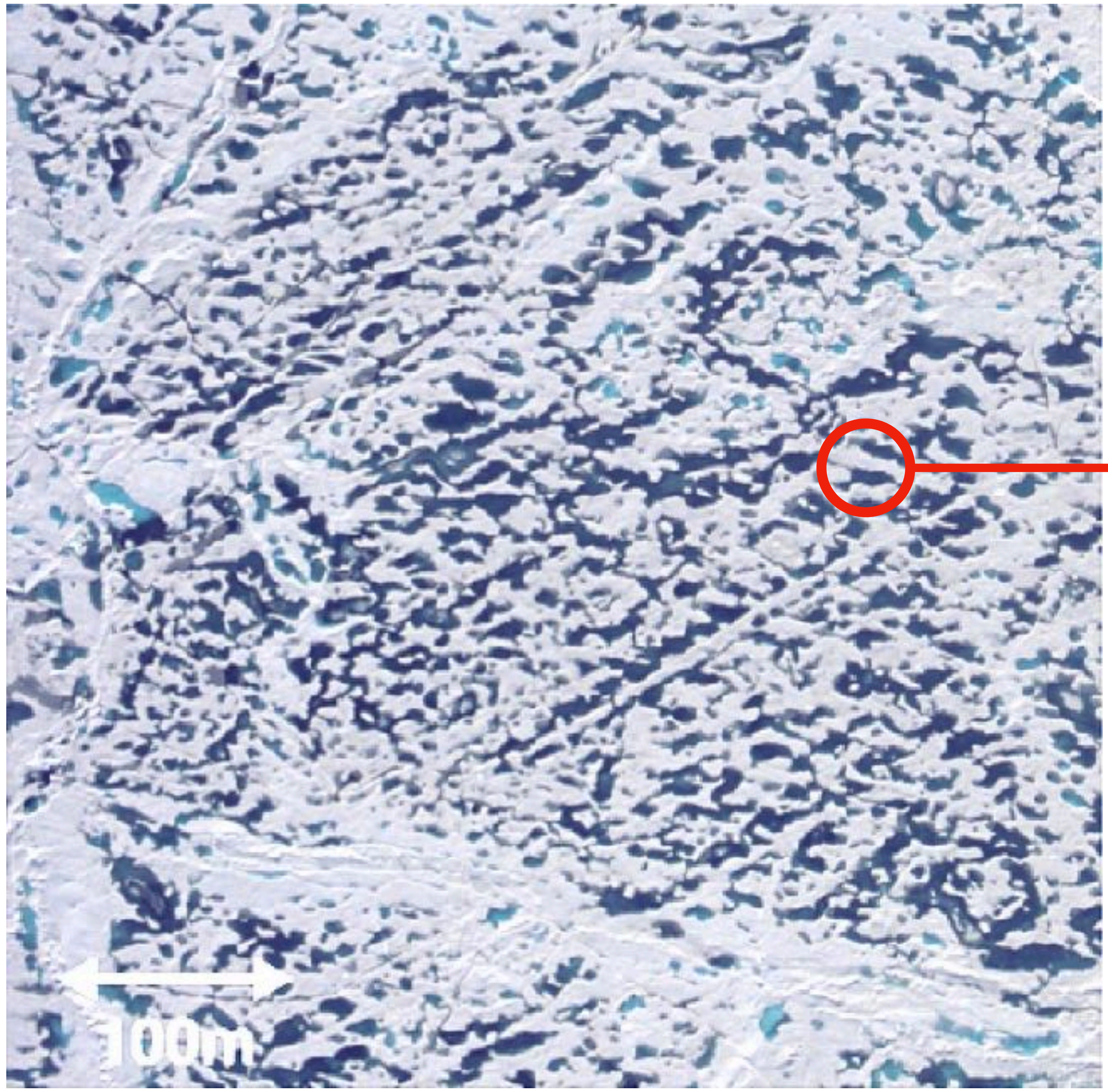

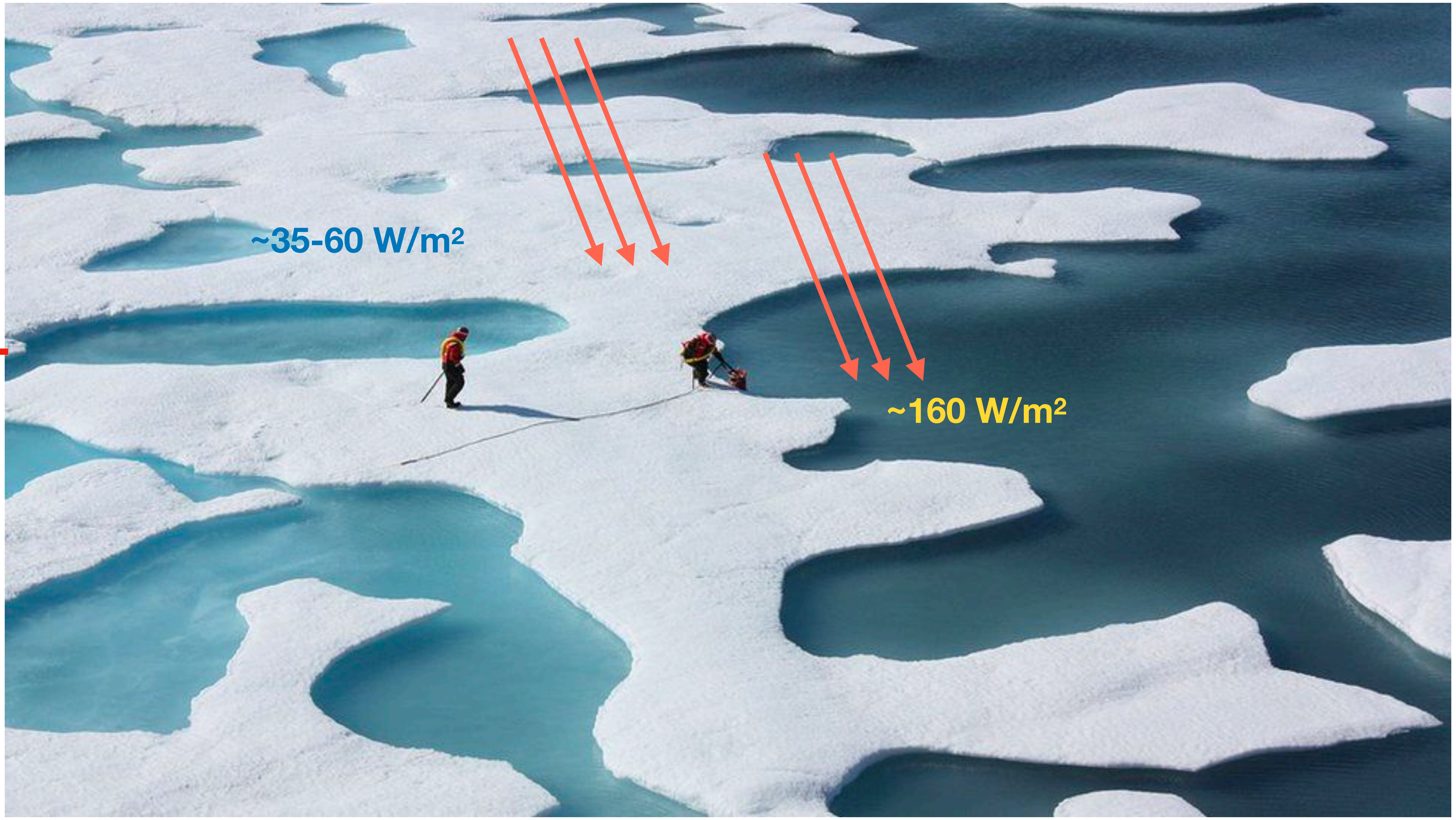

Popović, et al., Phys. Rev. Lett. 2018

Melting on smaller scale: Melt ponds:

Essential for radiative heat balance of earth (lowers albedo)

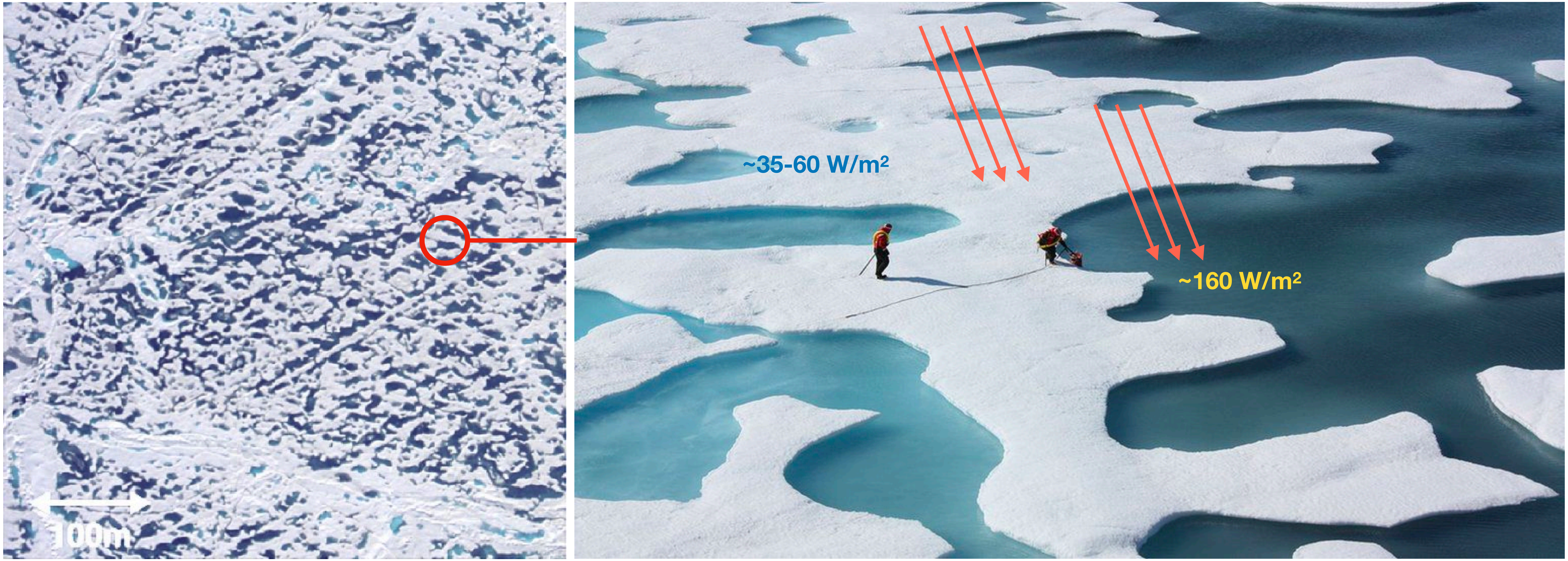

Popović, et al., Phys. Rev. Lett. 2018

Under what condition do these melt ponds form?

Mechanism: Convection in melt ponds

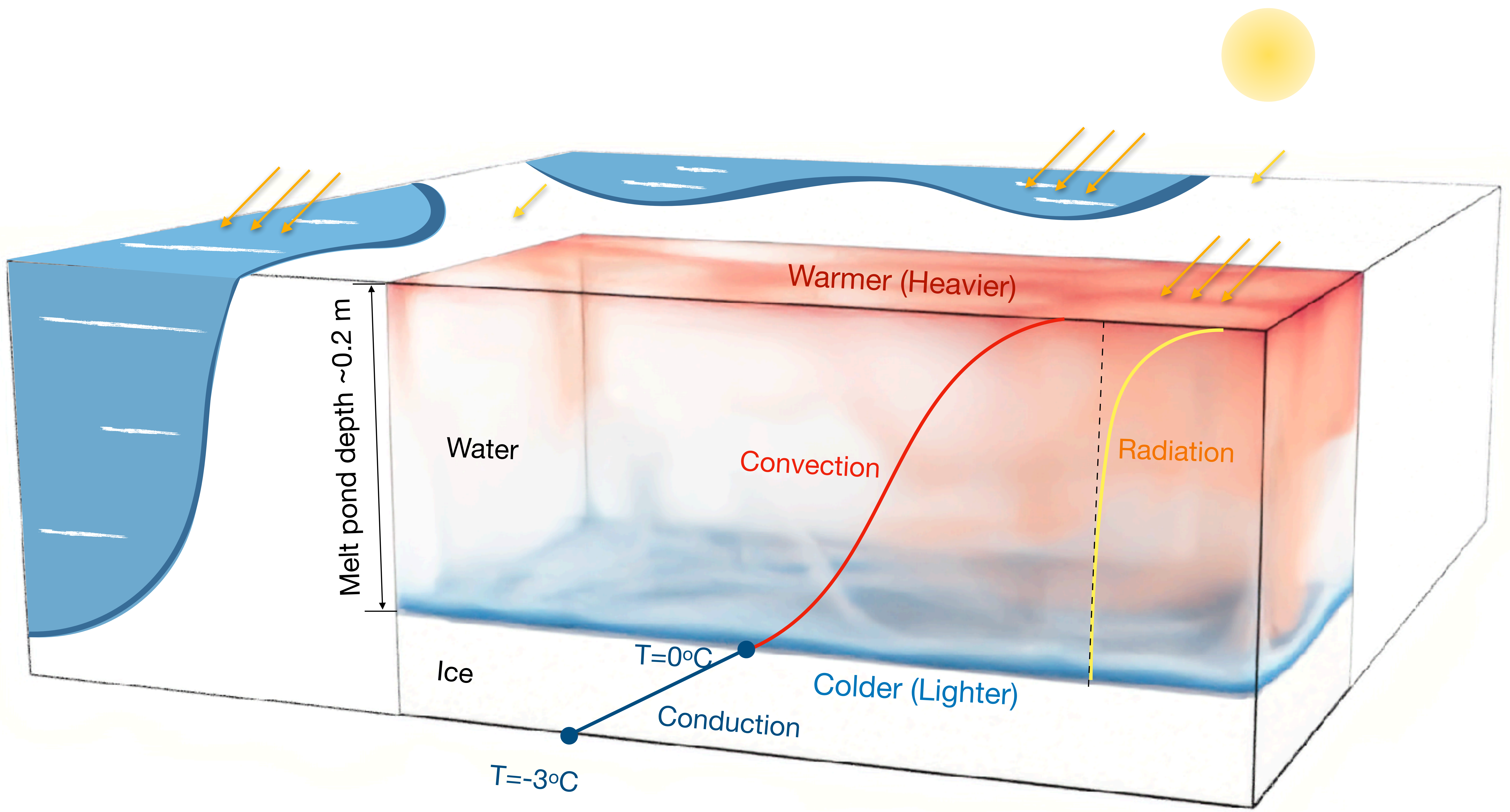

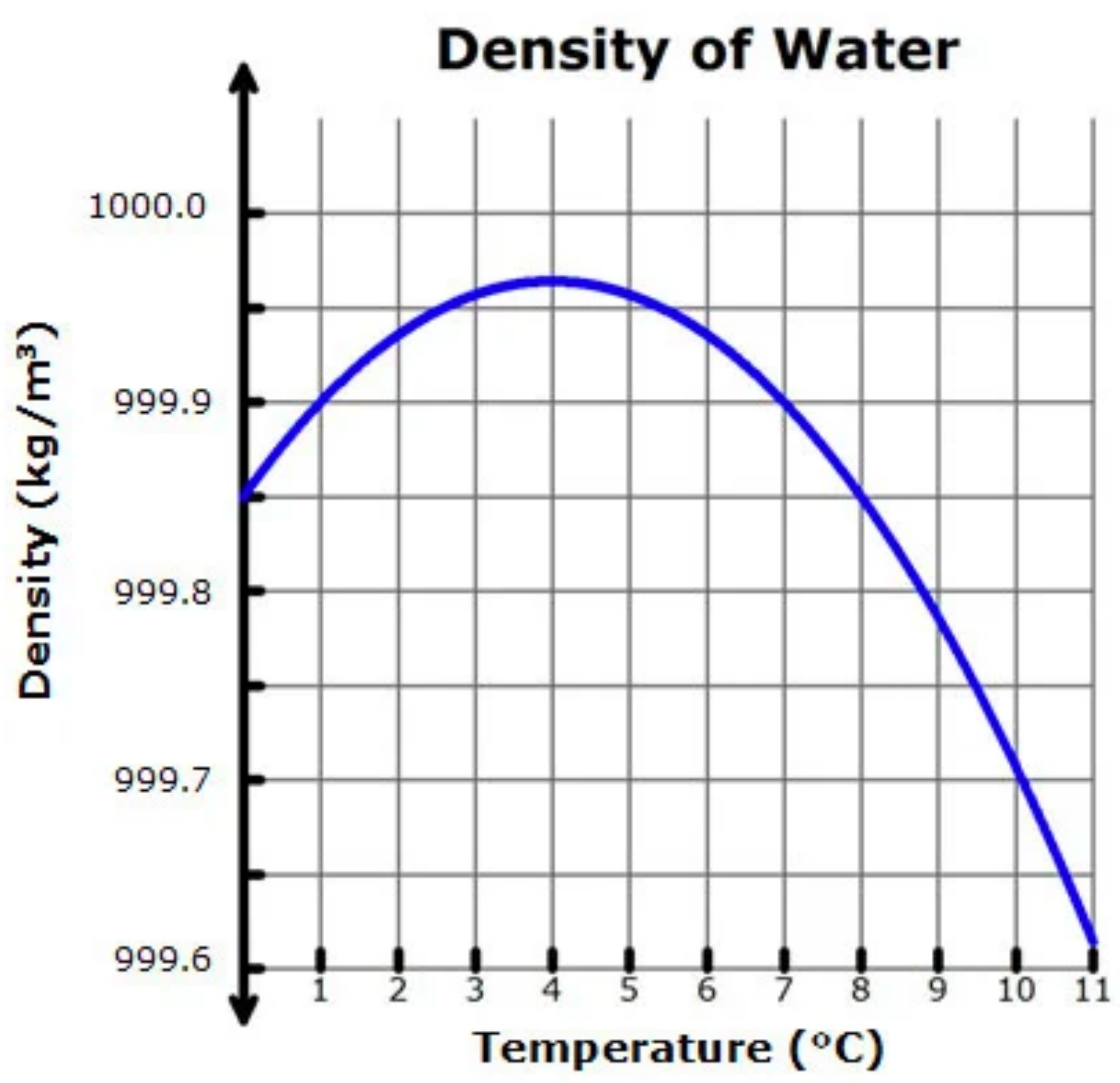

Under what condition do these melt ponds form?

Relevance of Stefan problem: buoyancy driven flow

Melting in geophysical context

$$\boxed{\rho(T, S)}$$

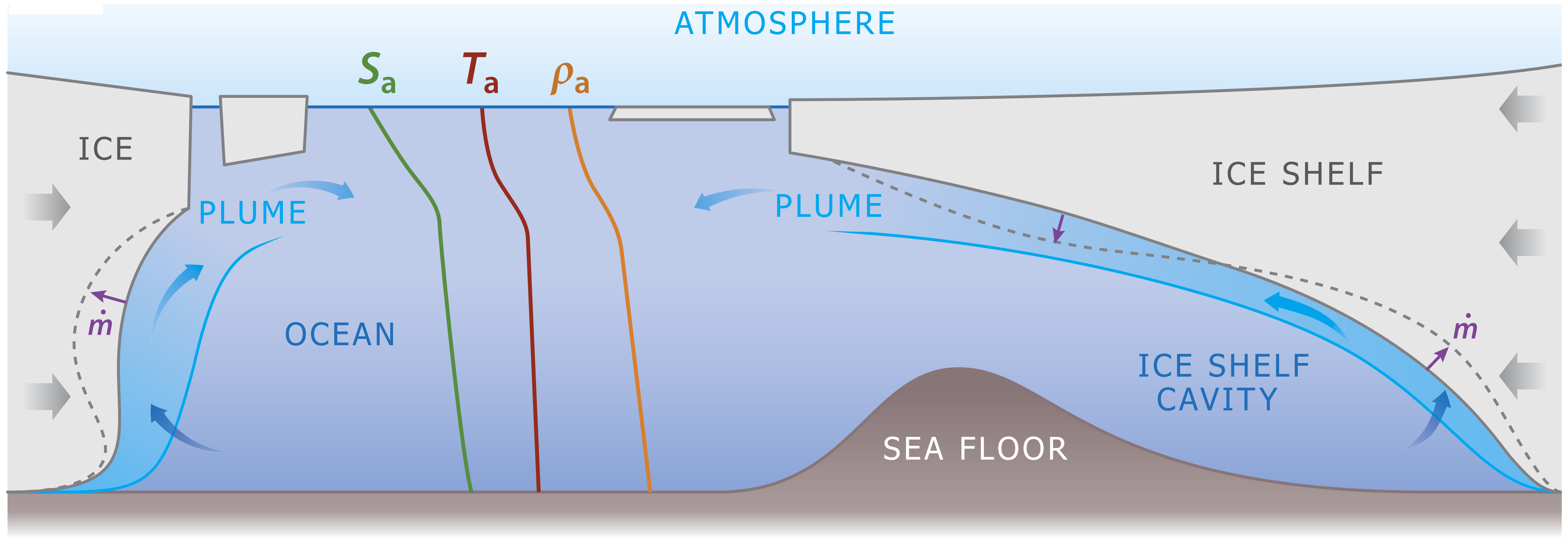

Relevance of Stefan problem: buoyancy driven flow

$$\boxed{\rho(T, S)}$$

Melting in geophysical context

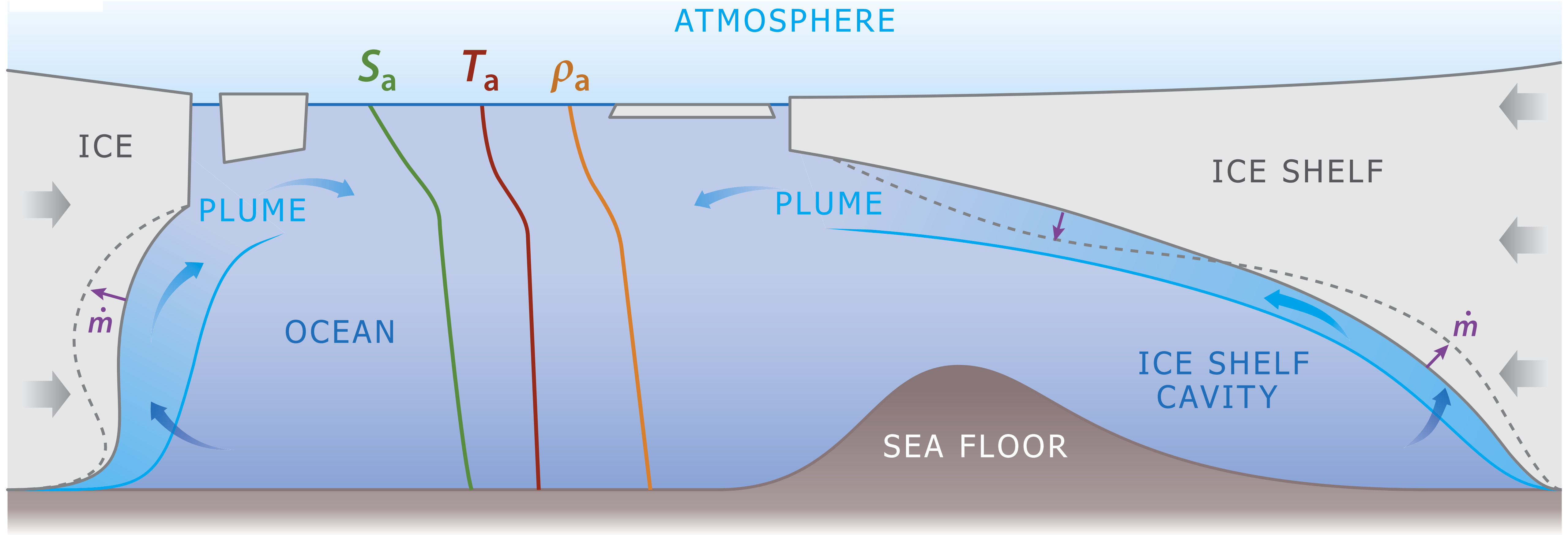

CO_2 sequestration in brine: negative emission

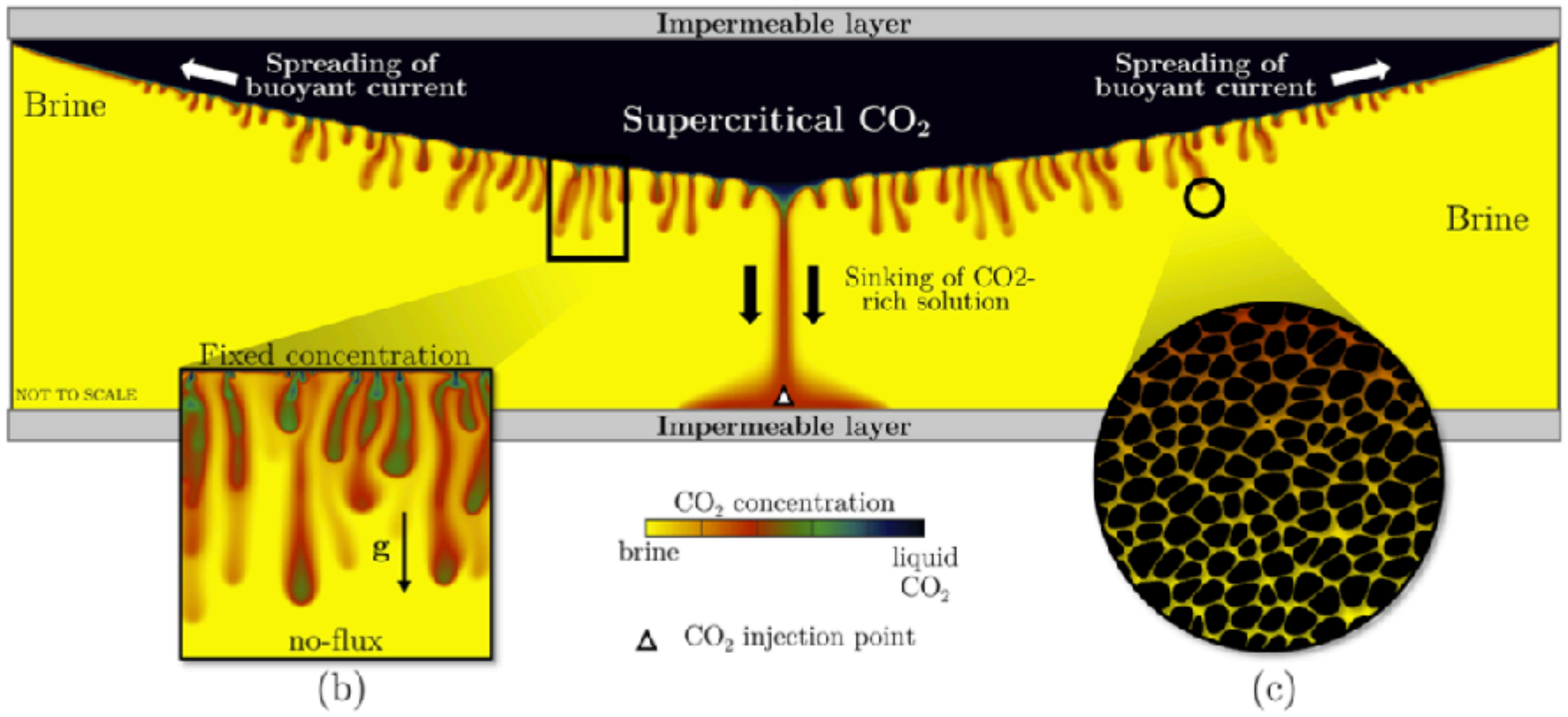

Relevance of Stefan problem: buoyancy driven flow

$$\boxed{\rho(T, S)}$$

Melting in geophysical context

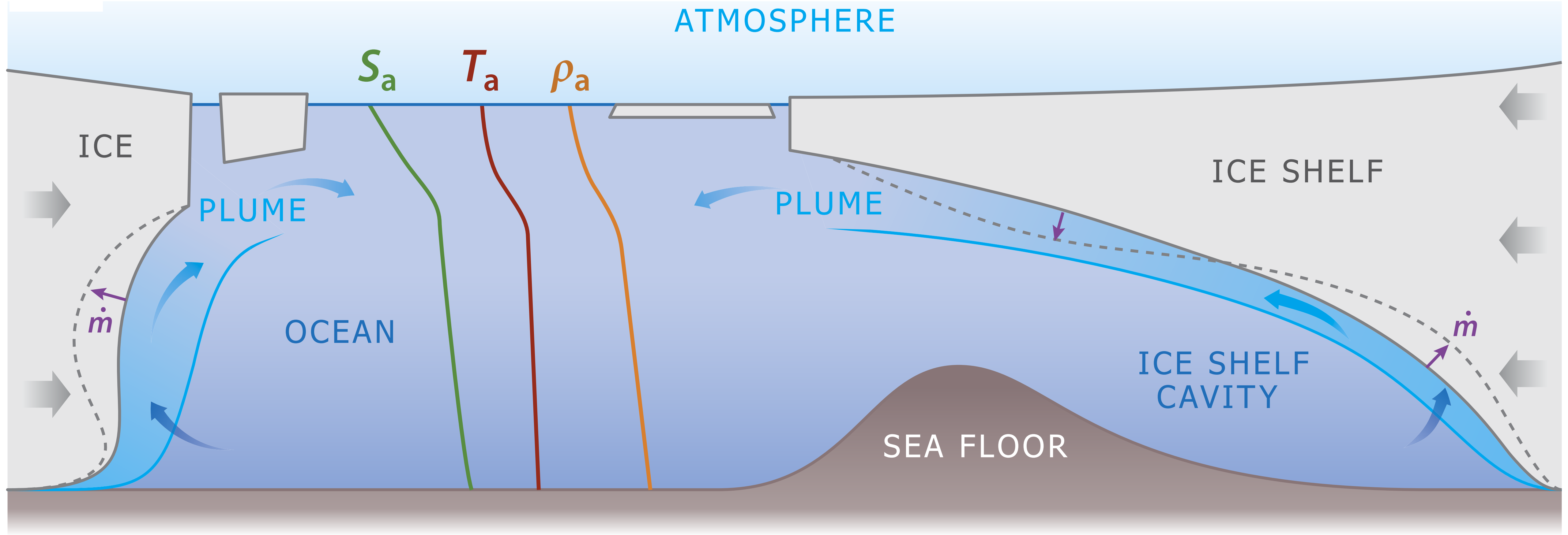

CO_2 sequestration in brine: negative emission

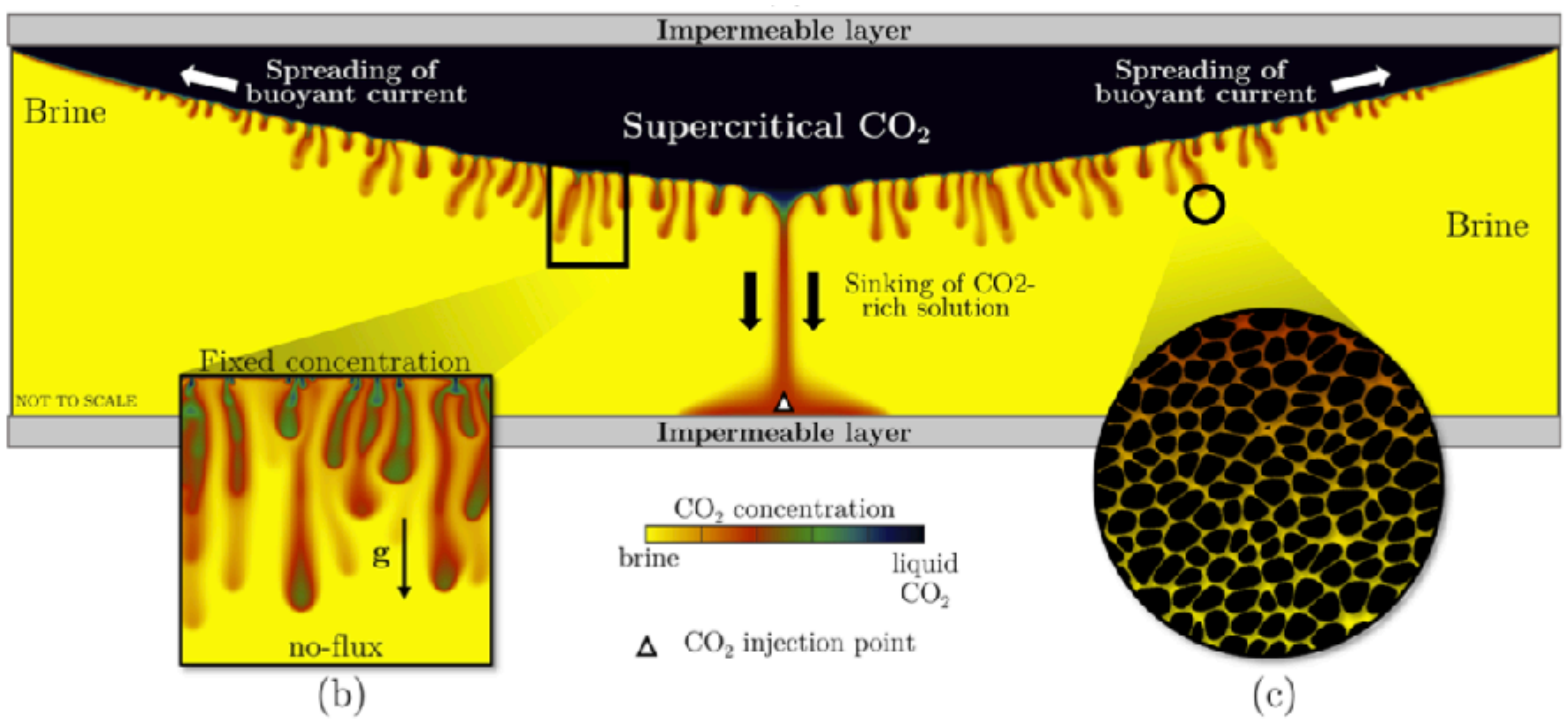

Latent thermal energy storage:

Phase change materials

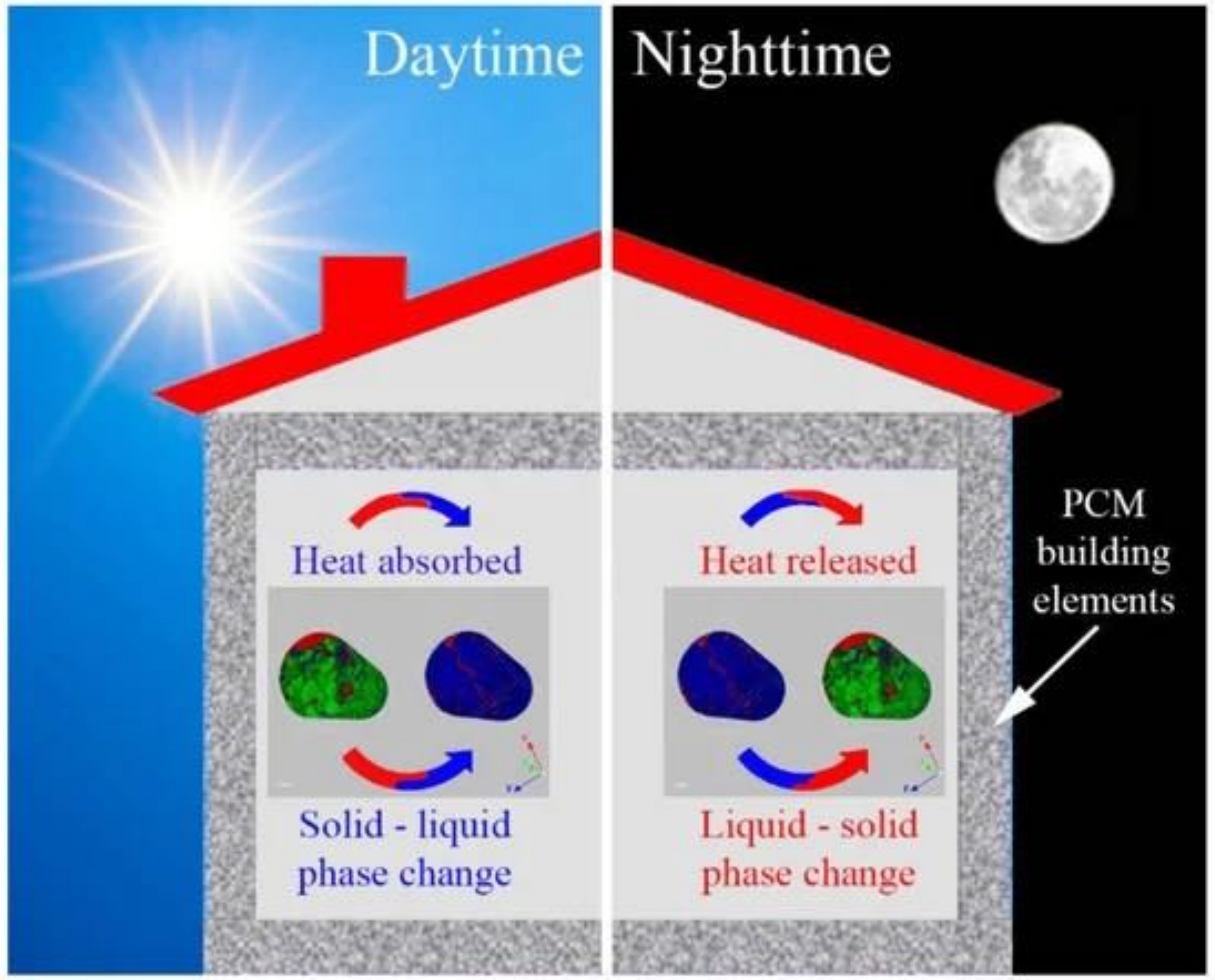

Podara *et al.*, Appl. Sci. 11, 1490 (2021)

Relevance of Stefan problem: buoyancy driven flow

Melting in geophysical context

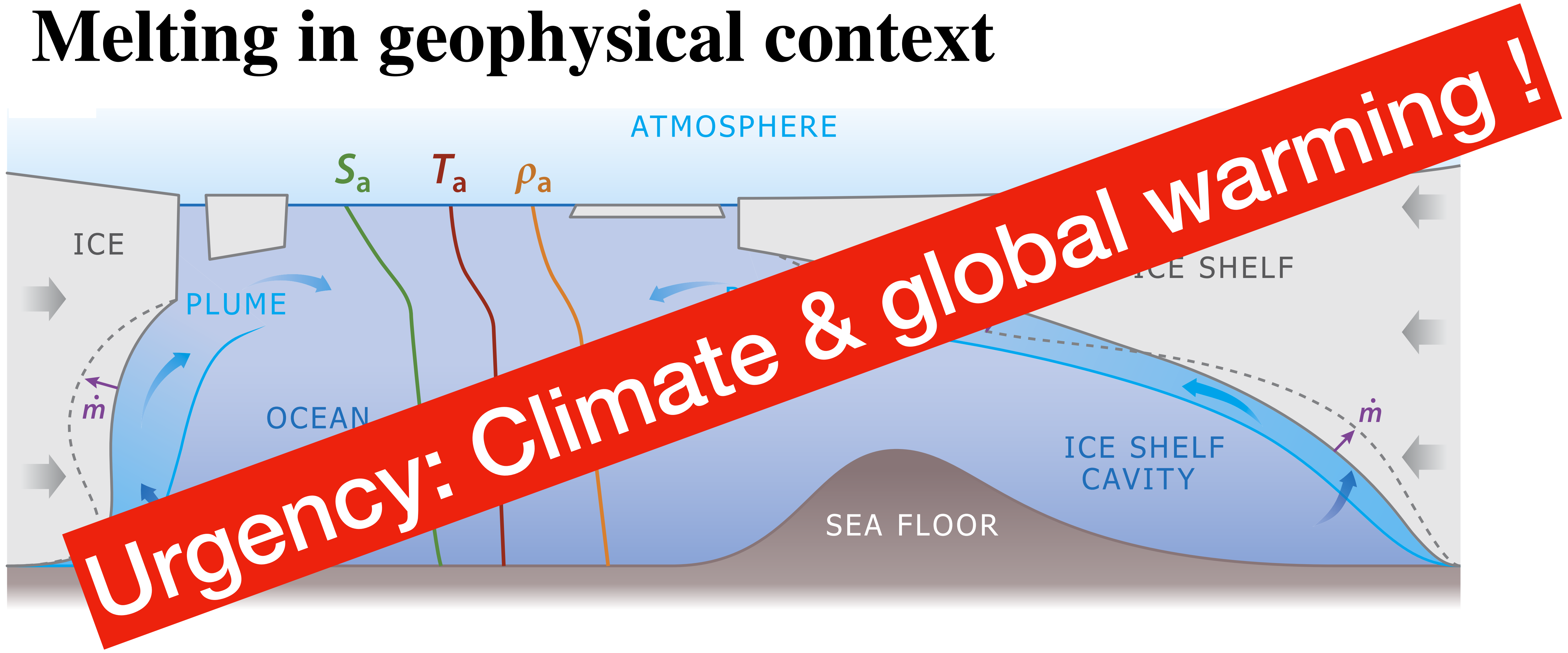

CO_2 sequestration in brine: negative emission

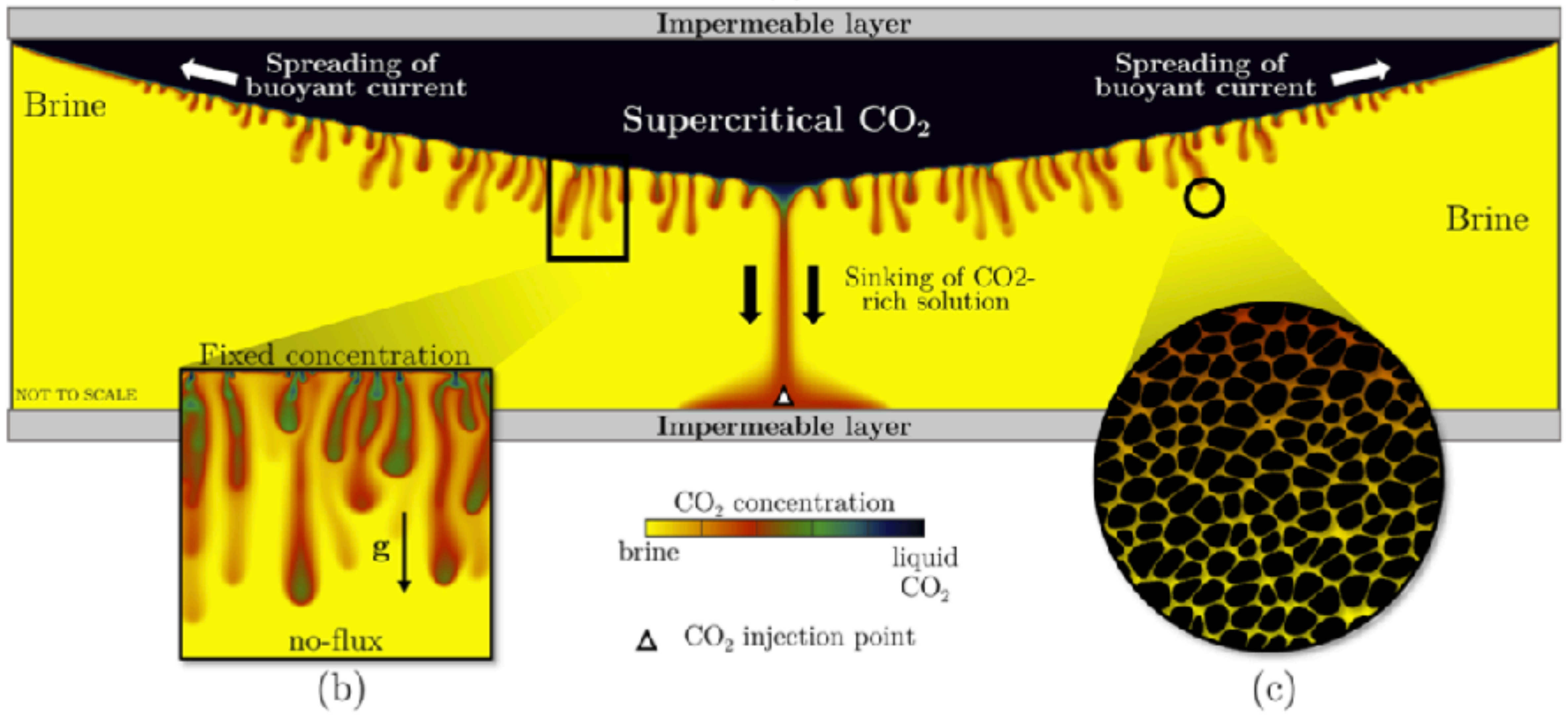

$$\boxed{\rho(T, S)}$$

Latent thermal energy storage:

Phase change materials

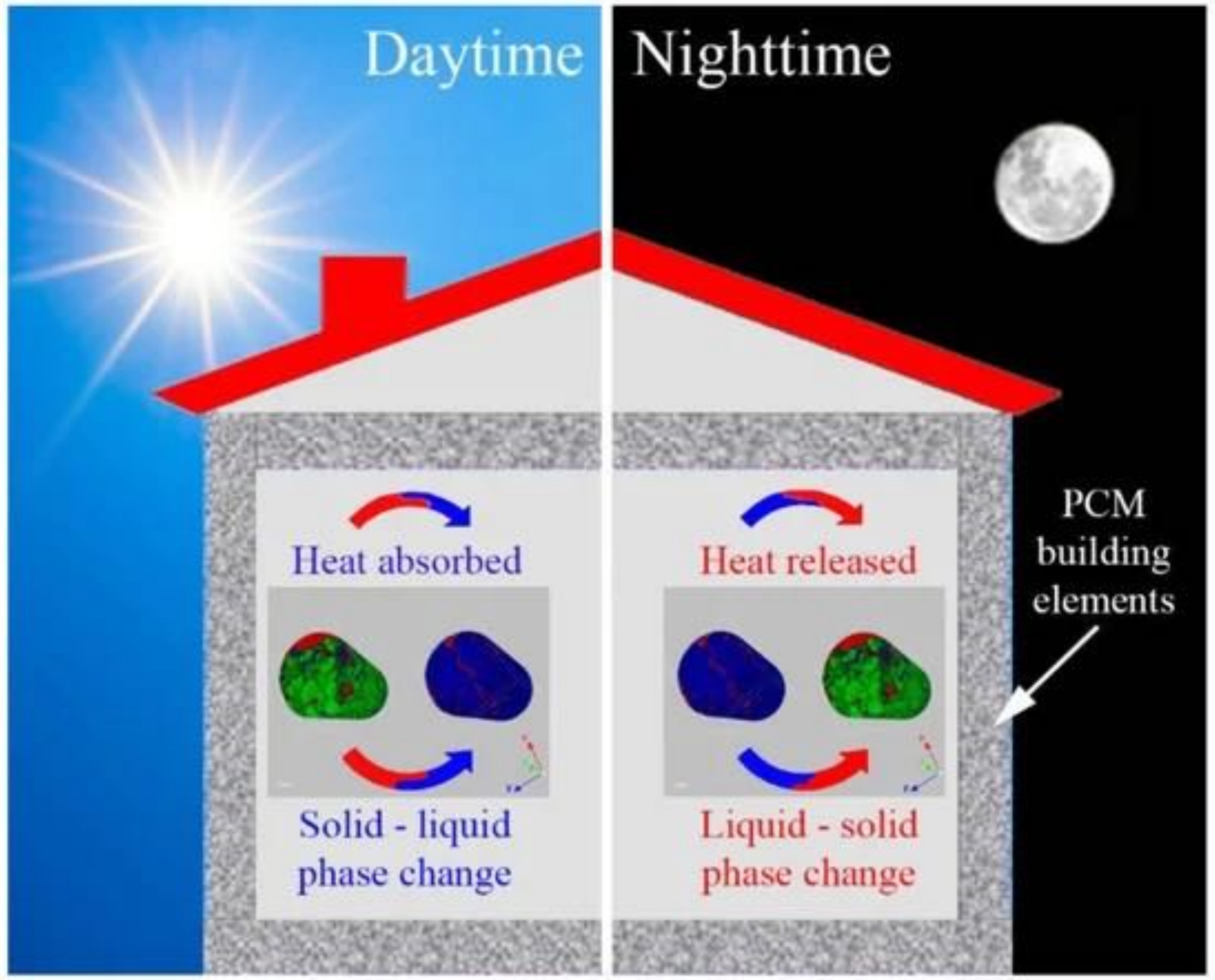

Podara *et al.*, Appl. Sci. 11, 1490 (2021)

Relevance of Stefan problem: buoyancy driven flow

$$\boxed{\rho(T, S)}$$

Melting in geophysical context

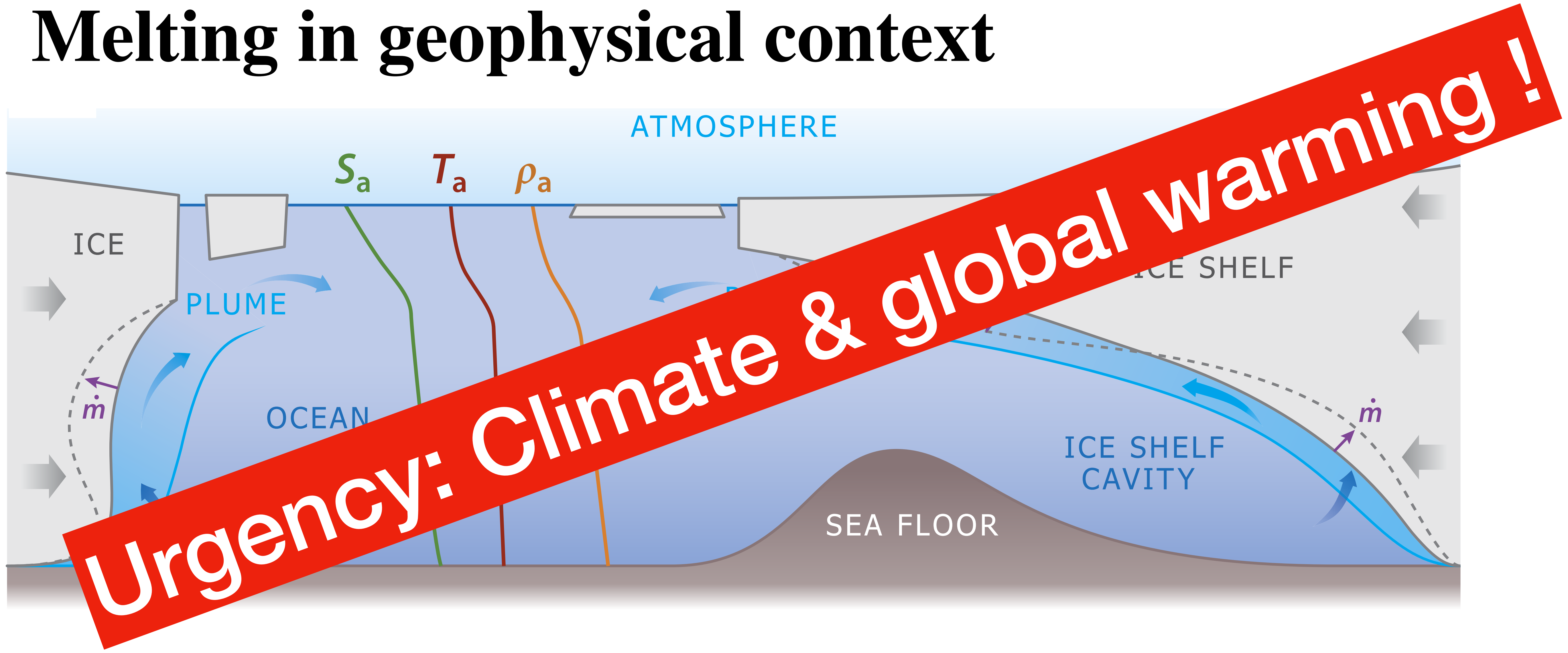

Latent thermal energy storage:

Phase change materials

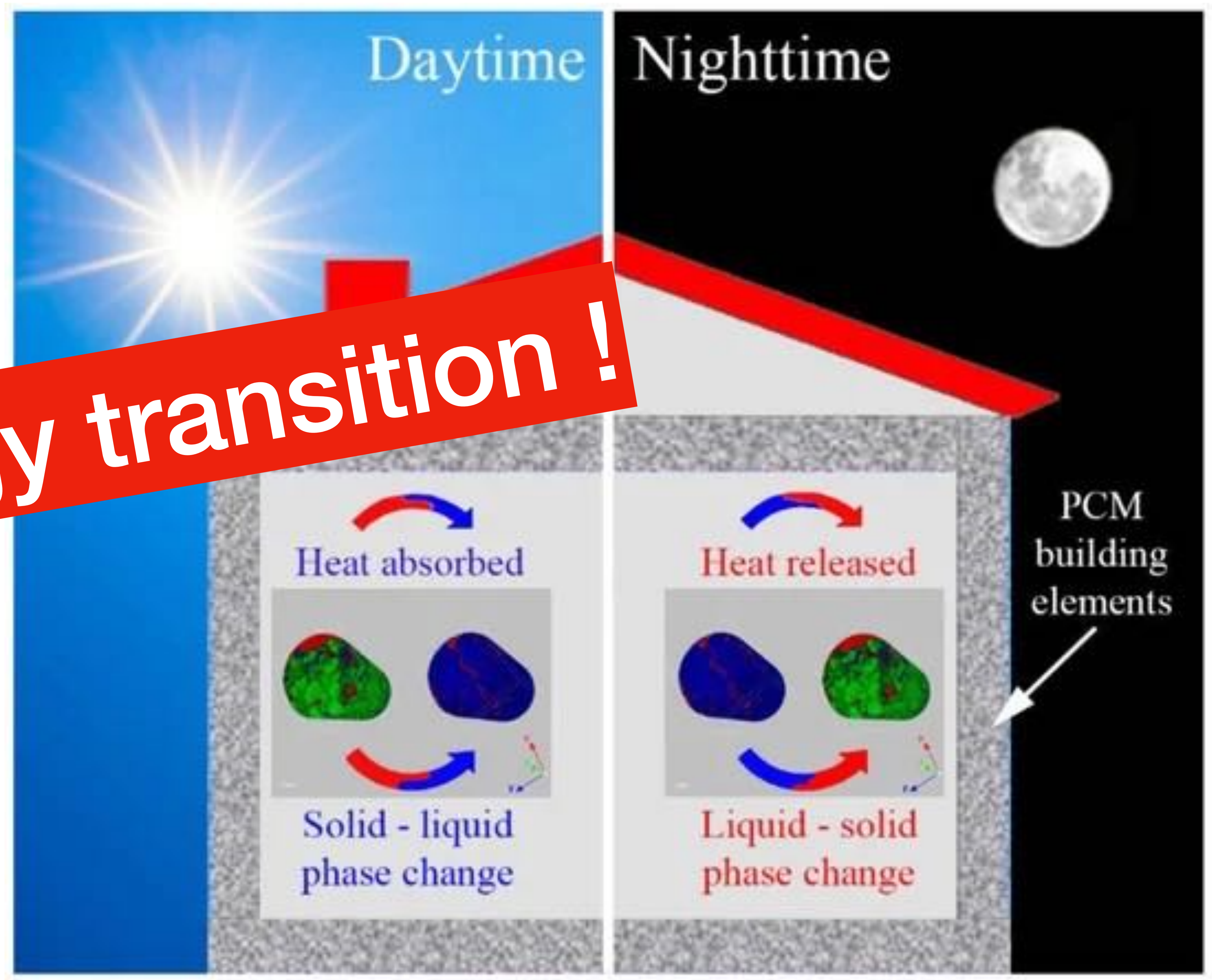

CO_2 sequestration in brine: negative emission

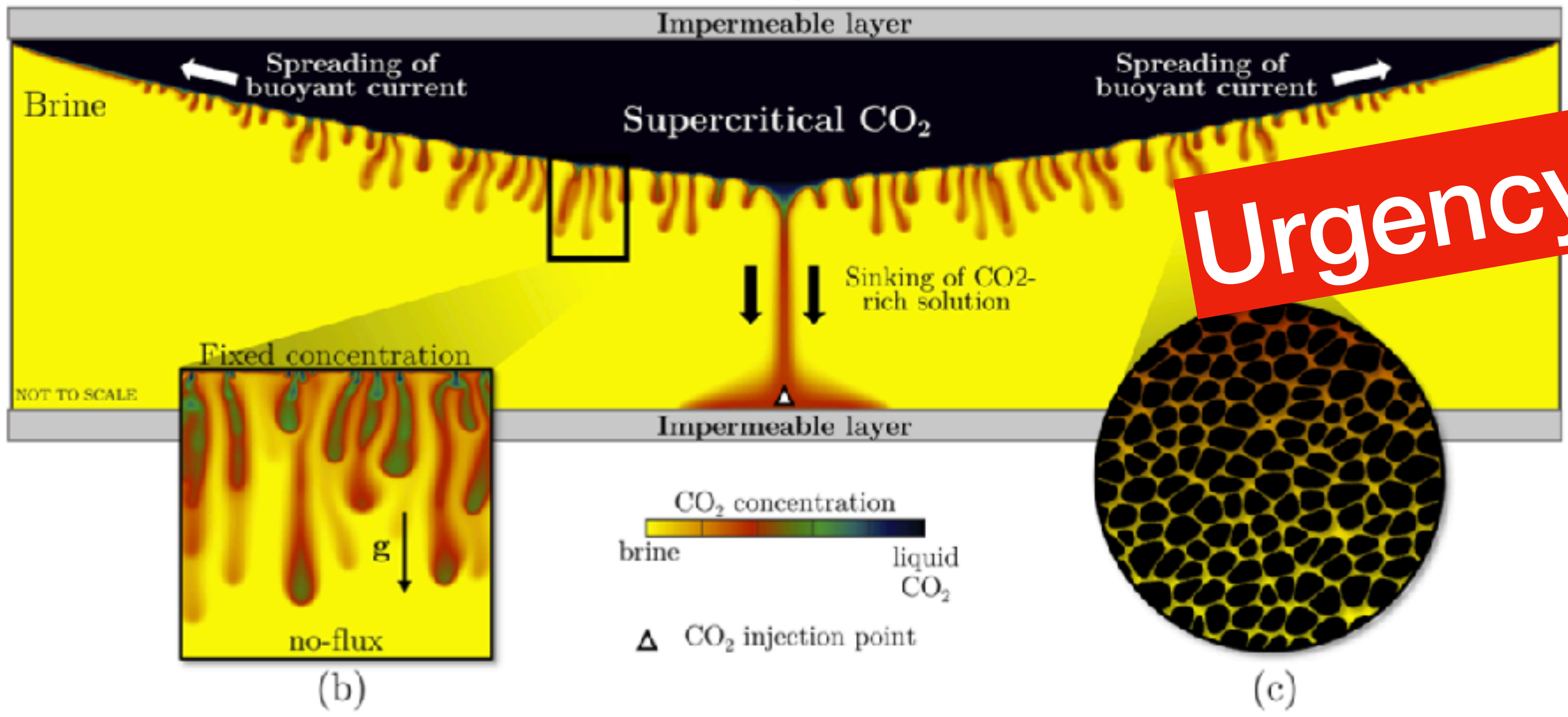

Podara *et al.*, Appl. Sci. 11, 1490 (2021)

Objective of research line

- **Quantitative understanding** of melting & dissolution processes in multicomponent, multiphase systems, across all scales and on a fundamental level
- Perform controlled experiments & numerical simulations for **idealized setups** on various length scales
- Allow for a **one-to-one comparison** between experiments and numerics/theory

Objective of research line

- **Quantitative understanding** of melting & dissolution processes in multicomponent, multiphase systems, across all scales and on a fundamental level
- Perform controlled experiments & numerical simulations for **idealized setups** on various length scales
- Allow for a **one-to-one comparison** between experiments and numerics/theory
- **Local** measurements of velocity, salt concentration, and temperature and connect them to **global transport processes**, to arrive at a fundamental understanding of such Stefan problems in multicomponent systems

Cast the melting problem into Rayleigh-Bénard geometry!

“Drosophila” of Physics of Fluids

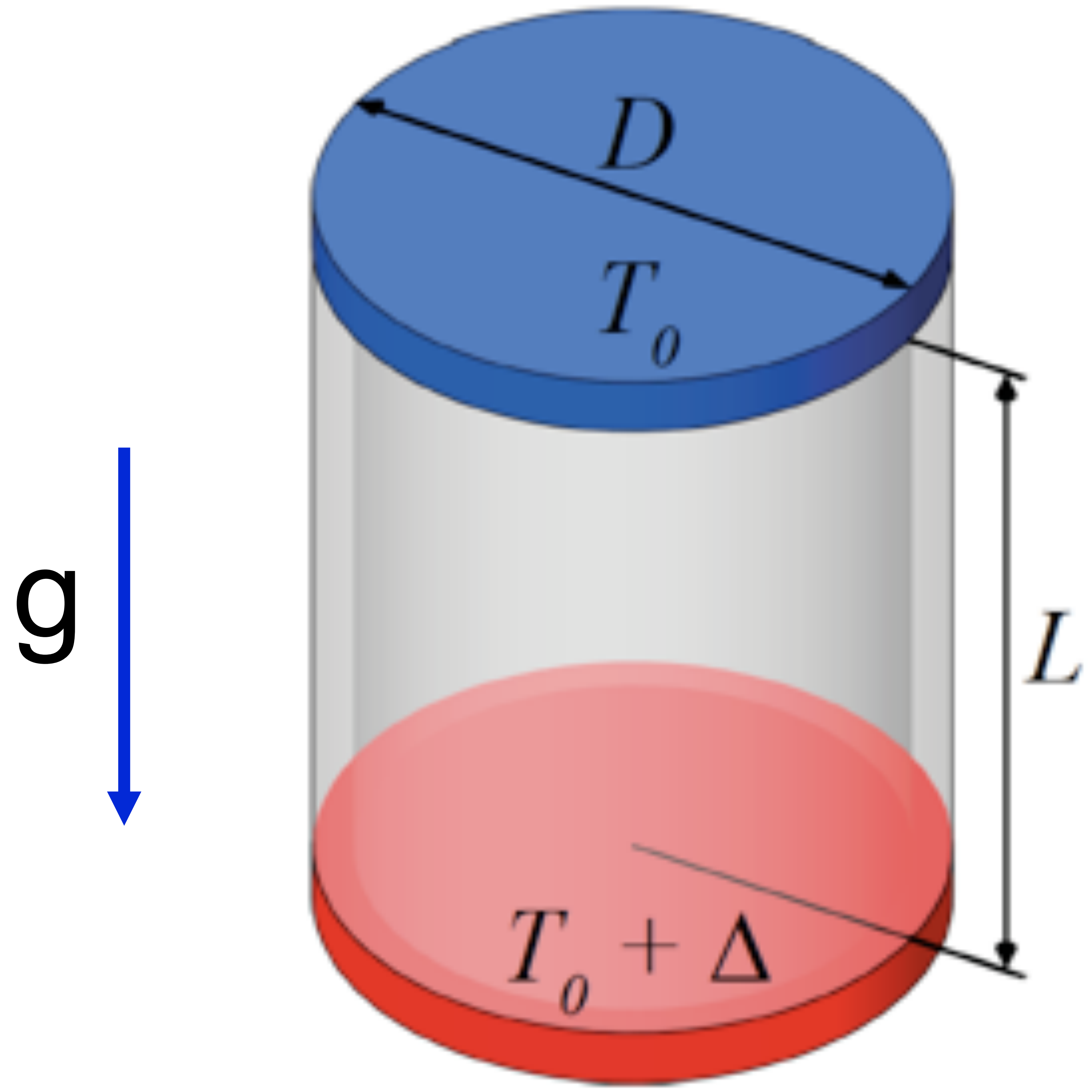

Rayleigh-Bénard:

Heat transfer

-- closed systems -- global balances -- mathematically well defined

Rayleigh-Bénard convection

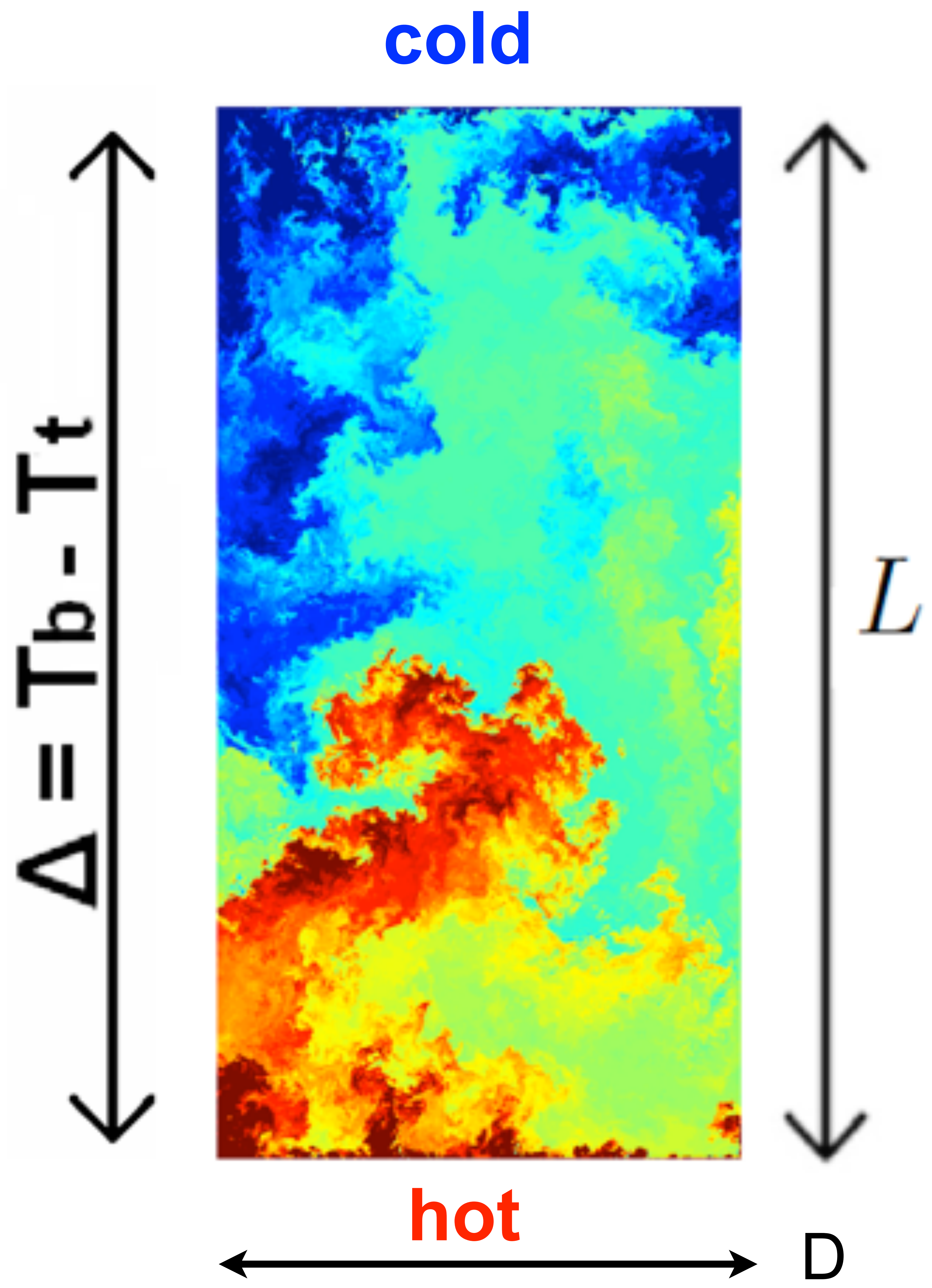

Control parameters:

Rayleigh number

$$Ra = \frac{\beta g L^3 \Delta}{\nu \kappa}$$

Prandtl number

$$Pr = \frac{\nu}{\kappa}$$

Aspect ratio

$$\Gamma = \frac{D}{L}$$

Rayleigh-Bénard convection

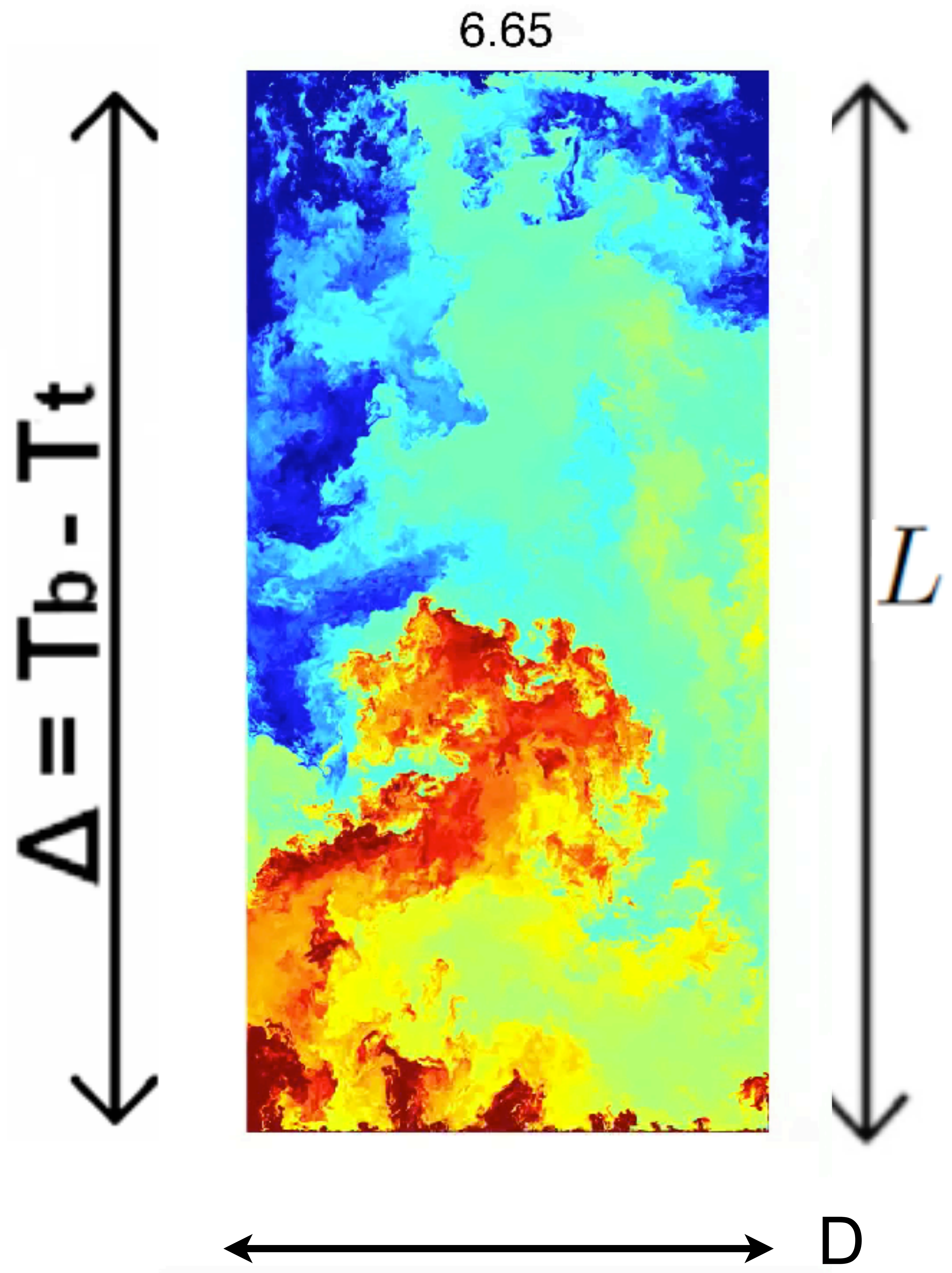

Control parameters:

Rayleigh number

$$Ra = \frac{\beta g L^3 \Delta}{\nu \kappa}$$

Prandtl number

$$Pr = \frac{\nu}{\kappa}$$

Aspect ratio

$$\Gamma = \frac{D}{L}$$

Rayleigh-Bénard convection

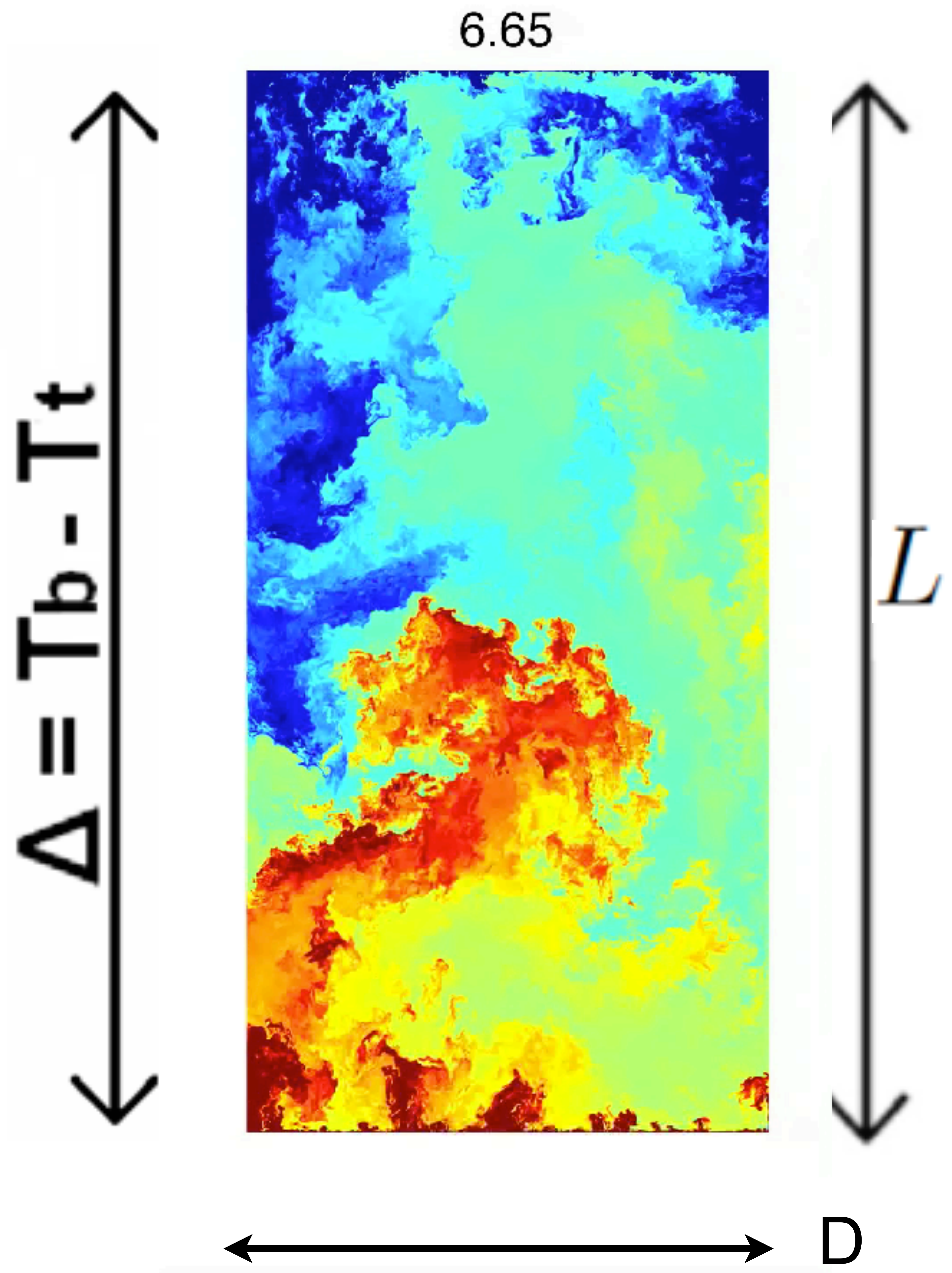

Control parameters:

Rayleigh number

$$Ra = \frac{\beta g L^3 \Delta}{\nu \kappa}$$

Prandtl number

$$Pr = \frac{\nu}{\kappa}$$

Aspect ratio

$$\Gamma = \frac{D}{L}$$

Rayleigh-Bénard convection

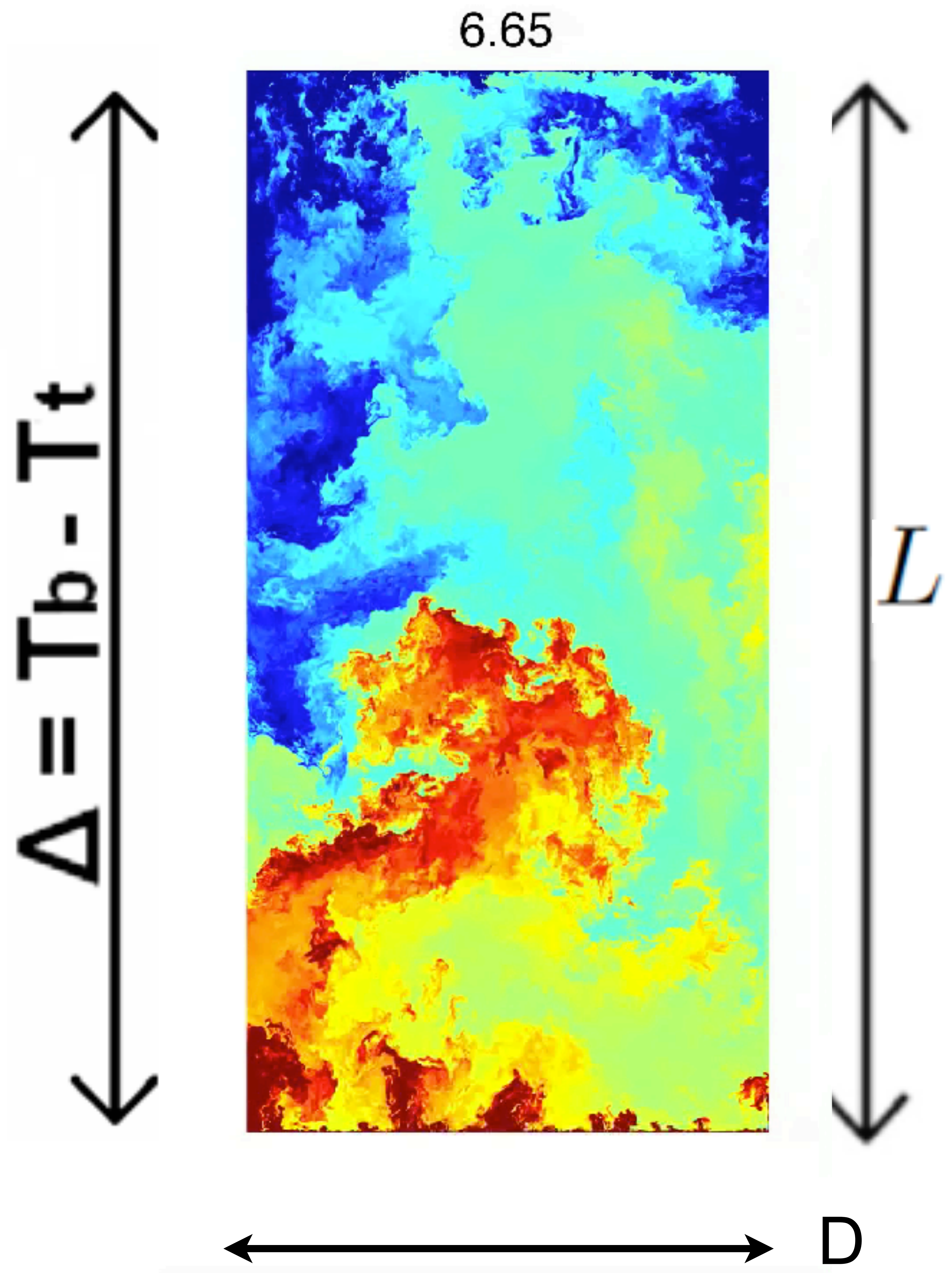

Control parameters:

Rayleigh number

$$Ra = \frac{\beta g L^3 \Delta}{\nu \kappa}$$

Prandtl number

$$Pr = \frac{\nu}{\kappa}$$

Aspect ratio

$$\Gamma = \frac{D}{L}$$

Global response of the system

$$\boxed{\begin{array}{c} \mathbf{Nu\ (Ra,\ Pr,\ \Gamma)\ ?} \\ \mathbf{Re\ (Ra,\ Pr,\ \Gamma)\ ?} \end{array}}$$

Nu = dimensionless heat transfer = $J/J_{conductive}$

Re = dimensionless turbulence intensity

Turbulent Rayleigh-Bénard flow

Turbulent Rayleigh-Bénard flow

Rayleigh-Bénard convection

$Ra = 10^9$

$Pr = 1$

$\Gamma = 1$

Movie by Olga Shishkina
Goldfish-code

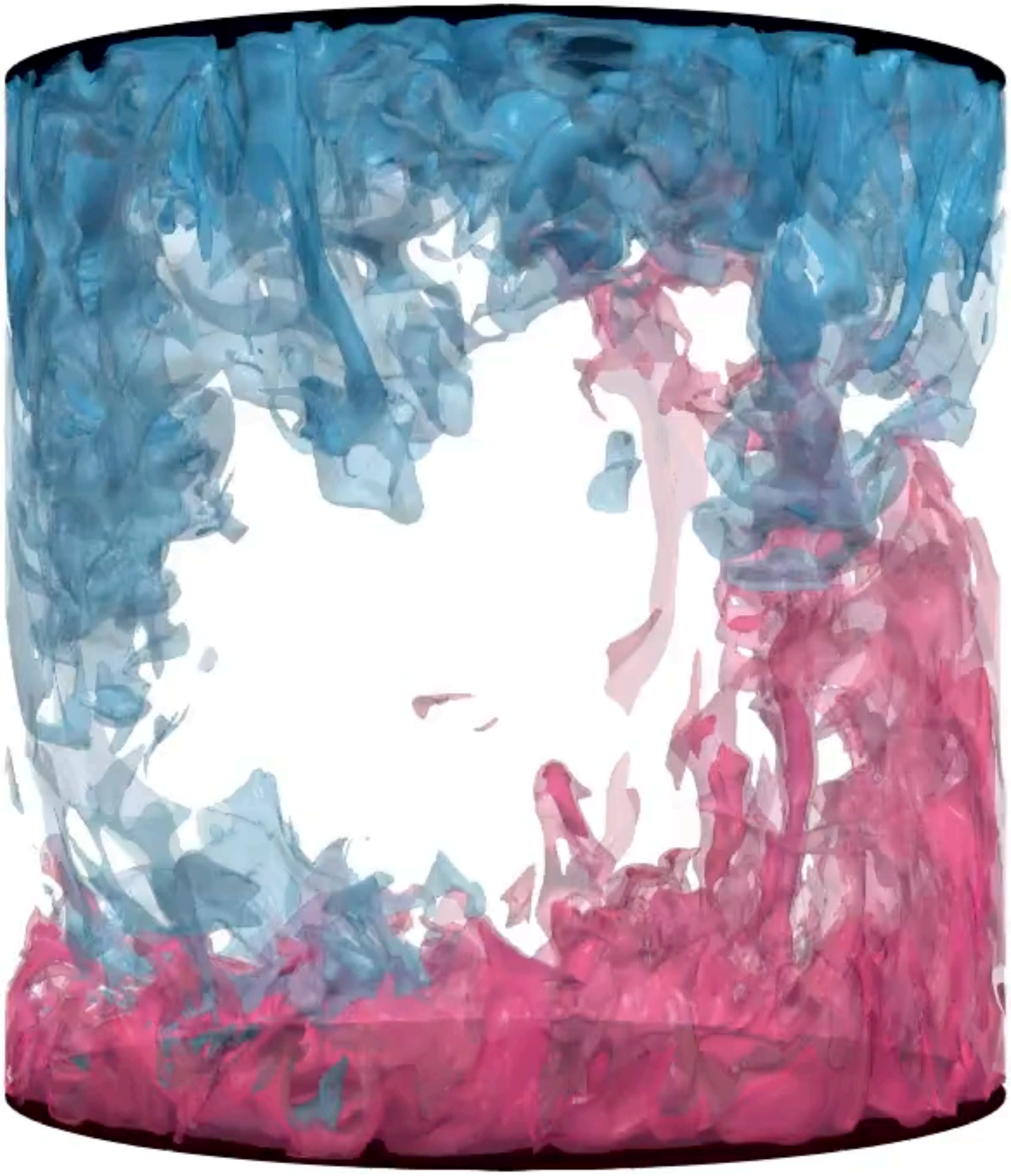

Rayleigh-Bénard convection

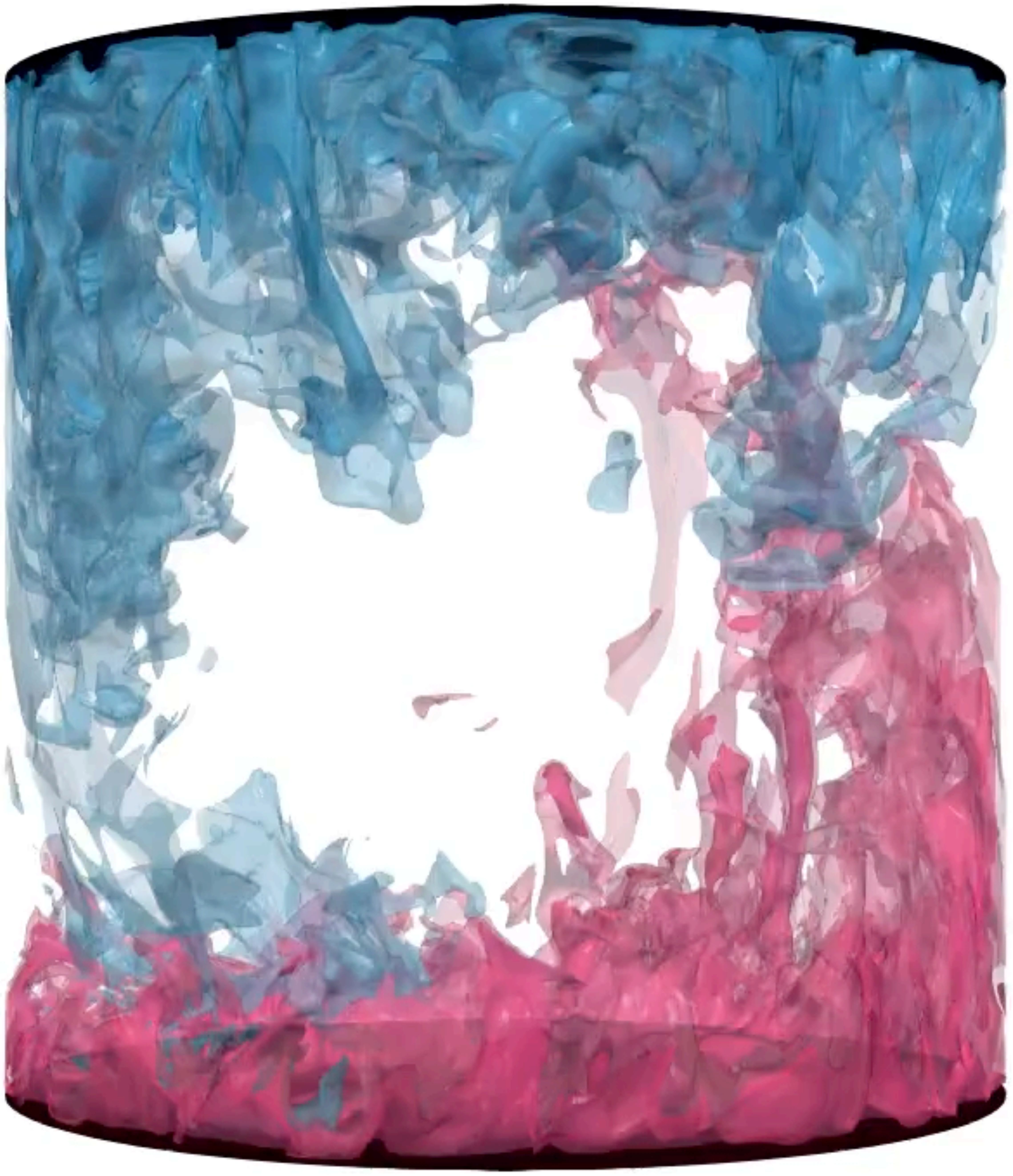

$\mathrm{Ra} = 10^9$

$\mathrm{Pr} = 1$

$\Gamma = 1$

Movie by Olga Shishkina
Goldfish-code

Cast the melting problem into Rayleigh-Bénard geometry!

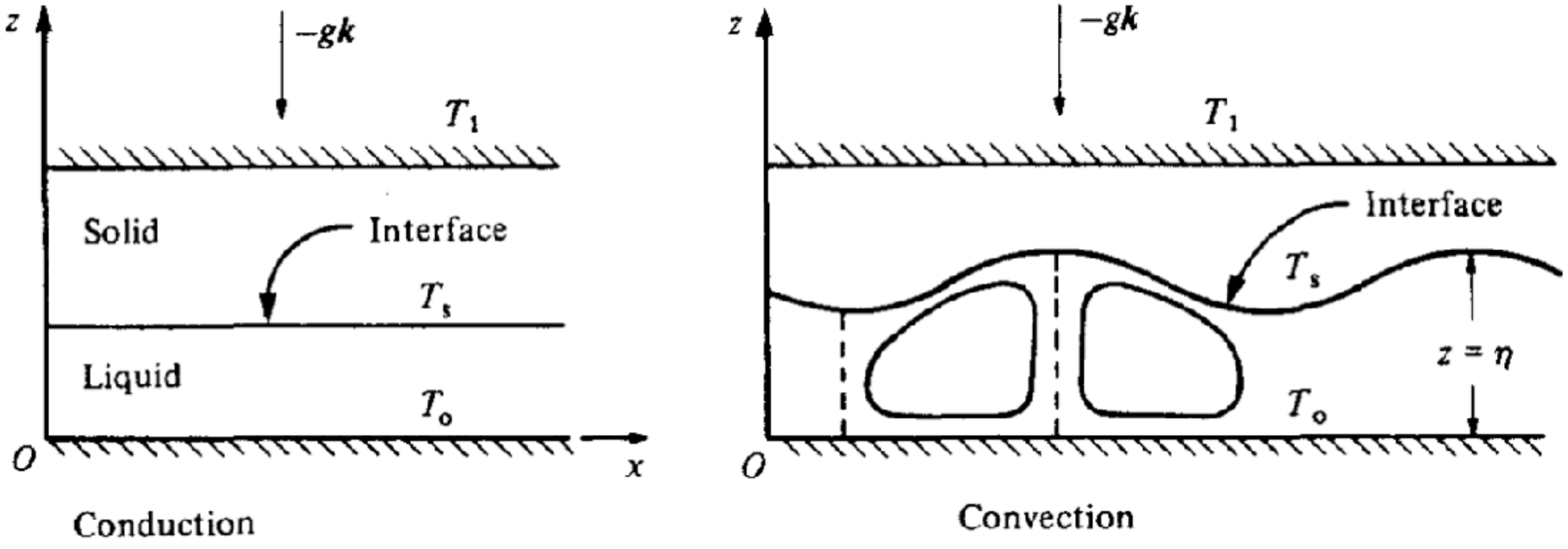

S. H. Davis, U. Müller, C. Dietsche, JFM 144, 133 (1984)

Cast the melting problem into Rayleigh-Bénard geometry!

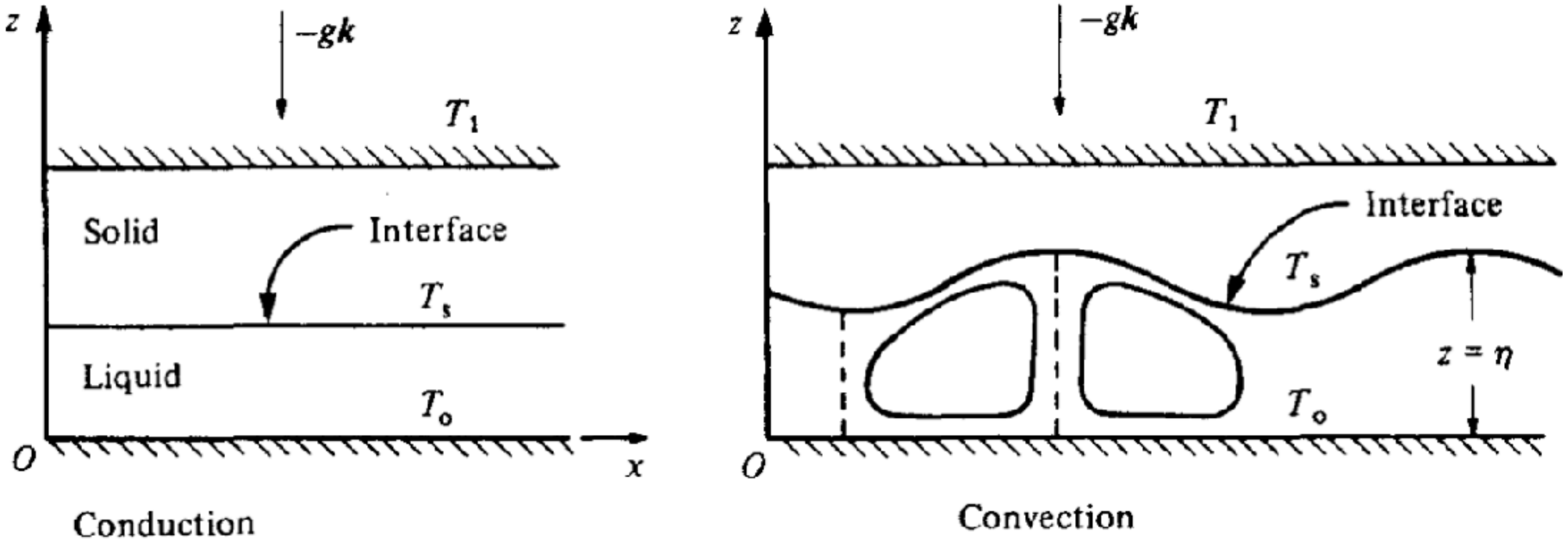

S. H. Davis, U. Müller, C. Dietsche, JFM 144, 133 (1984)

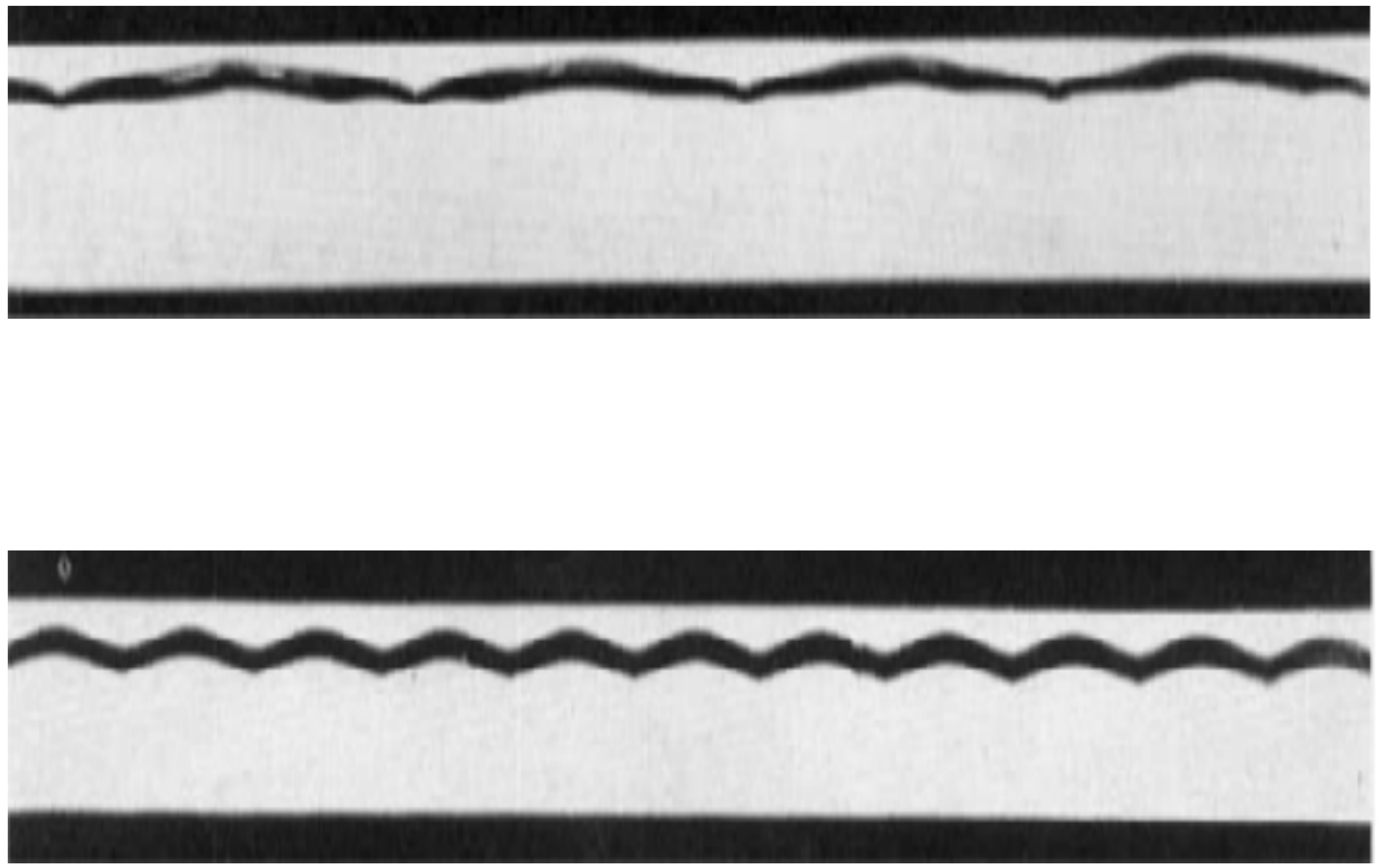

C. Dietsche, U. Müller, JFM 161, 249 (1985)

Cast the melting problem into Rayleigh-Bénard geometry!

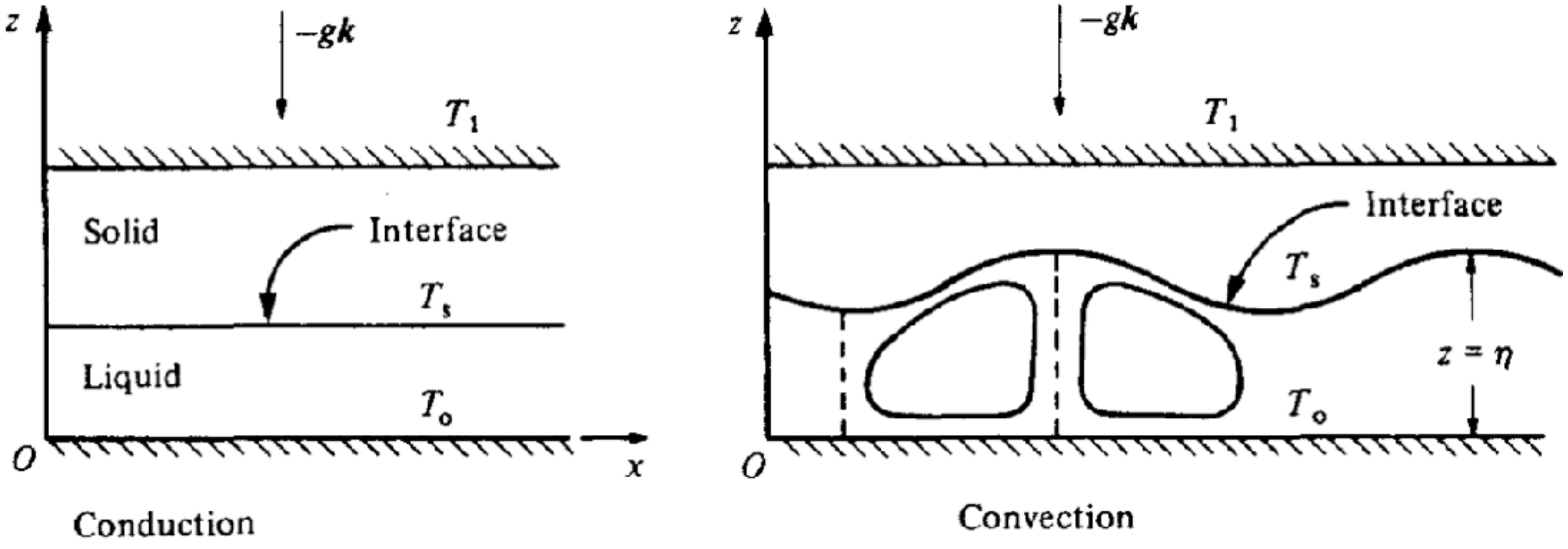

S. H. Davis, U. Müller, C. Dietsche, JFM 144, 133 (1984)

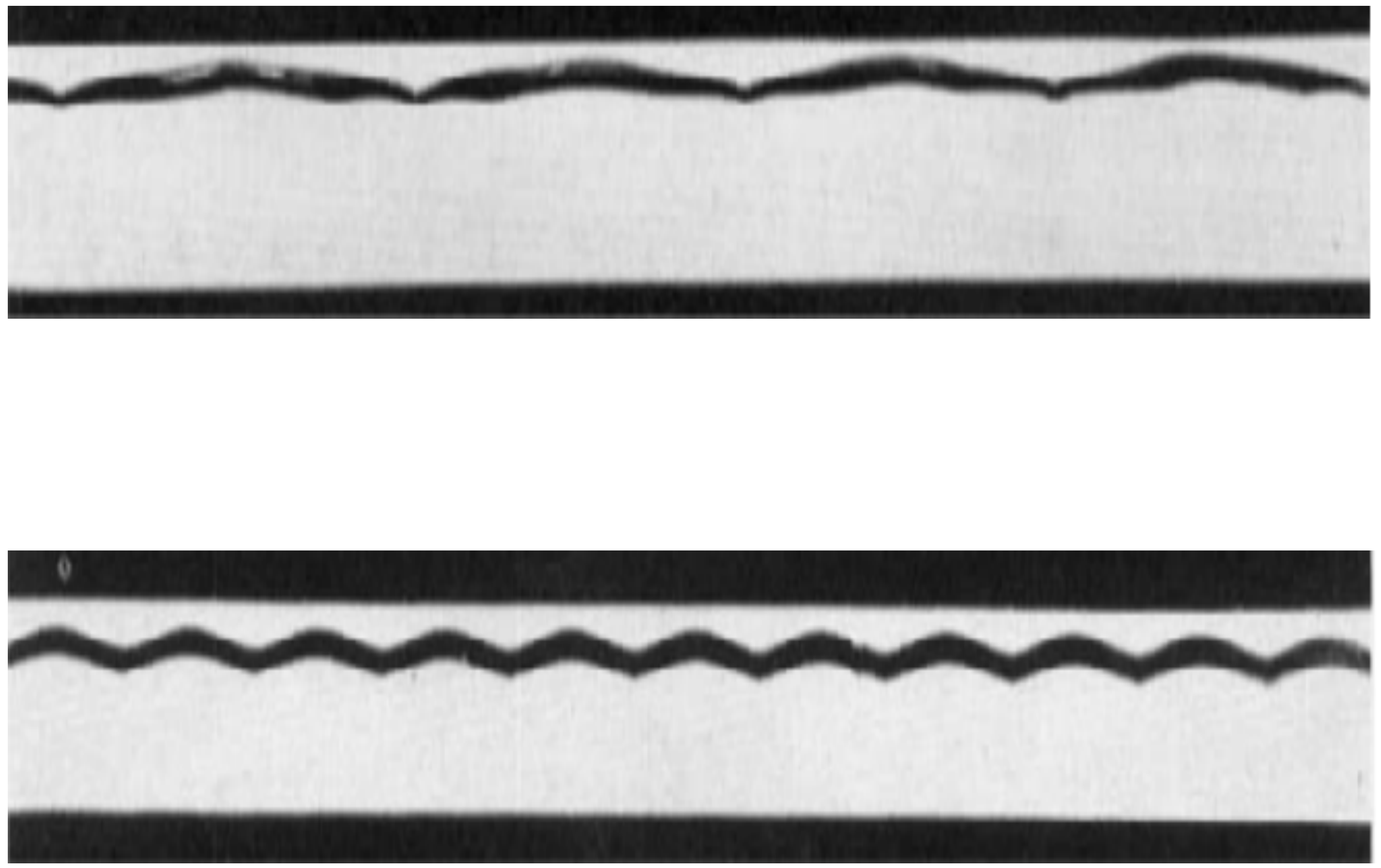

C. Dietsche, U. Müller, JFM 161, 249 (1985)

but in these papers: Ra $< 10^6$

Flipping of iceberg exposes engraved structures

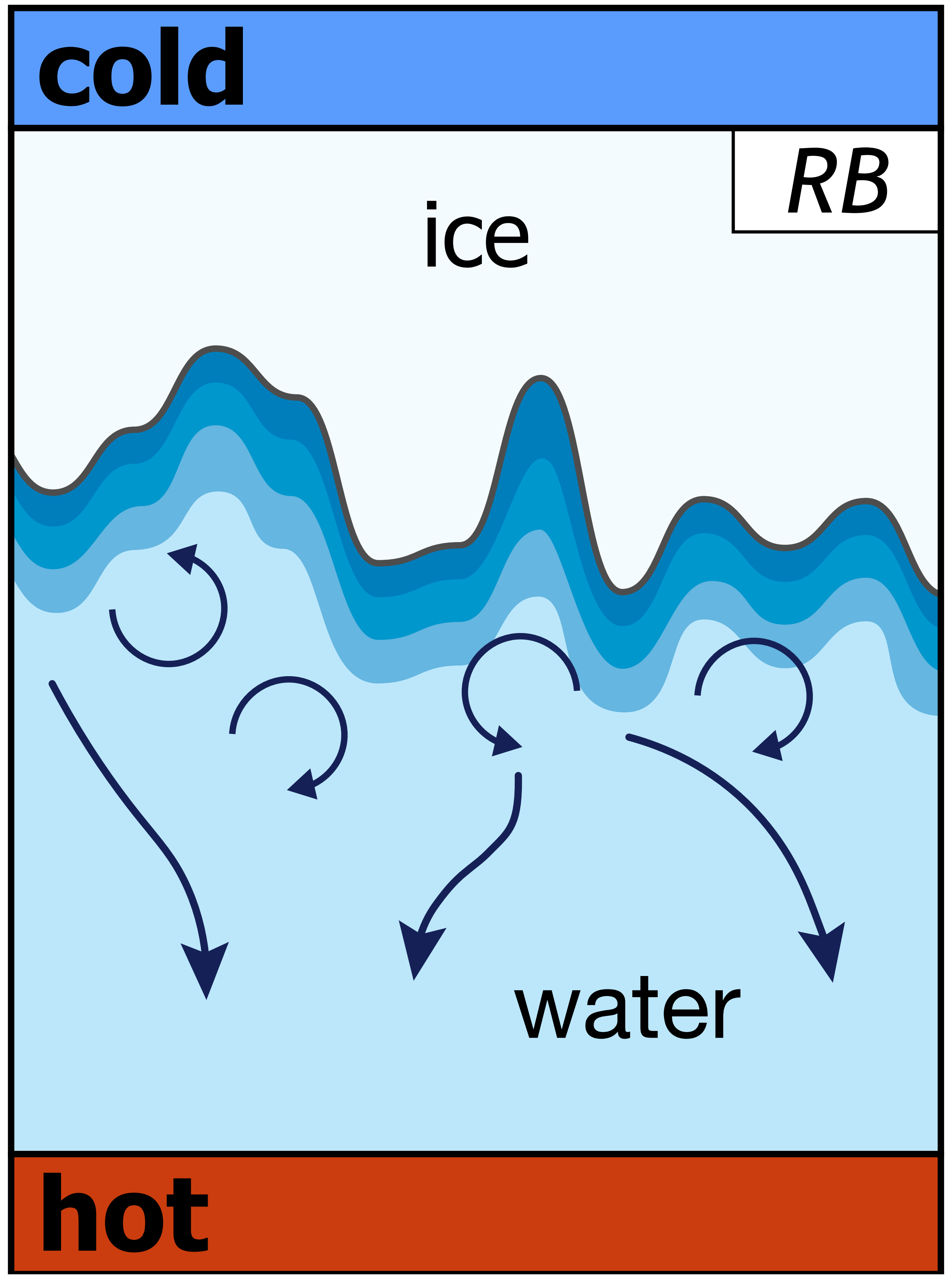

Flipping of iceberg exposes engraved structures

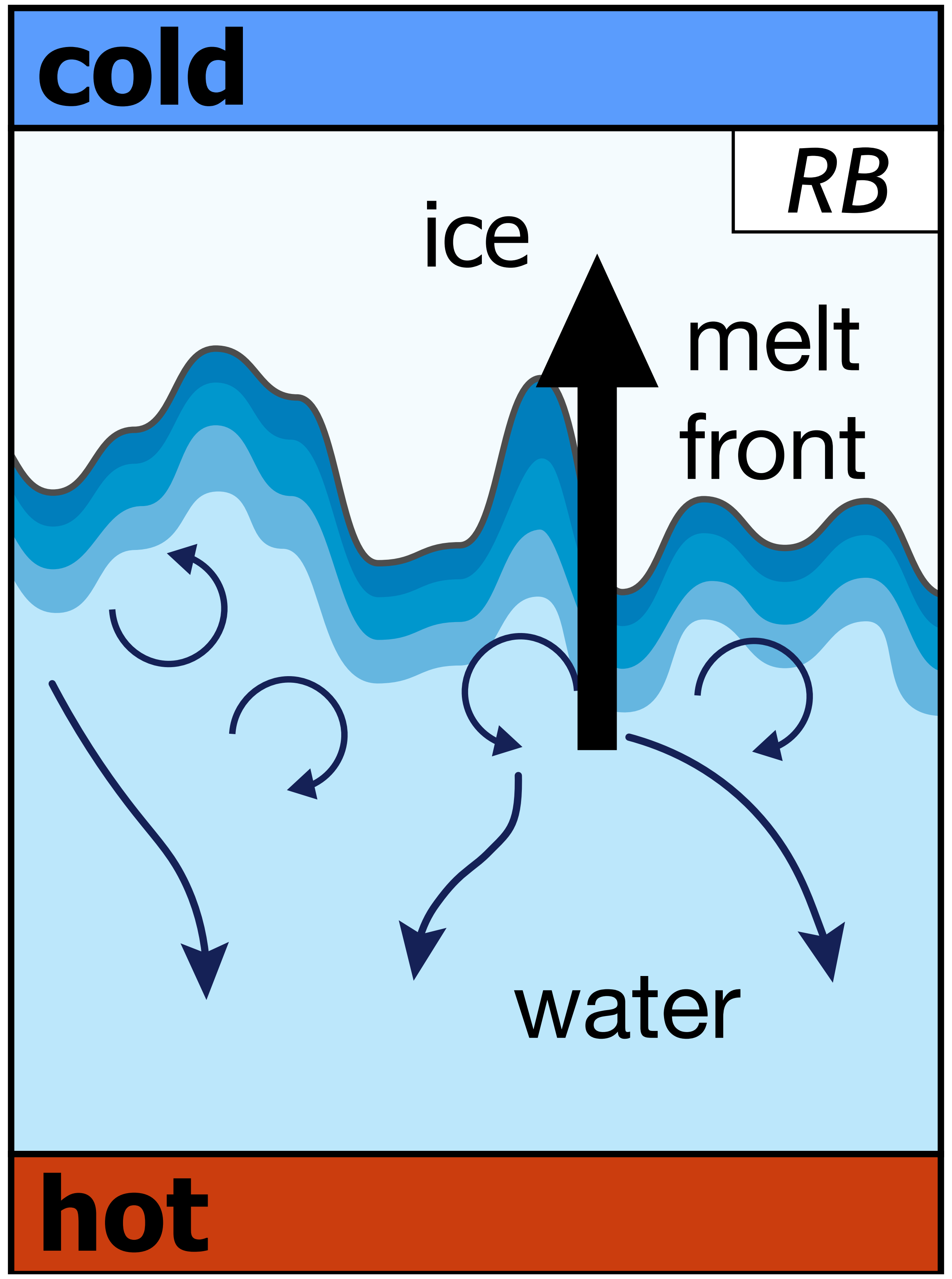

Flipping of iceberg exposes engraved structures

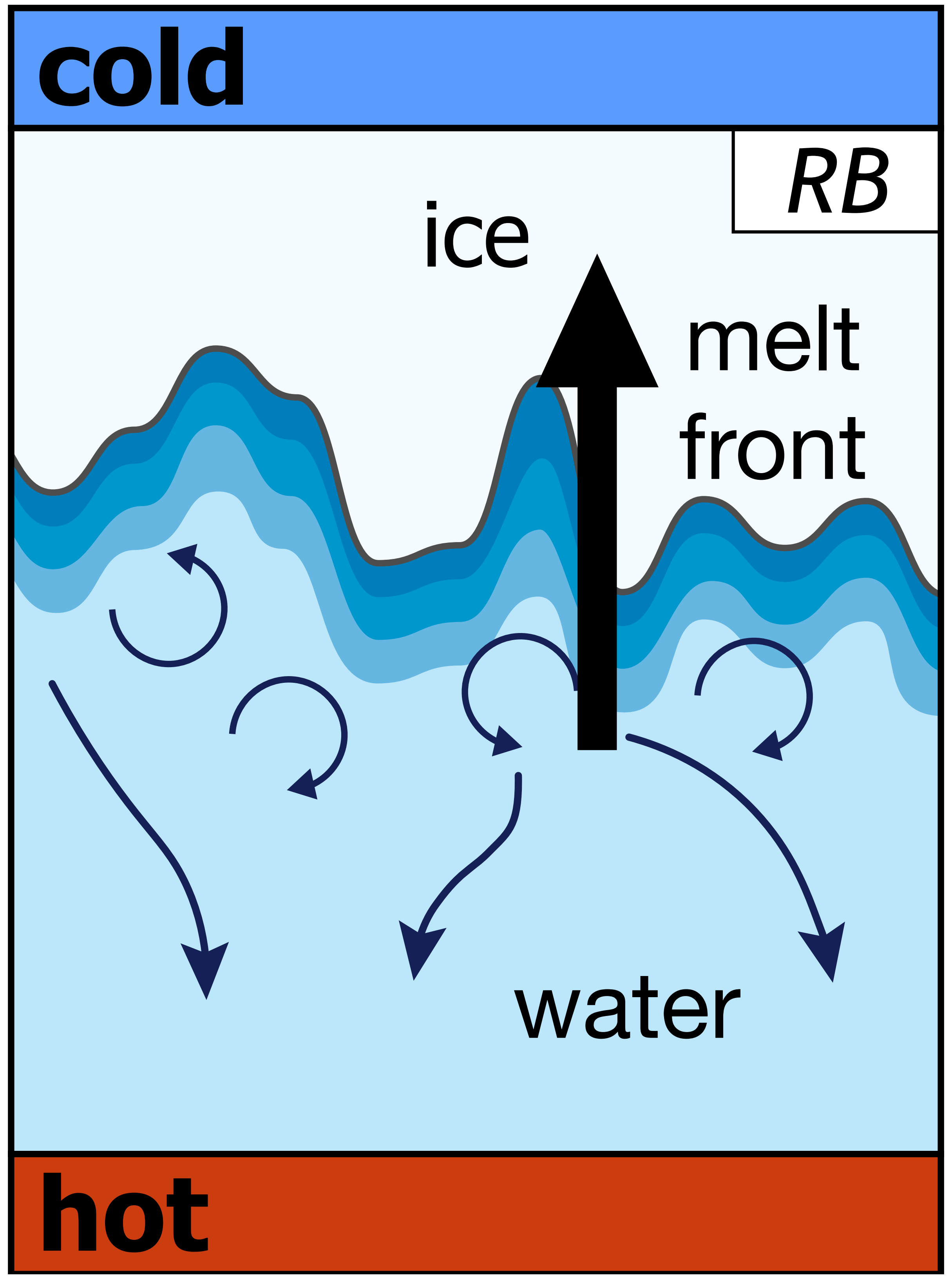

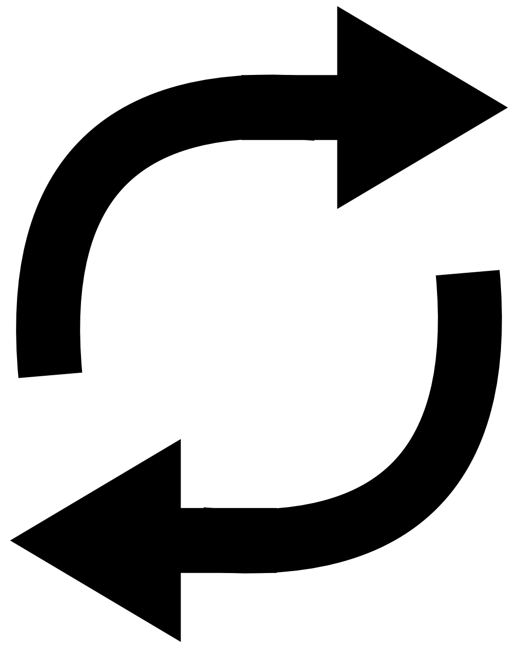

Flipping of iceberg exposes engraved structures

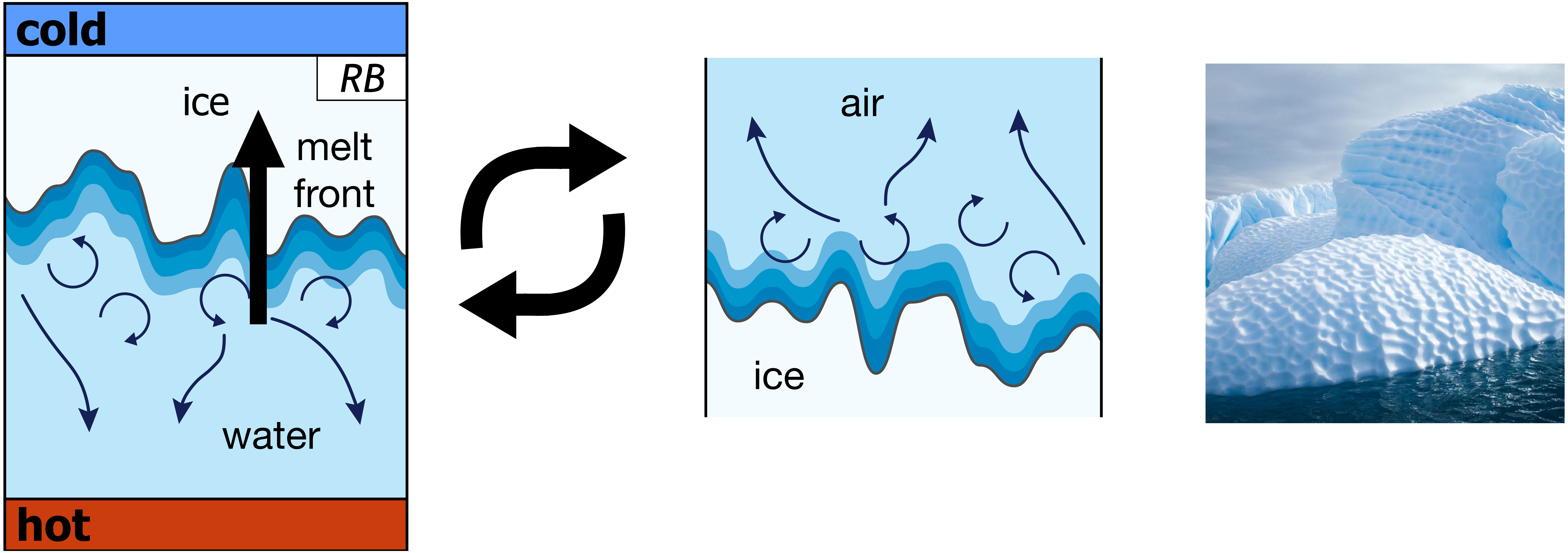

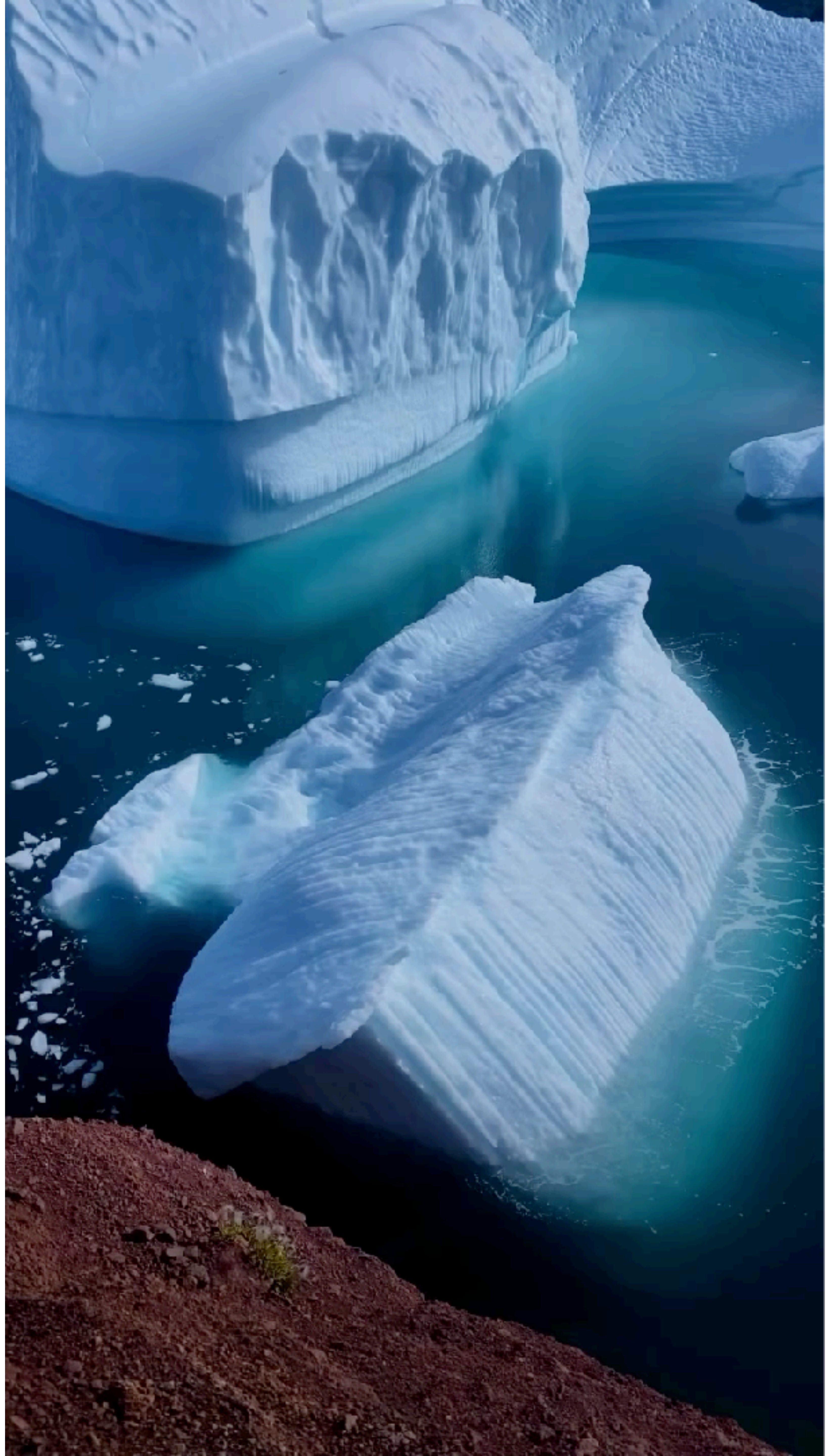

Flipping of iceberg exposes engraved structures

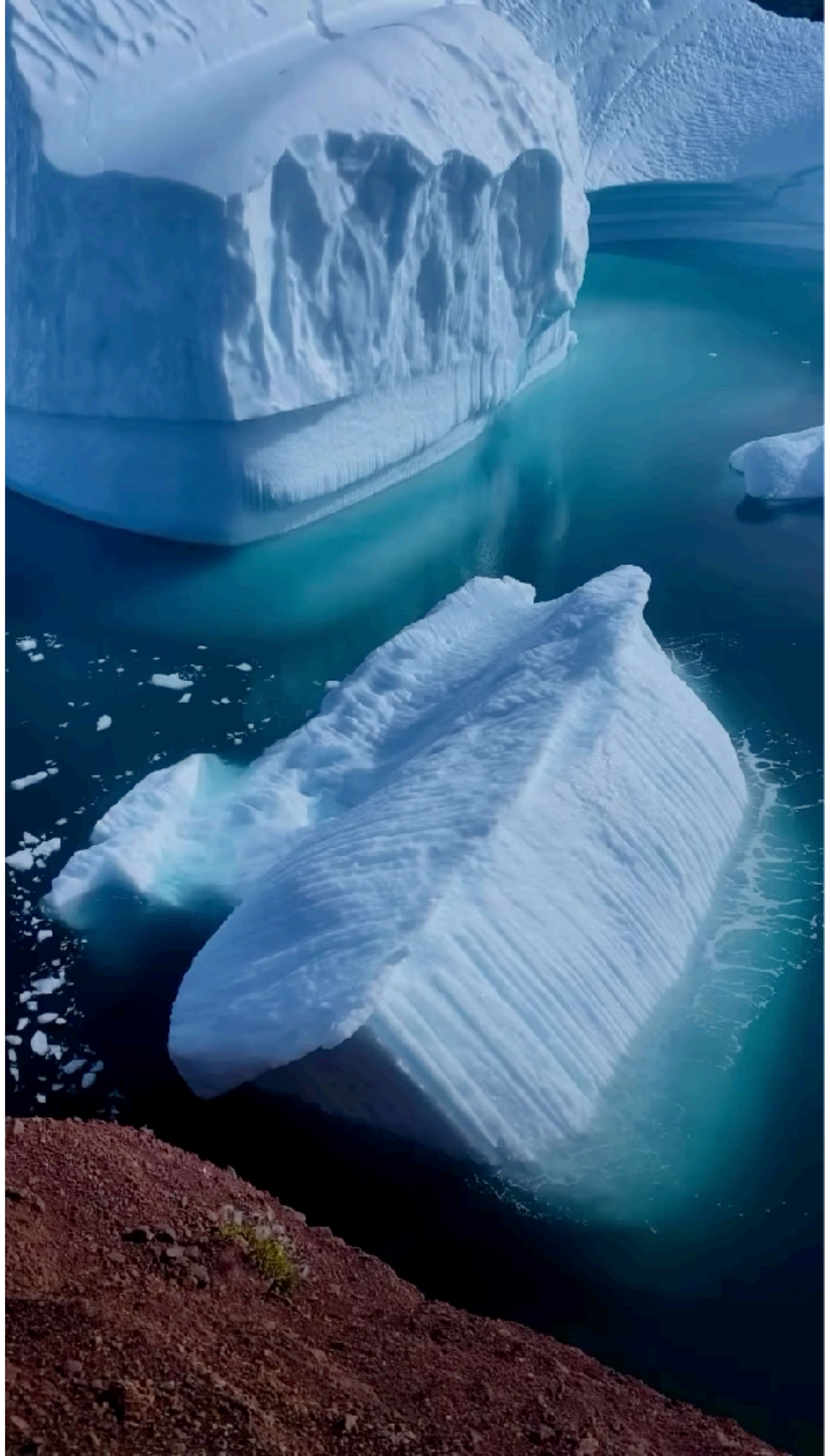

Flipping of iceberg exposes engraved structures

How to achieve very large Ra in numerics?

- DNS, 2nd order finite difference method
- no turbulence modelling!
- Massive parallelization (10^4 cores!)
- petaflop computing
- extremely efficient Poisson solver
- scalar lives on finer grid to achieve large Pr or Sc
- GPU version available
- coupled to Immersed Boundary Method (IBM)

Richard Stevens

Rodolfo Ostilla-Monico

Erwin vd Poel

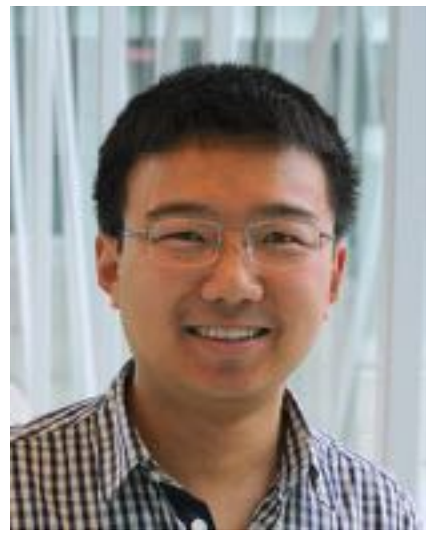

Yantao Yang

Xiaojue Zhu

Vamsi Spandan

Roberto Verzicco

How to achieve very large Ra in numerics?

- DNS, 2nd order finite difference method
- no turbulence modelling!
- Massive parallelization (10^4 cores!)
- petaflop computing
- extremely efficient Poisson solver
- scalar lives on finer grid to achieve large Pr or Sc
- GPU version available
- coupled to Immersed Boundary Method (IBM)

Advanced Finite Difference

AFiD

Richard
Stevens

Rodolfo
Ostilla-
Monico

Erwin
vd Poel

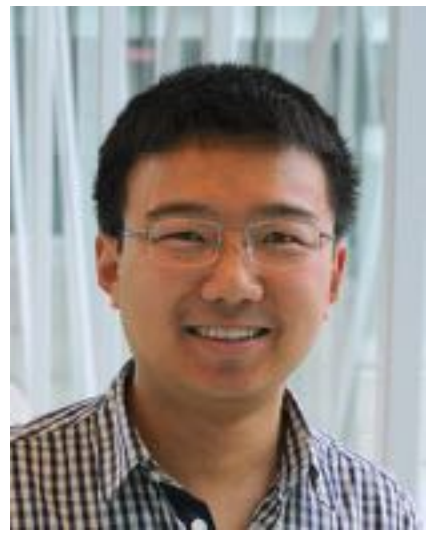

Yantao
Yang

Xiaojue
Zhu

Vamsi
Spandan

Roberto Verzicco

Flows to which we applied AFiD

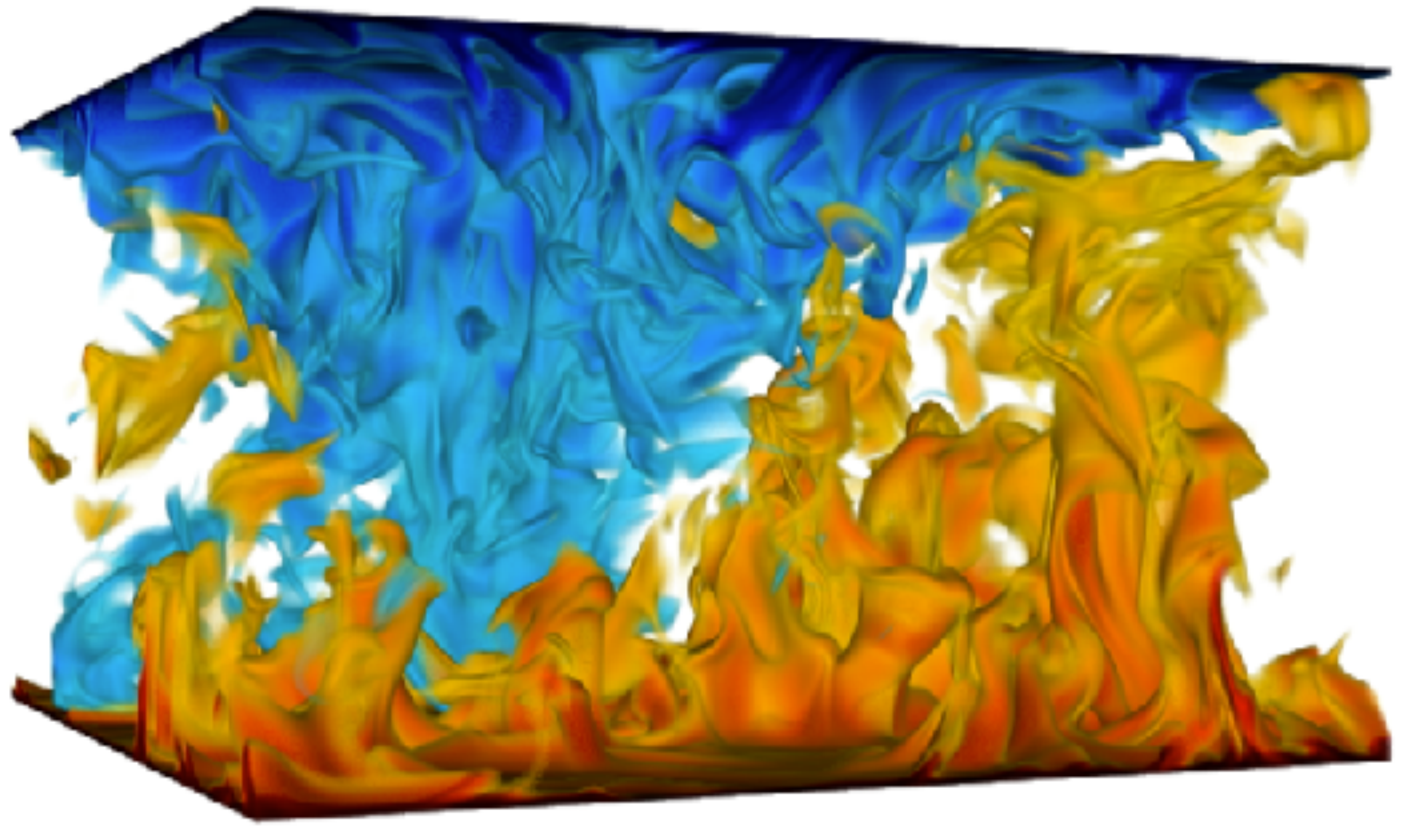

Rayleigh-Bénard convection

Flows to which we applied AFiD

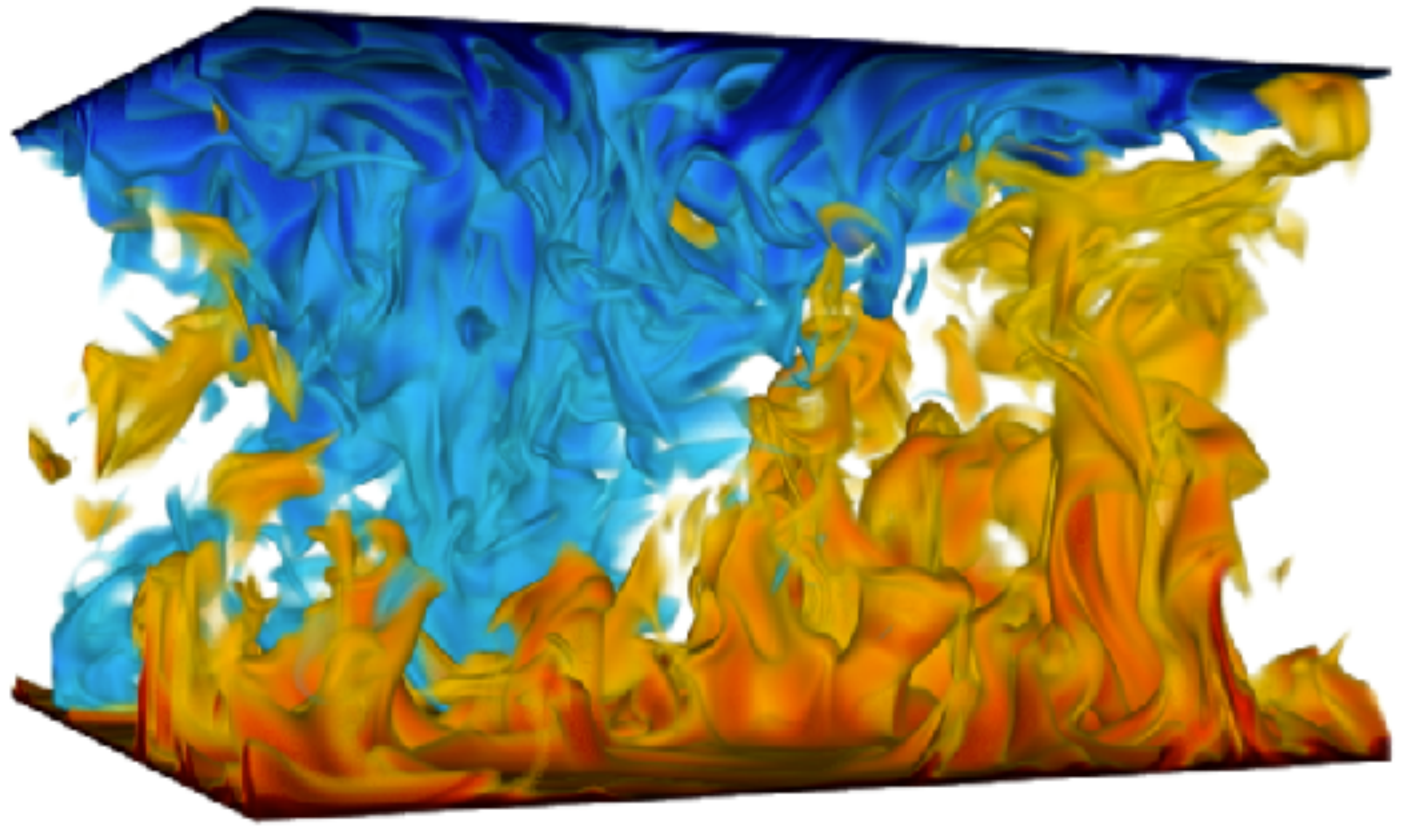

Rayleigh-Bénard convection

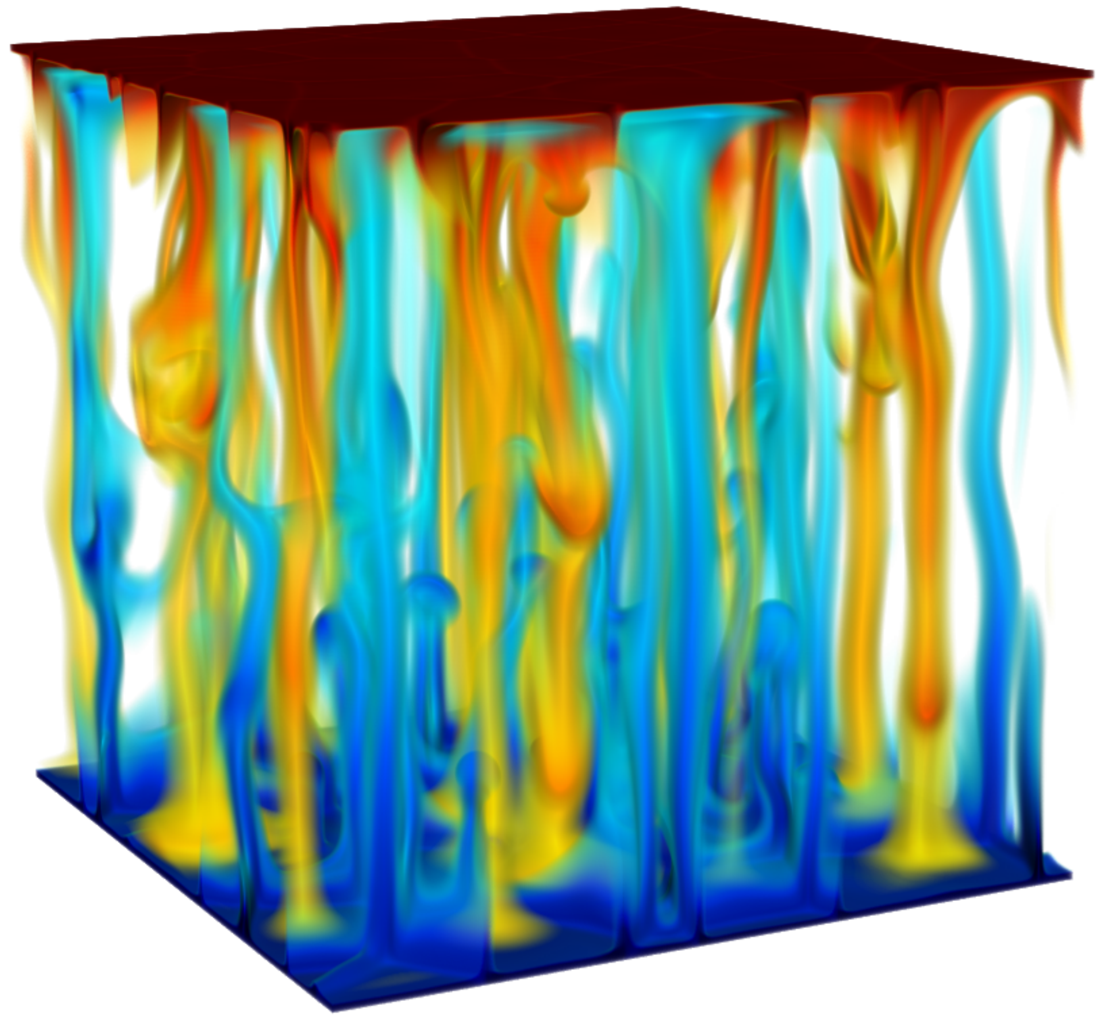

Double Diffusive convection

Flows to which we applied AFiD

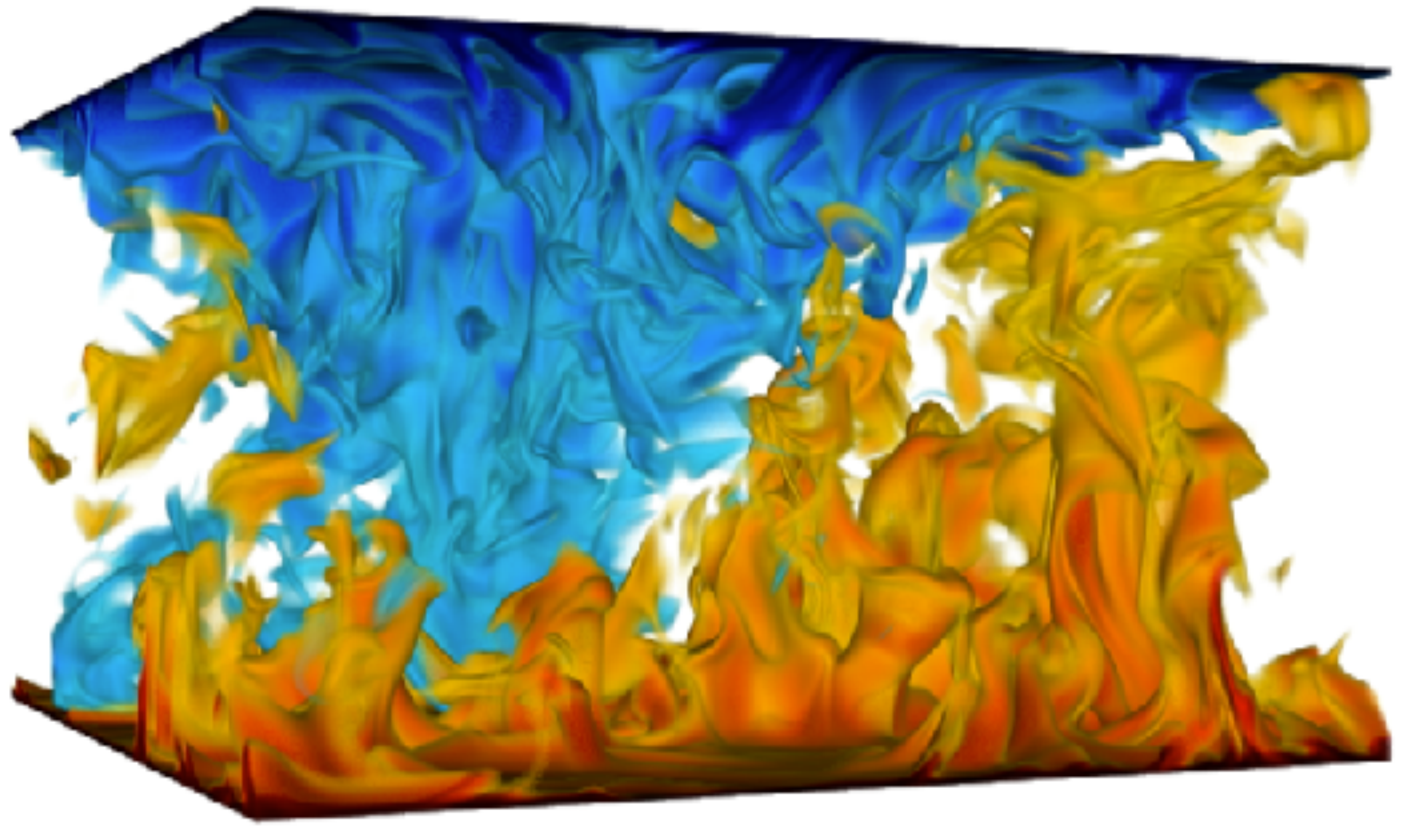

Rayleigh-Bénard convection

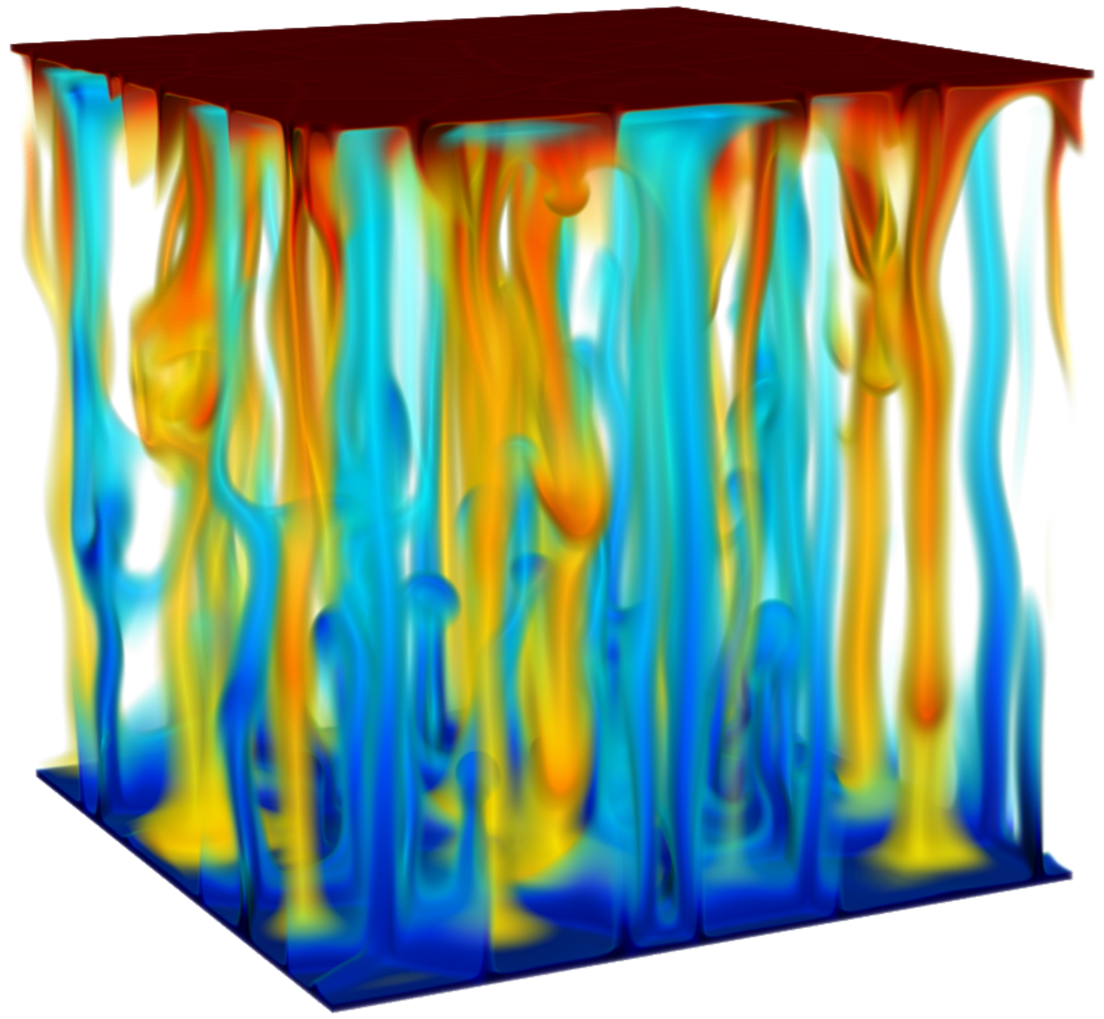

Double Diffusive convection

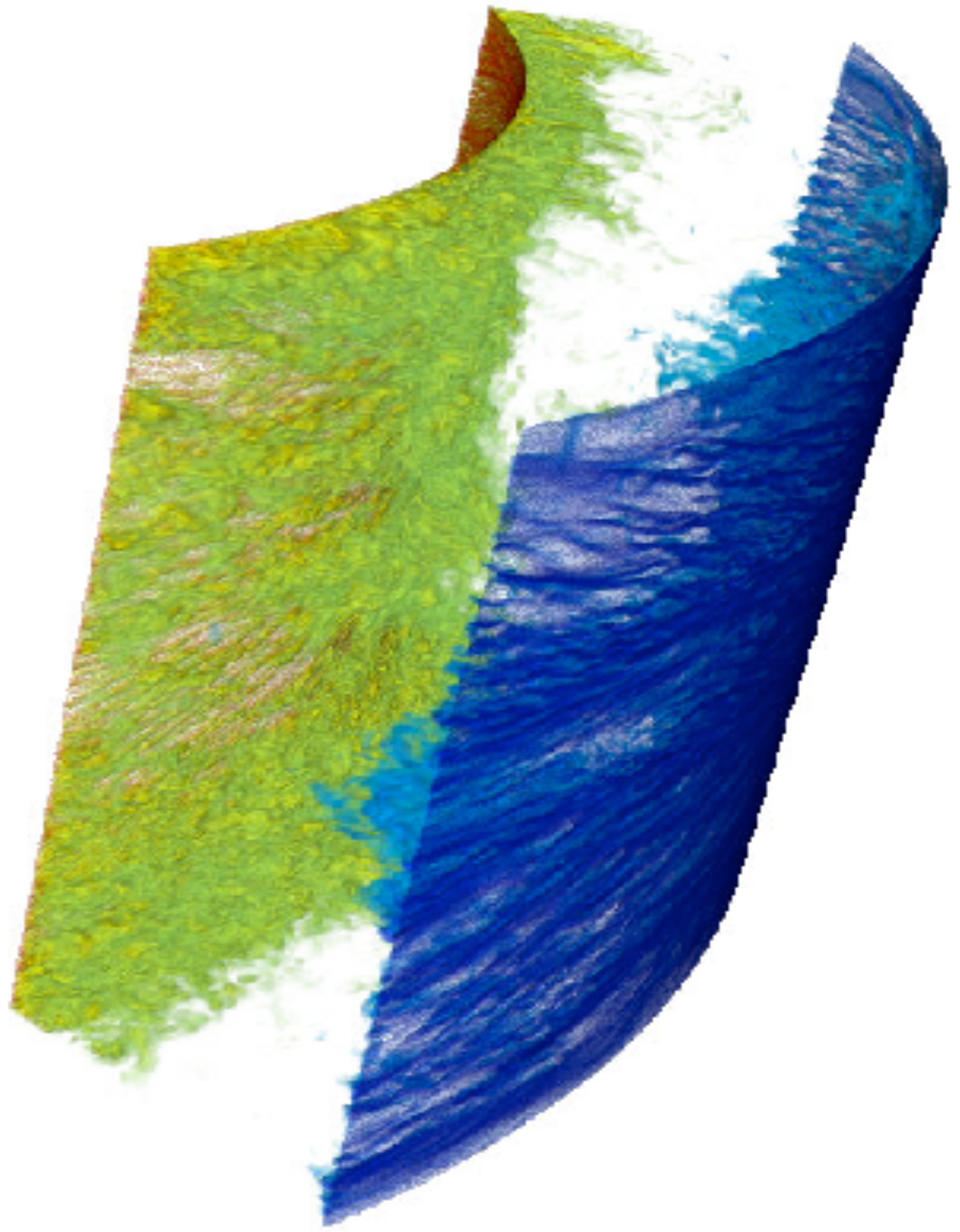

Taylor-Couette flow

Flows to which we applied AFiD

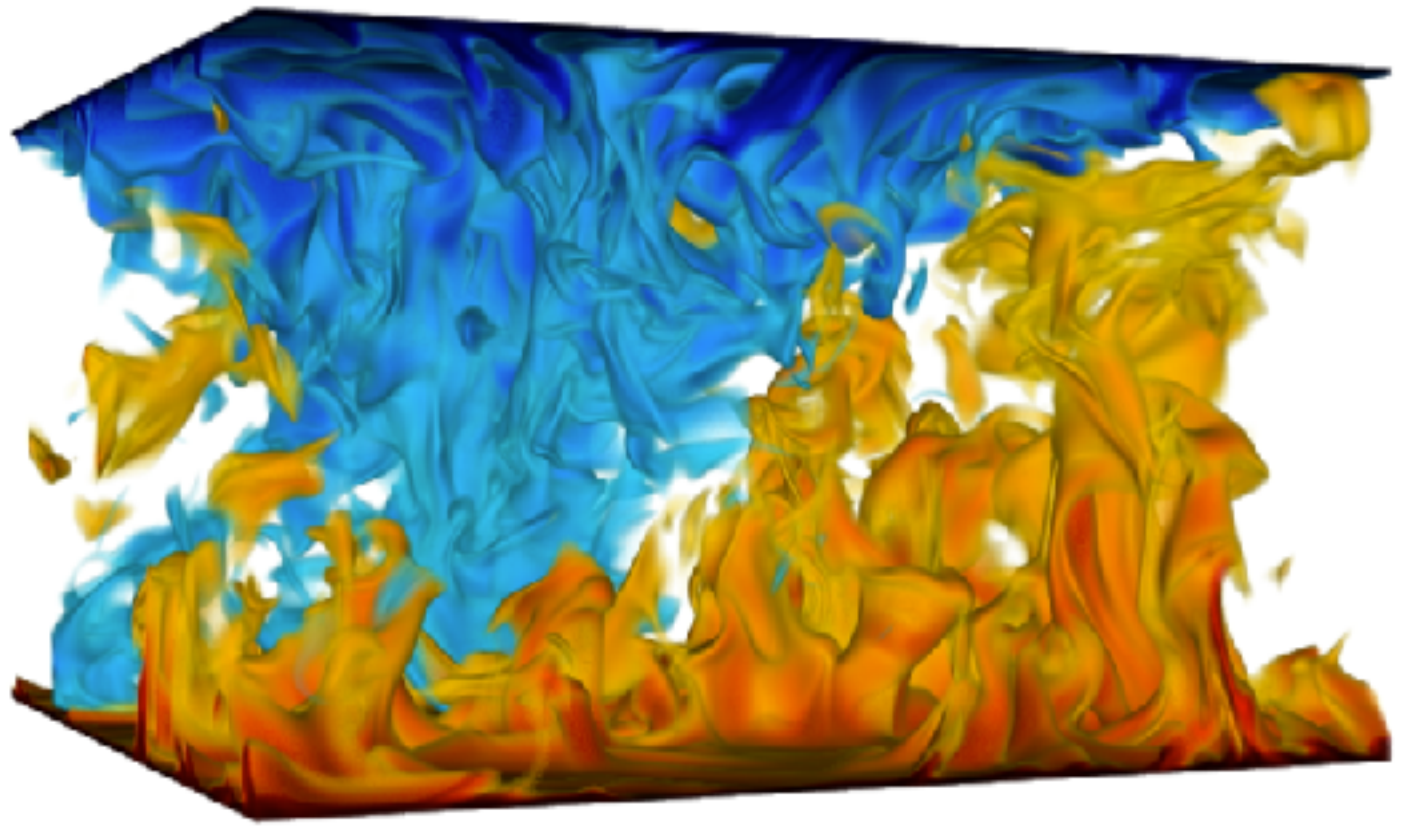

Rayleigh-Bénard convection

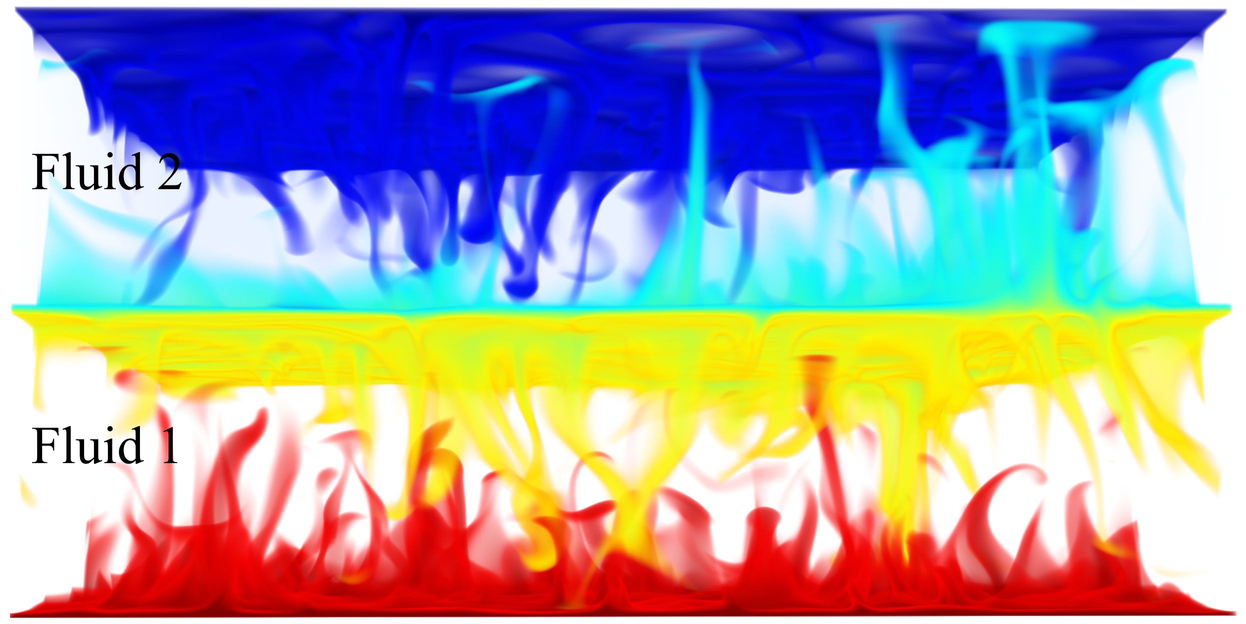

Two-layer systems

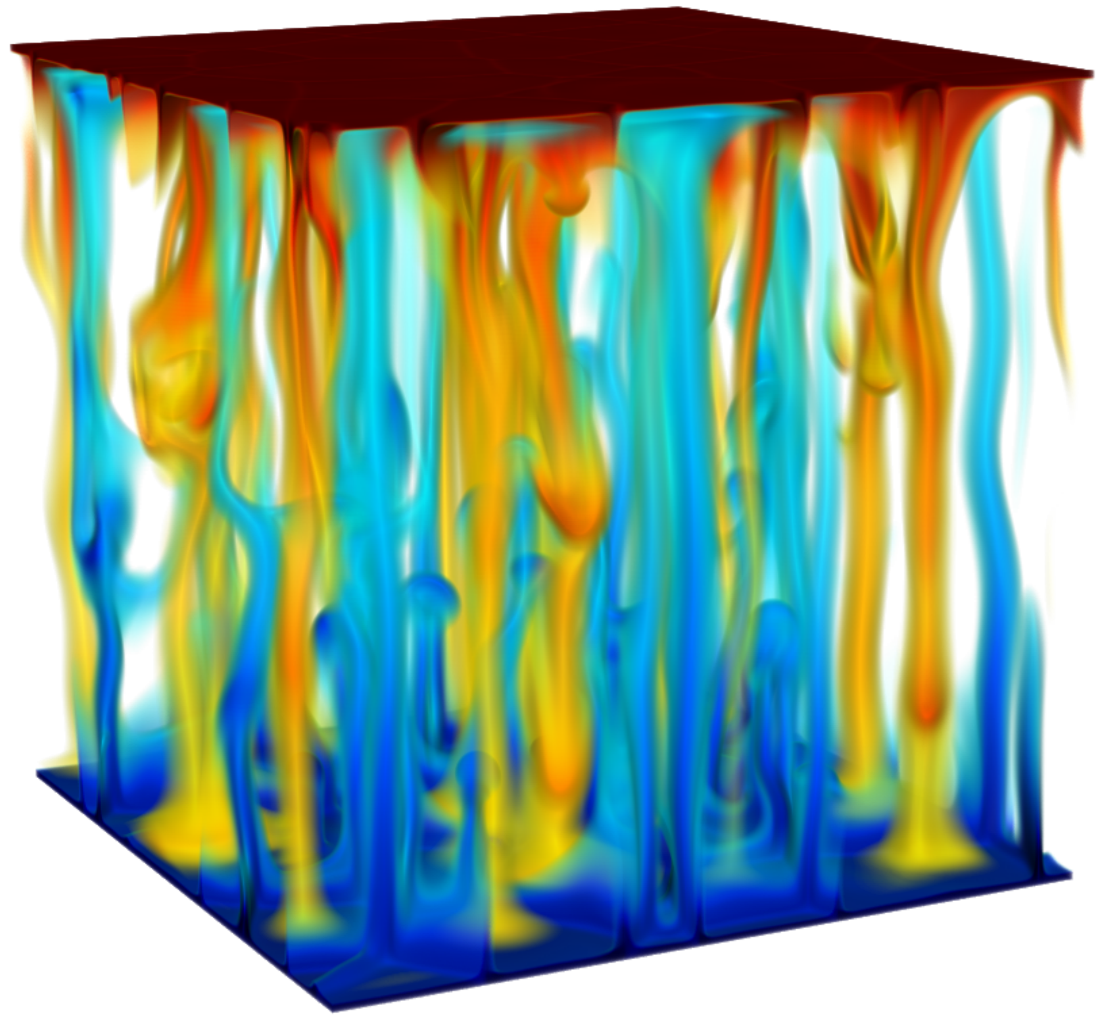

Double Diffusive convection

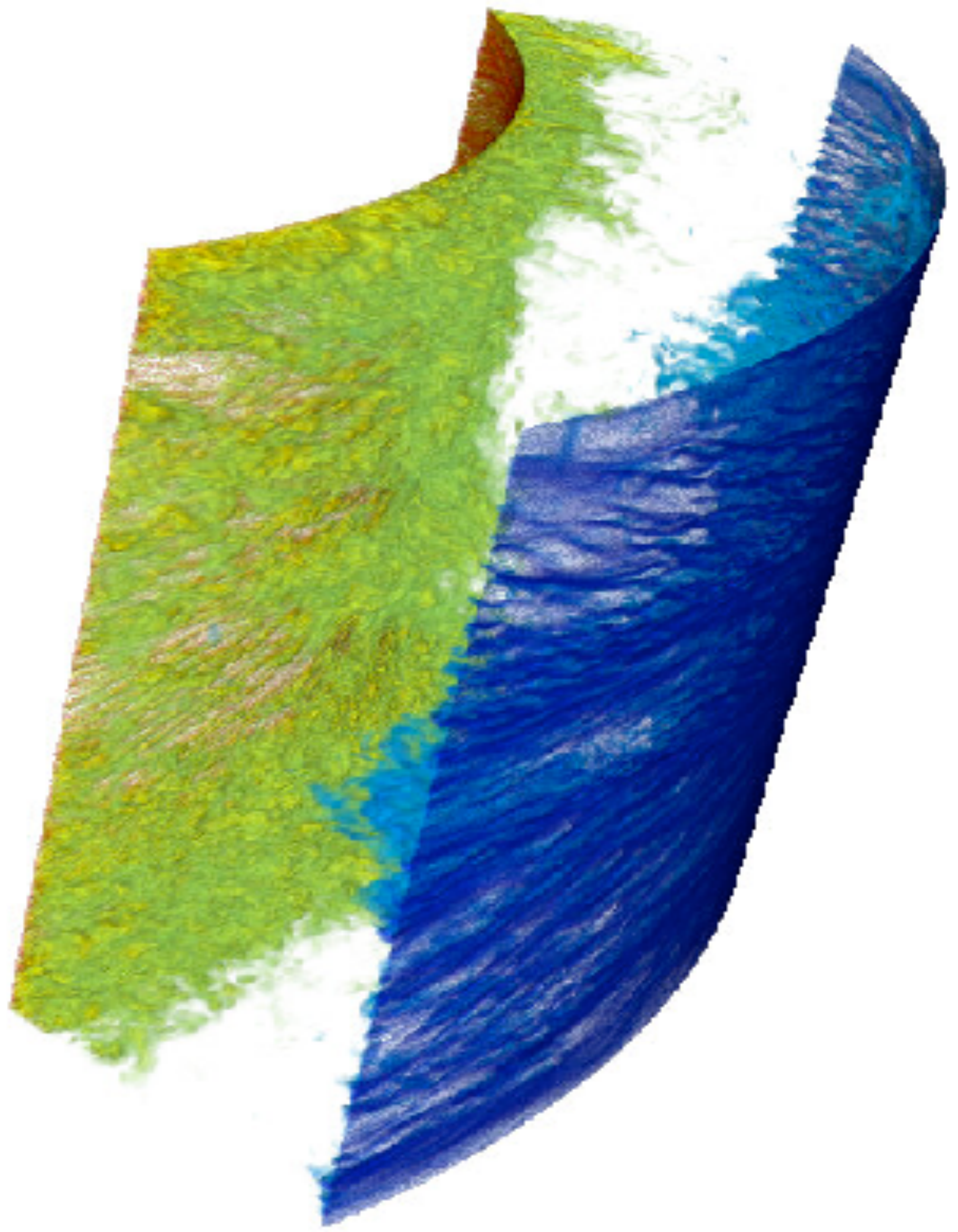

Taylor-Couette flow

Flows to which we applied AFiD

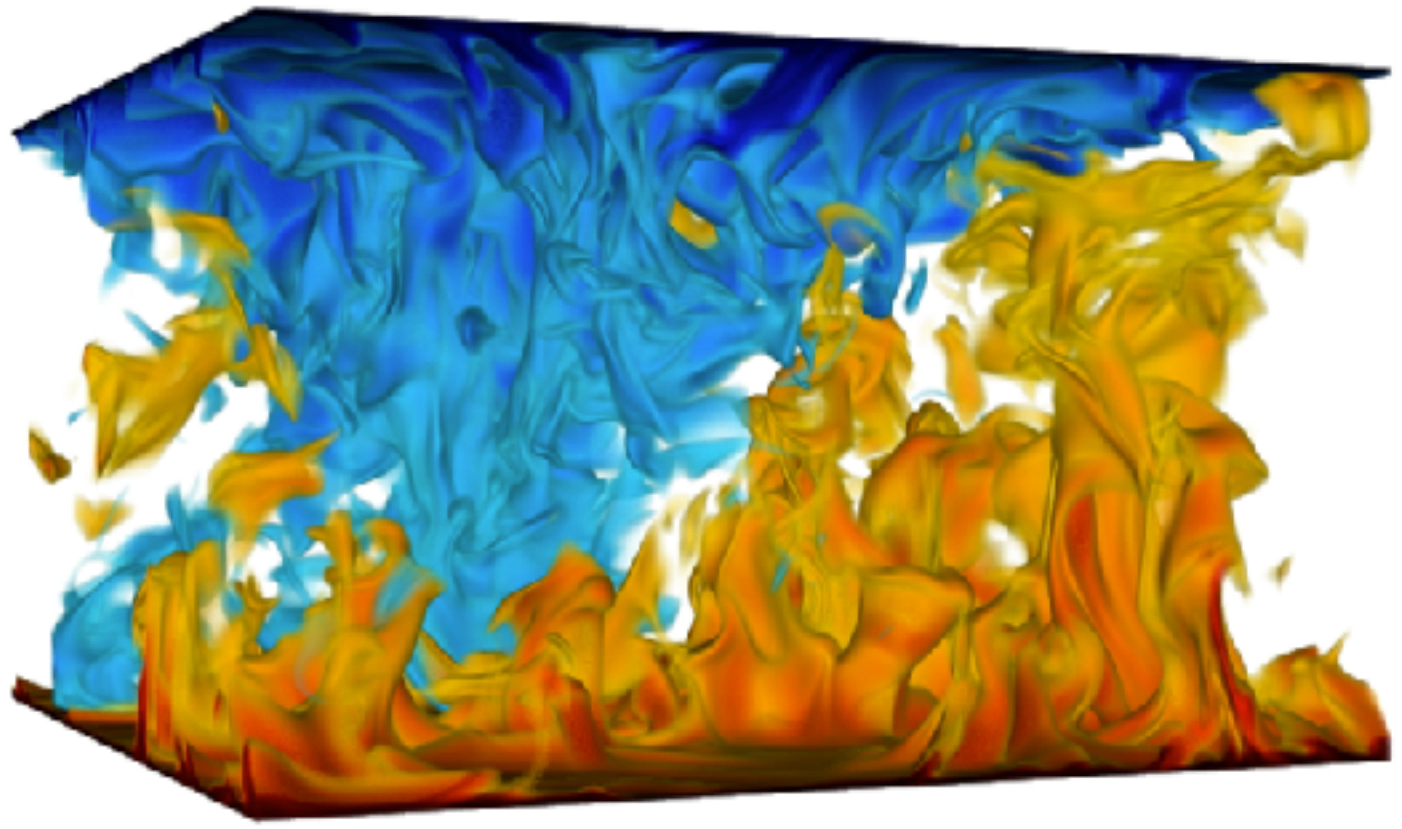

Rayleigh-Bénard convection

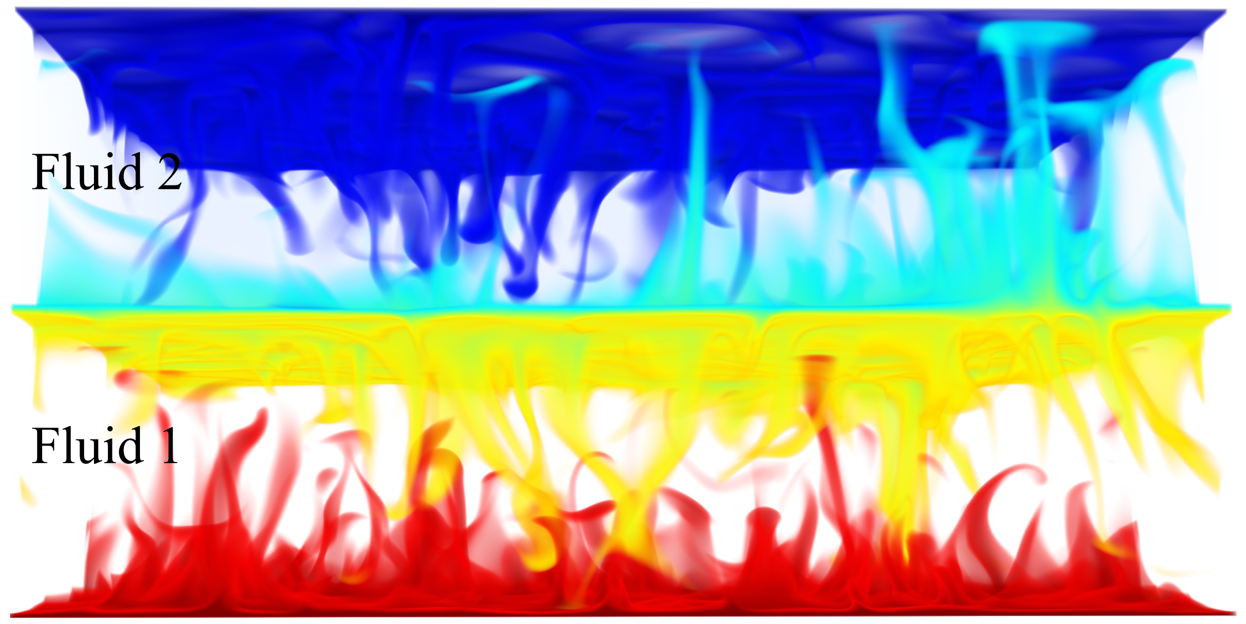

Two-layer systems

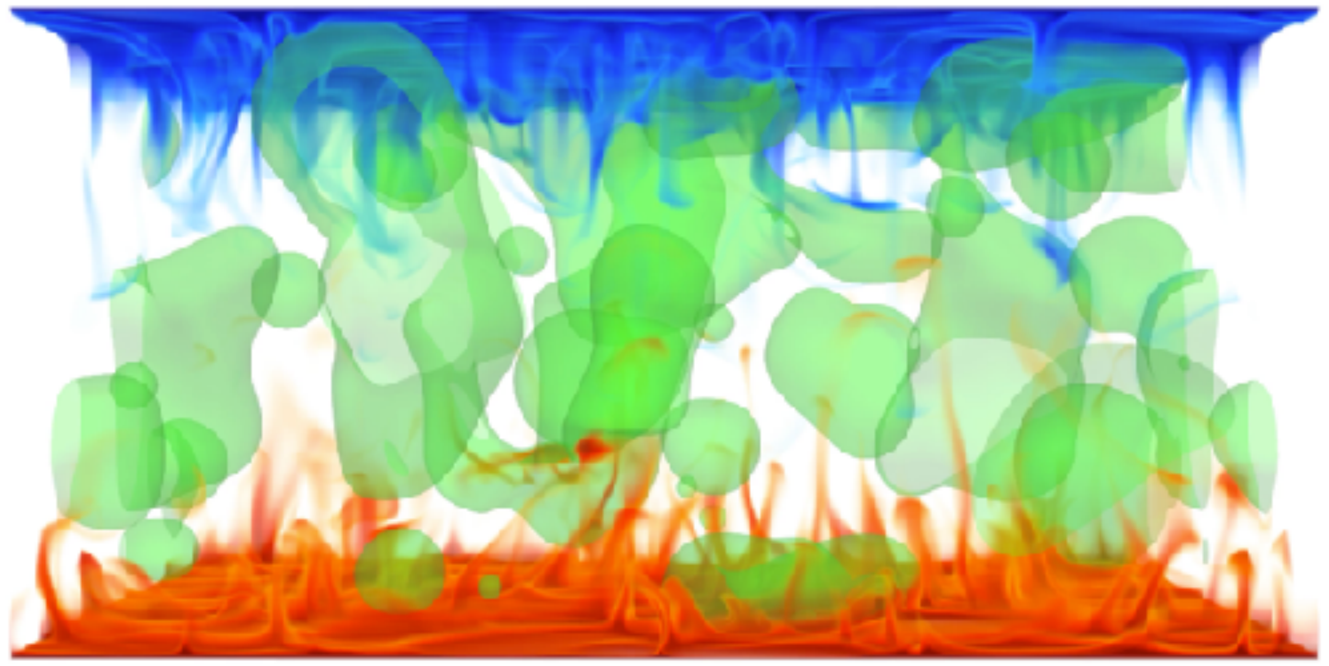

Dispersed systems

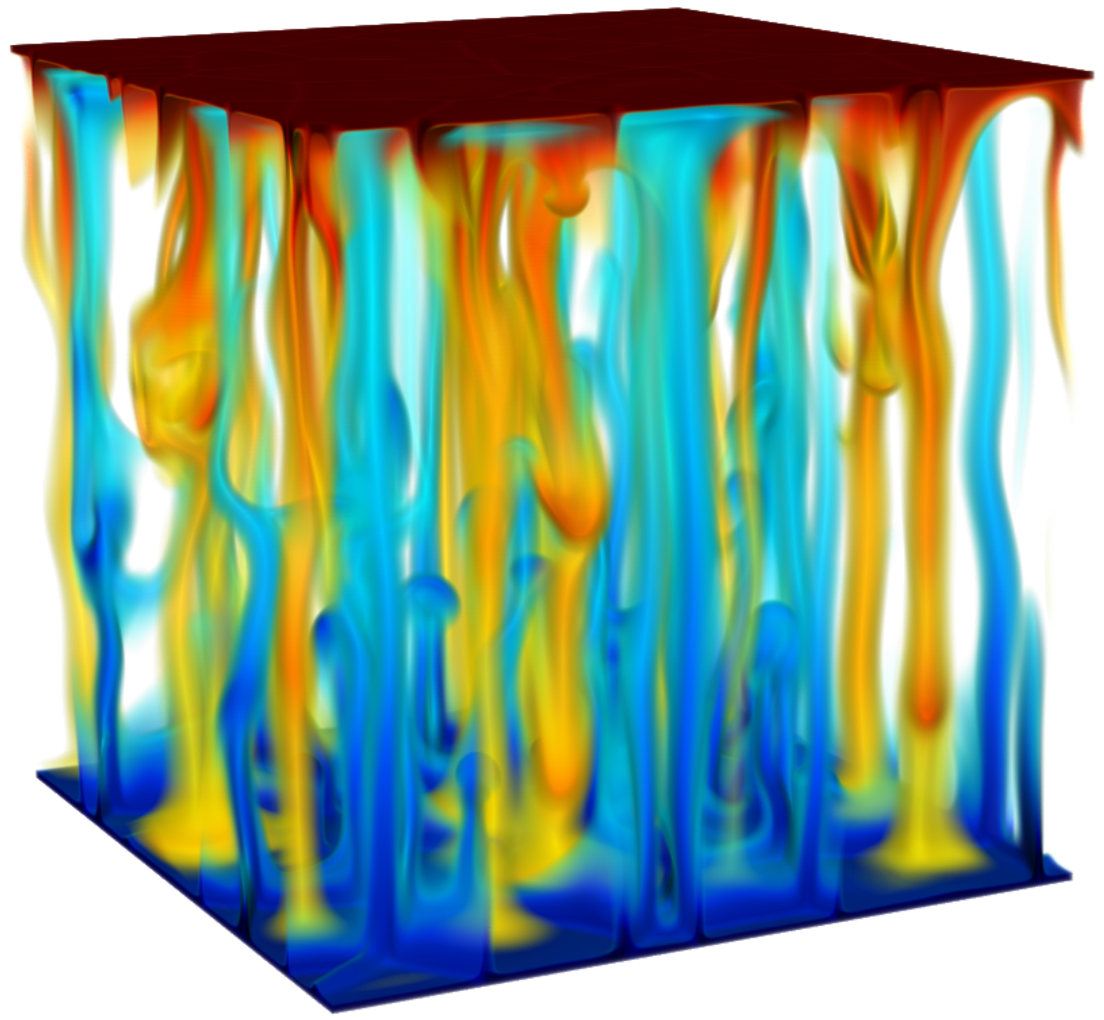

Double Diffusive convection

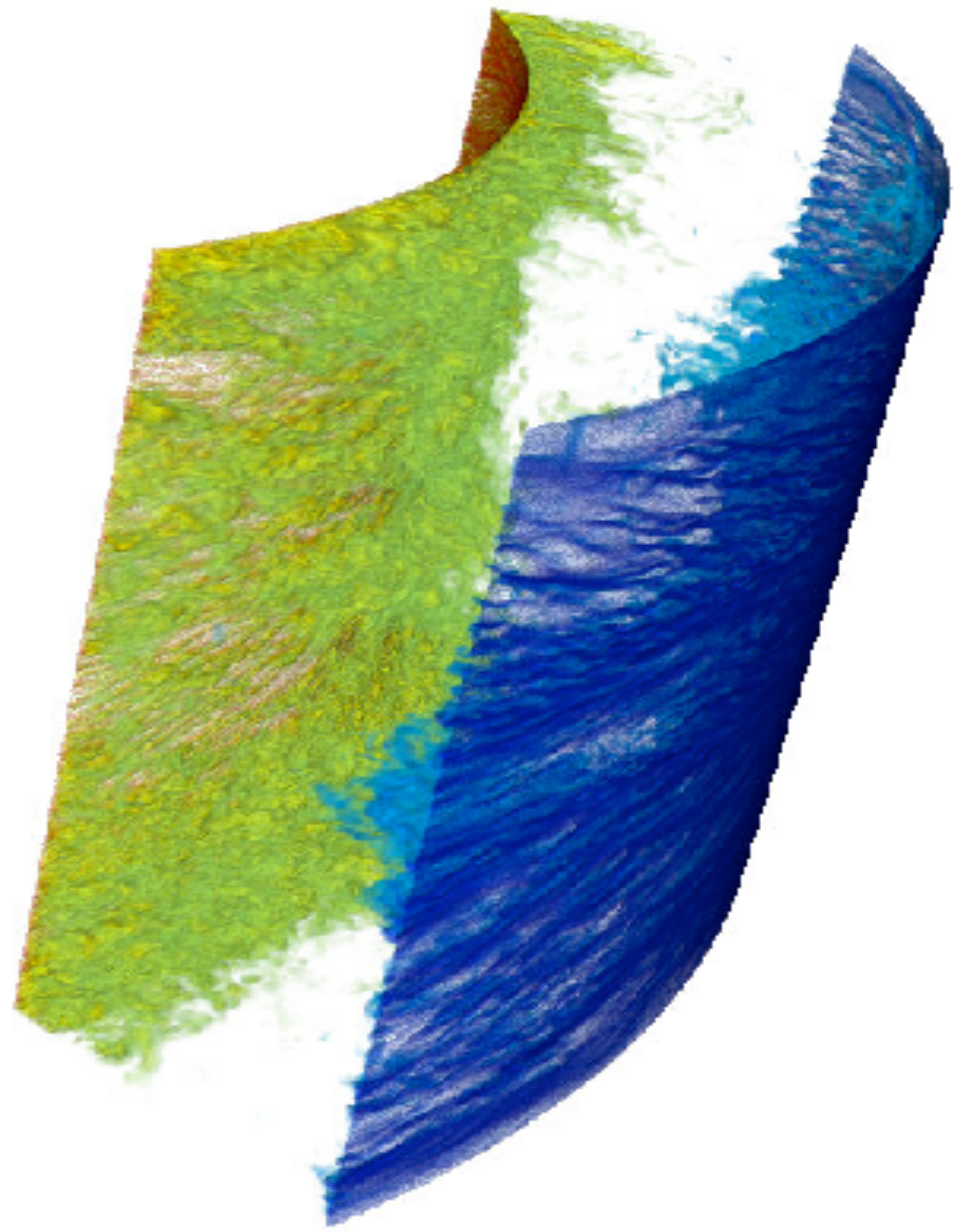

Taylor-Couette flow

Flows to which we applied AFiD

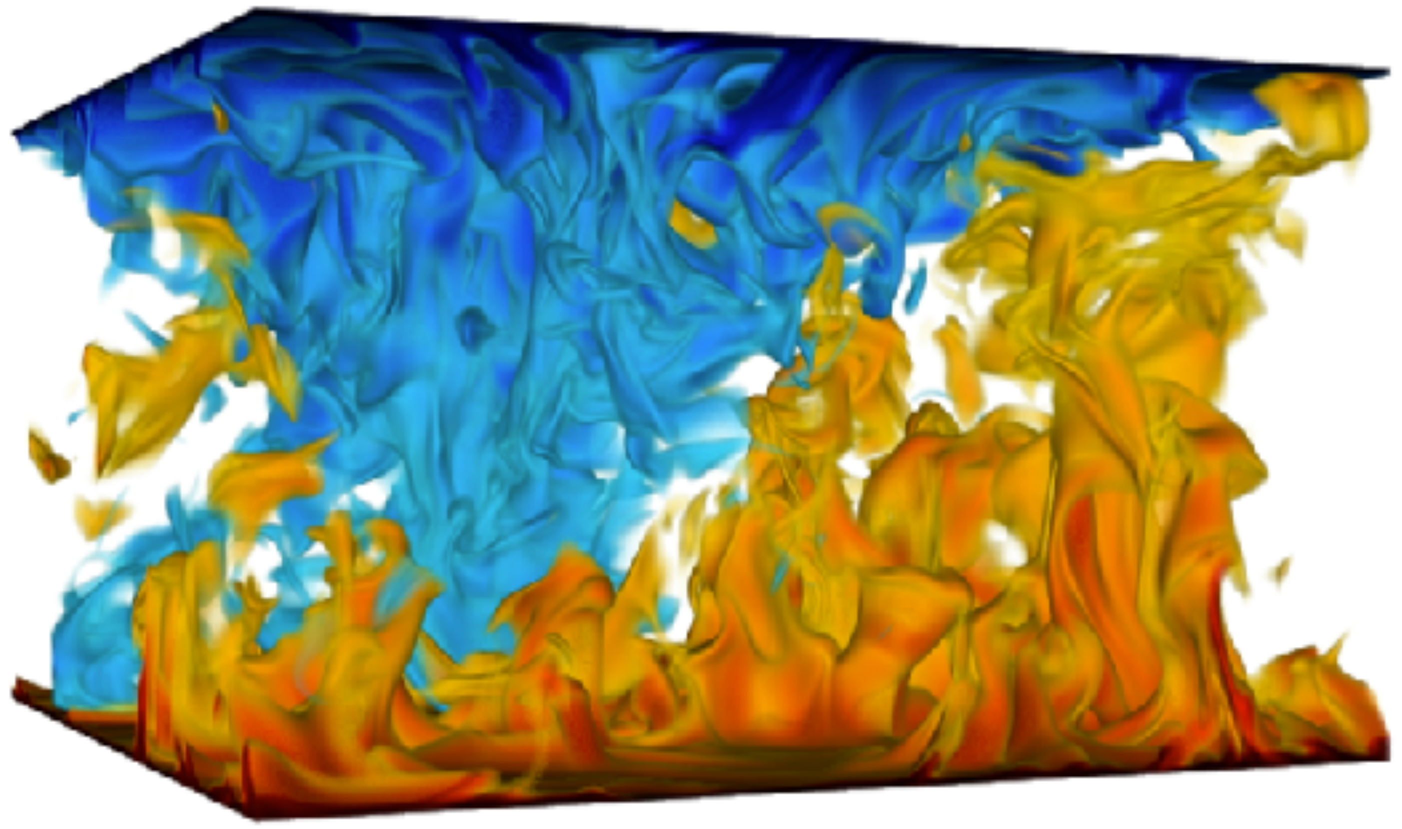

Rayleigh-Bénard convection

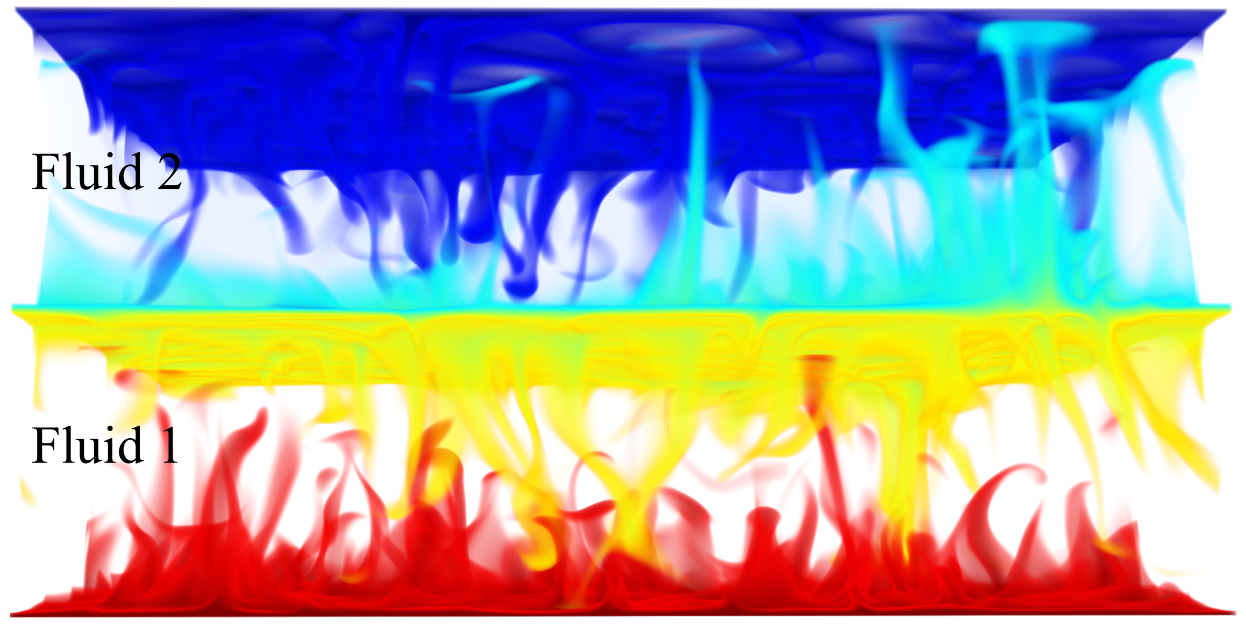

Two-layer systems

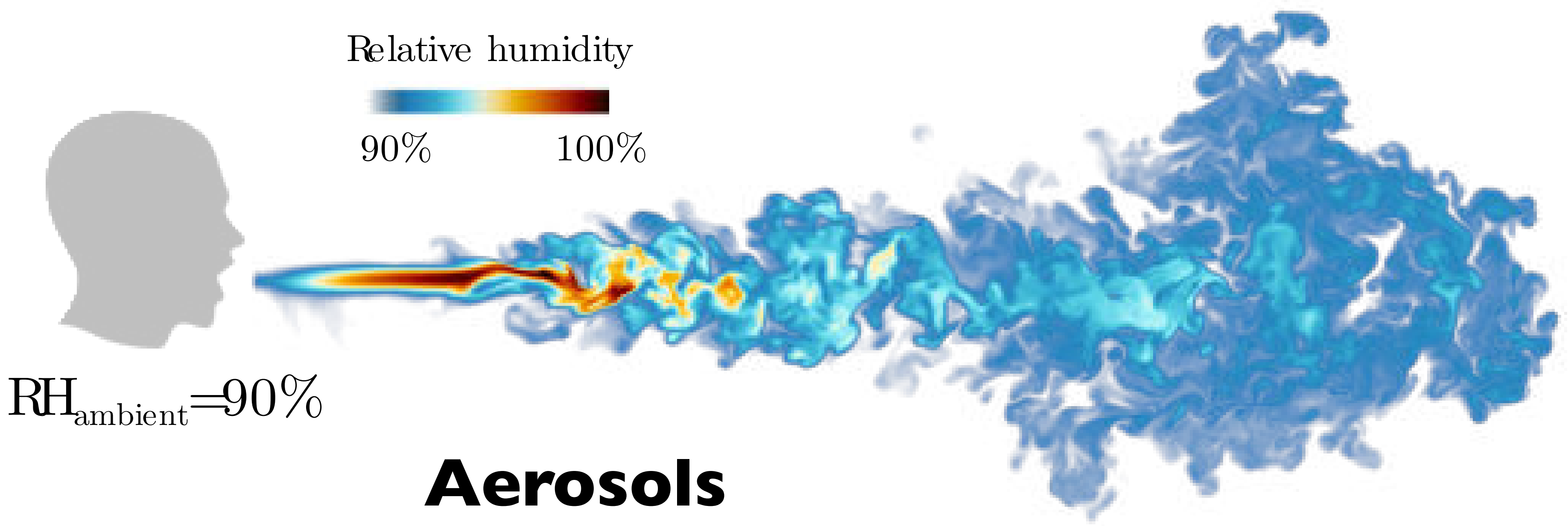

Aerosols

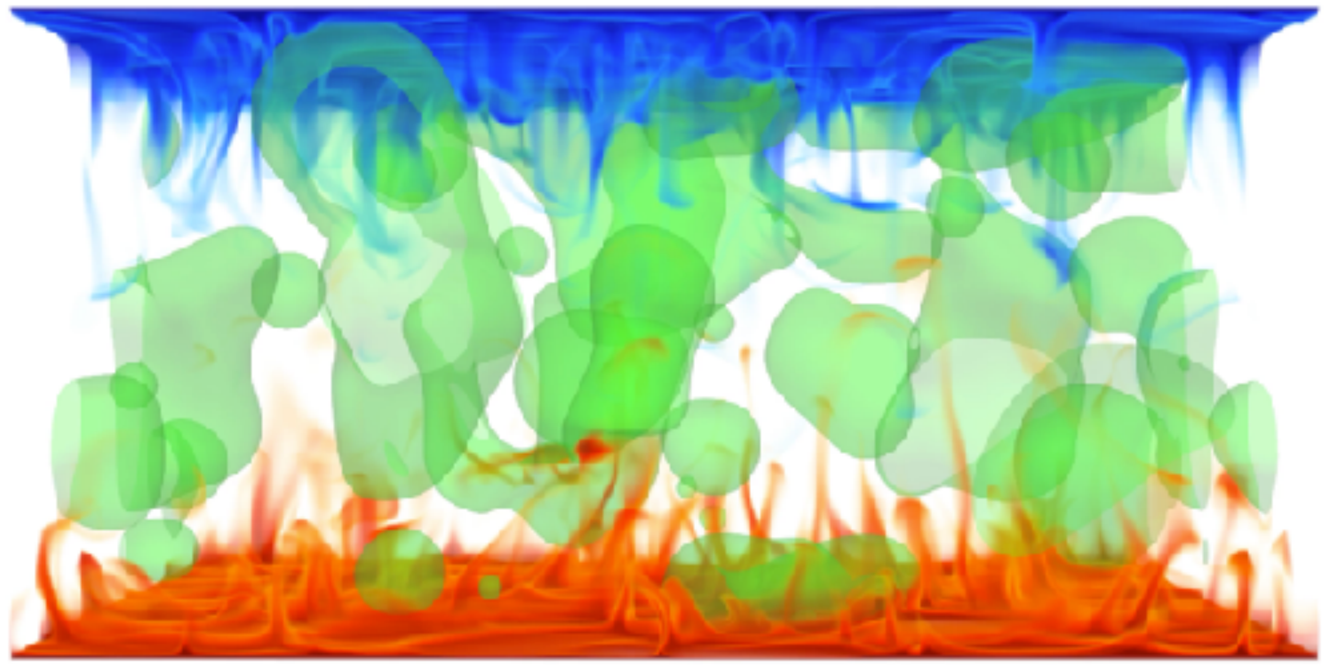

Dispersed systems

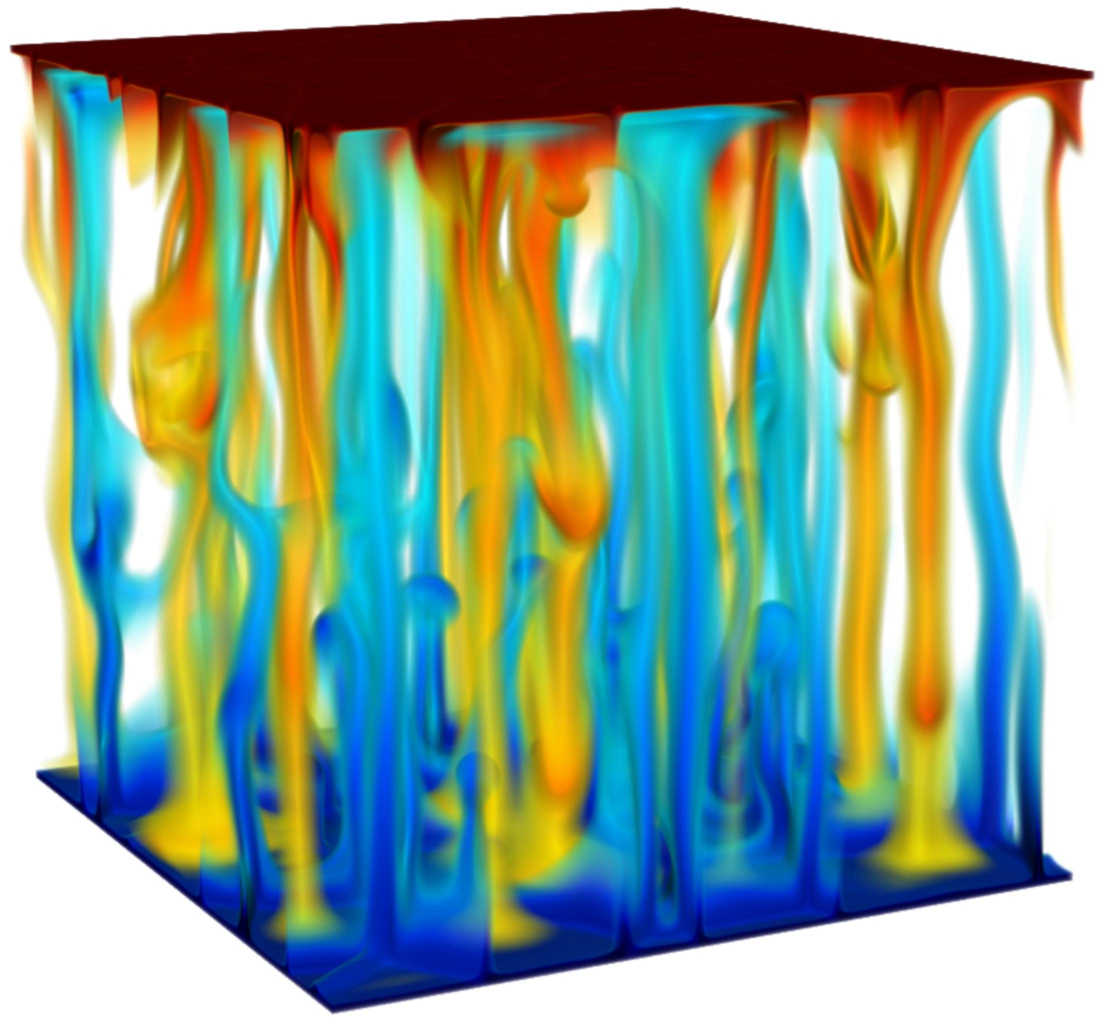

Double Diffusive convection

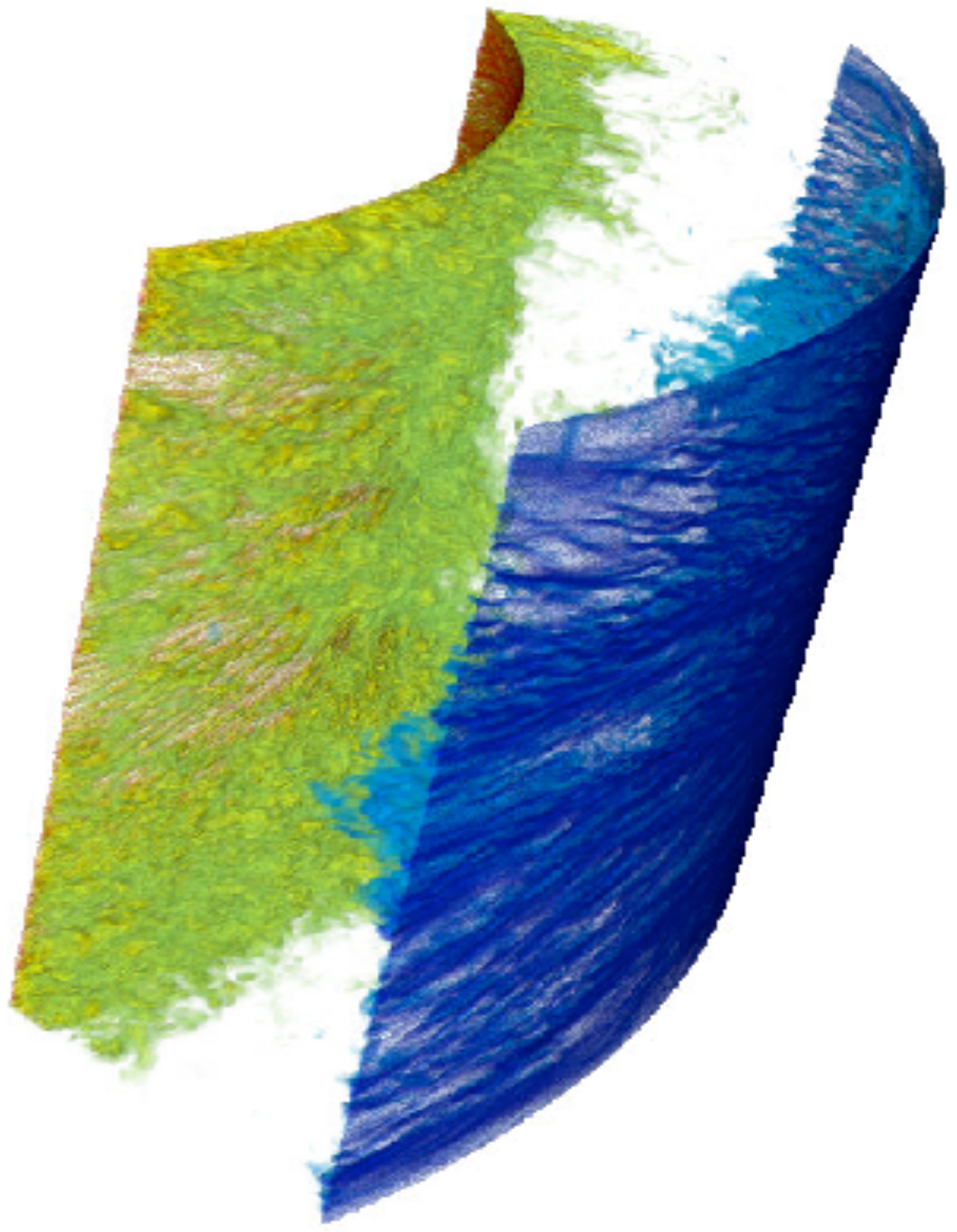

Taylor-Couette flow

Flows to which we applied AFiD

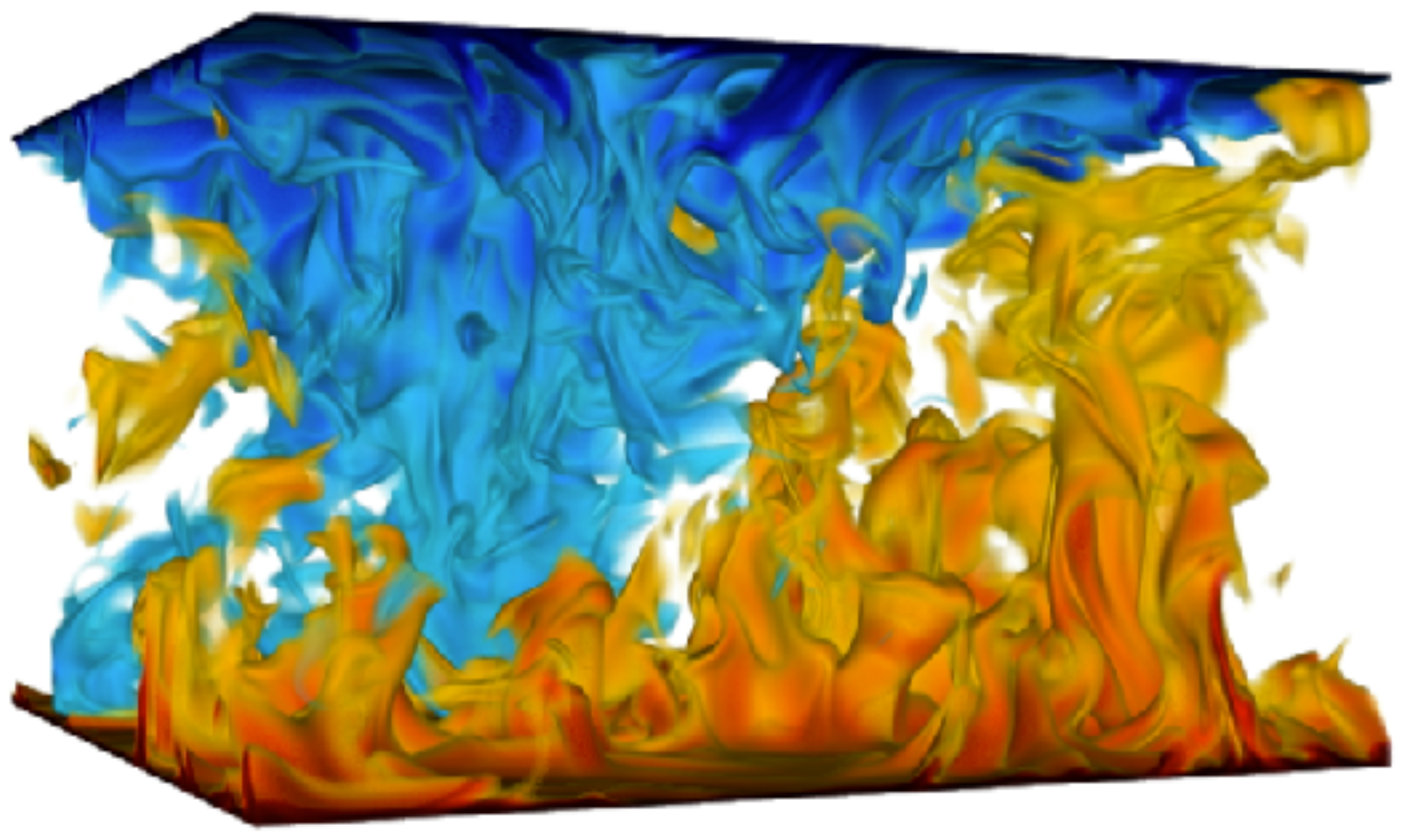

Rayleigh-Bénard convection

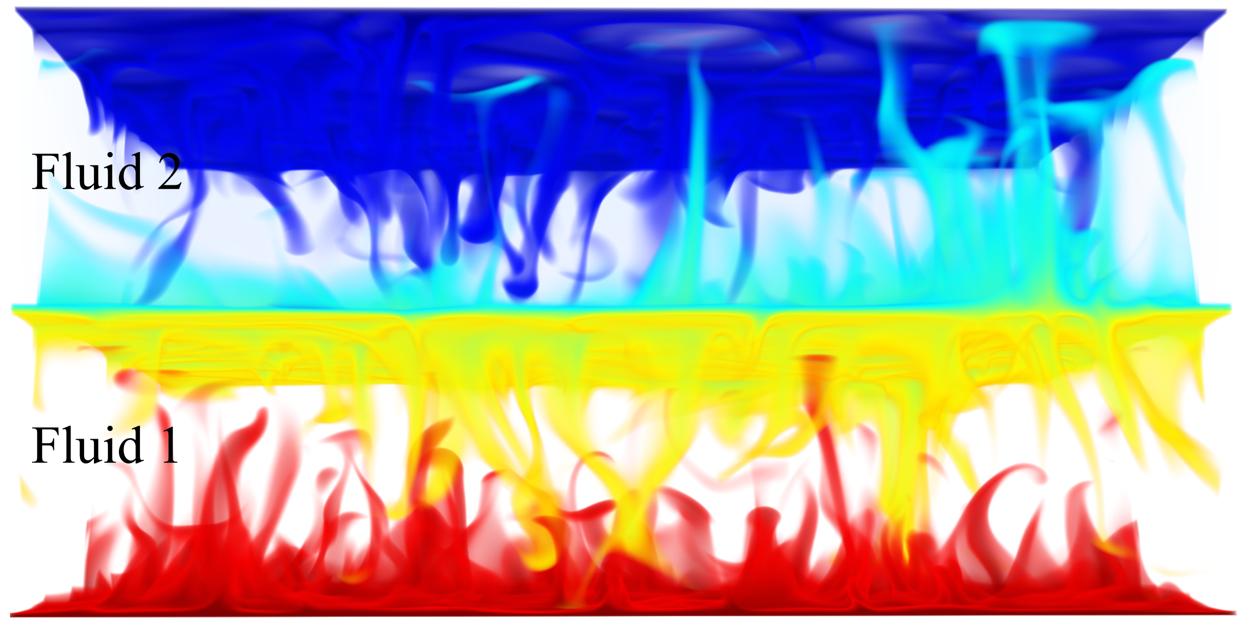

Two-layer systems

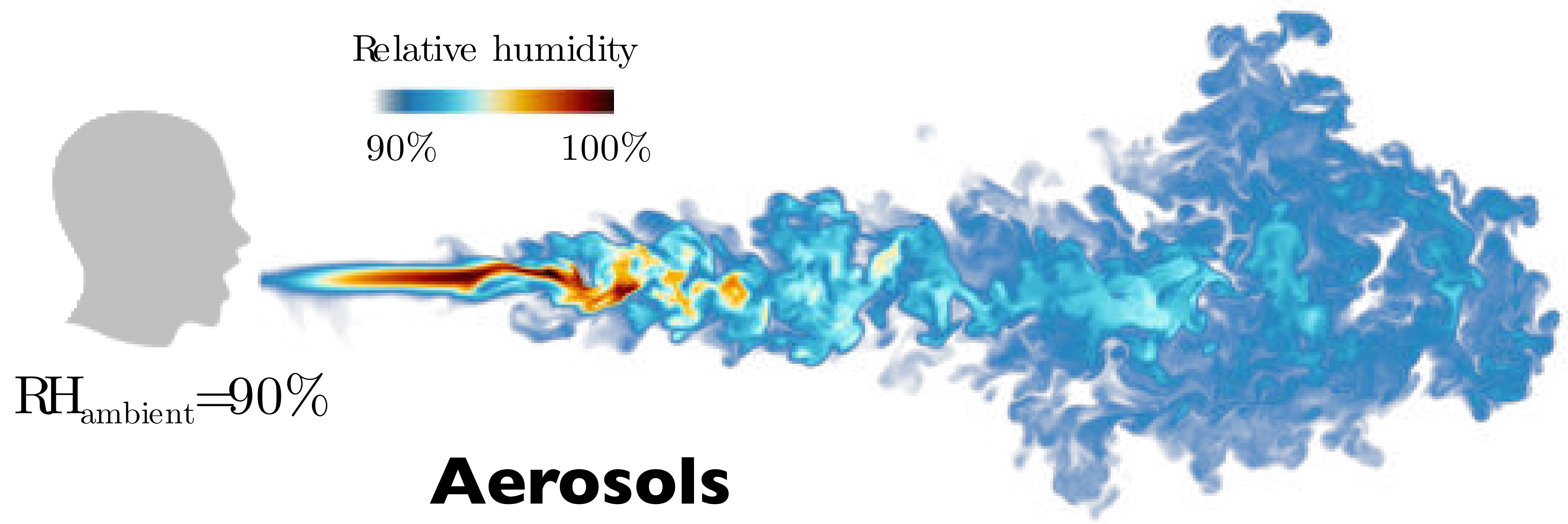

Aerosols

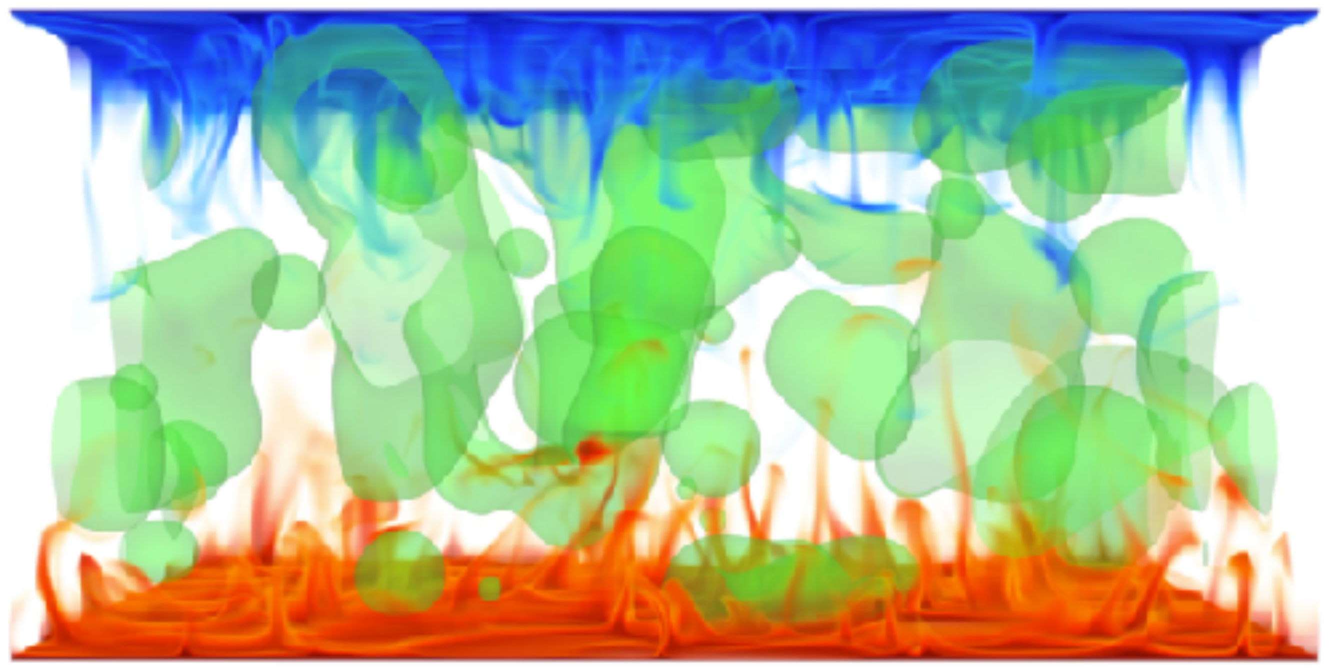

Dispersed systems

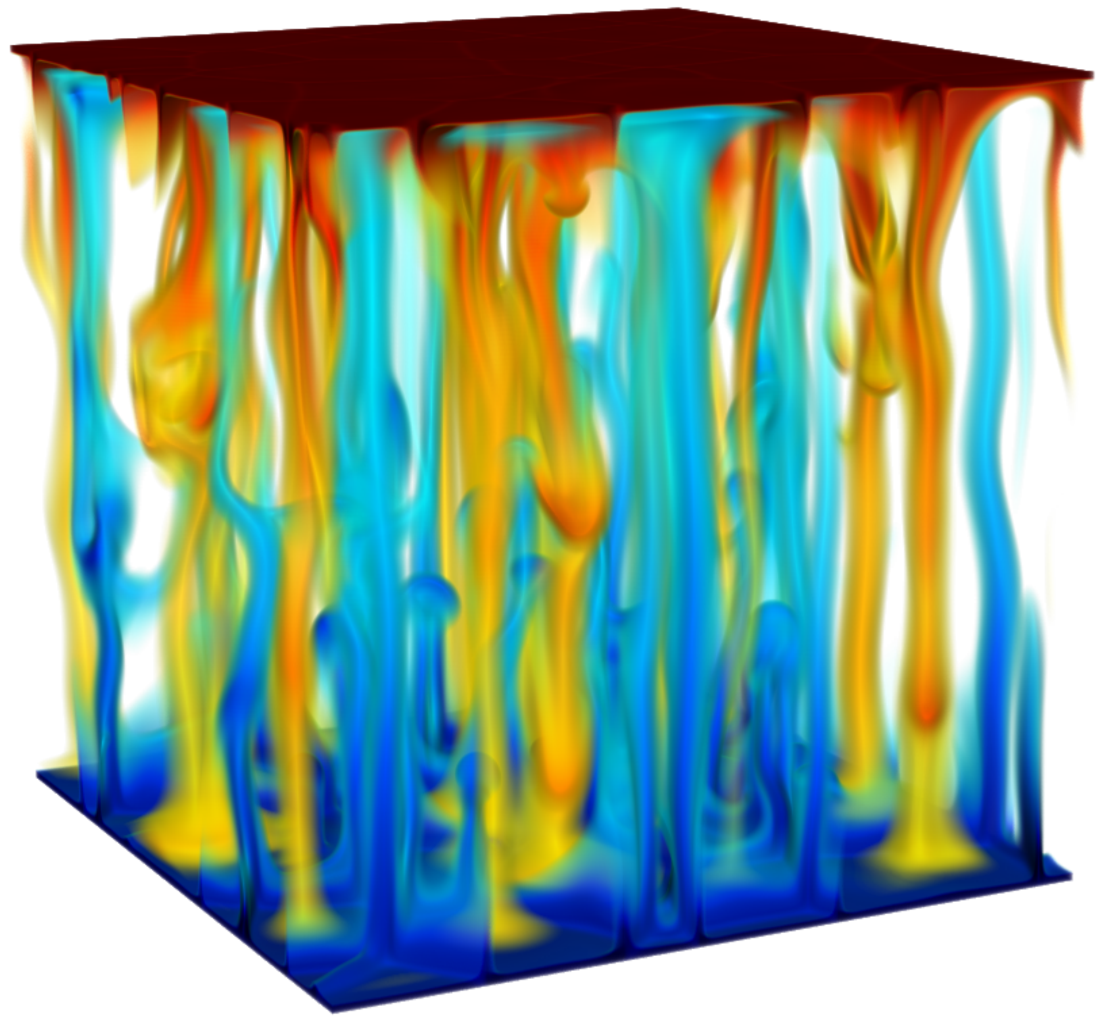

Double Diffusive convection

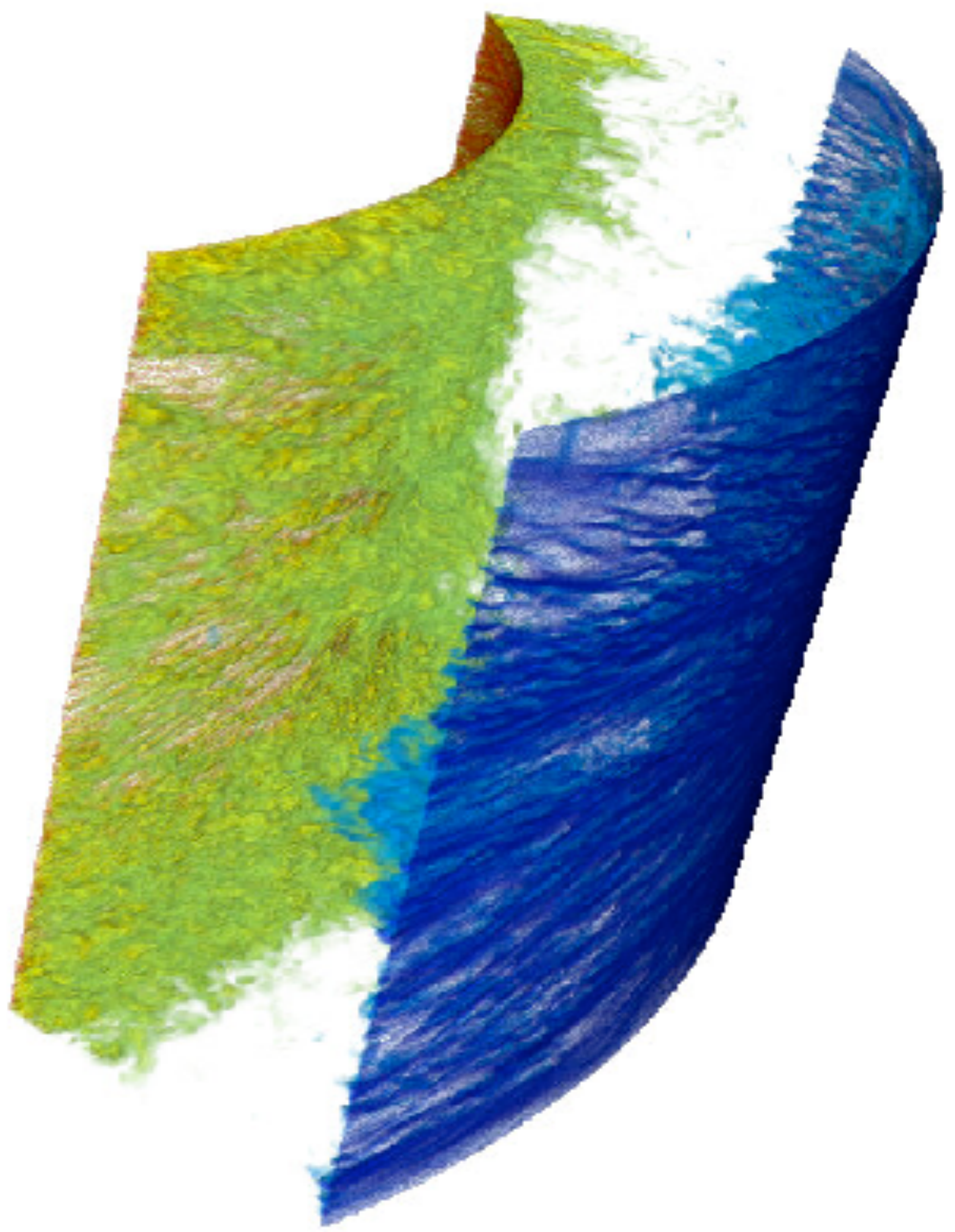

Taylor-Couette flow

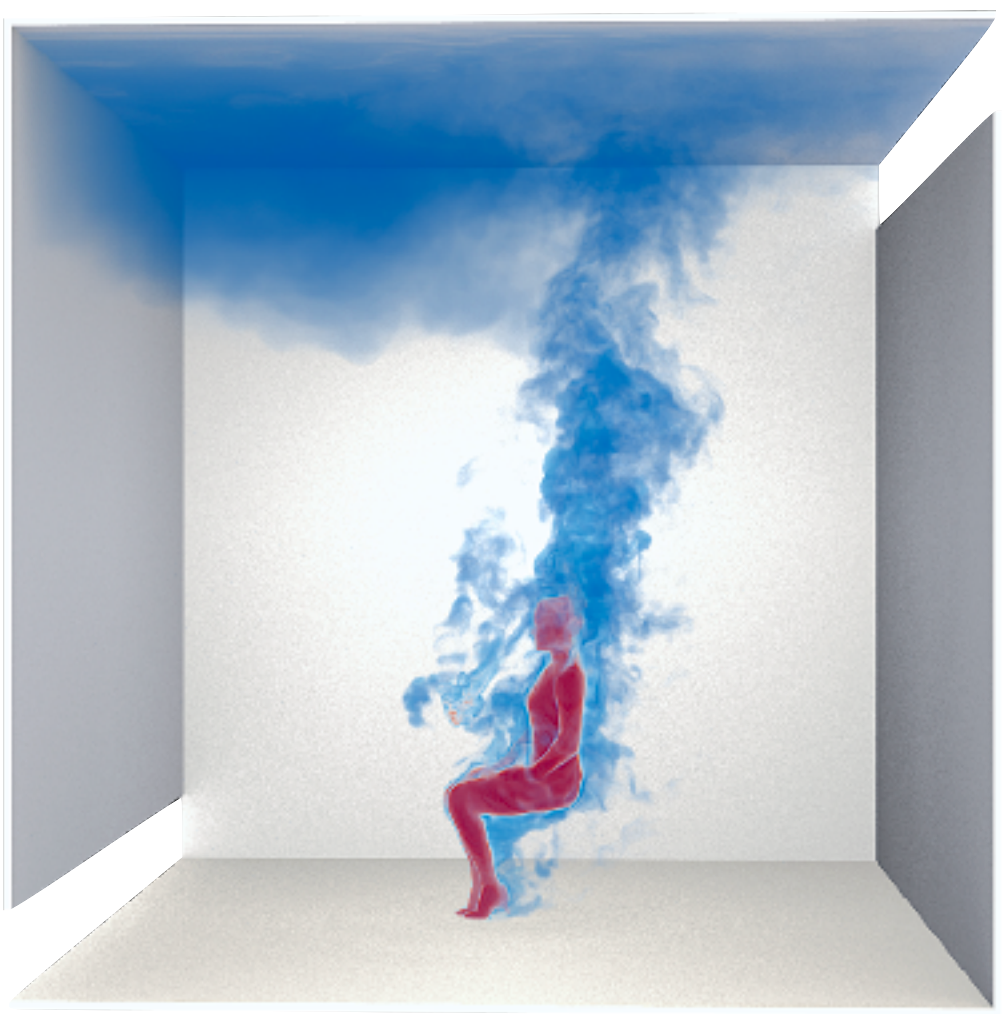

Ventilation

Flows to which we applied AFiD

... and many more

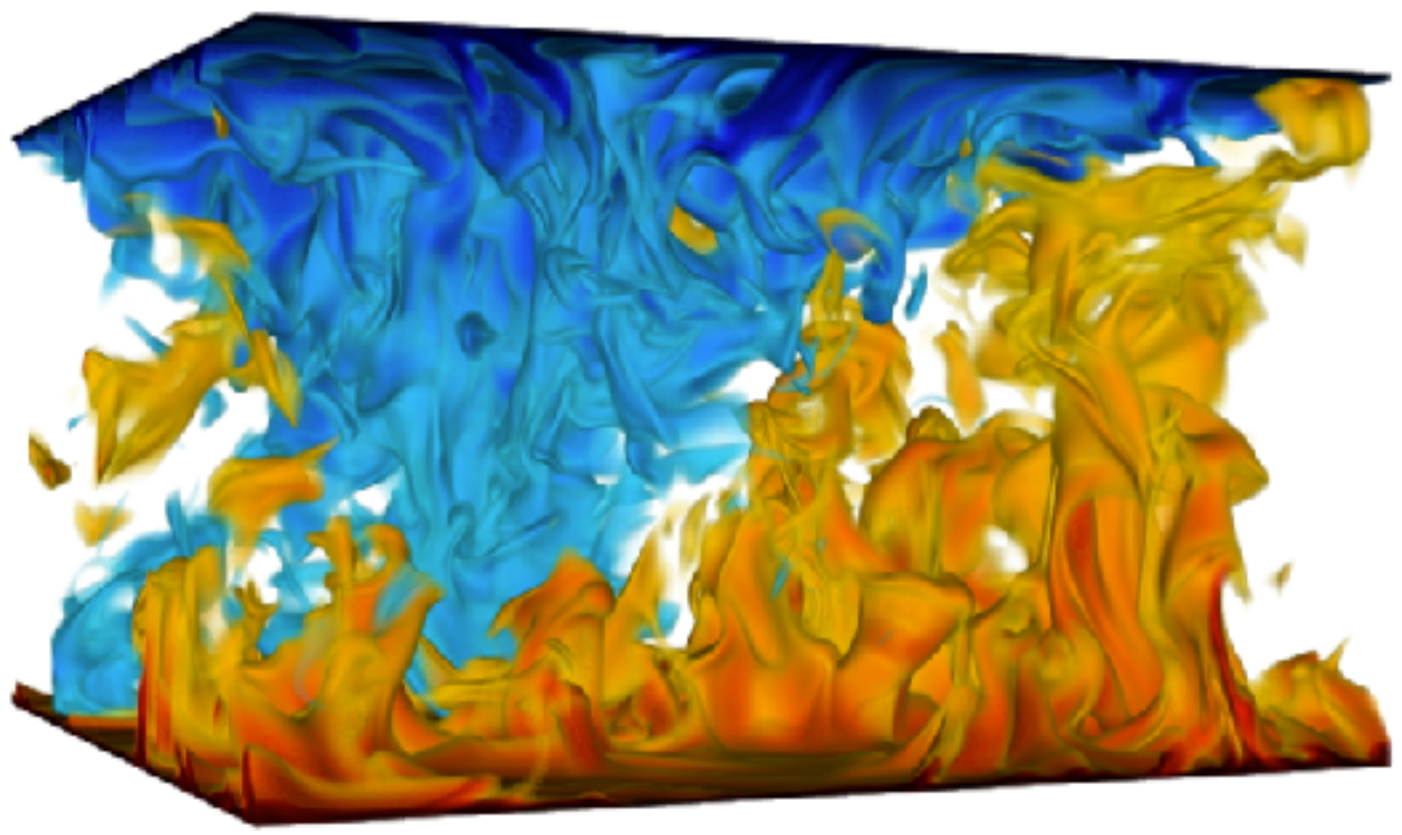

Rayleigh-Bénard convection

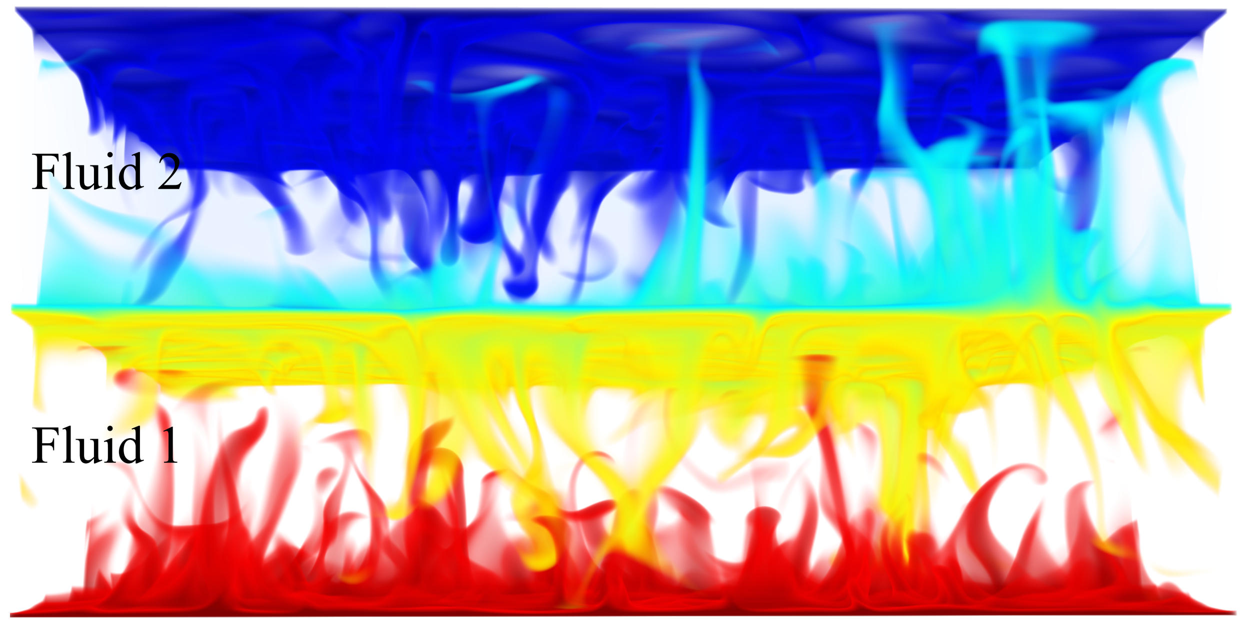

Two-layer systems

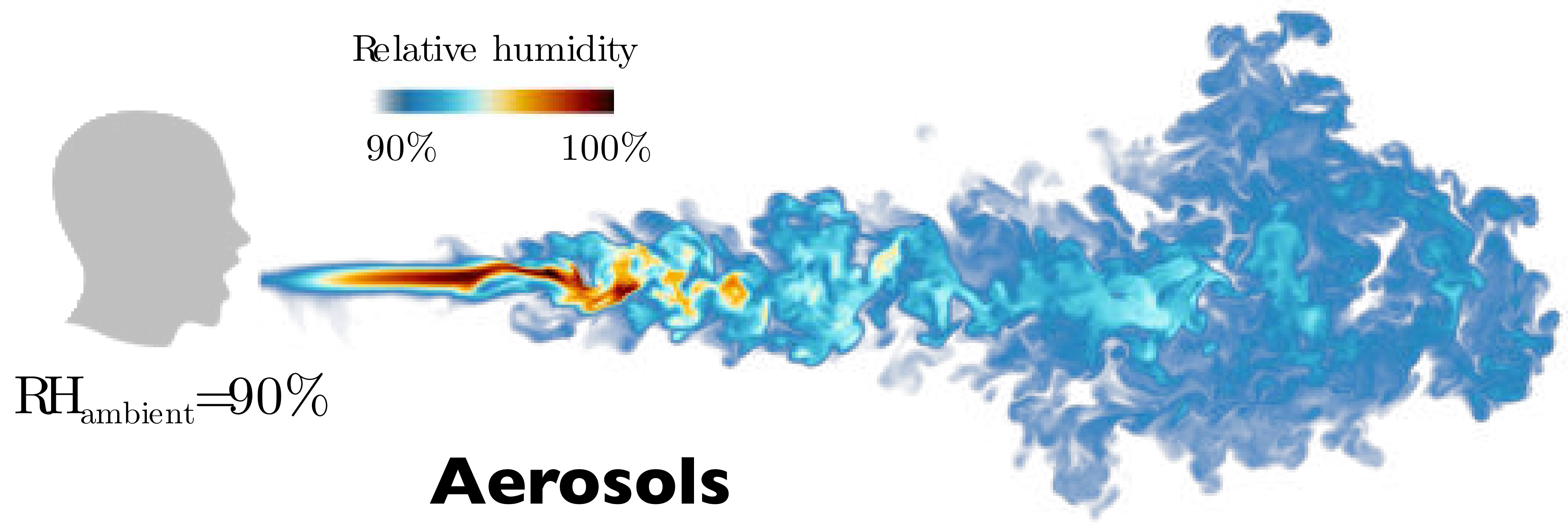

Aerosols

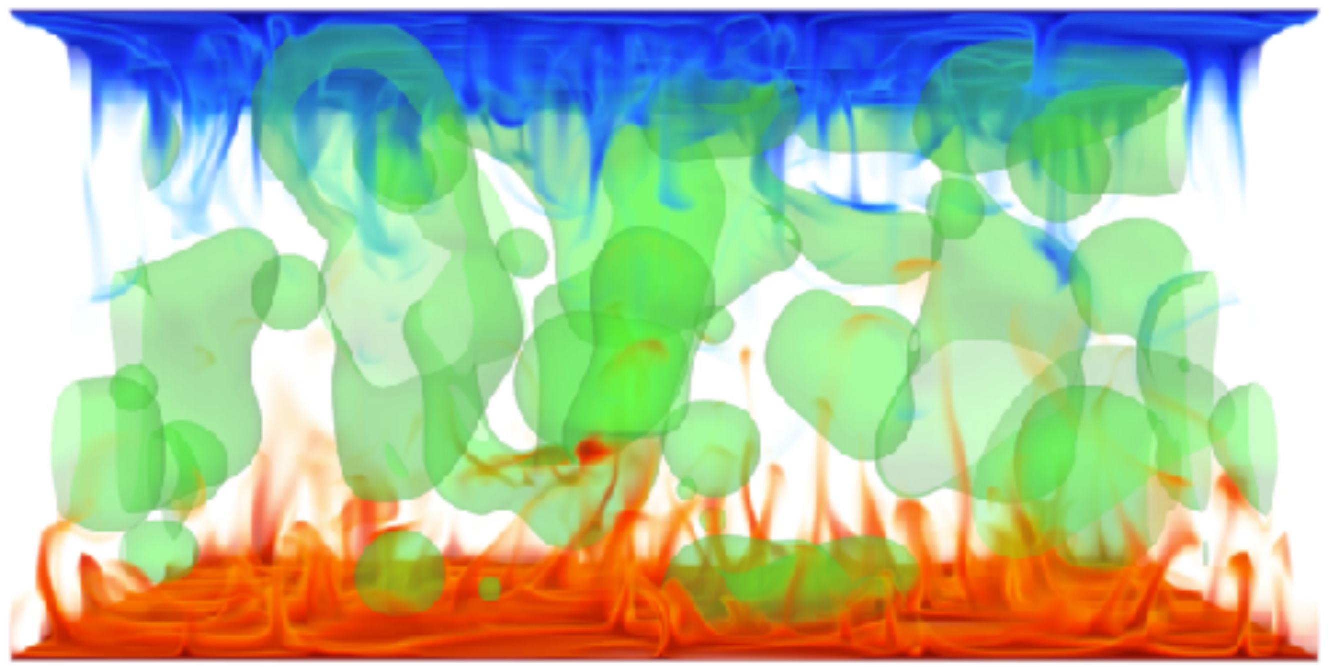

Dispersed systems

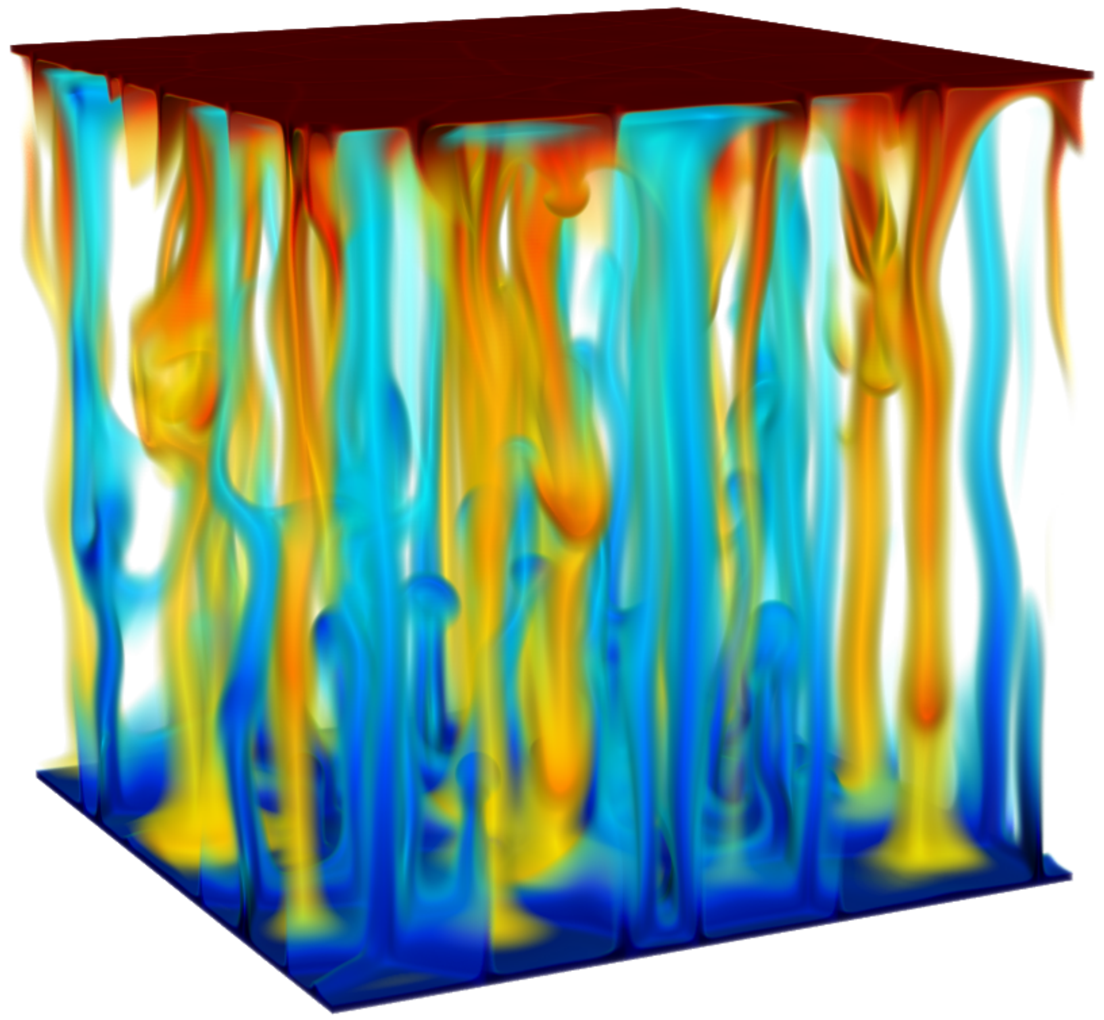

Double Diffusive convection

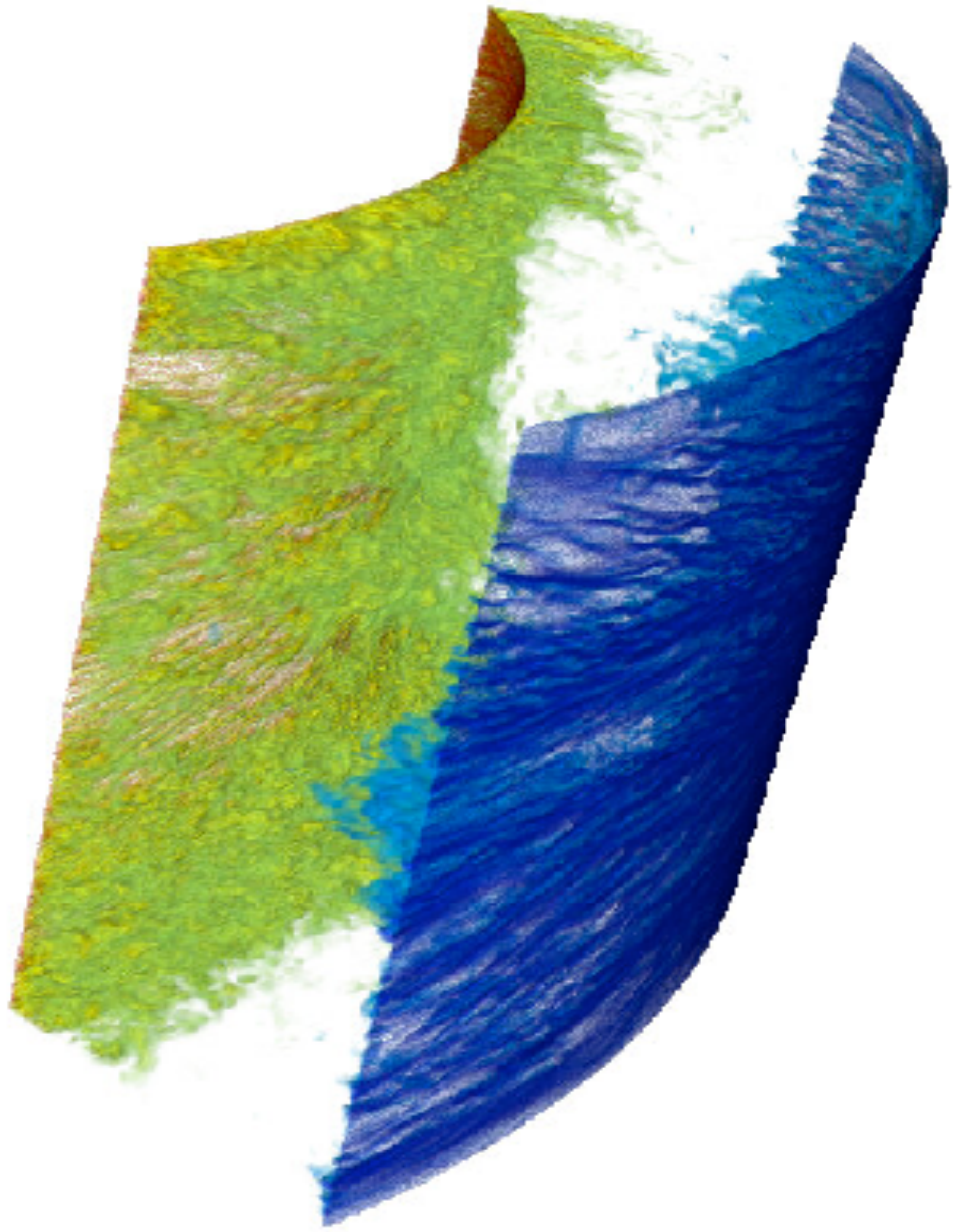

Taylor-Couette flow

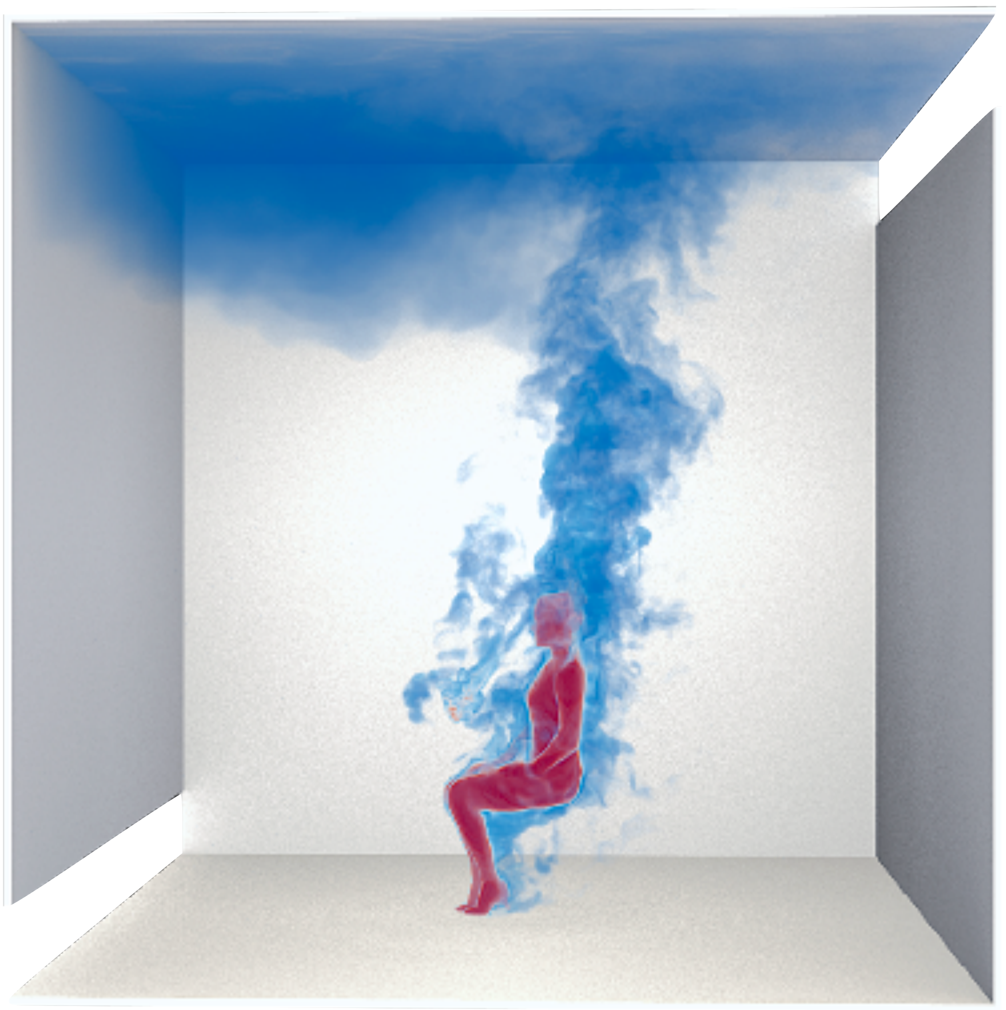

Ventilation

Presently largest 3D RB DNS: Top view on boundary layer

Pr = 1
Ra = 10^{13}

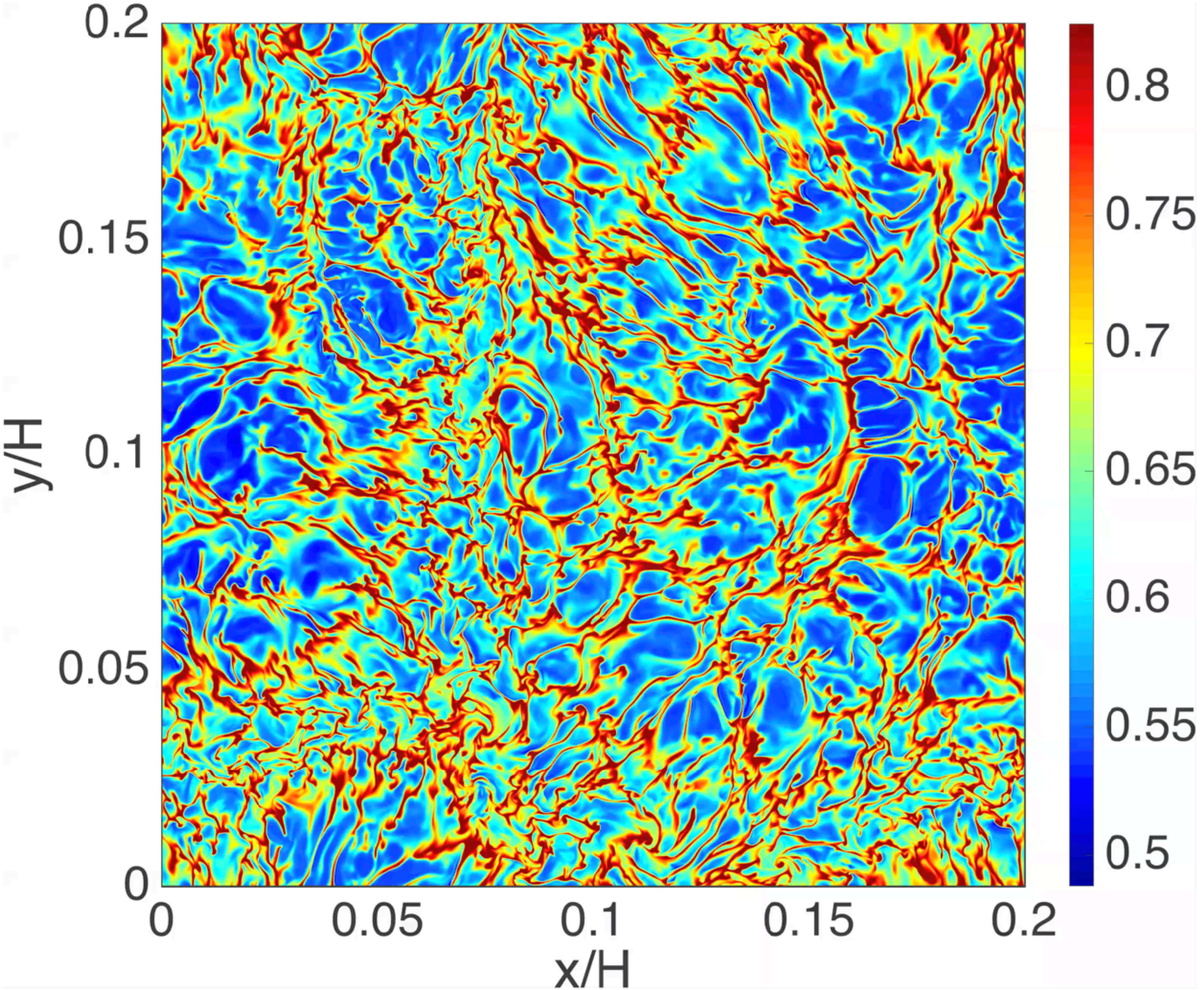

Presently largest 3D RB DNS: Top view on boundary layer

Pr = 1
Ra = 10^{13}

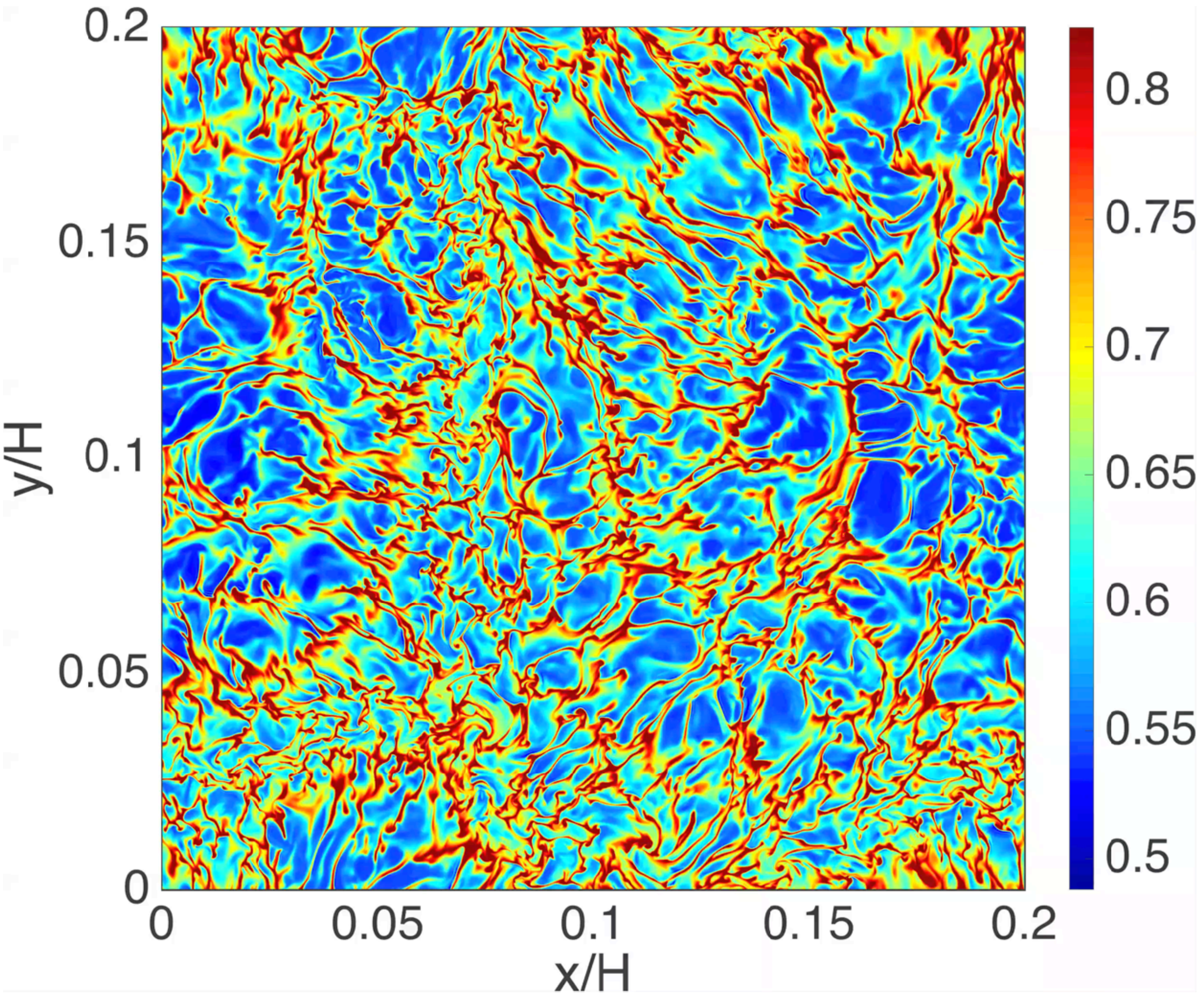

PHYSICS TODAY

November 2023 • volume 76, number 11

A publication of the American Institute of Physics

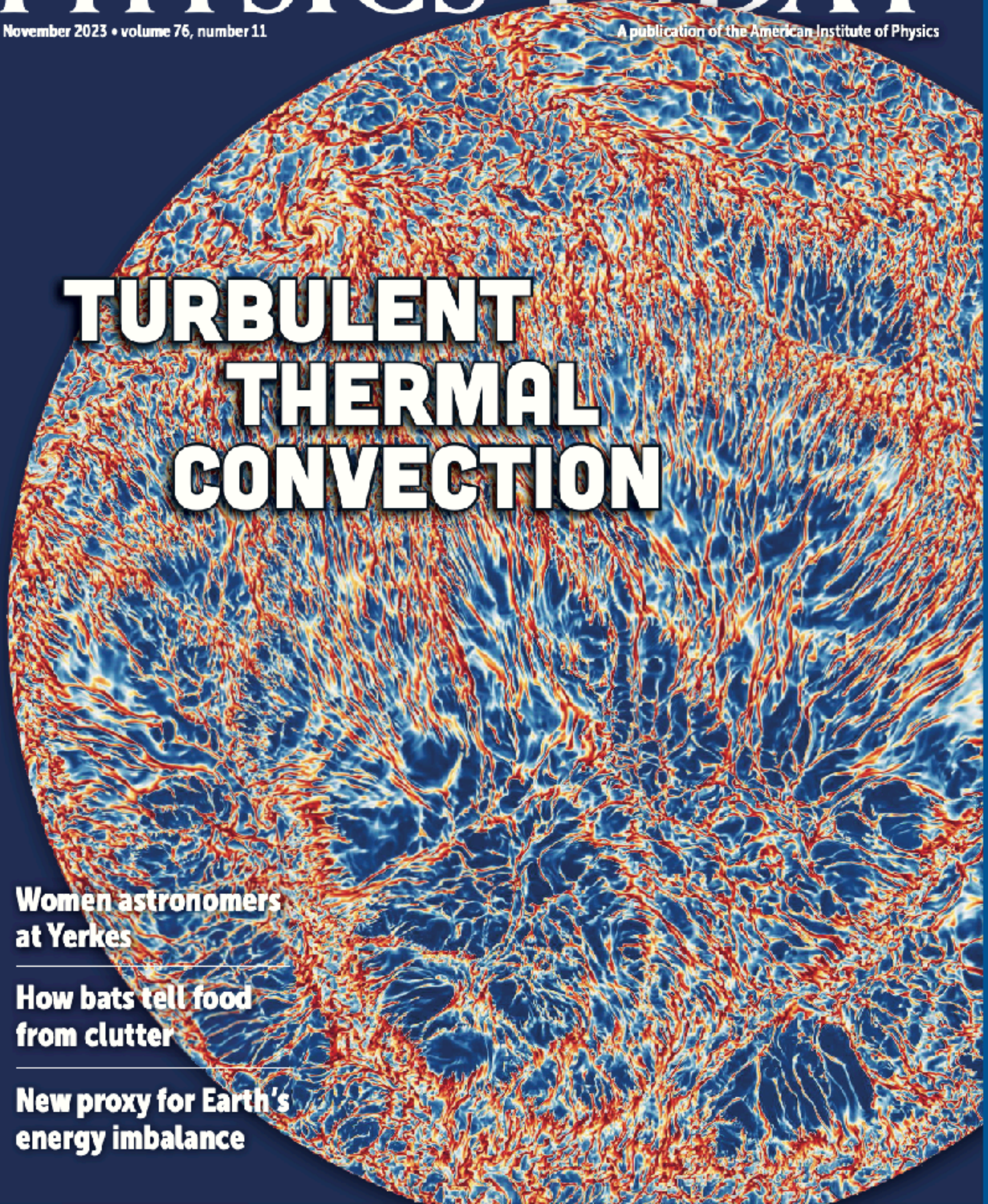

TURBULENT THERMAL CONVECTION

Women astronomers at Yerkes

How bats tell food from clutter

New proxy for Earth's energy imbalance

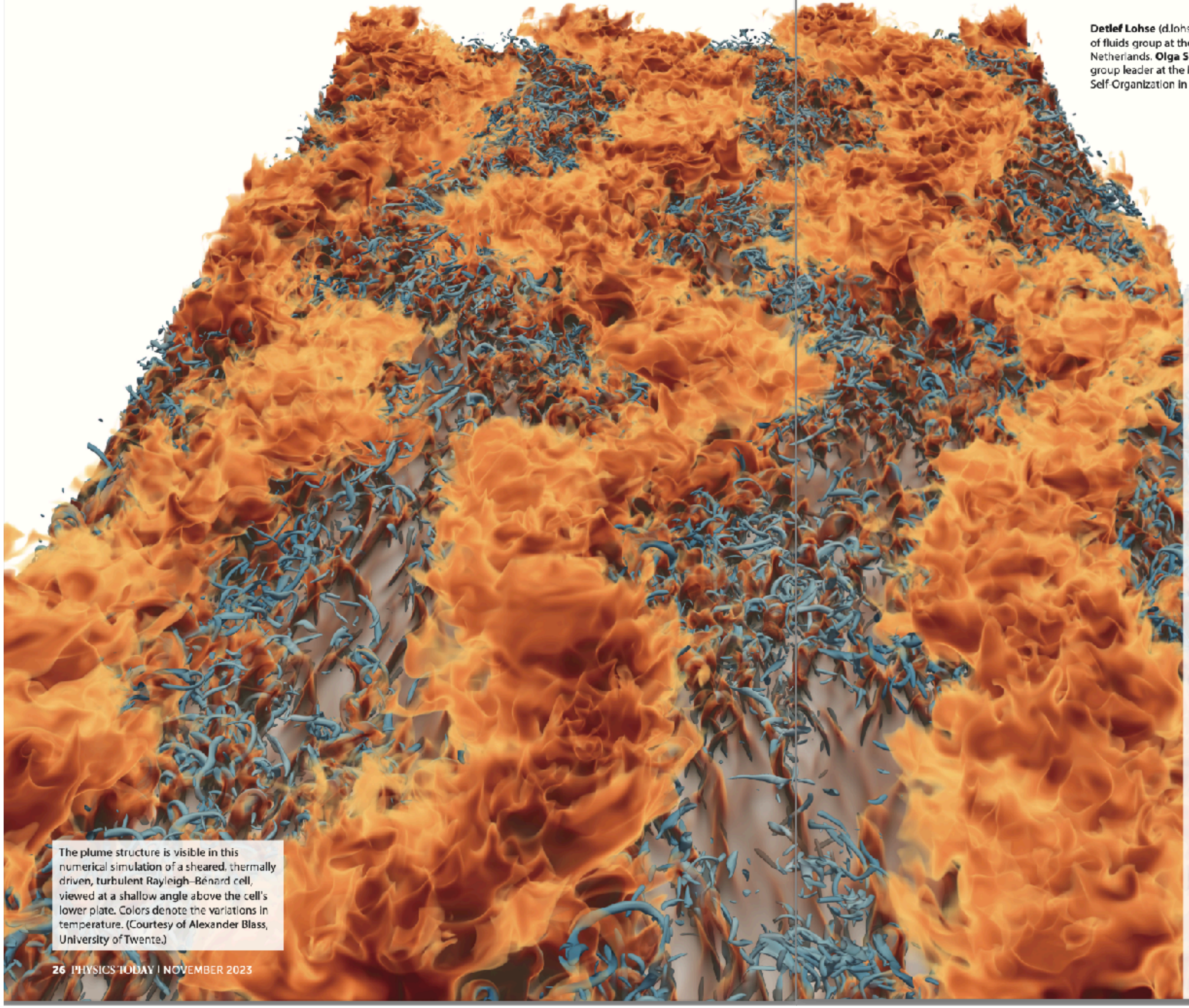

The plume structure is visible in this numerical simulation of a sheared, thermally driven, turbulent Rayleigh–Bénard cell, viewed at a shallow angle above the cell's lower plate. Colors denote the variations in temperature. (Courtesy of Alexander Blass, University of Twente.)

Detlef Lohse (d.lohse@utwente.nl) is the chair of the physics of fluids group at the University of Twente in Enschede, the Netherlands. **Olga Shishkina** (olga.shishkina@ds.mpg.de) is group leader at the Max Planck Institute for Dynamics and Self-Organization in Göttingen, Germany.

Ultimate turbulent thermal convection

Detlef Lohse and Olga Shishkina

Recent studies of a model system—a fluid in a box heated from below and cooled from above—provide insights into the physics of turbulent thermal convection. But upscaling the system to extremely strong turbulence remains difficult.

Thermally driven turbulent flow can be found throughout nature and technology. Such flow transports not only heat but also mass and momentum. Comprehending what determines that transport is key to understanding numerous geophysical and astrophysical flows and to being able to control the industrial and more general flows that people experience every day.

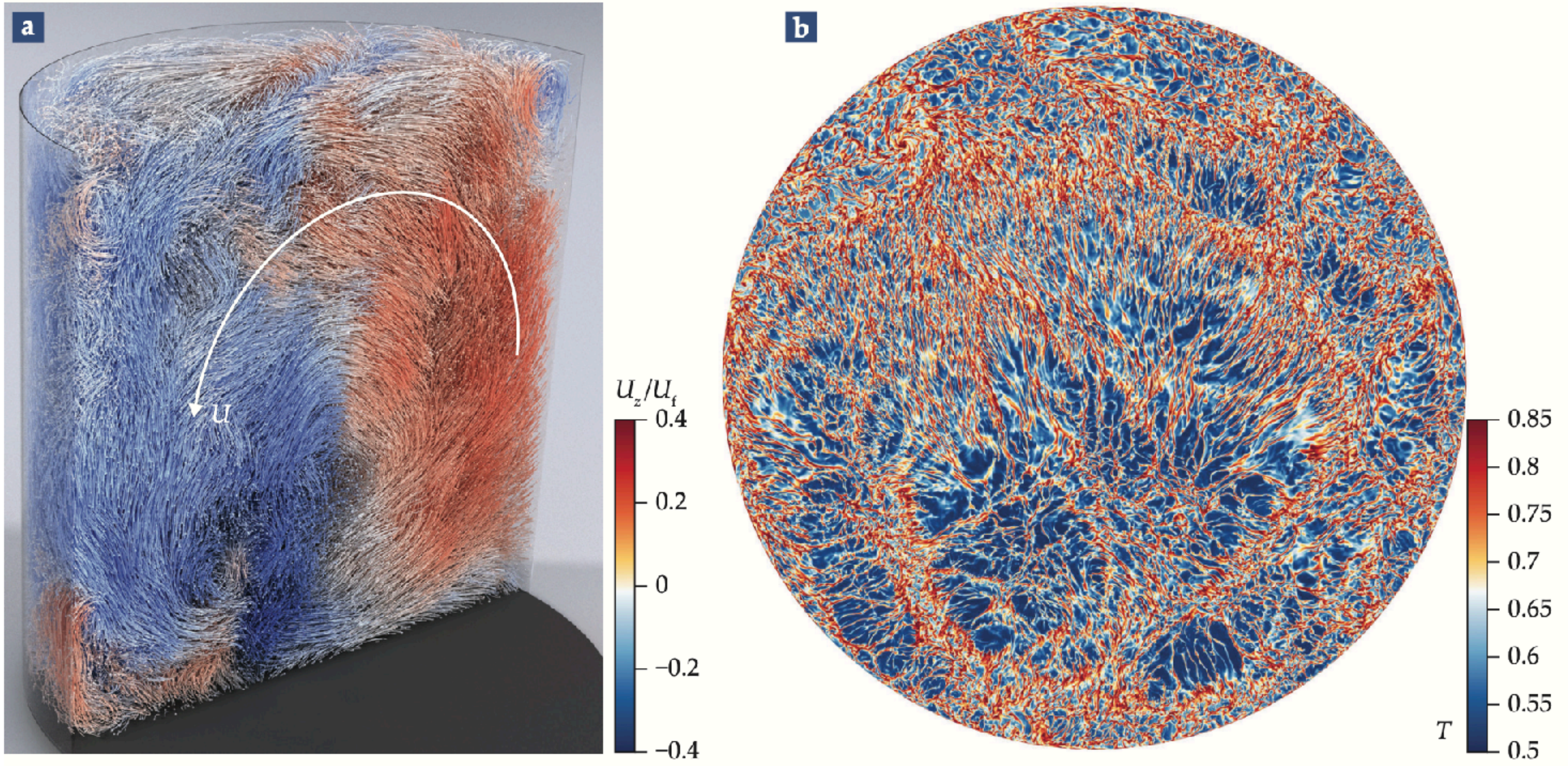

FIGURE 1. THREE-DIMENSIONAL VISUALIZATION of experimental turbulent structures **(a)** in half of a cylindrical Rayleigh–Bénard cell with diameter-to-height aspect ratio Γ = ½, Rayleigh number $Ra = 1.5 \times 10^9$, and Prandtl number $Pr \approx 0.7$ (see the main text for definitions). The particles with trails reveal small turbulent structures in the dominating large-scale convection, which has typical velocity U. The vertical component of the velocity, U_z, is plotted here, normalized by the so-called free-fall velocity $U_f \equiv \sqrt{\beta \Delta g L}$. (Adapted from P. Godbersen et al., *Phys. Rev. Fluids* **6**, 110509, 2021.) **(b)** This cross-sectional snapshot from a fully resolved direct numerical simulation of a cylindrical convection cell with $Ra = 10^{13}$, $Pr = 1$, and Γ = ½ shows the dimensionless temperature field T, which varies from 0 at the top of the cell to 1 at the bottom. It reveals the tiny detaching plume structure. (Courtesy of Richard Stevens, University of Twente; based on an advanced finite-difference code developed by Roberto Verzicco, Tor Vergata University of Rome.)

2D DNS: Ra=10^{14} at Pr=1

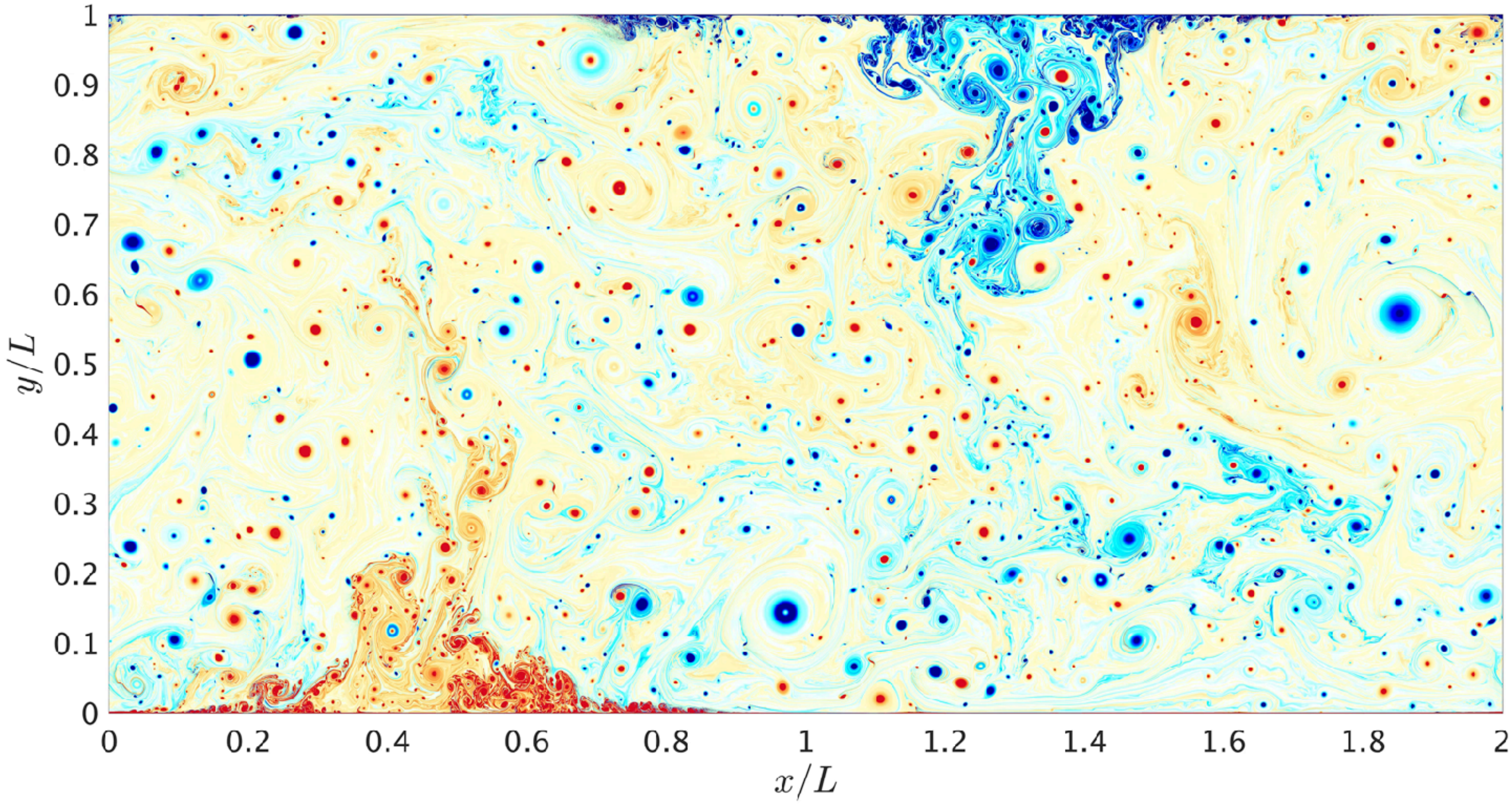

Zhu, Mathai, Stevens, Verzicco, Lohse, Phys. Rev. Lett. 120, 144502 (2018)

Resolution: 25600×12800 $\Gamma = 2$

2D DNS: Ra=10^{14} at Pr=1

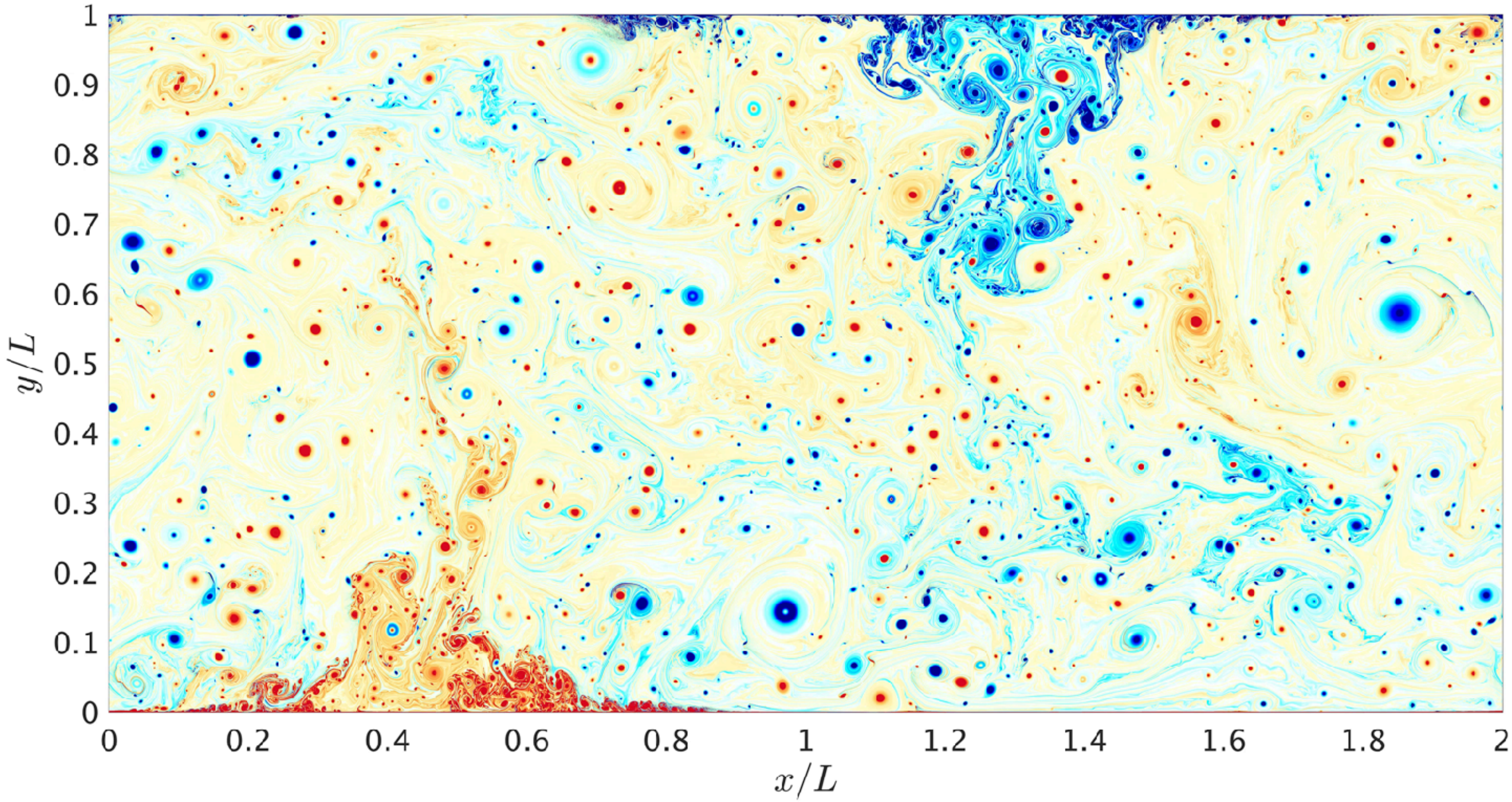

Resolution: 25600×12800

$\Gamma = 2$

Zhu, Mathai, Stevens, Verzicco, Lohse, Phys. Rev. Lett. 120, 144502 (2018)

PRL Cover Designer likes RB numerics

Rotating Rayleigh-Bénard

Zhong *et al.*, PRL 102, 044502 (2009)

Double Diffusive convection

Yang *et al.*, PRL 117, 184501 (2016)

Ultimate Rayleigh-Bénard

Zhu *et al.*, PRL 120, 144502 (2018)

Convection with aerosols

Chong *et al.*, PRL 126, 034502 (2021)

Extend AFiD to multi-phase flow: Phase Field Method

DNS solver (AFiD)

$$\tilde{\rho}\left(\frac{\partial \mathbf{u}}{\partial t}+\mathbf{u}\cdot\nabla\mathbf{u}\right)=-\nabla P+\sqrt{\frac{Pr}{Ra}}\nabla\cdot[\tilde{\mu}(\nabla\mathbf{u}+\nabla\mathbf{u}^{T})]+\underbrace{\mathbf{F}_{st}}_{\text{surface forces}}+\underbrace{\mathbf{G}}_{\text{buoyancy}},$$

$$\tilde{\rho}\tilde{c_p}\left(\frac{\partial \theta}{\partial t}+\mathbf{u}\cdot\nabla\theta\right)=\sqrt{\frac{1}{Pr\,Ra}}\nabla\cdot(\tilde{k}\nabla\theta),$$

$$\nabla\cdot\mathbf{u}=0,$$

For details of AFiD-PFM, see: H.-R. Liu, C. S. Ng, K. L. Chong, D. Lohse & R. Verzicco, *J. Comput. Phys.* 446, 110659 (2021)

Extend AFiD to multi-phase flow: Phase Field Method

DNS solver (AFiD)

$$\tilde{\rho}\left(\frac{\partial \mathbf{u}}{\partial t} + \mathbf{u}\cdot\nabla\mathbf{u}\right) = -\nabla P + \sqrt{\frac{Pr}{Ra}}\nabla\cdot\left[\tilde{\mu}(\nabla\mathbf{u} + \nabla\mathbf{u}^T)\right] + \mathbf{F}_{st} + \mathbf{G},$$

surface forces

buoyancy

$$\tilde{\rho}\tilde{c_p}\left(\frac{\partial \theta}{\partial t} + \mathbf{u}\cdot\nabla\theta\right) = \sqrt{\frac{1}{Pr\,Ra}}\nabla\cdot(\tilde{k}\nabla\theta),$$

$$\nabla\cdot\mathbf{u} = 0,$$

For details of AFiD-PFM, see: H.-R. Liu, C. S. Ng, K. L. Chong, D. Lohse & R. Verzicco, *J. Comput. Phys.* 446, 110659 (2021)

Extend AFiD to multi-phase flow: Phase Field Method

DNS solver (AFiD)

$$\tilde{\rho}\left(\frac{\partial \mathbf{u}}{\partial t} + \mathbf{u}\cdot\nabla\mathbf{u}\right) = -\nabla P + \sqrt{\frac{Pr}{Ra}}\nabla\cdot[\tilde{\mu}(\nabla\mathbf{u} + \nabla\mathbf{u}^T)] + \underbrace{\mathbf{F}_{st}}_{\text{surface forces}} + \underbrace{\mathbf{G}}_{\text{buoyancy}},$$

$$\tilde{\rho}\tilde{c_p}\left(\frac{\partial \theta}{\partial t} + \mathbf{u}\cdot\nabla\theta\right) = \sqrt{\frac{1}{Pr\,Ra}}\nabla\cdot(\tilde{k}\nabla\theta),$$

$$\nabla\cdot\mathbf{u} = 0,$$

Phase field model
for volume fraction C

Cahn-Hilliard equation: $$\frac{\partial C}{\partial t} + \nabla\cdot(\mathbf{u}C) = \frac{1}{Pe}\nabla^2\psi$$

Chemical potential: $$\psi = C^3 - 1.5C^2 + 0.5C - Cn^2\nabla^2 C$$

Cn = Cahn number
Pe = 0.9/Cn

For details of AFiD-PFM, see: H.-R. Liu, C. S. Ng, K. L. Chong, D. Lohse & R. Verzicco, *J. Comput. Phys.* 446, 110659 (2021)

Phase field method in RB context

Melting process in RB convection

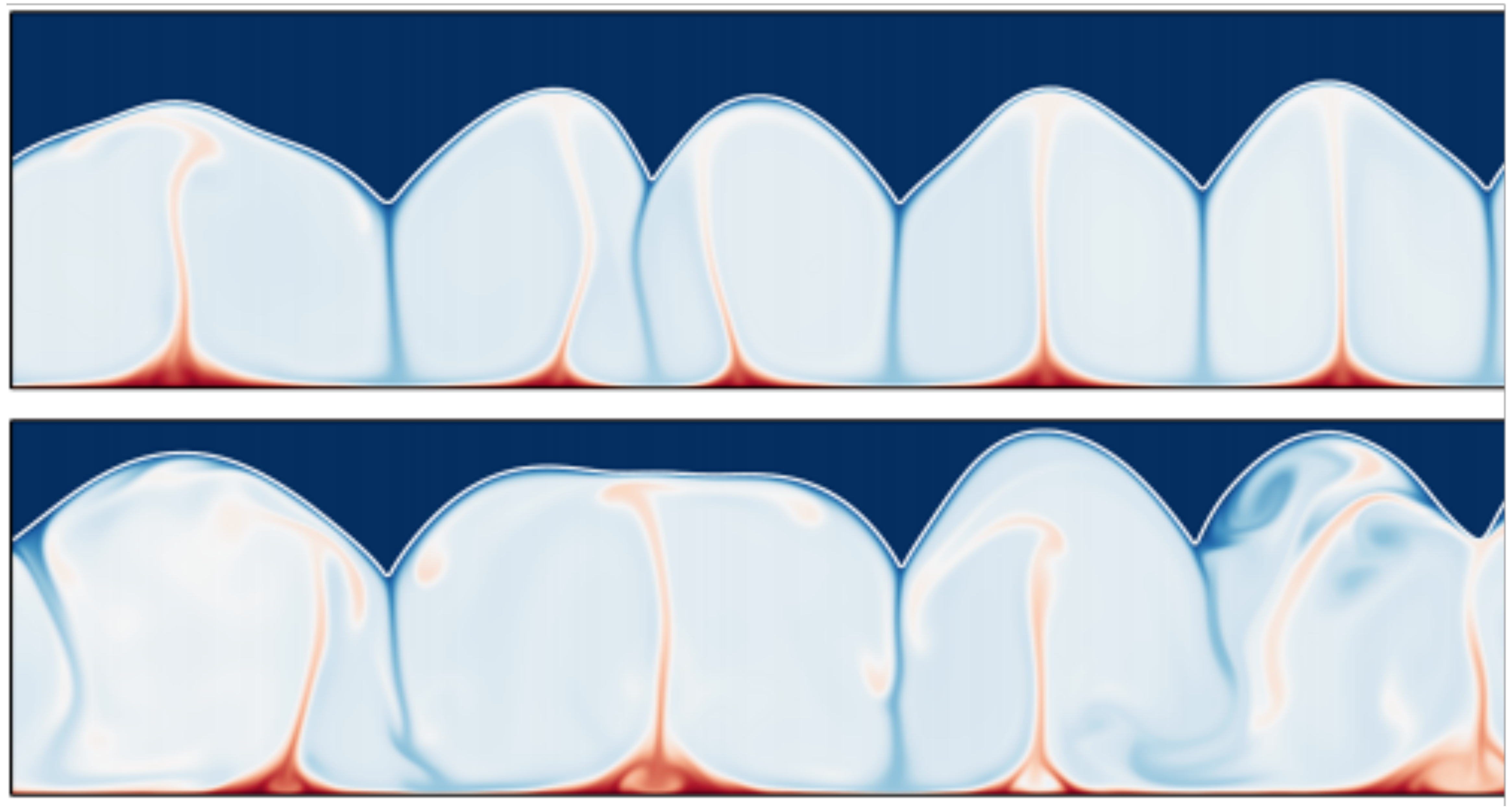

B. Favier, J. Purseed, L. Duchemin,
Rayleigh-Bénard convection with a melting boundary,
J. Fluid Mech. 858, 437 (2019).

(relatively small Ra)

Melting process in turbulent shear flow

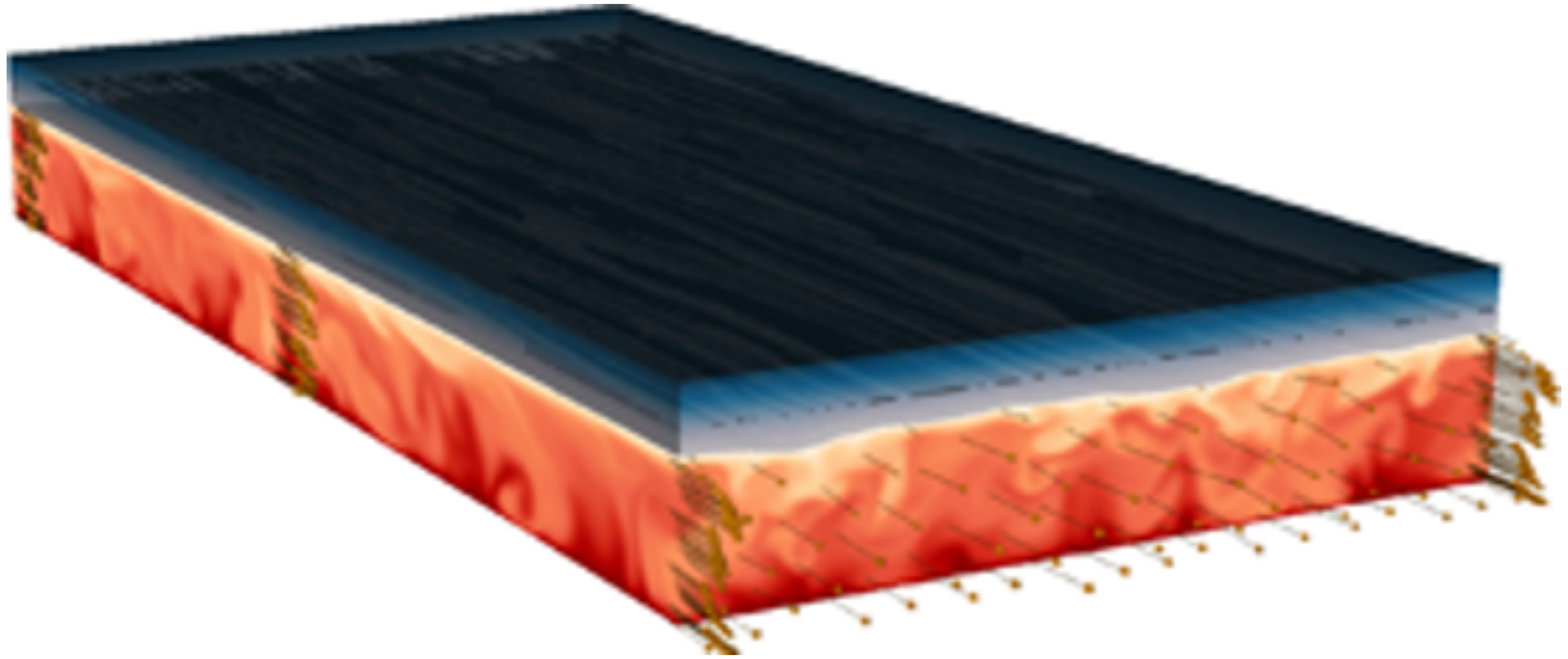

L. A. Couston, E. Hester, B. Favier, J. R. Taylor, P. R. Holland, A. Jenkins,
Topography generation by melting and freezing in a turbulent shear flow,
J. Fluid Mech. 911, A44 (2021).

Extend AFiD to include density anomaly

Momentum equation

$$\frac{\partial u_i}{\partial t} + u_j \frac{\partial u_i}{\partial x_j} = -\frac{\partial p}{\partial x_i} + \sqrt{\frac{Pr}{Ra}} \frac{\partial^2 u_i}{\partial x_j^2}$$

Temperature equation

$$\frac{\partial \theta}{\partial t} + u_i \frac{\partial \theta}{\partial x_i} = \sqrt{\frac{1}{RaPr}} \frac{\partial^2 \theta}{\partial x_j^2}$$

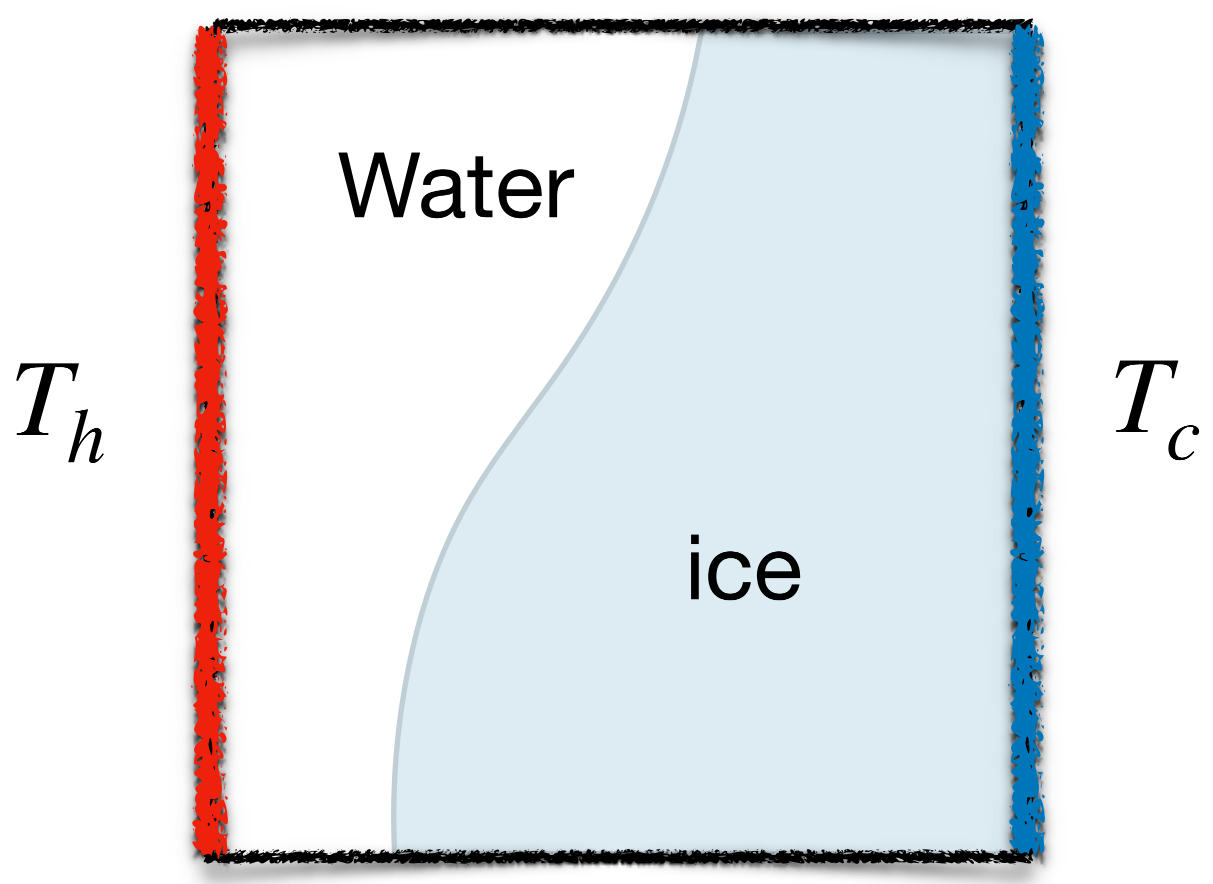

Extend AFiD to include density anomaly

Momentum equation

$$\frac{\partial u_i}{\partial t} + u_j \frac{\partial u_i}{\partial x_j} = - \frac{\partial p}{\partial x_i} + \sqrt{\frac{Pr}{Ra}} \frac{\partial^2 u_i}{\partial x_j^2} + |\theta - \theta_{max}|^q \delta_{iz}$$

Temperature equation

$$\frac{\partial \theta}{\partial t} + u_i \frac{\partial \theta}{\partial x_i} = \sqrt{\frac{1}{RaPr}} \frac{\partial^2 \theta}{\partial x_j^2}$$

Water density anomaly:

$$\rho_w = \rho_0(1 - \beta^* |T - T_{max}|^q)$$

$$T_{max} = 4^{o}\mathrm{C}$$

$$q = 1.895$$

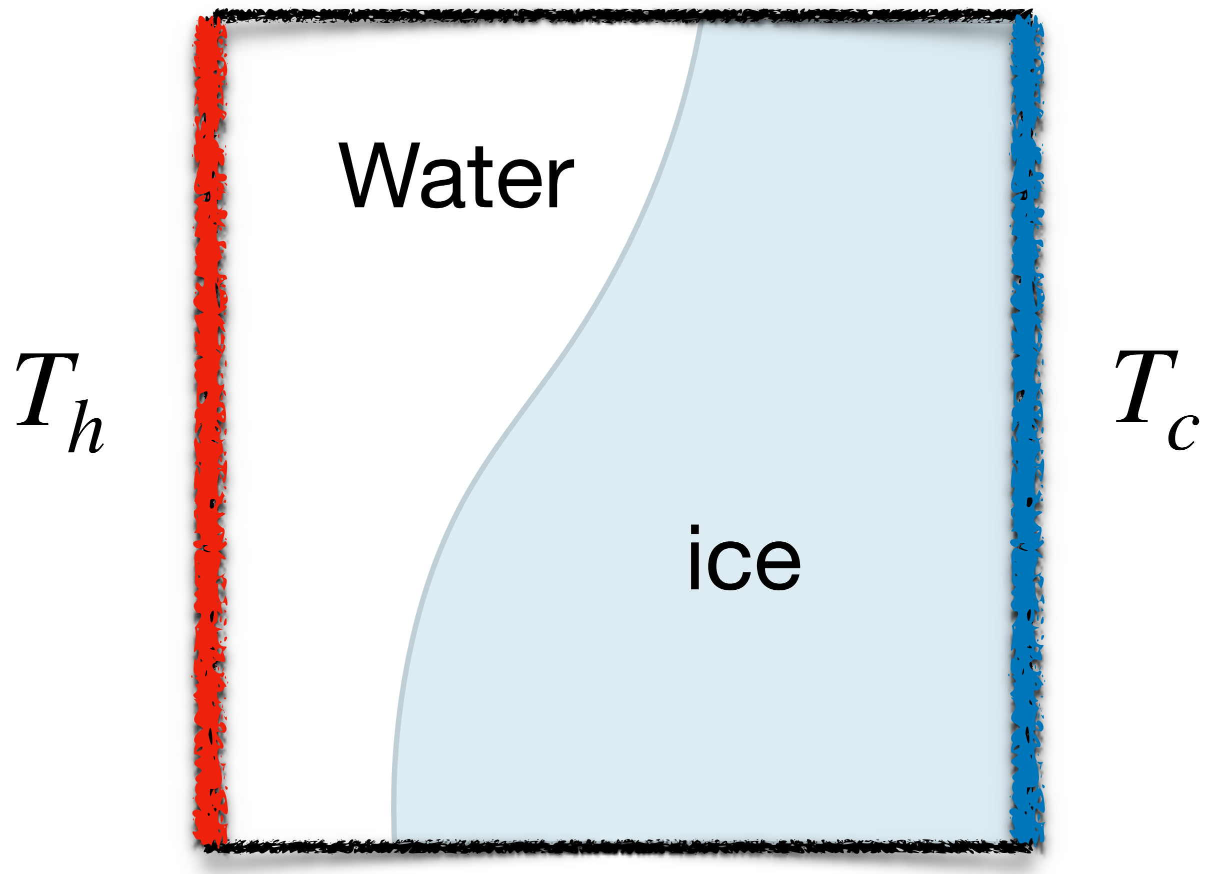

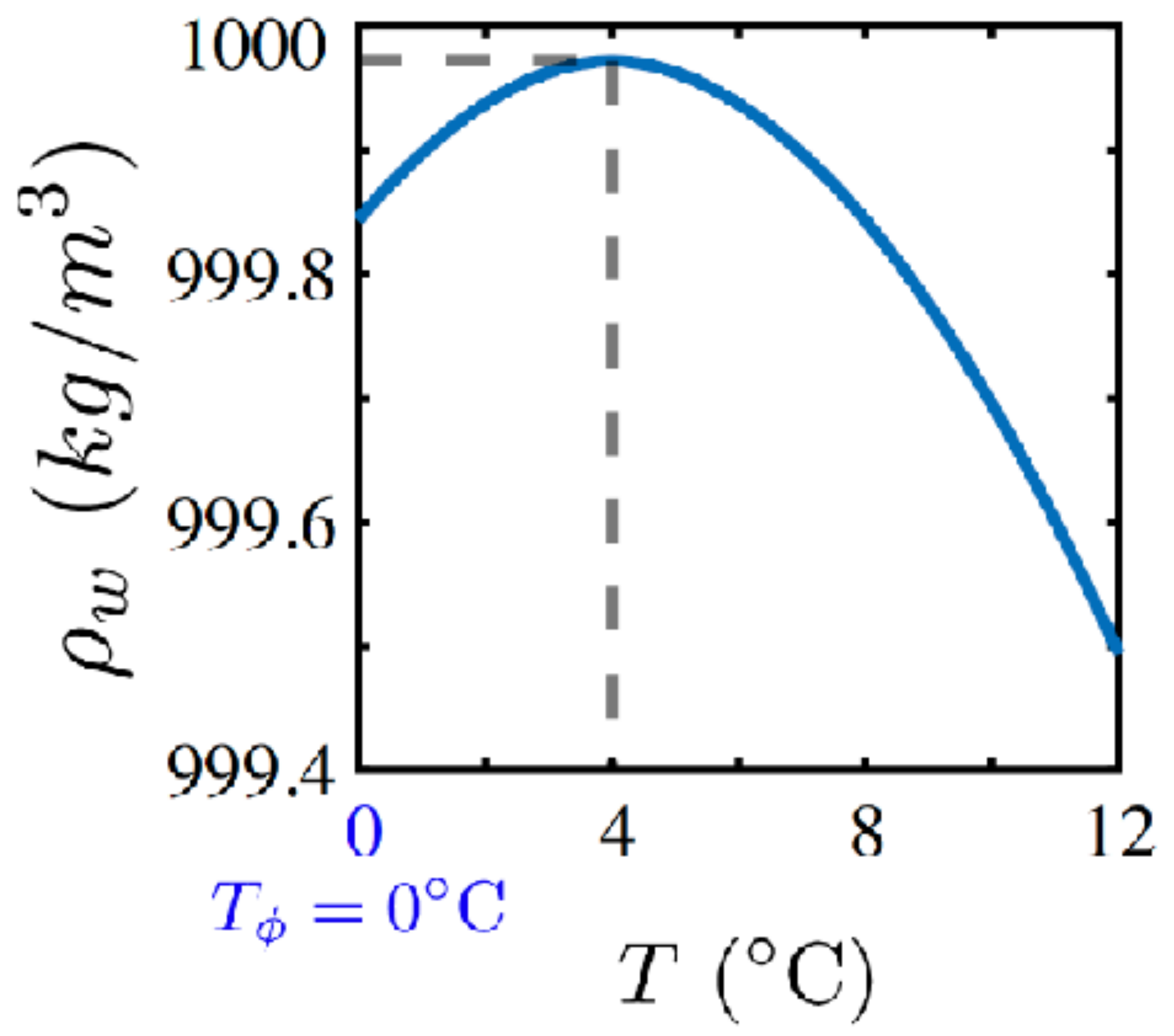

Further extend AFiD to include latent heat

$\phi = 0$ Solid

$\phi = 1$ Liquid

Momentum equation

$$\frac{\partial u_i}{\partial t} + u_j \frac{\partial u_i}{\partial x_j} = -\frac{\partial p}{\partial x_i} + \sqrt{\frac{Pr}{Ra}} \frac{\partial^2 u_i}{\partial x_j^2} + |\theta - \theta_{max}|^q \delta_{iz}$$

Temperature equation

$$\frac{\partial \theta}{\partial t} + u_i \frac{\partial \theta}{\partial x_i} = \sqrt{\frac{1}{RaPr}} \frac{\partial^2 \theta}{\partial x_j^2}$$

Phase field equation

$$\frac{\epsilon^2}{M} \frac{\partial \phi}{\partial t} = \epsilon^2 \frac{\partial^2 \phi}{\partial x_j^2} + \alpha \epsilon St(\theta - \theta_M) \frac{dQ(\phi)}{d\phi} - \frac{1}{4} \frac{dG(\phi)}{d\phi}$$

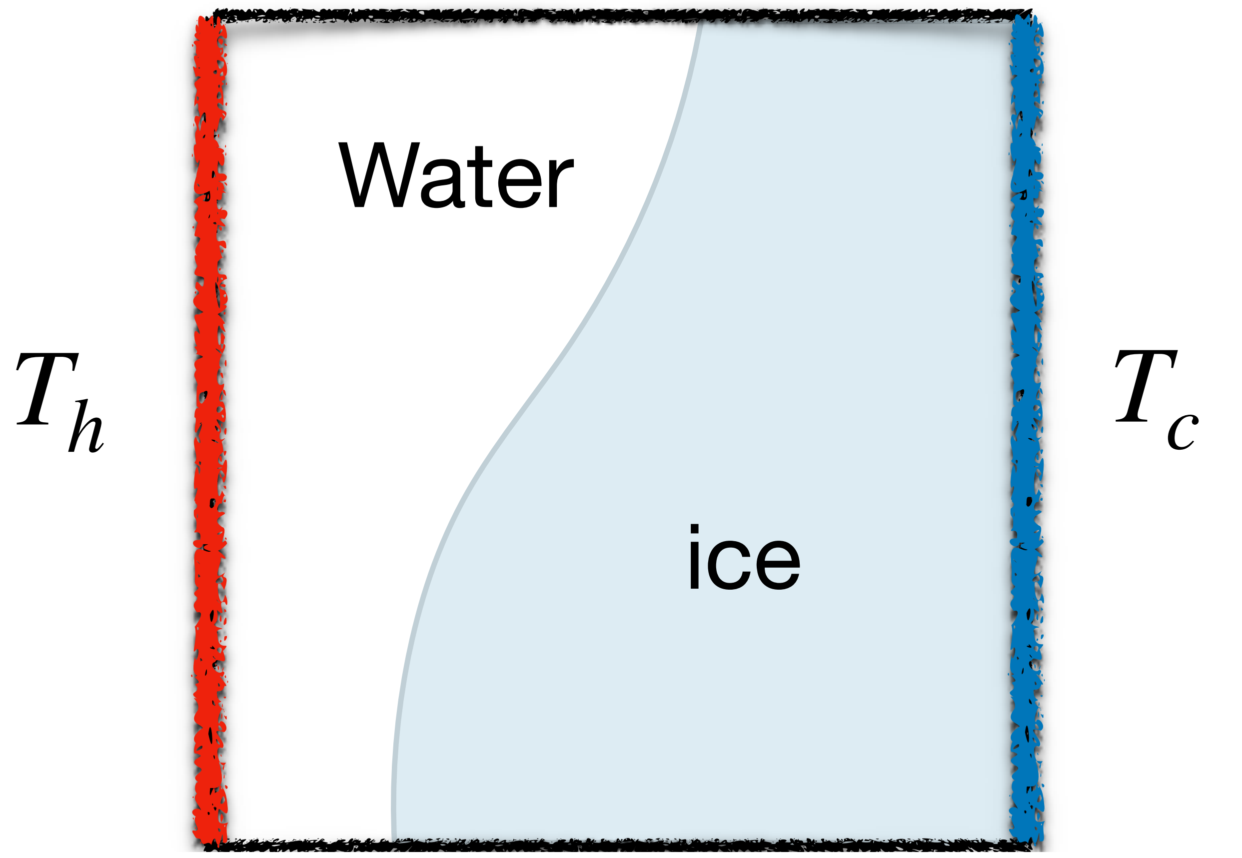

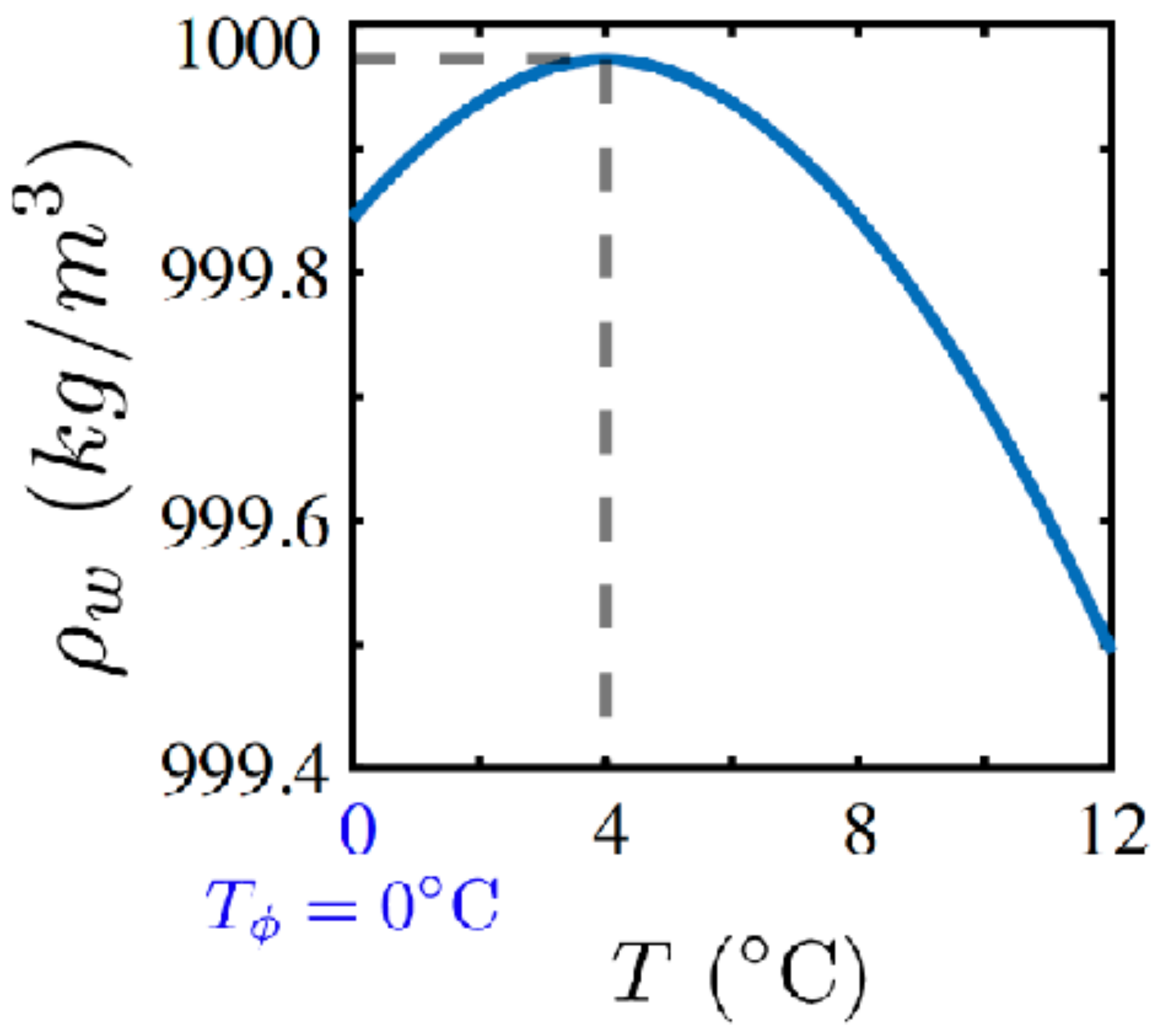

Further extend AFiD to include latent heat

$\phi = 0$ Solid

$\phi = 1$ Liquid

Momentum equation

$$\frac{\partial u_i}{\partial t} + u_j \frac{\partial u_i}{\partial x_j} = -\frac{\partial p}{\partial x_i} + \sqrt{\frac{Pr}{Ra}} \frac{\partial^2 u_i}{\partial x_j^2} + |\theta - \theta_{max}|^q \delta_{iz} - \frac{(1-\phi)^2 u_i}{\eta}$$

Penalty term

Temperature equation

$$\frac{\partial \theta}{\partial t} + u_i \frac{\partial \theta}{\partial x_i} = \sqrt{\frac{1}{RaPr}} \frac{\partial^2 \theta}{\partial x_j^2}$$

Phase field equation

$$\frac{\epsilon^2}{M} \frac{\partial \phi}{\partial t} = \epsilon^2 \frac{\partial^2 \phi}{\partial x_j^2} + \alpha \epsilon St(\theta - \theta_M) \frac{dQ(\phi)}{d\phi} - \frac{1}{4} \frac{dG(\phi)}{d\phi}$$

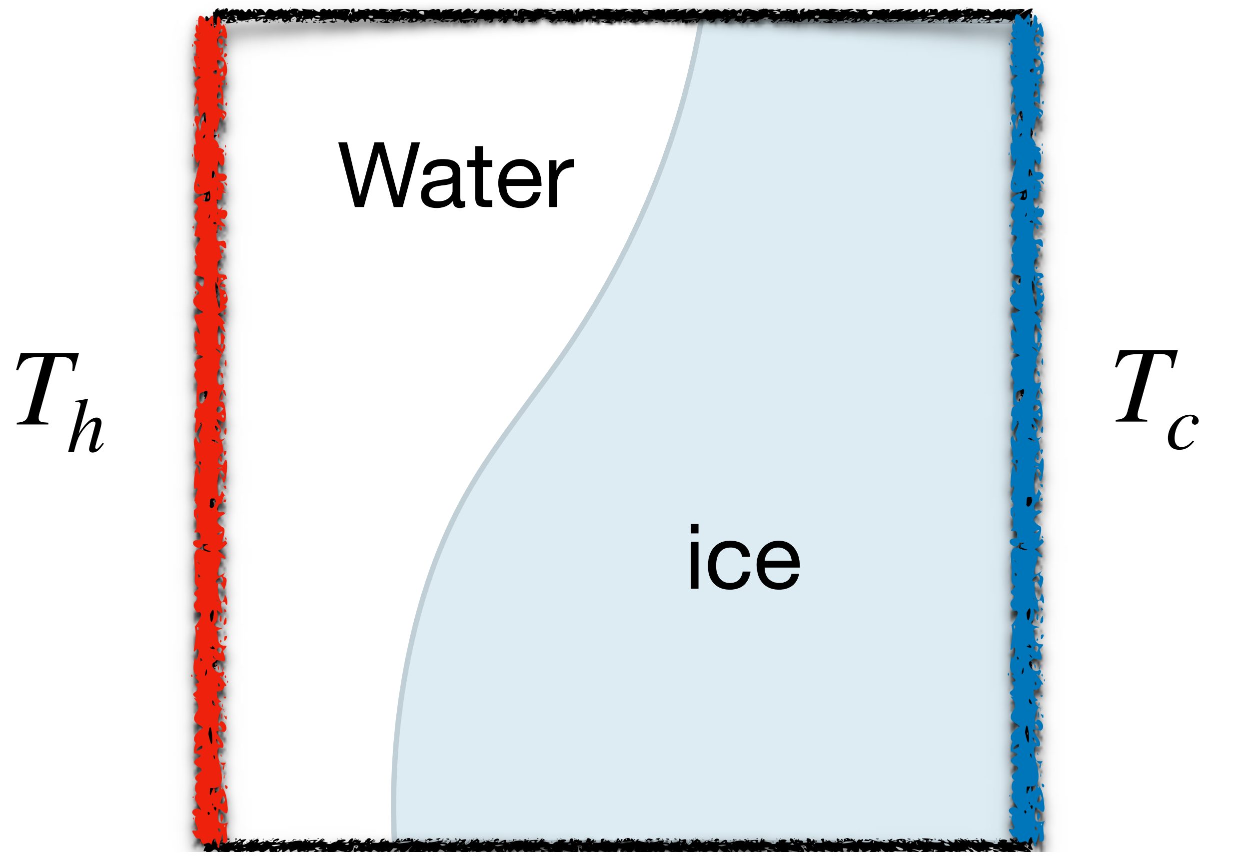

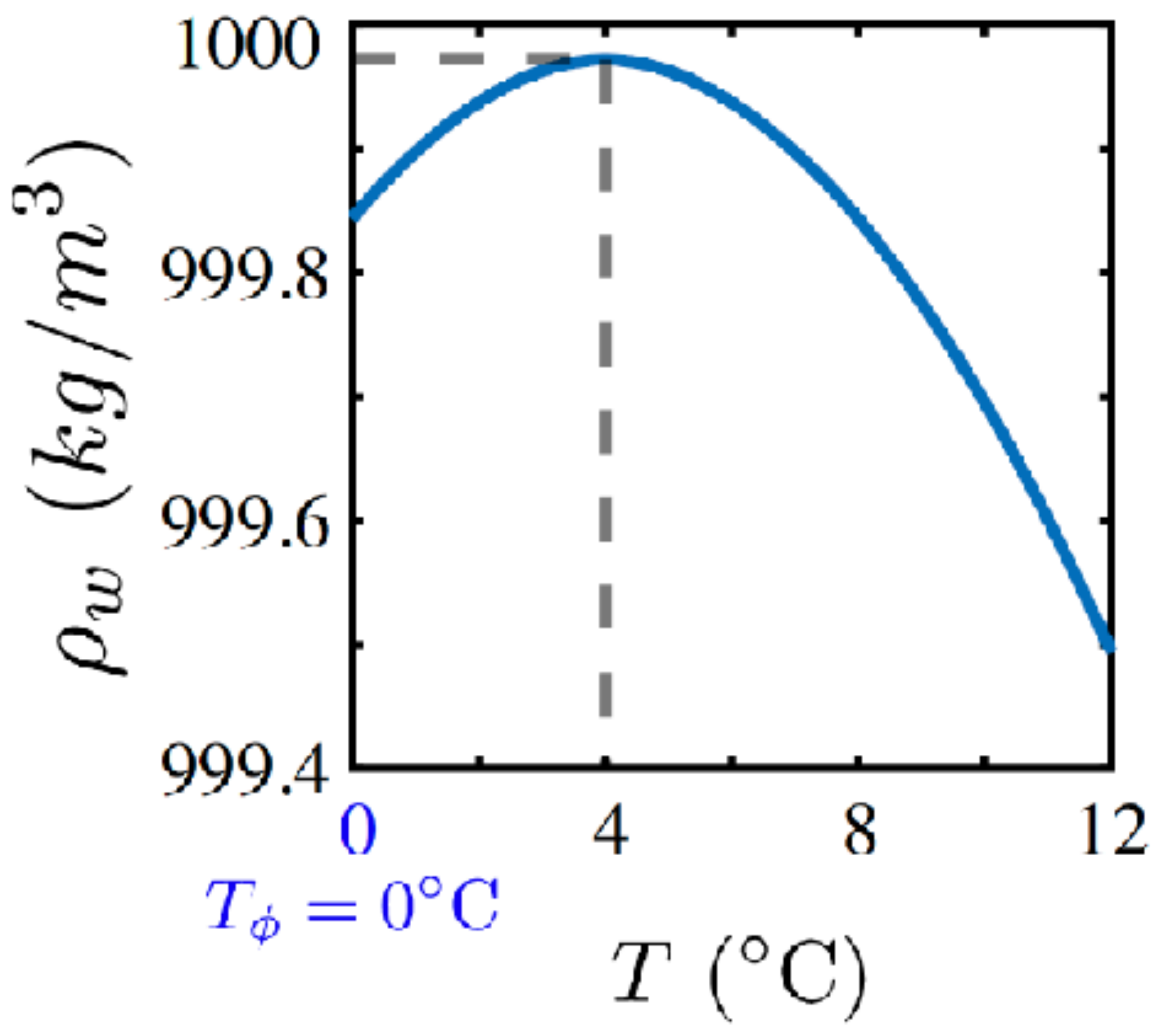

Further extend AFiD to include latent heat

$\phi = 0$ Solid

$\phi = 1$ Liquid

Momentum equation

$$\frac{\partial u_i}{\partial t} + u_j \frac{\partial u_i}{\partial x_j} = -\frac{\partial p}{\partial x_i} + \sqrt{\frac{Pr}{Ra}} \frac{\partial^2 u_i}{\partial x_j^2} + |\theta - \theta_{max}|^q \delta_{iz} - \frac{(1-\phi)^2 u_i}{\eta}$$

Penalty term

Temperature equation

$$\frac{\partial \theta}{\partial t} + u_i \frac{\partial \theta}{\partial x_i} = \sqrt{\frac{1}{RaPr}} \frac{\partial^2 \theta}{\partial x_j^2} - \frac{1}{St} \frac{dQ(\phi)}{d\phi} \frac{d\phi}{dt}$$

Latent heat

Phase field equation

$$\frac{\epsilon^2}{M} \frac{\partial \phi}{\partial t} = \epsilon^2 \frac{\partial^2 \phi}{\partial x_j^2} + \alpha \epsilon St(\theta - \theta_M) \frac{dQ(\phi)}{d\phi} - \frac{1}{4} \frac{dG(\phi)}{d\phi}$$

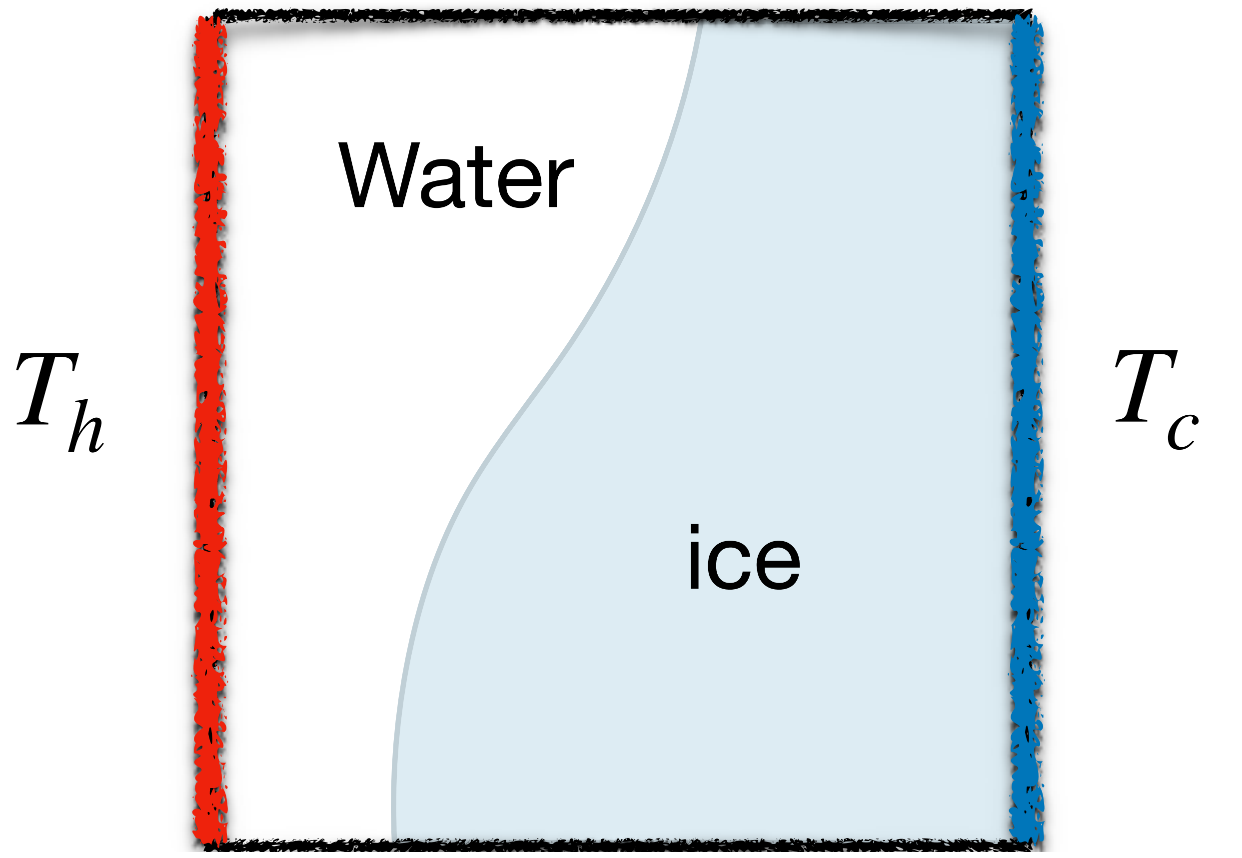

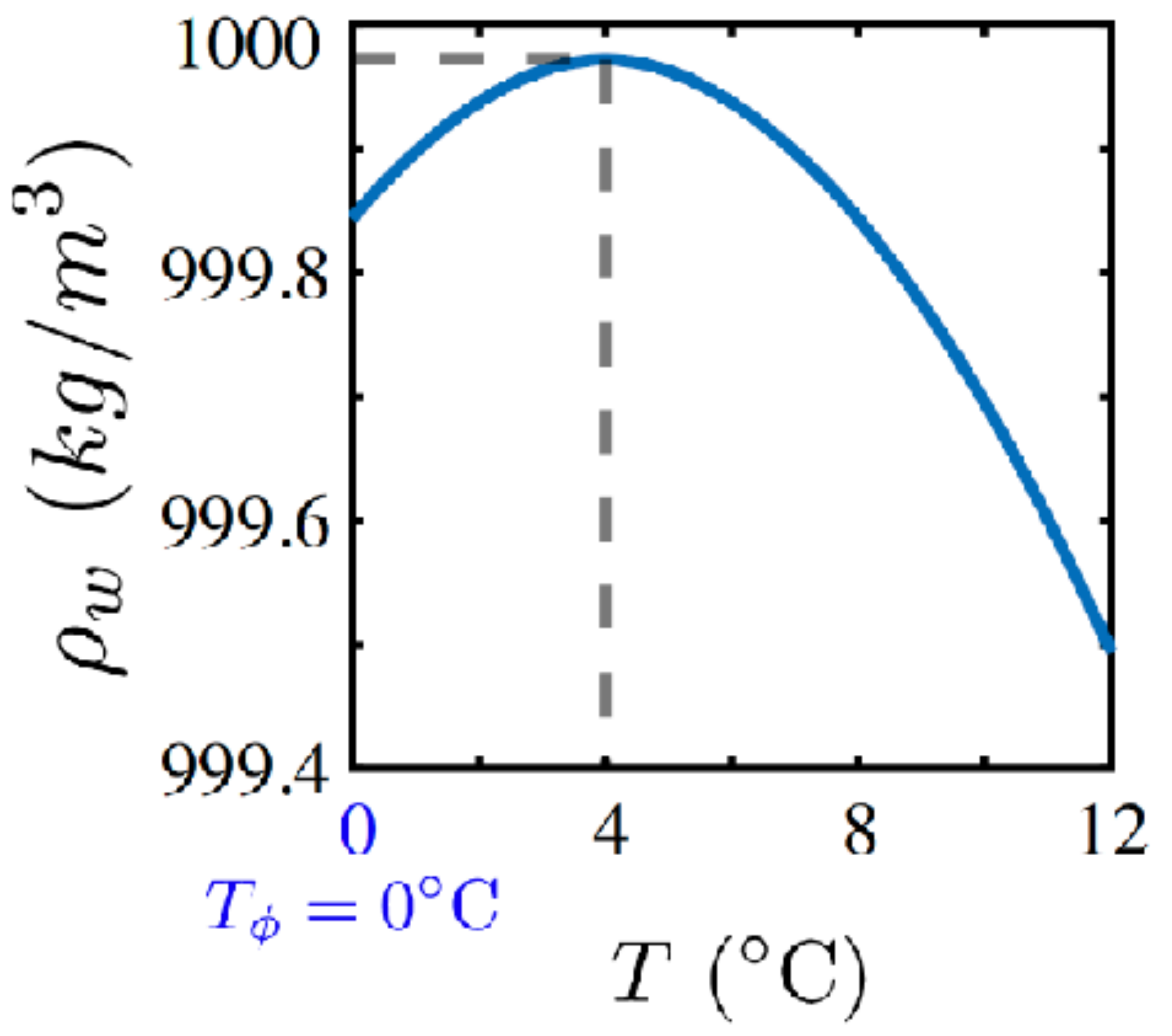

Further extend AFiD to include latent heat

$\phi = 0$ Solid

$\phi = 1$ Liquid

Momentum equation

$$\frac{\partial u_i}{\partial t} + u_j \frac{\partial u_i}{\partial x_j} = -\frac{\partial p}{\partial x_i} + \sqrt{\frac{Pr}{Ra}} \frac{\partial^2 u_i}{\partial x_j^2} + |\theta - \theta_{max}|^q \delta_{iz} - \frac{(1-\phi)^2 u_i}{\eta}$$

Penalty term

Temperature equation

$$\frac{\partial \theta}{\partial t} + u_i \frac{\partial \theta}{\partial x_i} = \sqrt{\frac{1}{RaPr}} \frac{\partial^2 \theta}{\partial x_j^2} - \frac{1}{St} \frac{dQ(\phi)}{d\phi} \frac{d\phi}{dt}$$

Latent heat

Phase field equation

$$\frac{\epsilon^2}{M} \frac{\partial \phi}{\partial t} = \epsilon^2 \frac{\partial^2 \phi}{\partial x_j^2} + \alpha \epsilon St(\theta - \theta_M) \frac{dQ(\phi)}{d\phi} - \frac{1}{4} \frac{dG(\phi)}{d\phi}$$

Double-well function $G(\phi) = \phi^2(1-\phi)^2$

Latent heat function (interpolated) $Q(\phi) = \phi^3(10 - 15\phi + 6\phi^2)$

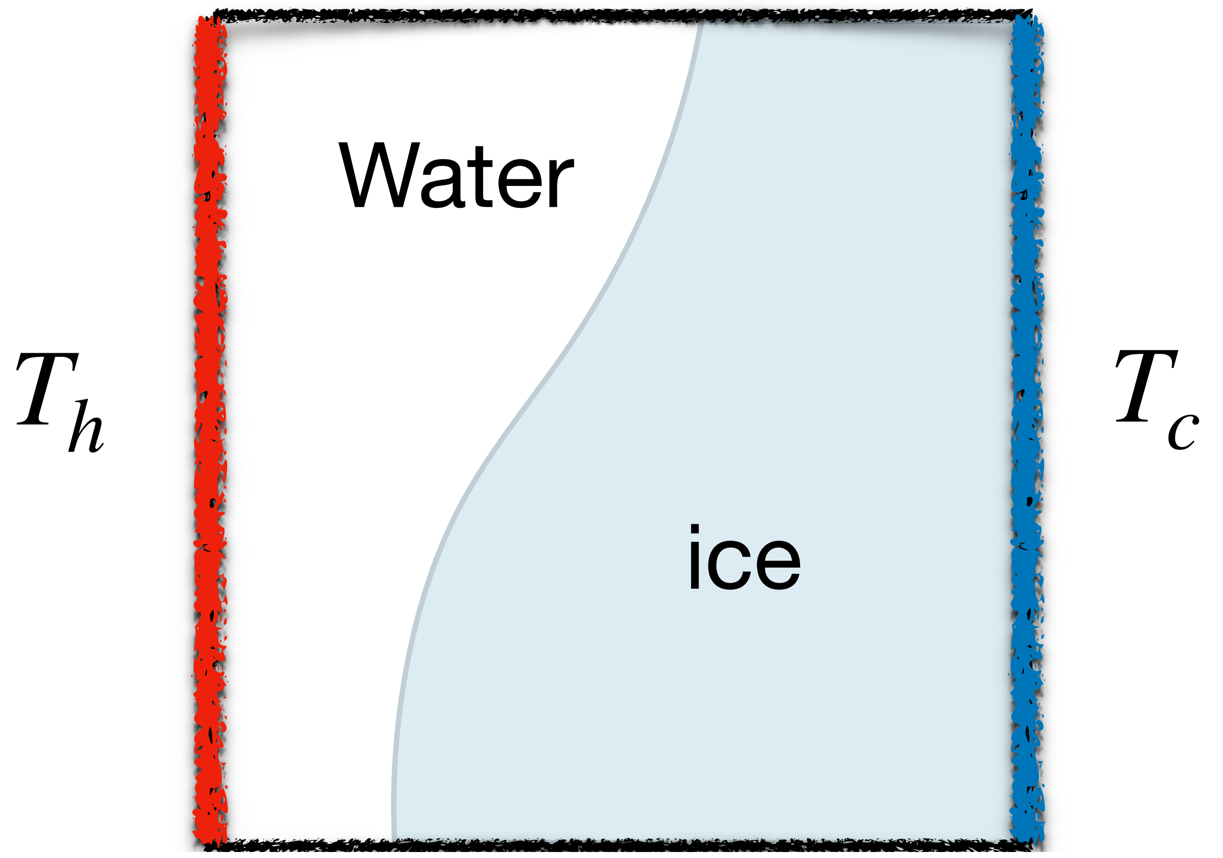

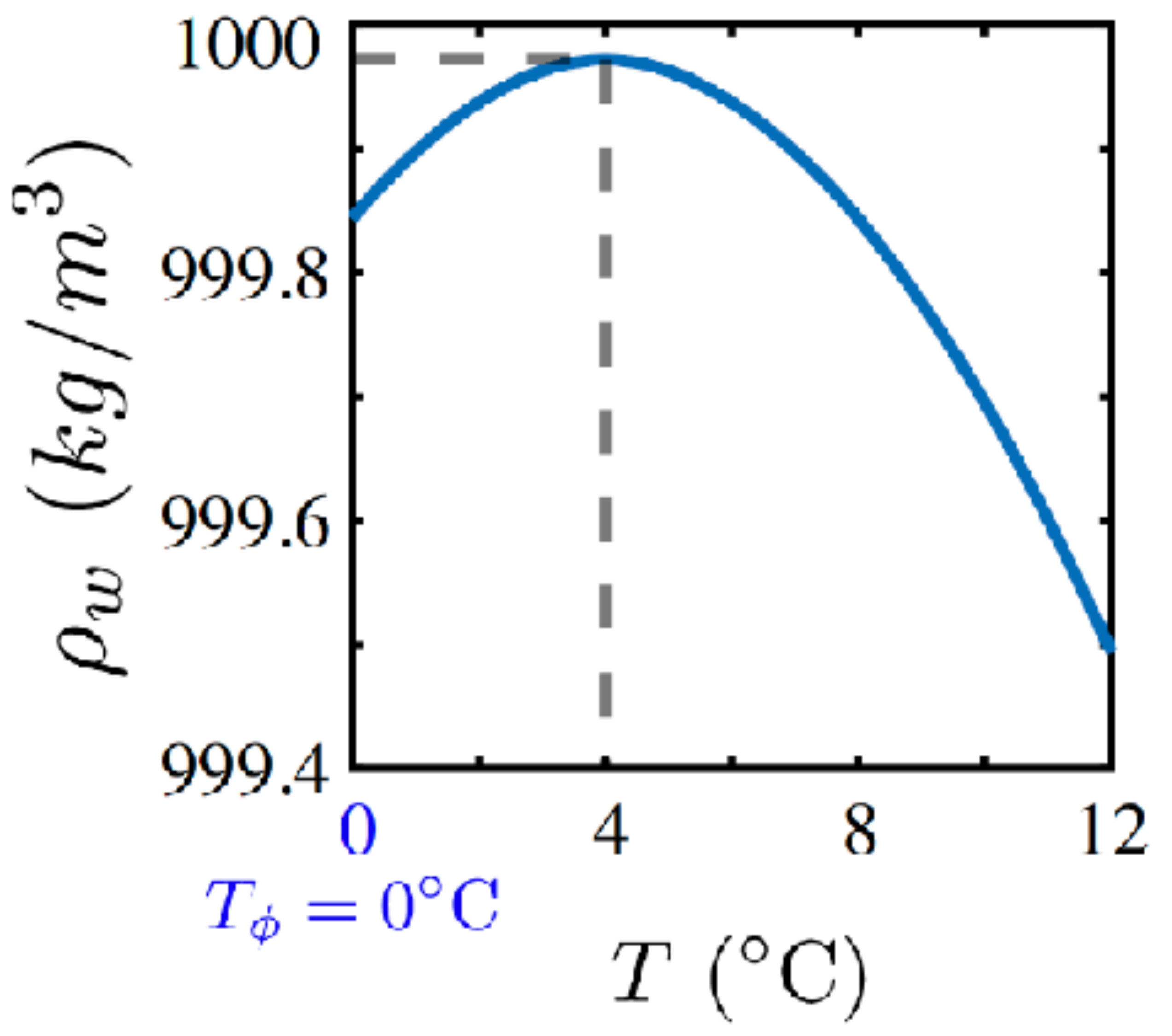

Summary of numerical methods that make DNS on melting in and with turbulence possible

Summary of numerical methods that make DNS on melting in and with turbulence possible

1. Original highly efficient AFiD code

vd Poel, Ostilla-Monico *et al.*
Comp. Fluids 116, 10 (2015)

Summary of numerical methods that make DNS on melting in and with turbulence possible

1. Original highly efficient AFiD code

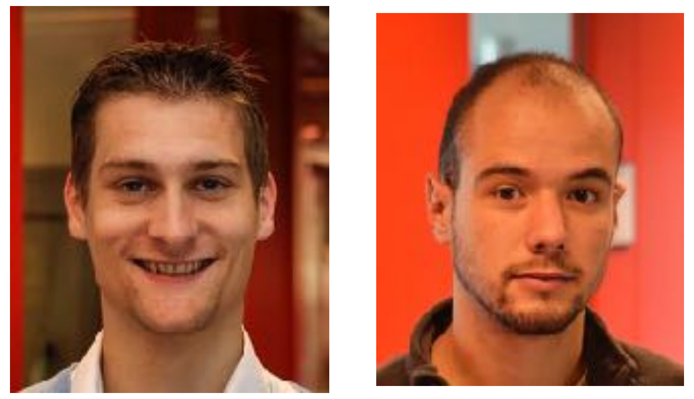

vd Poel, Ostilla-Monico *et al.*
Comp. Fluids 116, 10 (2015)

2. Multiple grid resolution for DDC

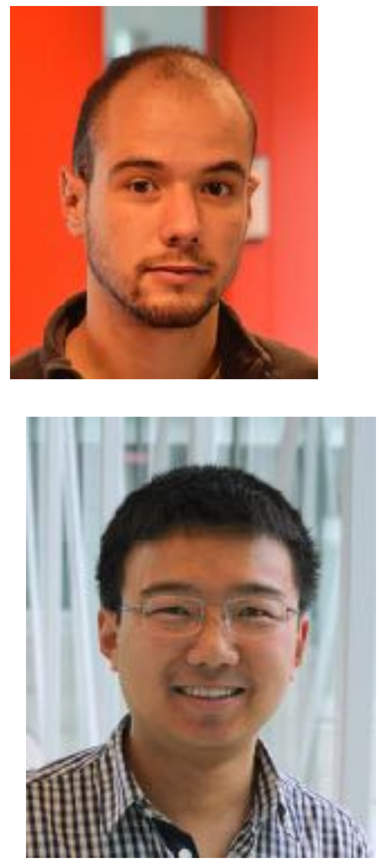

Ostilla-Monico, Yang *et al.*
J. Comp. Phys. 301, 308 (2015)

Summary of numerical methods that make DNS on melting in and with turbulence possible

1. Original highly efficient AFiD code


vd Poel, Ostilla-Monico *et al.*
Comp. Fluids 116, 10 (2015)

2. Multiple grid resolution for DDC

Ostilla-Monico, Yang *et al.*
J. Comp. Phys. 301, 308 (2015)

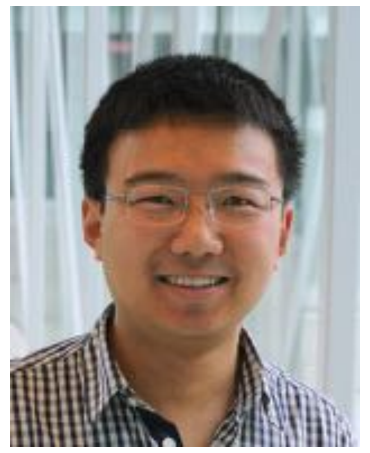

3. Immersed Boundary Method

Spandan *et al.*
J. Comp. Phys. 348, 567 (2016)

Summary of numerical methods that make DNS on melting in and with turbulence possible

1. Original highly efficient AFiD code


vd Poel, Ostilla-Monico *et al.*
Comp. Fluids 116, 10 (2015)

2. Multiple grid resolution for DDC


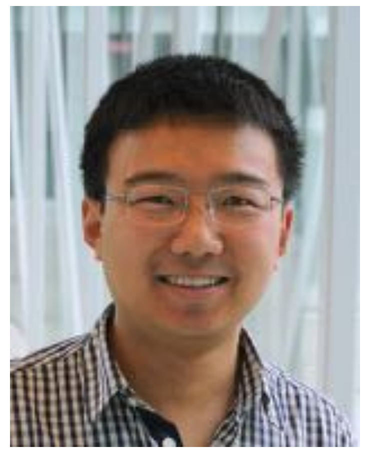

Ostilla-Monico, Yang *et al.*
J. Comp. Phys. 301, 308 (2015)

3. Immersed Boundary Method

Spandan *et al.*
J. Comp. Phys. 348, 567 (2016)

4. Phase Field Method with phase transitions

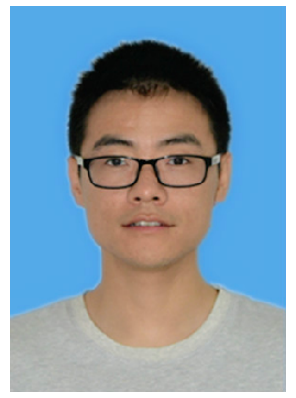

Haoran Liu *et al.*
J. Comp. Phys. 446, 110659 (2021)

Summary of numerical methods that make DNS on melting in and with turbulence possible

1. Original highly efficient AFiD code


vd Poel, Ostilla-Monico *et al.*
Comp. Fluids 116, 10 (2015)

2. Multiple grid resolution for DDC


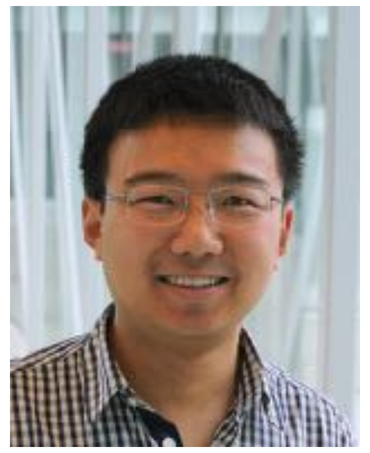

Ostilla-Monico, Yang *et al.*
J. Comp. Phys. 301, 308 (2015)

3. Immersed Boundary Method

Spandan *et al.*
J. Comp. Phys. 348, 567 (2016)

4. Phase Field Method with phase transitions

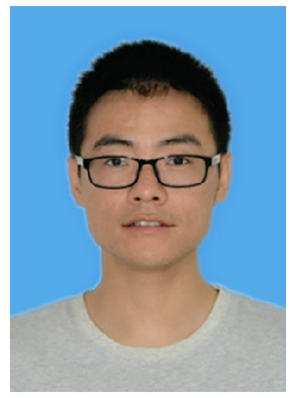


Haoran Liu *et al.*
J. Comp. Phys. 446, 110659 (2021)

Code validations: Compare to experiments & LBM simulations

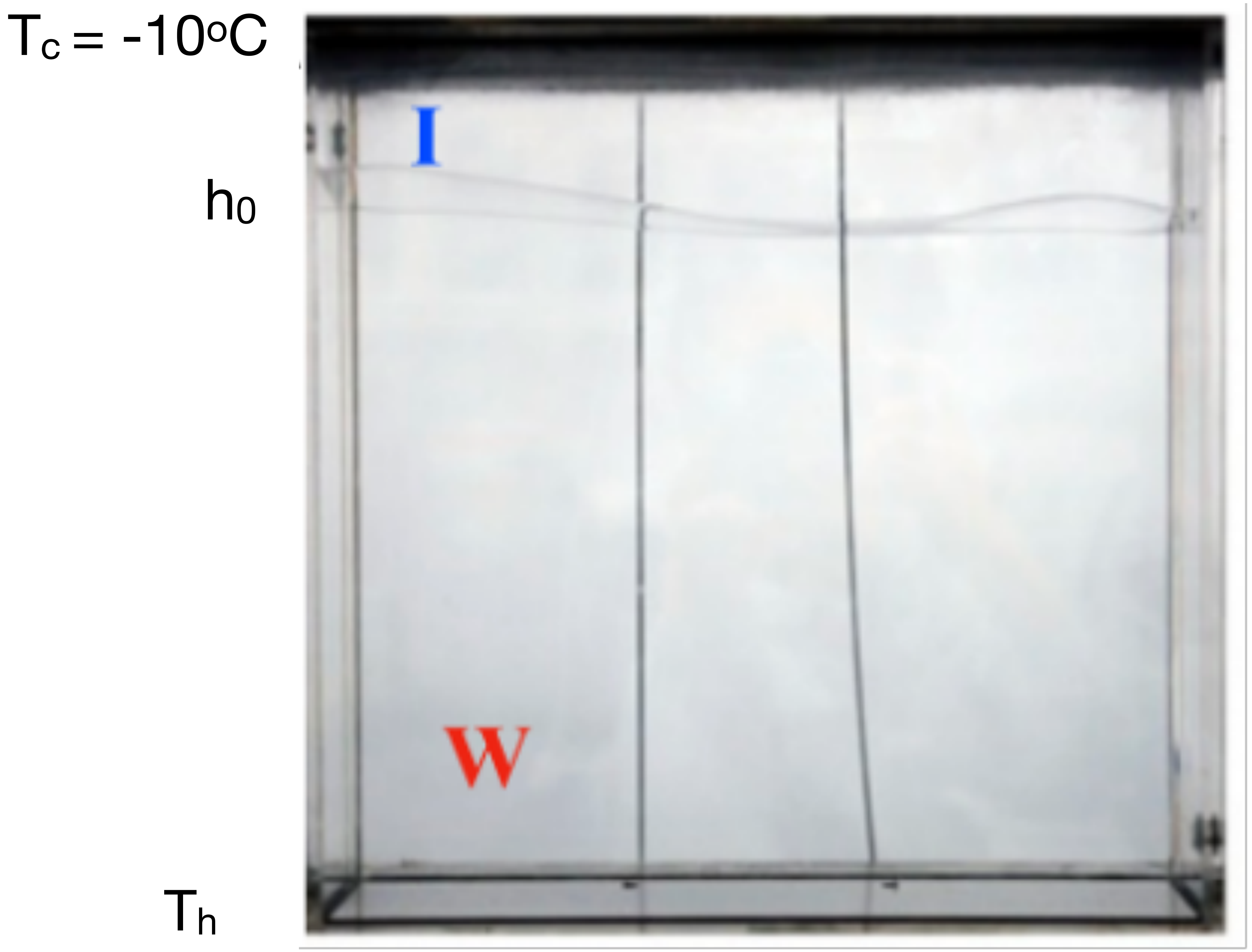

Experiment setup*

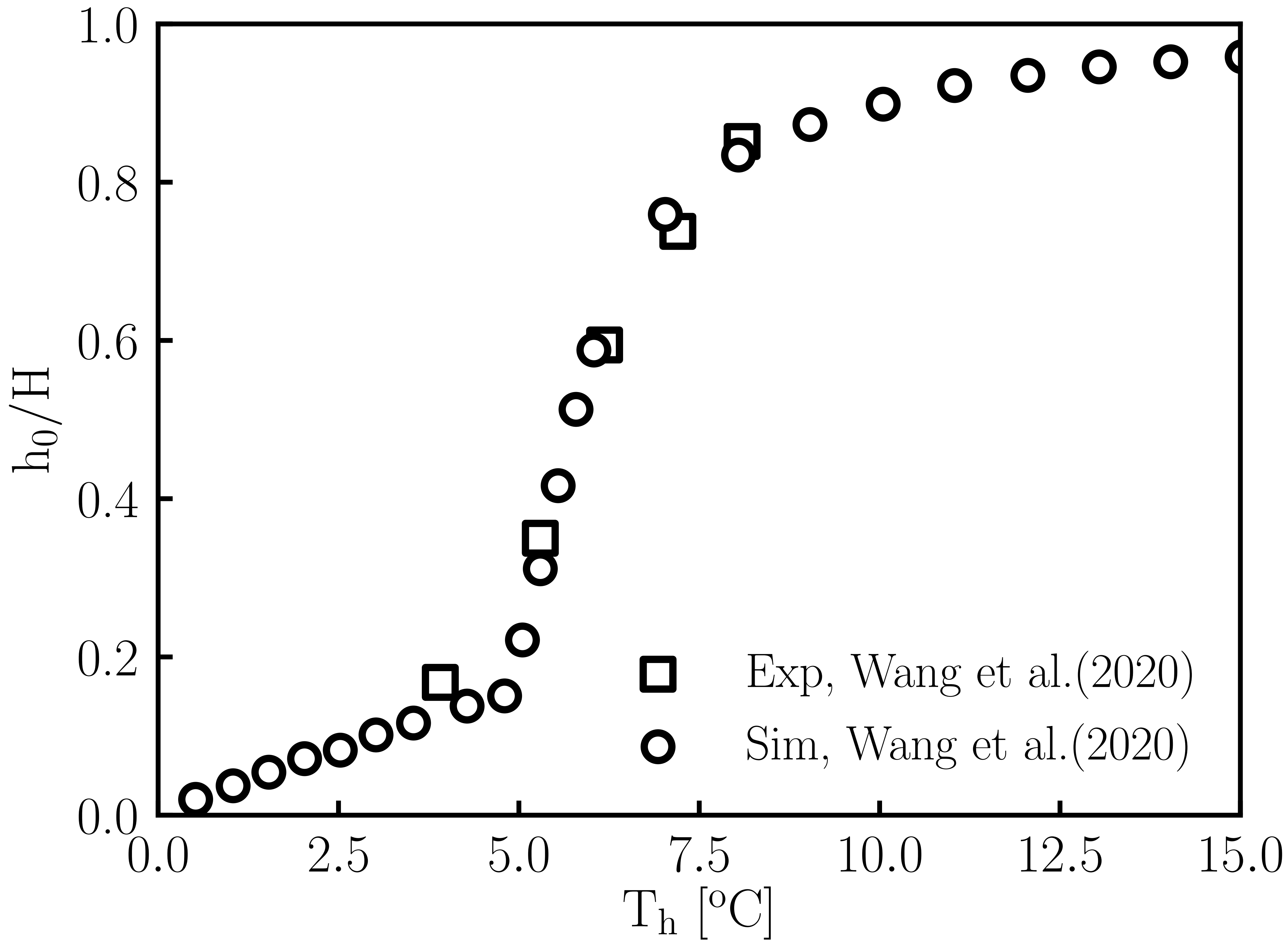

*Z. Wang, E. Calzavarini, C. Sun, & F. Toschi. How the growth of ice depends on the fluid dynamics underneath. PNAS 118, no. 10. (2021)

Code validations: Compare to experiments & LBM simulations

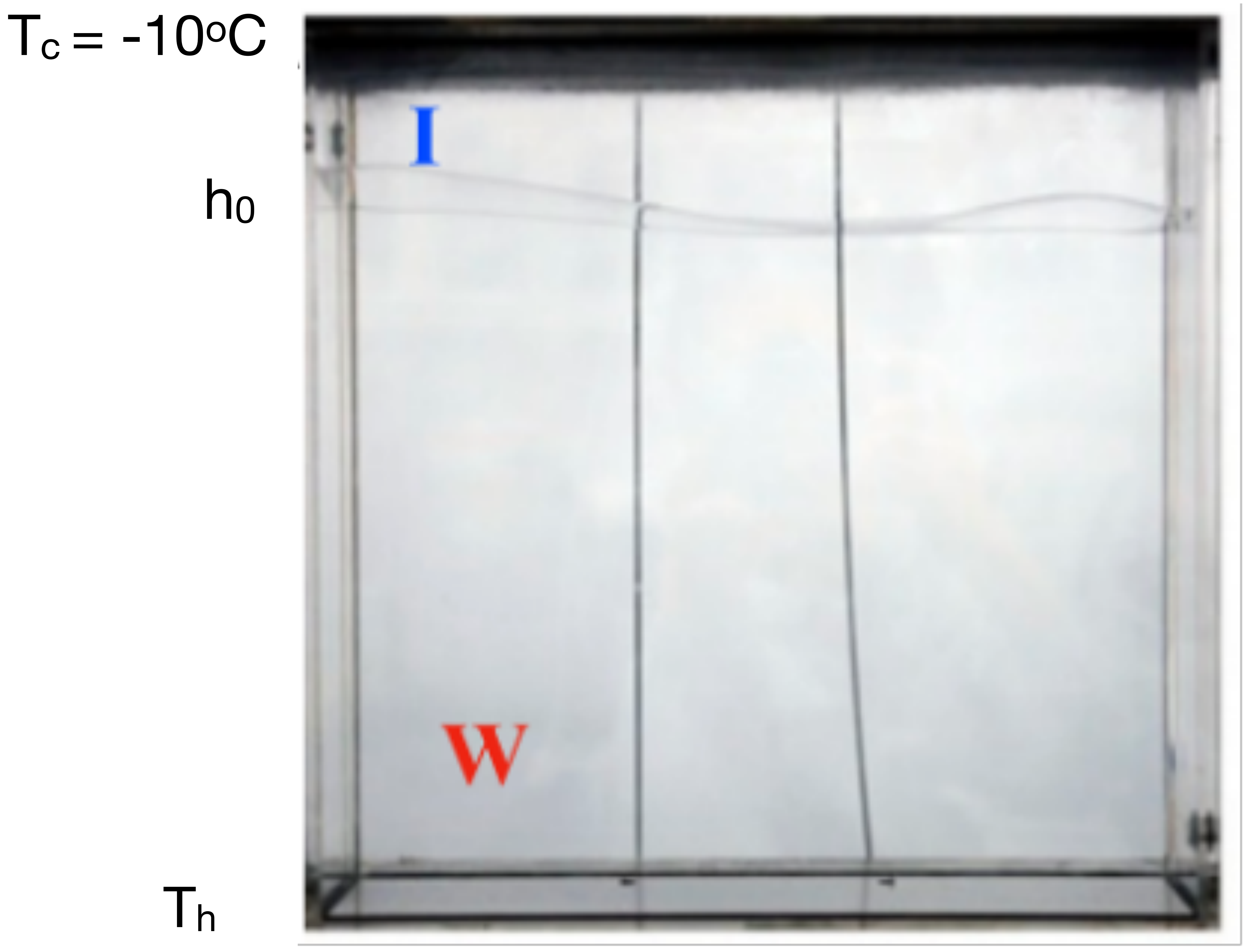

Experiment setup*

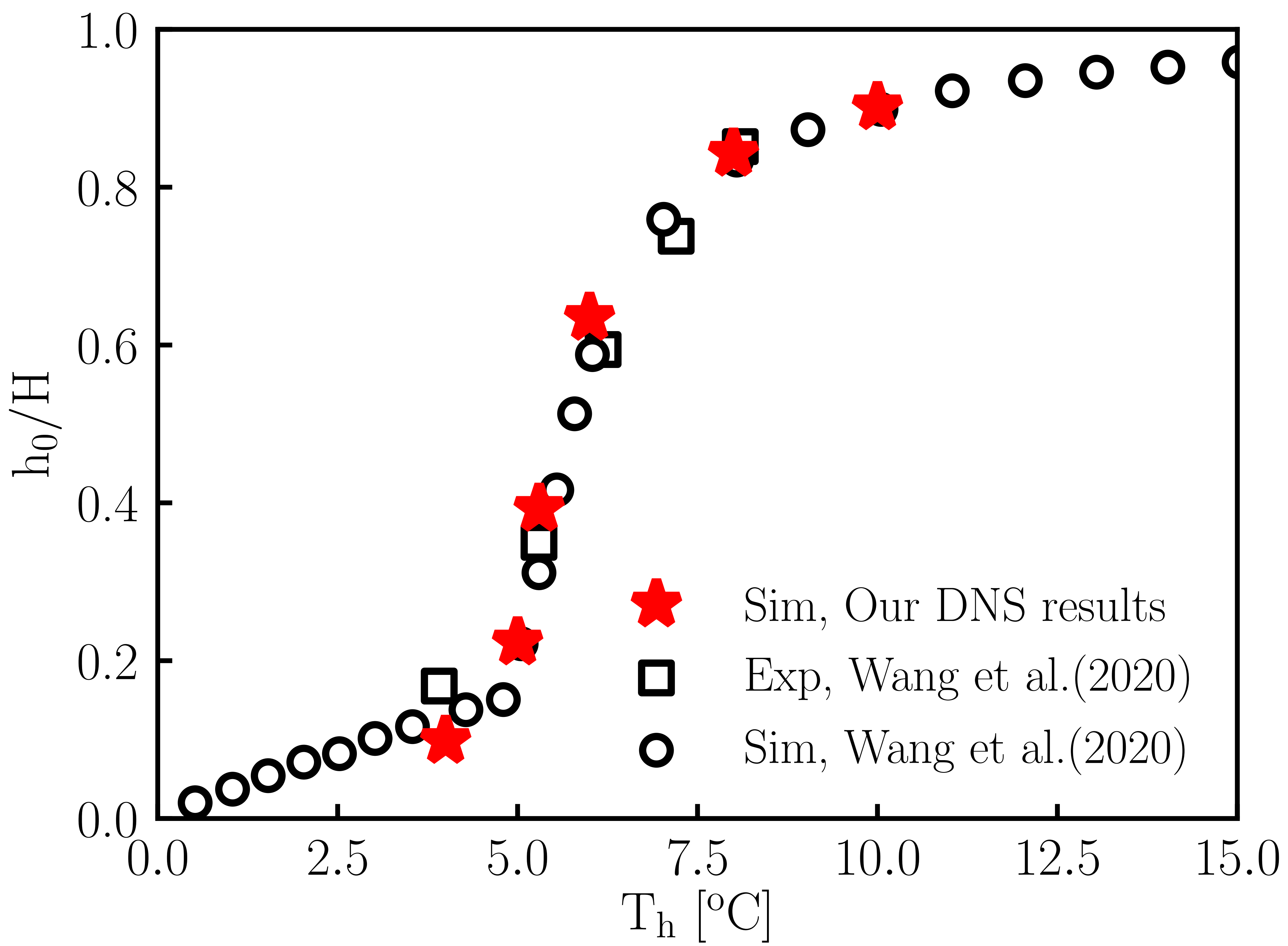

*Z. Wang, E. Calzavarini, C. Sun, & F. Toschi. How the growth of ice depends on the fluid dynamics underneath. PNAS 118, no. 10. (2021)

I. Bistability in radiatively heated melt ponds

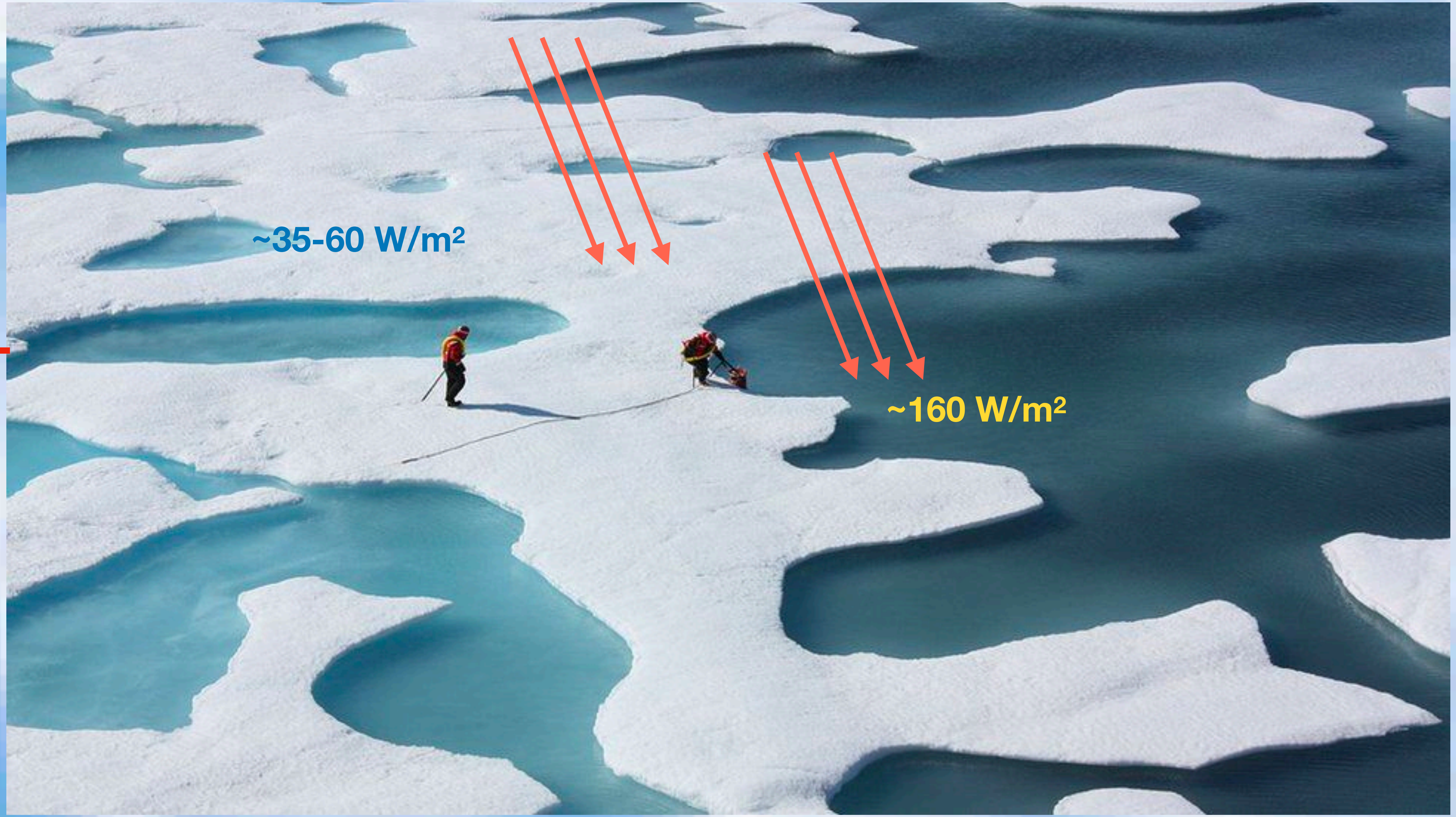

Yang, Howland, Liu, Verzicco, Lohse, Phys. Rev. Lett. 131, 234002 (2023)

Convection in melt ponds

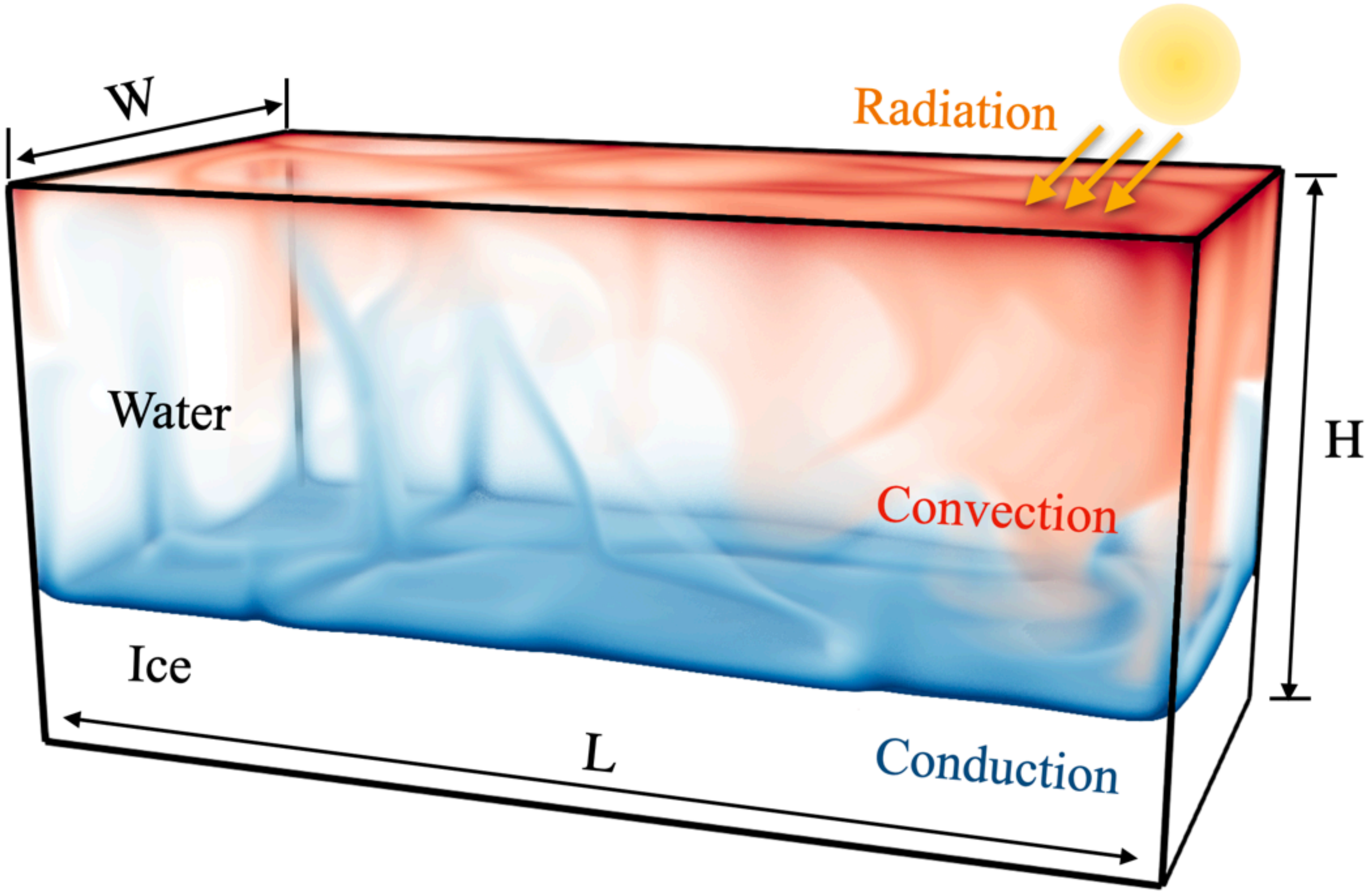

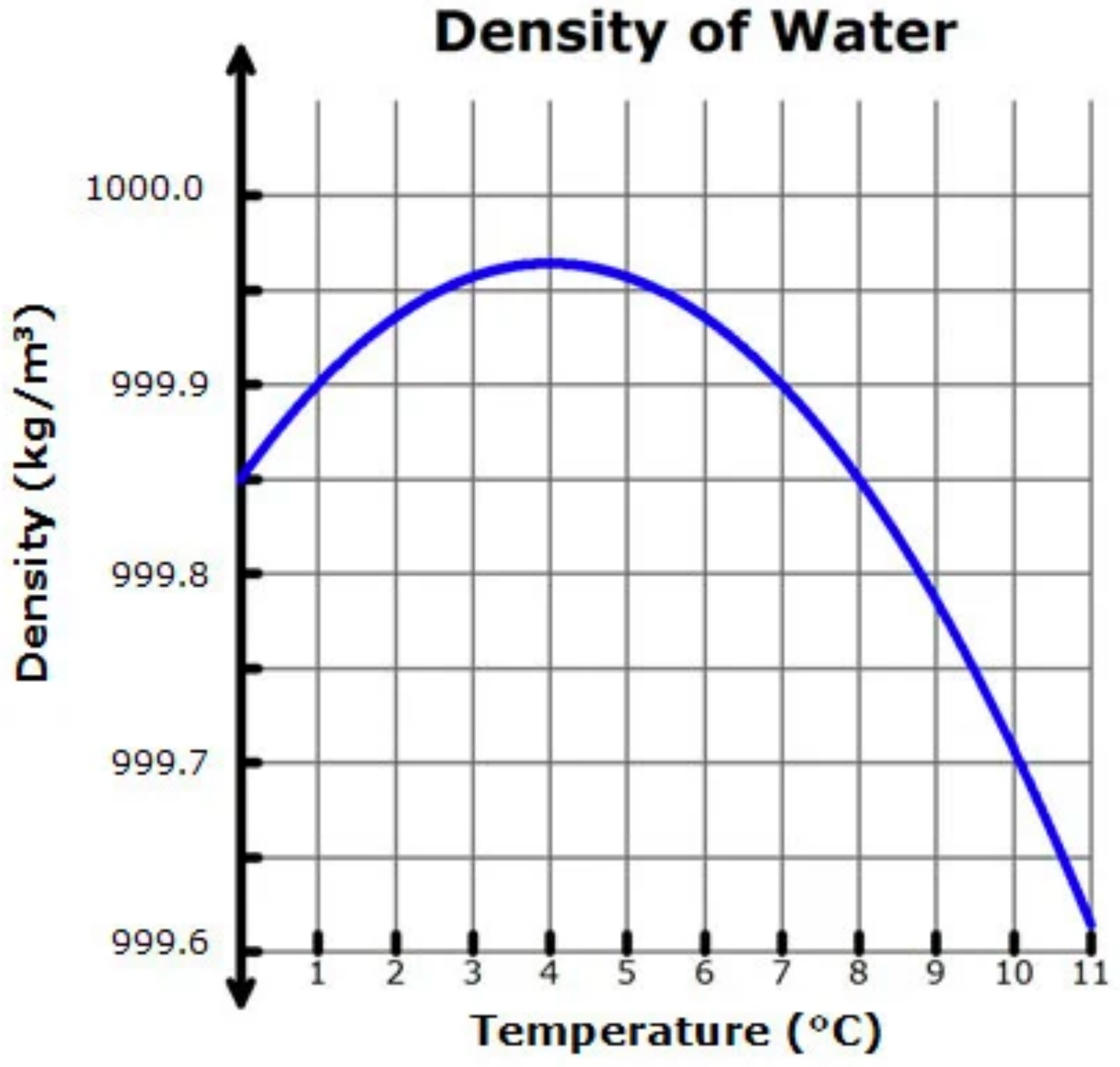

Under what conditions do these melt ponds form?

Flow structure

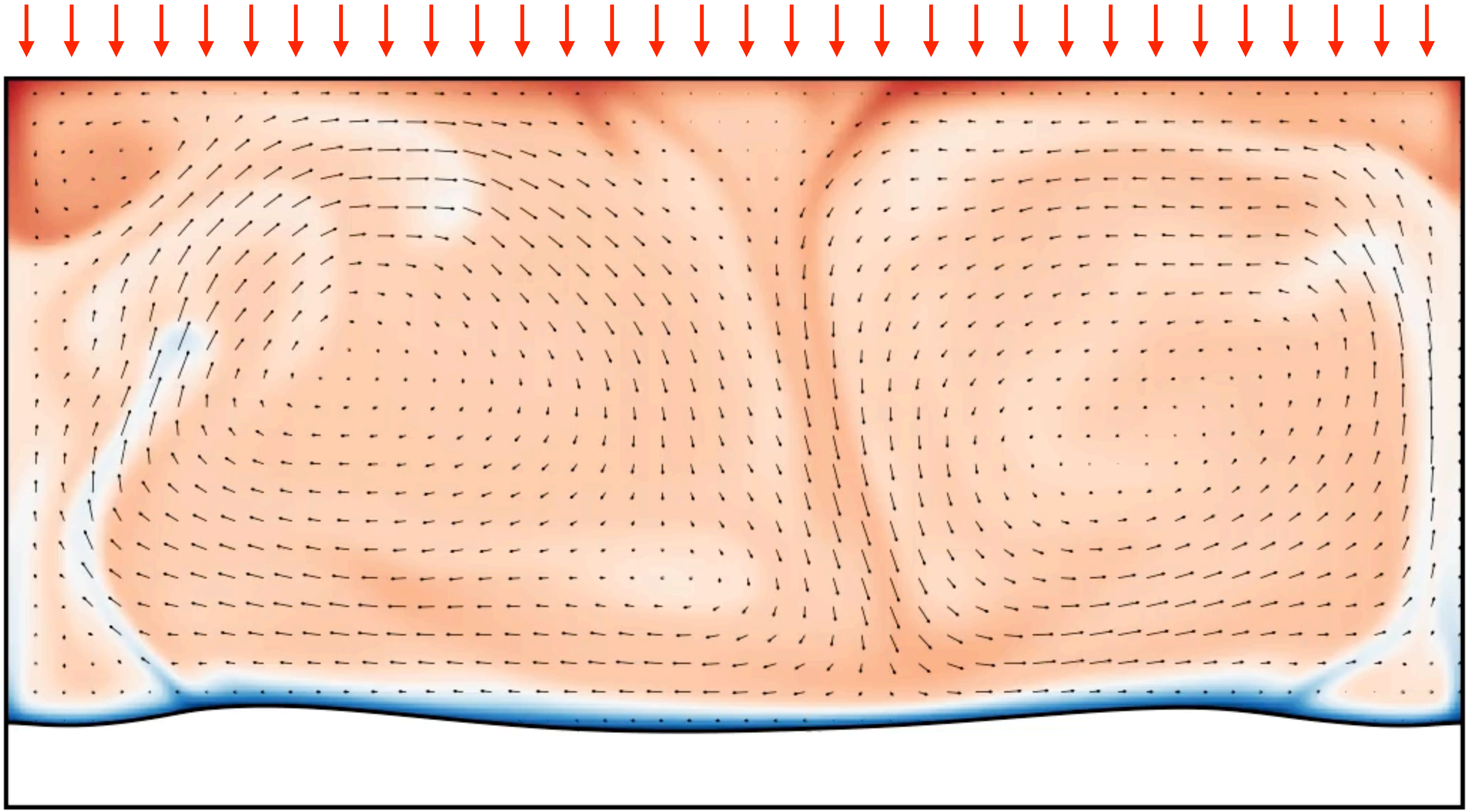

Flow structure

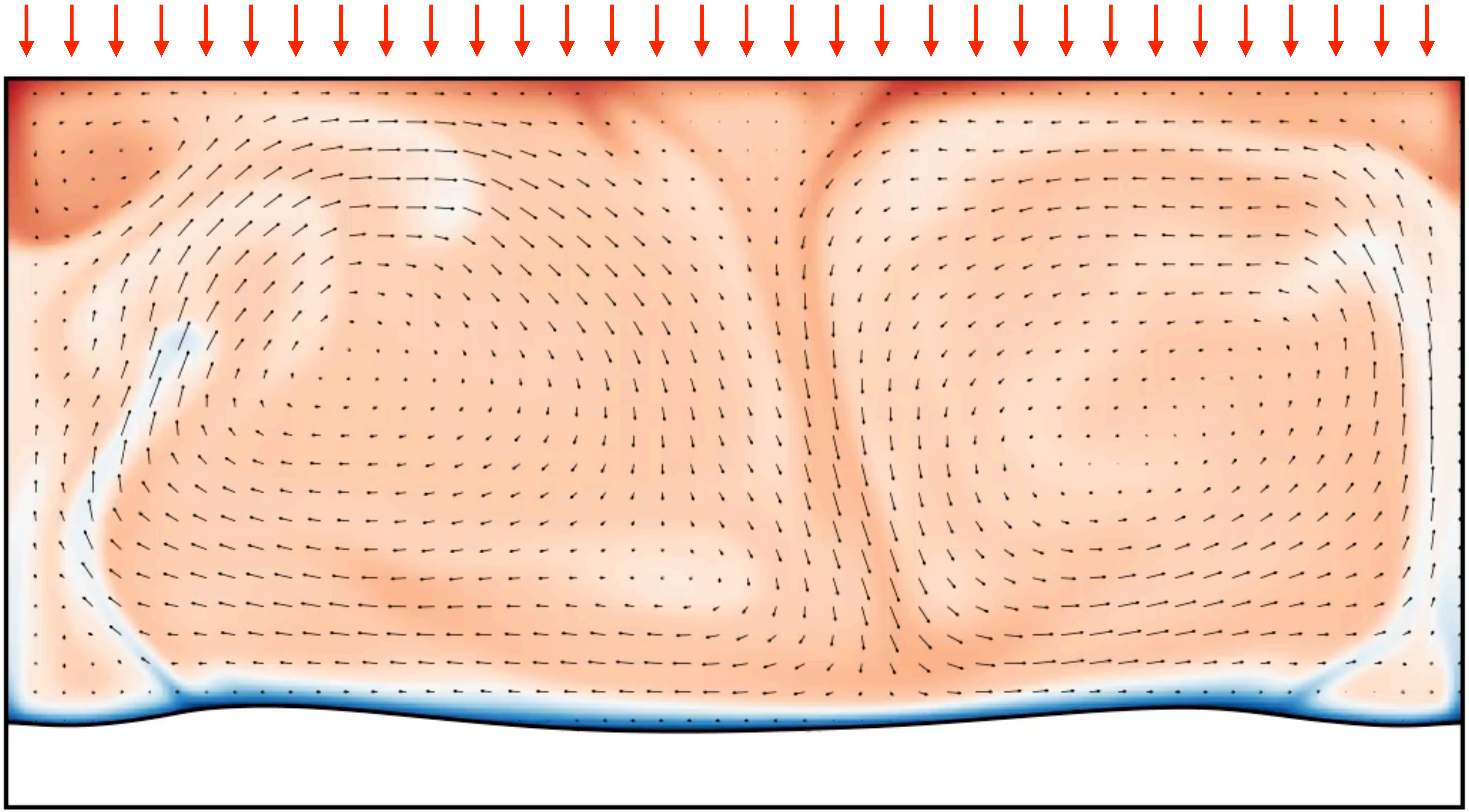

Key question:
Under what conditions do melt ponds form?

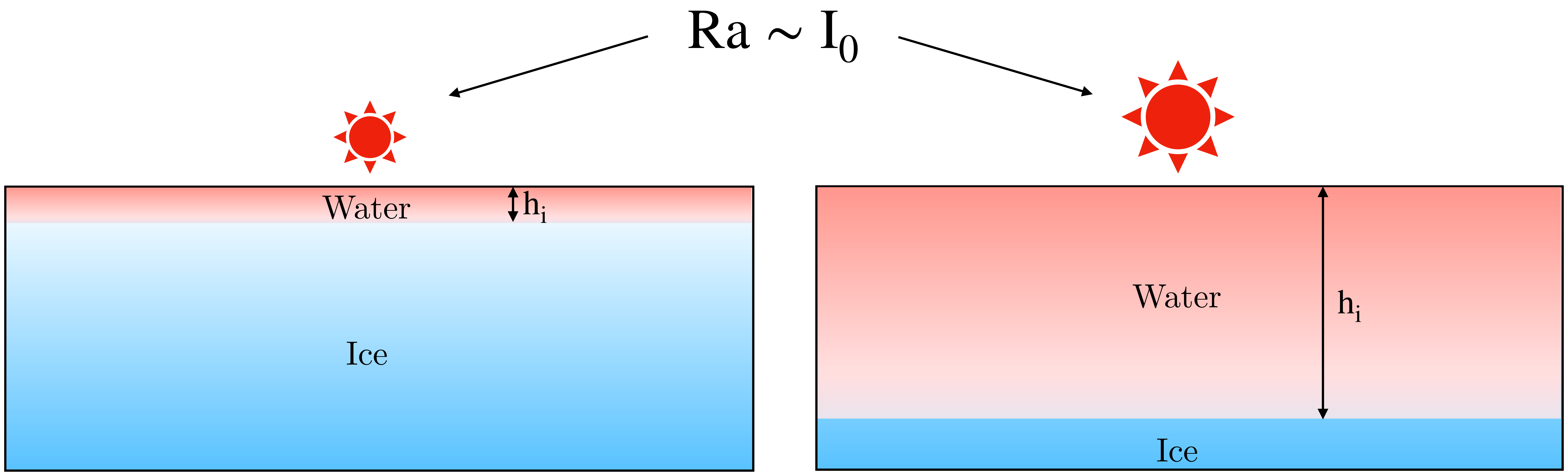

Vary: h_i & $Ra \sim I_0$

Modeling of solar radiation profile according to Lambert-Beer

Heat absorption:

$$\boxed{F_r(z) = I_0 \, \Sigma_{m=1,2,3,4} \, P_m(1 - e^{-K_m z})}$$

Table 1. Band Characteristics Used to Determine the Shortwave Radiation Absorbed in a Freshwater Layer[a]

Wavelength Range	350–700 nm, m = 1	700–900 nm, m = 2	900–1100 nm, m = 3	>1100 nm, m = 4
P_m	0.481	0.194	0.123	0.202
K_m [m^{-1}]	0.18	3.25	27.5	300

Skyllingstad, 2007

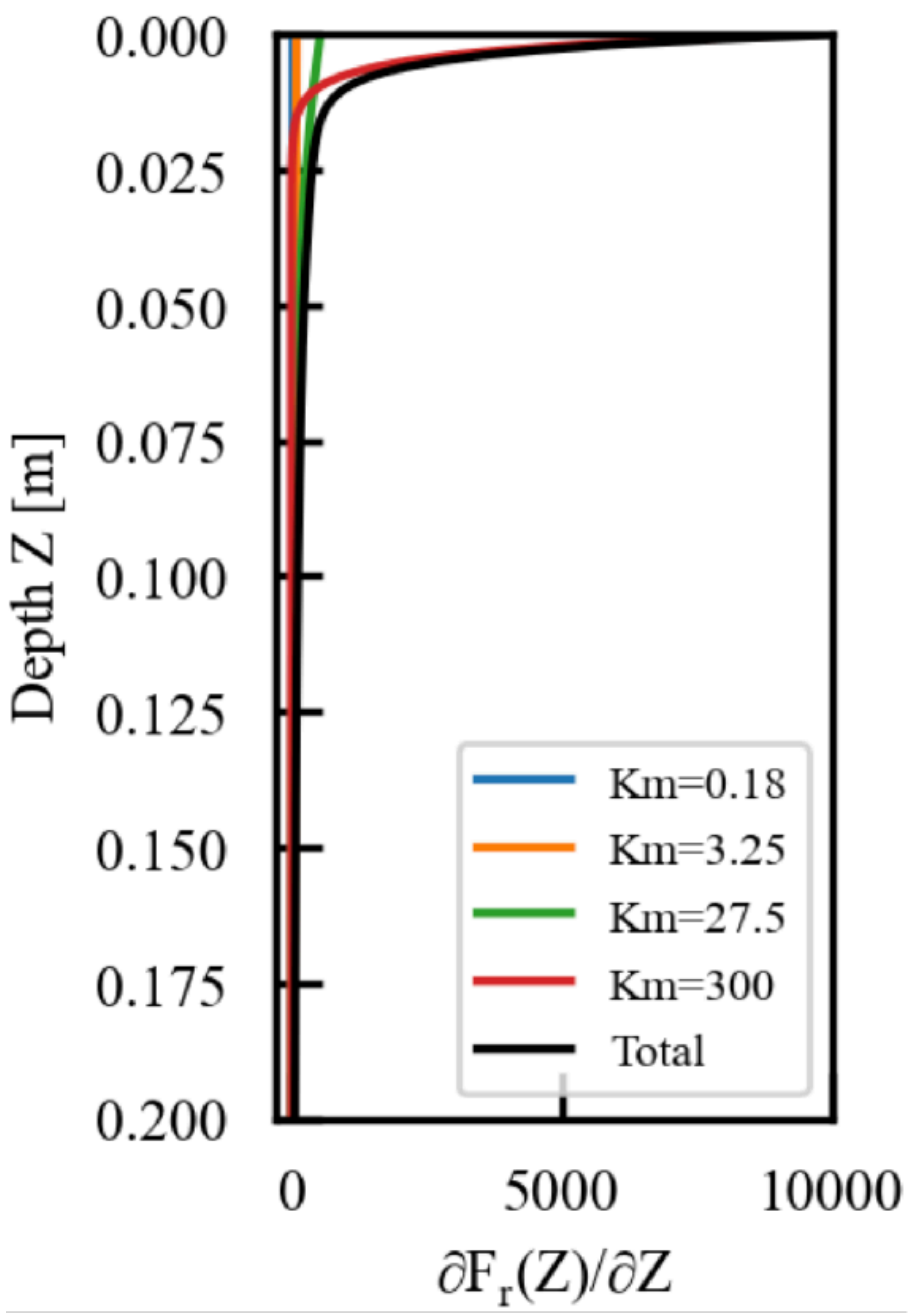

Governing equations: Boussinesq + phase field method

$$\frac{\partial u_i}{\partial t} + u_j \frac{\partial u_i}{\partial x_j} = -\frac{\partial p}{\partial x_i} + T\delta_{iz} + \sqrt{\frac{Pr}{Ra}} \frac{\partial^2 u_i}{\partial x_j^2} - \frac{\phi u_i}{\eta}$$

$$\frac{\partial \theta}{\partial t} + u_i \frac{\partial \theta}{\partial x_i} = \sqrt{\frac{1}{RaPr}} \frac{\partial^2 \theta}{\partial x_j^2} - St \frac{\partial \phi}{\partial t} + \underbrace{(1-\phi)\sqrt{\frac{1}{RaPr}} \Sigma \left(P_m K_m H e^{-K_m H z}\right)}_{\text{Heat source term}}$$

$$\partial_t \phi = D \nabla^2 \phi - \frac{D}{\epsilon^2} \phi (1-\phi) \Big(1 - 2\phi + A\left(T - T_m\right) \Big)$$

Dimensionless temperature $\Delta = \frac{I_0 H}{\rho c_p \kappa}$

Control parameters:

$$Ra = \frac{g\alpha H^3 \Delta}{\nu\kappa} = \frac{g\alpha H^4 I_0}{\rho c_p \nu \kappa^2}$$

$$Pr = \frac{\nu}{\kappa}$$

$$St = \frac{c_p \Delta}{\mathscr{L}} = \frac{I_0 H}{\rho \kappa \mathscr{L}}$$

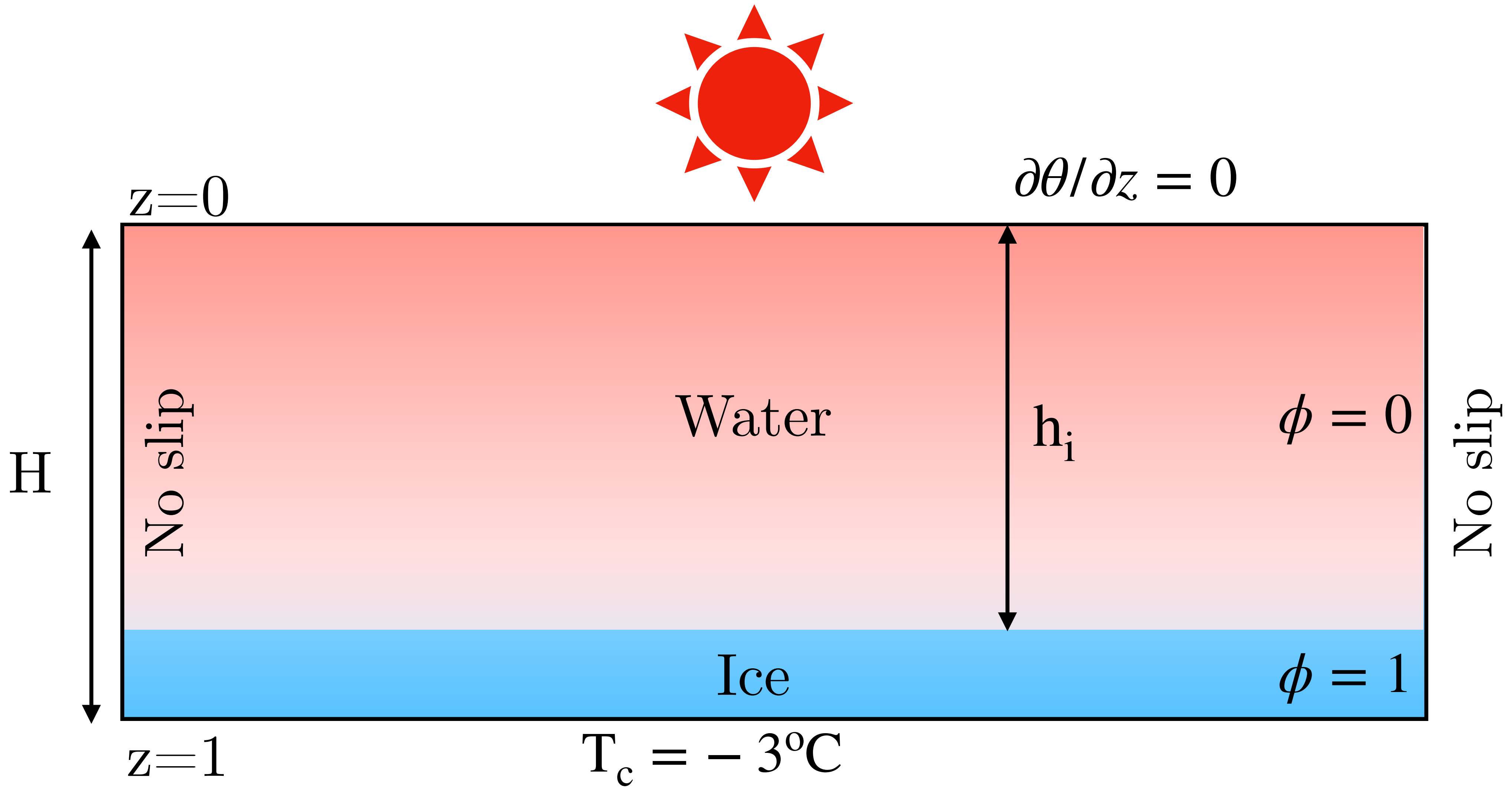

Phase diagram

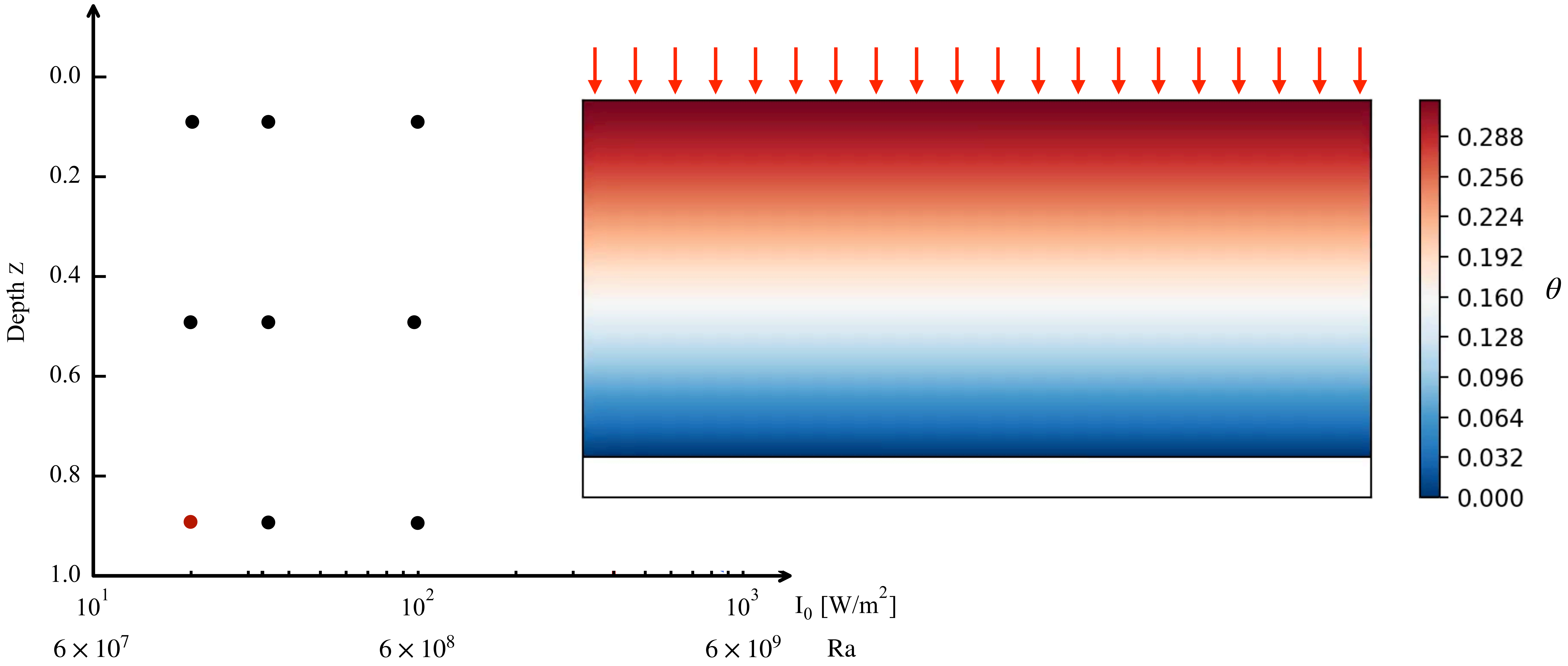

Phase diagram

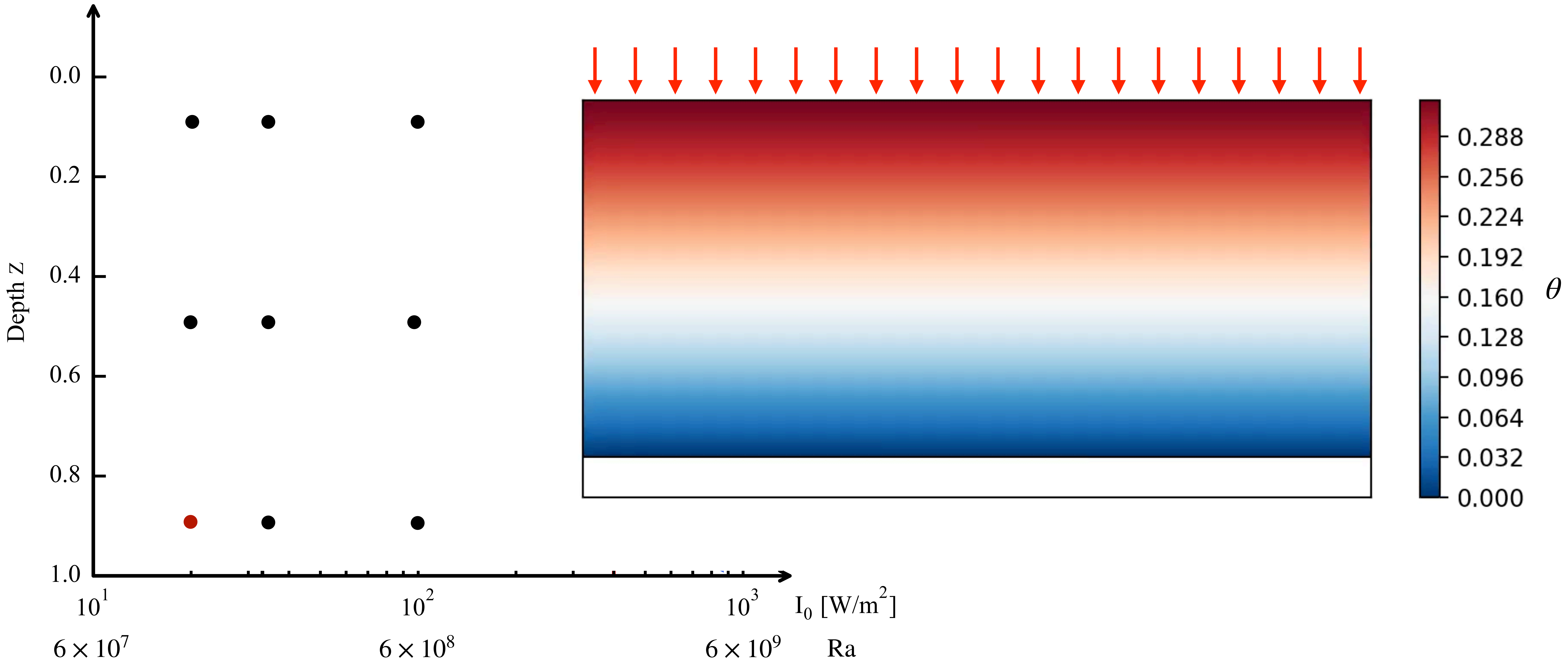

Phase diagram

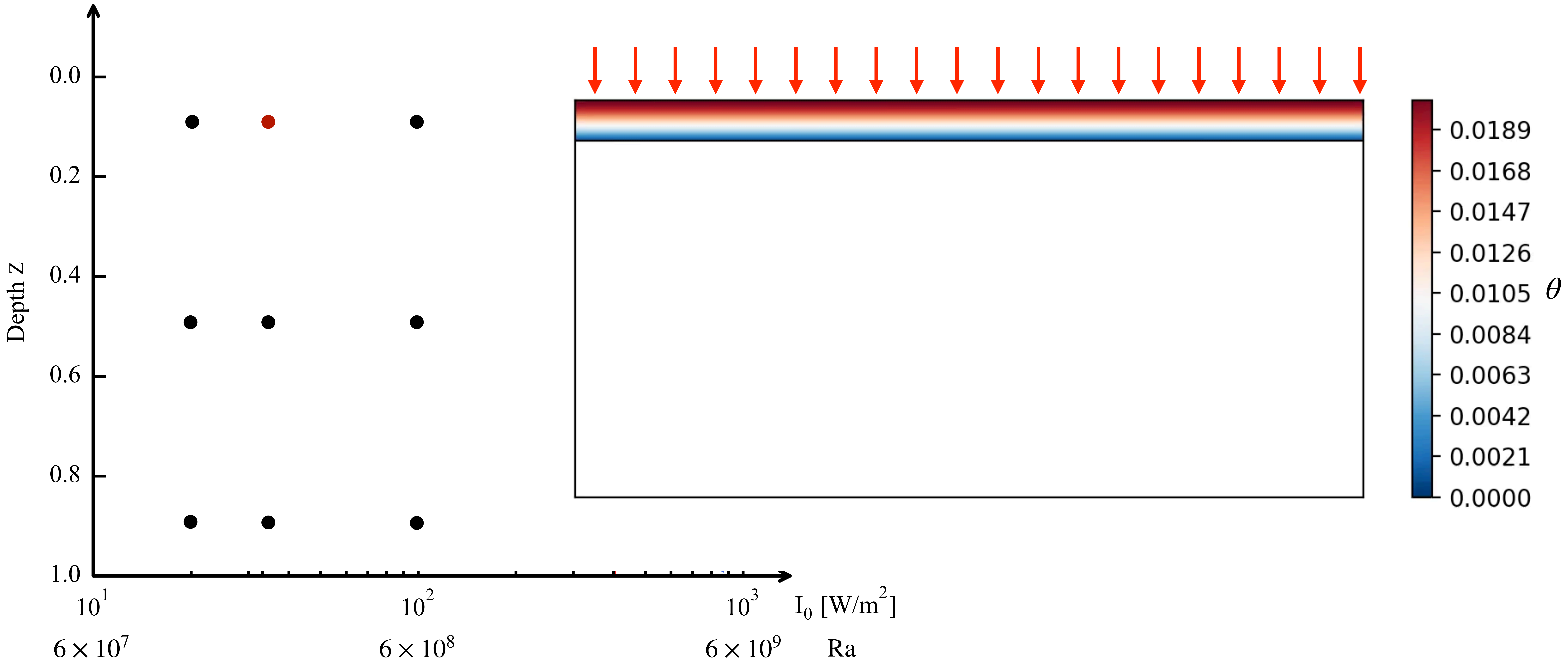

Phase diagram

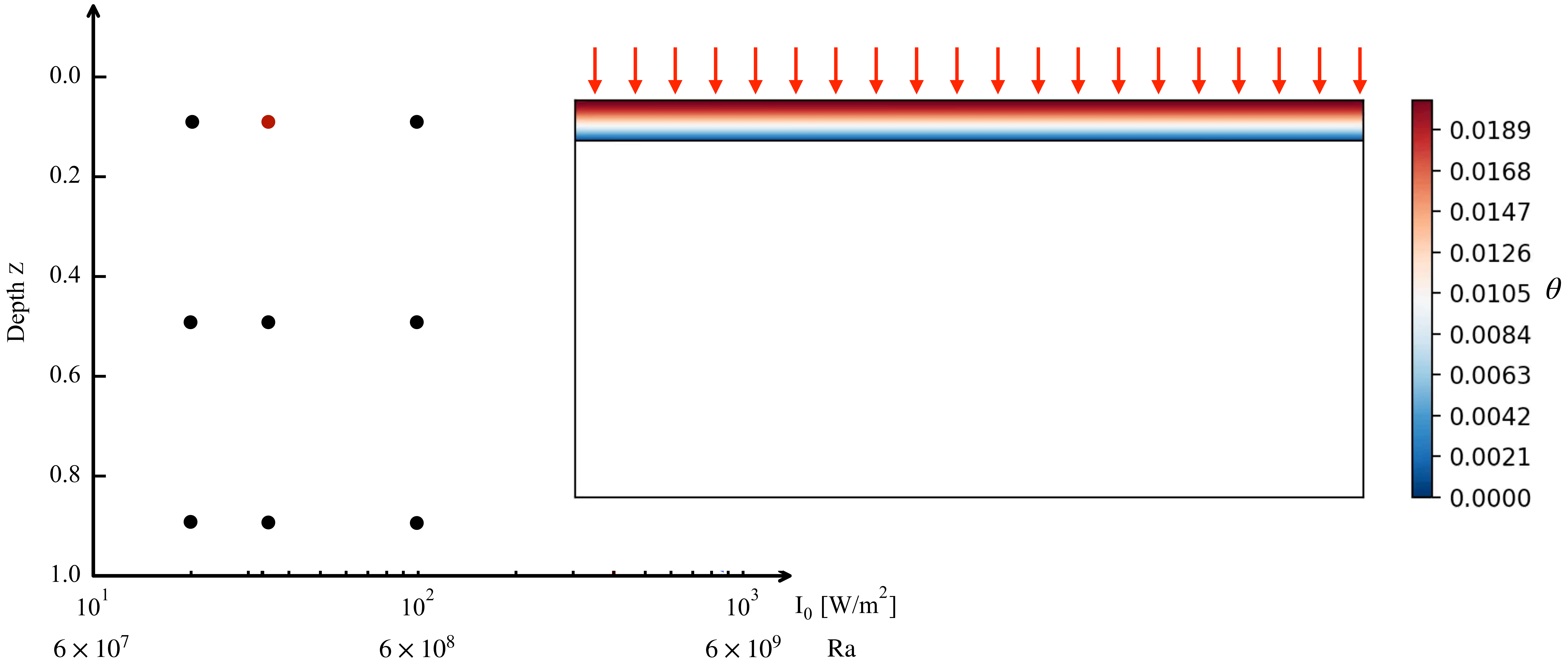

Phase diagram

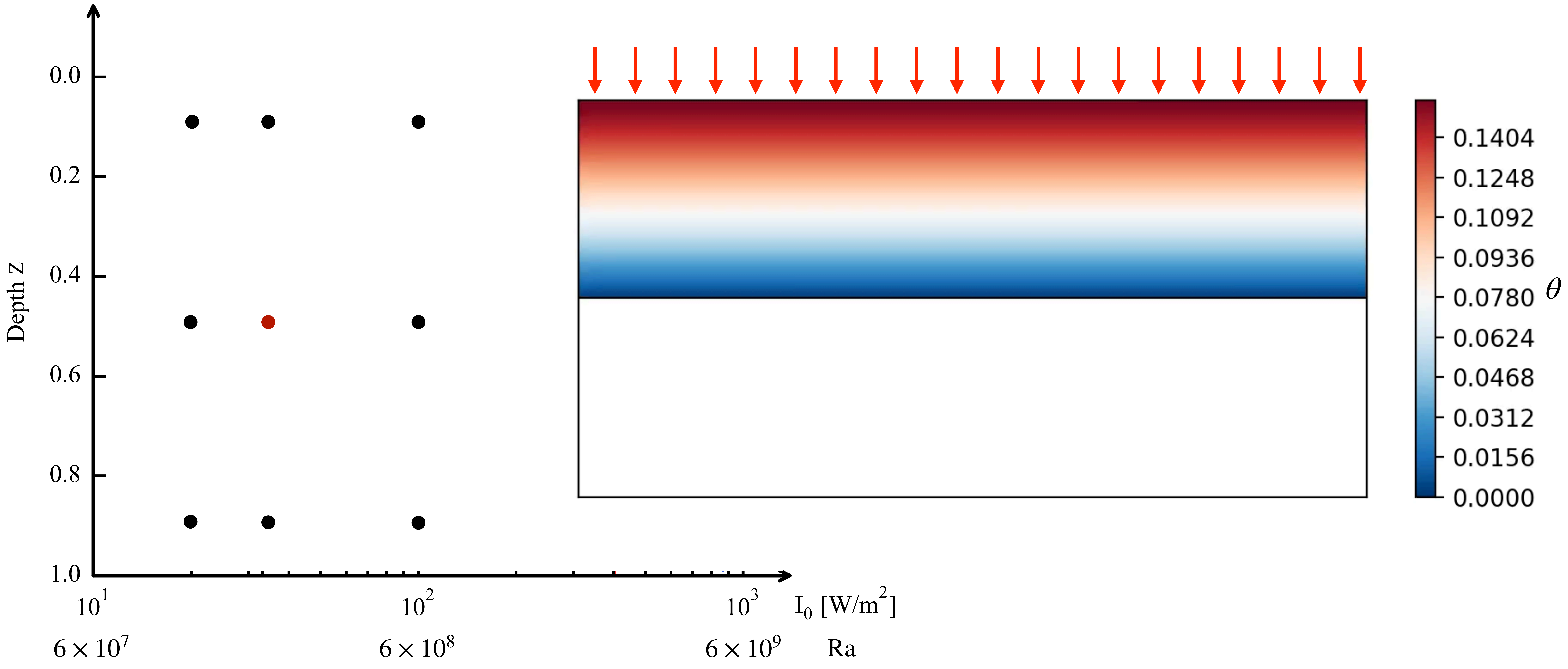

Phase diagram

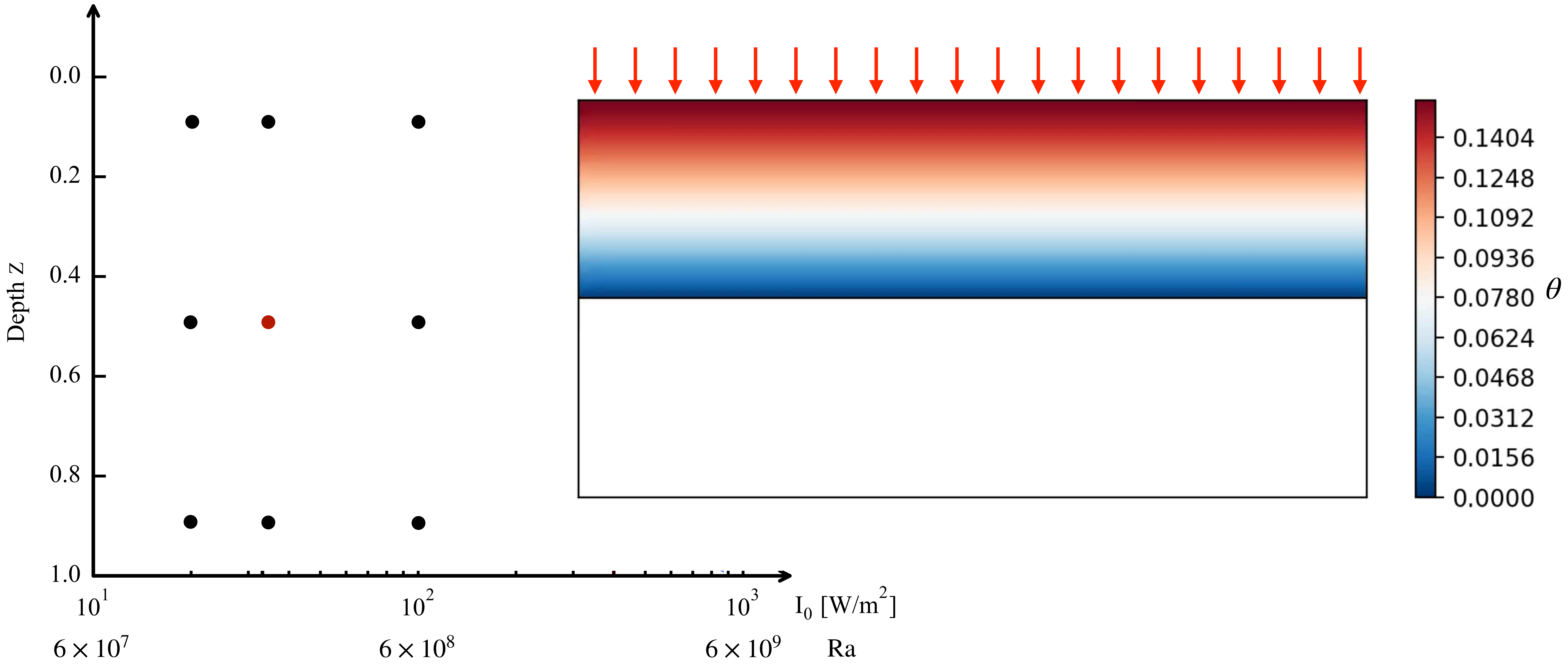

Phase diagram

“tipping point”: no full recovery of the ice!

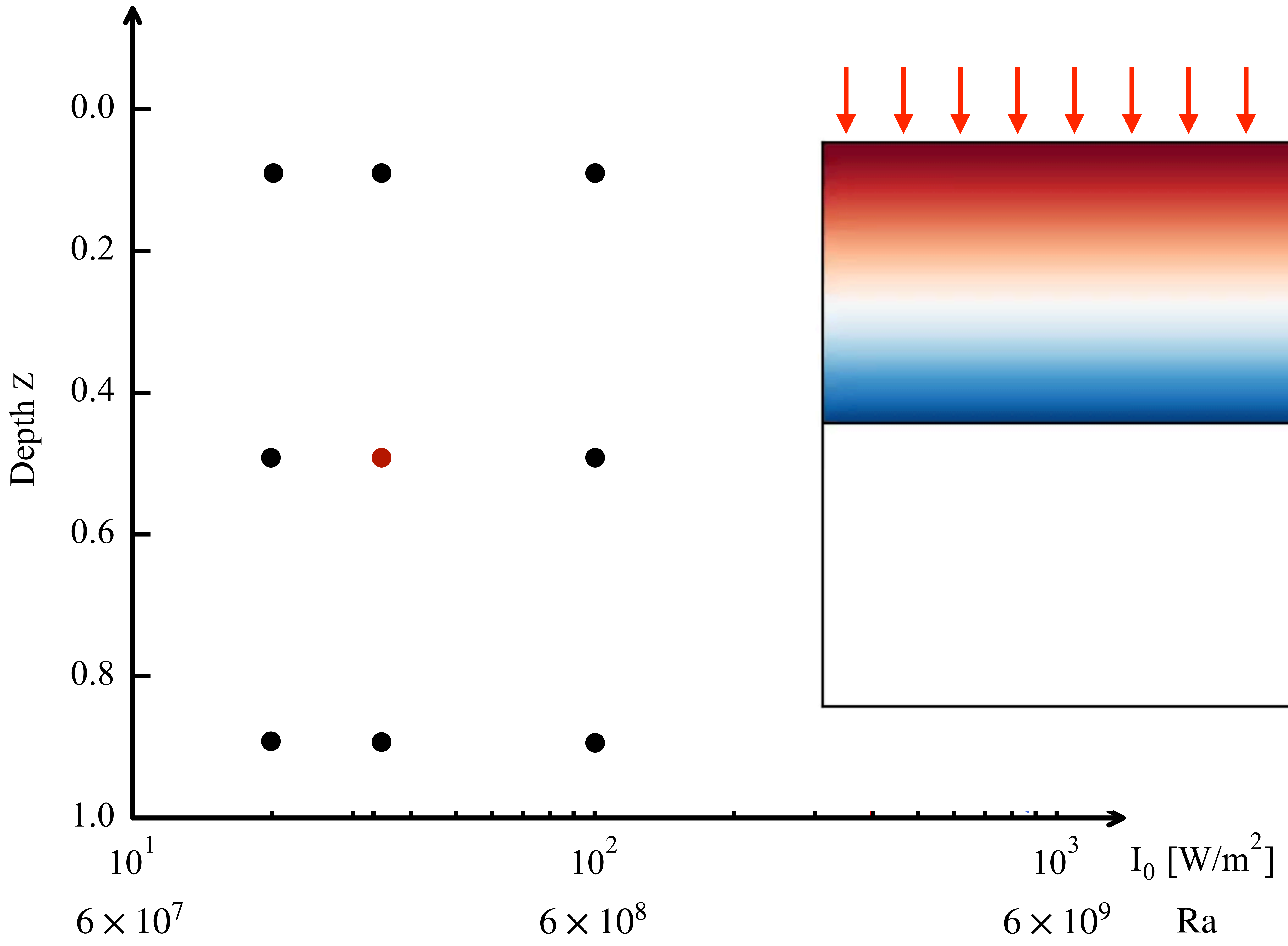

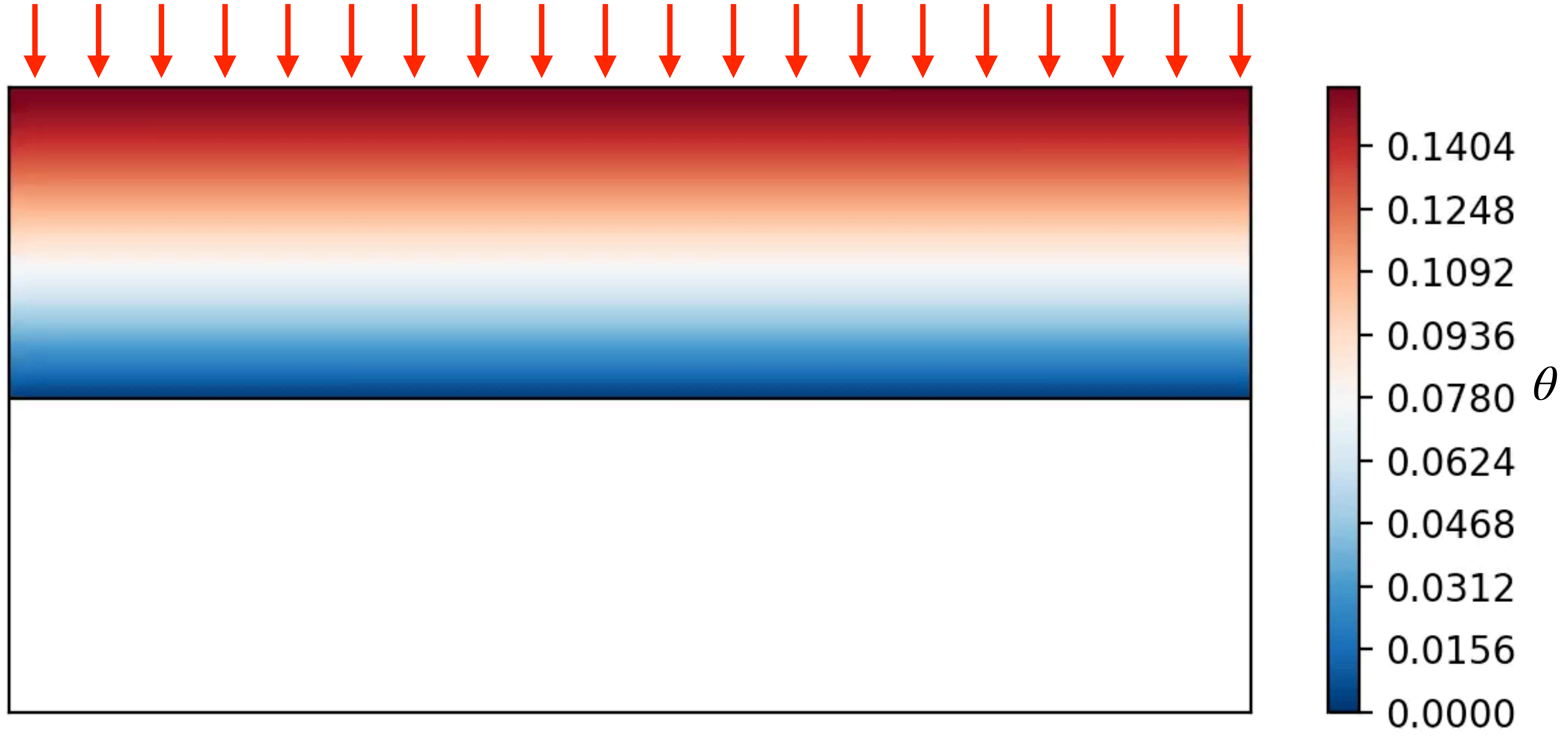

Phase diagram

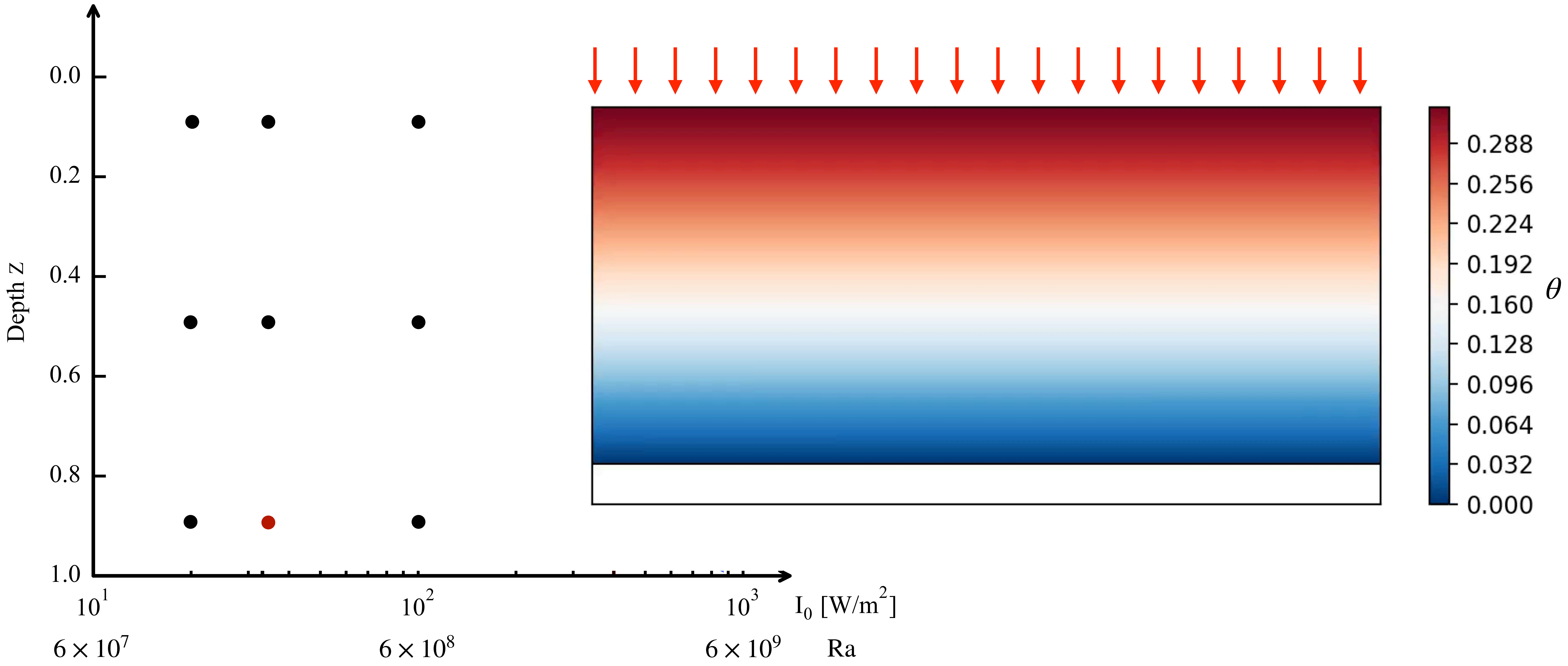

Phase diagram

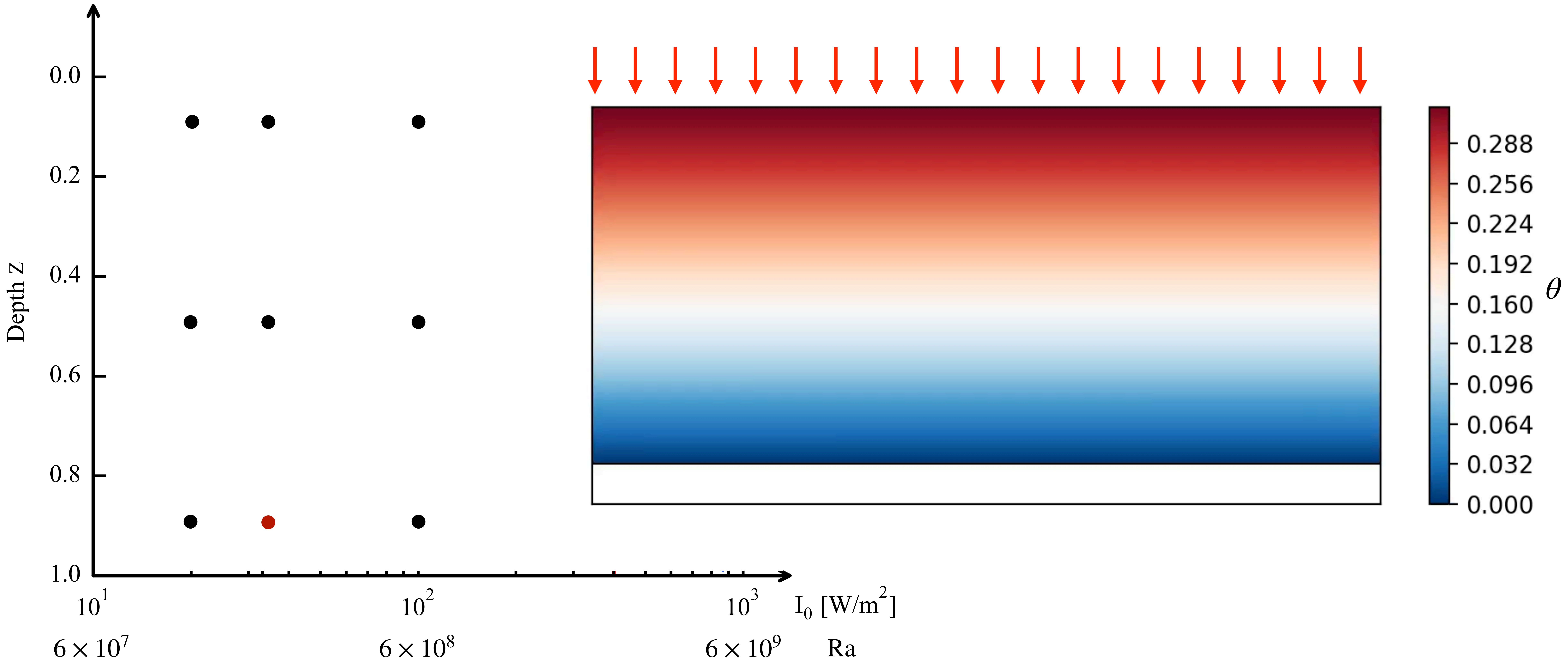

Phase diagram

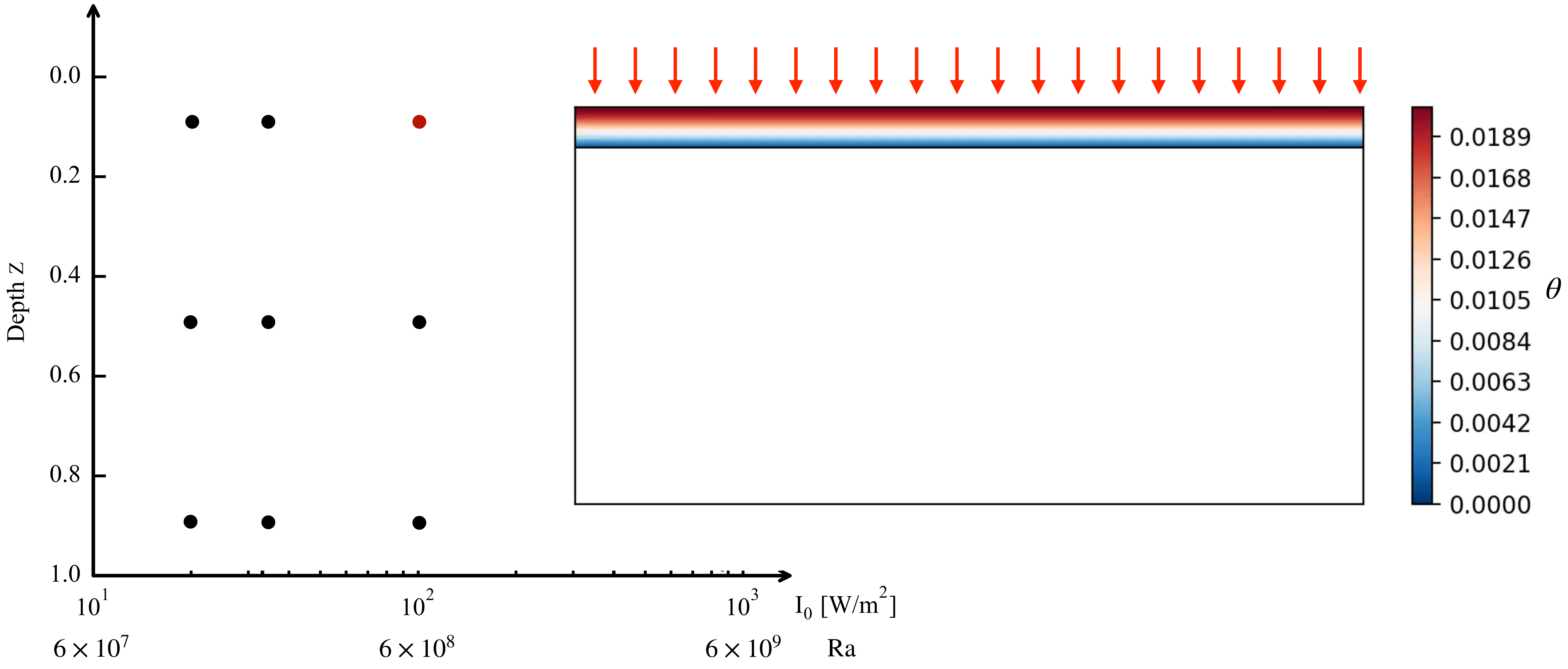

Phase diagram

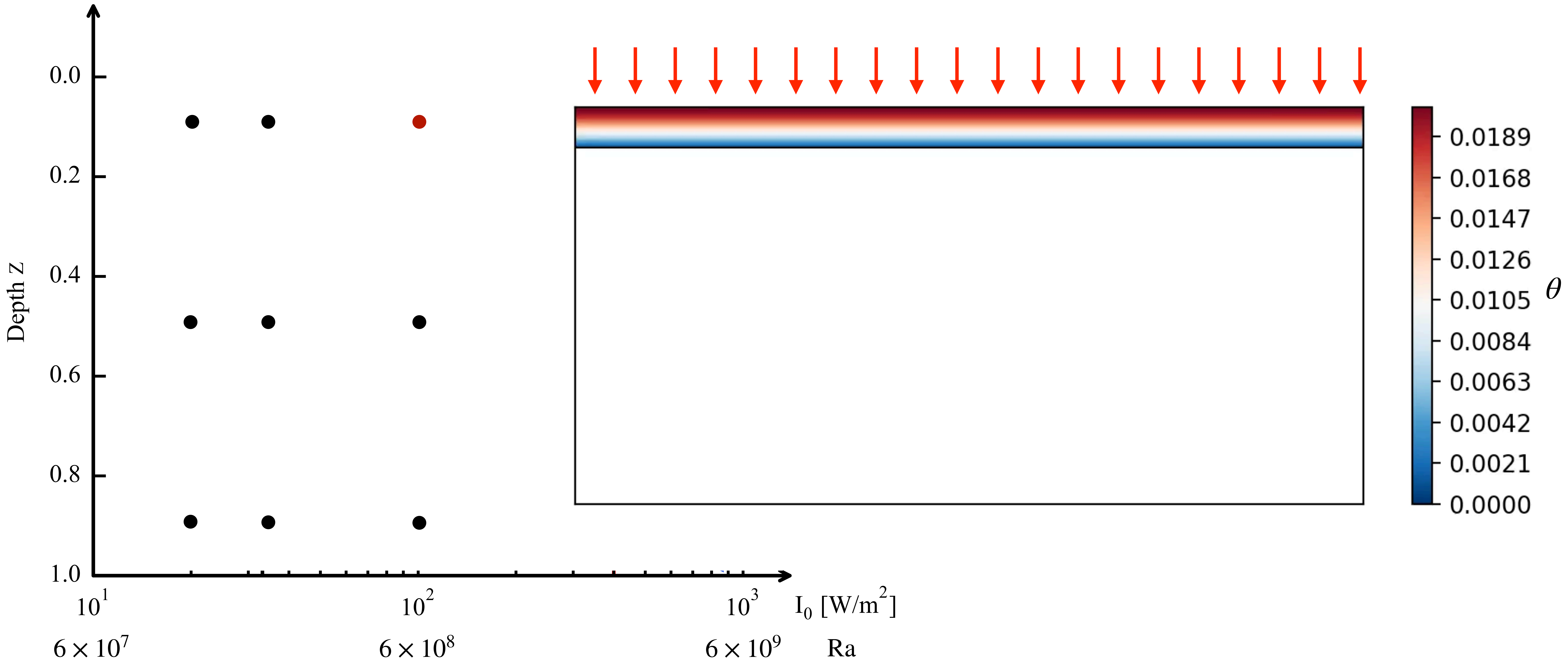

Phase diagram

“tipping point”

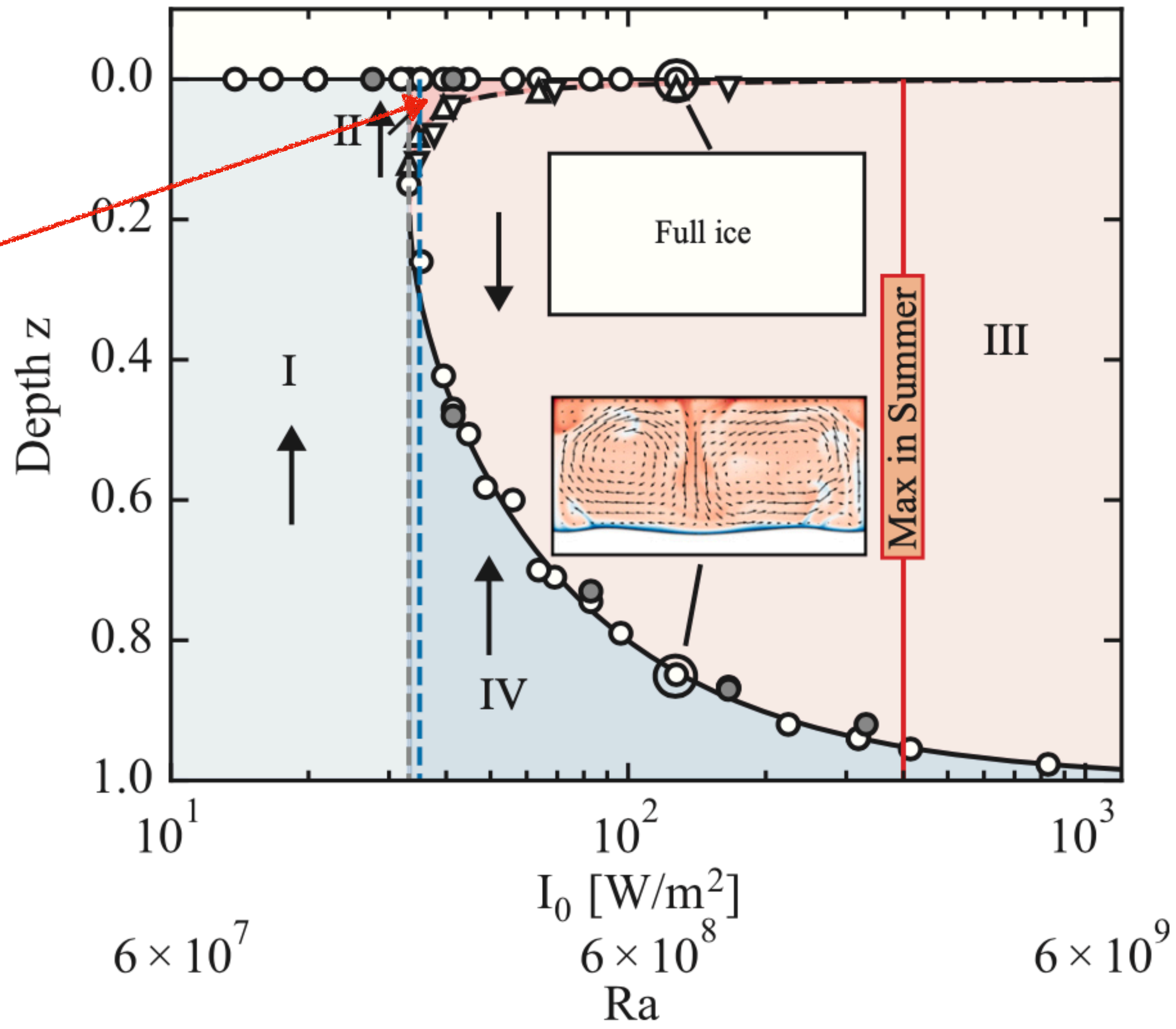

Nature of equilibria

h_i - initial depth
h_0 - final depth

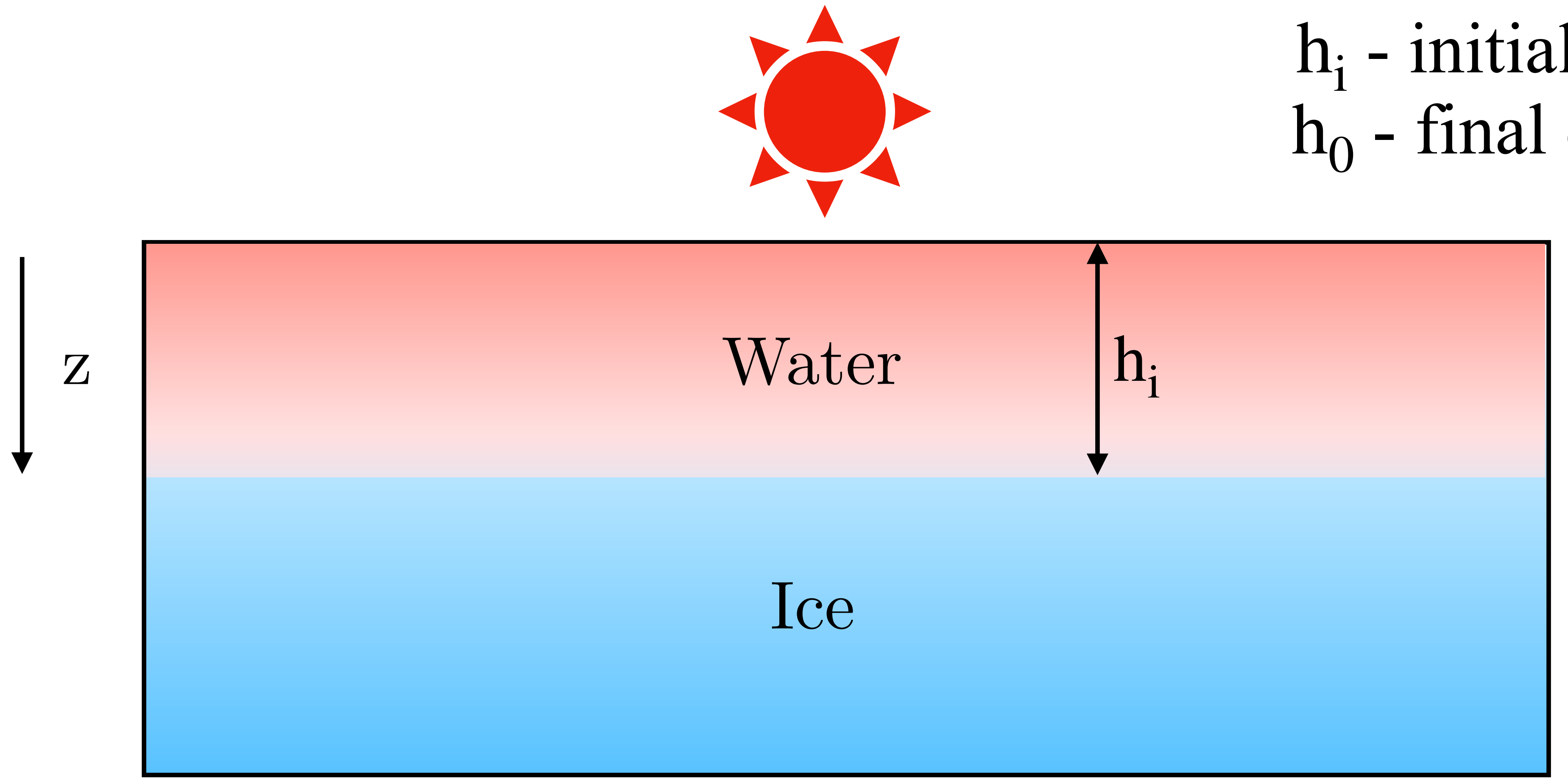

$\theta_c = 3K/\Delta$

Advection-diffusion equation with latent heat & radiation

$$\frac{\partial \theta}{\partial t} + u_i \frac{\partial \theta}{\partial x_i} = \sqrt{\frac{1}{RrPr}} \frac{\partial^2 \theta}{\partial x_j^2} - St \frac{d\phi}{dt} + (1-\phi)\sqrt{\frac{1}{RrPr}} \Sigma \left(P_m K_m H e^{-K_m H z} \right)$$

Nature of equilibria

Advection-diffusion equation with latent heat & radiation

$$\frac{\partial \theta}{\partial t} + u_i \frac{\partial \theta}{\partial x_i} = \sqrt{\frac{1}{RrPr}} \frac{\partial^2 \theta}{\partial x_j^2} - St \frac{d\phi}{dt} + (1-\phi)\sqrt{\frac{1}{RrPr}} \Sigma \left(P_m K_m H e^{-K_m H z} \right)$$

not relevant for equilibrium

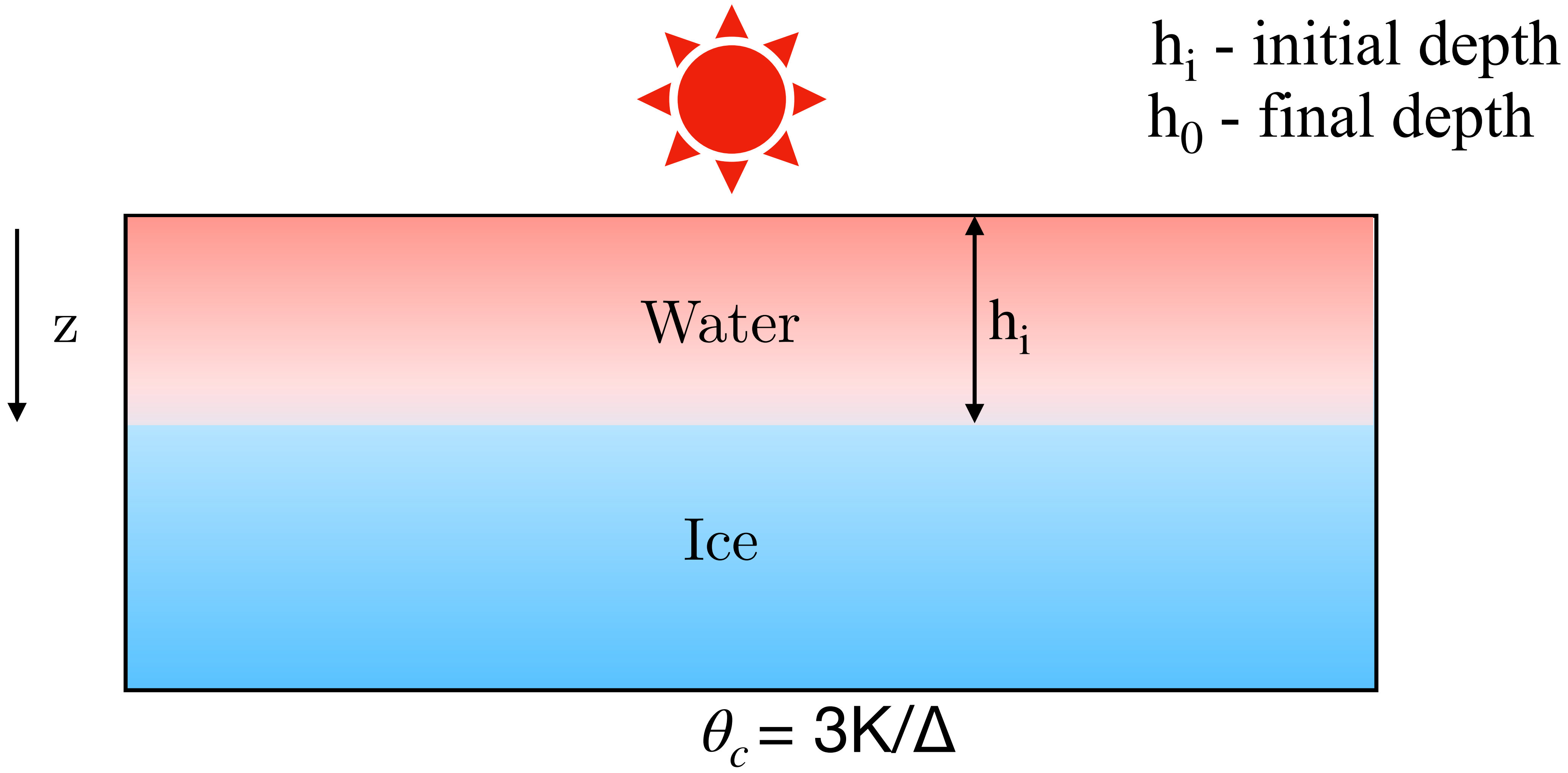

Nature of equilibria

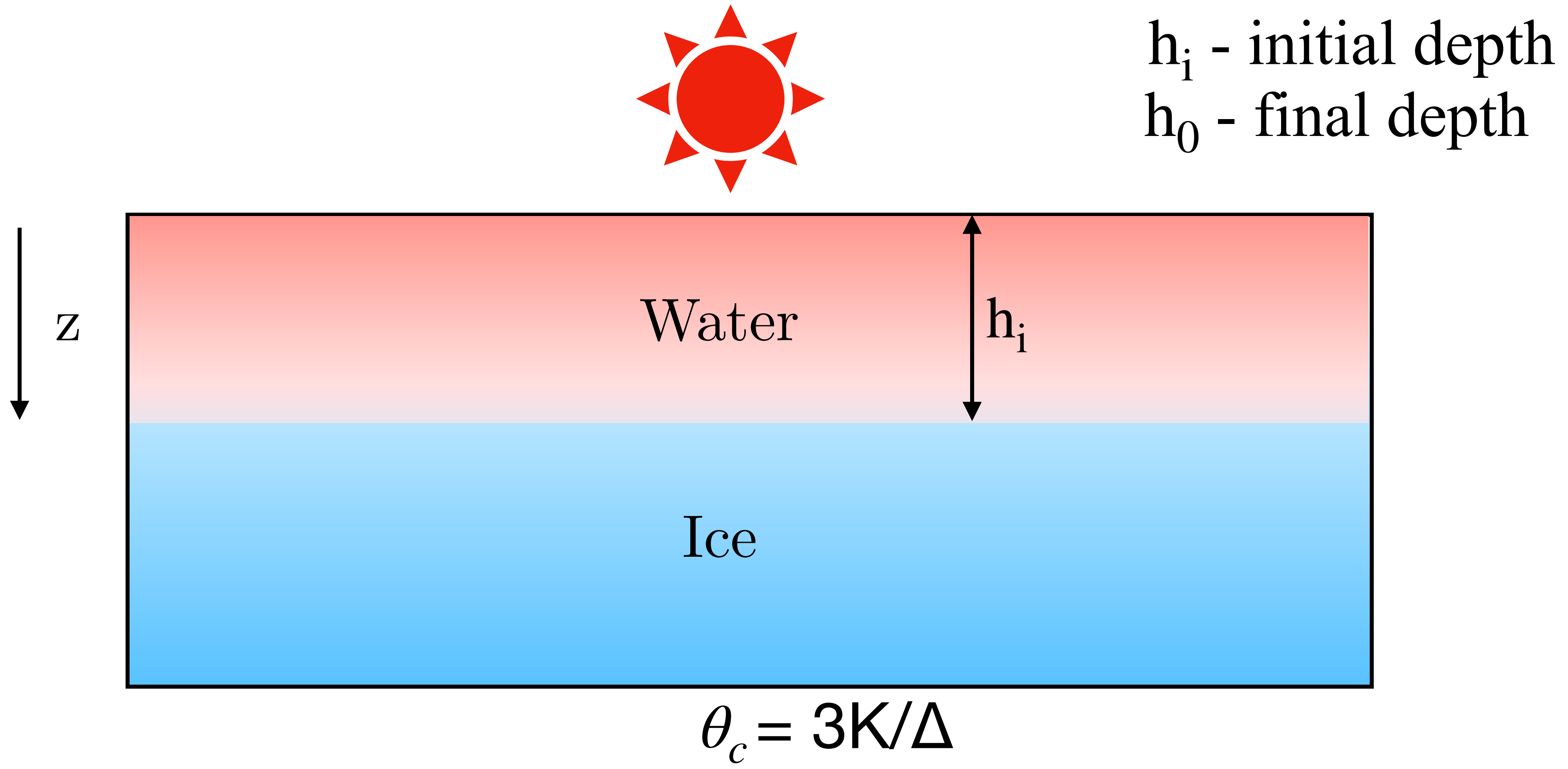

Advection-diffusion equation with latent heat & radiation

$$\frac{\partial\theta}{\partial t} + u_i\frac{\partial\theta}{\partial x_i} = \sqrt{\frac{1}{RrPr}}\frac{\partial^2\theta}{\partial x_j^2} - St\frac{d\phi}{dt} + (1-\phi)\sqrt{\frac{1}{RrPr}}\Sigma\left(P_m K_m H e^{-K_m H z}\right)$$

not relevant for equilibrium

Heat flux balance at the ice-water interface:

$$\boxed{Q(h_0) = \Sigma P_m(1 - e^{-K_m H h_0}) = \frac{\theta_c(I_0)}{1 - h_0}}$$

radiation

heat conduction through ice

—> solve for h_0 (equilibrium thickness of melt pond)

Nature of equilibria

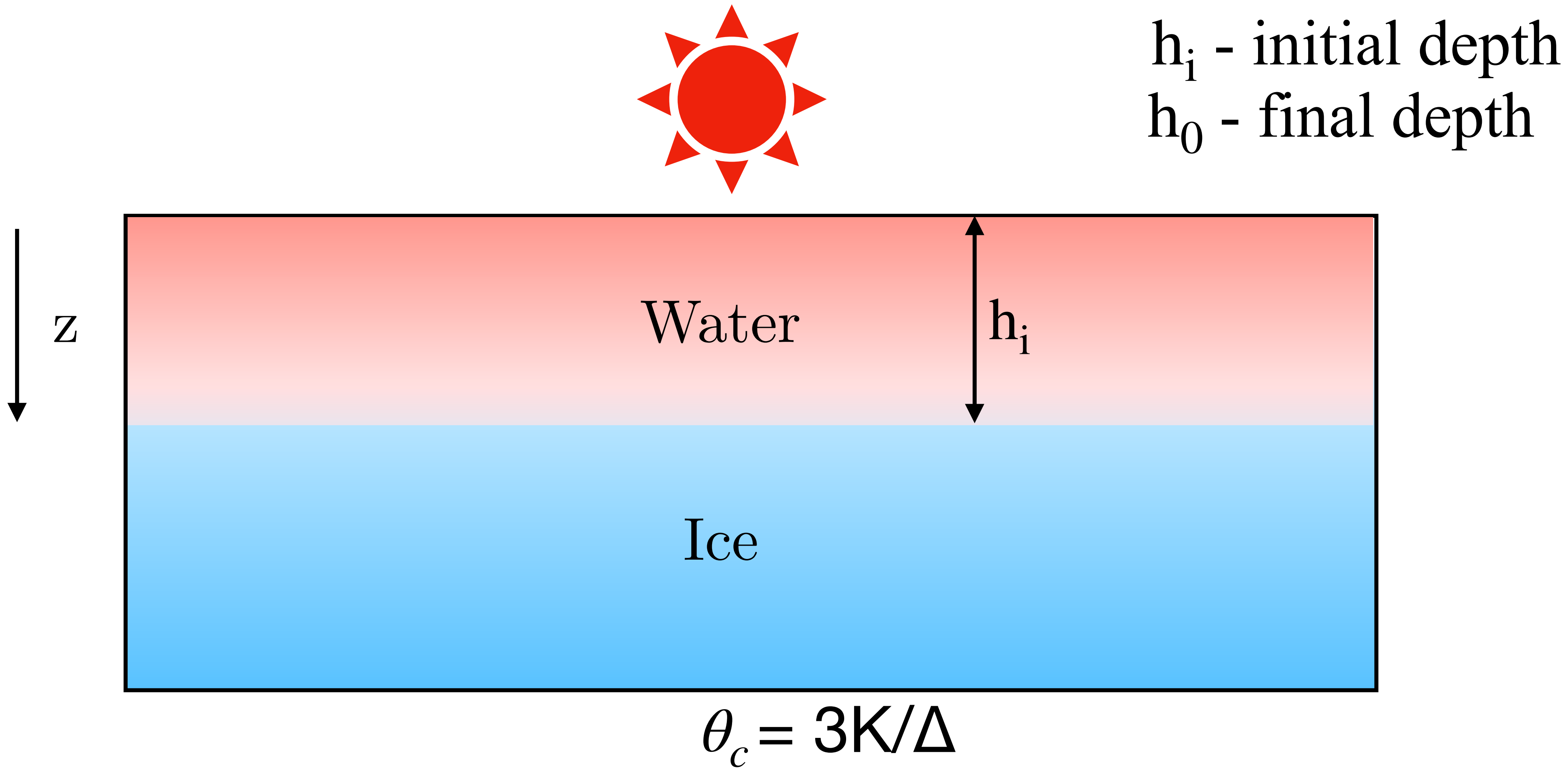

Advection-diffusion equation with latent heat & radiation

$$\frac{\partial\theta}{\partial t} + u_i\frac{\partial\theta}{\partial x_i} = \sqrt{\frac{1}{RrPr}}\frac{\partial^2\theta}{\partial x_j^2} - St\frac{d\phi}{dt} + (1-\phi)\sqrt{\frac{1}{RrPr}}\Sigma\left(P_m K_m H e^{-K_m H z}\right)$$

not relevant for equilibrium

Heat flux balance at the ice-water interface:

$$\boxed{Q(h_0) = \Sigma P_m(1 - e^{-K_m H h_0}) = \frac{\theta_c(I_0)}{1 - h_0}}$$

radiation

heat conduction through ice

—> solve for h_0 (equilibrium thickness of melt pond)

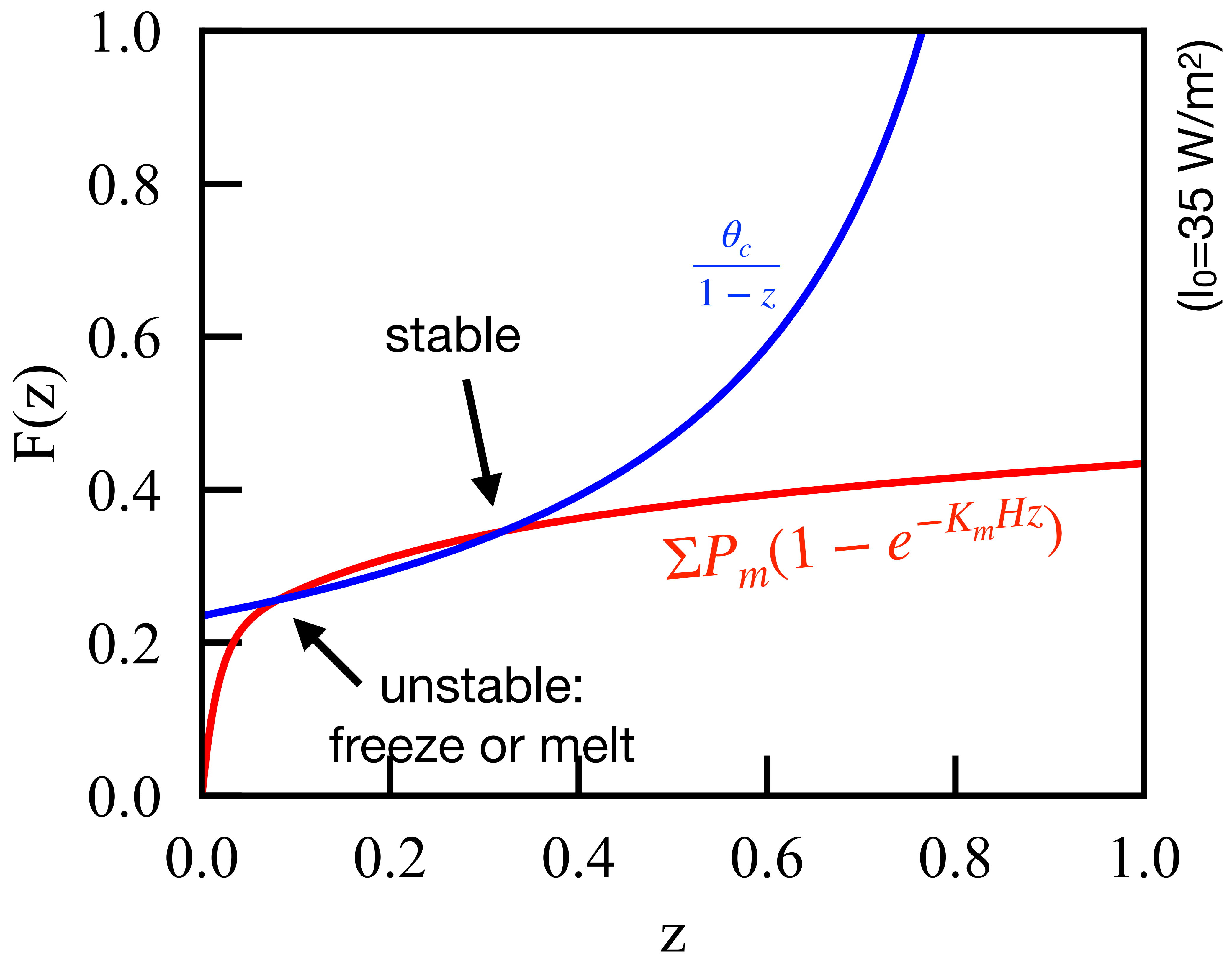

Result for depth of melt pond

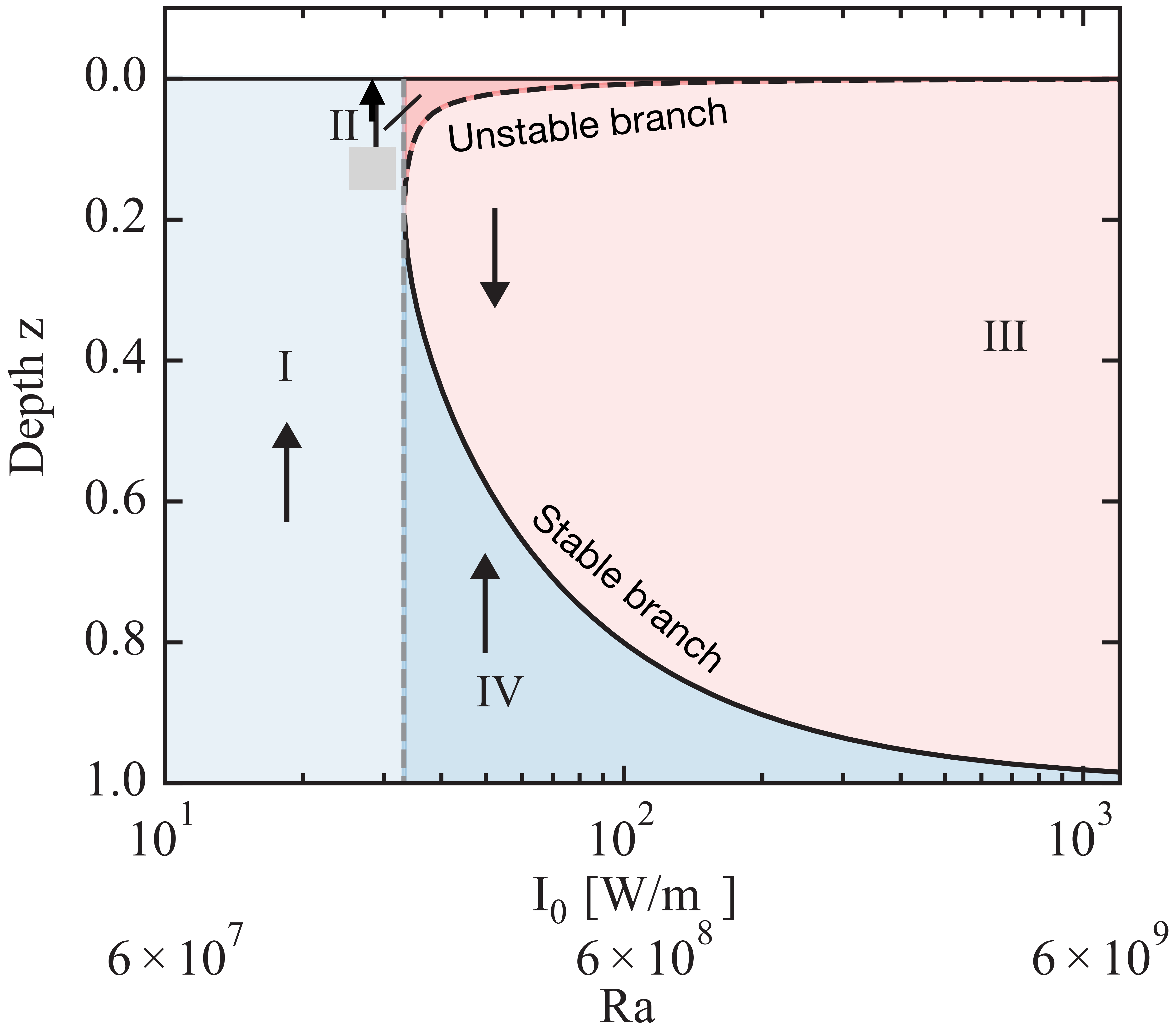

Result for depth of melt pond

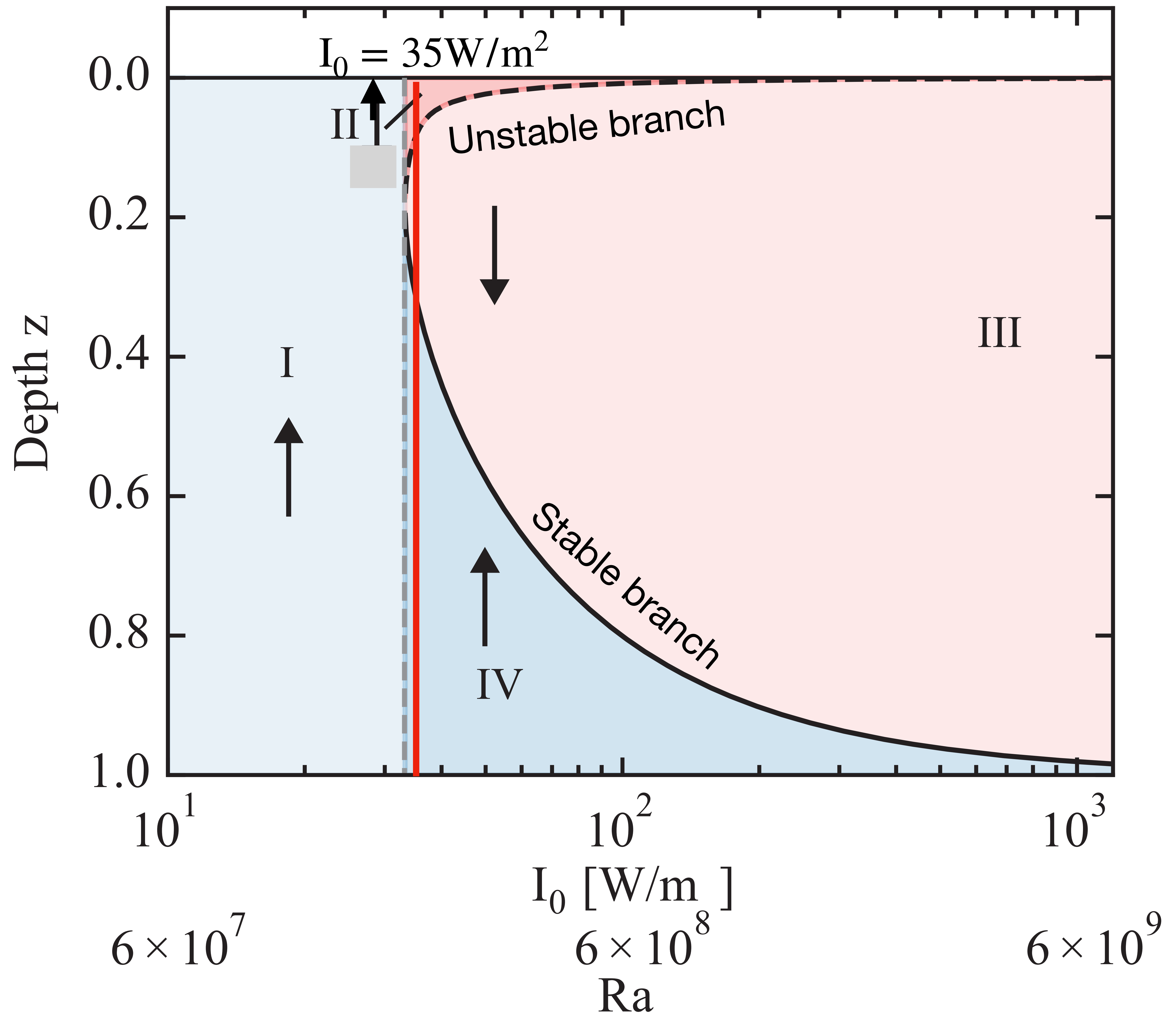

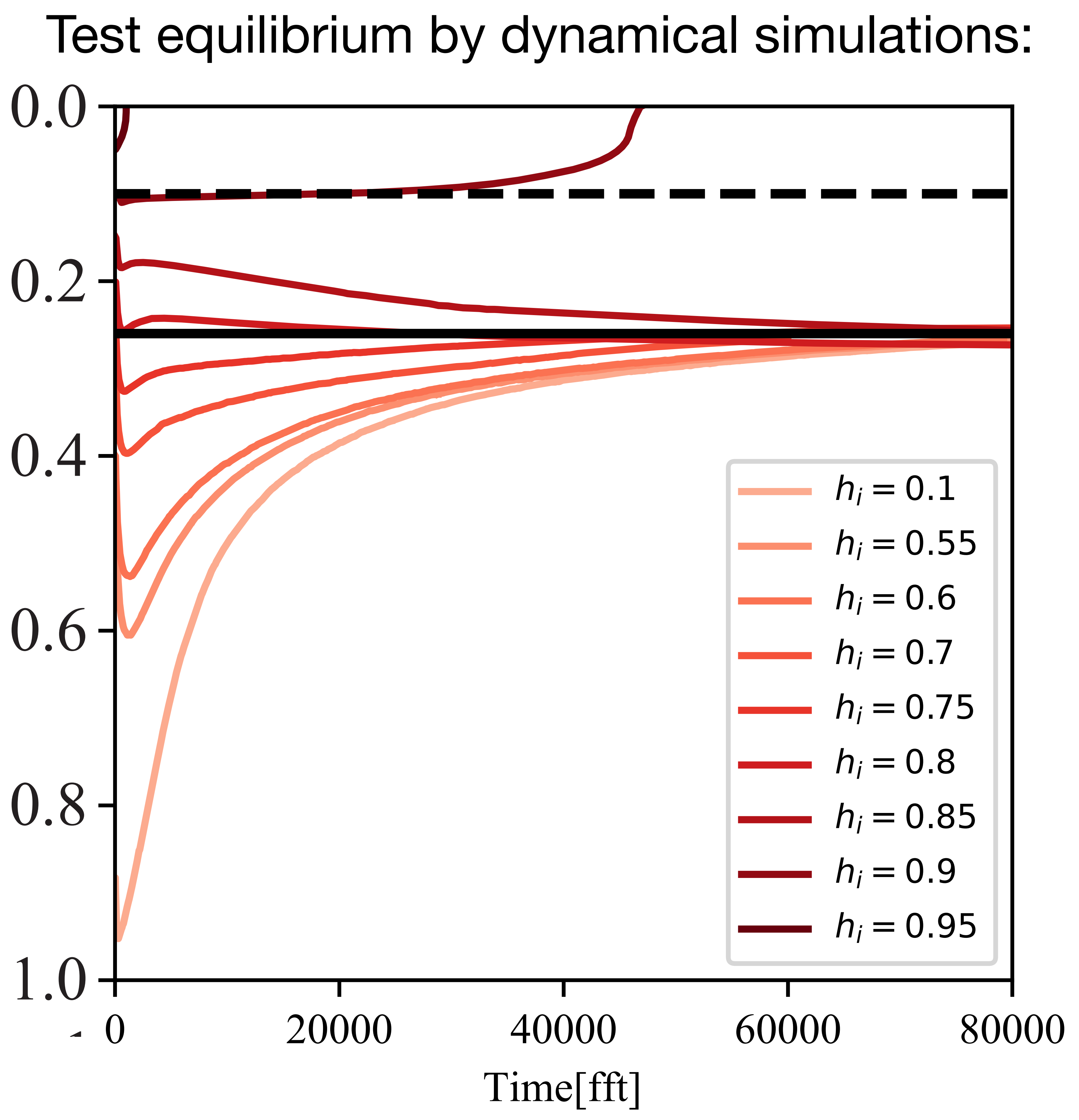

Phase diagram

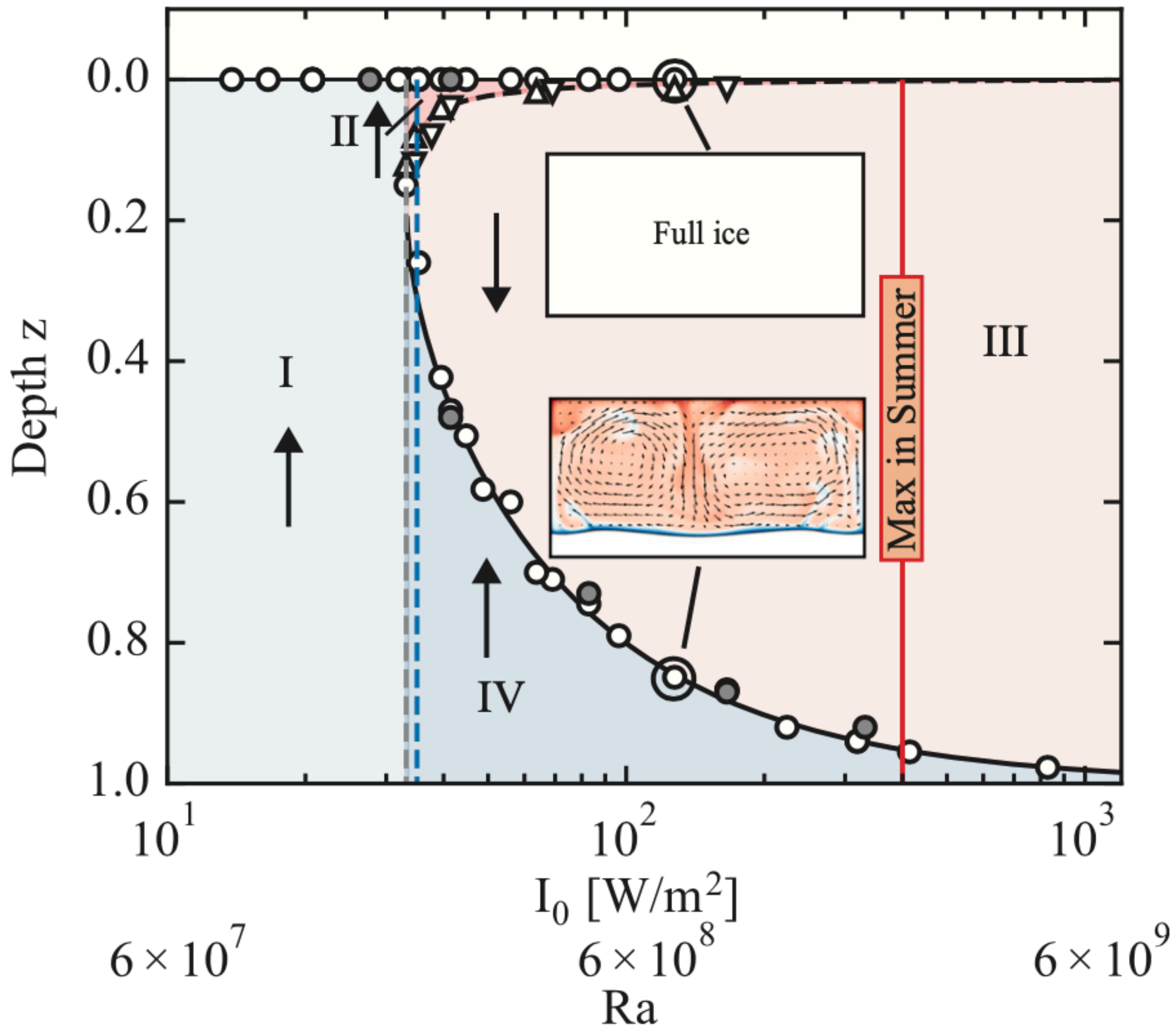

Equilibrium data points from dynamical simulations exactly on stable equilibrium curves

Can we predict the mean flow velocity and the mean bulk temperature as the radiation I_0 intensifies?

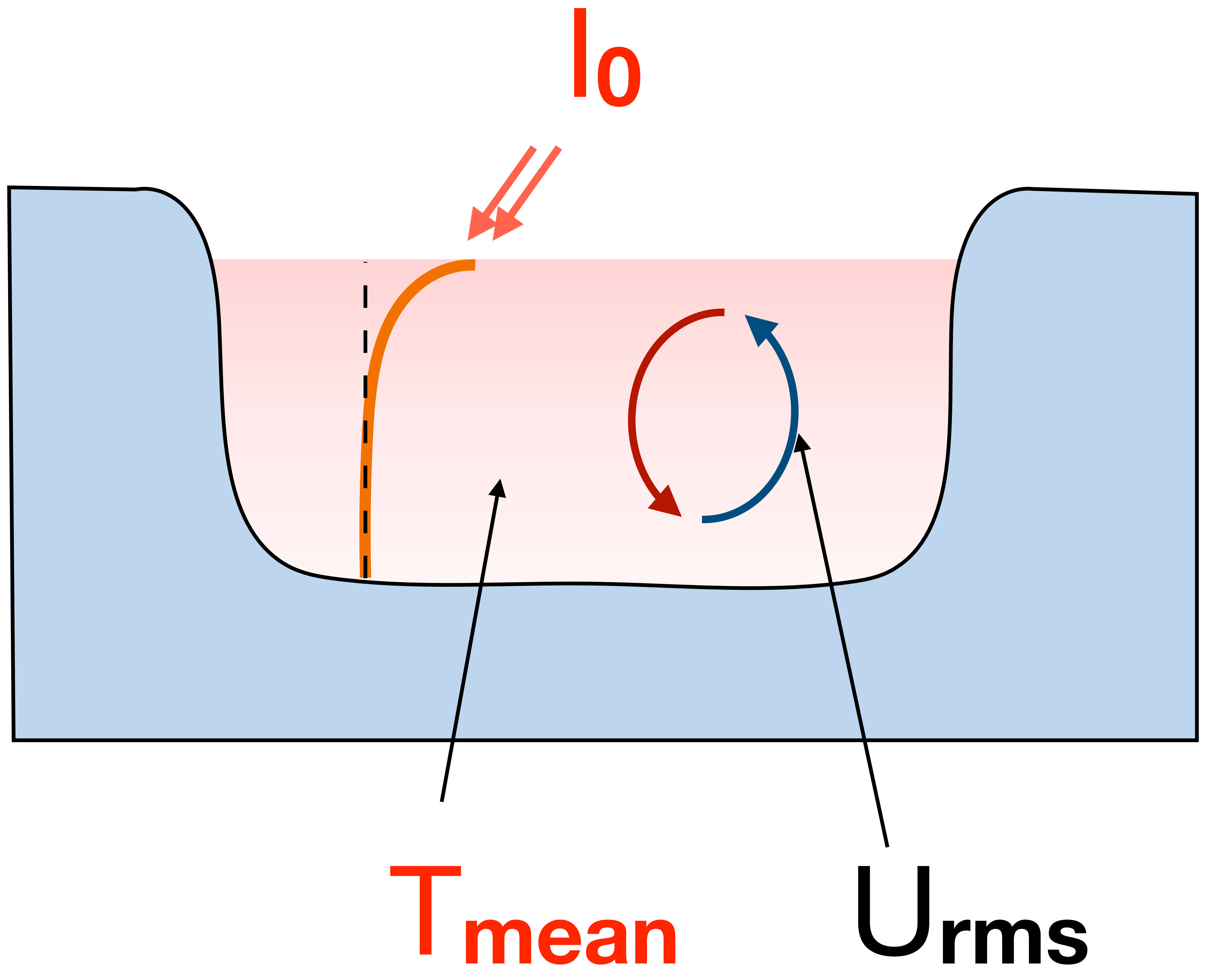

Can we predict the mean flow velocity and the mean bulk temperature as the radiation I_0 intensifies?

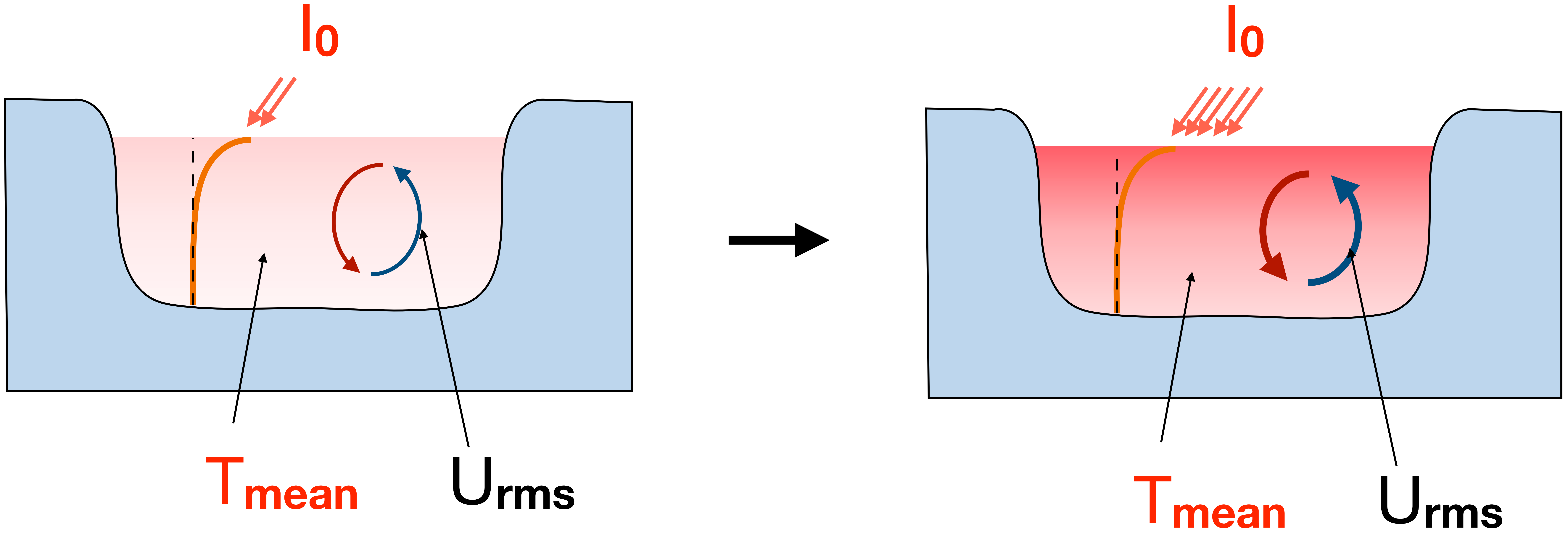

Mean bulk temperature and mean flow velocity

$h_0(I_0)$ = equlibrium depth from calculation

$$\rightarrow \quad Ra_{eff} \sim I_0 \cdot (h_0(I_0))^3$$

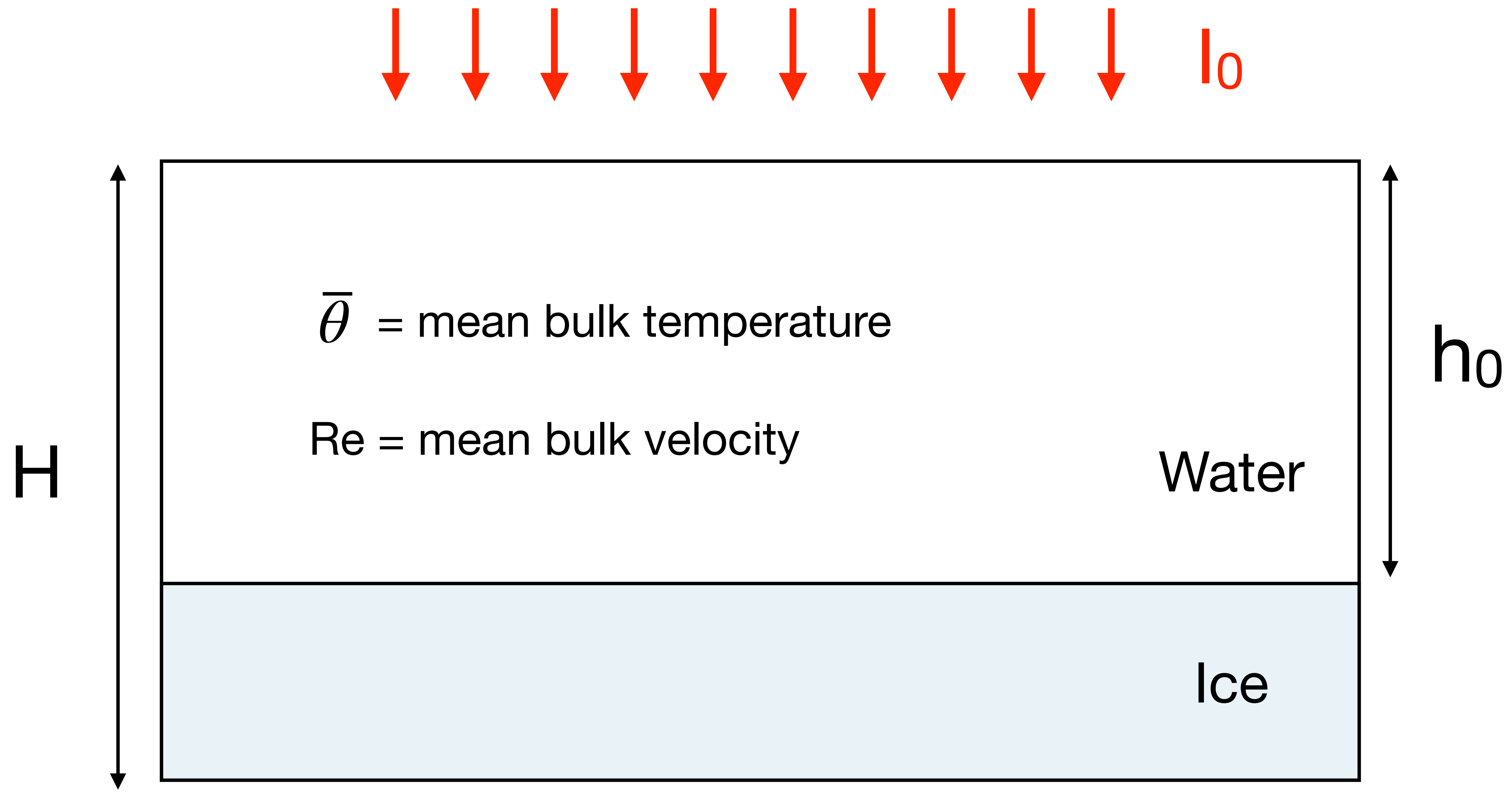

Mean bulk temperature and mean flow velocity

$h_0(I_0)$ = equlibrium depth from calculation

$$\rightarrow \quad Ra_{eff} \sim I_0 \cdot (h_0(I_0))^3$$

GL theory for **internal heating**[1]:

$$\bar{\theta} \sim Ra_{eff}^{-1/5}, \quad Re \sim Ra_{eff}^{1/2}$$

—> functional dependence of mean bulk temperature & mean flow velocity on radiation strength

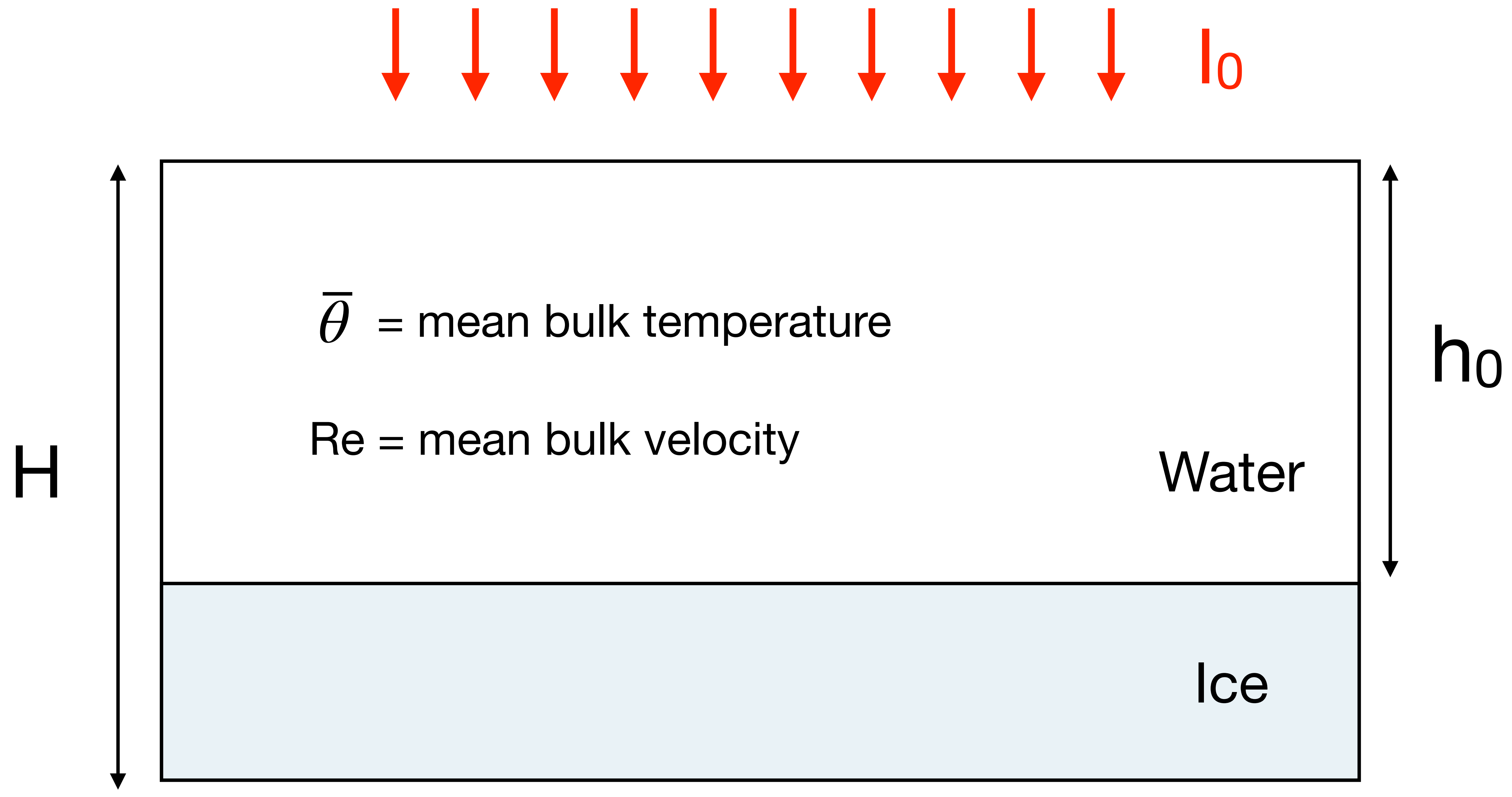

[1] Q. Wang, D. Lohse, O. Shishkina,
Scaling in internally heated convection: a unifying theory,
Geophys. Res. Lett. 48, e2020GL091198 (2021).

Mean bulk temperature and mean flow velocity

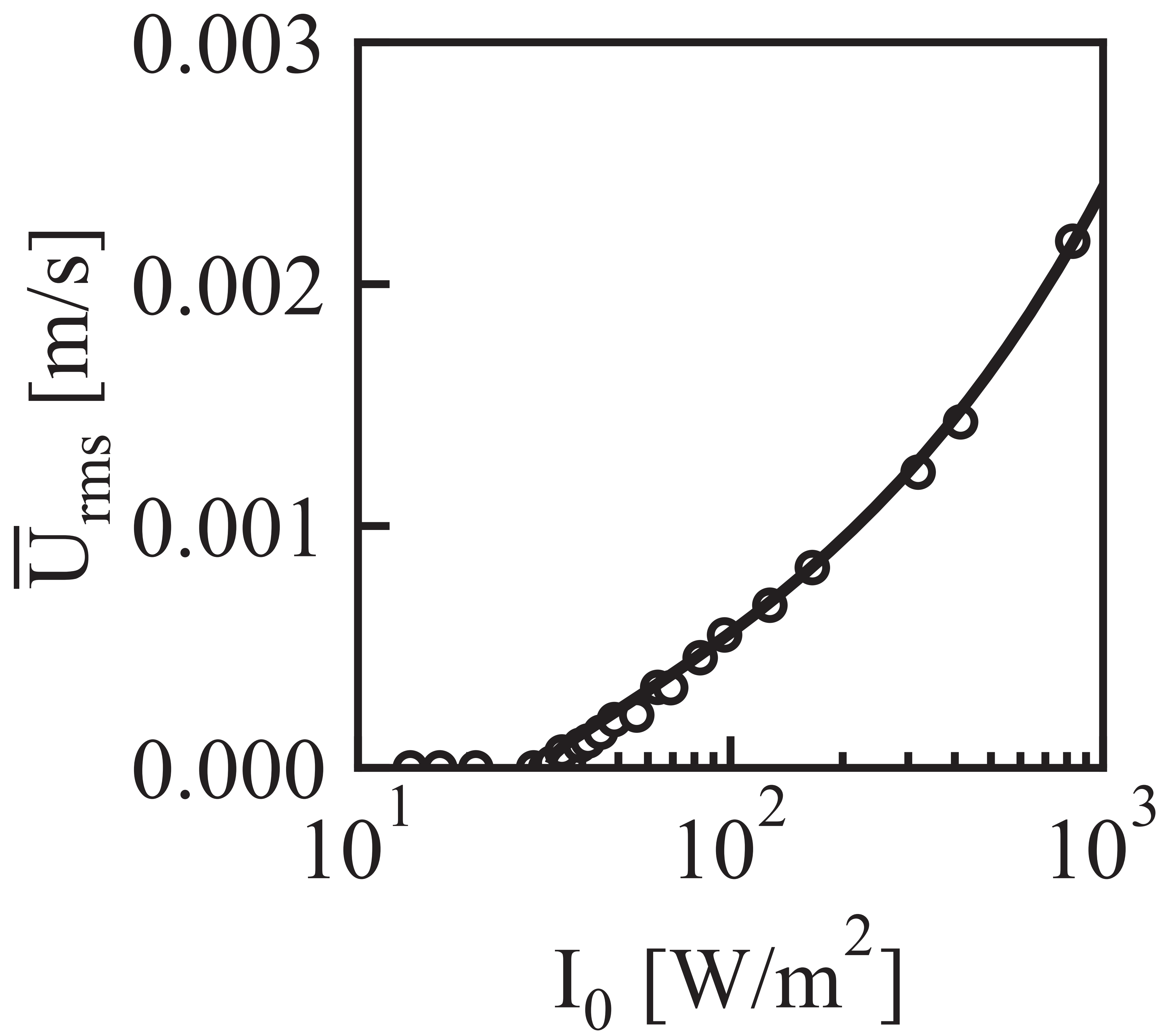

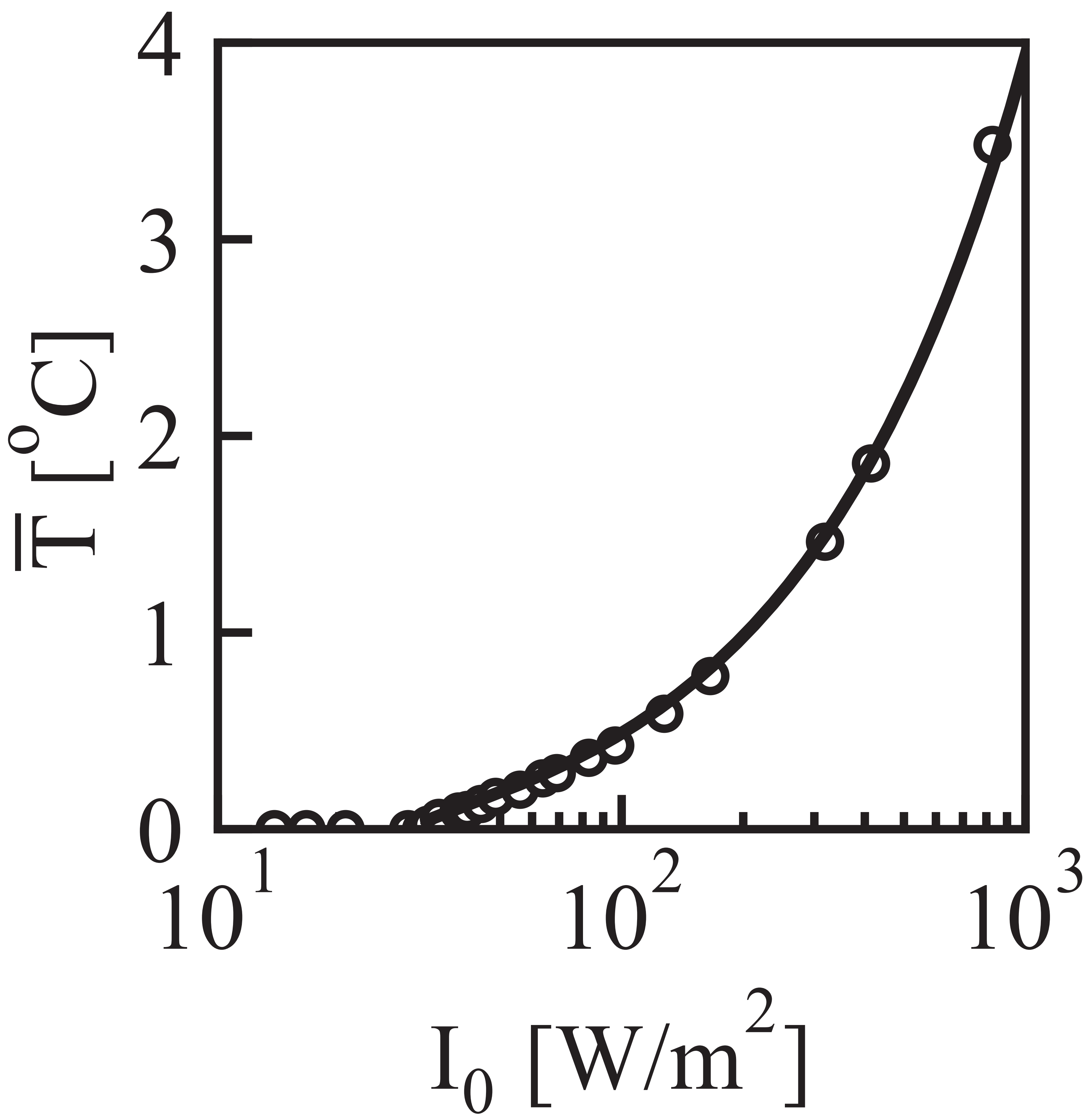

Predictions (o) vs GL theory (—)

Conclusions on melt ponds

- bistability
- subcritical bifurcation
- tipping point
- GL-theory predictive power for functional dependence of bulk temperature & flow velocity on radiation strength

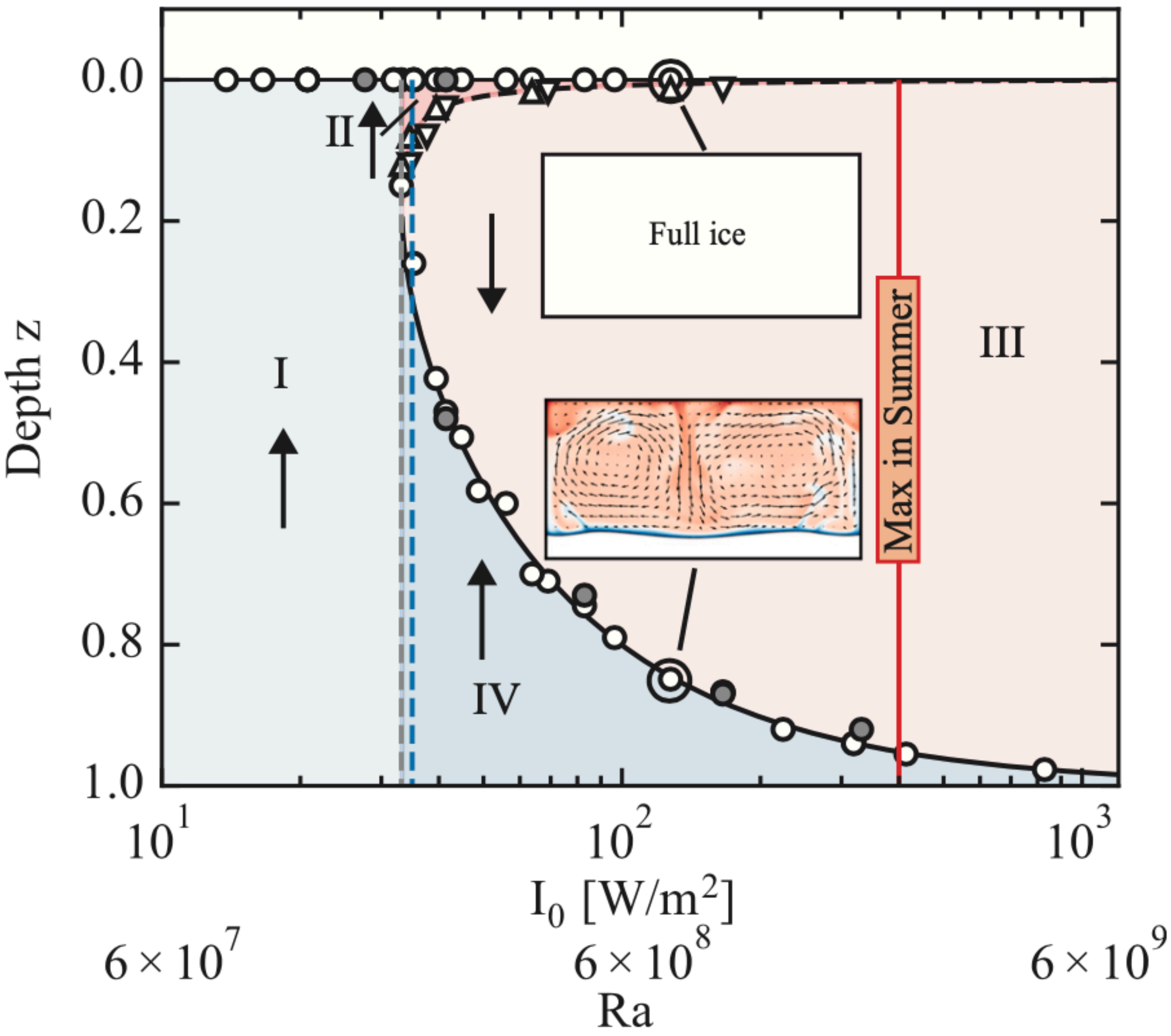

Yang, Howland, Liu, Verzicco, Lohse,
Phys. Rev. Lett. 131, 234002 (2023)

Where will the rest of the talk bring you?

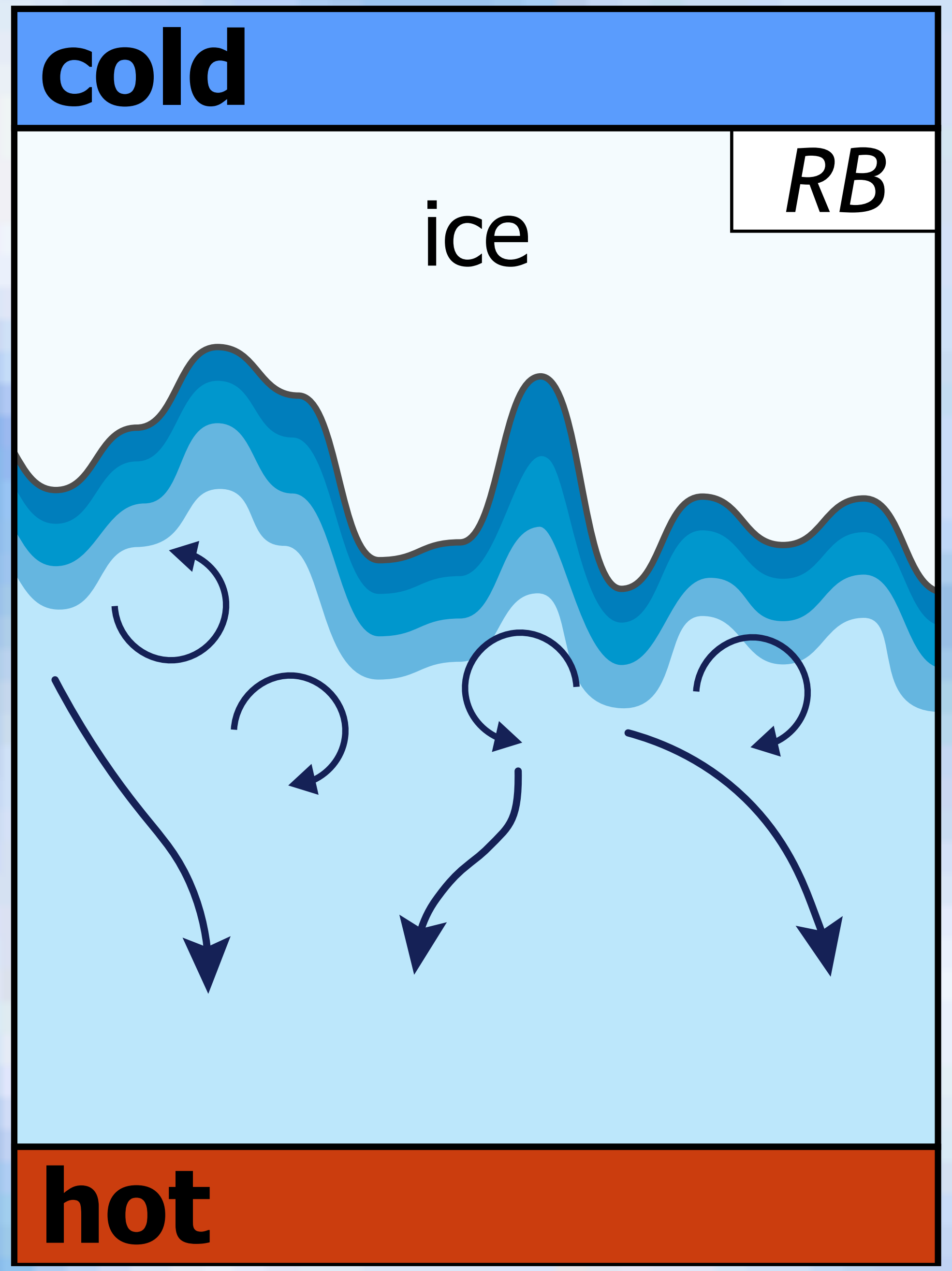

II. RB with fresh water at large Ra

Where will the rest of the talk bring you?

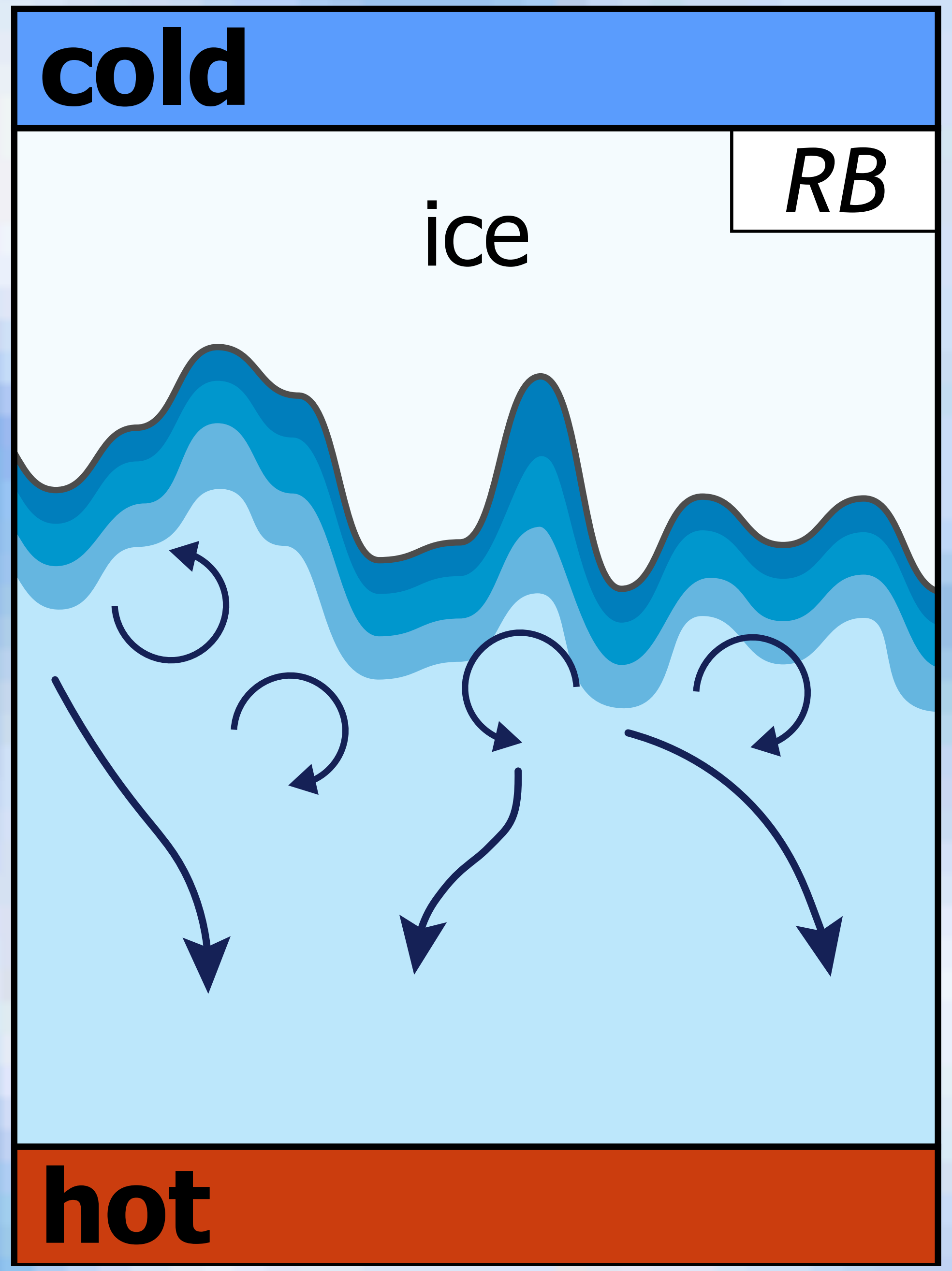

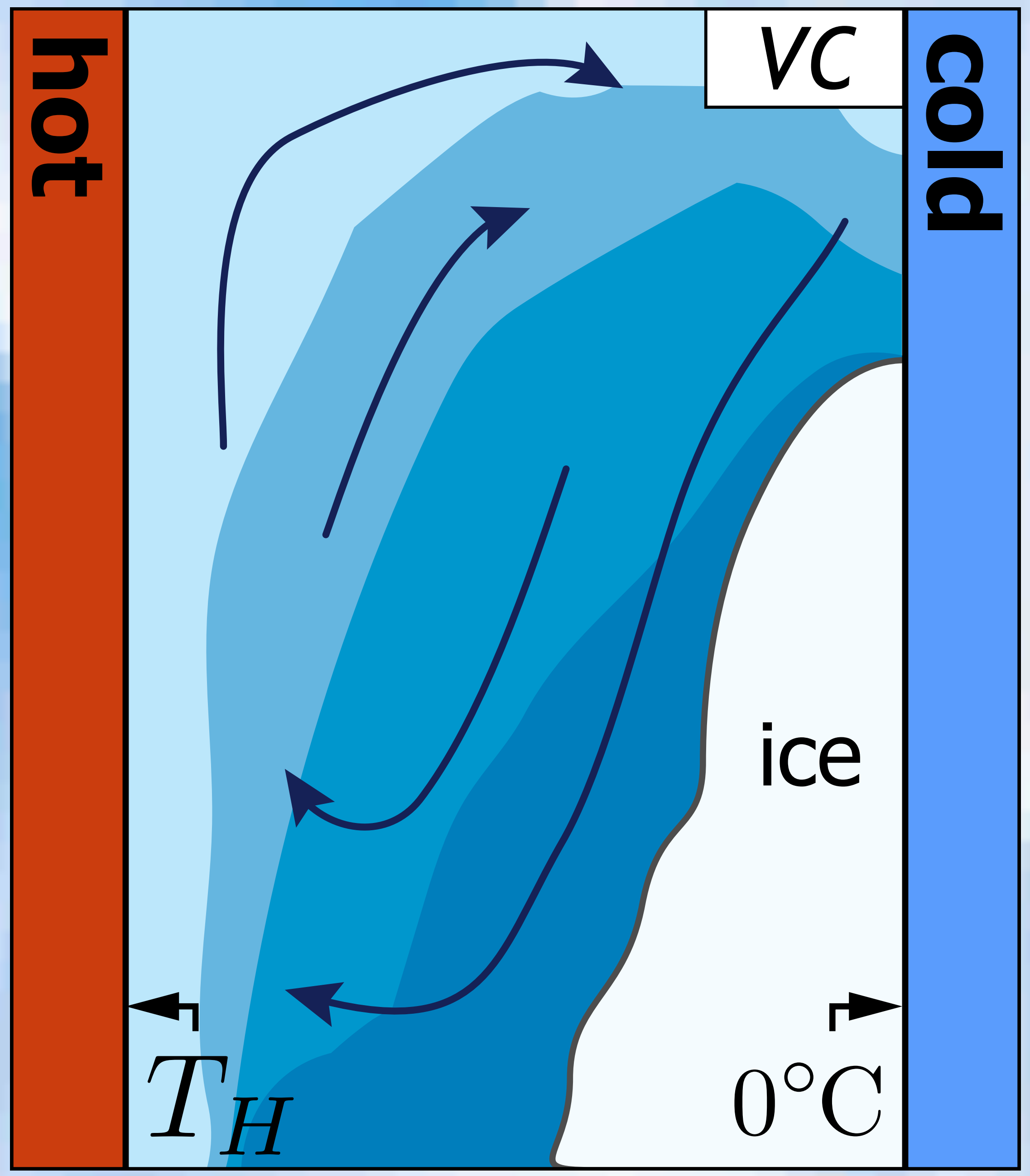

II. RB with fresh water at large Ra

III. Vertical convection with fresh water

Where will the rest of the talk bring you?

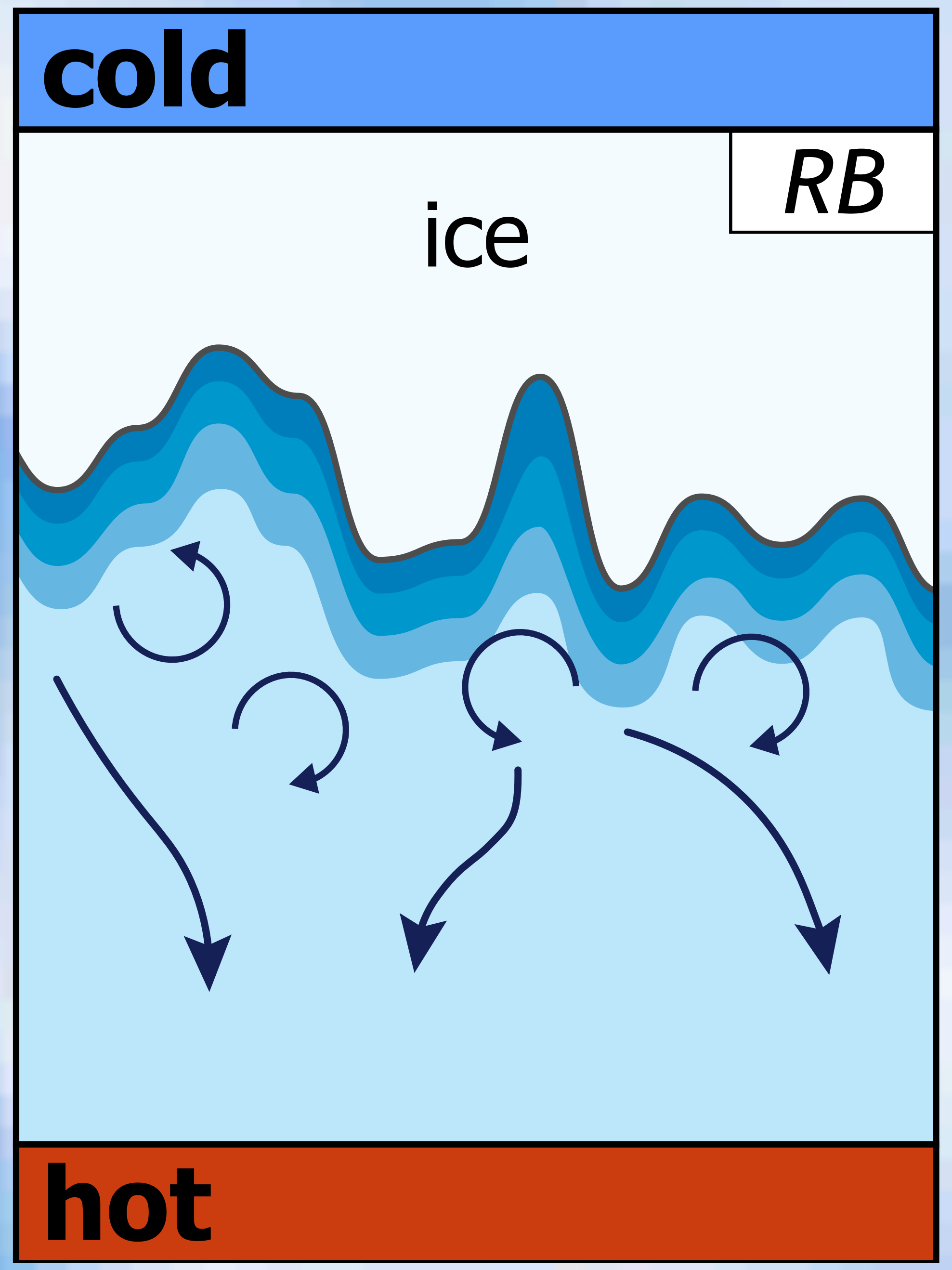

II. RB with fresh water at large Ra

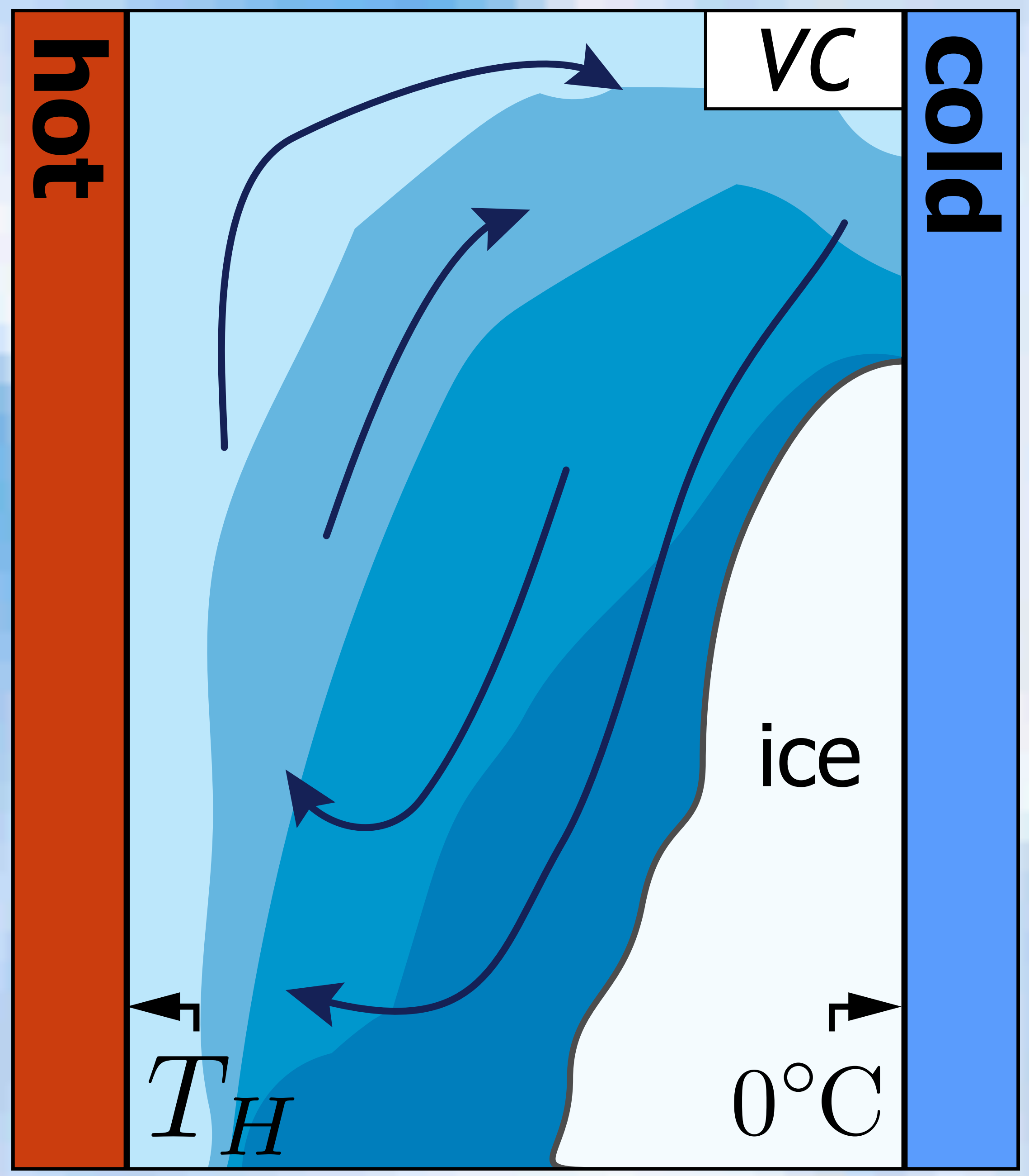

III. Vertical convection with fresh water

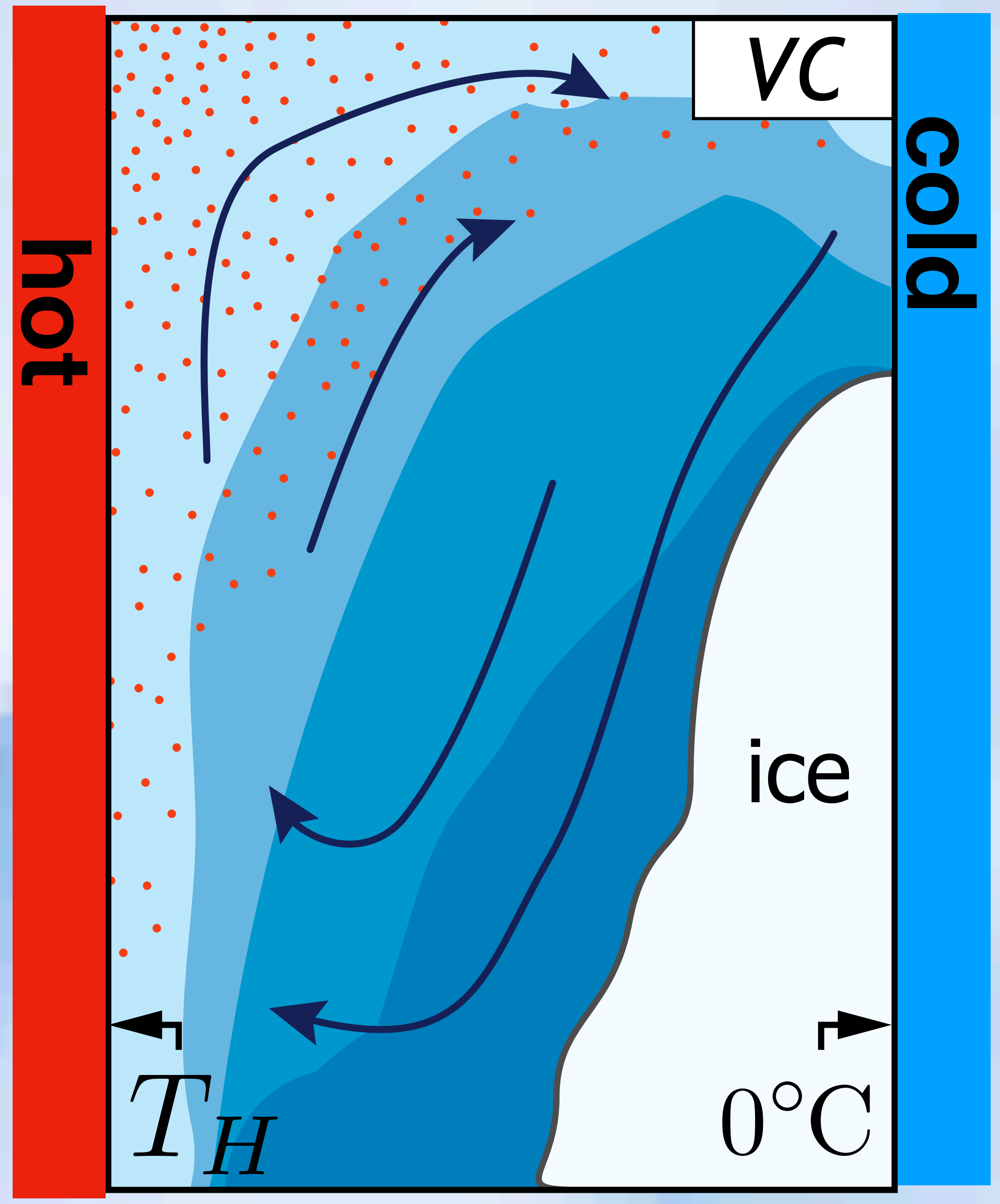

IV. Vertical convection with salty water

II. RB with fresh water at large Ra

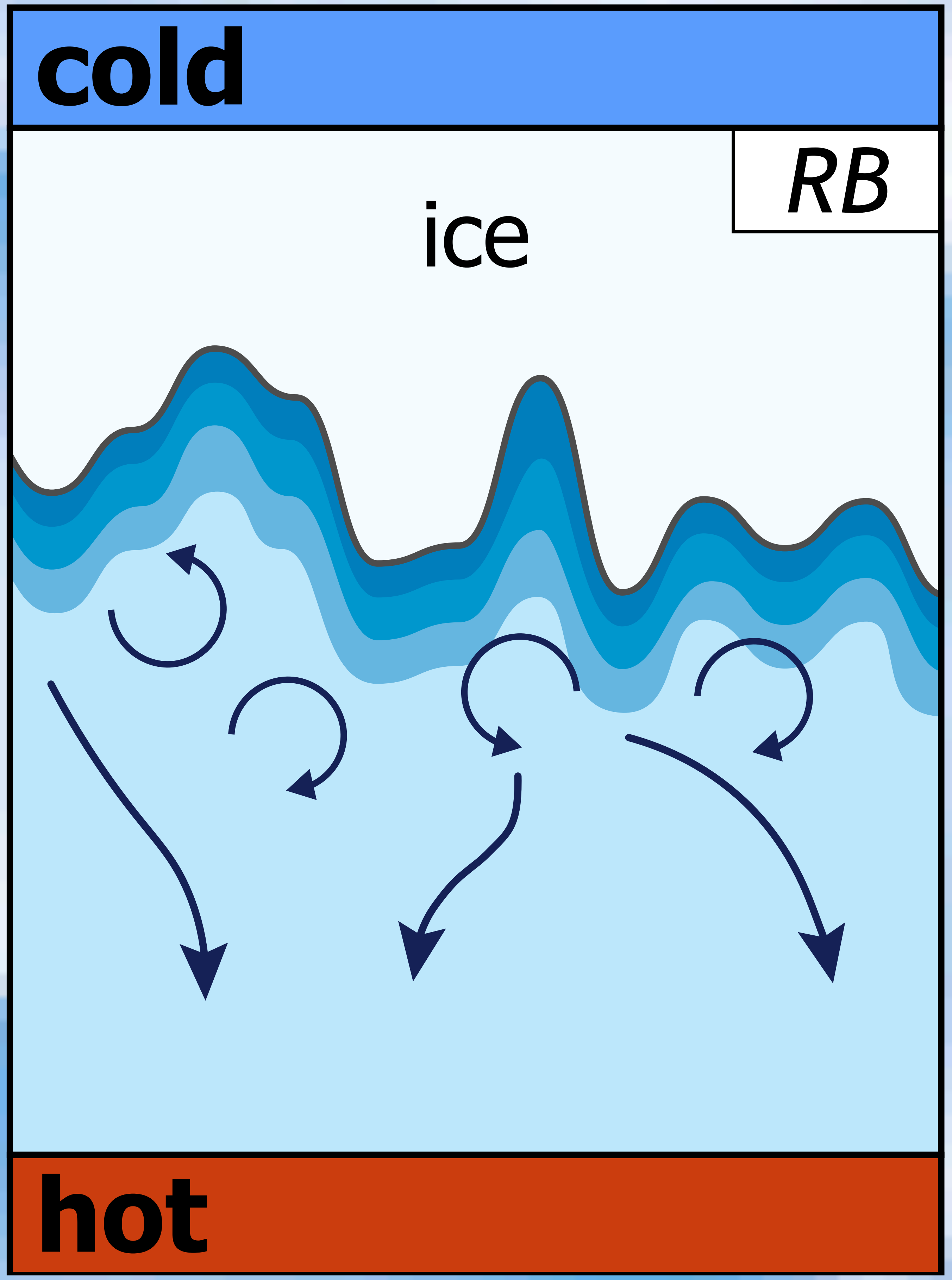

Morphology evolution of a melting solid layer above a liquid heated from below

Yang, Howland, Liu, Verzicco, Lohse, JFM 956, A23 (2023)

II. Ice melting above convection

Topography of melting solids in highly turbulent convection

Rui Yang, Christopher J. Howland, Hao-Ran Liu, Roberto Verzicco, Detlef Lohse

II. Ice melting above convection

Topography of melting solids in highly turbulent convection

Rui Yang, Christopher J. Howland, Hao-Ran Liu, Roberto Verzicco, Detlef Lohse

Alternative title:

How scallop patterns can emerge

Rui Yang, Christopher J. Howland, Hao-Ran Liu, Roberto Verzicco, Detlef Lohse

Alternative title:

How scallop patterns can emerge

Rui Yang, Christopher J. Howland, Hao-Ran Liu, Roberto Verzicco, Detlef Lohse

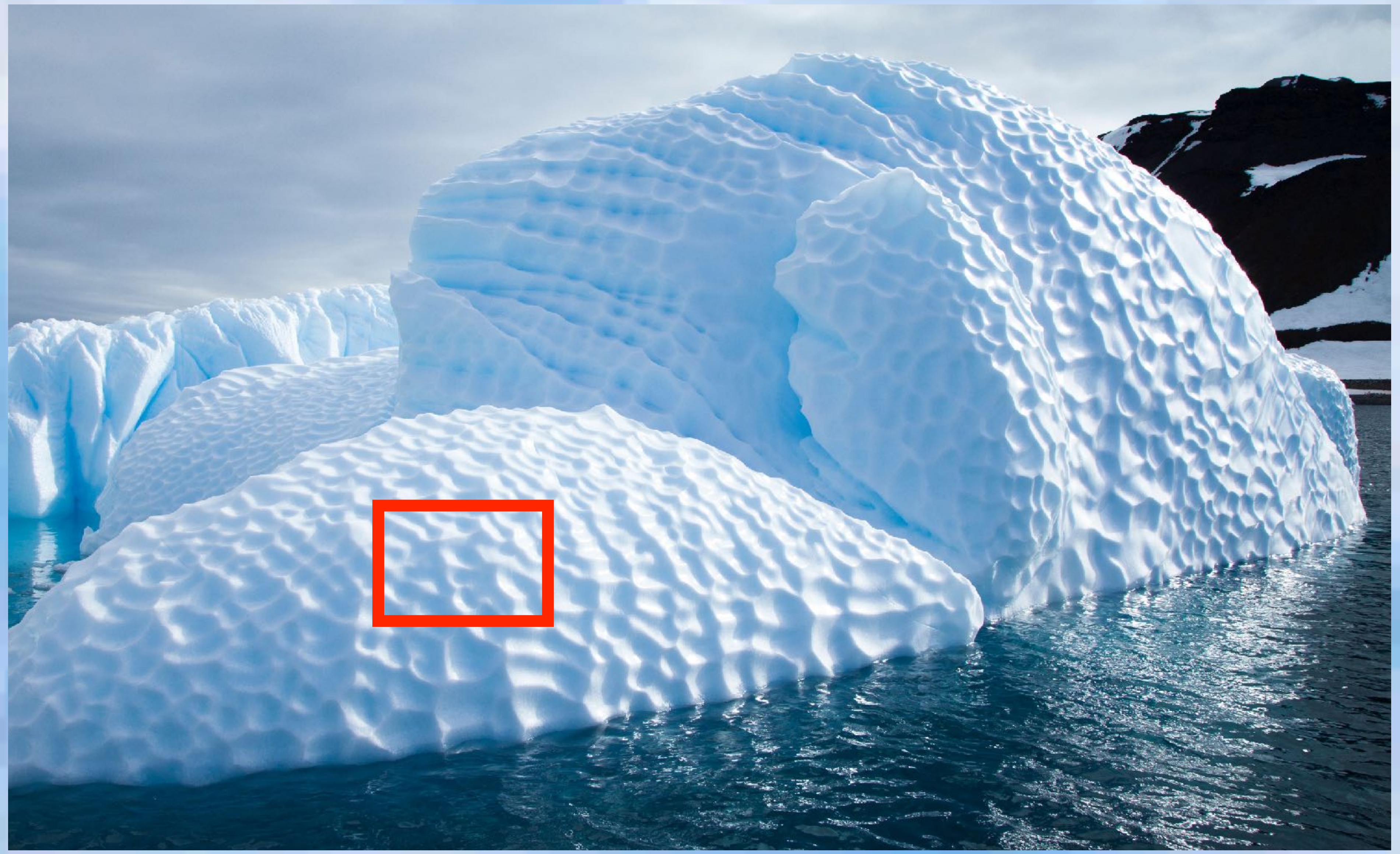

Alternative title:

How scallop patterns can emerge

Rui Yang, Christopher J. Howland, Hao-Ran Liu, Roberto Verzicco, Detlef Lohse

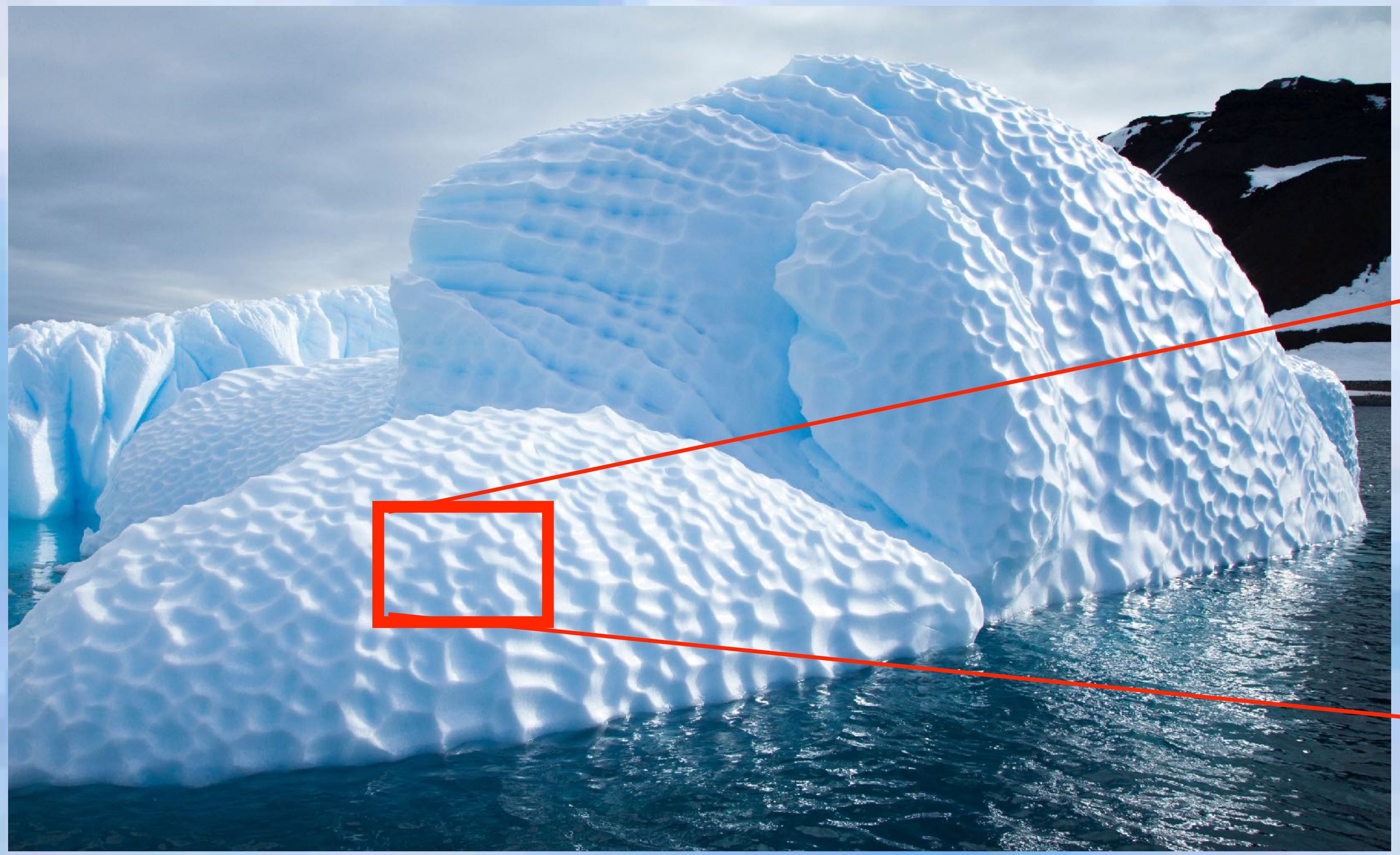

Control and response parameters

Control parameters:

$$Ra = \frac{\beta g \Delta H^3}{\nu\kappa} = 10^8,\ 10^9,\ 10^{10},\ 10^{11}$$

$$Pr = \frac{\nu}{\kappa} = 1,\ 10$$

$$\Gamma = \frac{W}{H} = 2$$

$$St = \frac{L}{c_p \Delta} = 1$$

Control and response parameters

Control parameters:

$$Ra = \frac{\beta g \Delta H^3}{\nu\kappa} = 10^8,\ 10^9,\ 10^{10},\ 10^{11}$$

$$Pr = \frac{\nu}{\kappa} = 1,\ 10$$

$$\Gamma = \frac{W}{H} = 2$$

$$St = \frac{L}{c_p \Delta} = 1$$

Response parameters:

- Roughness amplitude (std): σ
- Roughness wavelength: L_c
- Nusselt number: Nu

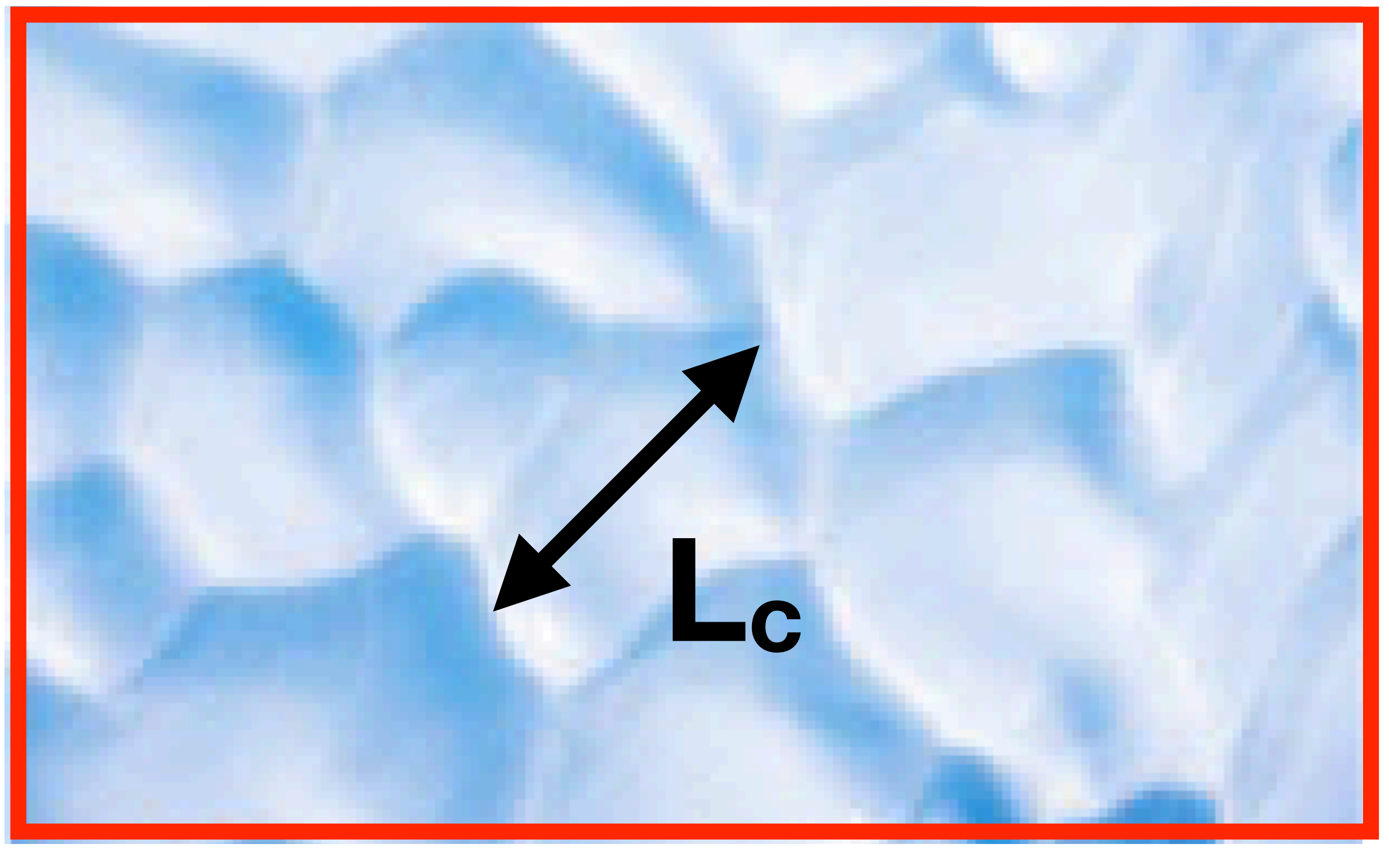

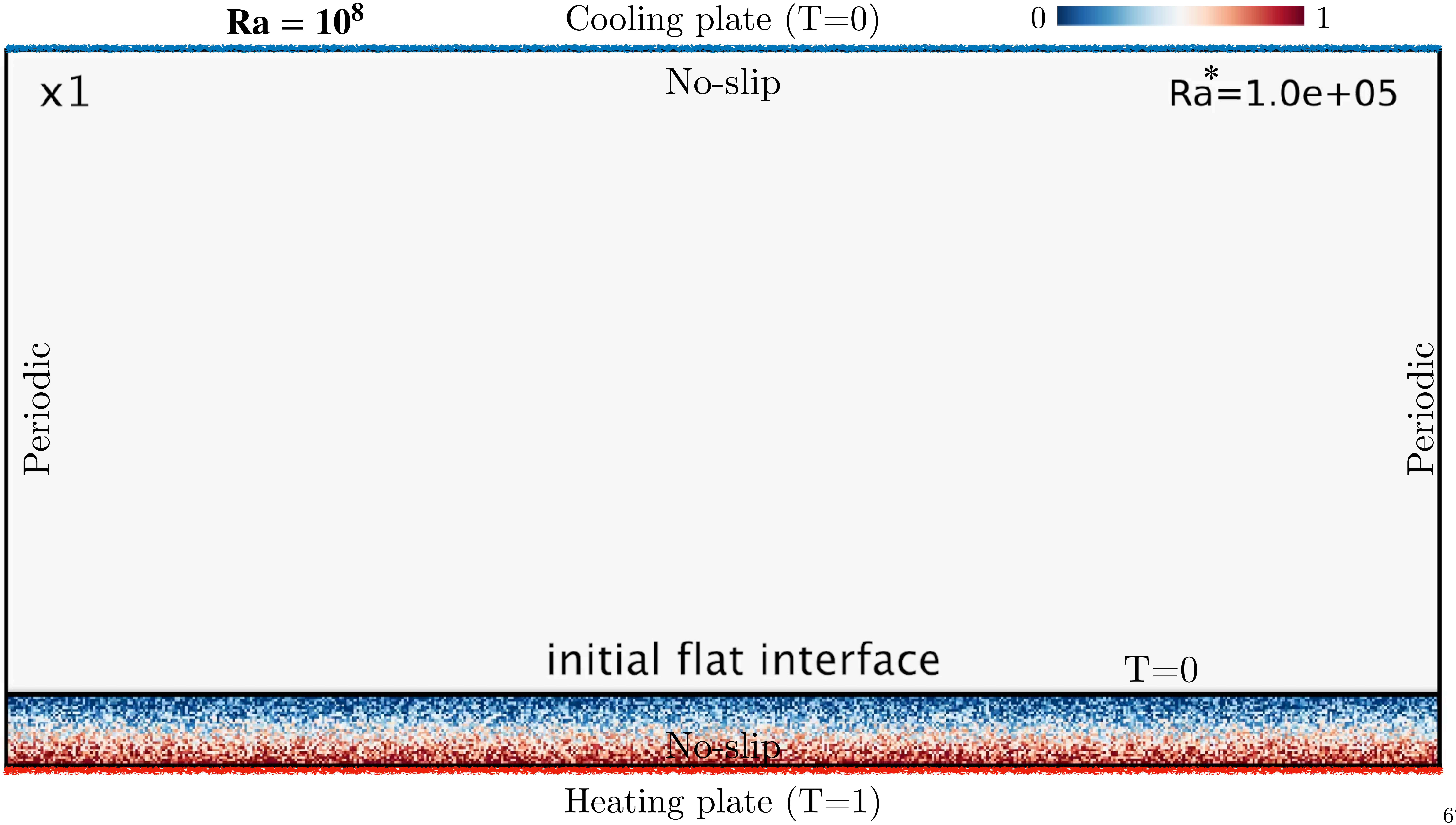

Ra = 10^8
Cooling plate (T=0)
0
1
No-slip
x1
Ra*=1.0e+05
Periodic
Periodic
initial flat interface
T=0
No-slip
Heating plate (T=1)

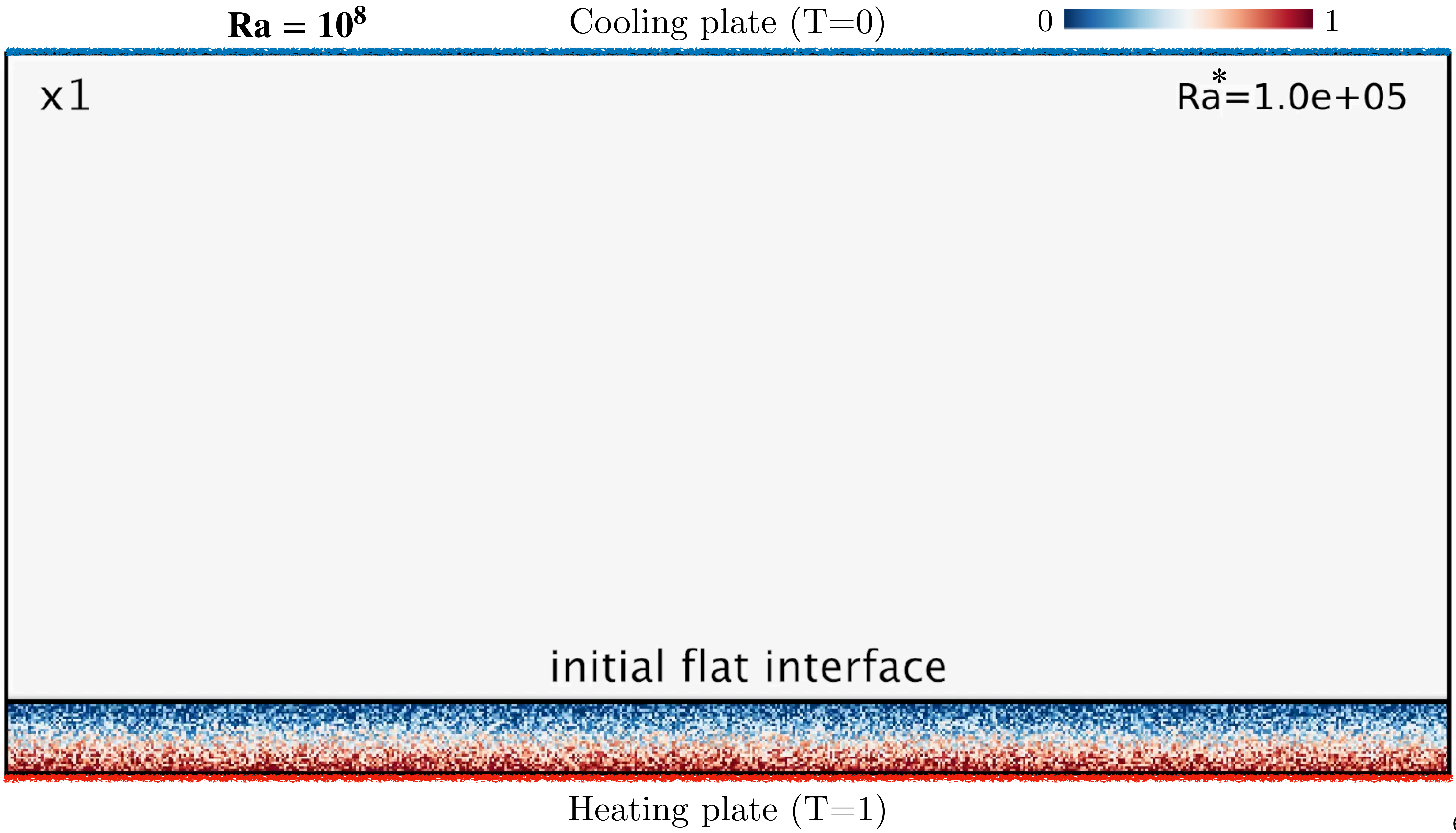

Ra = 10^8
Cooling plate (T=0)
0
1
x1
Ra*=1.0e+05
initial flat interface
Heating plate (T=1)

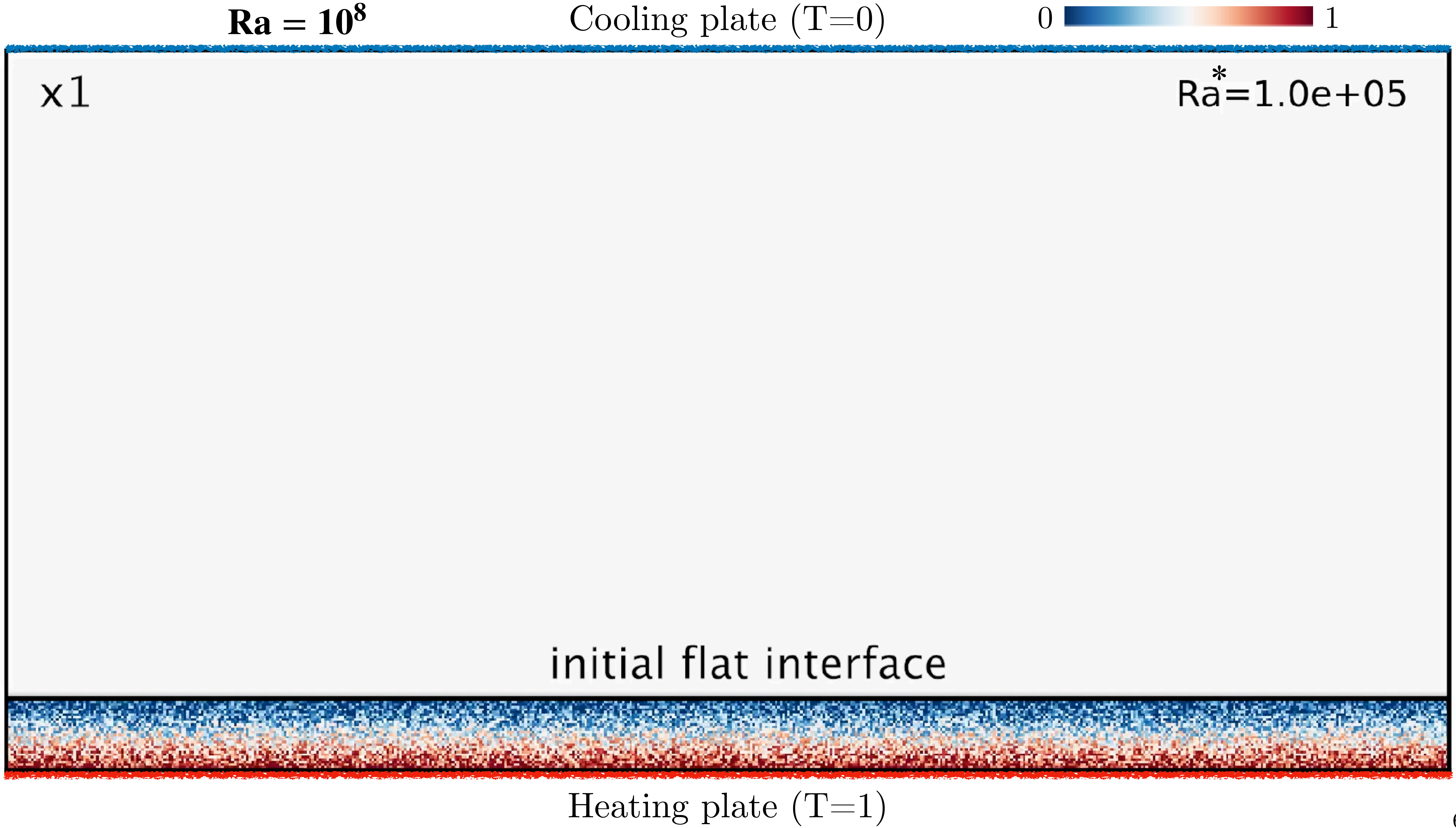

Ra = 10^8
Cooling plate (T=0)
0
1
x1
Ra*=1.0e+05
initial flat interface
Heating plate (T=1)

Flow & melt front structure at small Ra (in 2D RB)

- Non-uniform pattern induced by convection plumes underneath
- As height/time/Ra* increase, ice front deforms as the convection cells merge
- Cusp structure
- Strongest melting under impacting plumes

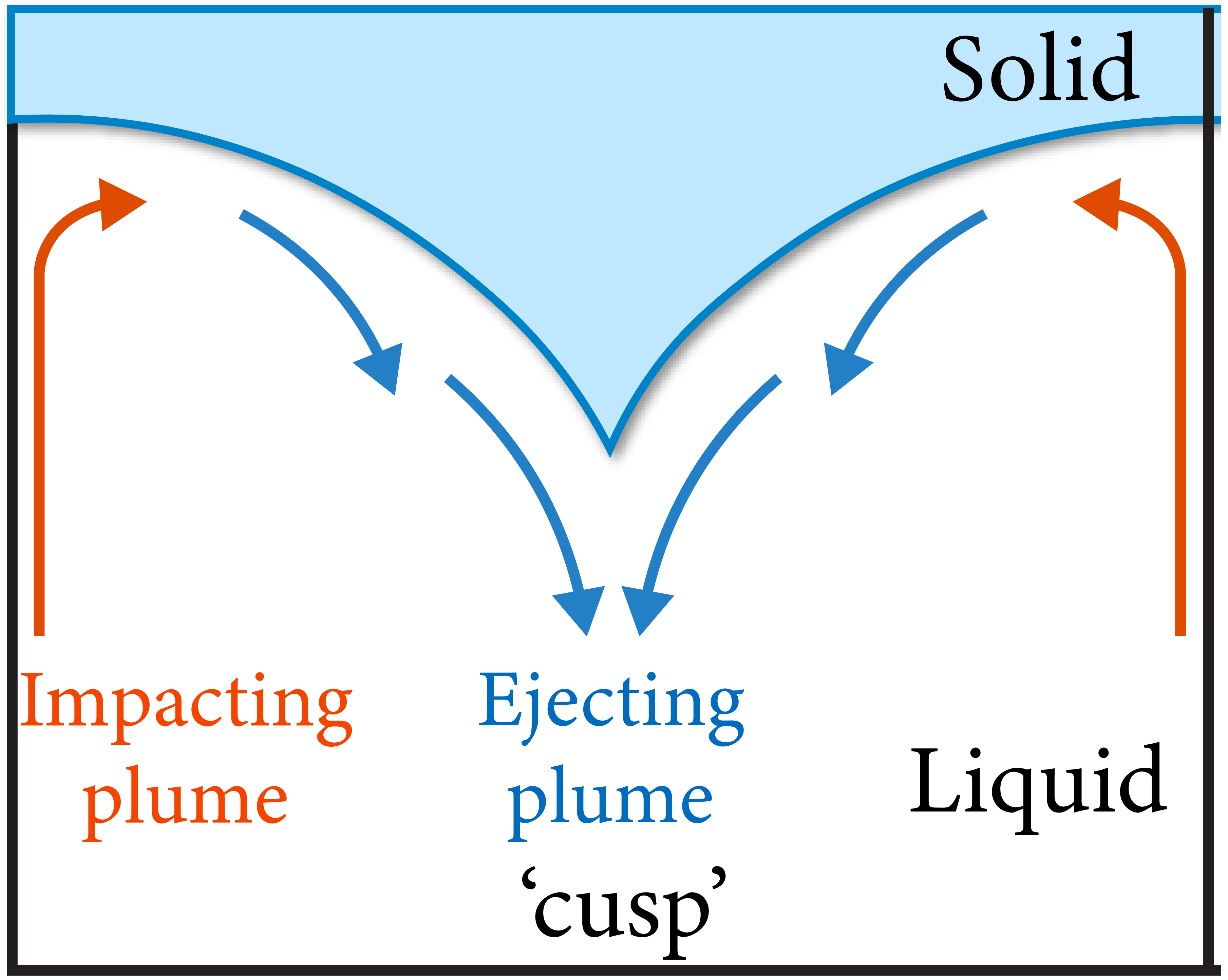

Flow & melt front structure at small Ra (in 2D RB)

- Non-uniform pattern induced by convection plumes underneath
- As height/time/Ra* increase, ice front deforms as the convection cells merge
- Cusp structure
- Strongest melting under impacting plumes

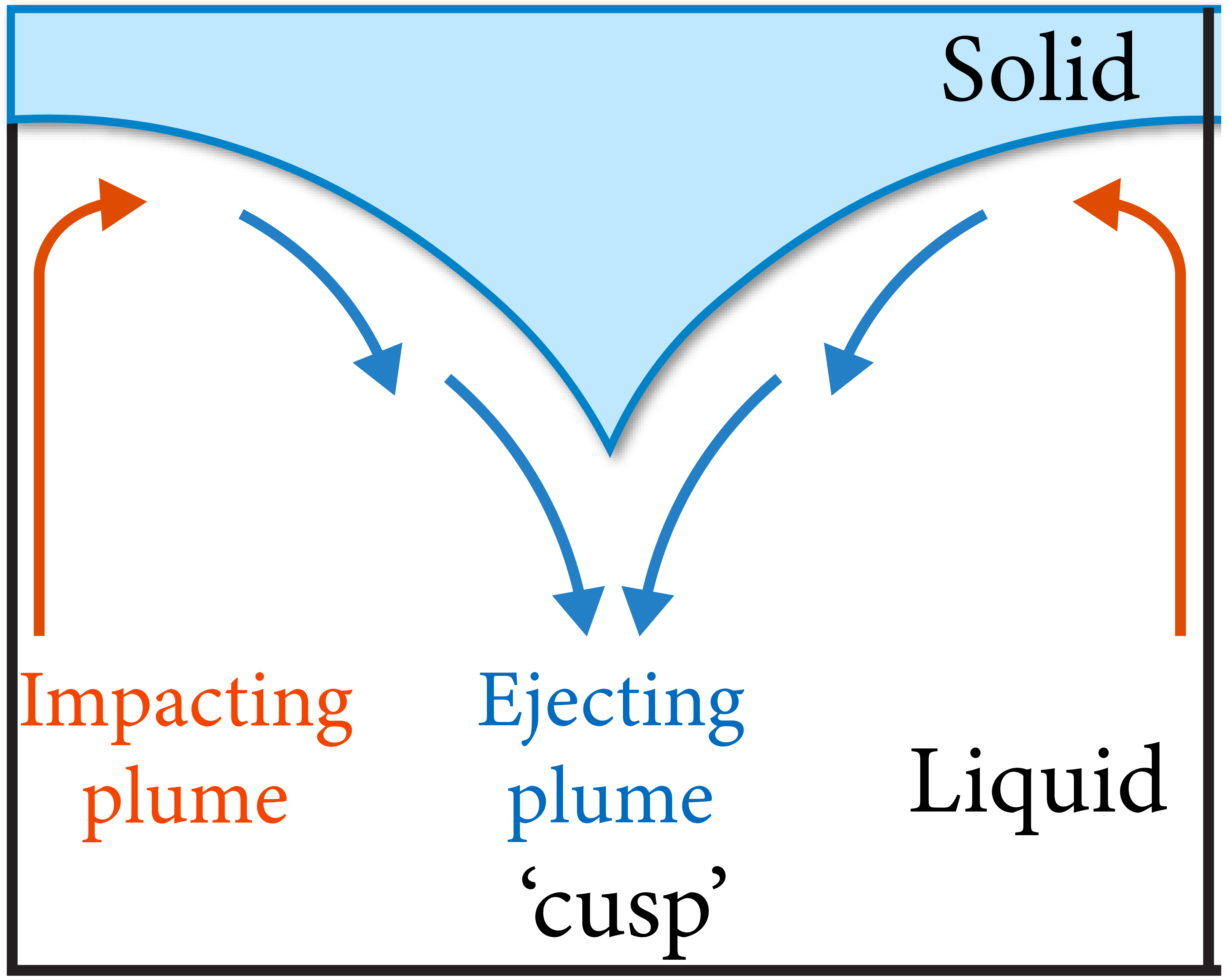

This changes when Ra and thus Ra* further increase!

Ra = 10^{11}
Cooling plate (T=0)
0.3
0.7
Ra*=1.0e+08
Heating plate (T=1)

Ra = 10^{11}

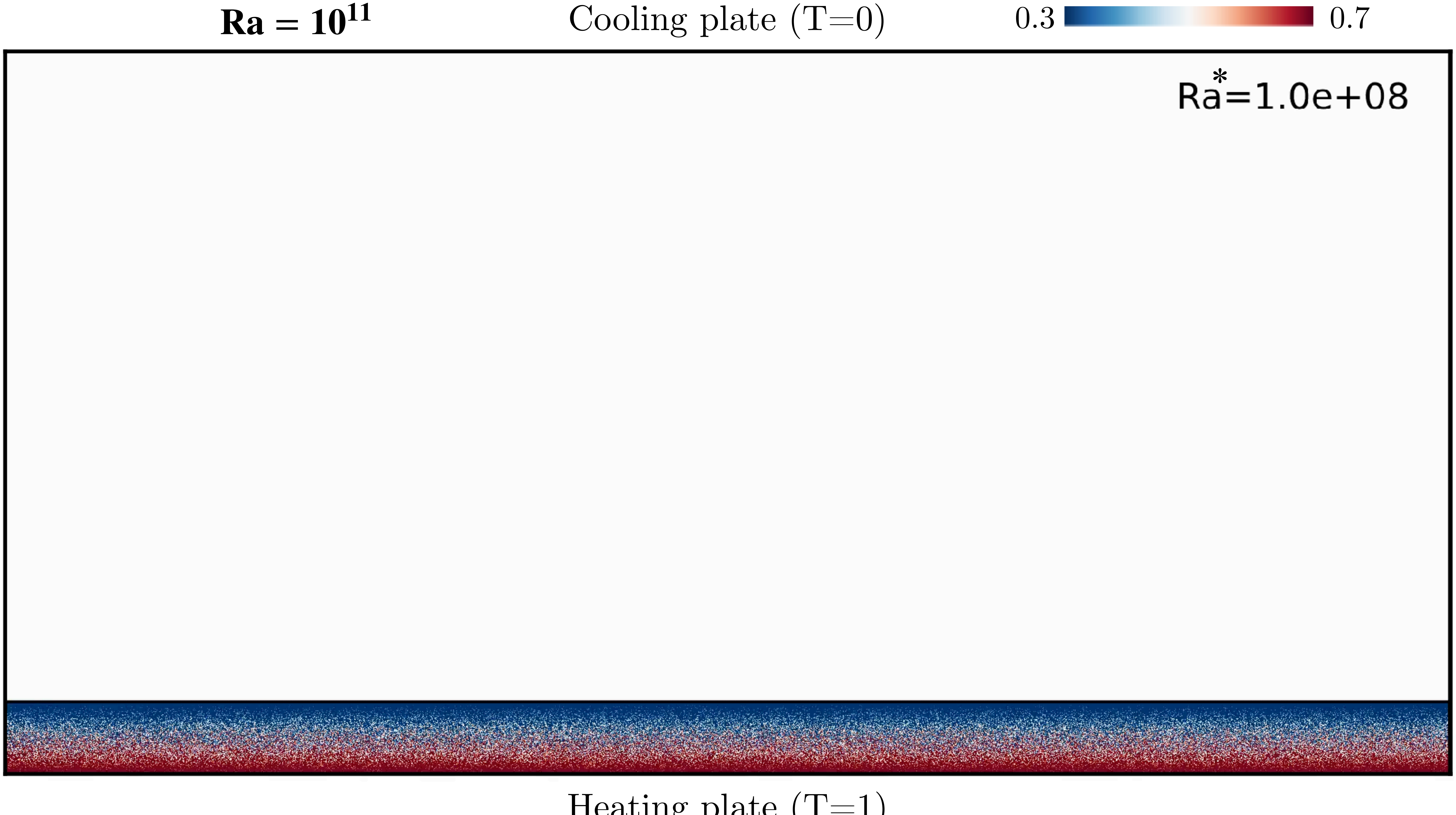

Flow & melt front structure at large Ra (in 2D RB)

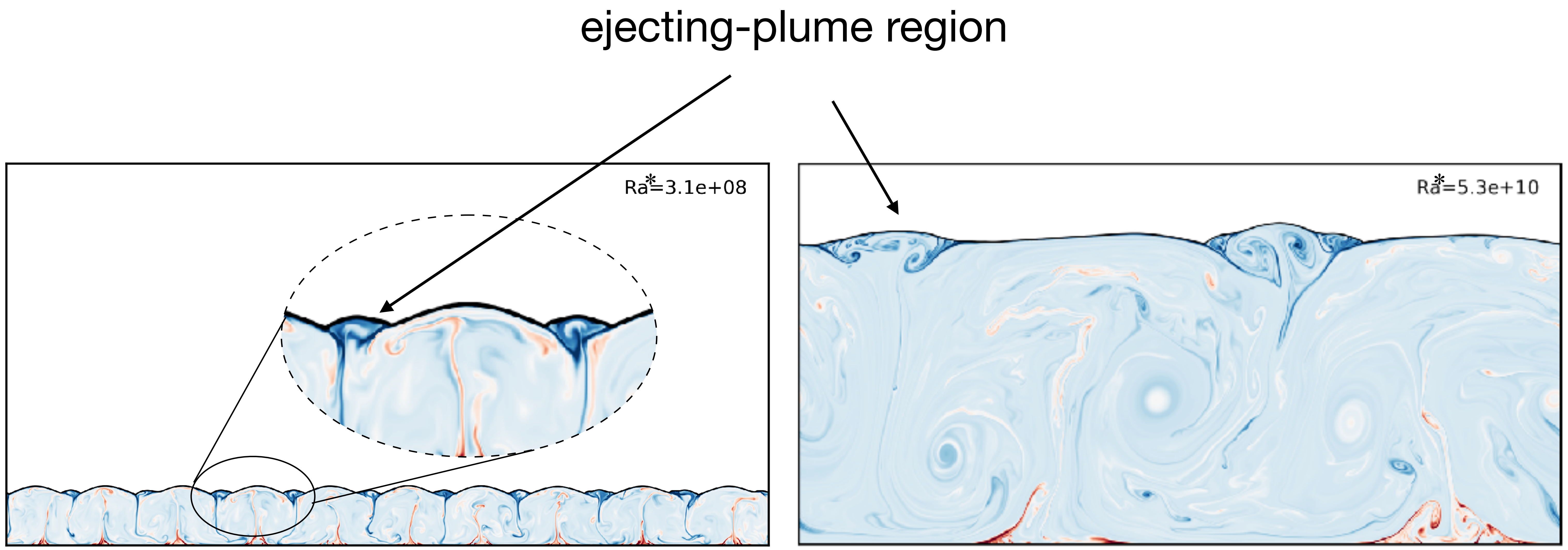

- As height/time/Ra* increase, ice front patterns in ejecting plume regions change from cusp to **cellular structure** ("2D scallops")

- Pattern in ice is no longer directly coupled to pattern of convection rolls

Flow & melt front structure at large Ra (in 2D RB)

- As height/time/Ra* increase, ice front patterns in ejecting plume regions change from cusp to **cellular structure** ("2D scallops")
- Pattern in ice is no longer directly coupled to pattern of convection rolls

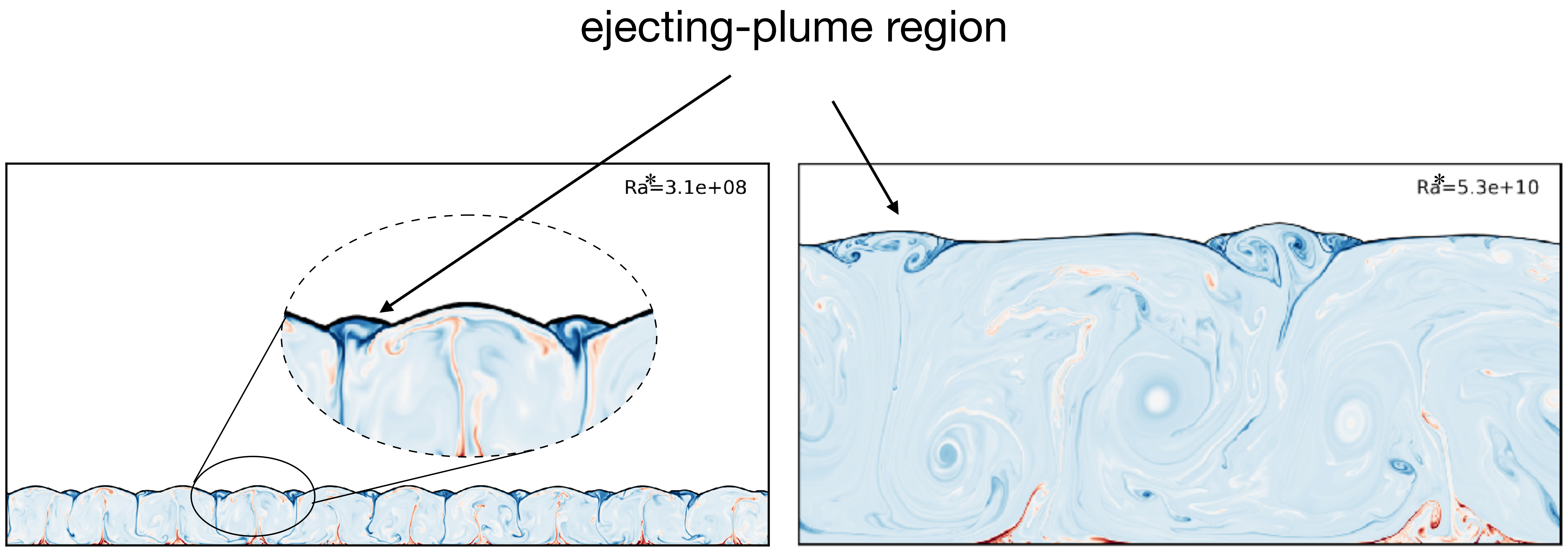

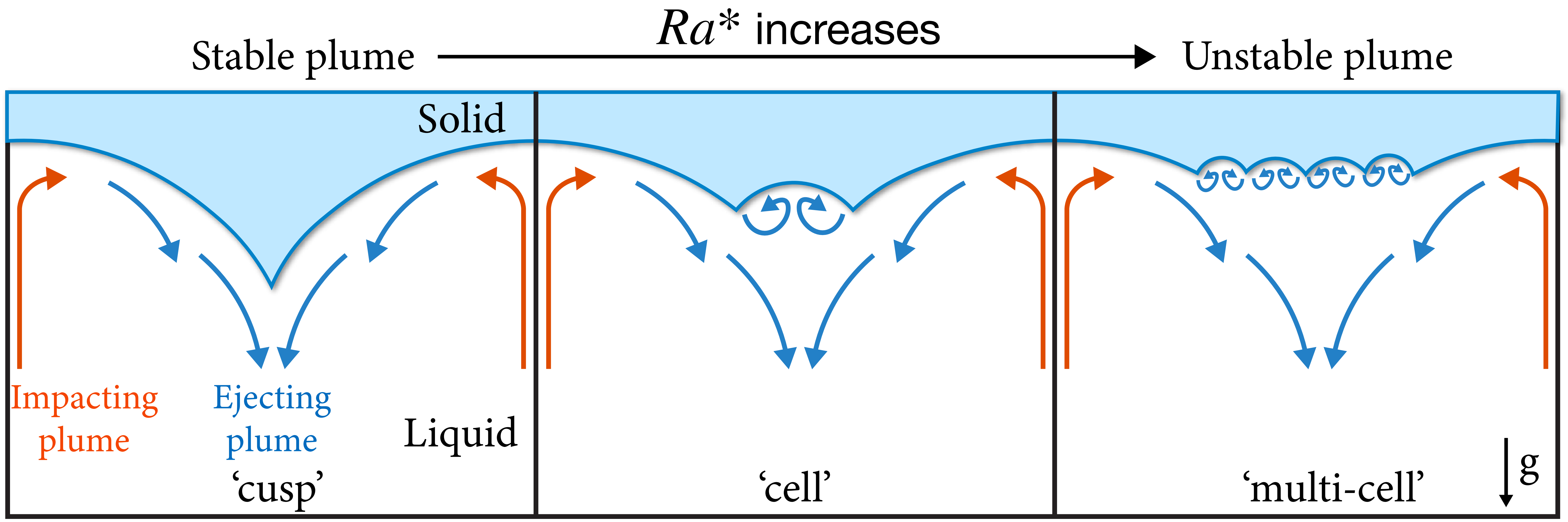

How do these cellular structures evolve in 3D?

How do these cellular structures evolve in 3D?

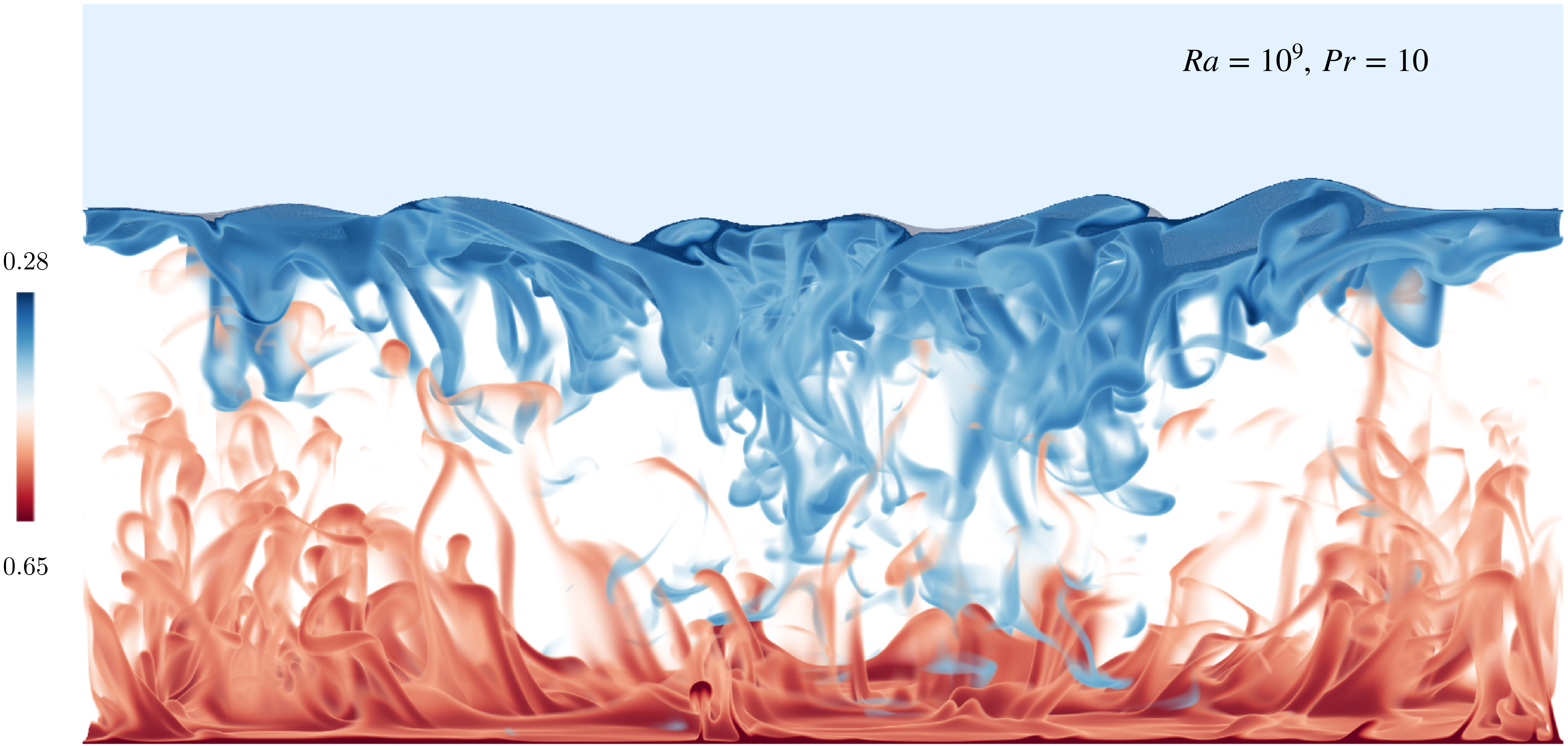

Evolution of flow & melt front structure (in 3D RB)

side view: middle 2D slice

$Ra = 10^9, Pr = 10$

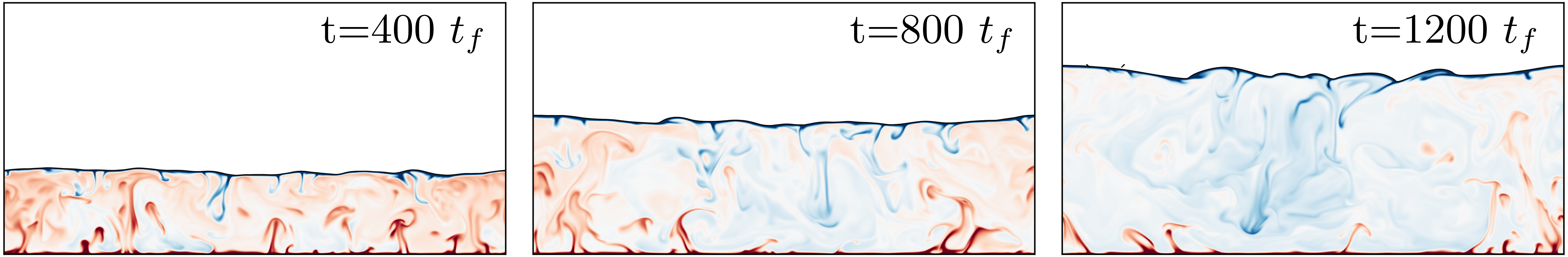

Evolution of flow & melt front structure (in 3D RB)

side view: middle 2D slice

$Ra = 10^9,\ Pr = 10$

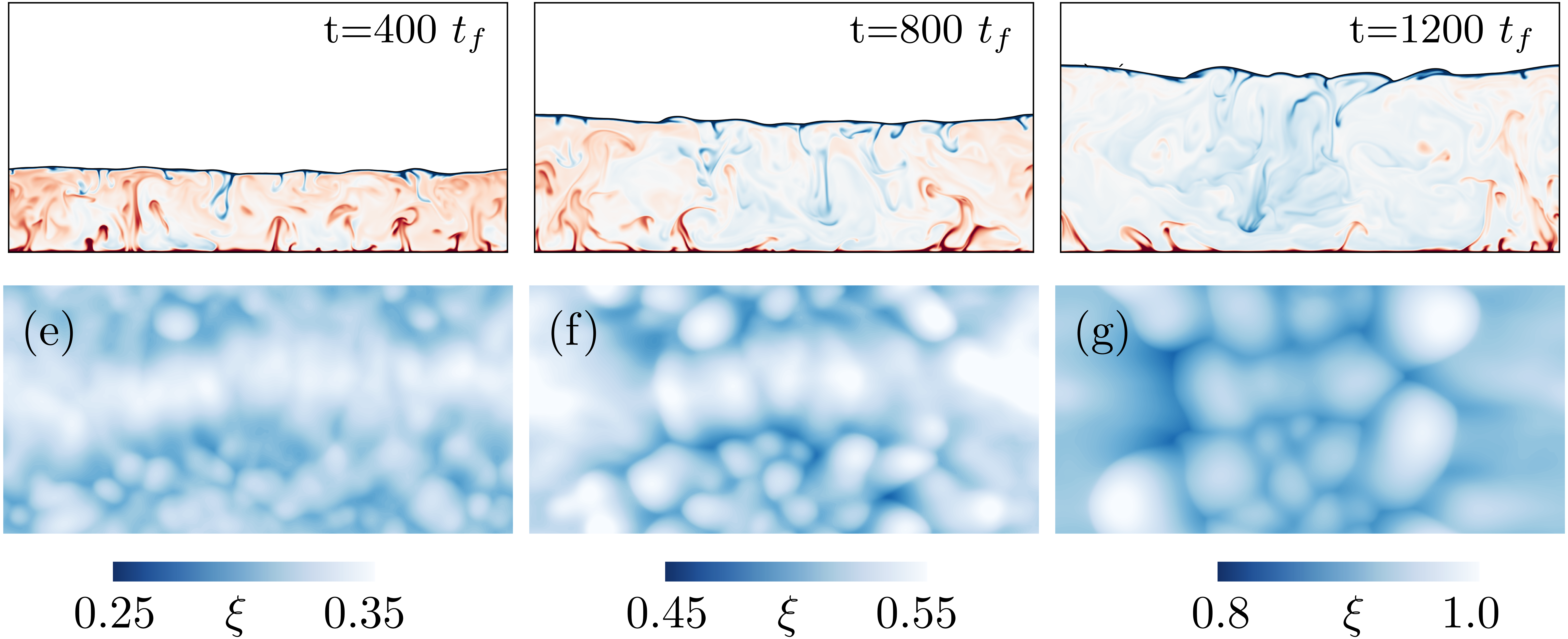

bottom view: interface topography

Length scale of structure evolves with time /with increasing Ra*

Evolution of flow & melt front structure (in 3D RB)

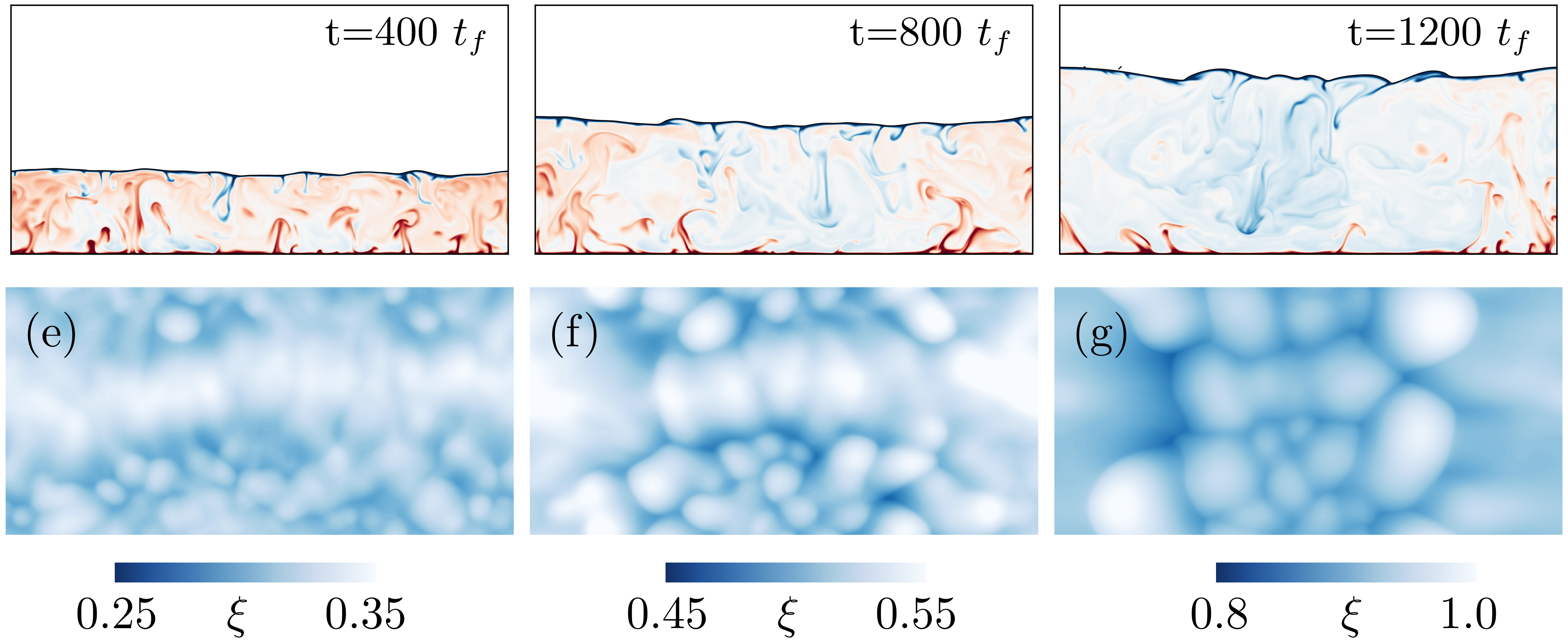

Very similar evolution as in 2D:

- Non-uniform pattern induced by convection plumes underneath
- As height/time/Ra* increase, ice front deforms as the convection cells merge
- As height/time/Ra* further increase, ice front patterns in ejecting plume regions change from cusp to **cellular structure ("scallops")**

Evolution of flow & melt front structure (in 3D RB)

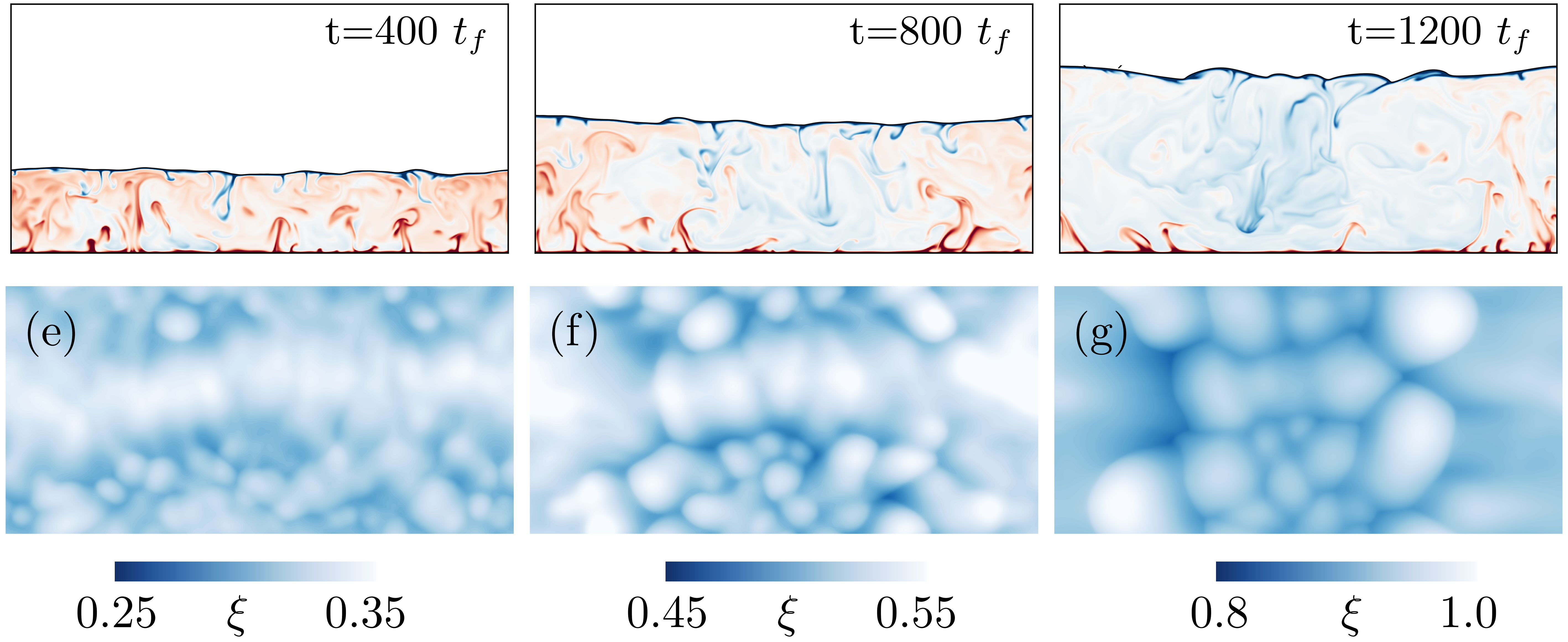

Very similar evolution as in 2D:

- Non-uniform pattern induced by convection plumes underneath
- As height/time/Ra* increase, ice front deforms as the convection cells merge
- As height/time/Ra* further increase, ice front patterns in ejecting plume regions change from cusp to **cellular structure ("scallops")**

How do these scallops compare with those from field measurements ?

Scallops from field measurements vs numerical ones

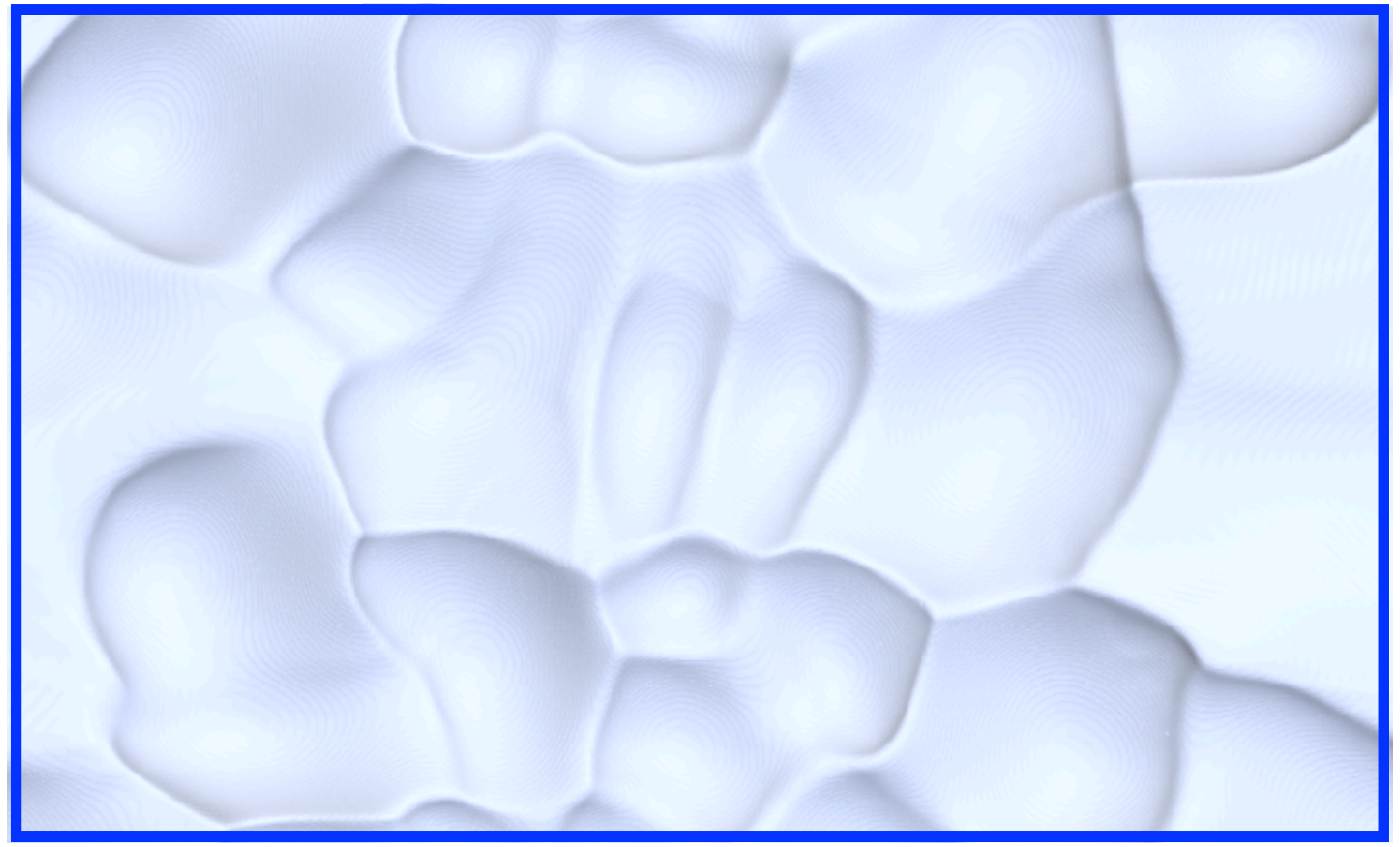

Scallops from field measurements vs numerical ones

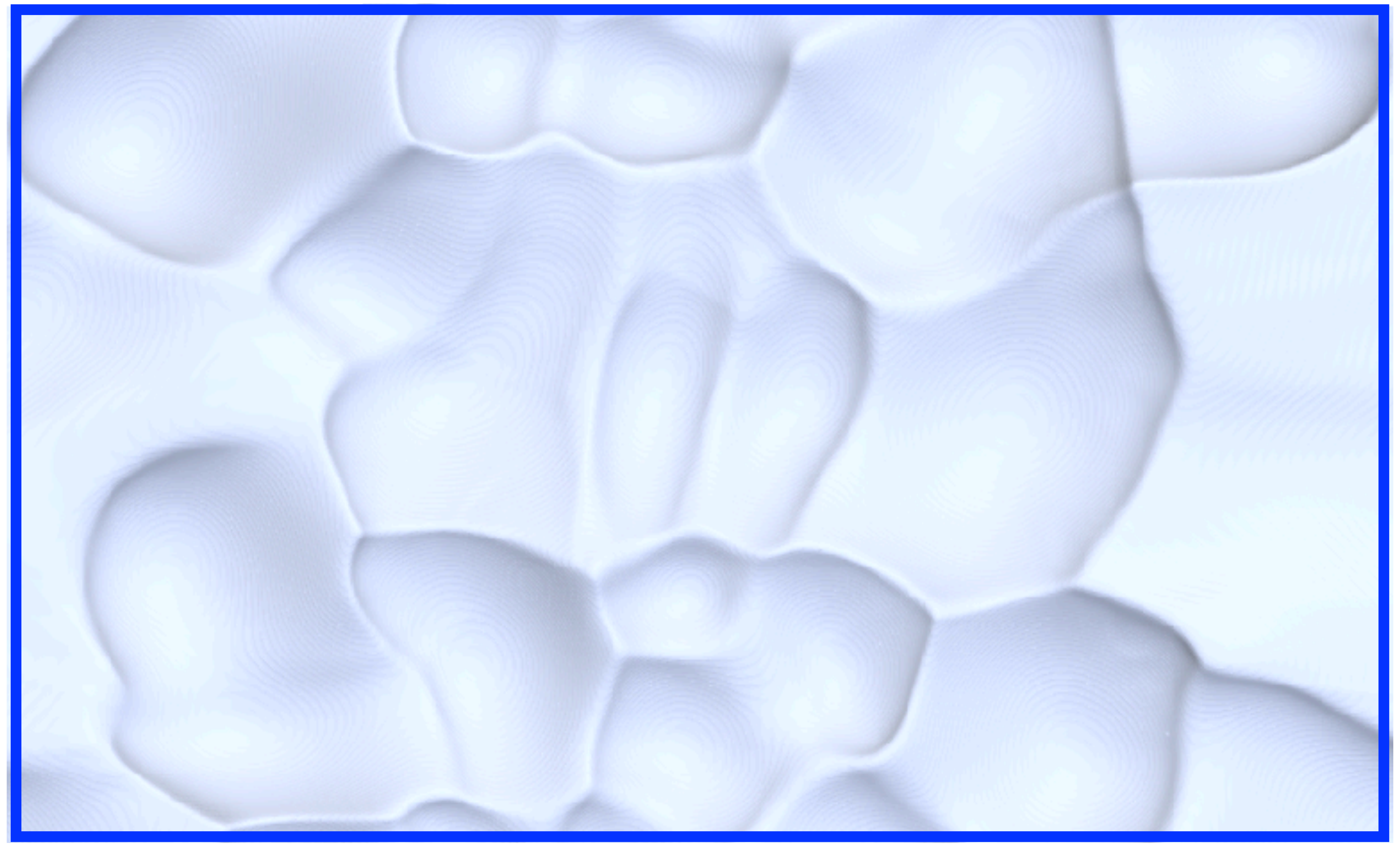

field measurements

DNS numerics

Scallops from field measurements vs numerical ones

But note:

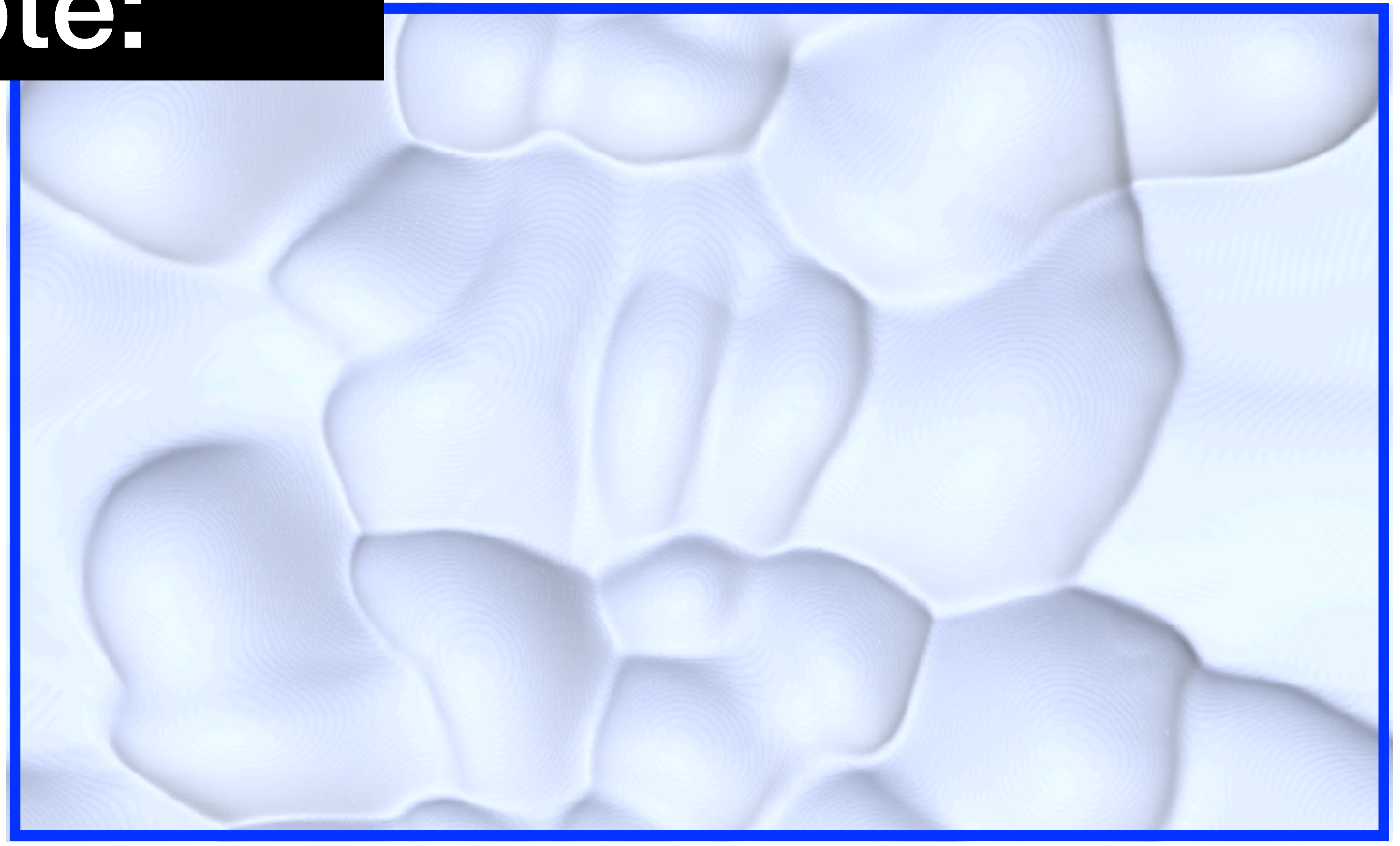

field
measurements

DNS
numerics

Scallops from field measurements vs numerical ones

But note:

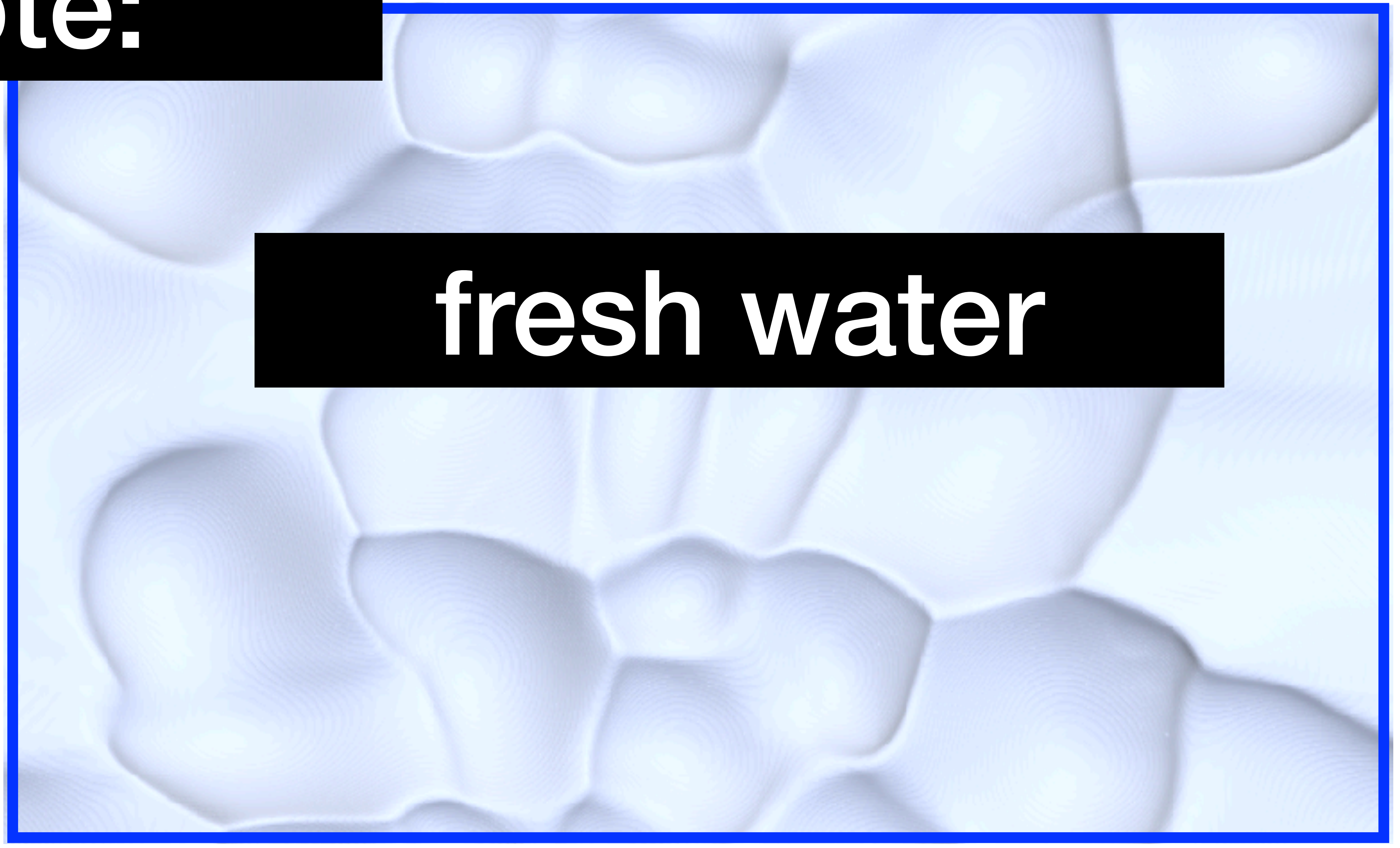

field measurements

DNS numerics

Scallops from field measurements vs numerical ones

But note:

salt water

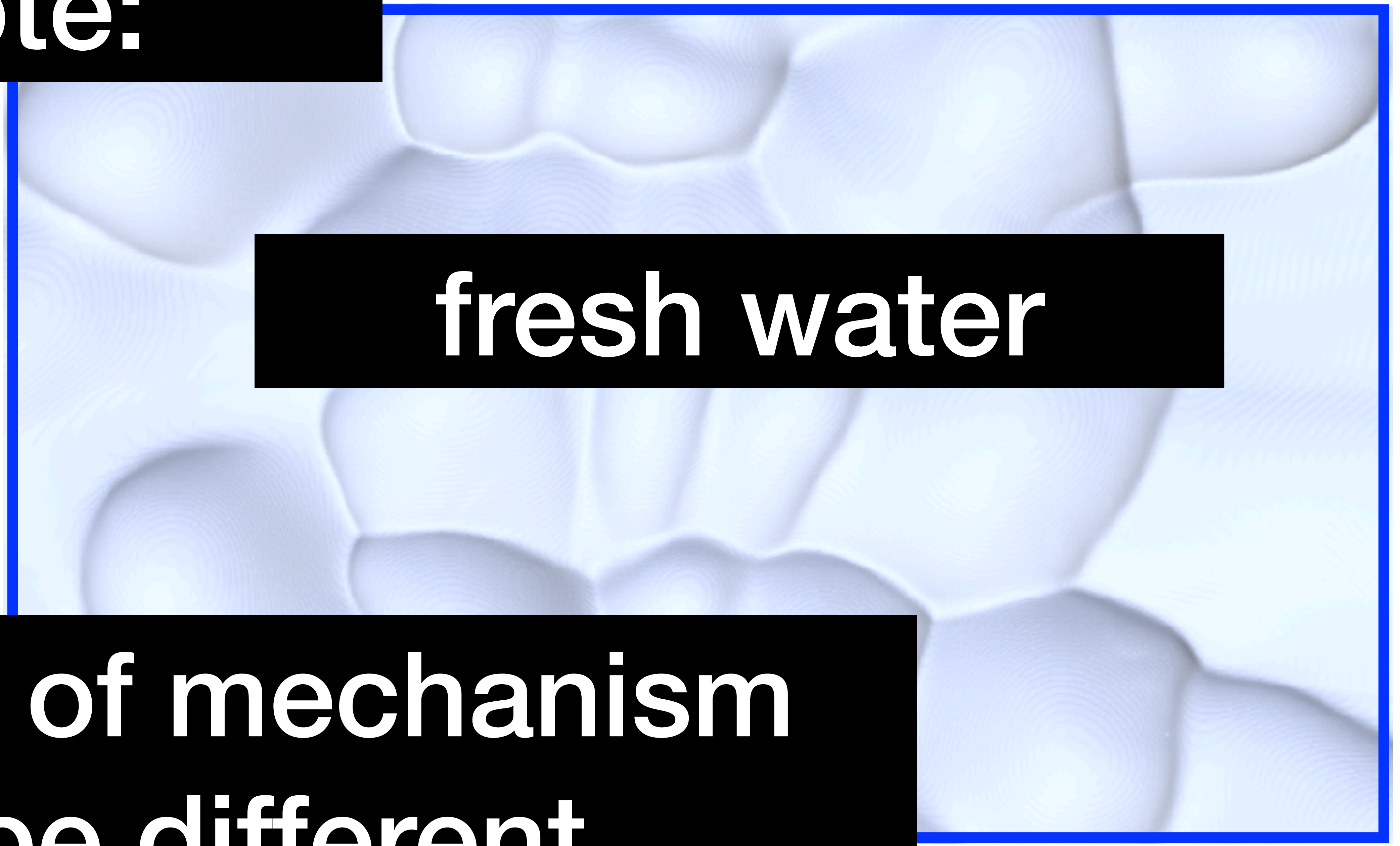

fresh water

So details of mechanism must be different

field measurements

DNS numerics

Quantification of evolution of wavelength

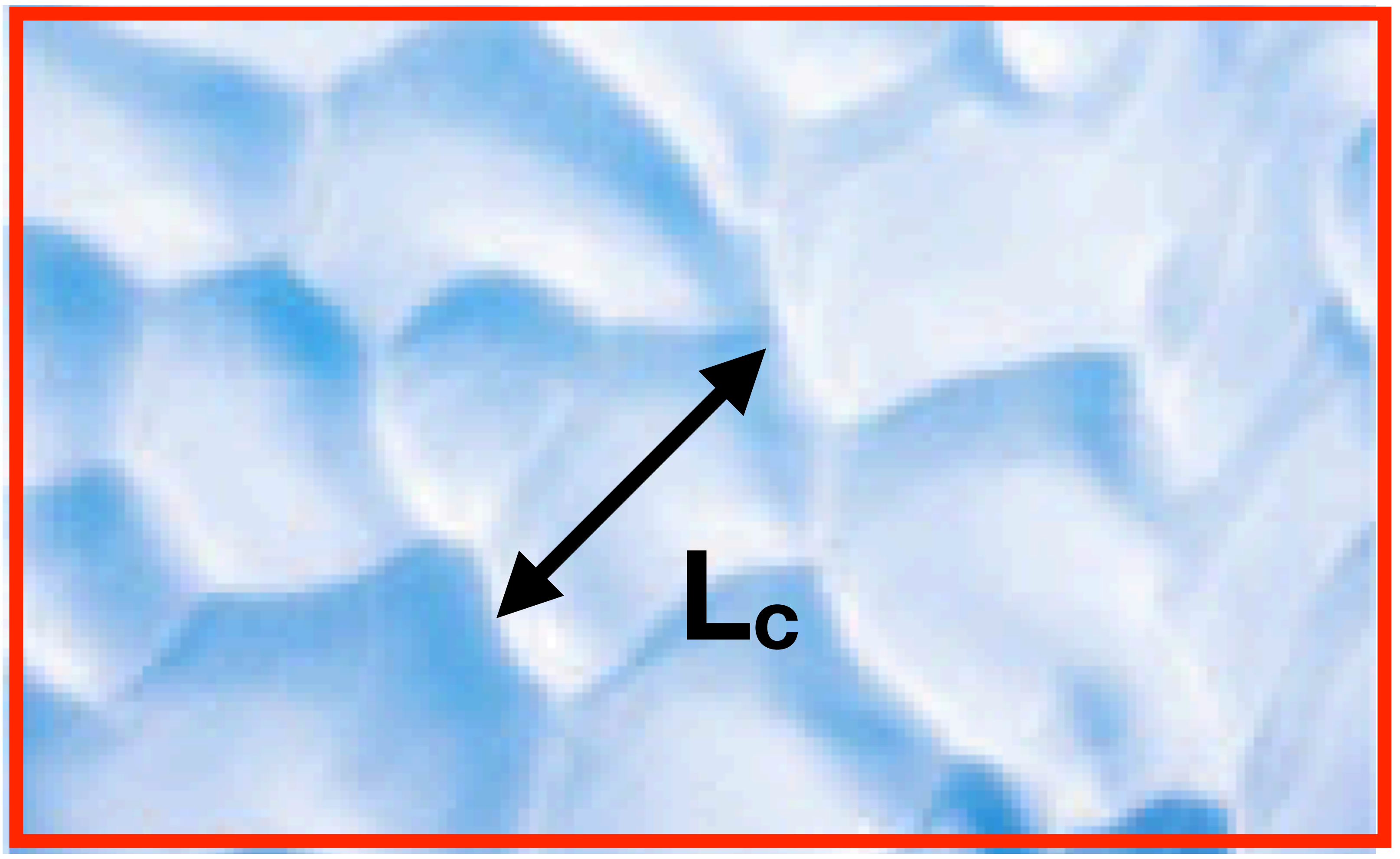

Quantification of evolution of wavelength

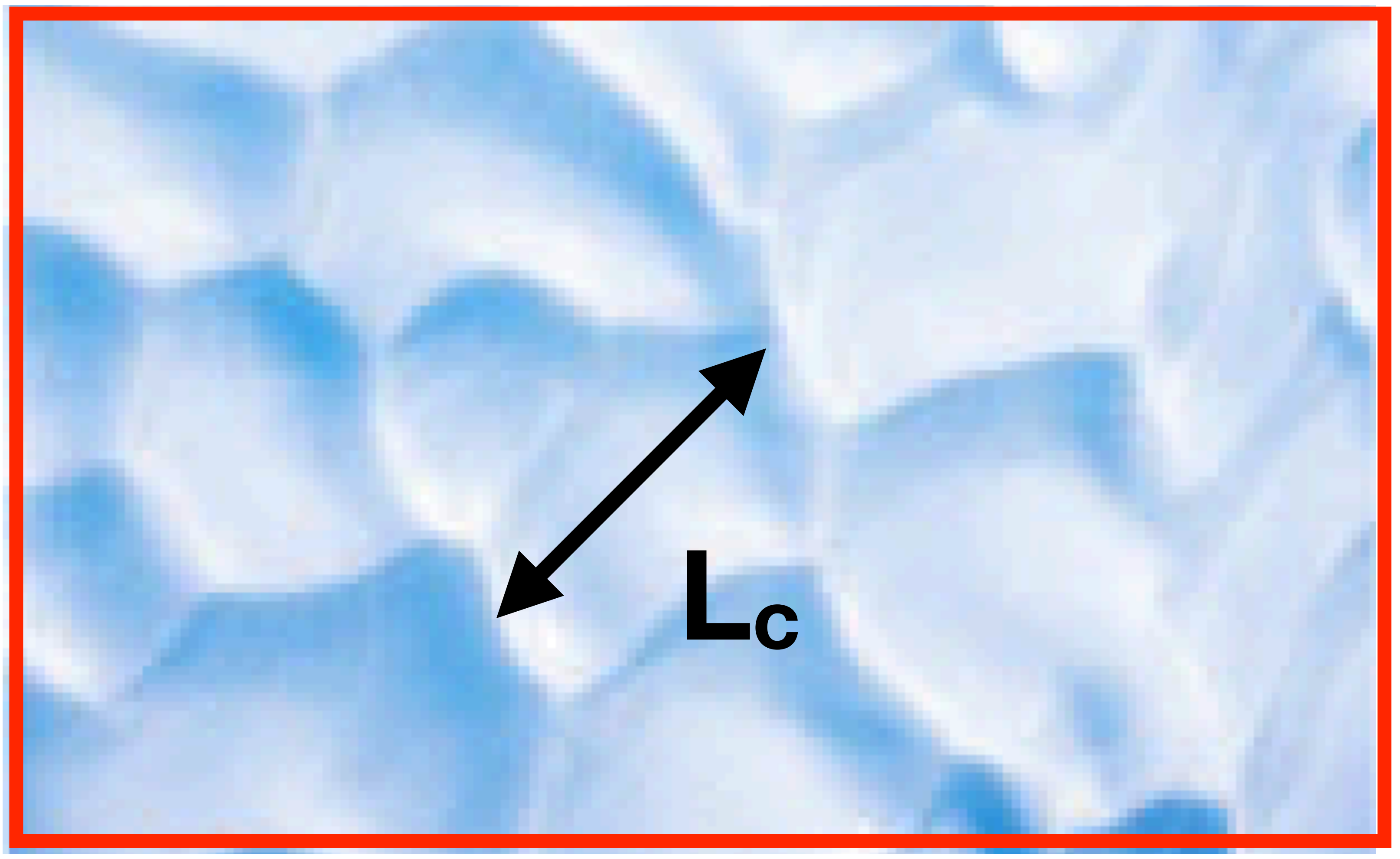

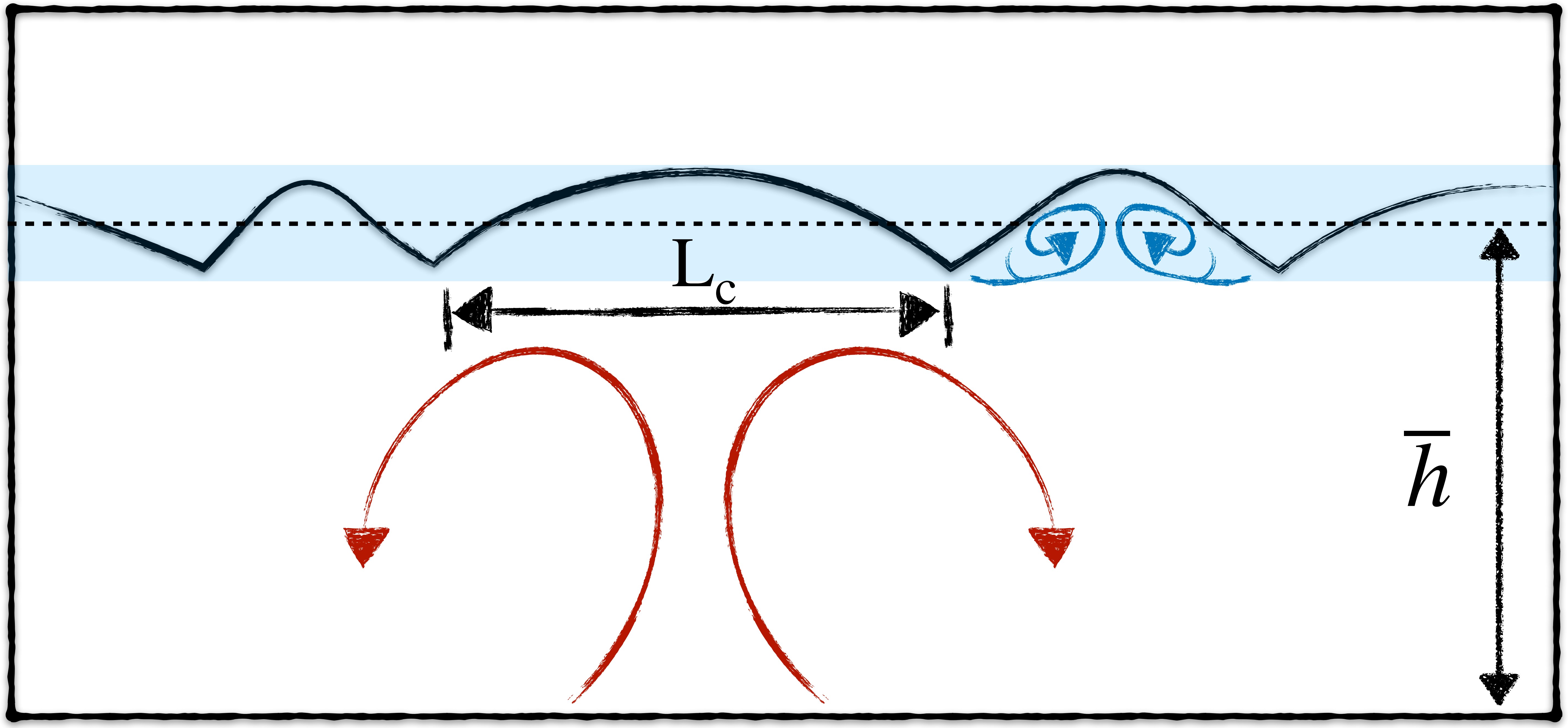

Quantification of evolution of wavelength

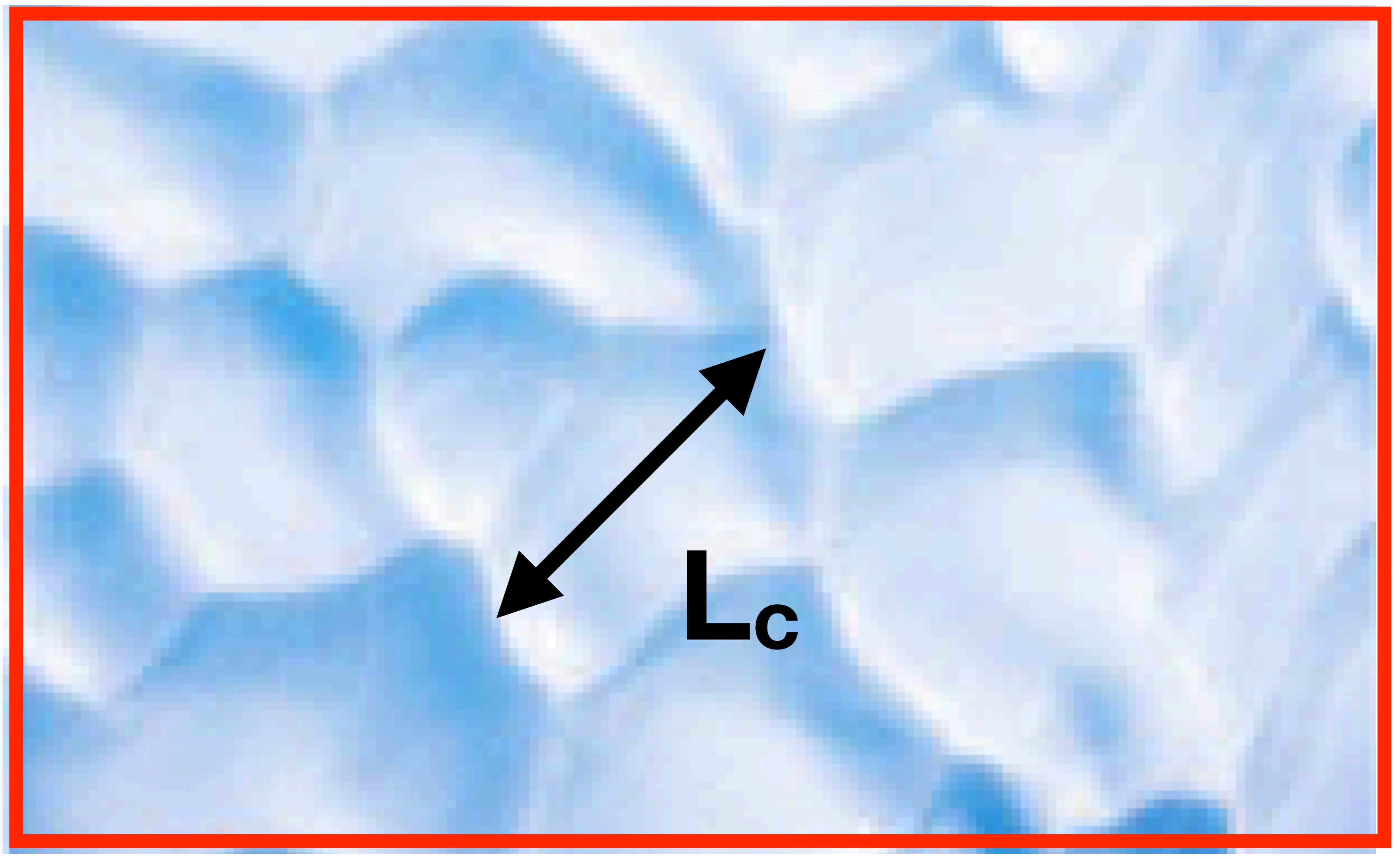

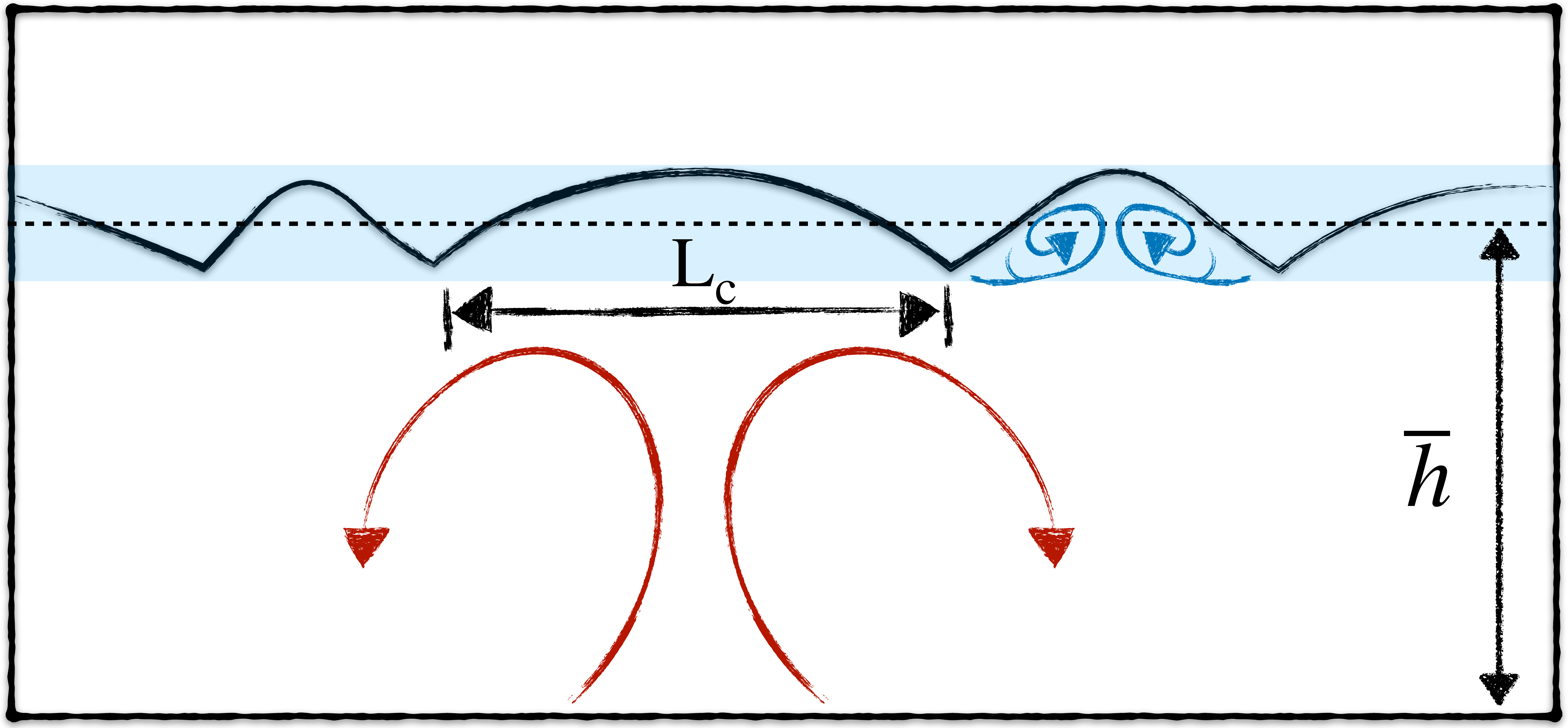

Aspect ratio: $\Gamma_c(t) = \dfrac{L_c(t)}{\bar{h}(t)}$

Quantification of evolution of wavelength

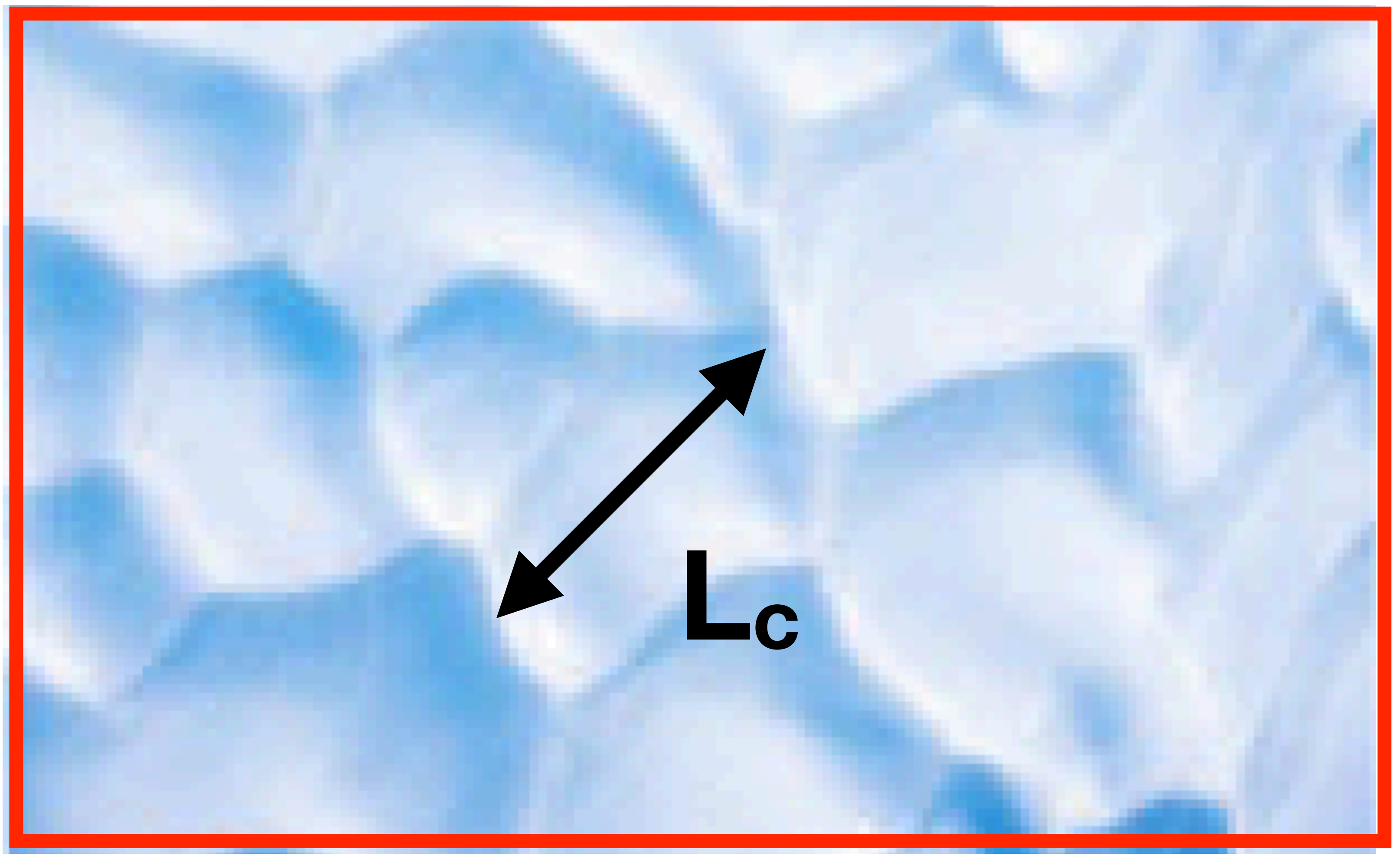

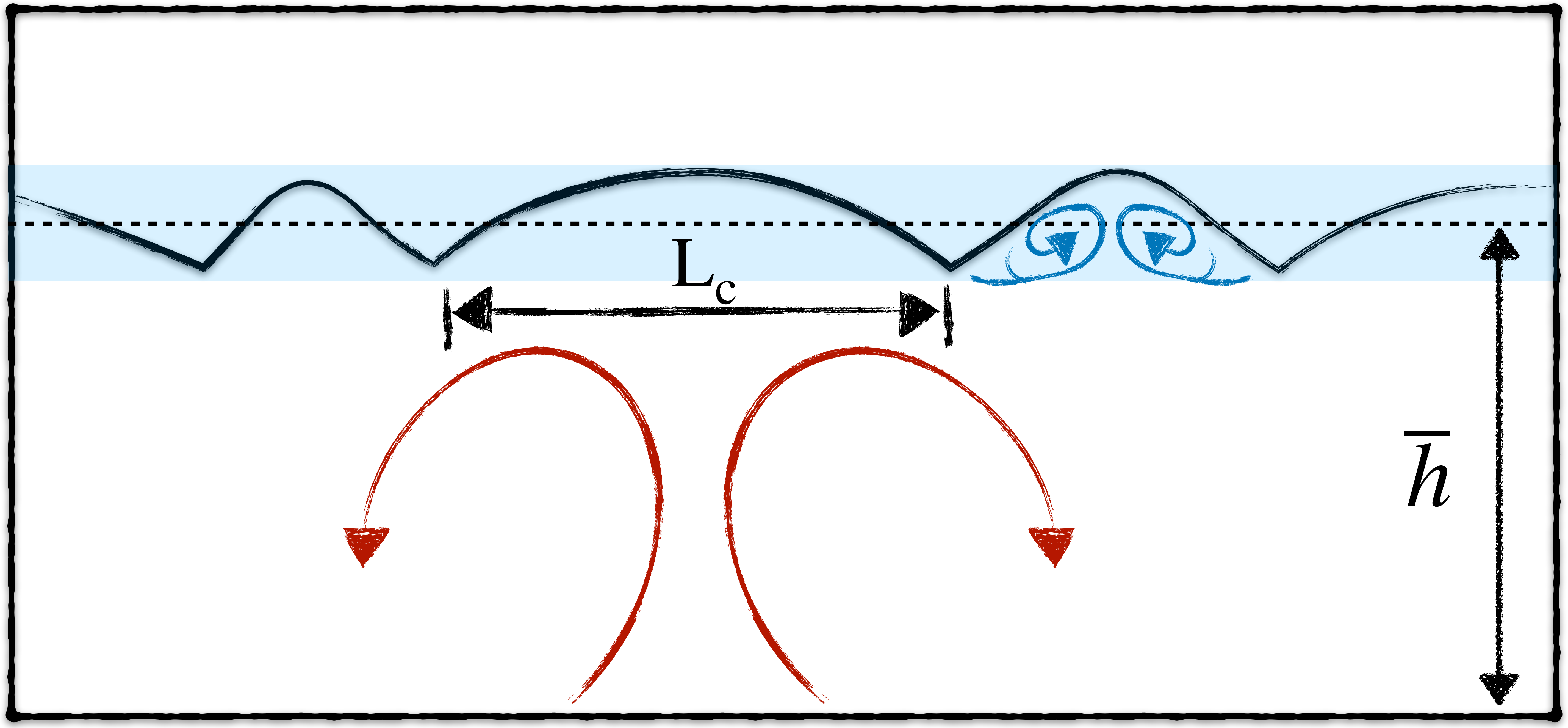

$\Gamma_c(t)?$

Aspect ratio: $\Gamma_c(t) = \dfrac{L_c(t)}{\bar{h}(t)}$

Quantification of evolution of wavelength

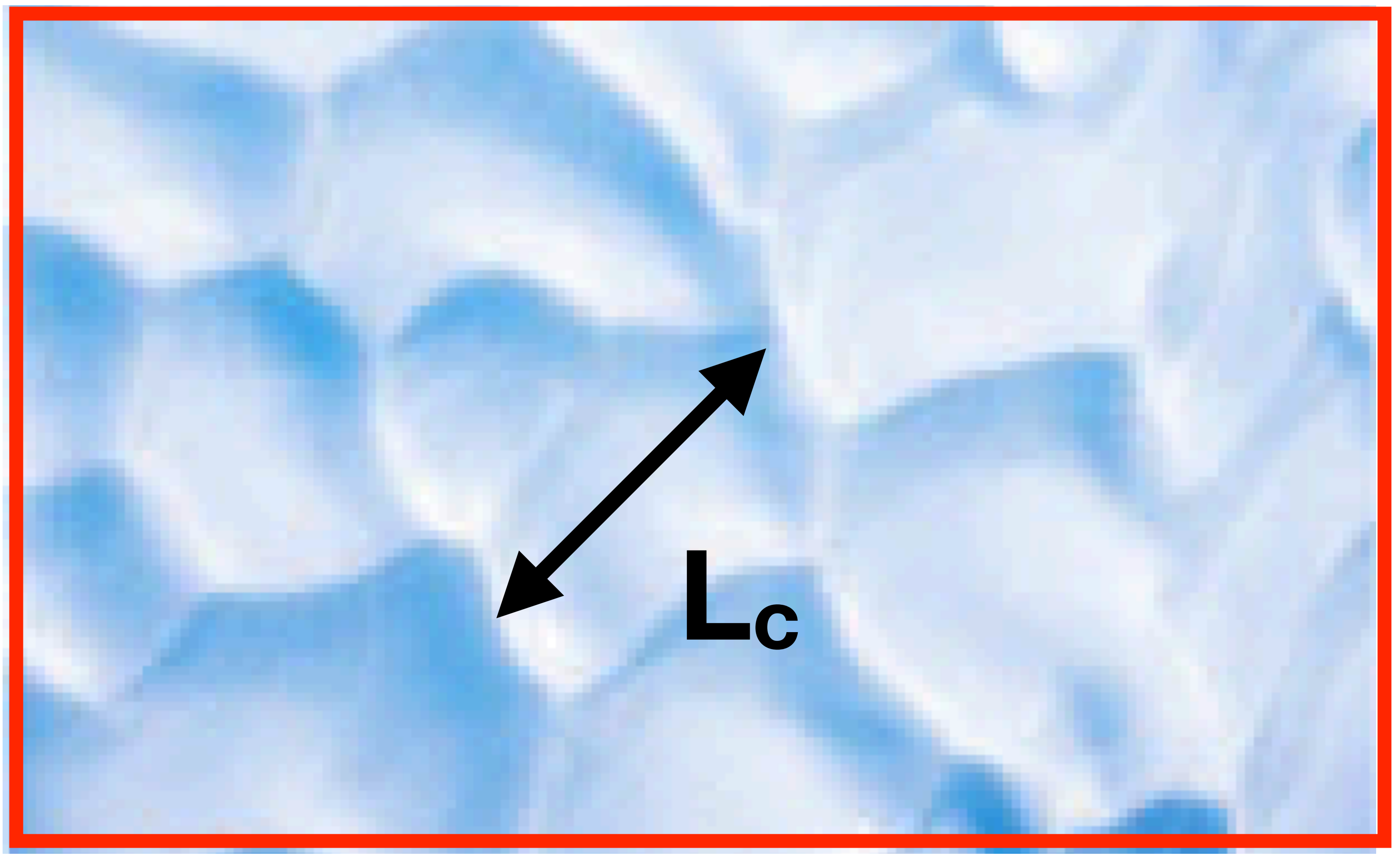

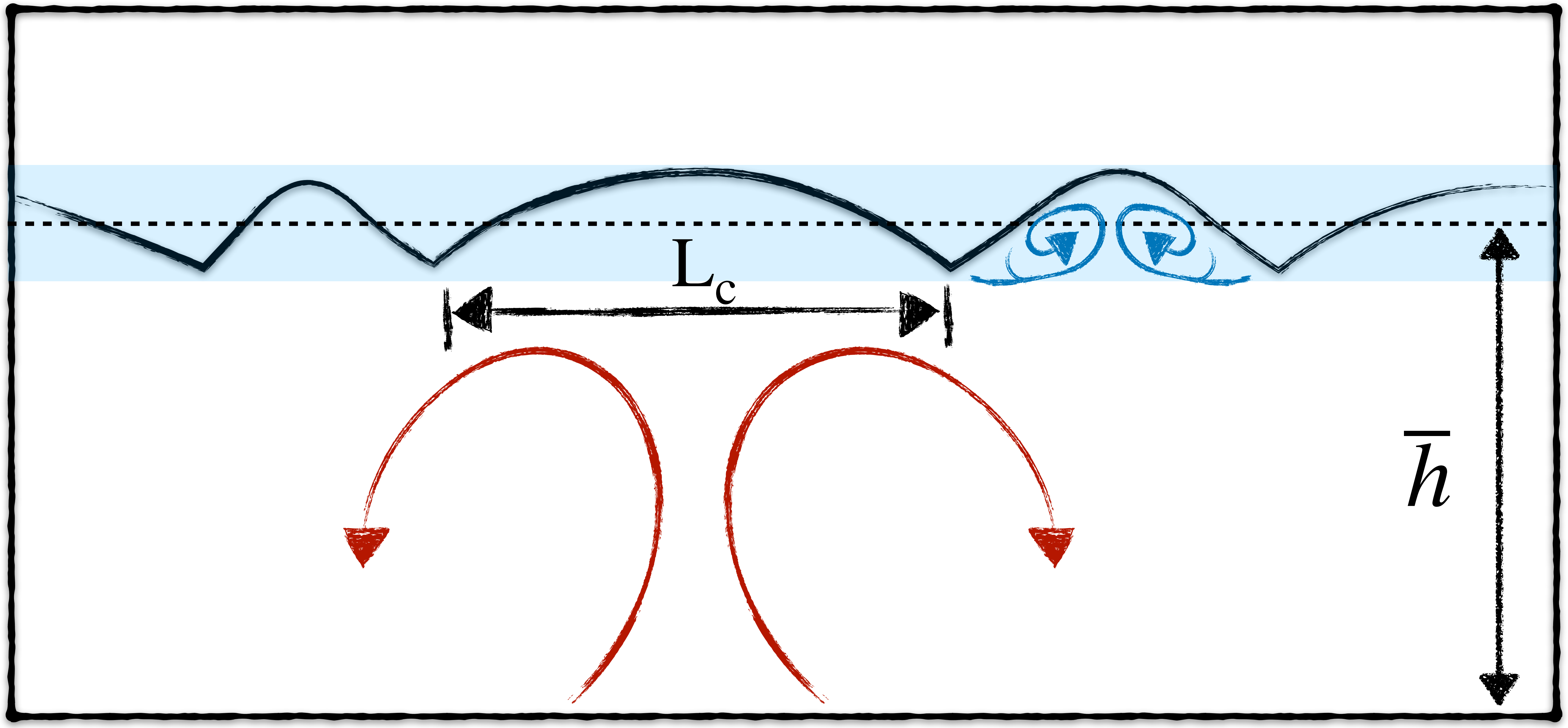

Aspect ratio: $\Gamma_c(t) = \dfrac{L_c(t)}{\overline{h}(t)}$

$\Gamma_c(t)$?

or: $\Gamma_c(\overline{h})$?

Quantification of evolution of wavelength

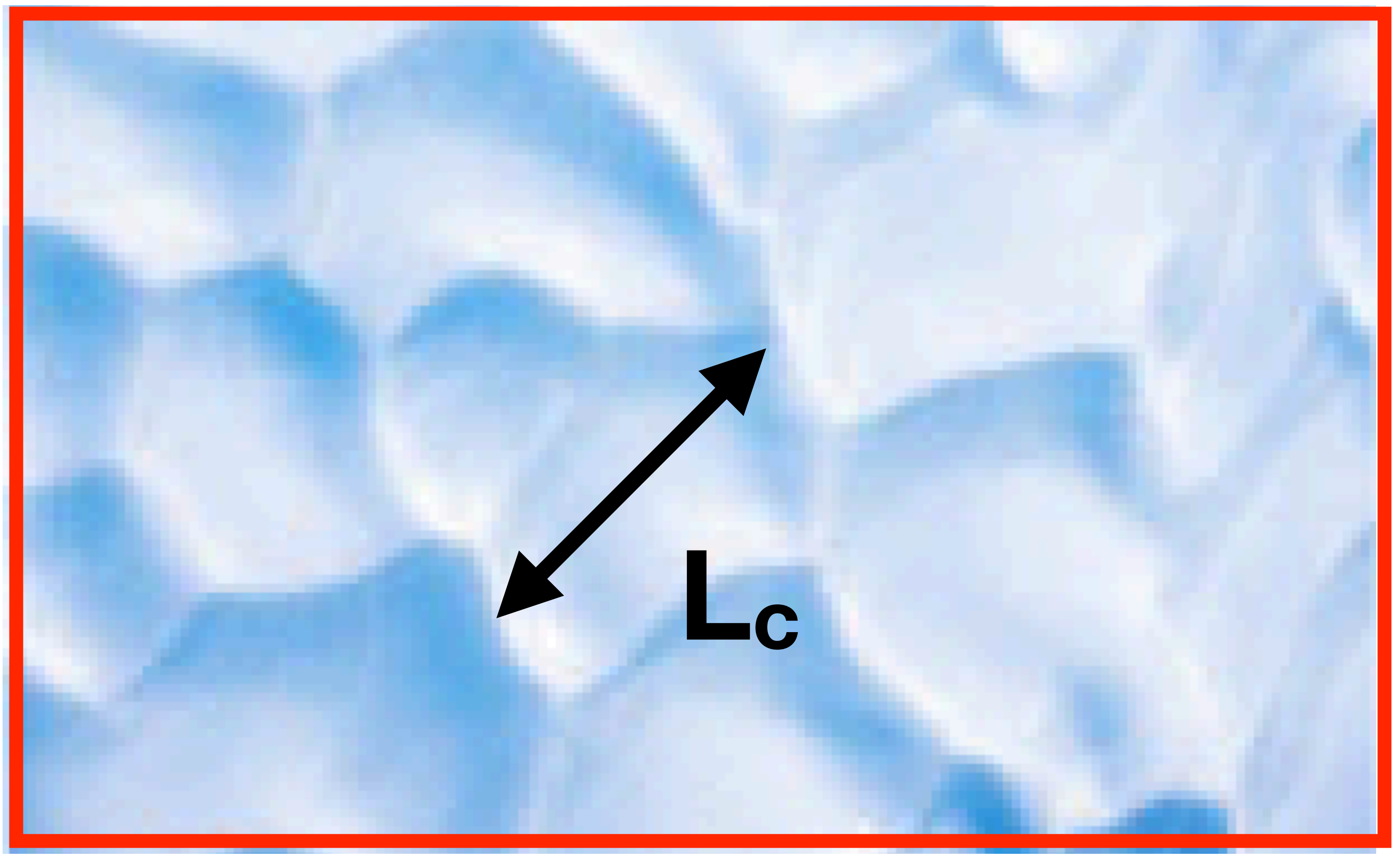

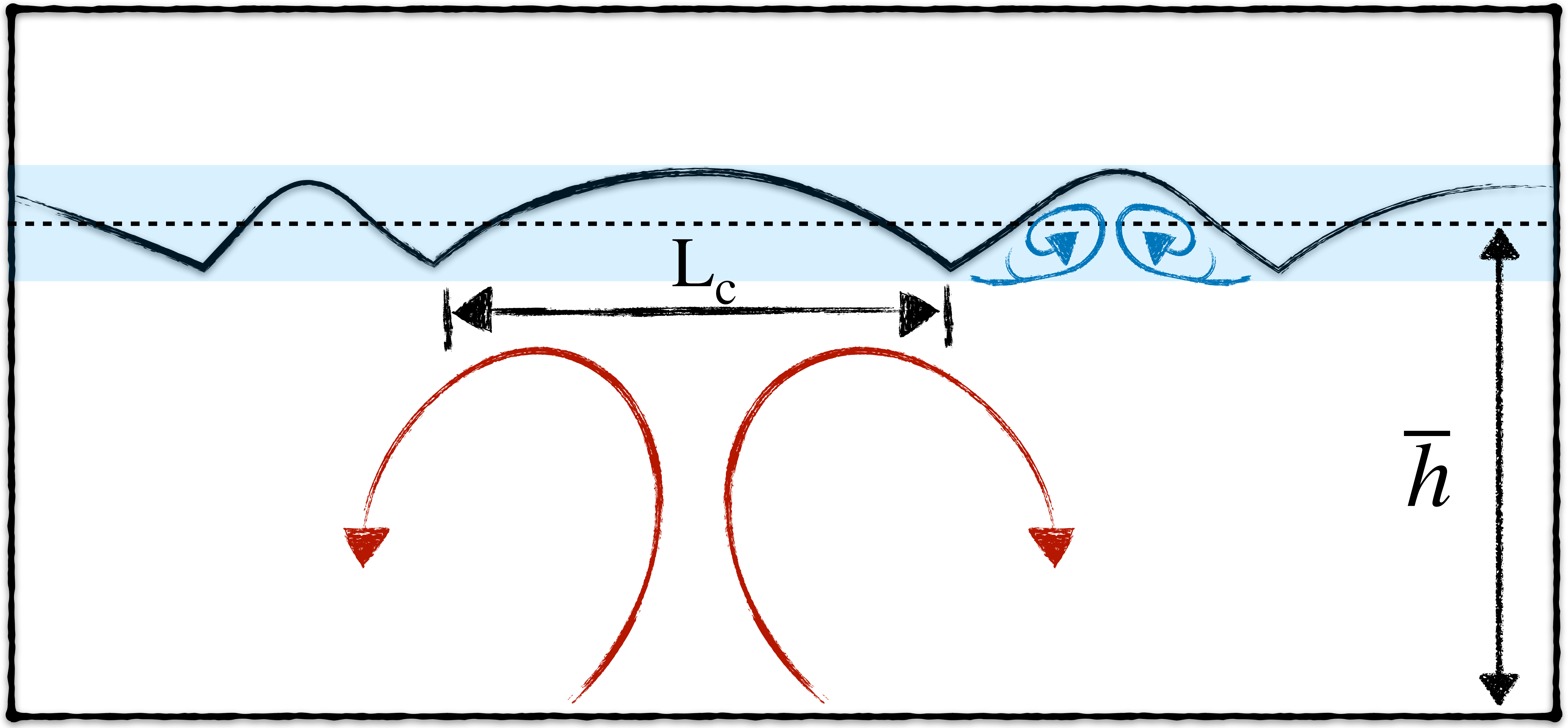

Aspect ratio: $\Gamma_c(t) = \dfrac{L_c(t)}{\overline{h}(t)}$

$\Gamma_c(t)$?

or: $\Gamma_c(\overline{h})$?

or: $\Gamma_c(Ra^*)$?

Evolution of typical wavelength

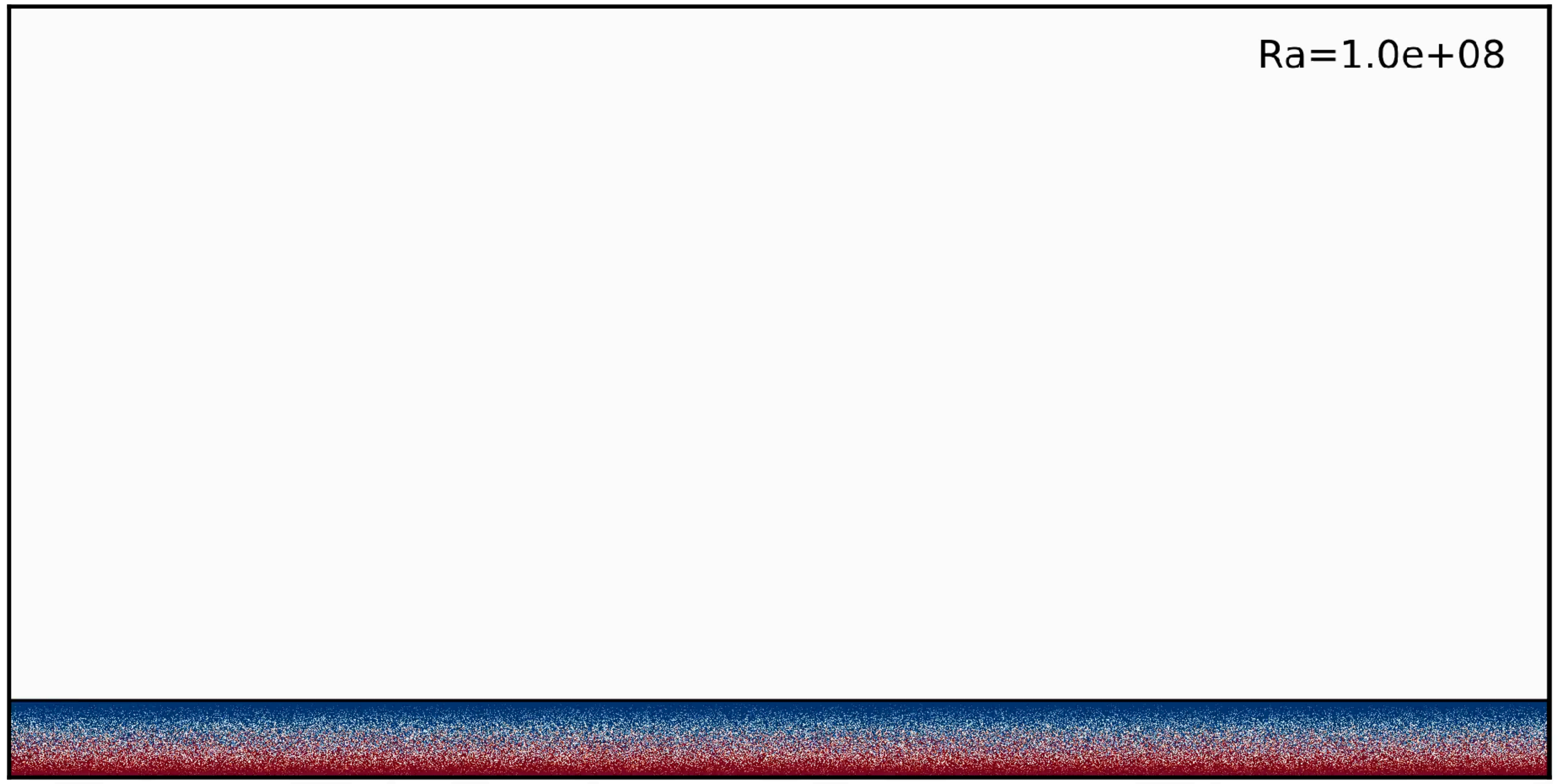

spectral analysis:

$$\frac{\lambda(t)}{H} = \frac{\int_0^\infty k^{-1} |\hat{h}(k,t)|^2 dk}{\int_0^\infty |\hat{h}(k,t)|^2 dk}$$

Evolution of typical wavelength

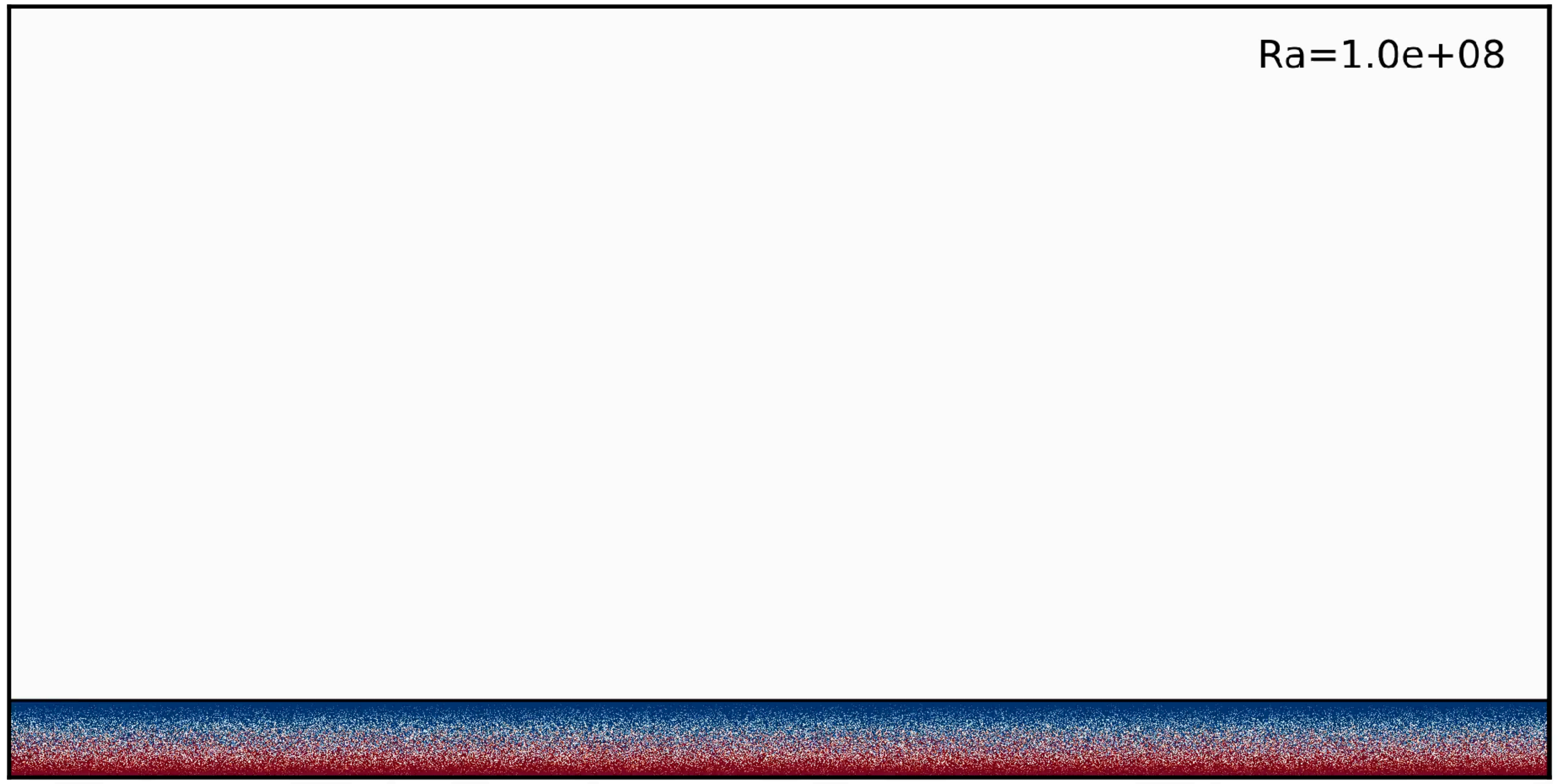

spectral analysis:

$$\frac{\lambda(t)}{H} = \frac{\int_0^\infty k^{-1}|\hat{h}(k,t)|^2 dk}{\int_0^\infty |\hat{h}(k,t)|^2 dk}$$

Evolution of typical wavelength

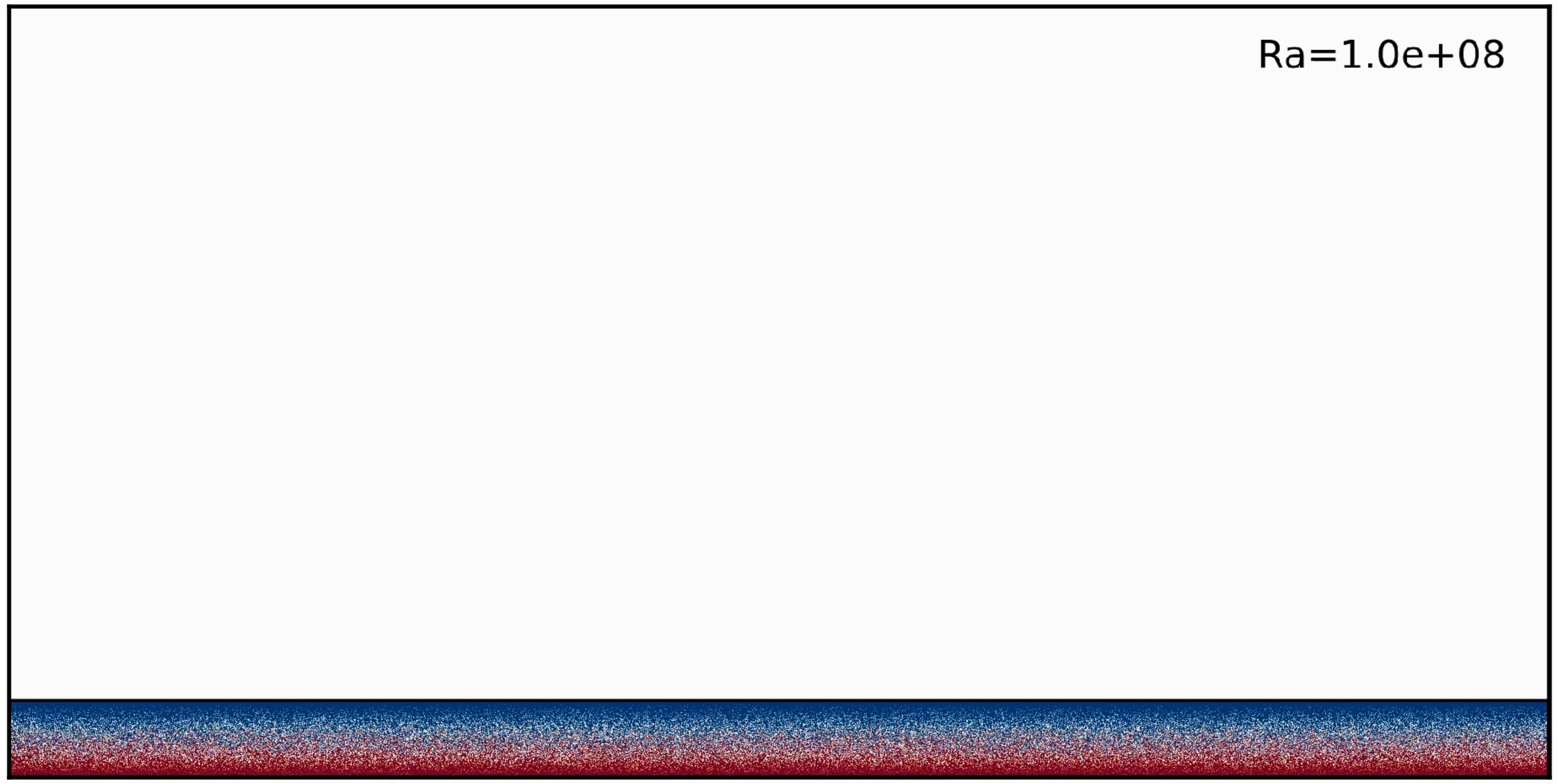

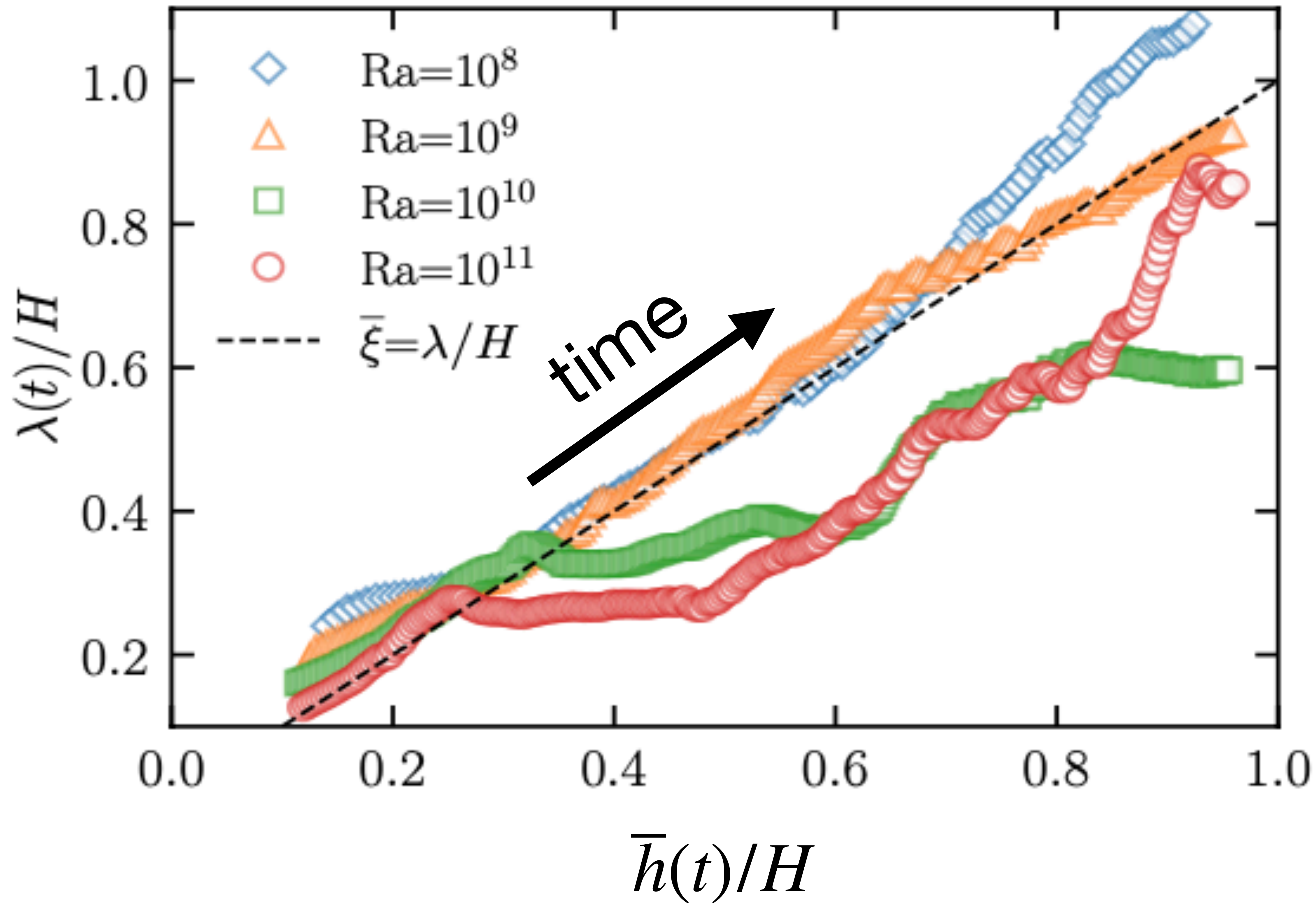

spectral analysis:

$$\frac{\lambda(t)}{H} = \frac{\int_0^\infty k^{-1}|\hat{h}(k,t)|^2 dk}{\int_0^\infty |\hat{h}(k,t)|^2 dk}$$

$$\boxed{\lambda(t) \sim \bar{h}(t)}$$

Evolution of typical wavelength

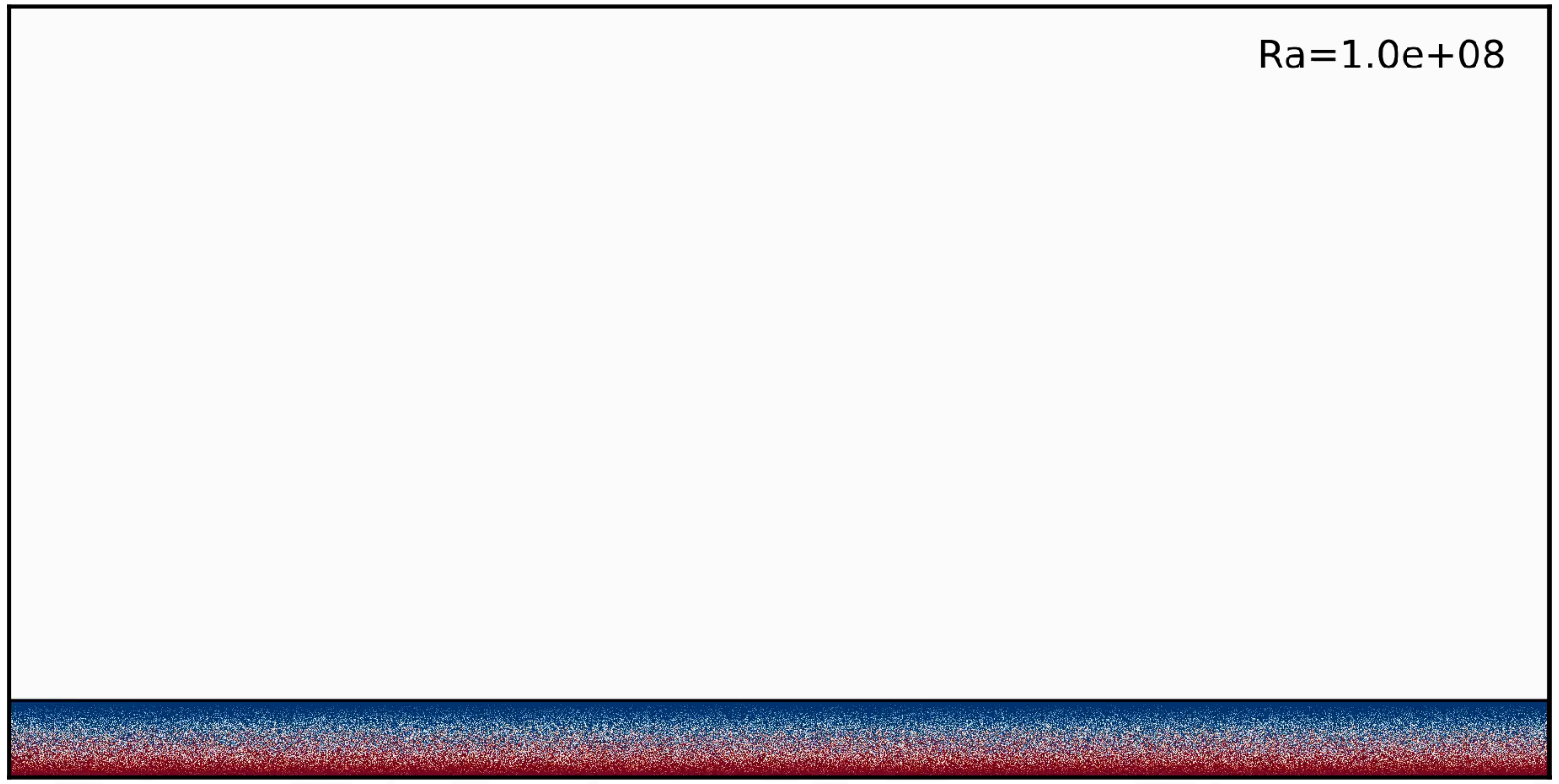

spectral analysis:

$$\frac{\lambda(t)}{H} = \frac{\int_0^\infty k^{-1}|\hat{h}(k,t)|^2 dk}{\int_0^\infty |\hat{h}(k,t)|^2 dk}$$

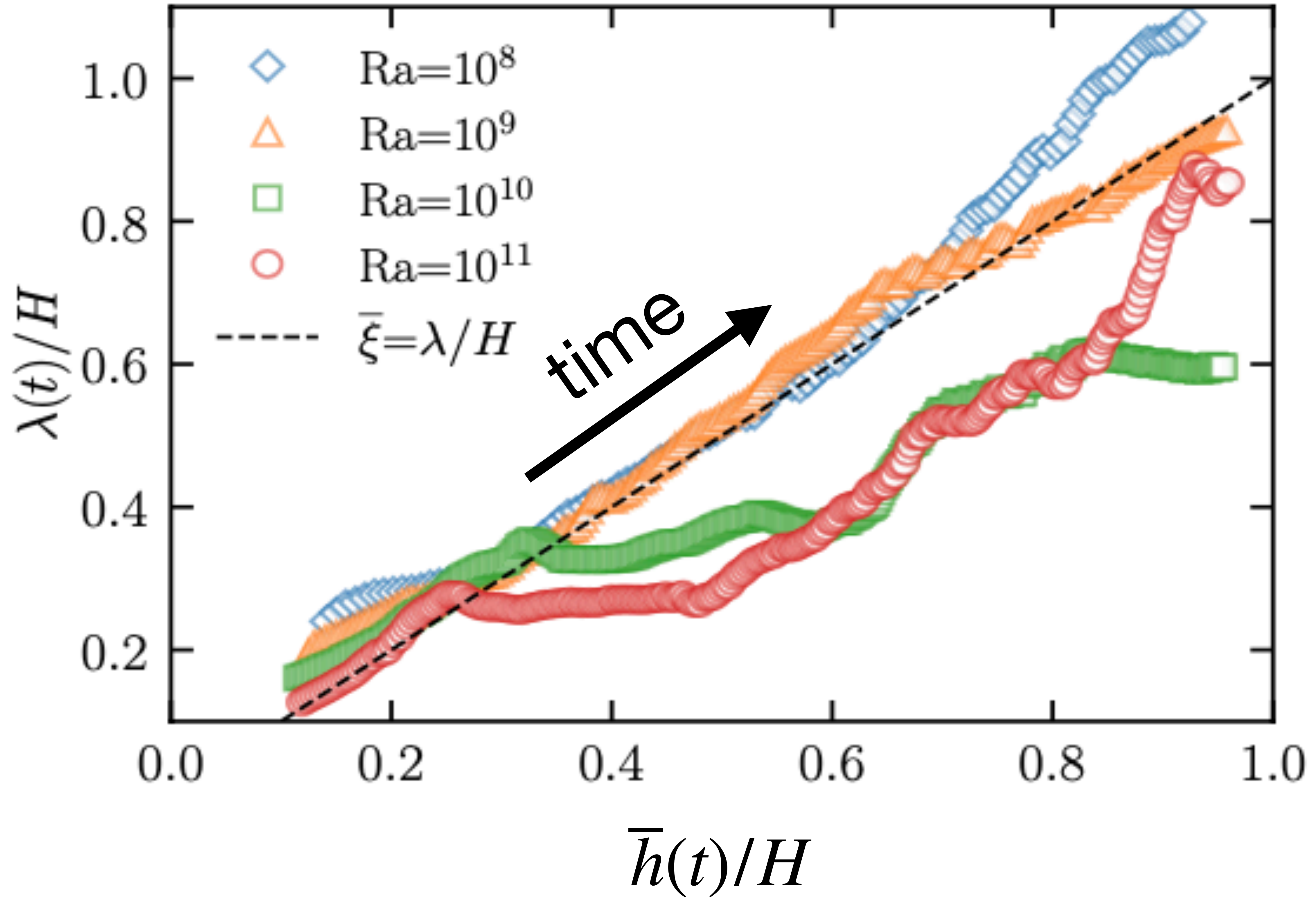

$$\boxed{\lambda(t) \sim \overline{h}(t)}$$

$$\boxed{\Gamma_c(t) = \frac{\lambda(t)}{\overline{h}(t)}}$$

cellular aspect ratio

Aspect ratio of cellular structure & of rolls

$$\boxed{\Gamma_c(t) = \frac{\lambda(t)}{\overline{h}(t)}}$$

cellular
aspect ratio

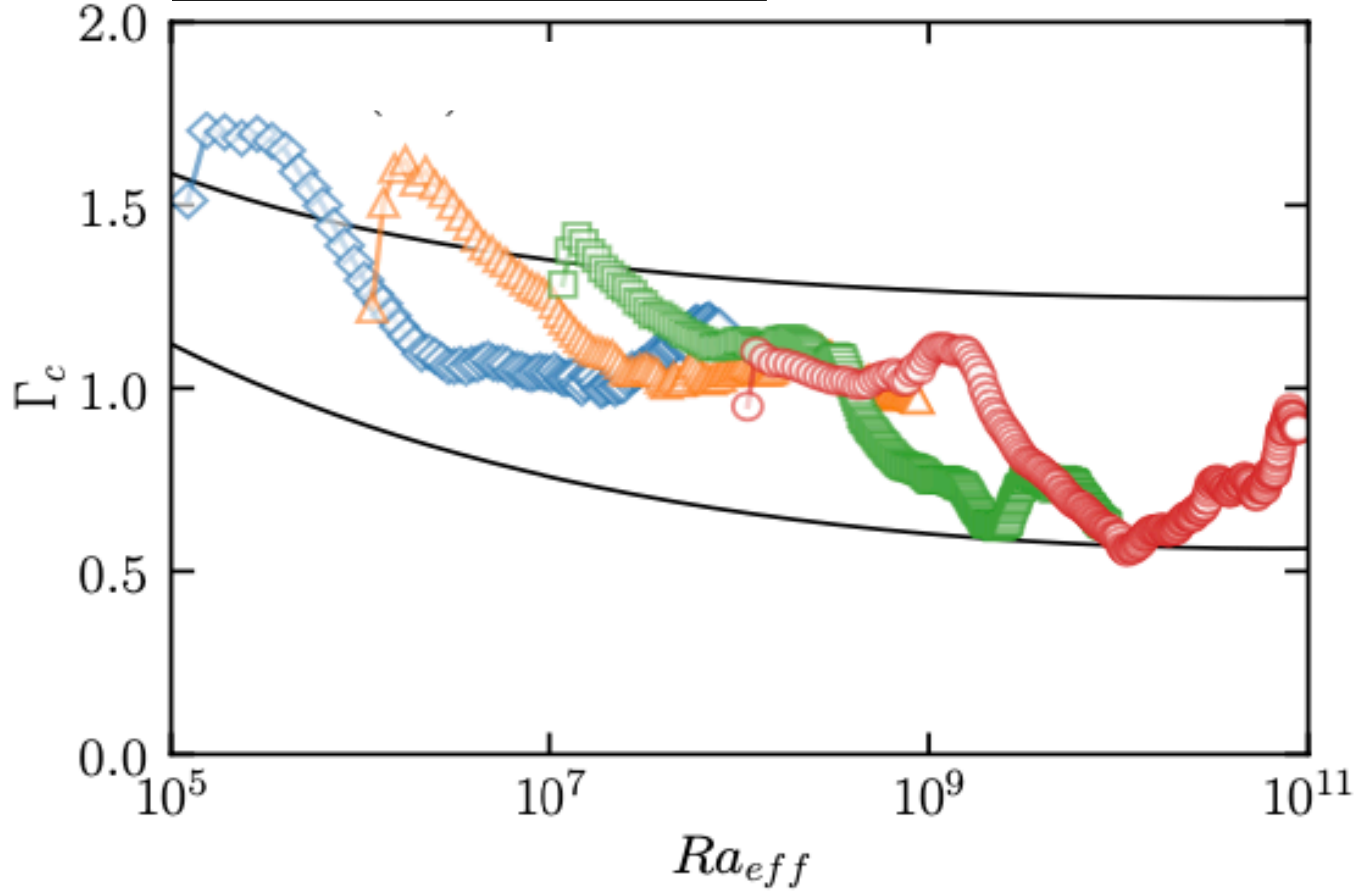

Aspect ratio of cellular structure & of rolls

$$\Gamma_c(t) = \frac{\lambda(t)}{\overline{h}(t)}$$

cellular aspect ratio

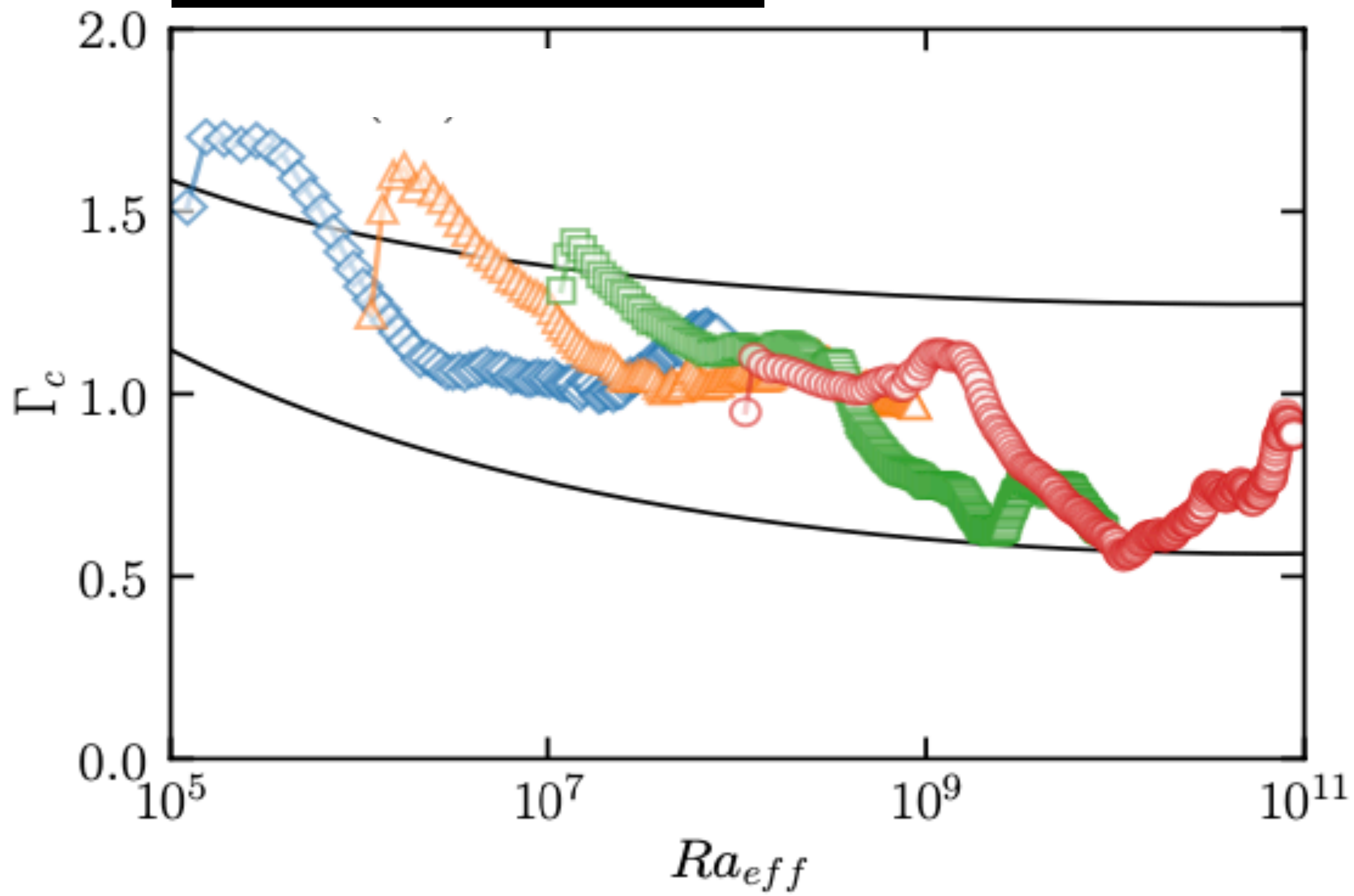

$$\Gamma_r(t) = \frac{\lambda_{roll}(t)}{\overline{h}(t)}$$

roll aspect ratio

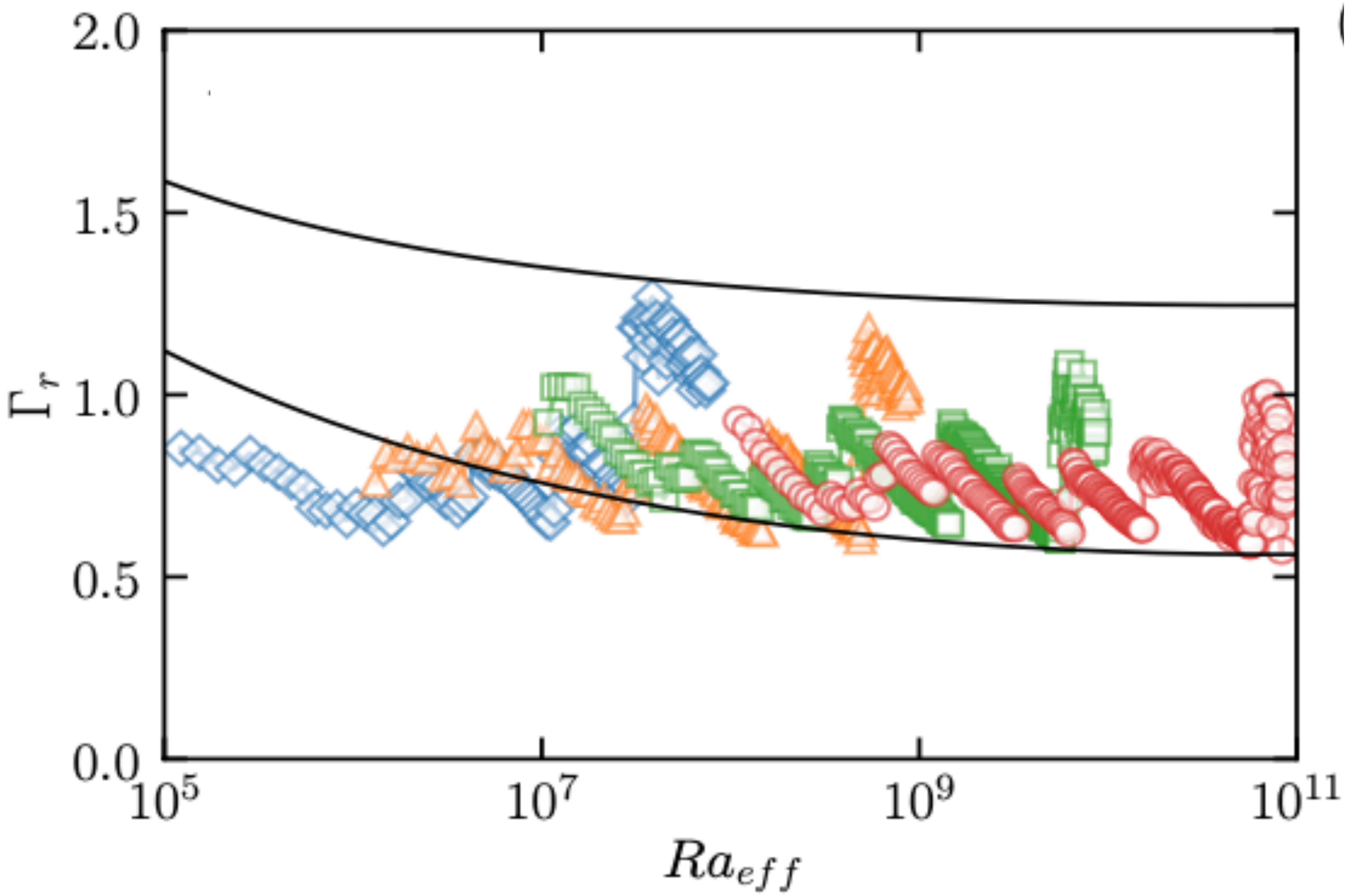

Aspect ratio of cellular structure & of rolls

$$\boxed{\Gamma_c(t) = \frac{\lambda(t)}{\overline{h}(t)}}$$

cellular
aspect ratio

$$\boxed{\Gamma_r(t) = \frac{\lambda_{roll}(t)}{\overline{h}(t)}}$$

roll
aspect ratio

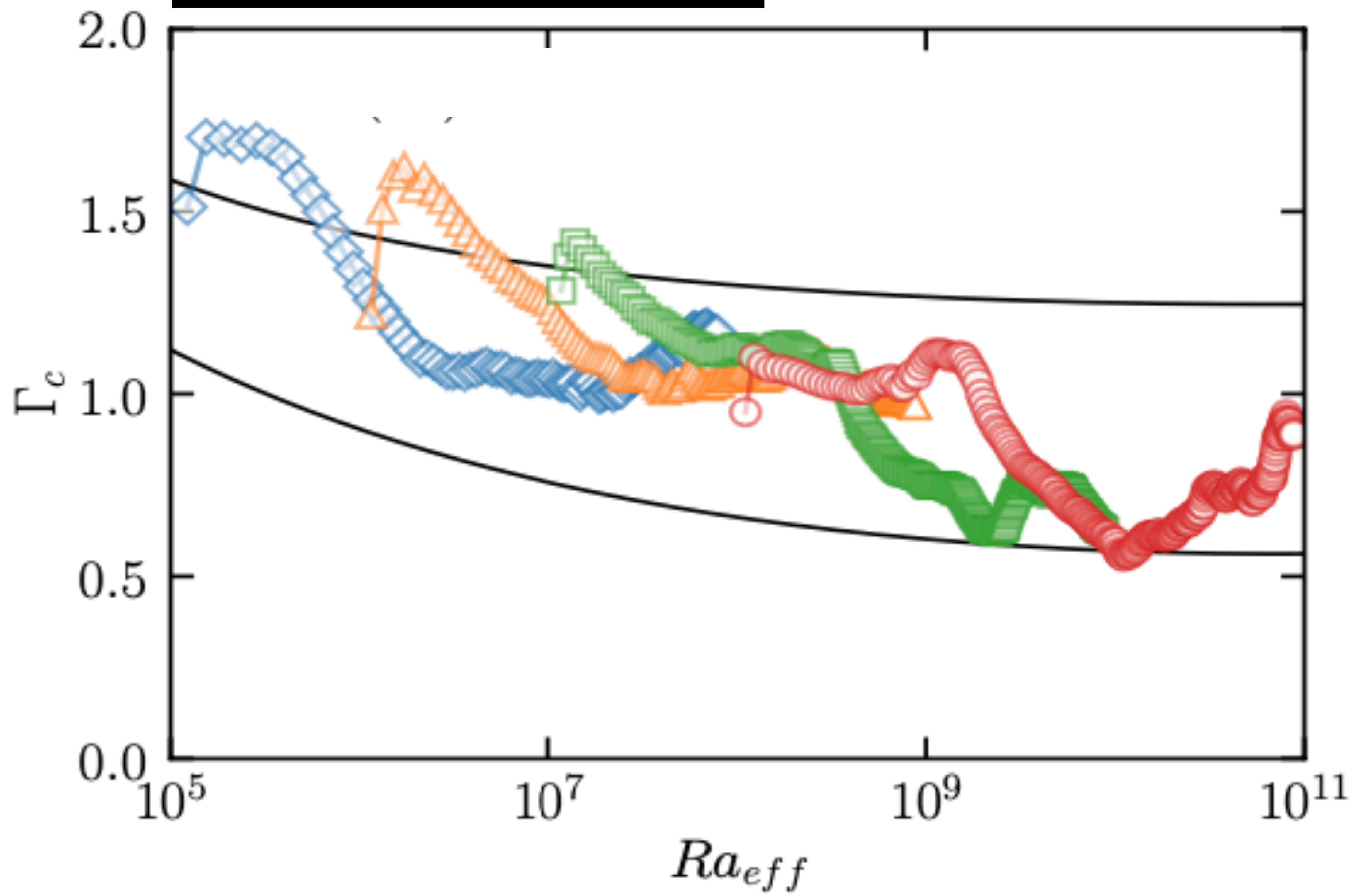

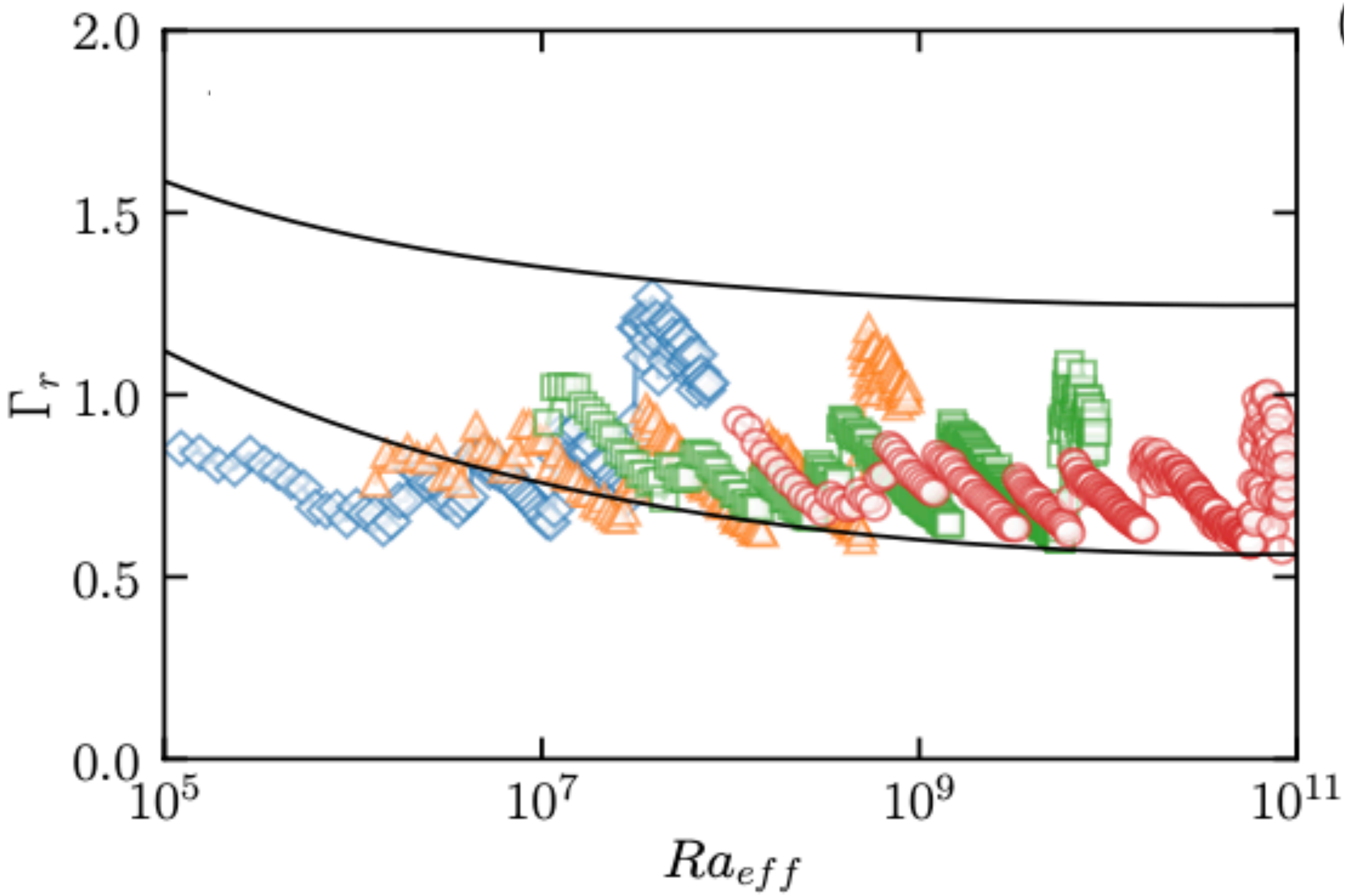

Lines: upper and lower bounds for **rolls** for **smooth walls** from theory:
Wang, Verzicco, Lohse, Shishkina, Phys. Rev. Lett. 125, 074501 (2020)

Allowed aspect ratios Γ_r

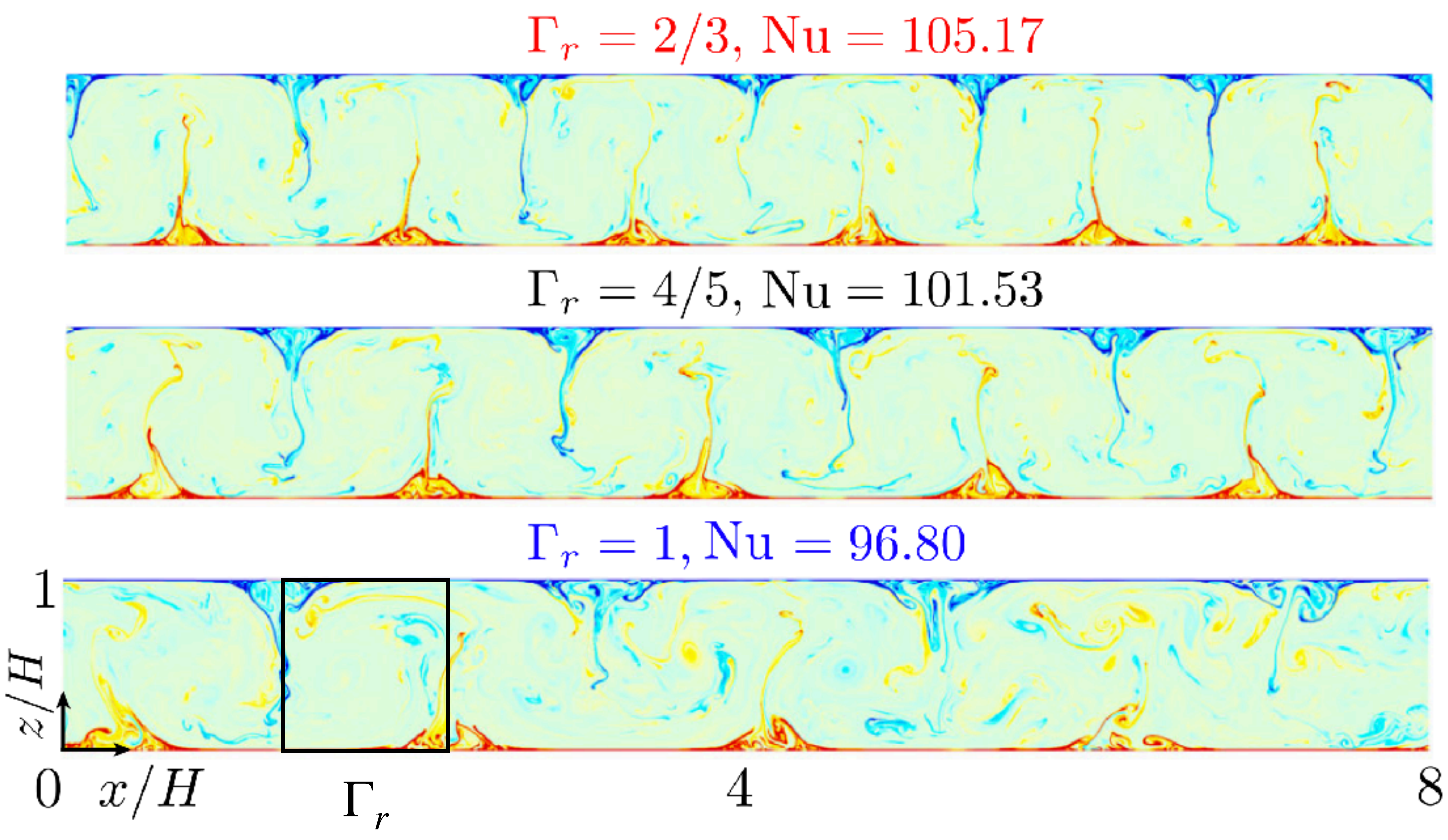

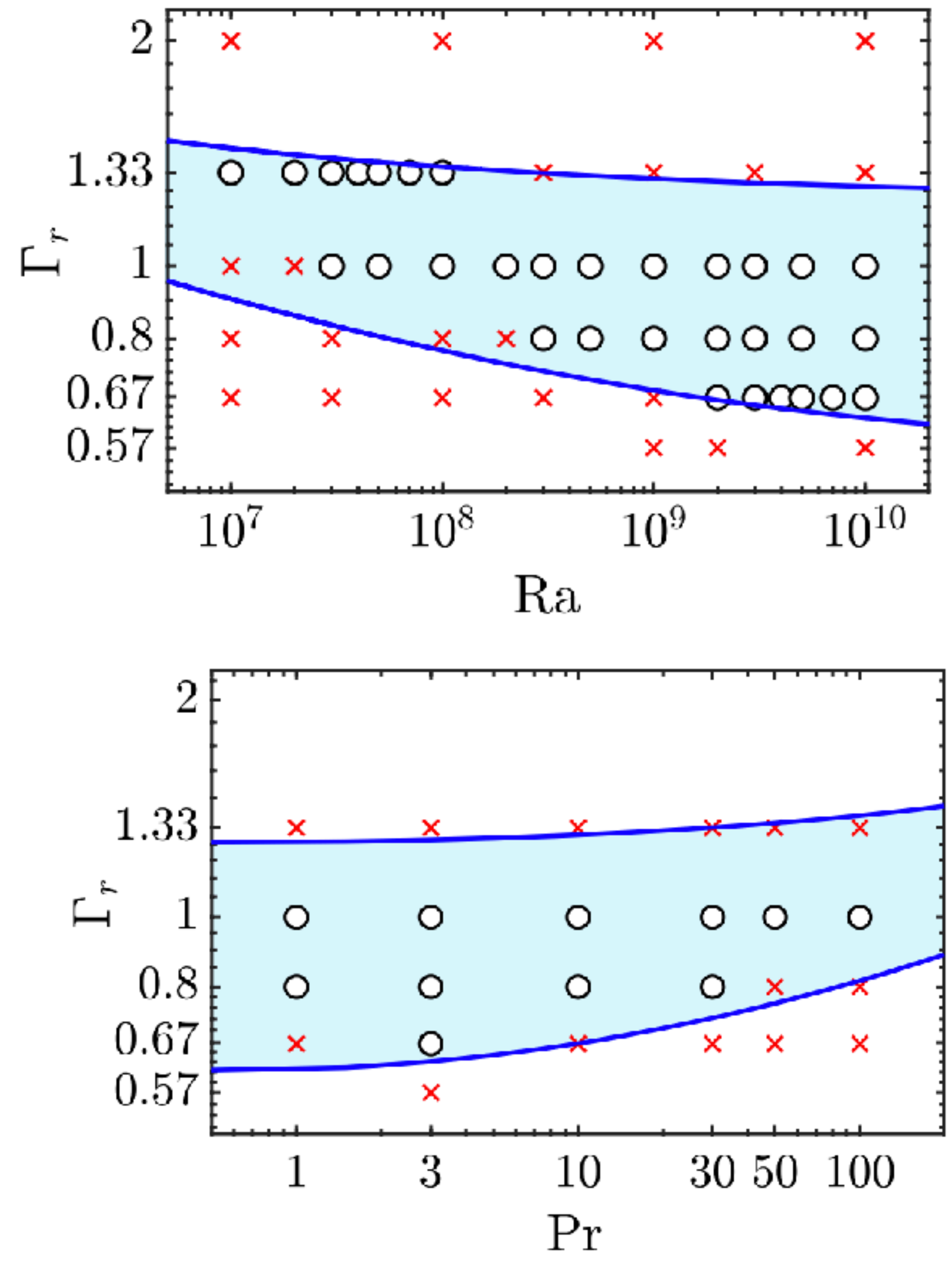

smooth wall case

Wang, Verzicco, Lohse, Shishkina, Phys. Rev. Lett. 125, 074501 (2020)

Aspect ratio of cellular structure & of rolls

$$\Gamma_c(t) = \frac{\lambda(t)}{\overline{h}(t)}$$

cellular aspect ratio

$$\Gamma_r(t) = \frac{\lambda_{roll}(t)}{\overline{h}(t)}$$

roll aspect ratio

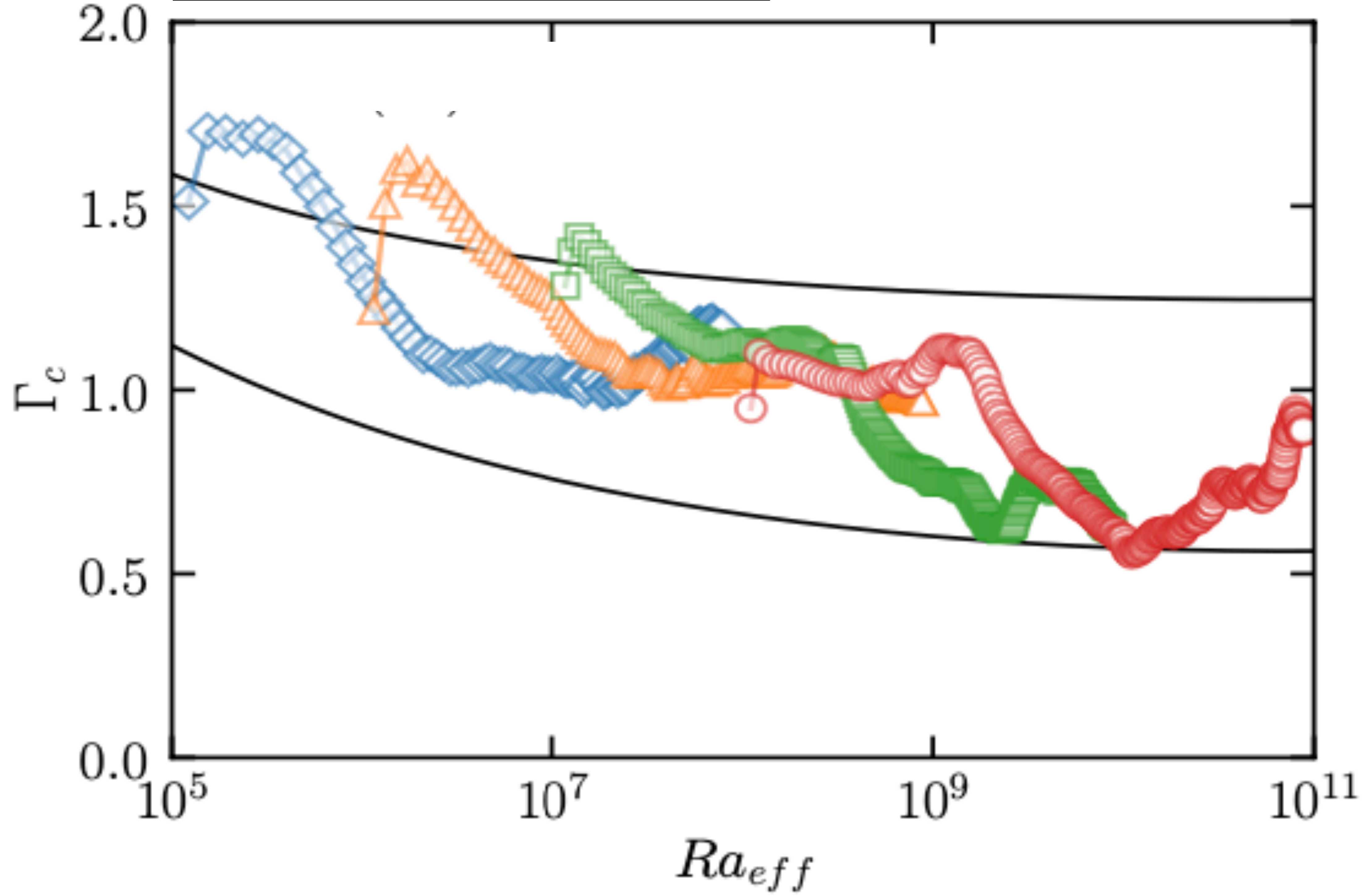

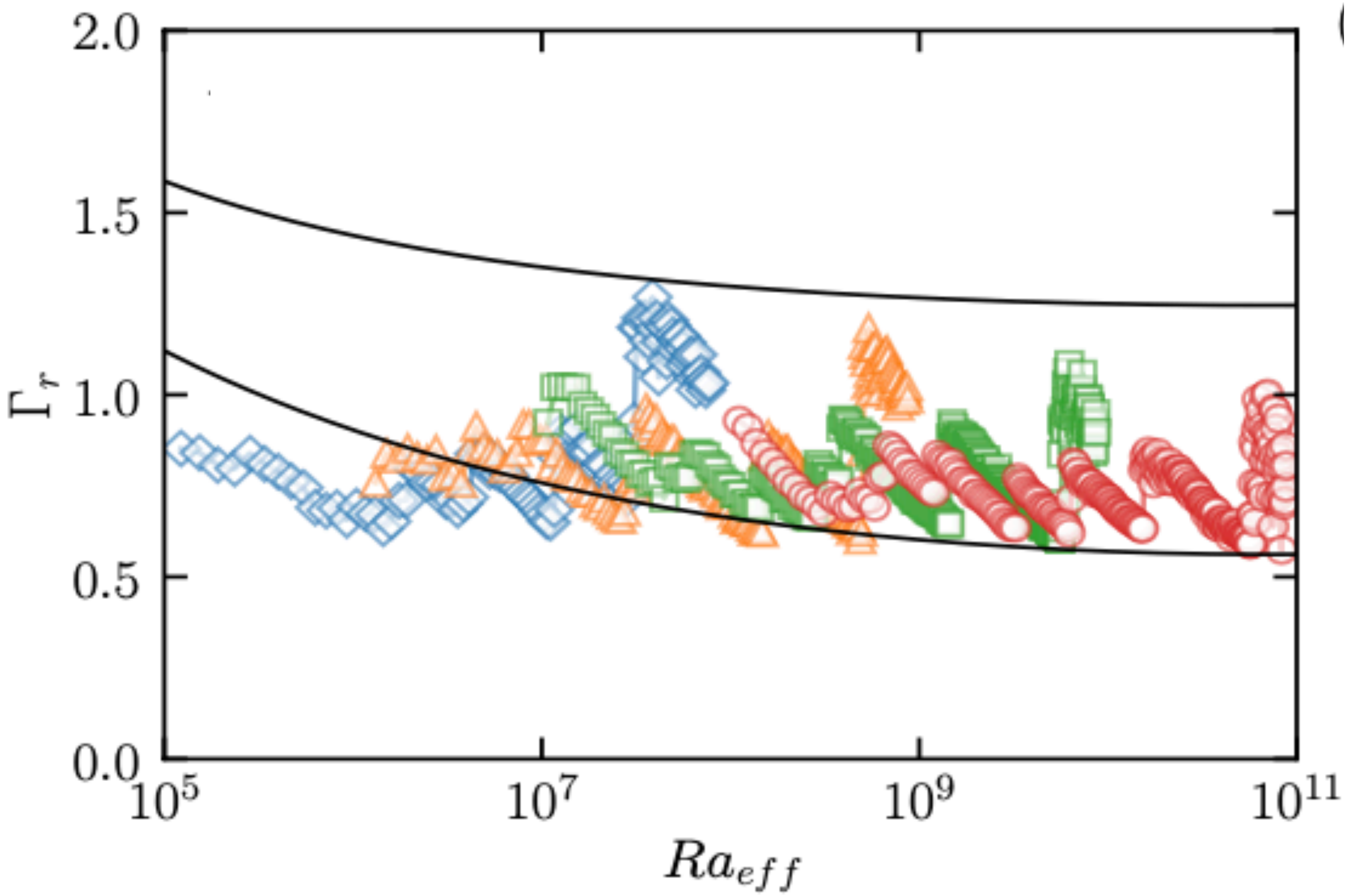

Lines: upper and lower bounds for **rolls** for **smooth walls** from theory:
Wang, Verzicco, Lohse, Shishkina, Phys. Rev. Lett. 125, 074501 (2020)

Conclusions on part II.

- For high Ra, scallops develop in ice layer
- Scallops resemble those in field measurements; connection to basal melting of glaciers?
- Wavelength of scallops grows in time and is given by length scale of convection rolls
- Roughness amplitude scales as ~ $Ra^{*1/3}$

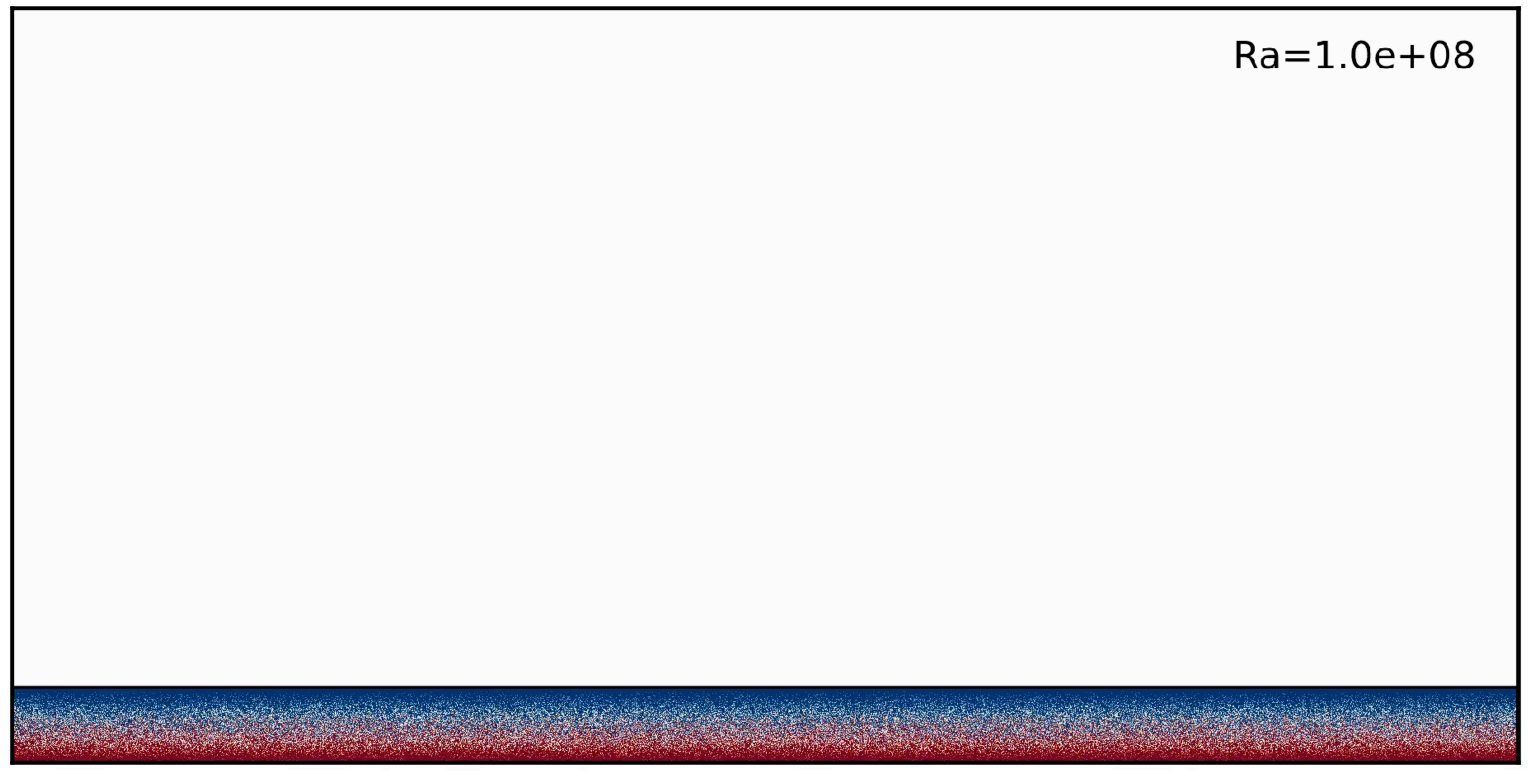

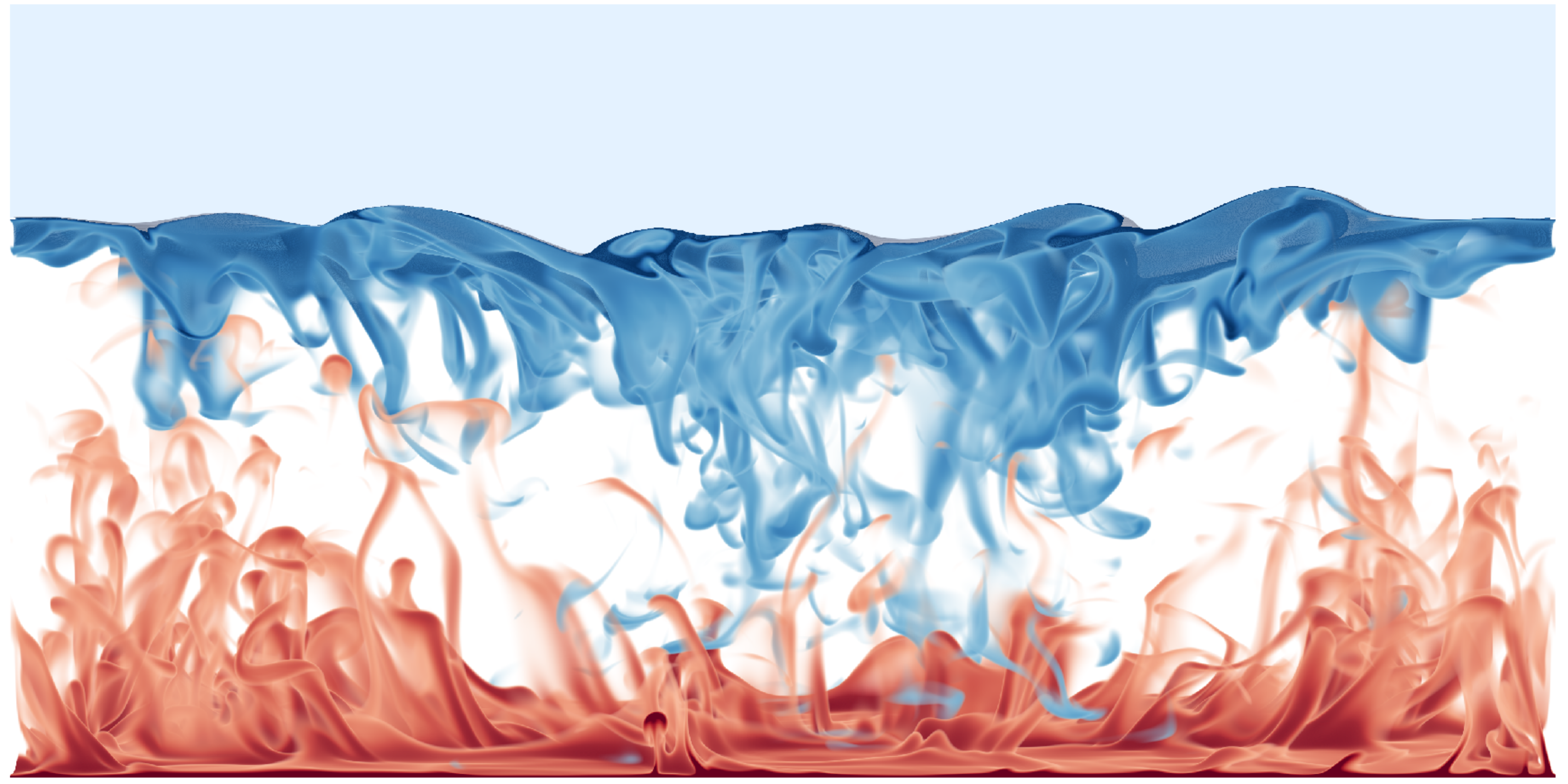

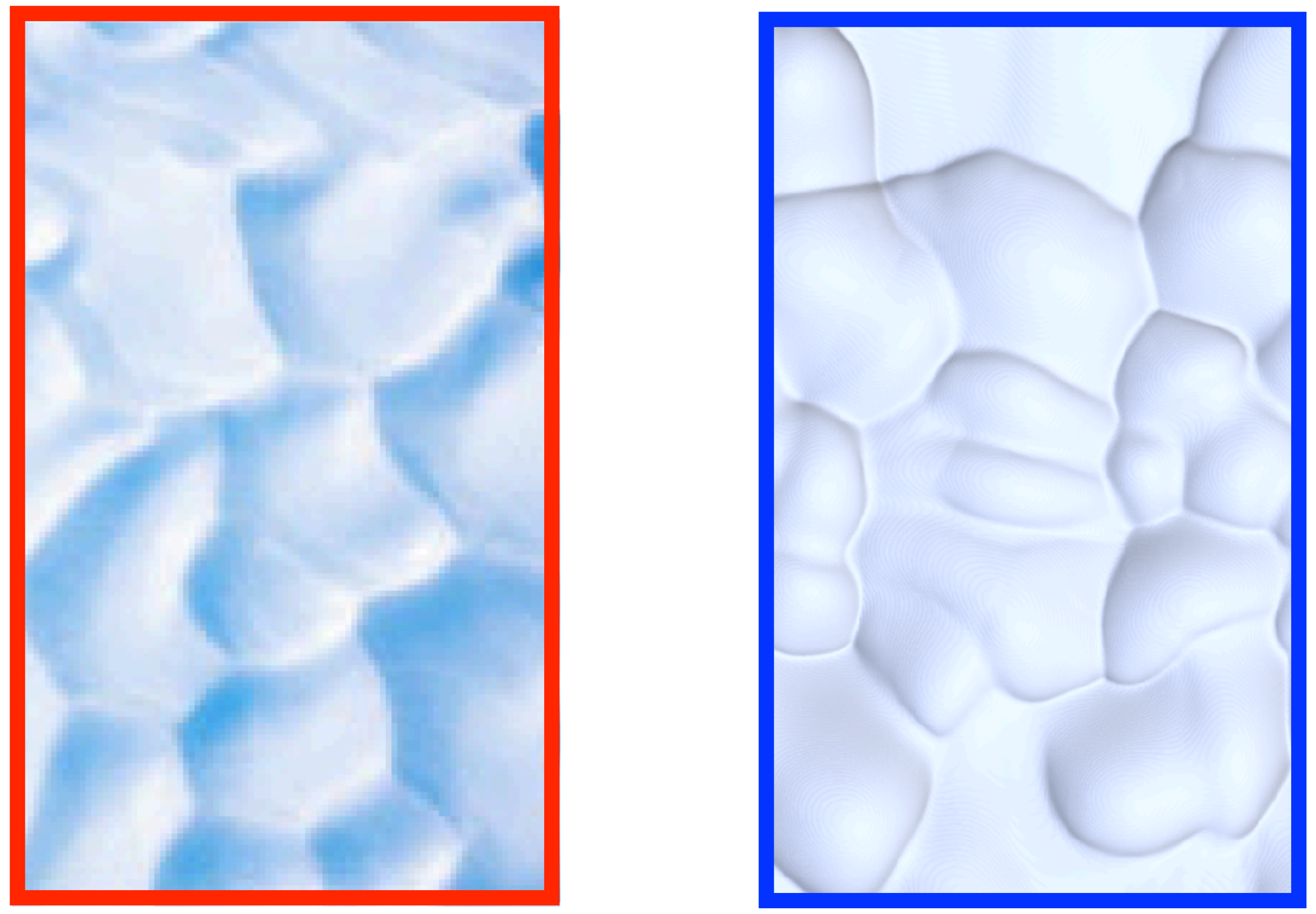

Conclusions on part II.

- For high Ra, scallops develop in ice layer

- Scallops resemble those in field measurements; connection to basal melting of glaciers?

- Wavelength of scallops grows in time and is given by length scale of convection rolls

- Roughness amplitude scales as ~ $Ra^{*1/3}$

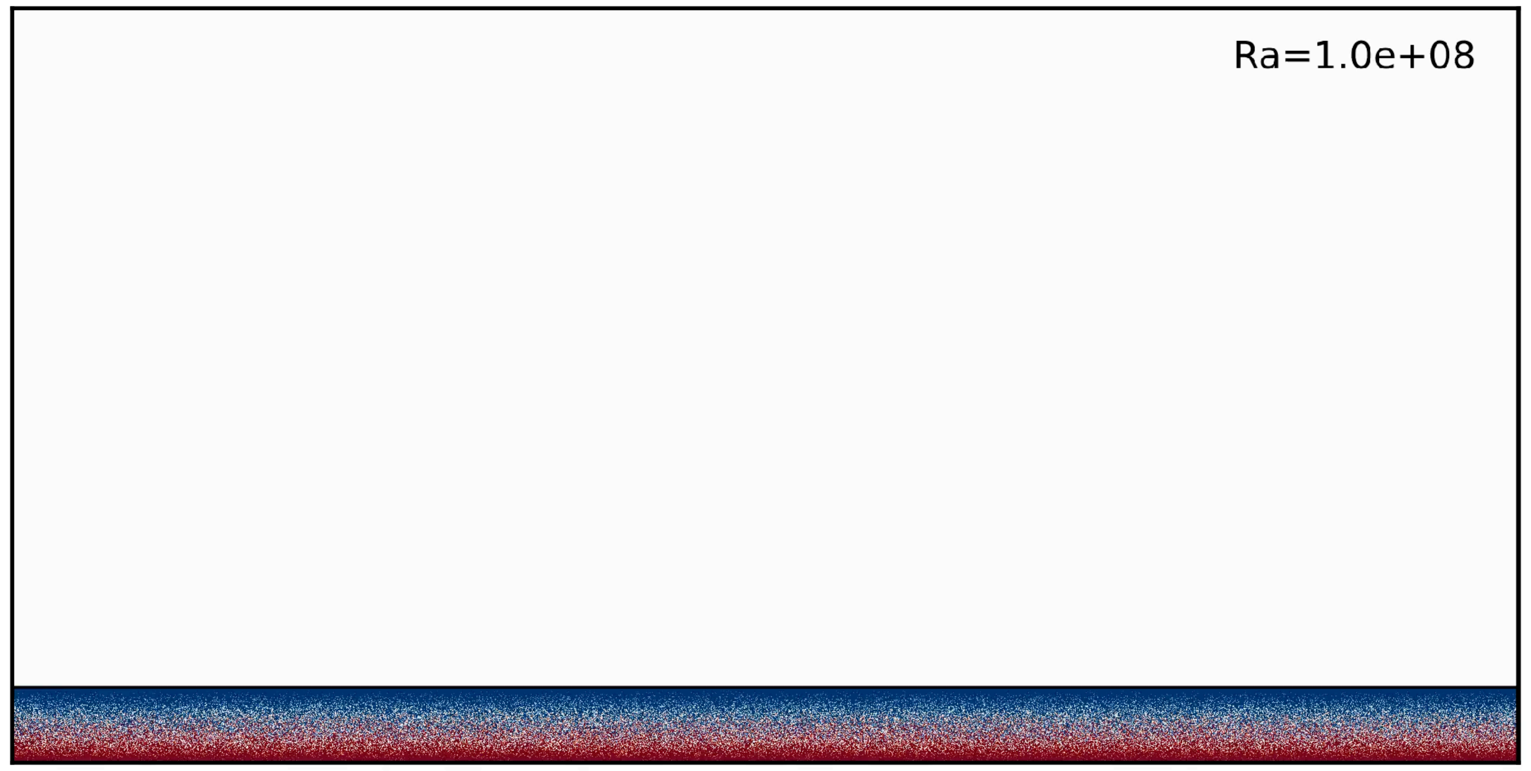

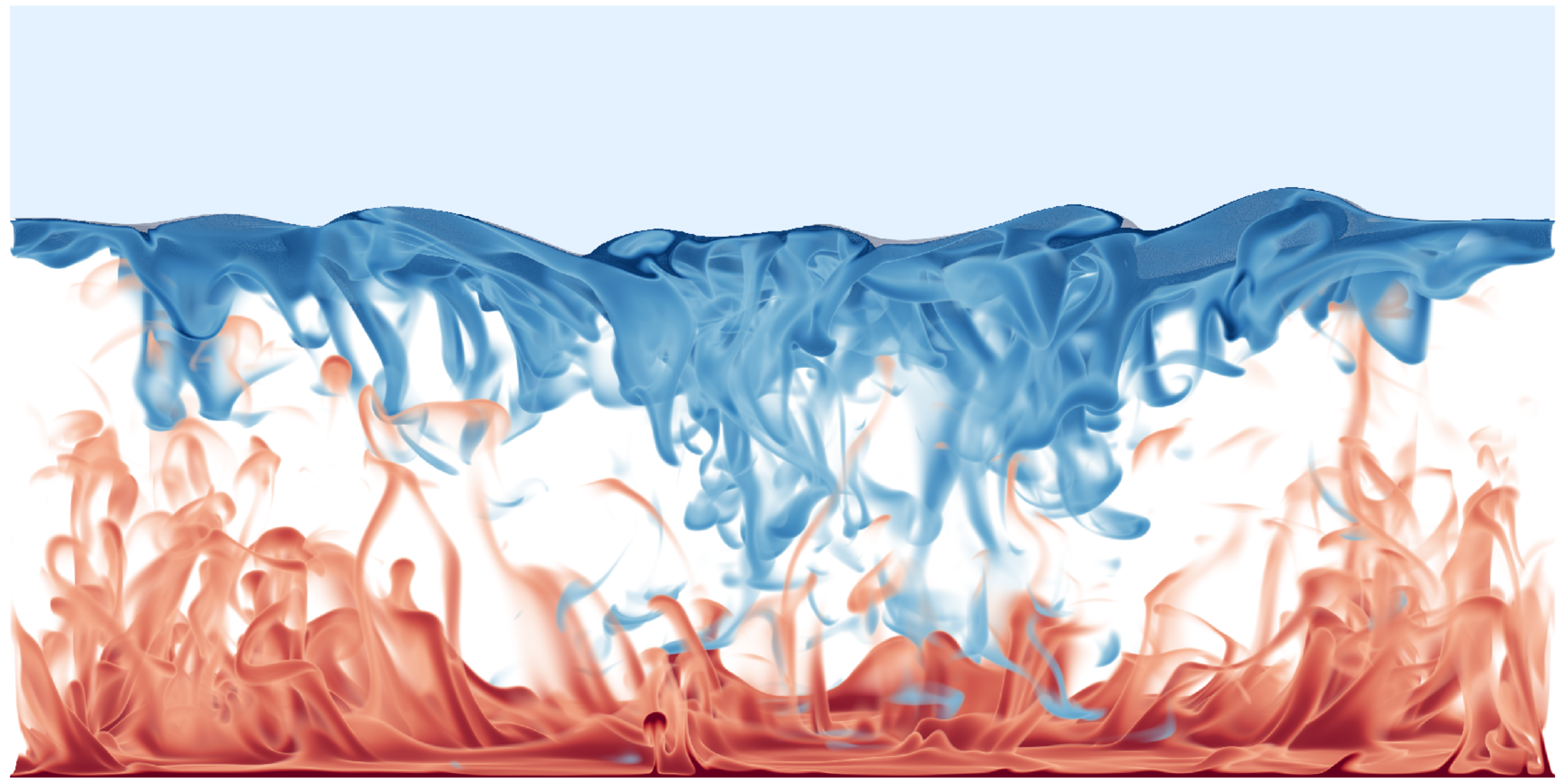

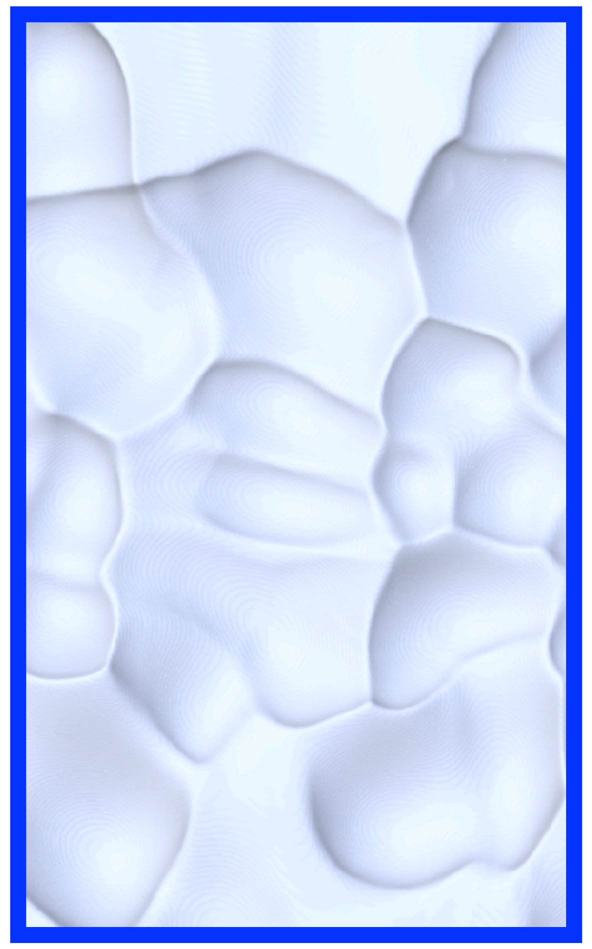

J. Fluid Mech. (2023), *vol.* 956, A23, doi:10.1017/jfm.2023.15

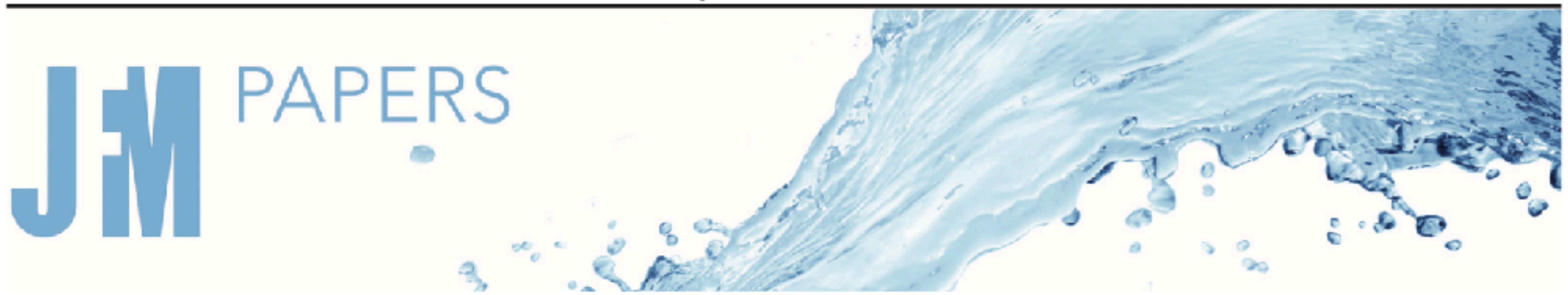

Morphology evolution of a melting solid layer above its melt heated from below

Rui Yang[1,†], Christopher J. Howland[1,†], Hao-Ran Liu[2,†], Roberto Verzicco[1,3,4,†] and Detlef Lohse[1,5,†]

III. Vertical convection with fresh water

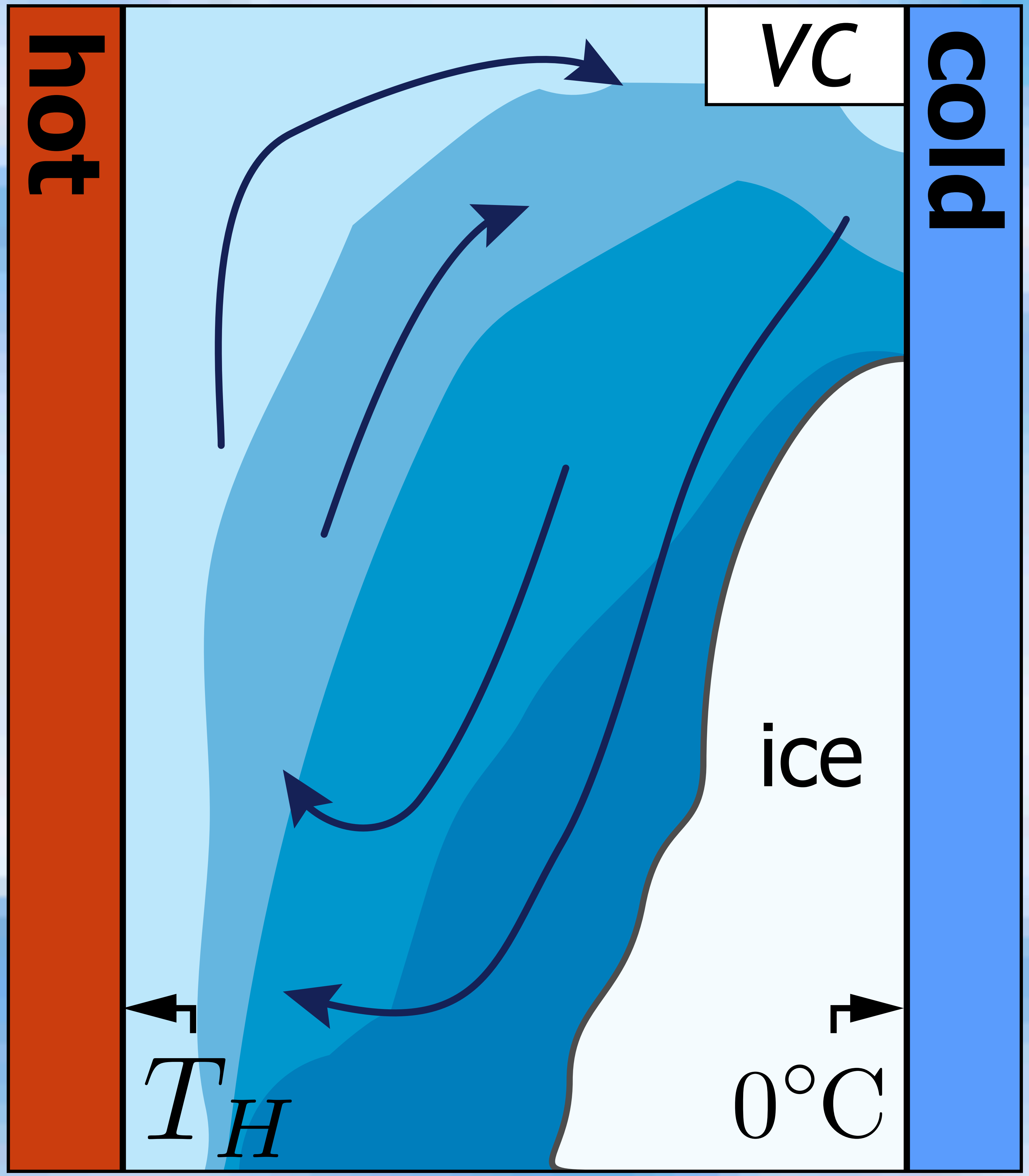

Abrupt transition from slow to fast melting

Yang, Chong, Liu, Verzicco, Lohse, Phys. Rev. Fluids 7, 083503 (2022)

Model system: Vertical convection, with one side frozen

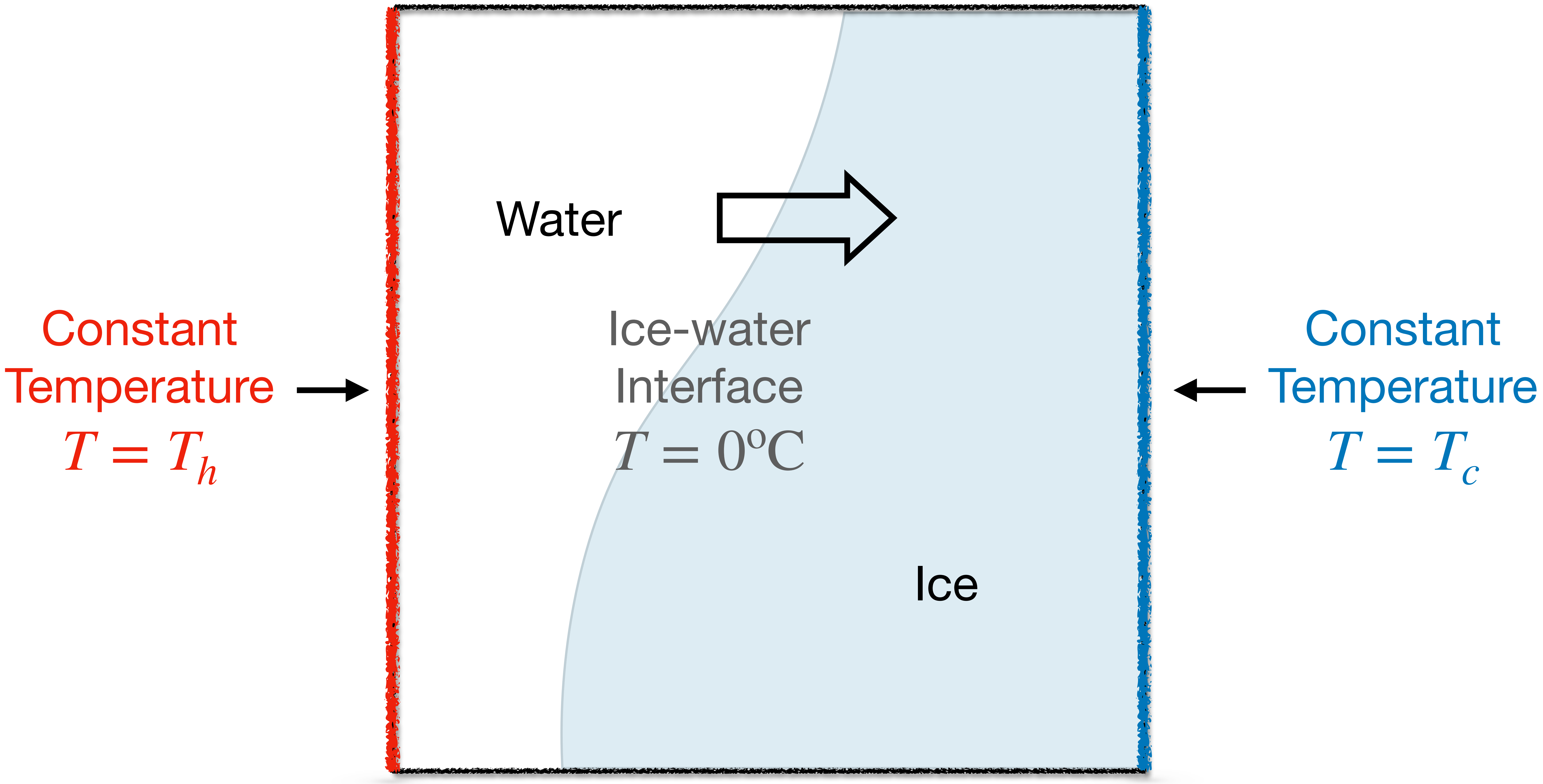

Model system: Vertical convection, with one side frozen

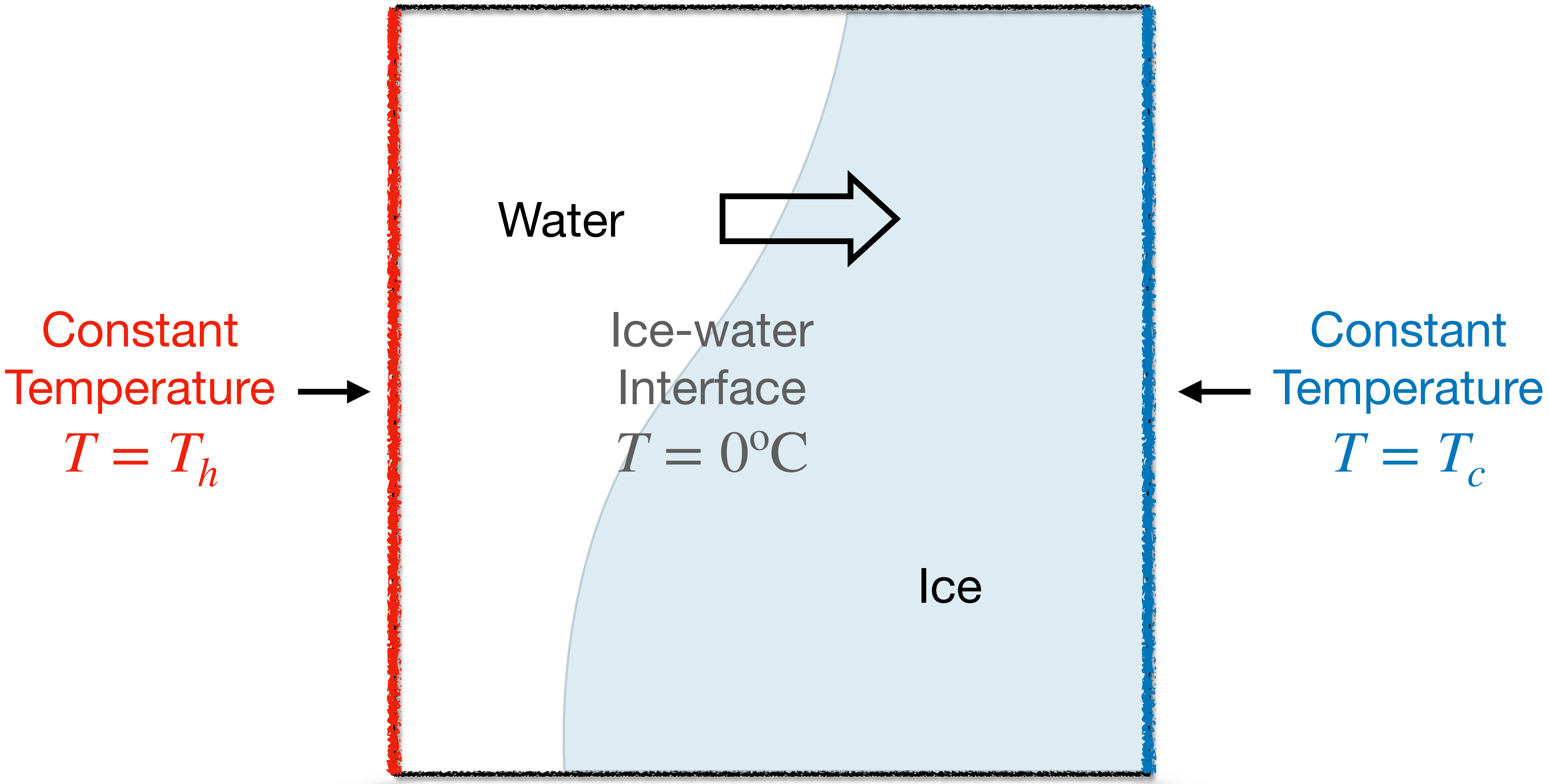

Objective: How does the melting rate depend on the heating temperature?

Control & response parameters

Control parameters (dimensional)

Heating temperature: T_h: $4^{o}\mathrm{C} < \mathrm{T_h} < 20^{o}\mathrm{C}$
Cooling temperature: T_c $\mathrm{T_c} = 0^{o}\mathrm{C}$

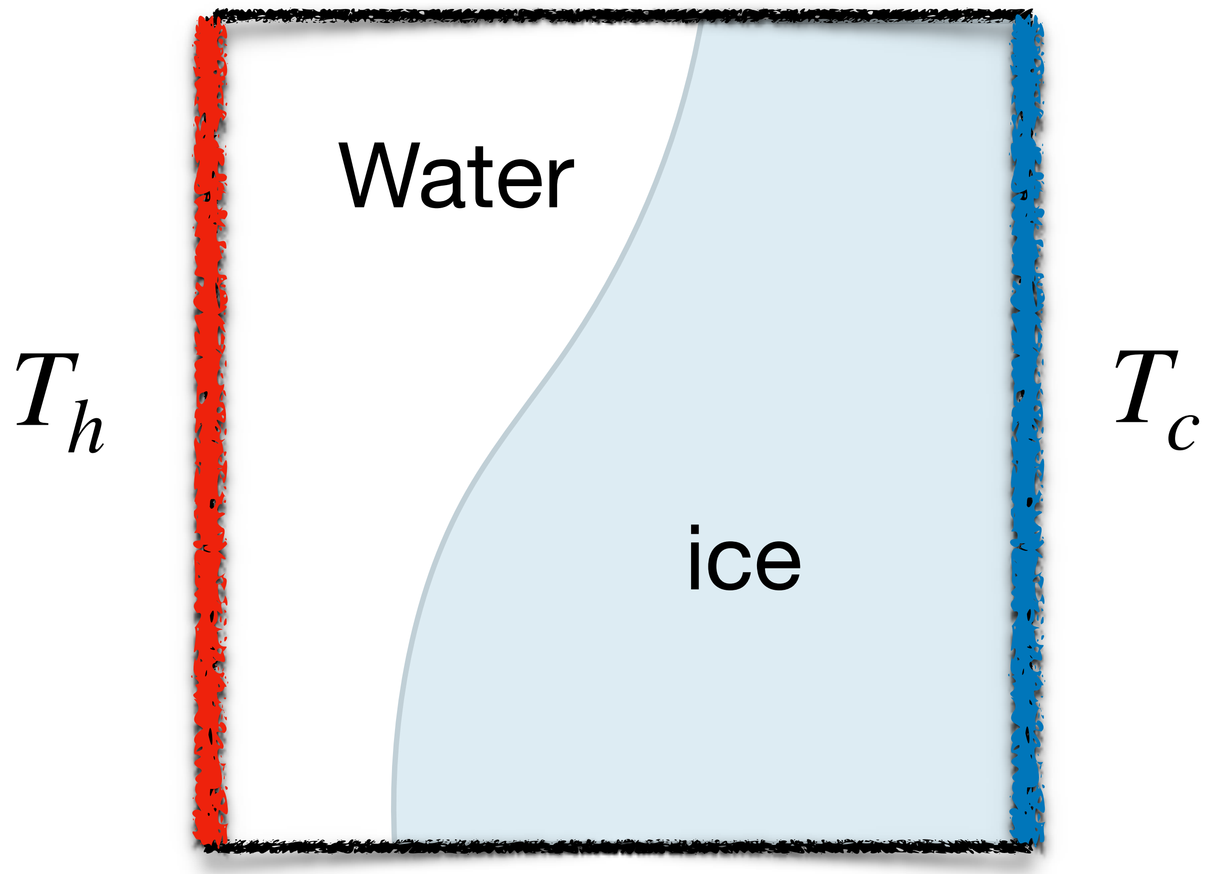

$$\rho_w = \rho_0(1 - \beta^* |T - T_{max}|^q)$$

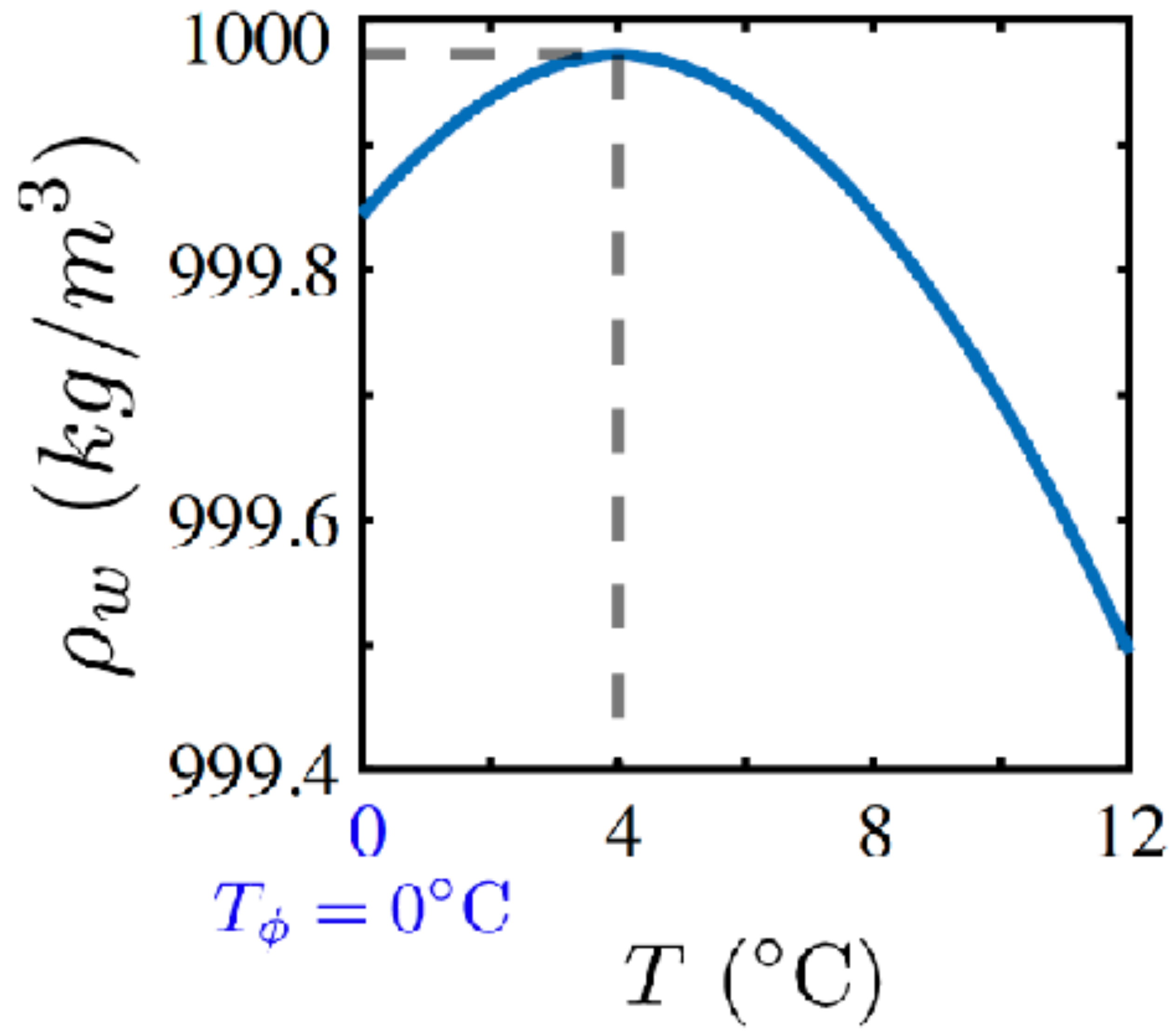

Control & response parameters

Control parameters (dimensional)

Heating temperature: T_h: $4^{o}\mathrm{C} < \mathrm{T_h} < 20^{o}\mathrm{C}$

Cooling temperature: T_c $\mathrm{T_c} = 0^{o}\mathrm{C}$

Control parameters (non-dimensional)

$$Ra = \frac{g\beta^*(T_h - T_c)^q H^3}{\nu\kappa}: \ 4 \times 10^7 < \mathrm{Ra} < 10^9$$

$$Pr = \frac{\nu}{\kappa} = 11.57$$

$$\theta_{max} = \frac{T_m - T_c}{T_h - T_c}$$

$$St = \frac{c_p(T_h - T_c)}{L}$$

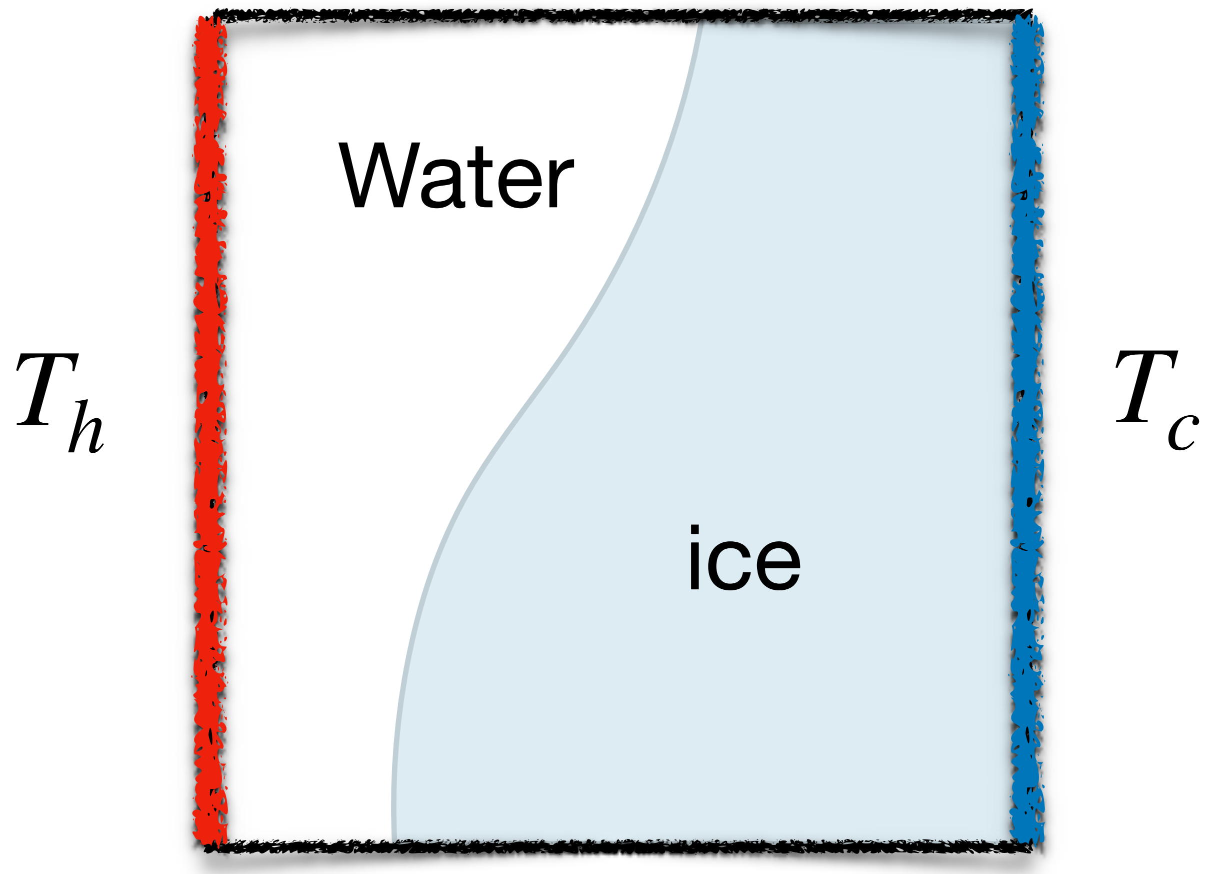

$$\rho_w = \rho_0(1 - \beta^* | T - T_{max} |^q)$$

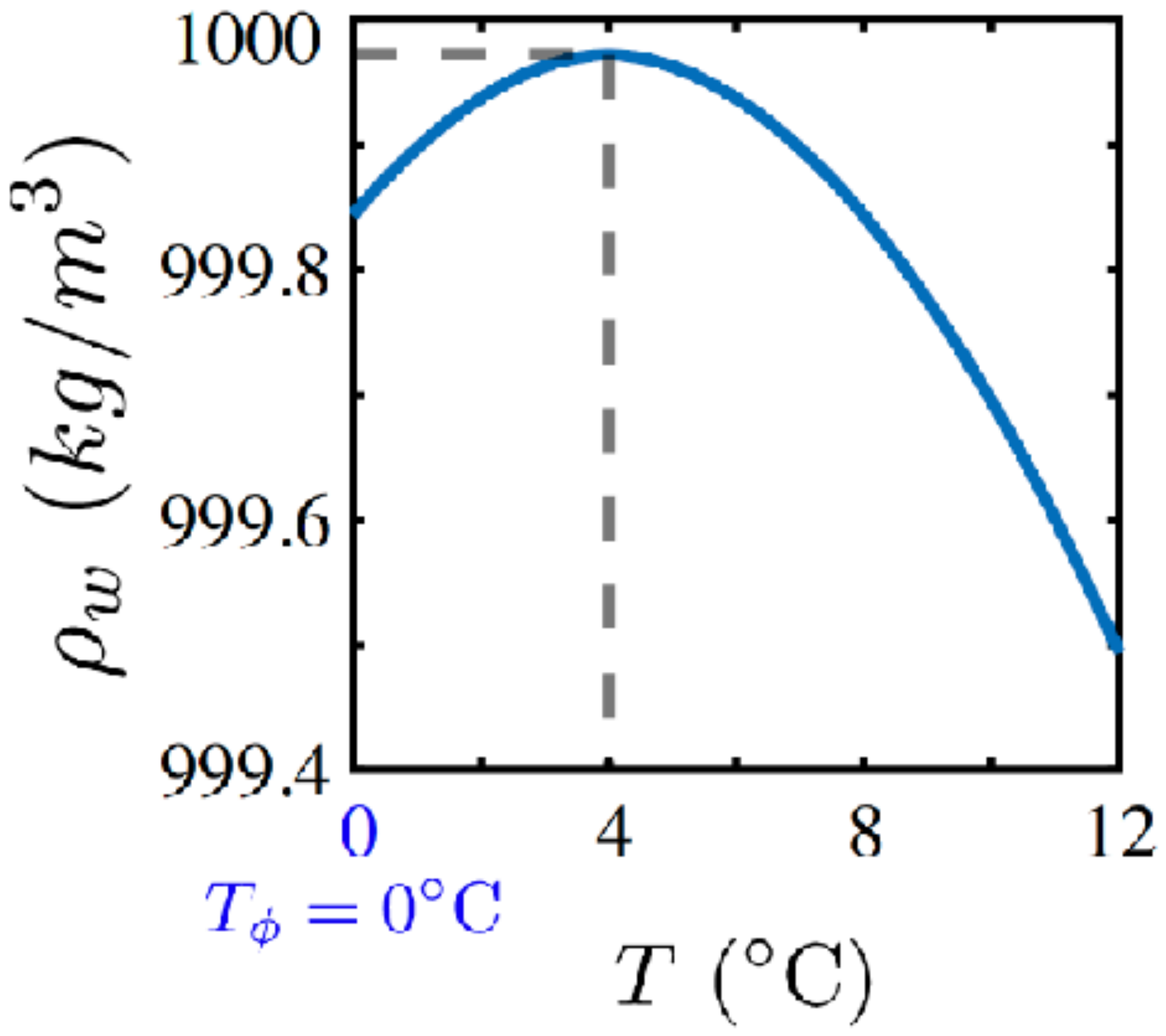

Control & response parameters

Control parameters (dimensional)

Heating temperature: T_h: $4^oC < T_h < 20^oC$

Cooling temperature: T_c $T_c = 0^oC$

Control parameters (non-dimensional)

$$Ra = \frac{g\beta^*(T_h - T_c)^q H^3}{\nu\kappa}: \ 4 \times 10^7 < Ra < 10^9$$

$$Pr = \frac{\nu}{\kappa} = 11.57$$

$$\theta_{max} = \frac{T_m - T_c}{T_h - T_c}$$

$$St = \frac{c_p(T_h - T_c)}{L}$$

Response parameters

Melting rate : f

Heat transfer: Nu

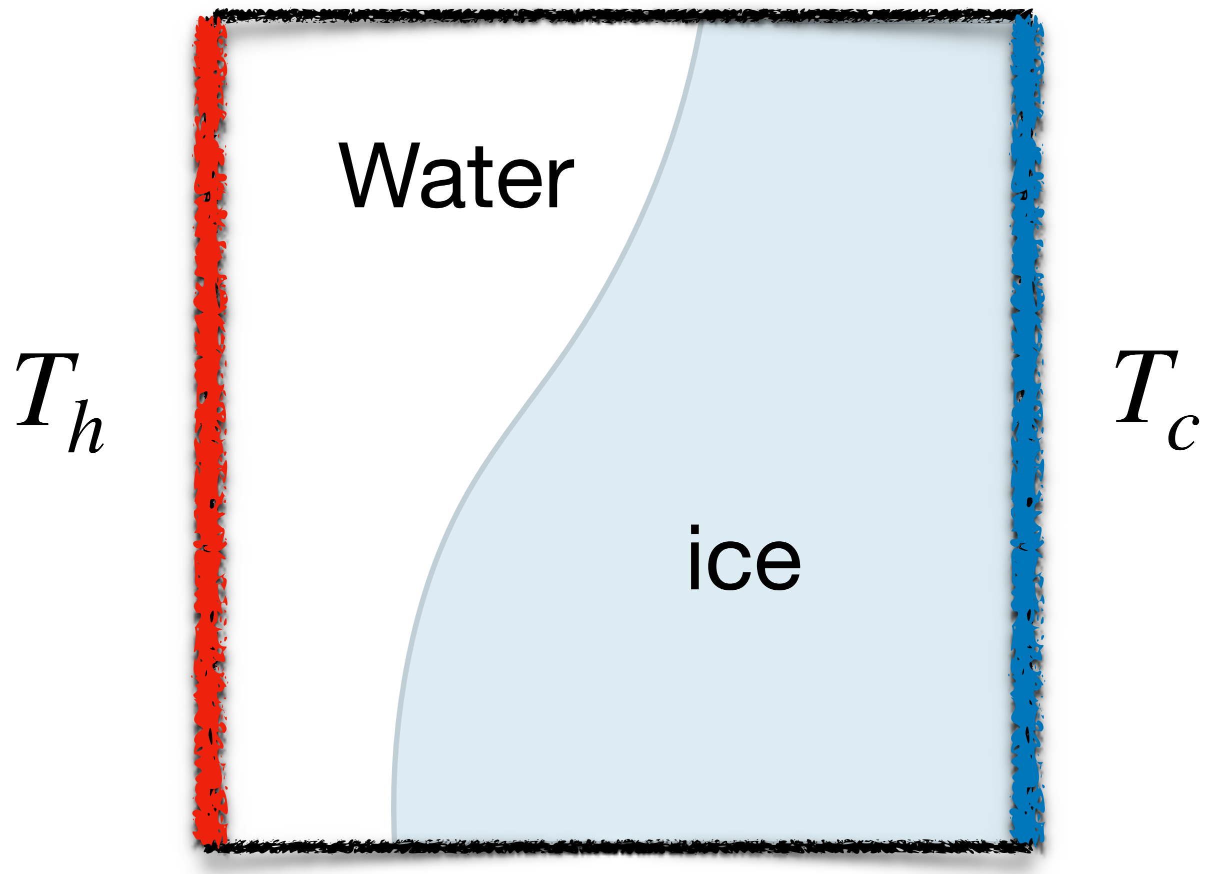

$$\rho_w = \rho_0(1 - \beta^* |T - T_{max}|^q)$$

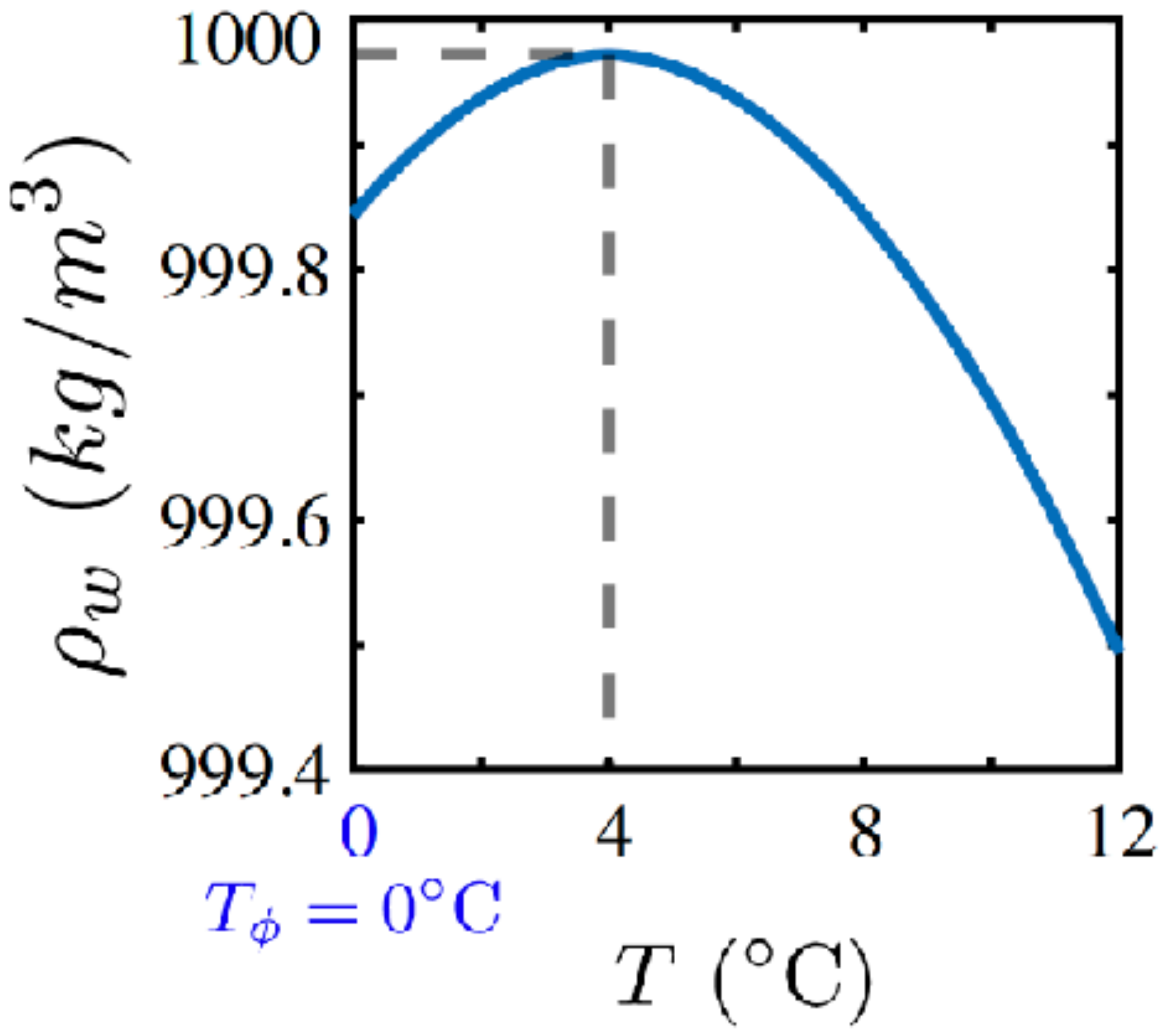

Control & response parameters

Control parameters (dimensional)

Heating temperature: T_h: $4^oC < T_h < 20^oC$

Cooling temperature: T_c $T_c = 0^oC$

Control parameters (non-dimensional)

$$Ra = \frac{g\beta^*(T_h - T_c)^q H^3}{\nu\kappa}: \; 4 \times 10^7 < Ra < 10^9$$

$$Pr = \frac{\nu}{\kappa} = 11.57$$

$$\theta_{max} = \frac{T_m - T_c}{T_h - T_c}$$

$$St = \frac{c_p(T_h - T_c)}{L}$$

Response parameters

Melting rate : f

Heat transfer: Nu

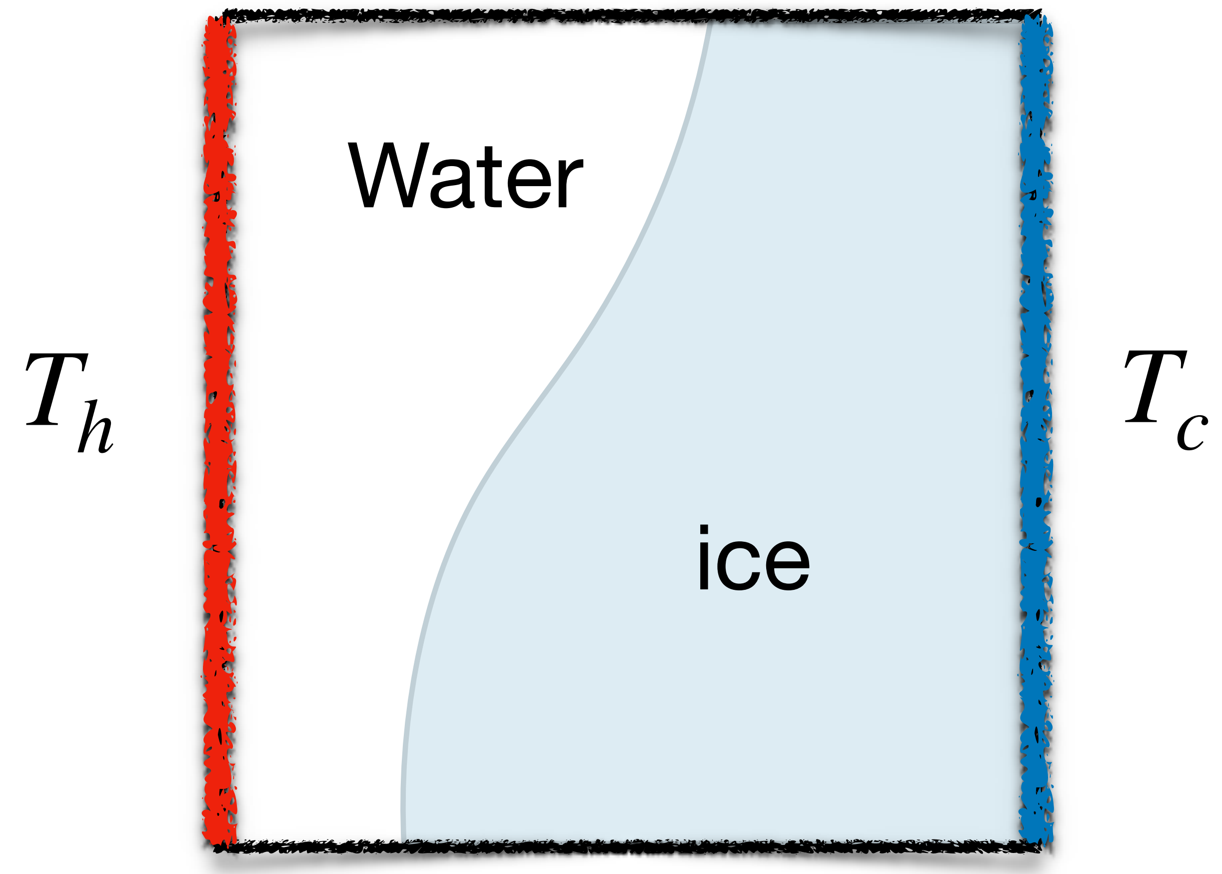

$$\rho_w = \rho_0(1 - \beta^* | T - T_{max} |^q)$$

Two groups of simulations

With density anomaly

$$F_{buoy} = \beta^* g | \theta - \theta_m |^q$$

Without density anomaly (OB)

$$F_{buoy} = \beta g \theta$$

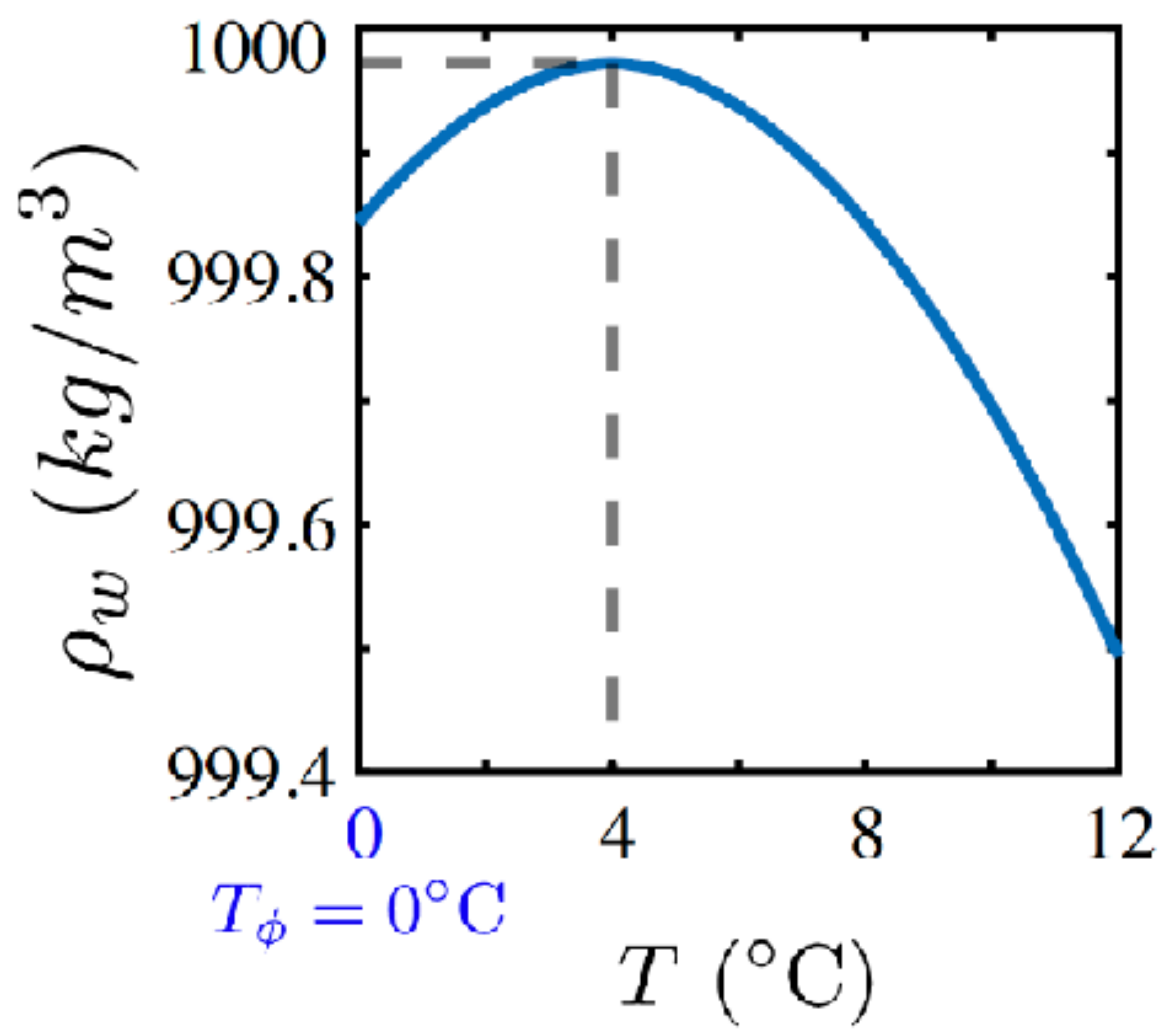

Control & response parameters

Control parameters (dimensional)

Heating temperature: T_h: $4^oC < T_h < 20^oC$

Cooling temperature: T_c $T_c = 0^oC$

Control parameters (non-dimensional)

$$Ra = \frac{g\beta^*(T_h - T_c)^q H^3}{\nu\kappa}: \; 4 \times 10^7 < Ra < 10^9$$

$$Pr = \frac{\nu}{\kappa} = 11.57$$

$$\theta_{max} = \frac{T_m - T_c}{T_h - T_c}$$

$$St = \frac{c_p(T_h - T_c)}{L}$$

Response parameters

Melting rate : f

Heat transfer: Nu

T_h

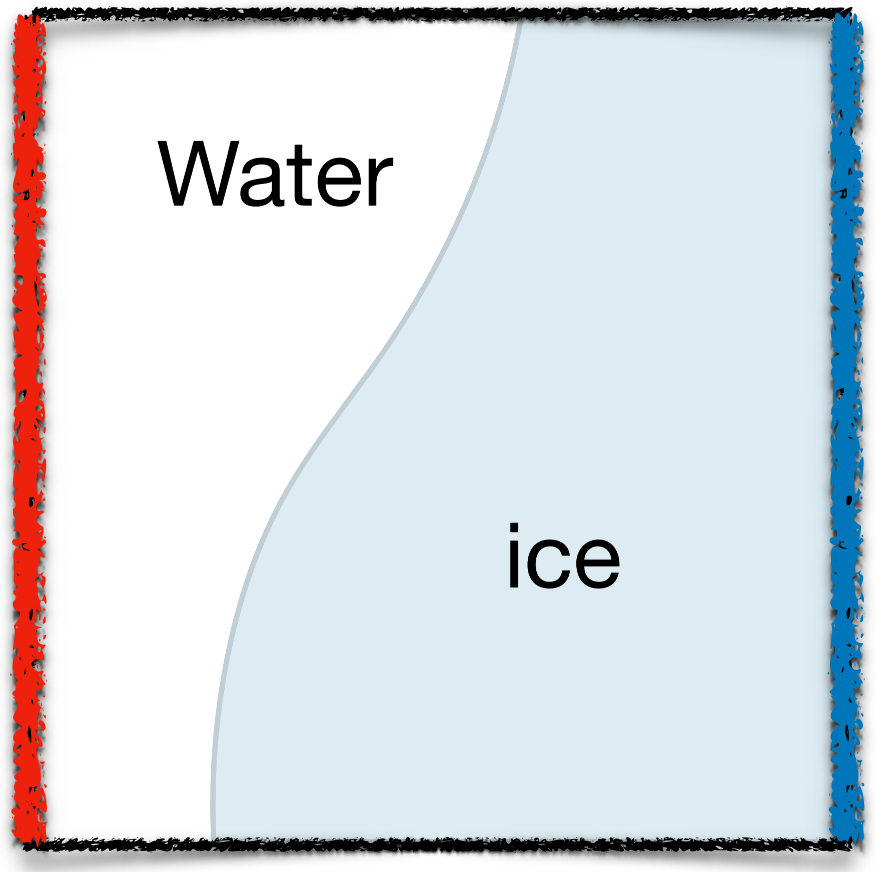

T_c

$$\rho_w = \rho_0(1 - \beta^* | T - T_{max} |^q)$$

Two groups of simulations

With density anomaly

$$F_{buoy} = \beta^* g | \theta - \theta_m |^q$$

Without density anomaly (OB)

$$F_{buoy} = \beta g \theta$$

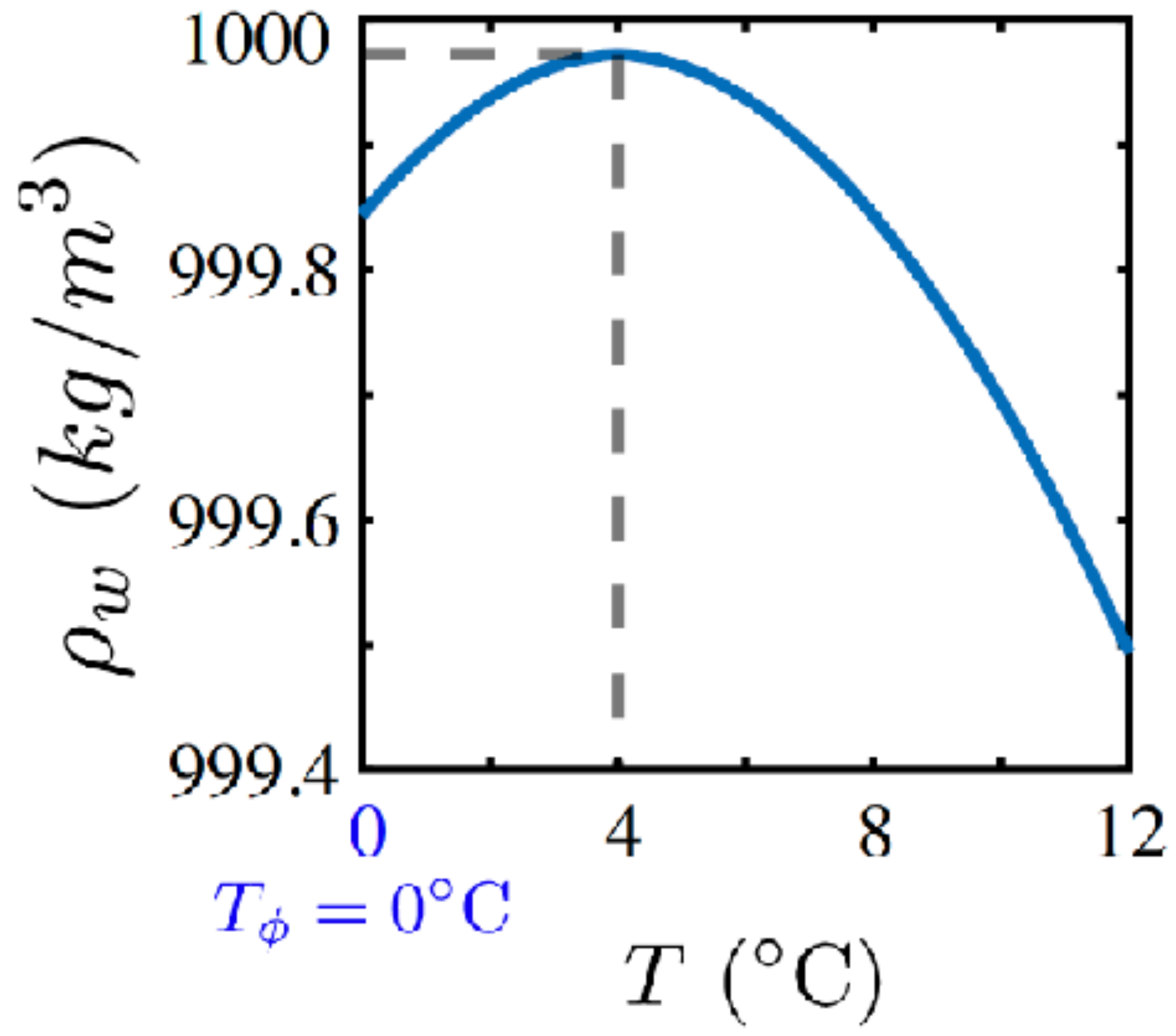

Objective:
How does the melting rate depend on the heating temperature?

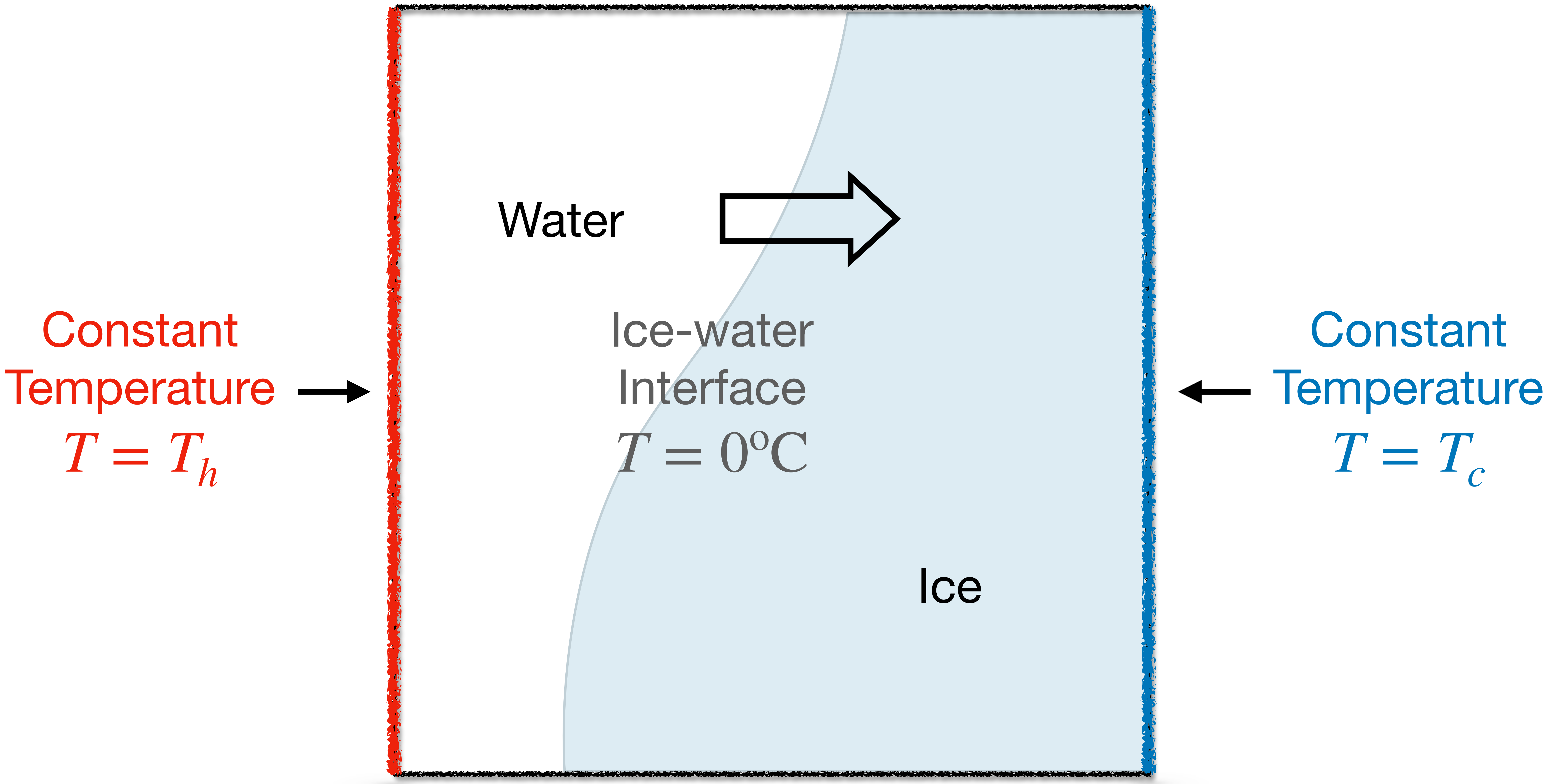

Finding: Morphological dynamics of melting ice depends on T_h

$T_h = 20^oC$

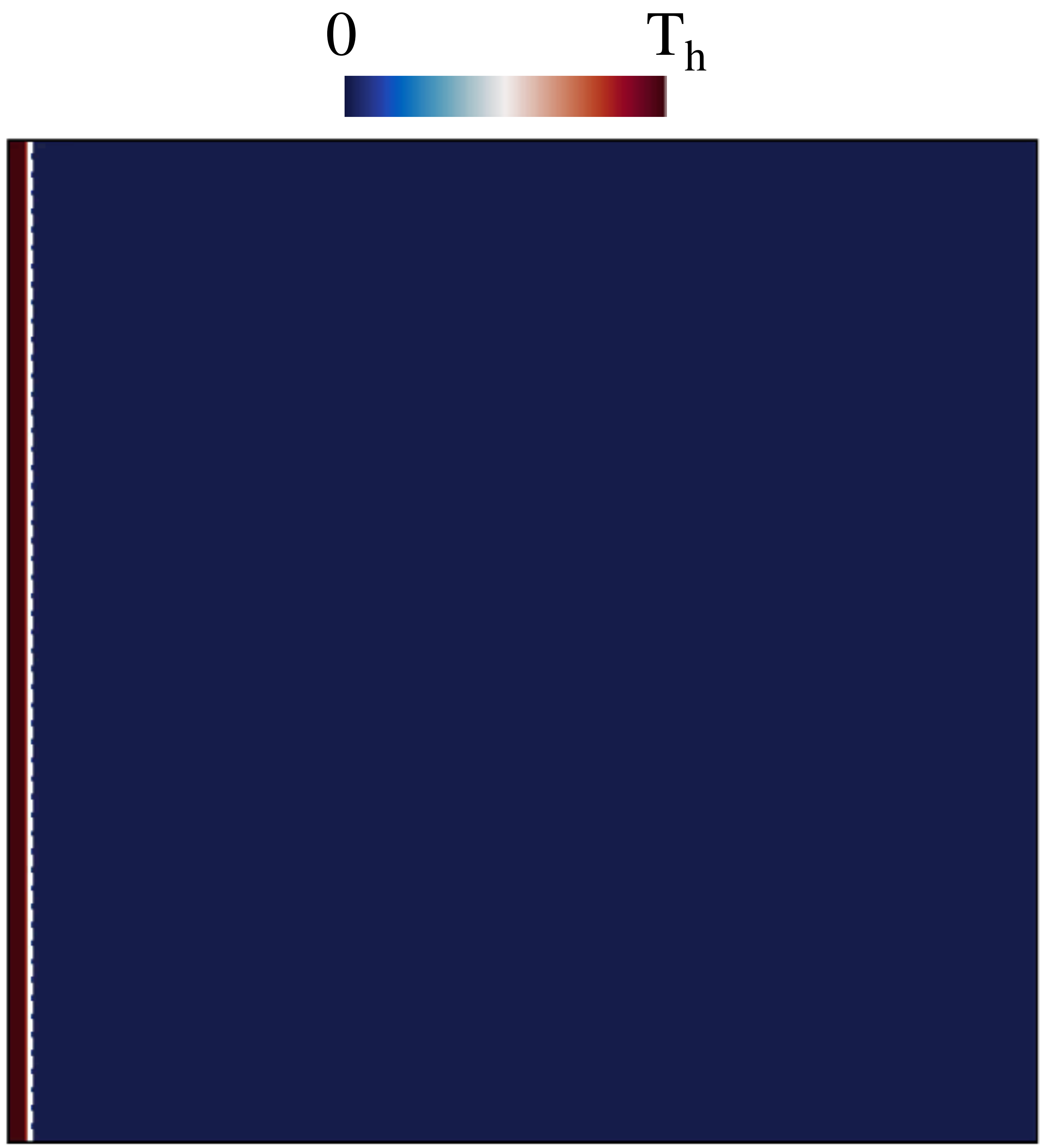

Finding: Morphological dynamics of melting ice depends on T_h

$T_h = 20^oC$

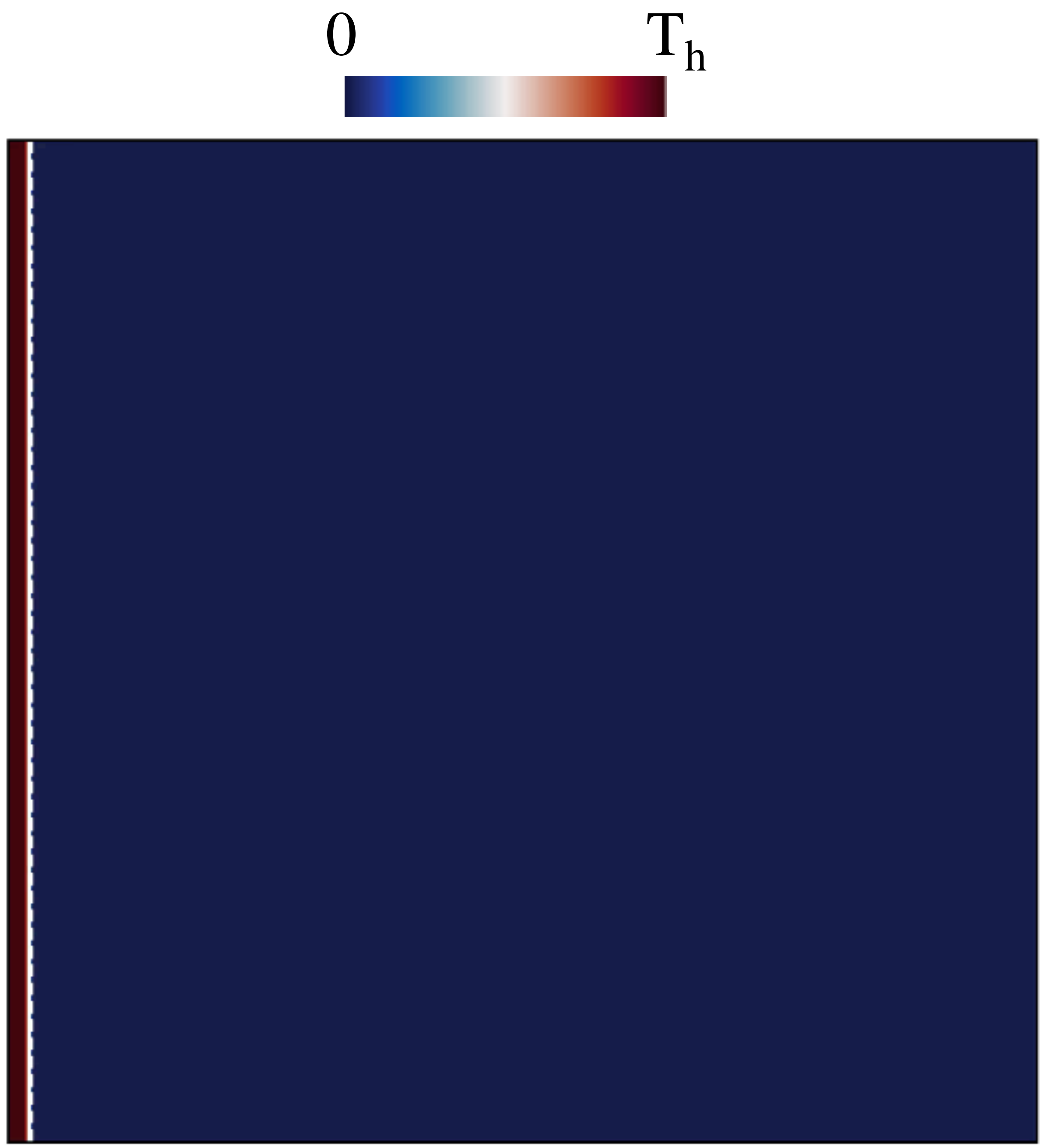

Finding: Morphological dynamics of melting ice depends on T_h

$T_h = 20^oC$

- Top part melts faster than the bottom part

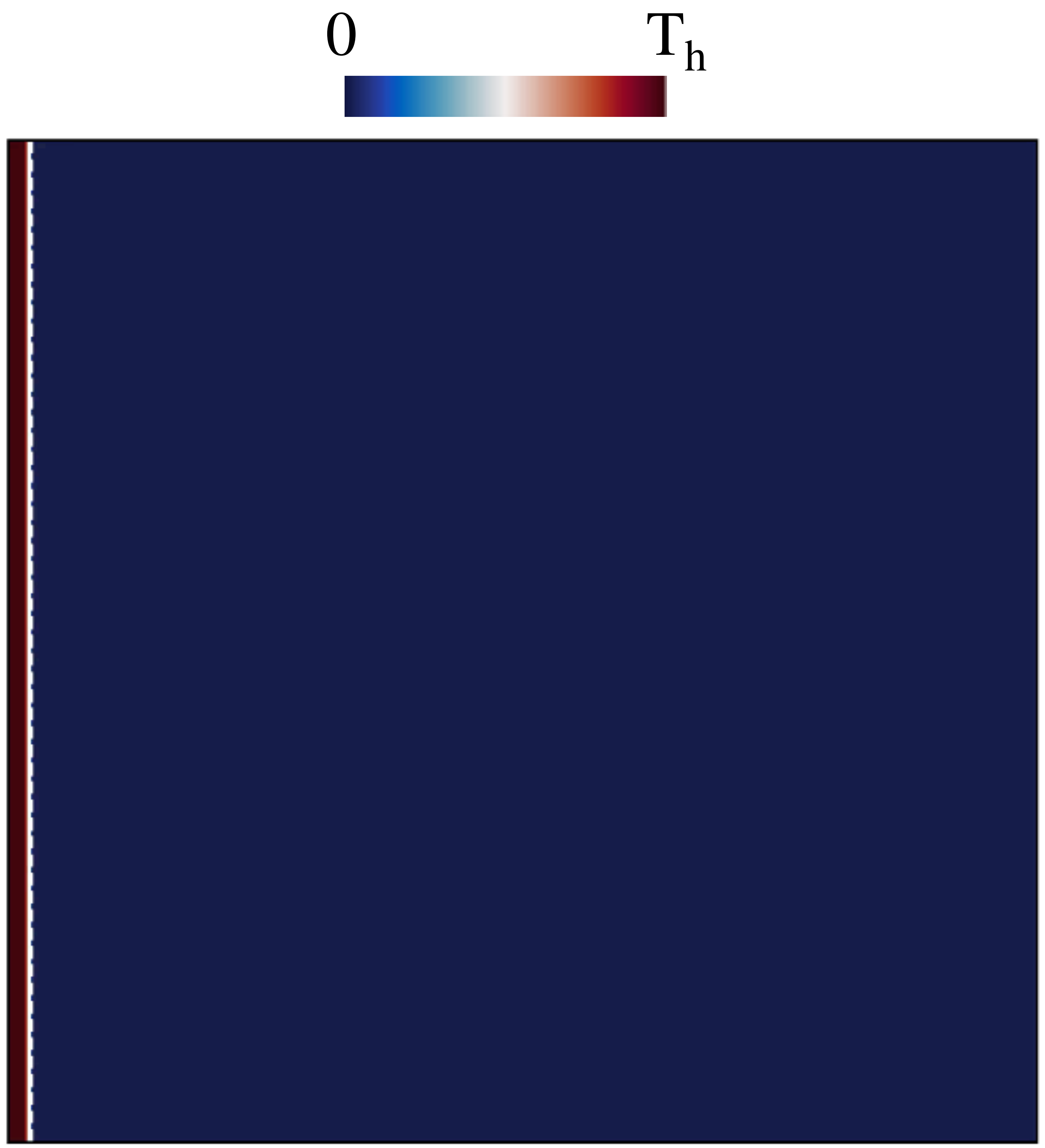

Finding: Morphological dynamics of melting ice depends on T_h

$$T_h = 20^oC$$

- Top part melts faster than the bottom part

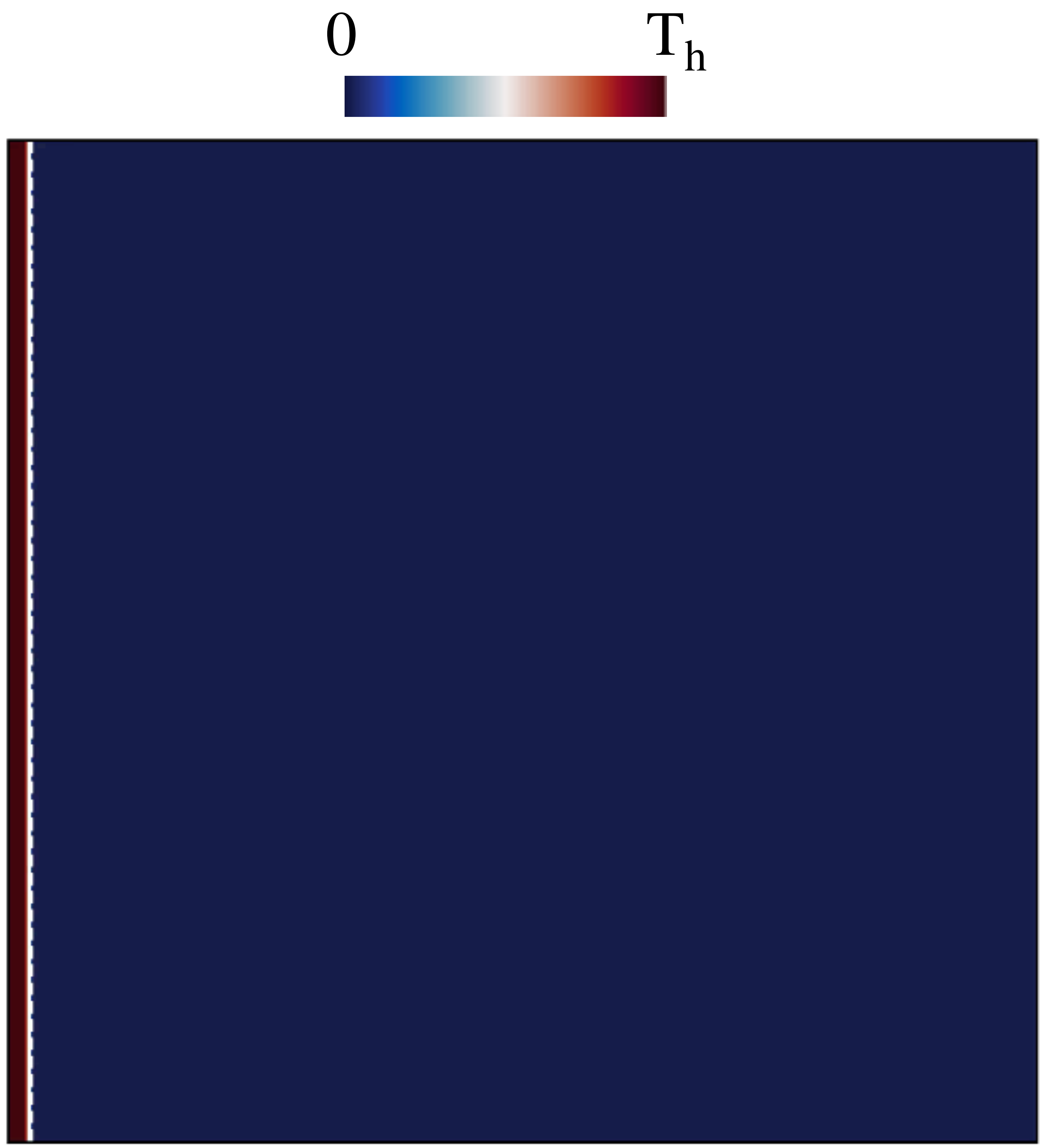

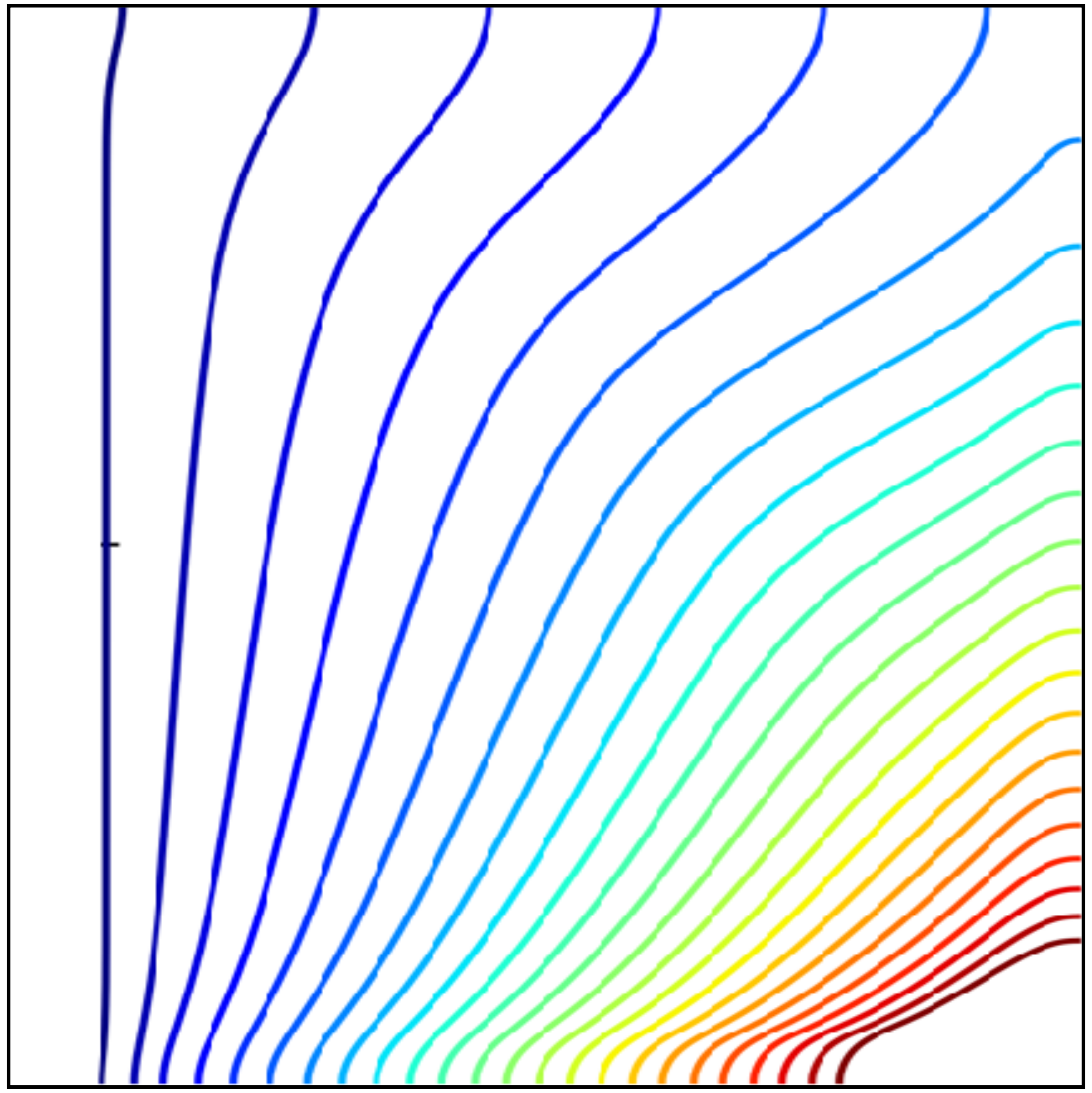

Finding: Morphological dynamics of melting ice depends on T_h

$T_h = 20^oC$

- Top part melts faster than the bottom part

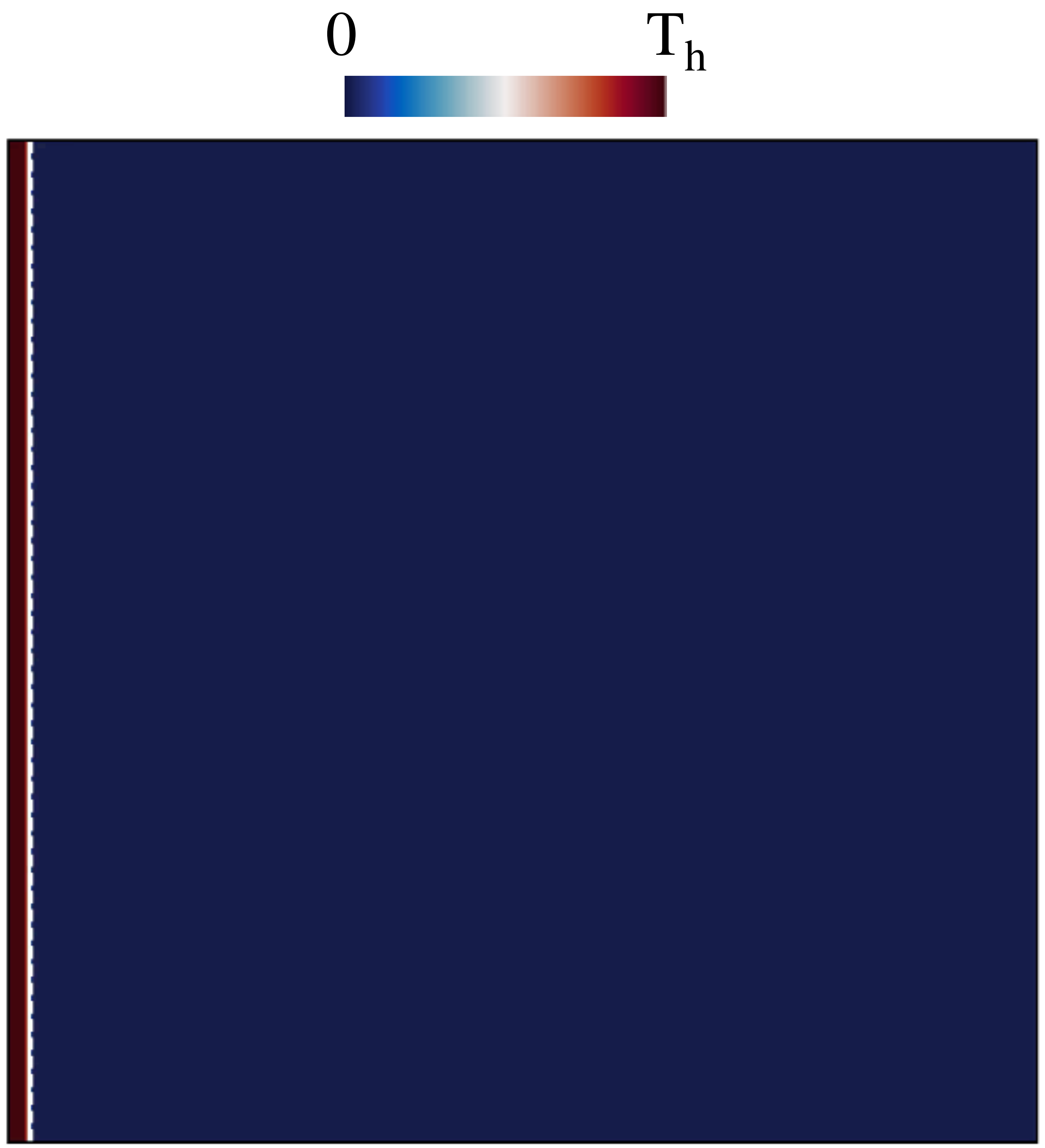

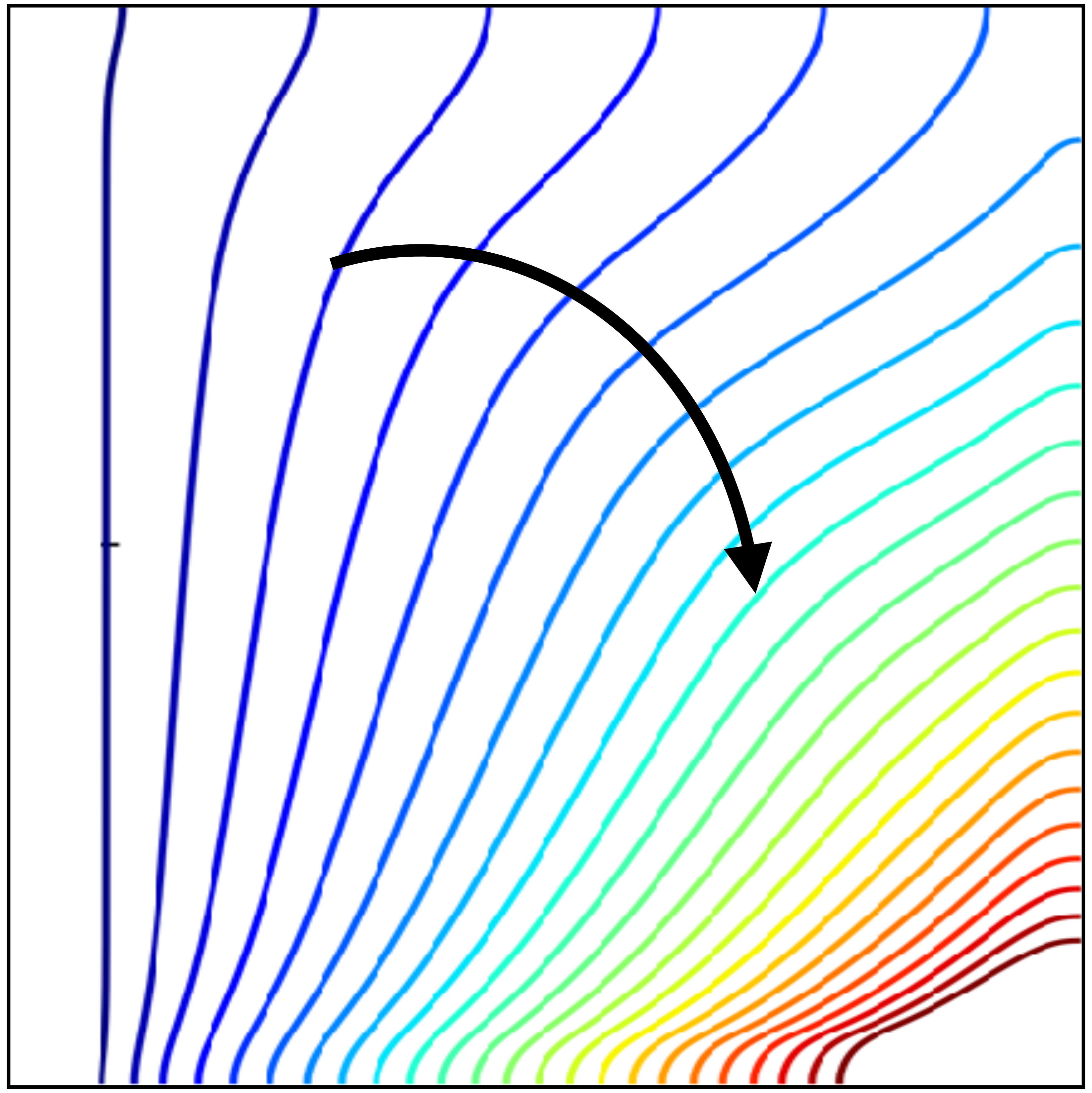

Finding: Morphological dynamics of melting ice depends on T_h

$T_h = 6.7^{o}C$

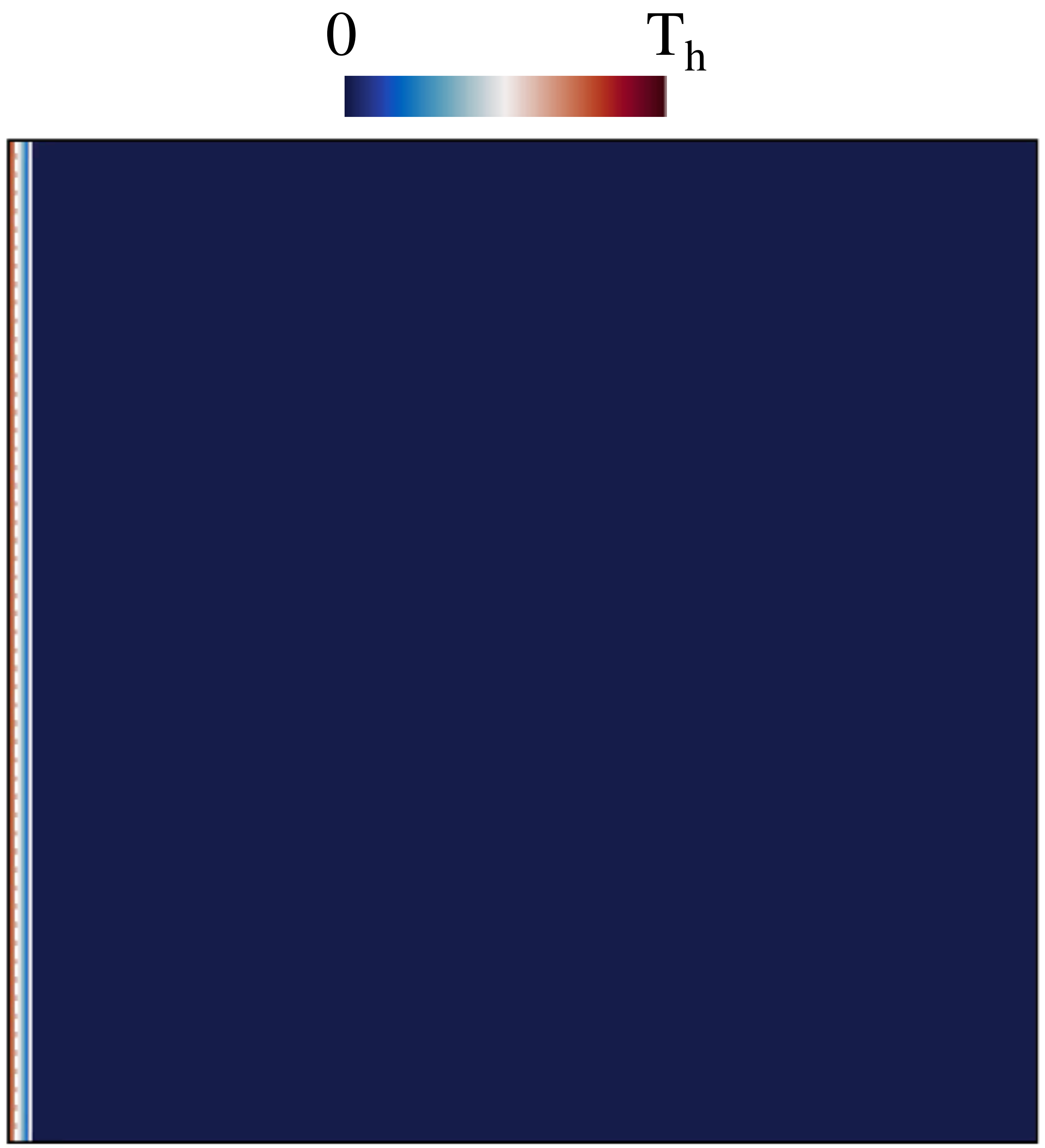

Finding: Morphological dynamics of melting ice depends on T_h

$T_h = 6.7^{o}C$

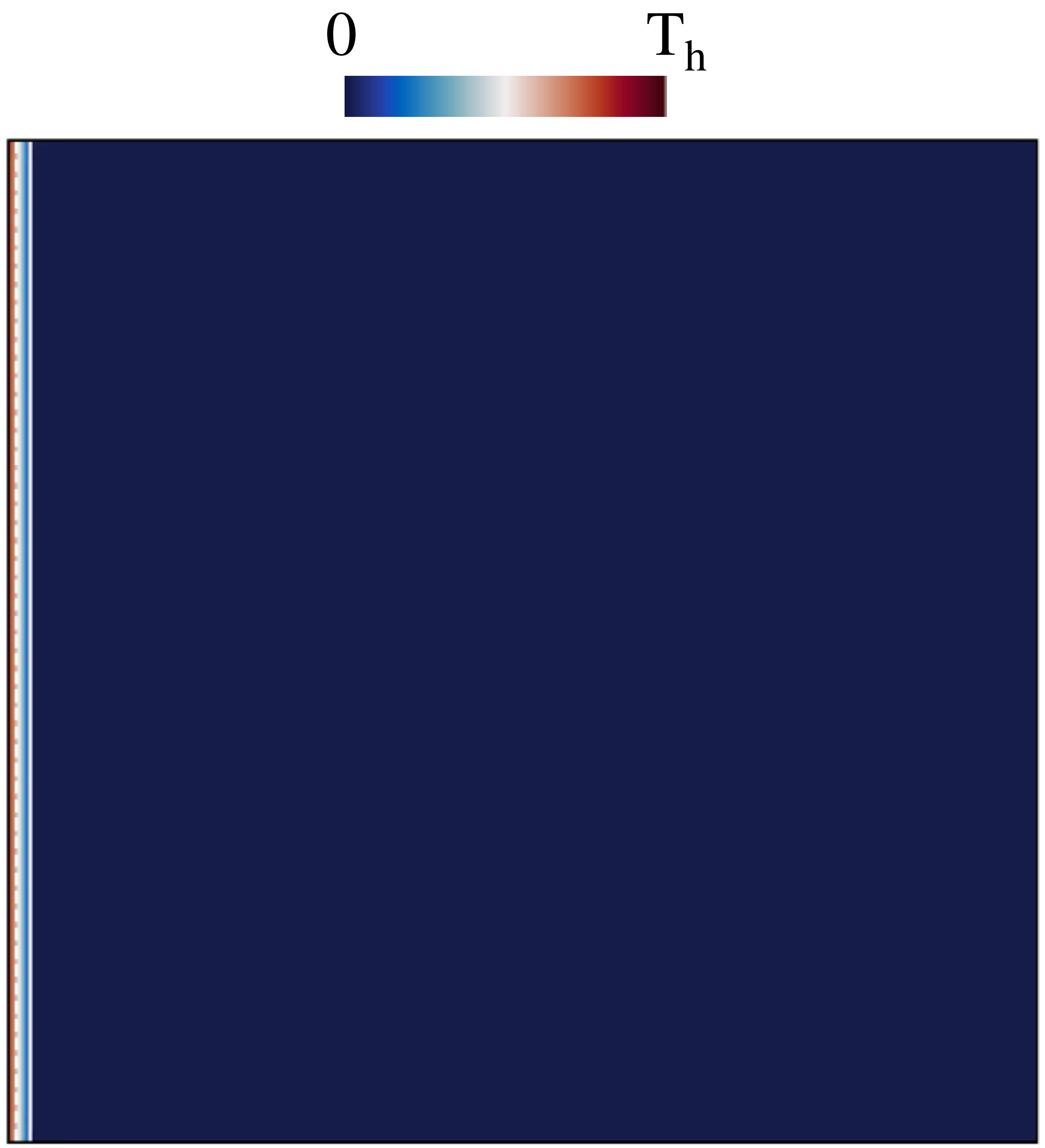

Finding: Morphological dynamics of melting ice depends on T_h

$$T_h = 6.7^{o}C$$

- Bottom part melts faster than top part

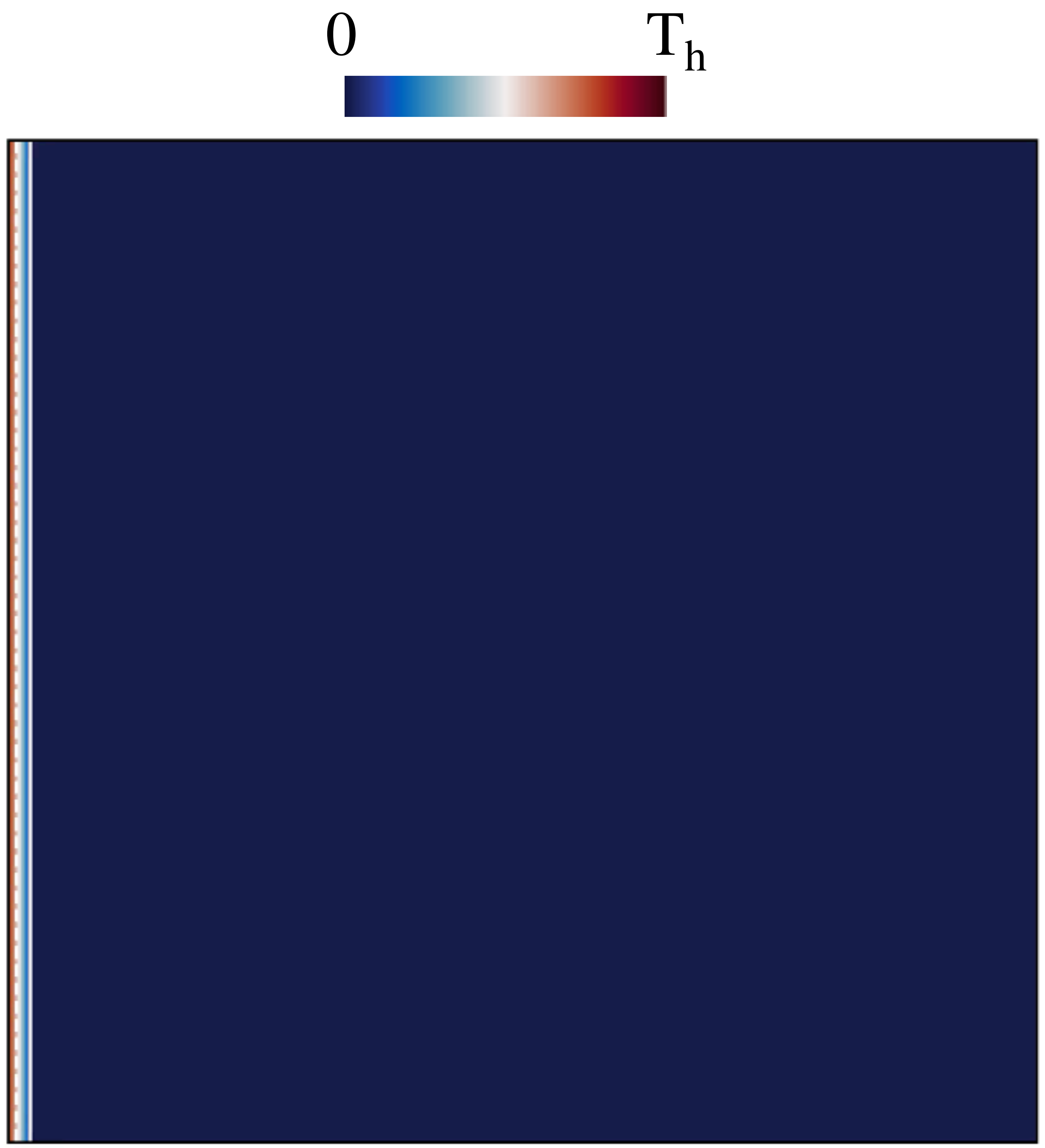

Finding: Morphological dynamics of melting ice depends on T_h

$$T_h = 6.7^{o}C$$

- Bottom part melts faster than top part

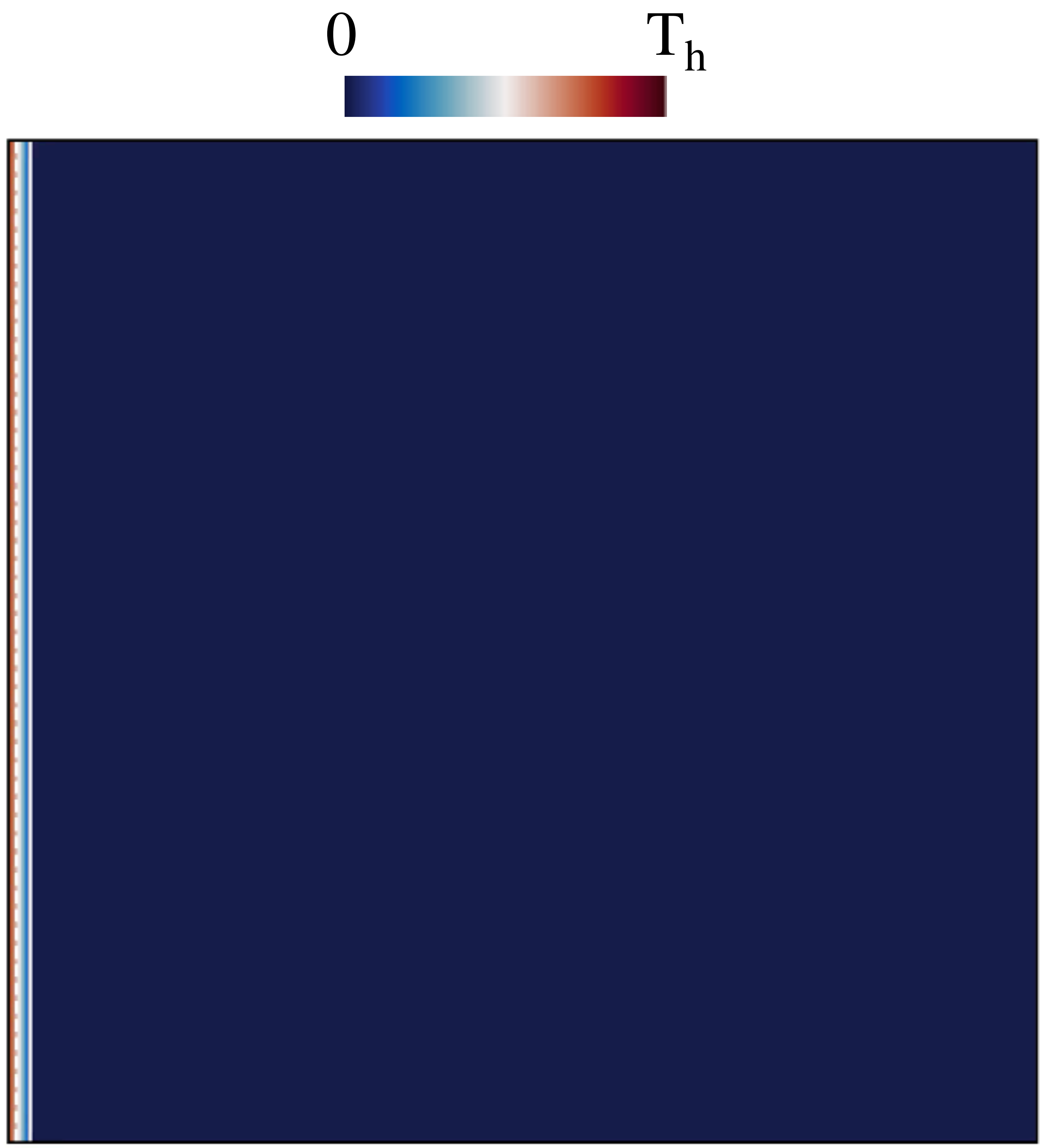

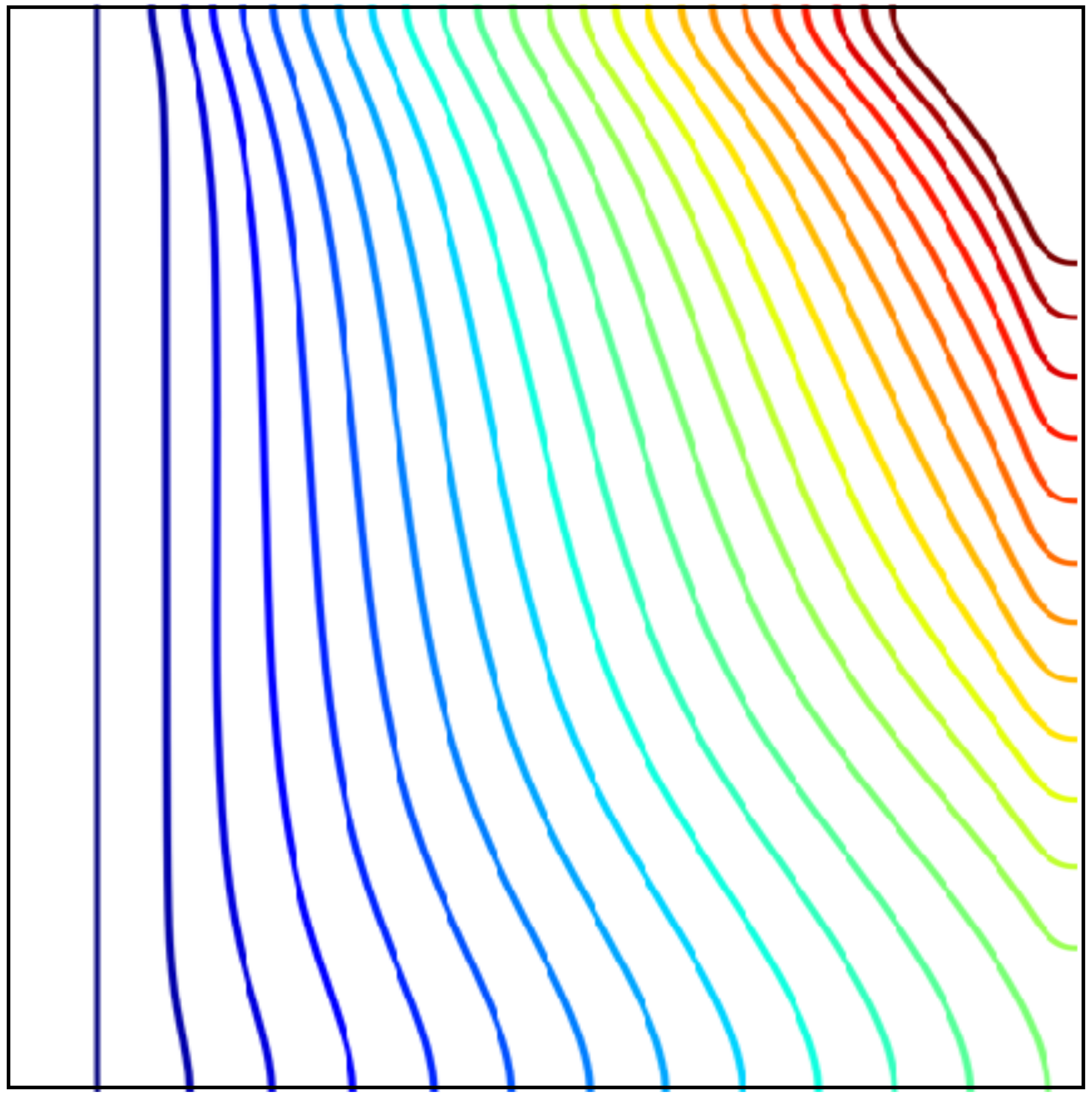

Finding: Morphological dynamics of melting ice depends on T_h

$T_h = 6.7^oC$

- Bottom part melts faster than top part

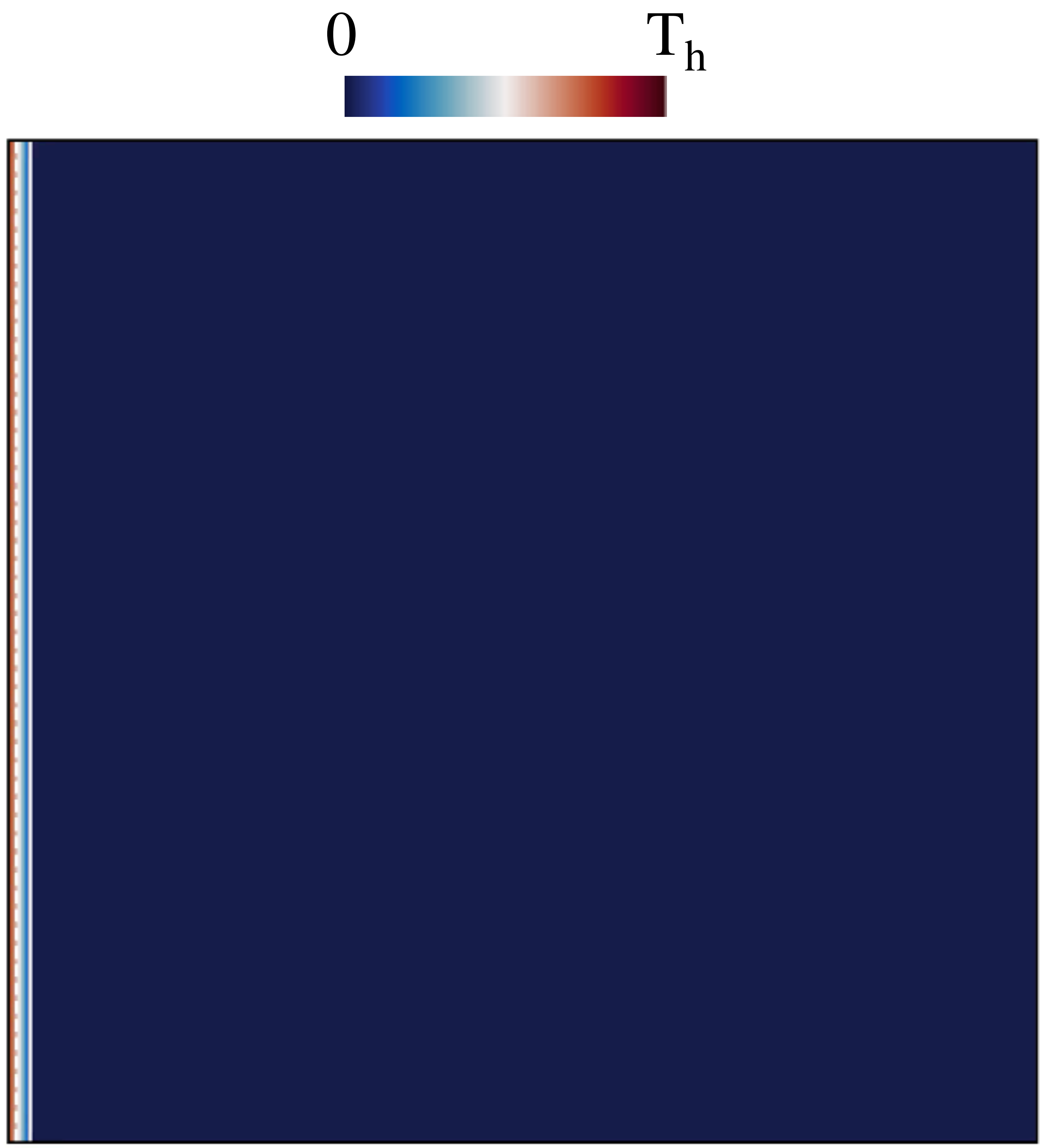

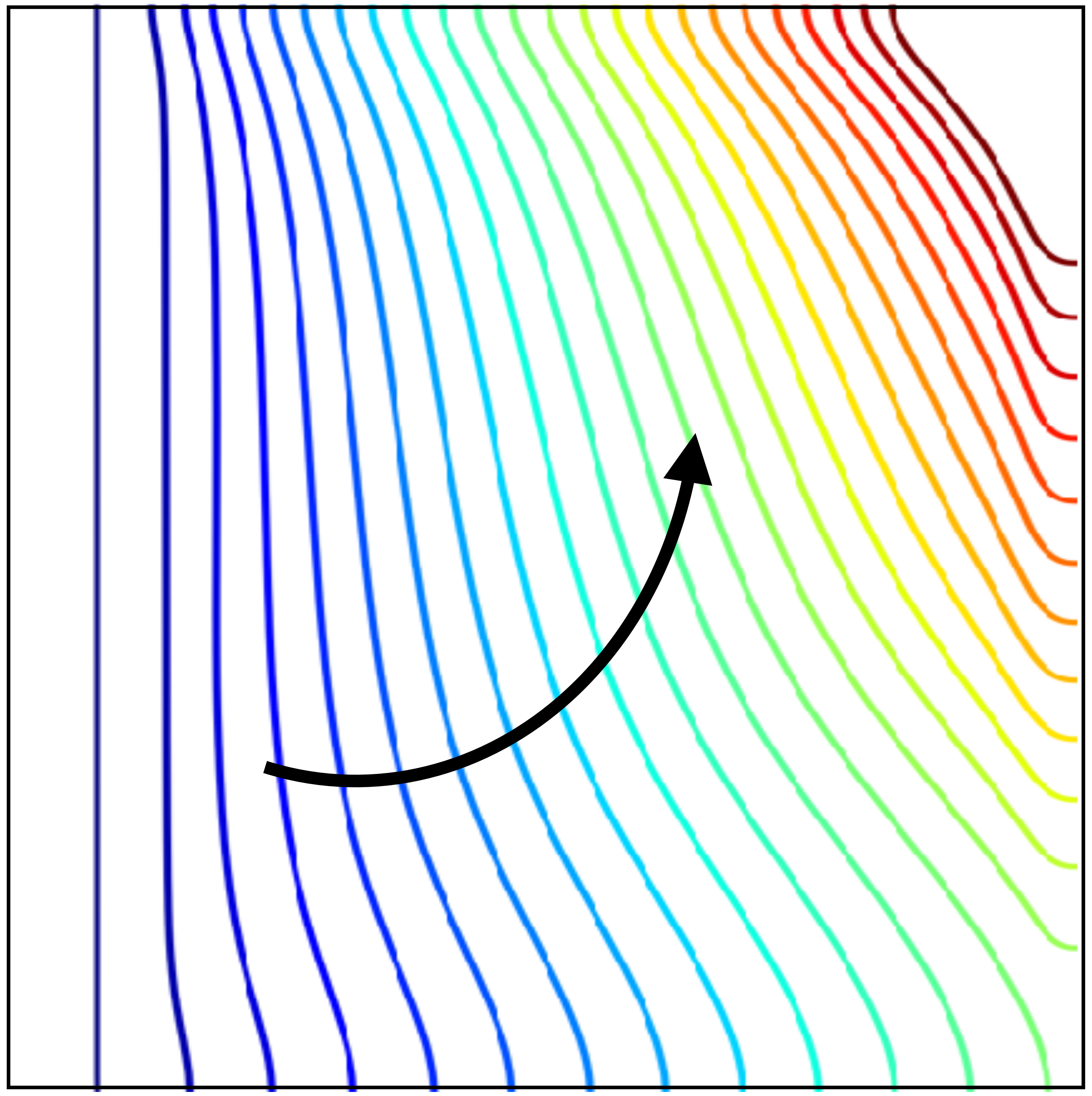

Finding: Morphological dynamics of melting ice depends on T_h

$T_h = 10^oC$

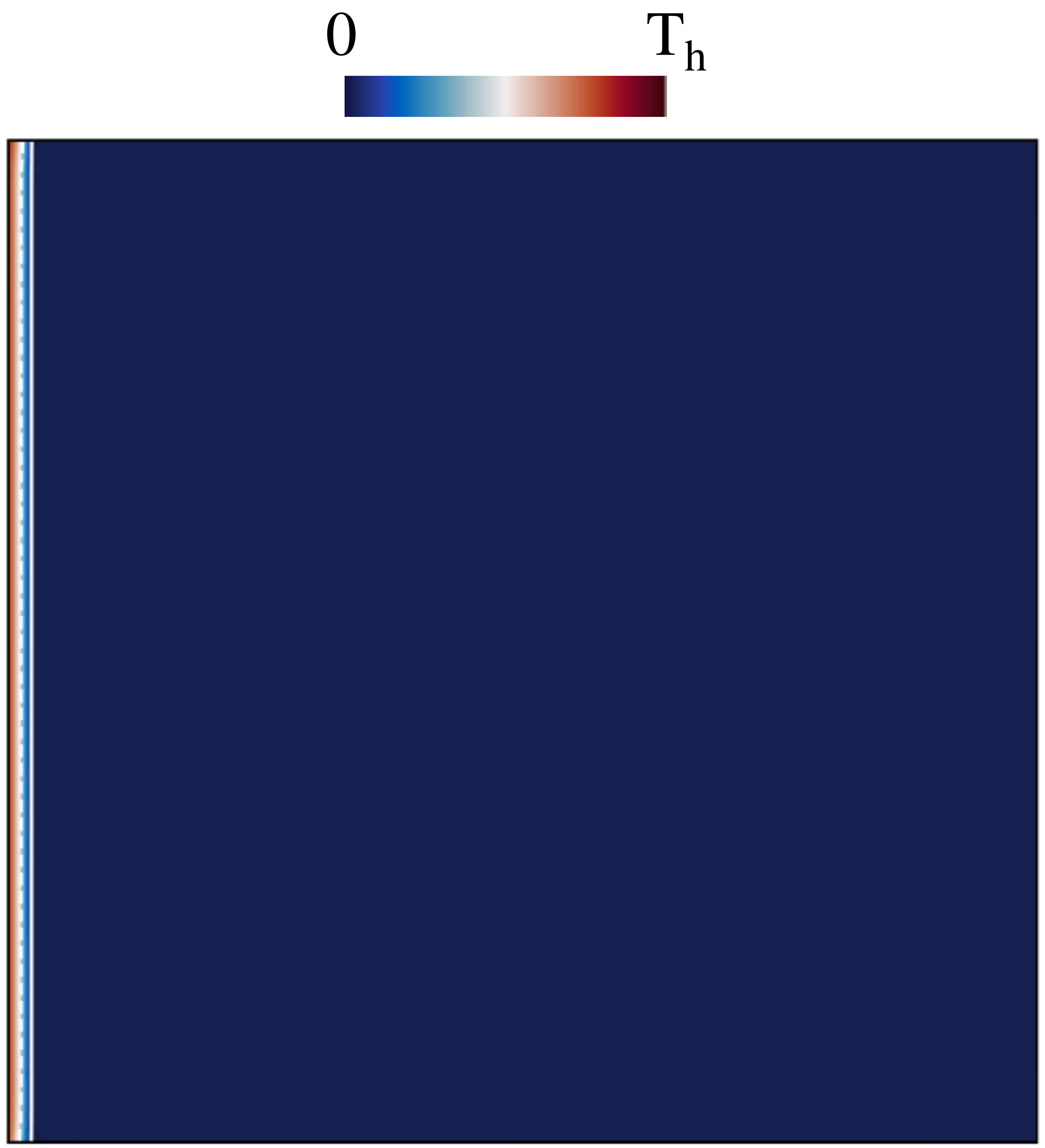

Finding: Morphological dynamics of melting ice depends on T_h

$T_h = 10^oC$

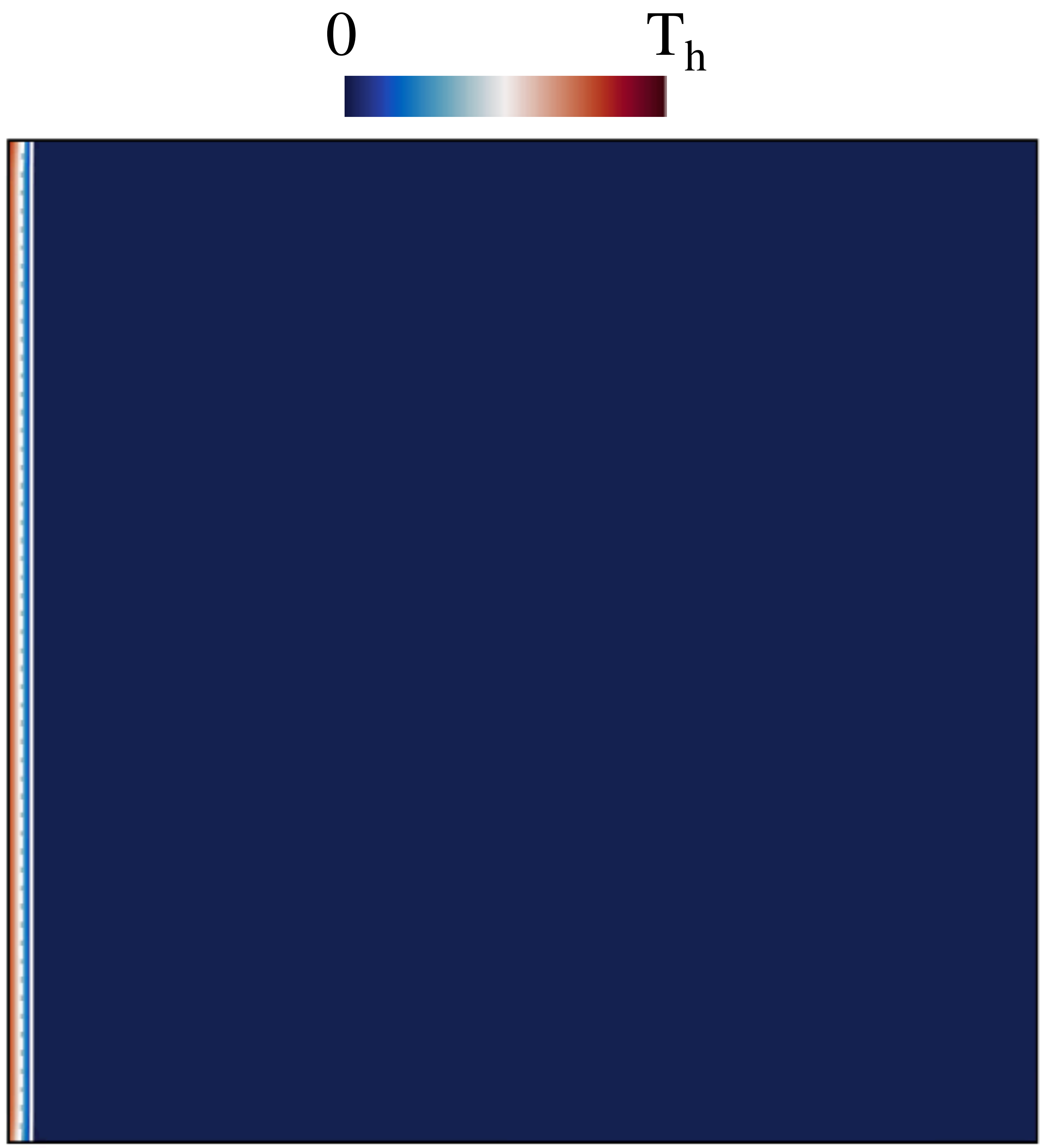

Finding: Morphological dynamics of melting ice depends on T_h

$T_h = 10^oC$

- Top part melts faster than bottom part
- Middle part melts the slowest

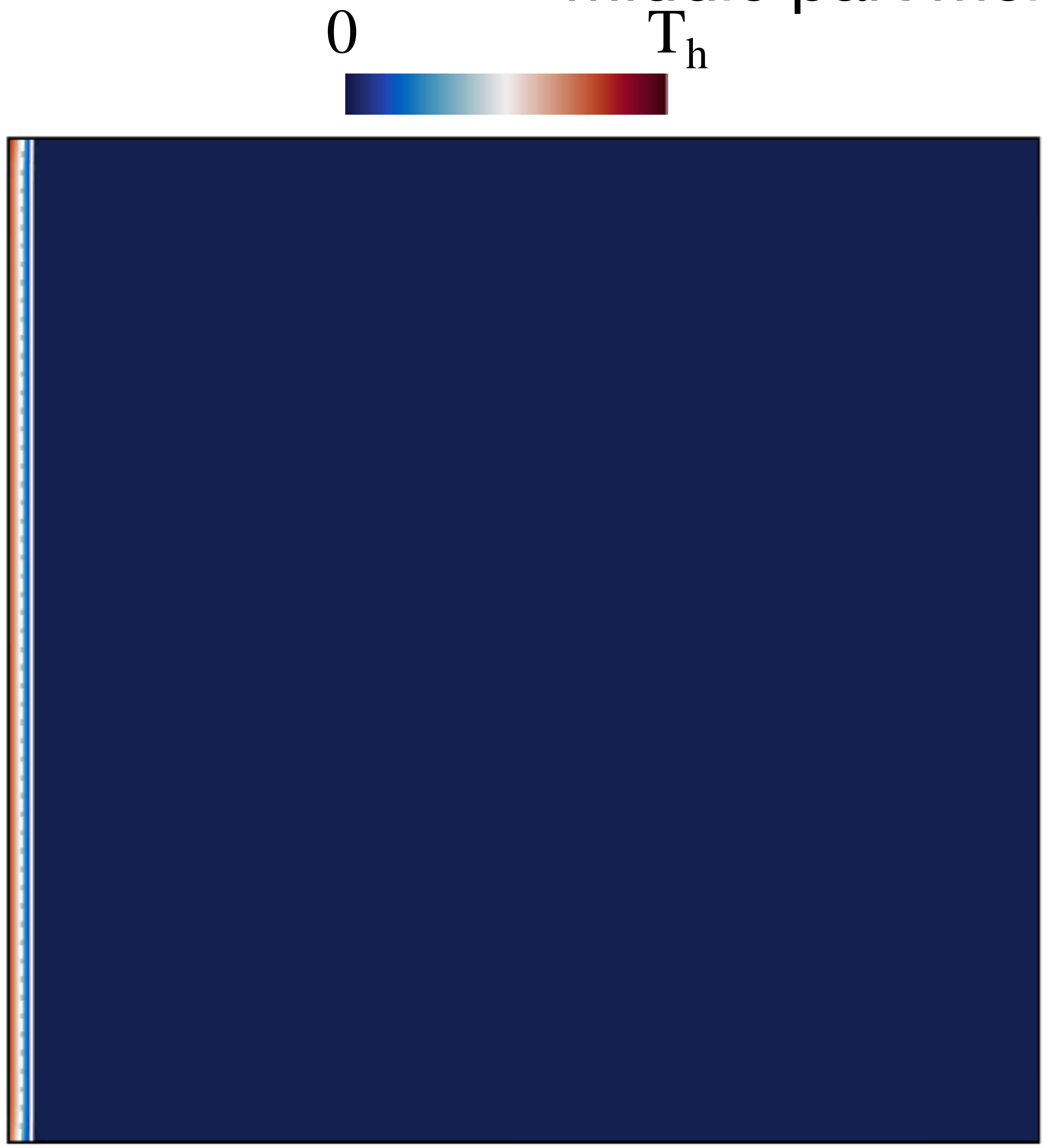

Finding: Morphological dynamics of melting ice depends on T_h

$T_h = 10^oC$

- Top part melts faster than bottom part
- Middle part melts the slowest

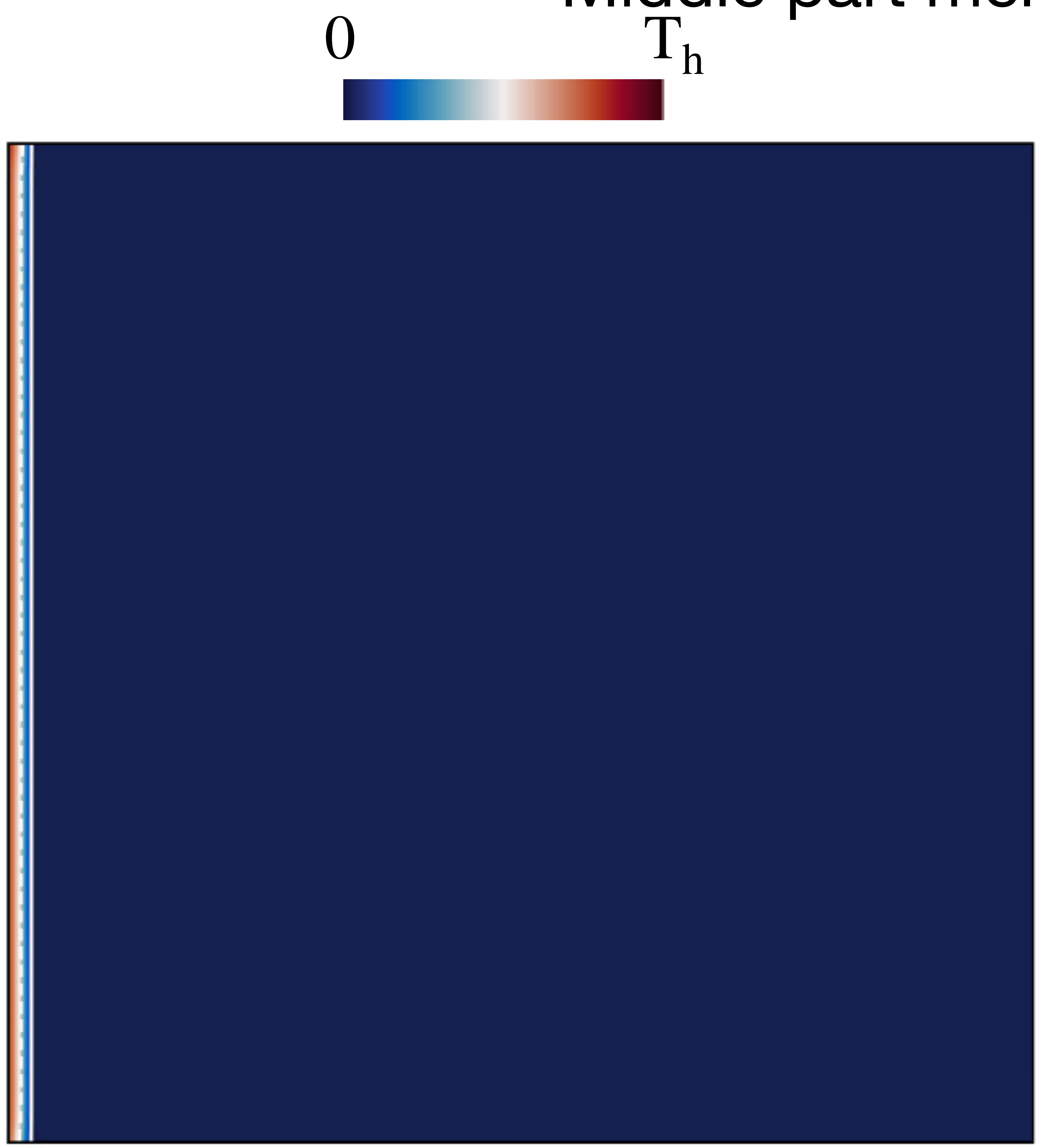

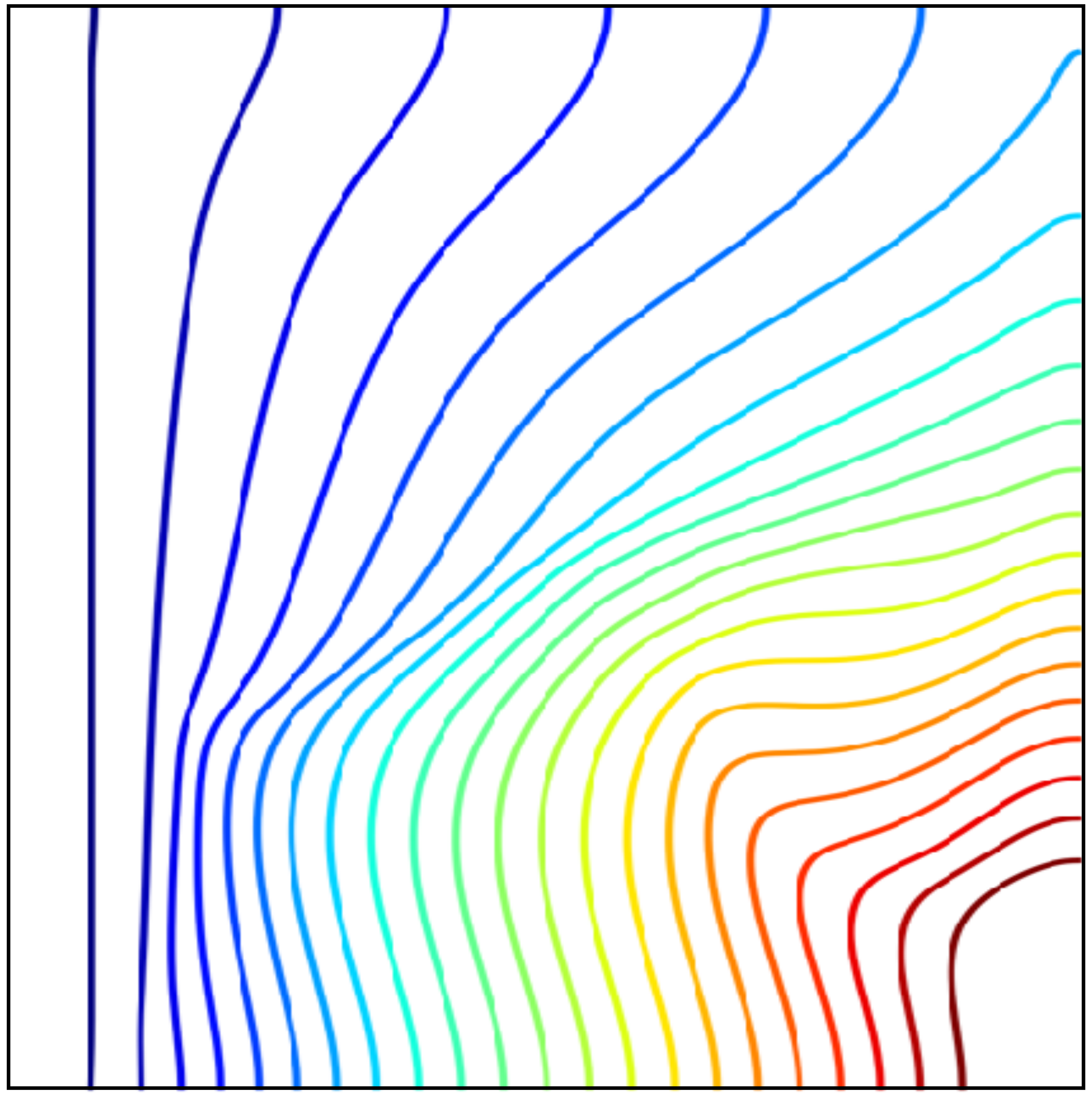

Finding: Morphological dynamics of melting ice depends on T_h

$T_h = 10^oC$

- Top part melts faster than bottom part
- Middle part melts the slowest

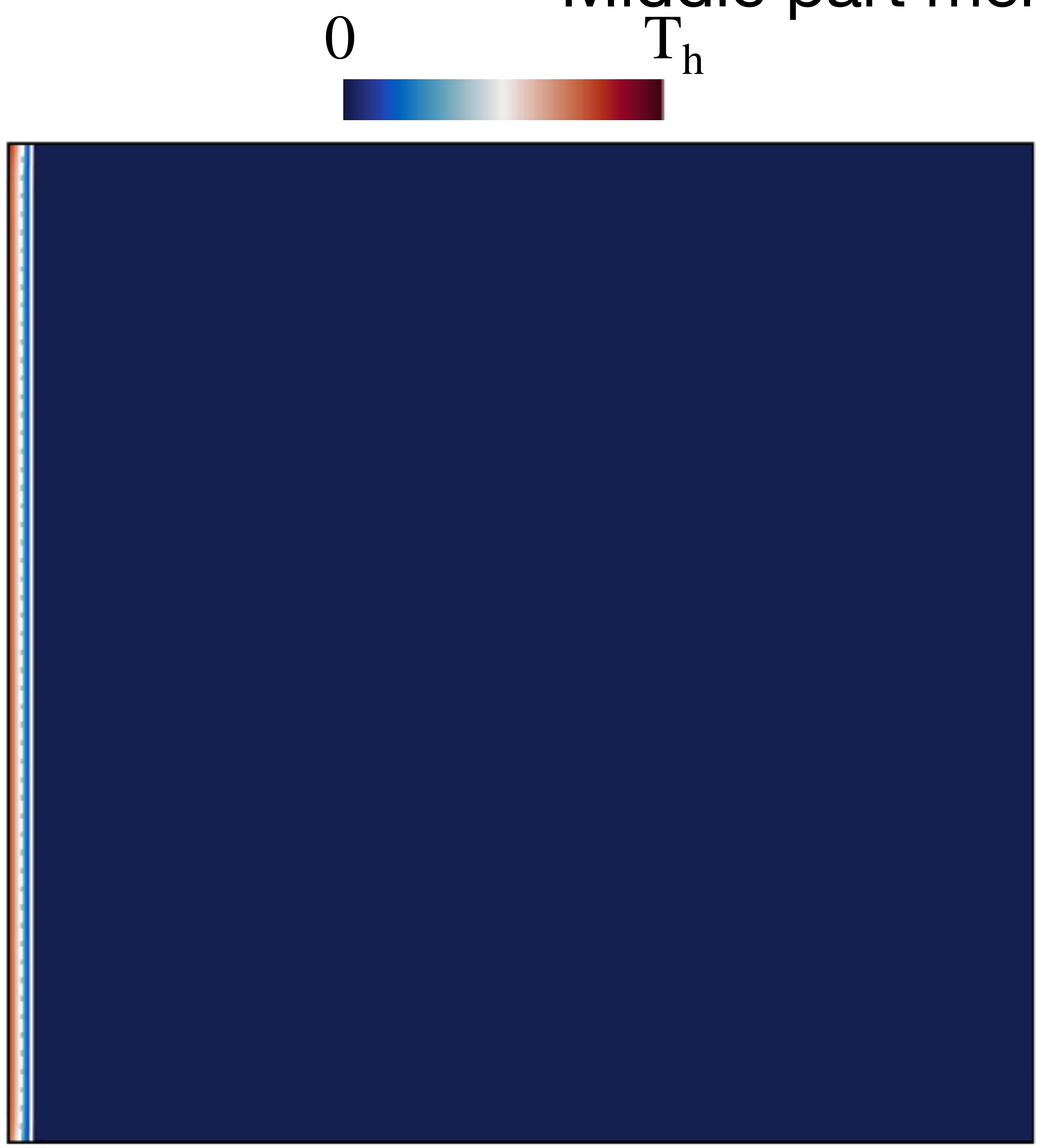

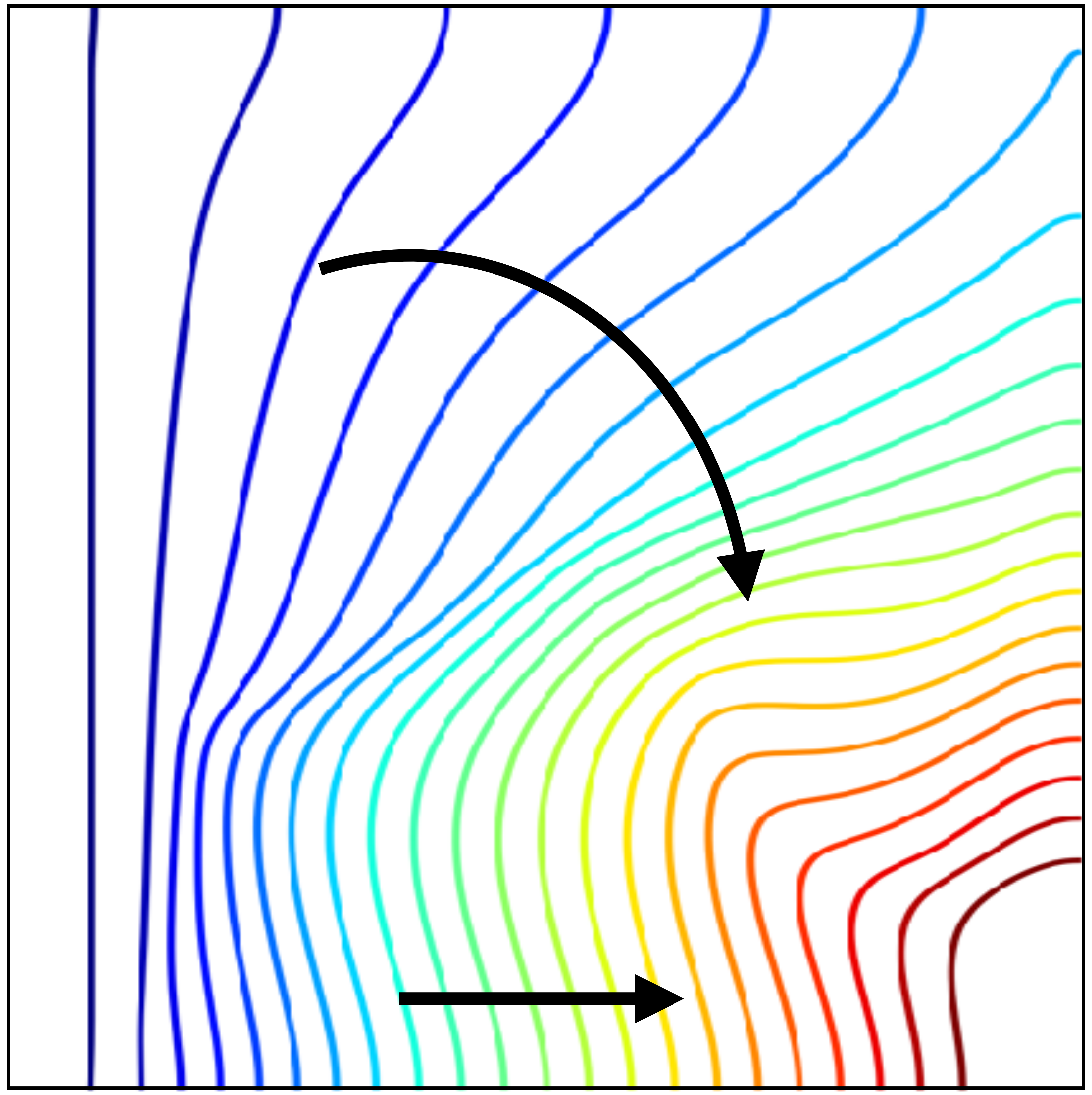

Summary of shape evolution

Without density anomaly

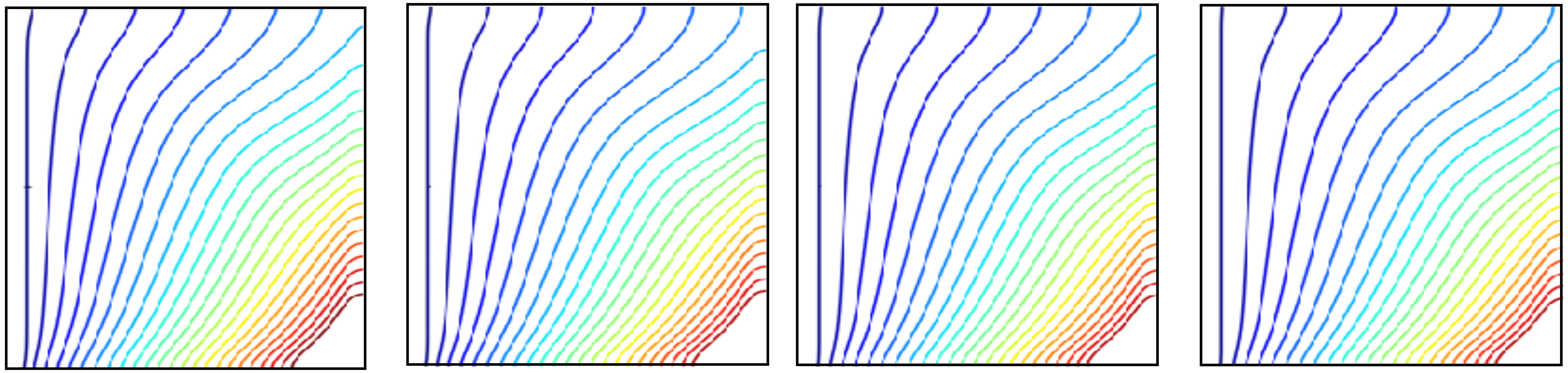

$T_h = 20^oC$ | $T_h = 10^oC$ | $T_h = 6.7^oC$ | $T_h = 5^oC$

With density anomaly

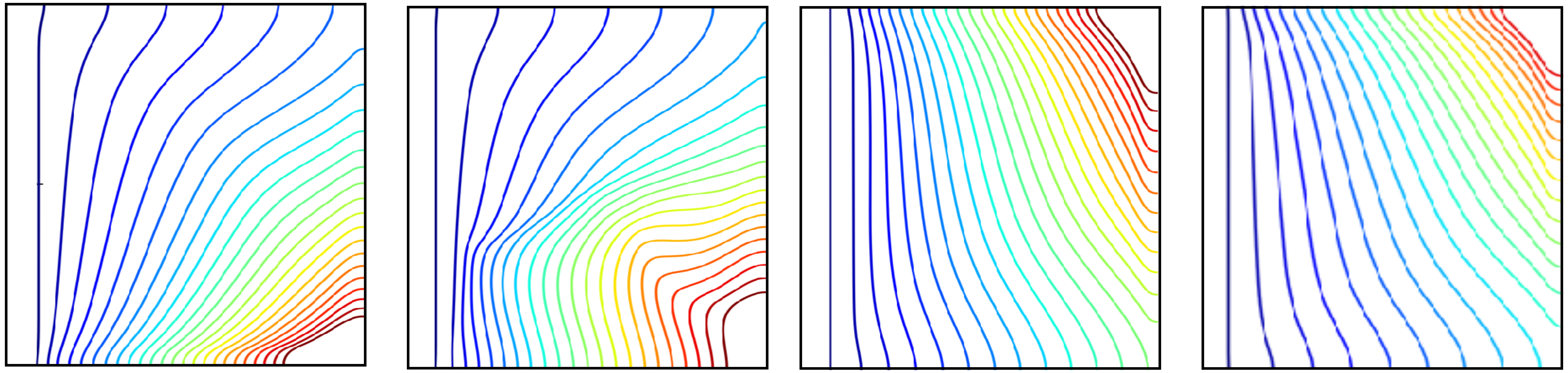

$T_h = 20^oC$, $\theta_m = 0.2$ | $T_h = 10^oC$, $\theta_m = 0.4$ | $T_h = 6.7^oC$, $\theta_m = 0.6$ | $T_h = 5^oC$, $\theta_m = 0.8$

Summary of shape evolution

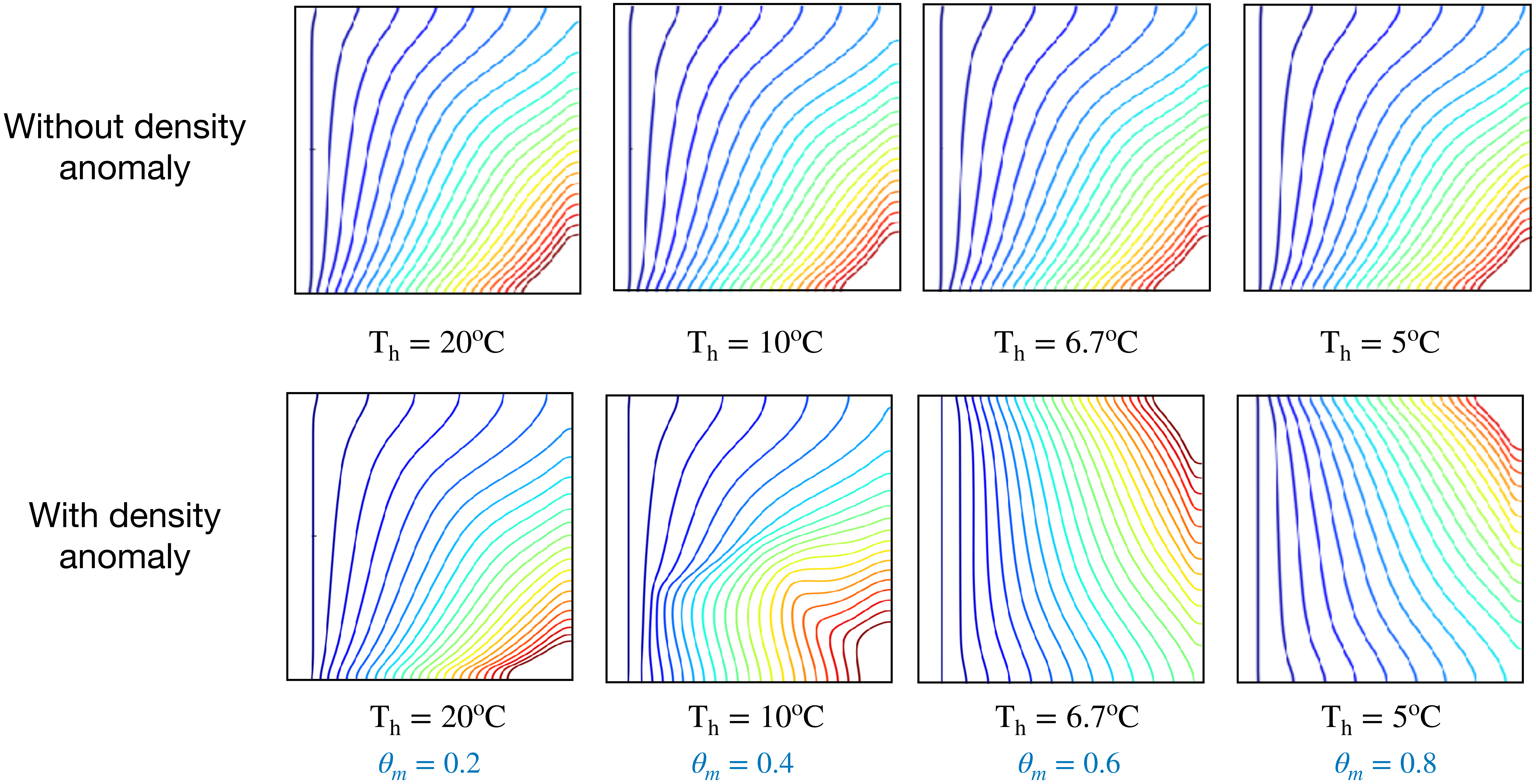

Locally reversed flow significantly affects the melt shape

Same features hold for 3D DNS

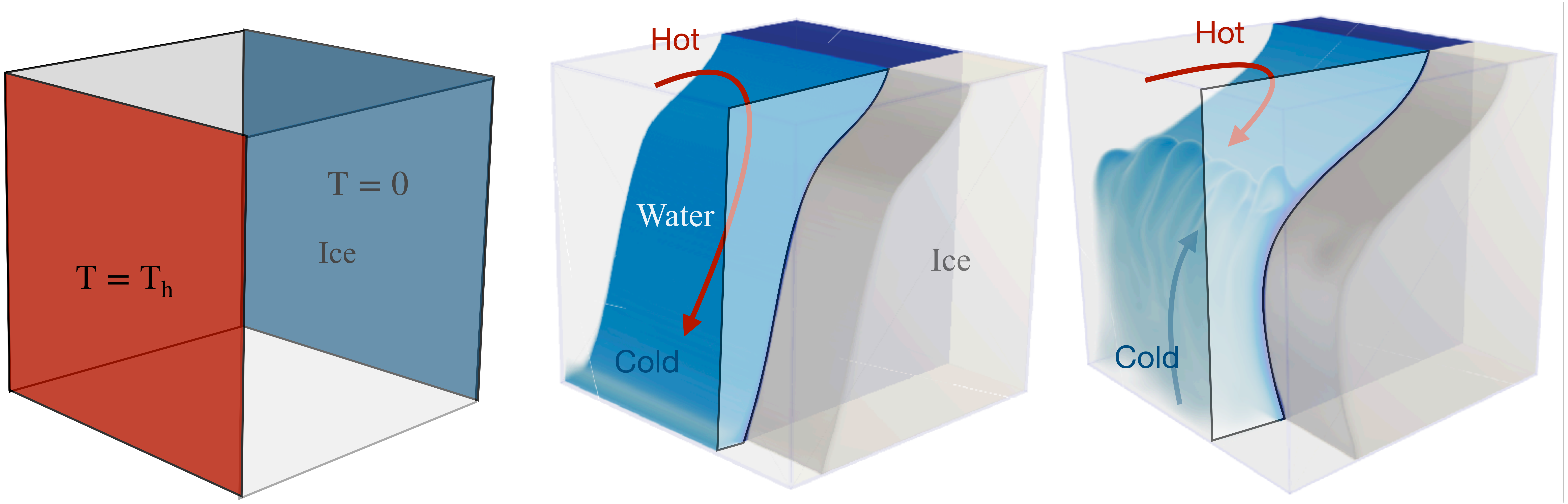

$T_h = 20^oC$ $T_h = 10^oC$

Same features hold for 3D DNS

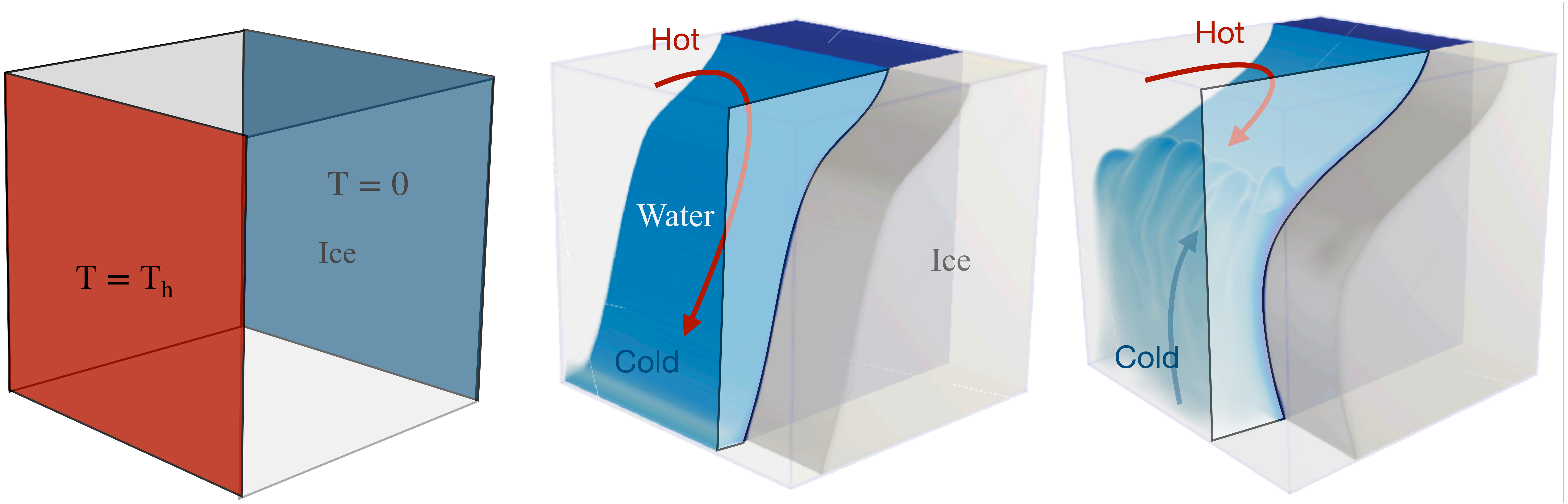

$T_h = 20^oC$ $T_h = 10^oC$

How does the melting rate change?

Impact of flow dynamics on melting rate

Without density anomaly

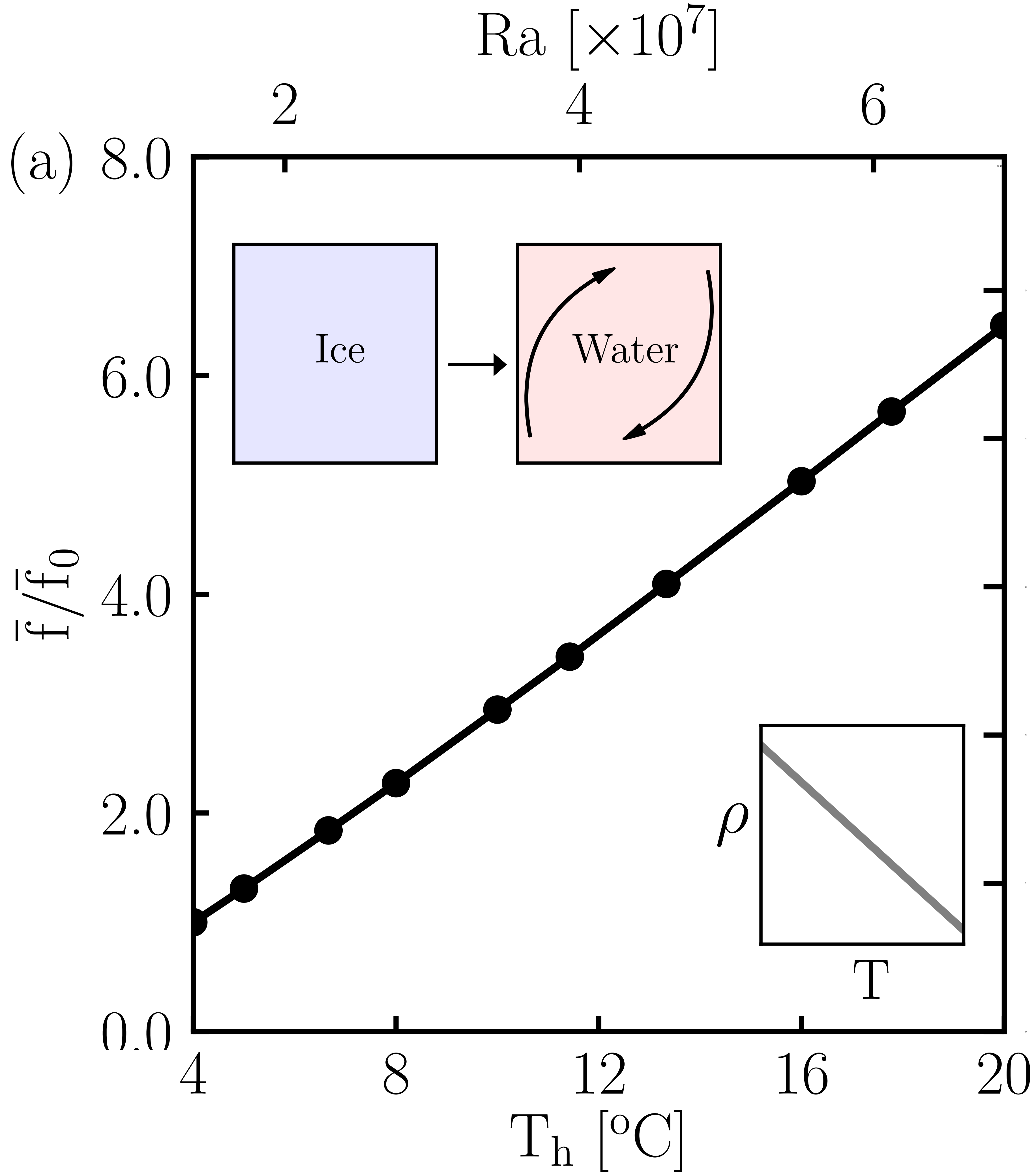

Impact of flow dynamics on melting rate

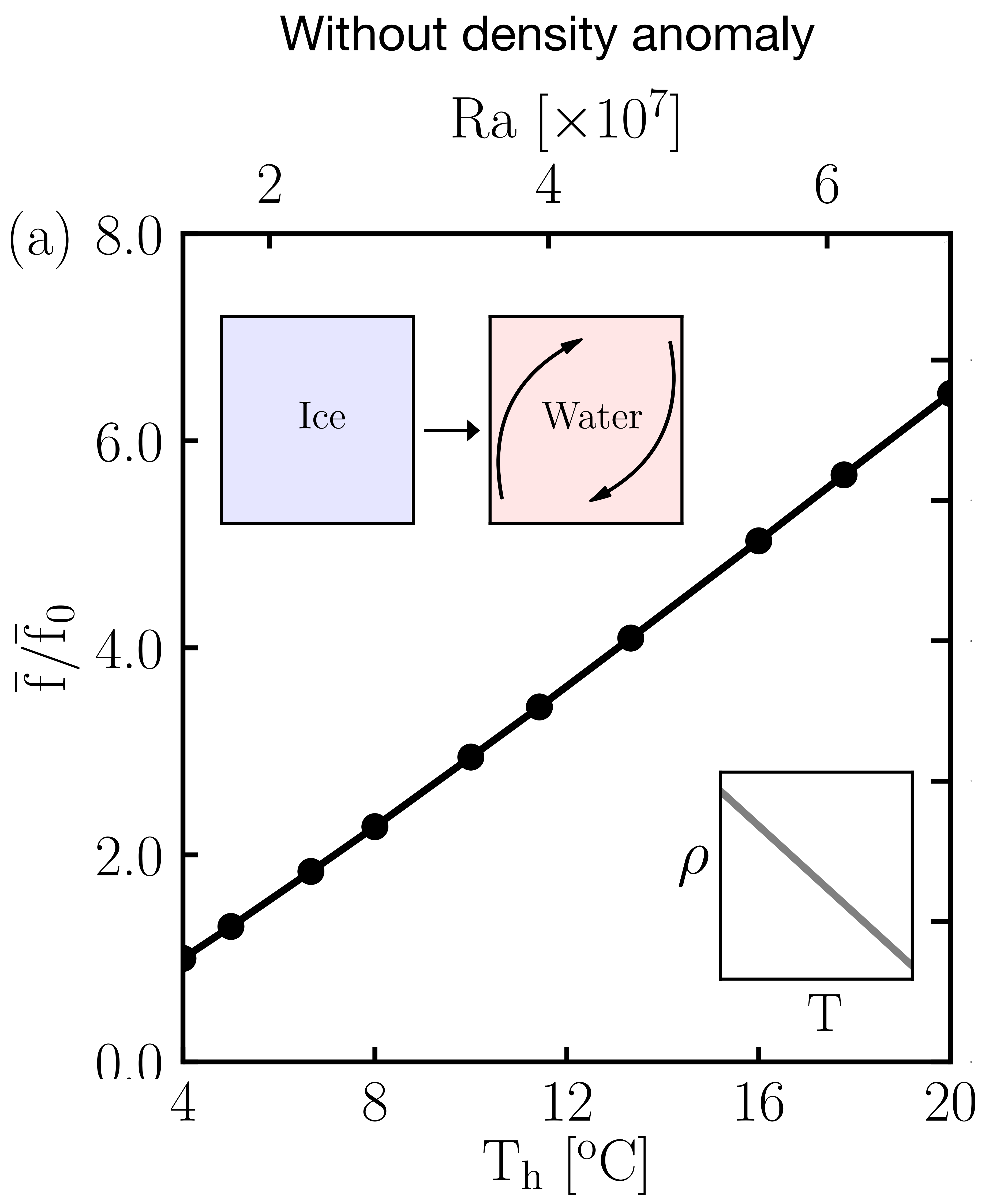

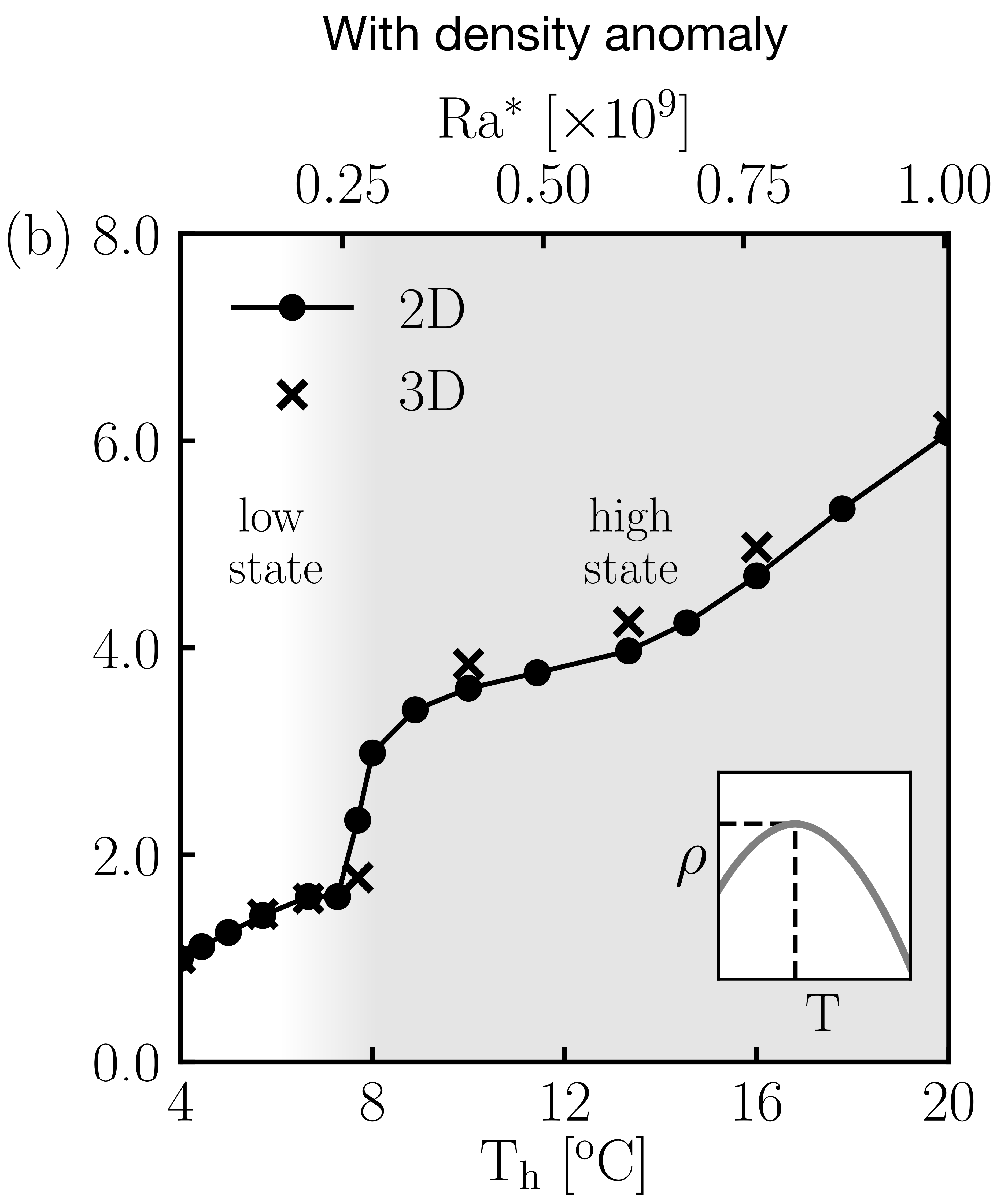

Impact of flow dynamics on melting rate

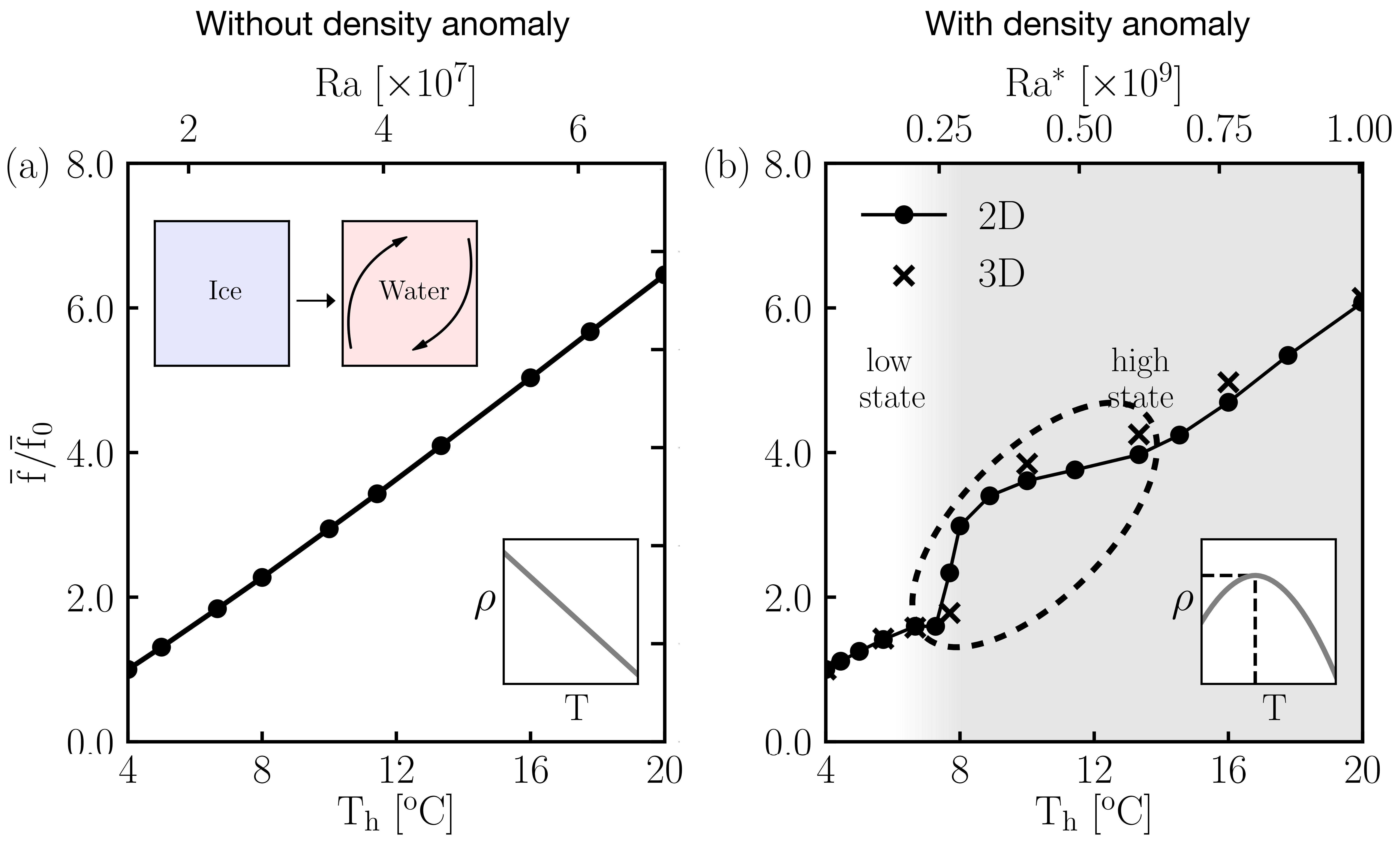

Impact of flow dynamics on melting rate

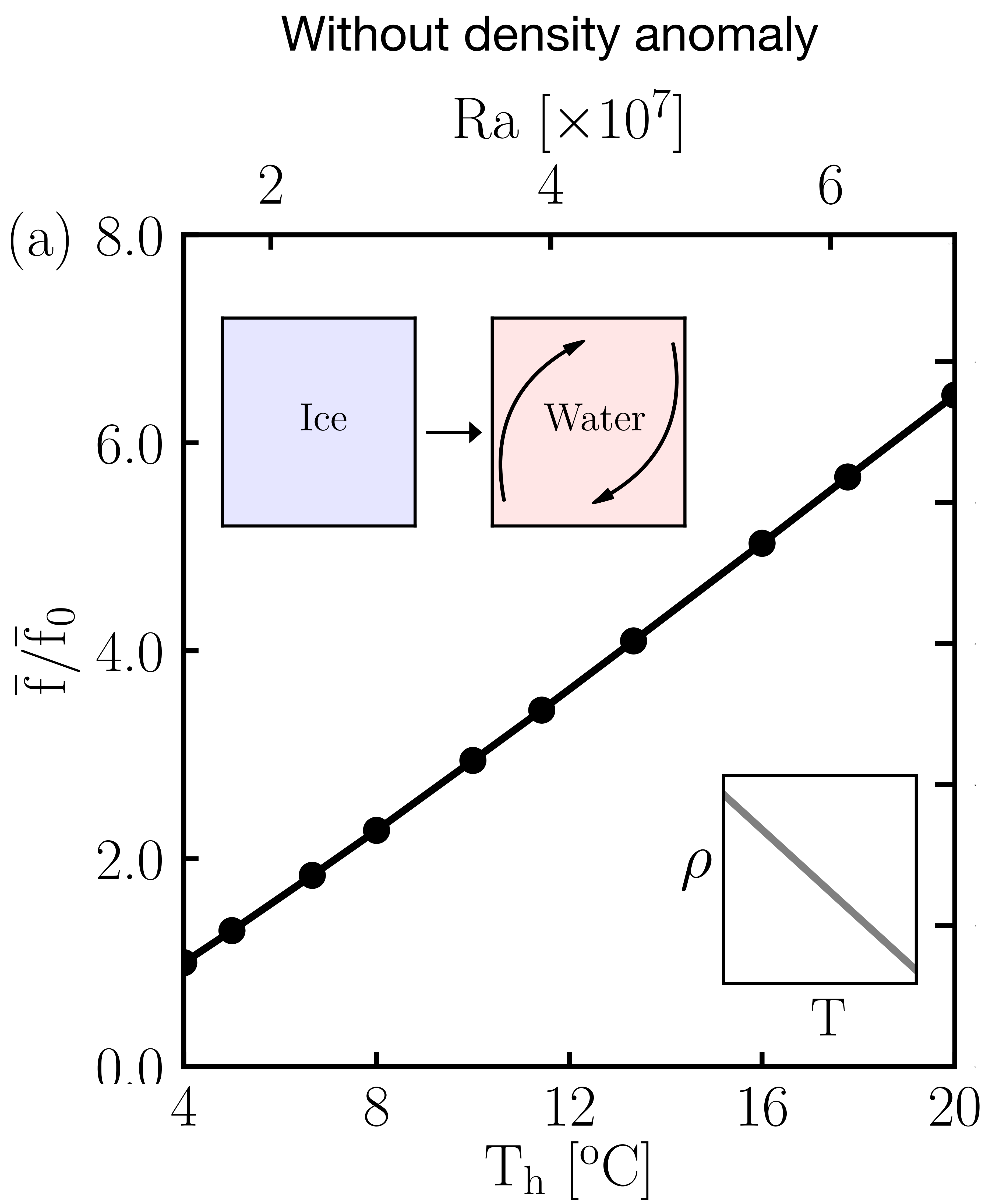

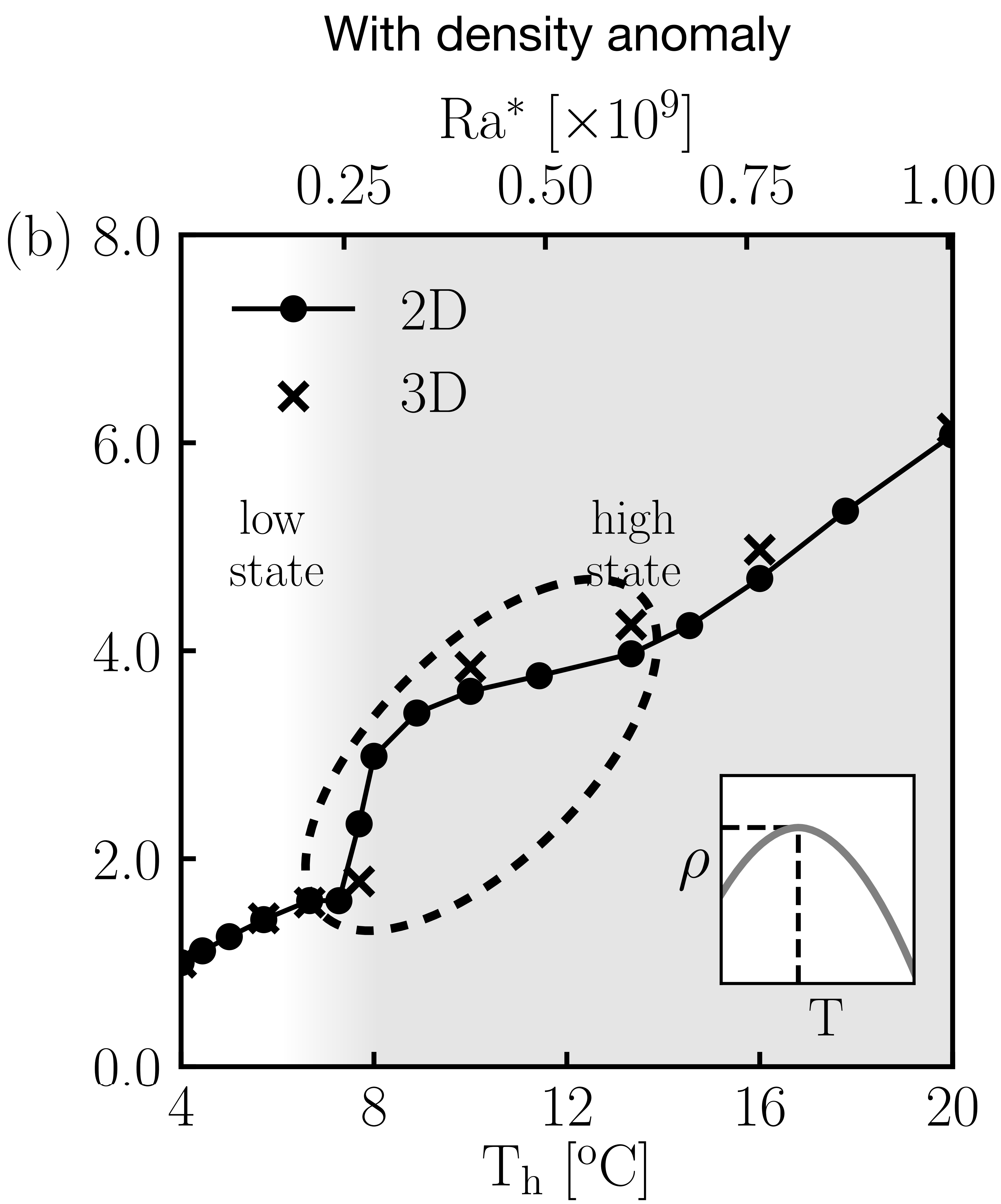

Tipping point towards enhanced melt regime due to density anomaly !

Heat transfer - Nu number

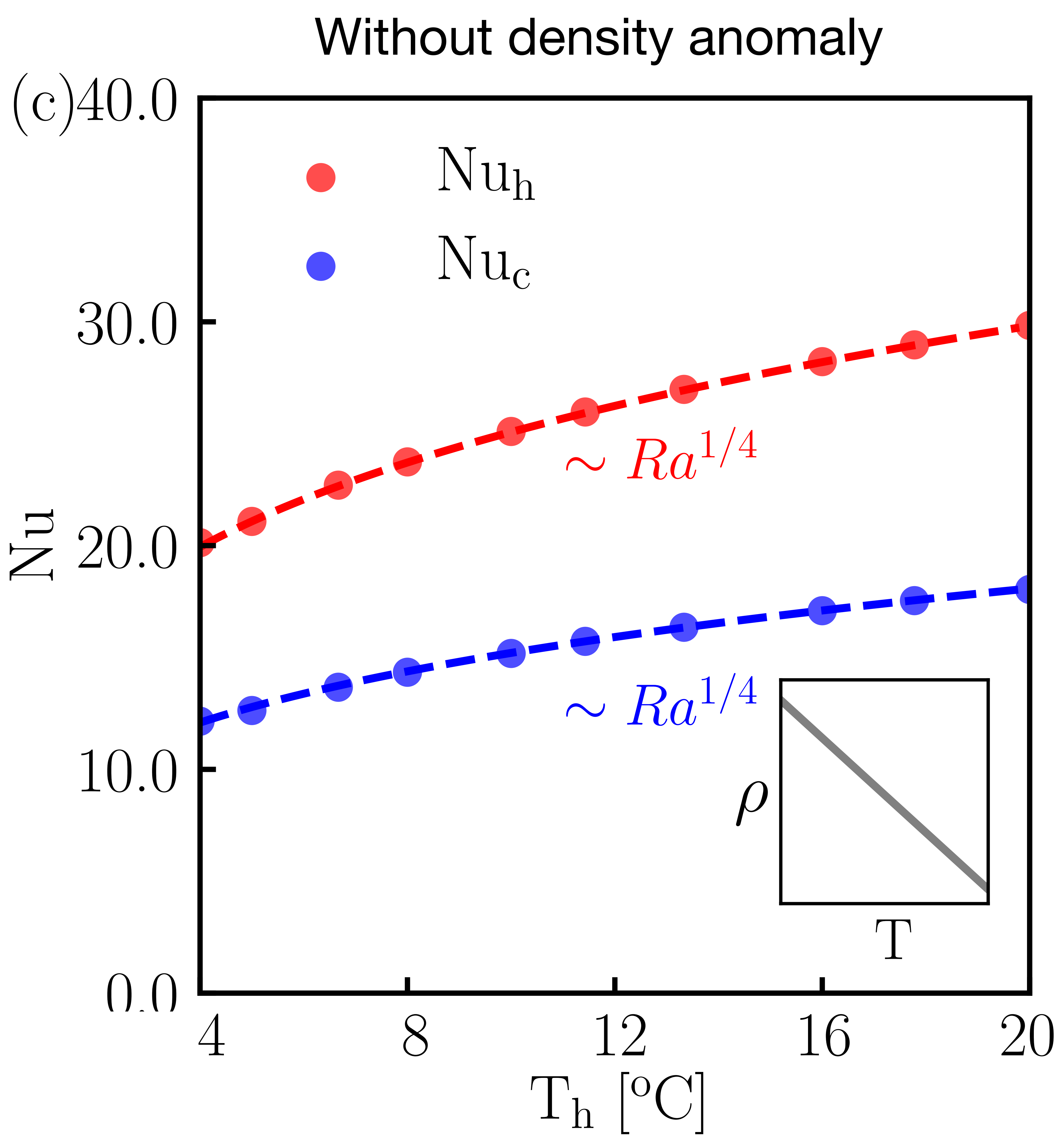

Heat transfer - Nu number

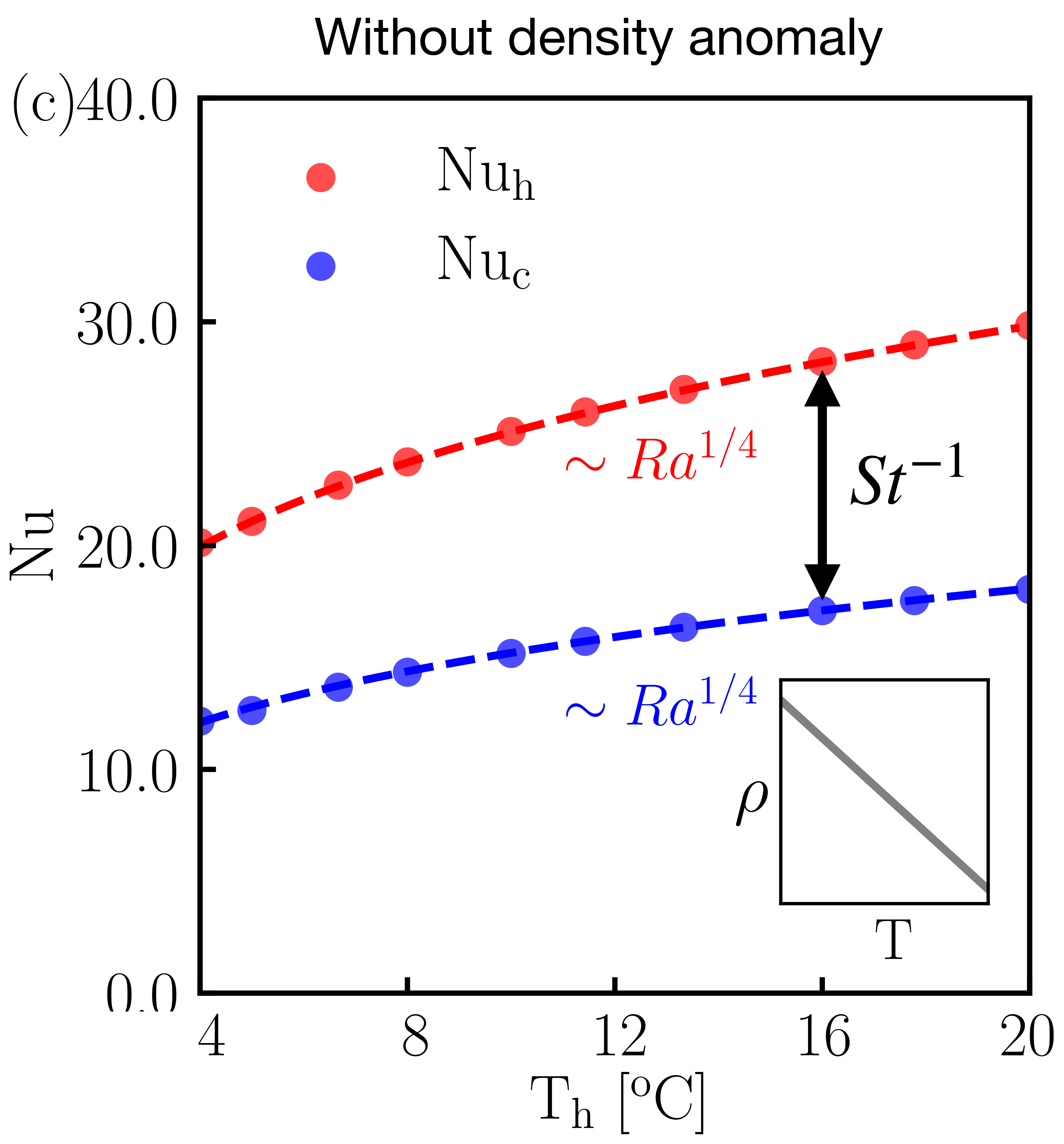

Heat transfer - Nu number

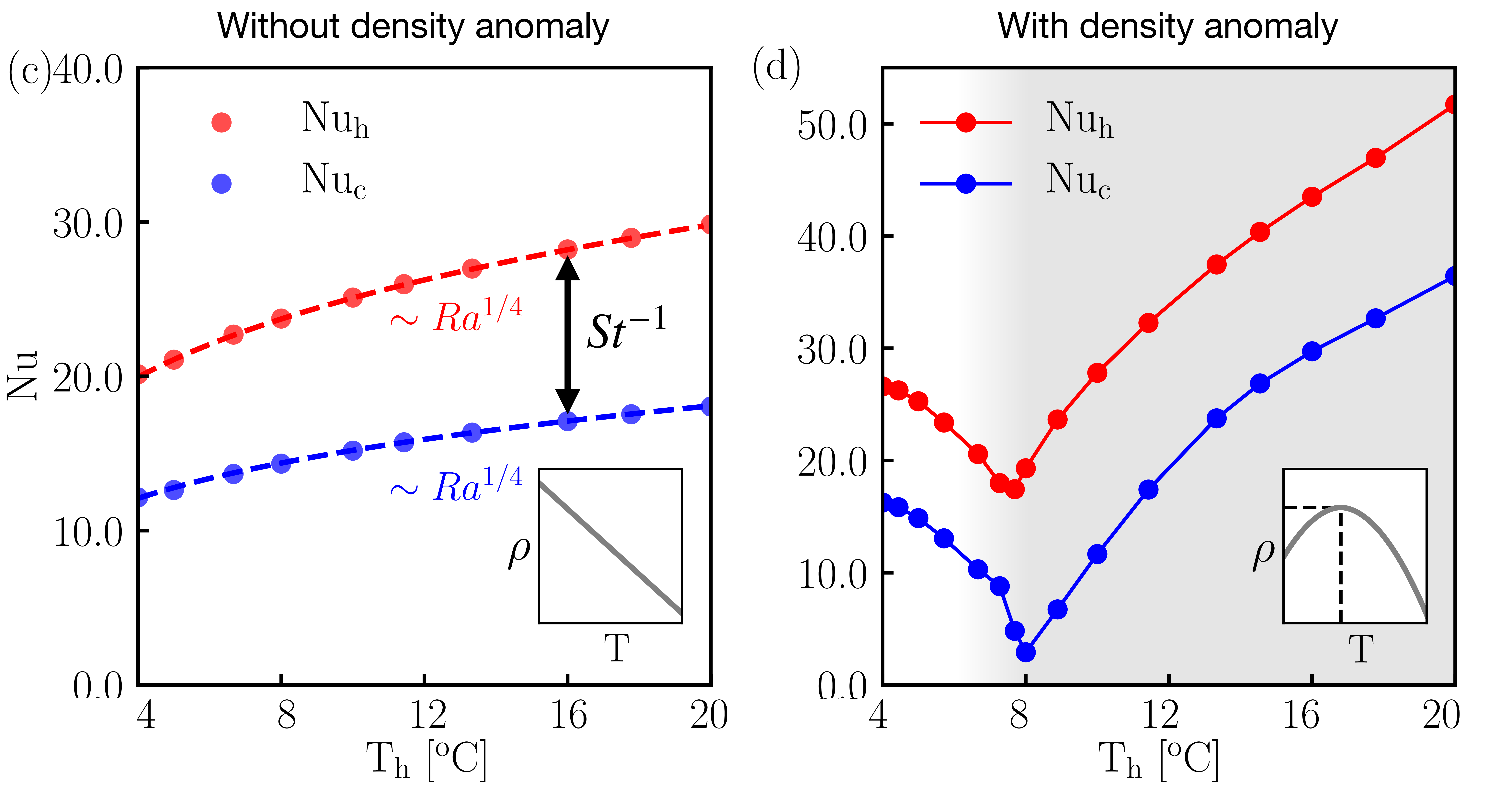

Heat transfer - Nu number

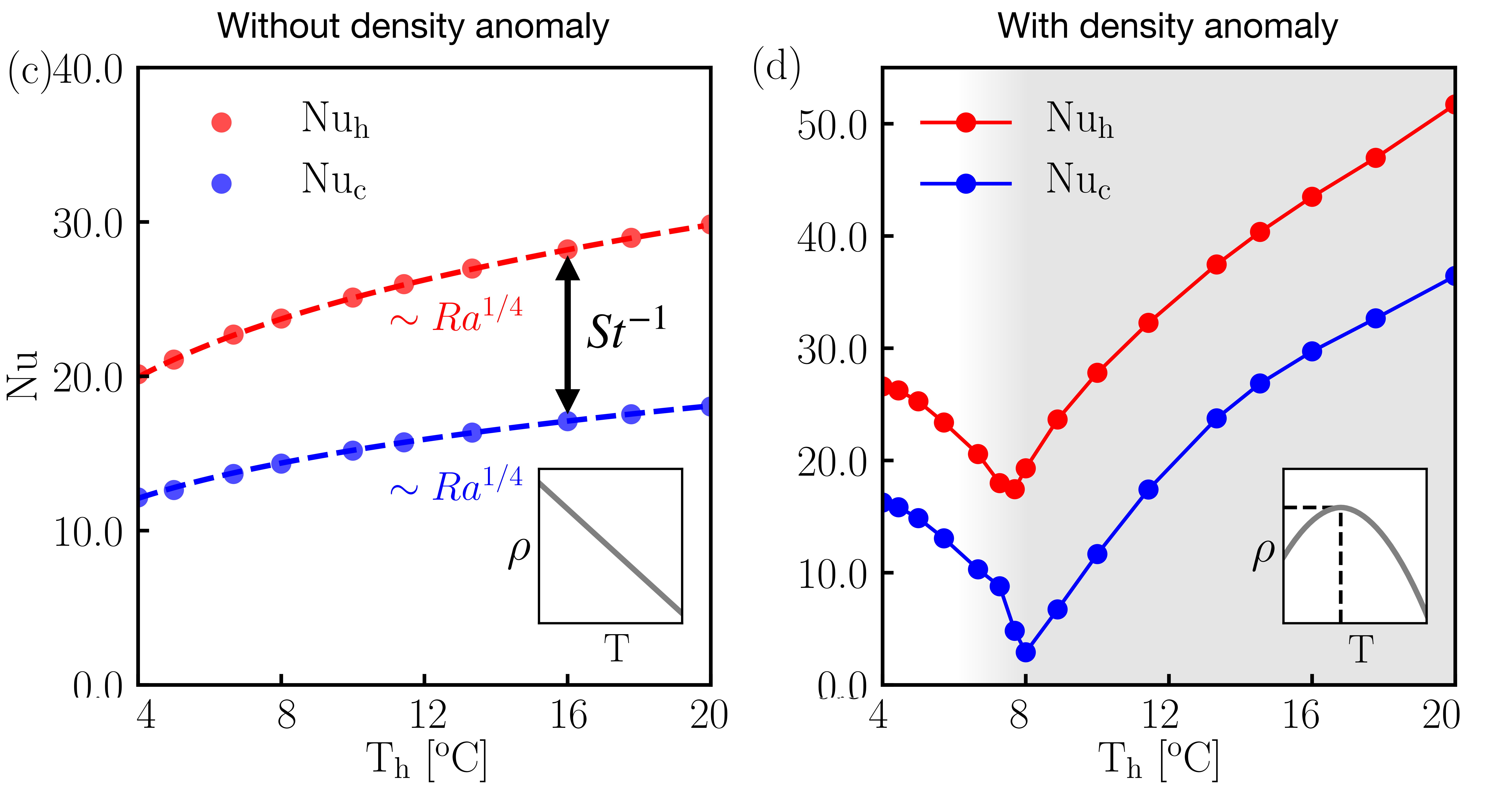

Non-monotonic trend of Nu numbers

Explanation for the Nu trend - locally reversed flow

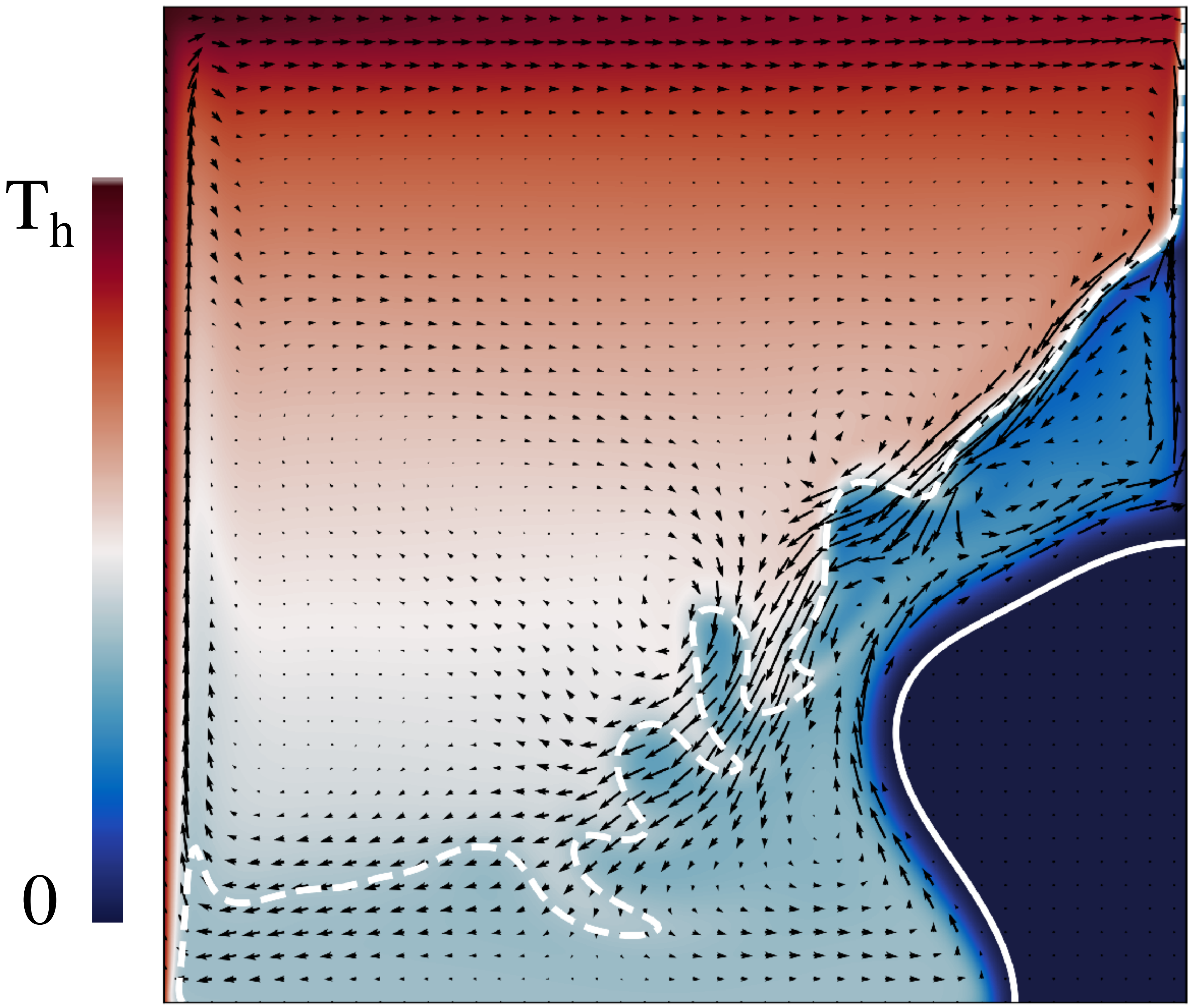

$T_h = 10^oC$

Explanation for the Nu trend - locally reversed flow

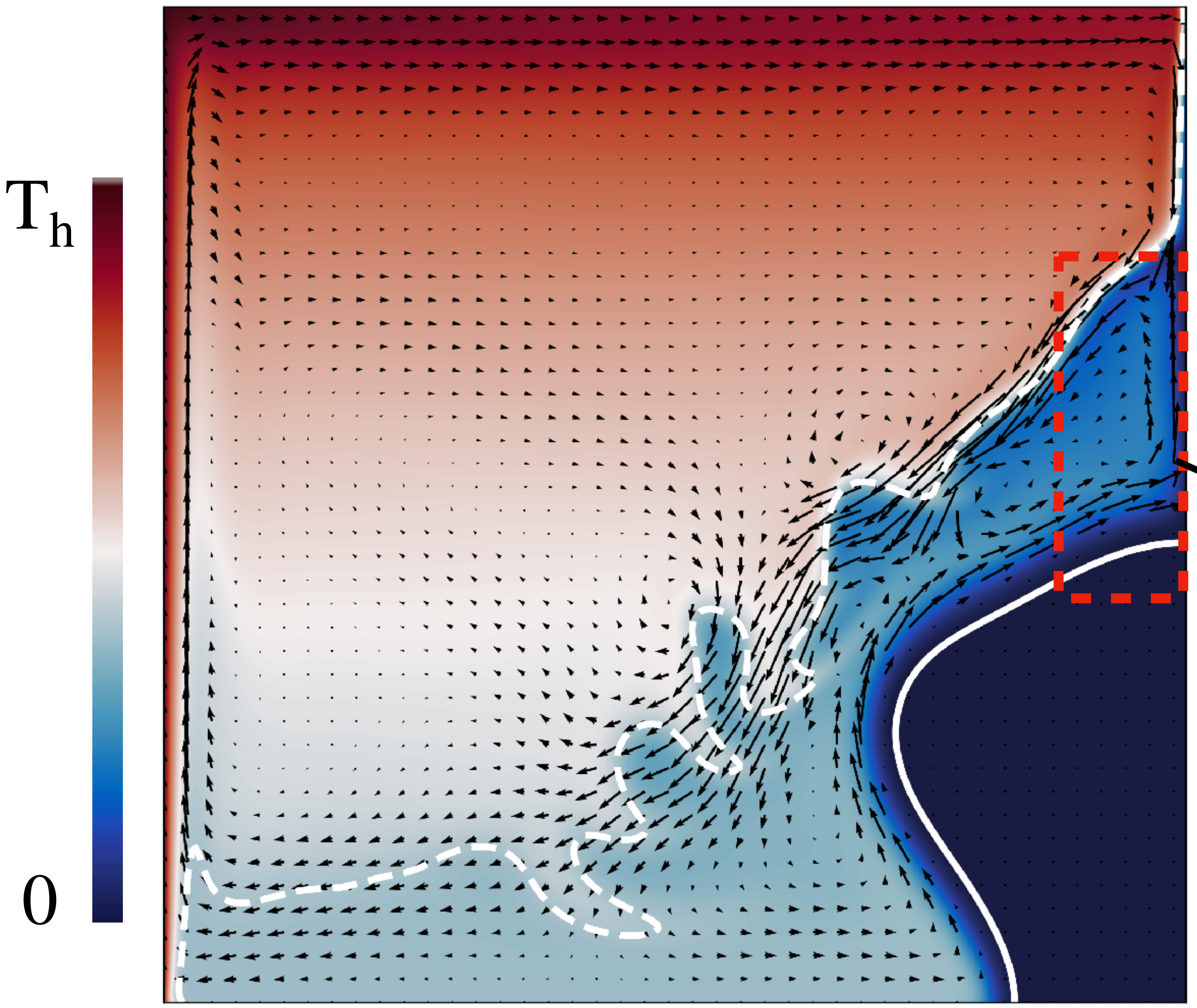

$T_h = 10^{o}C$

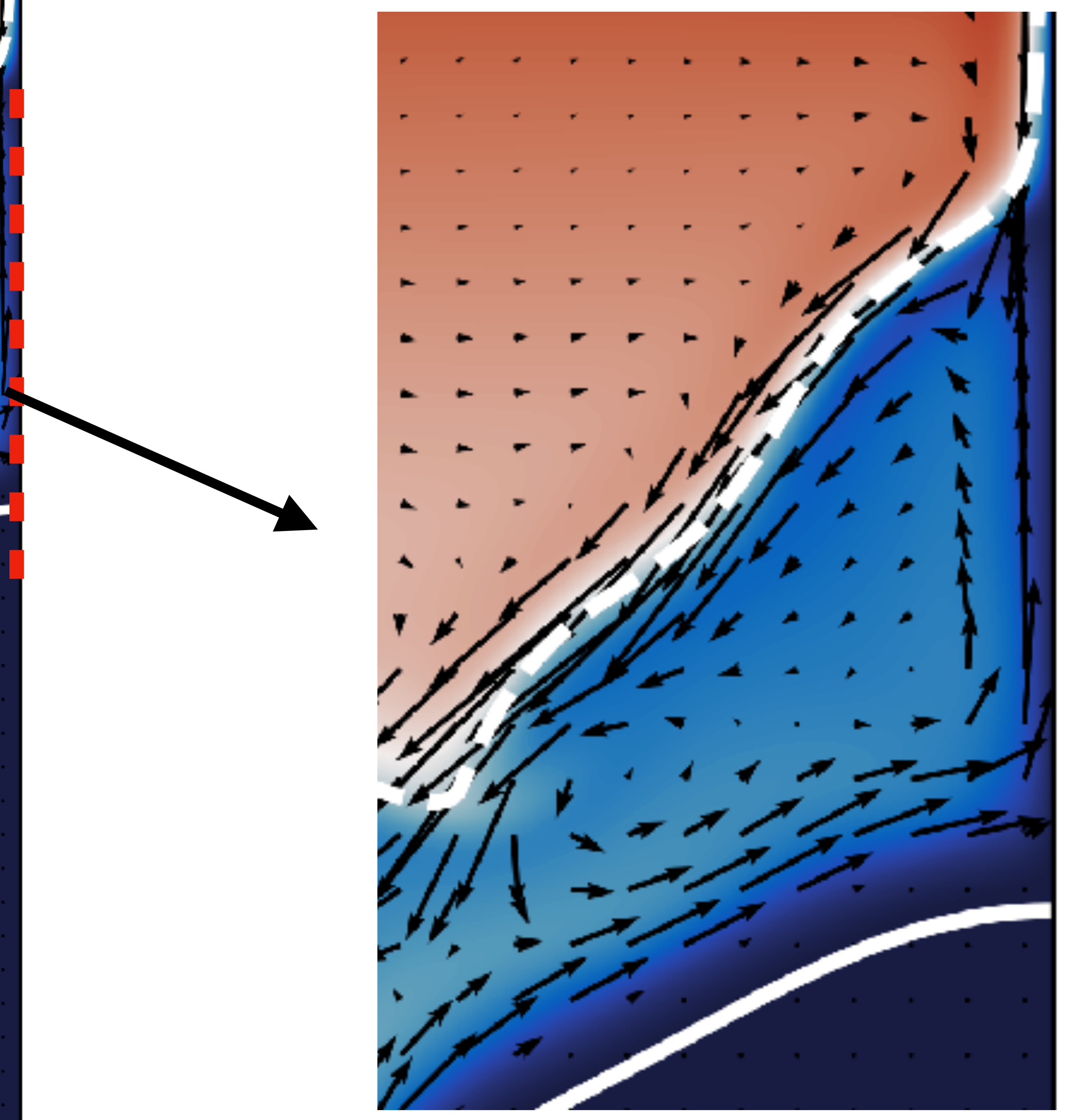

Locally reversed flow drives the melt fluid to protect the cold plate from heat loss

Explanation for the Nu trend - locally reversed flow

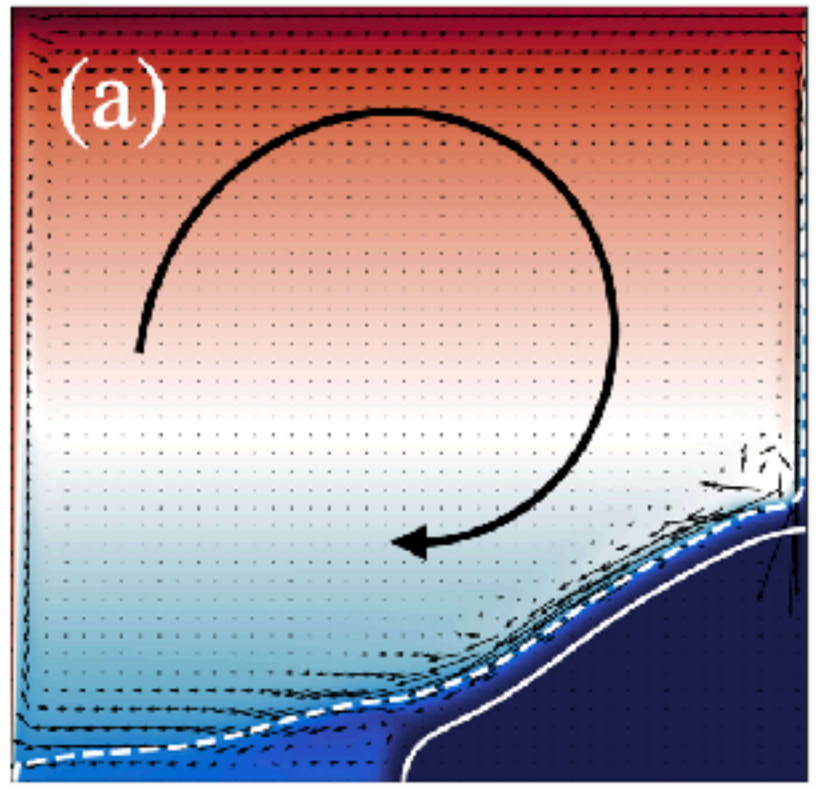

$T_h = 20^oC$

Explanation for the Nu trend - locally reversed flow

Explanation for the Nu trend - locally reversed flow

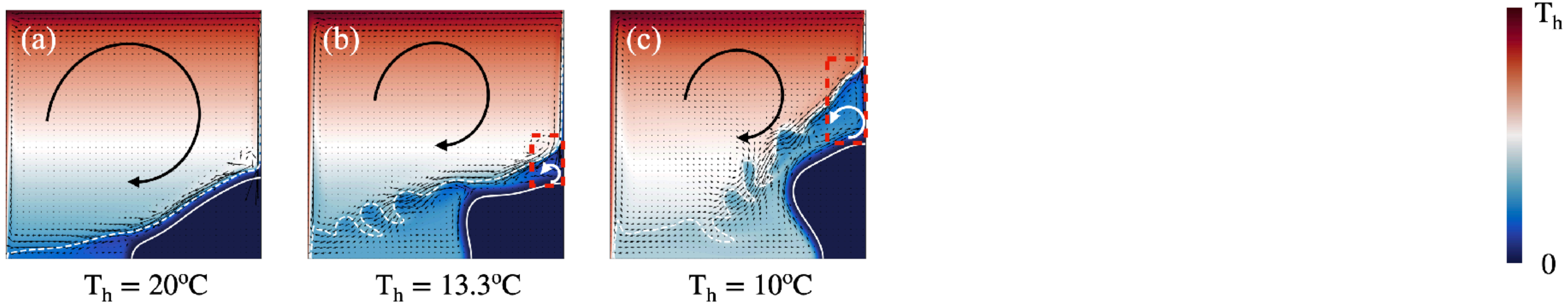

Explanation for the Nu trend - locally reversed flow

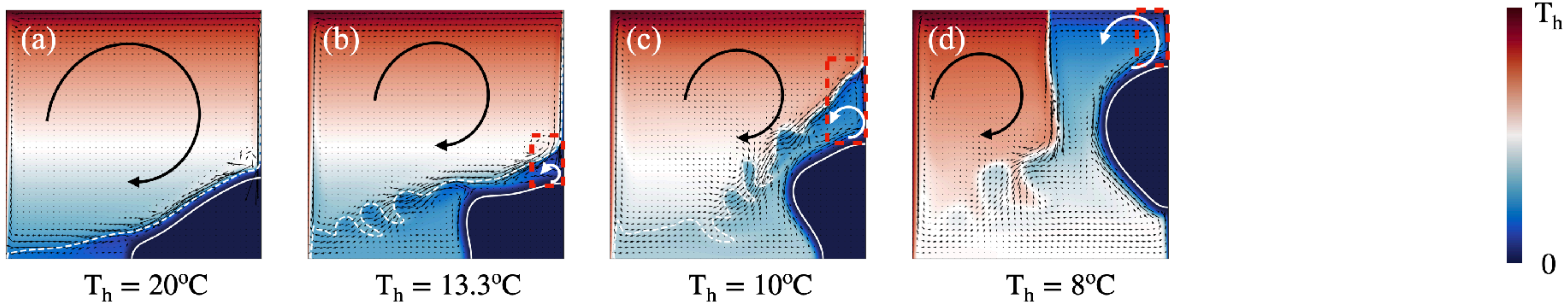

Explanation for the Nu trend - locally reversed flow

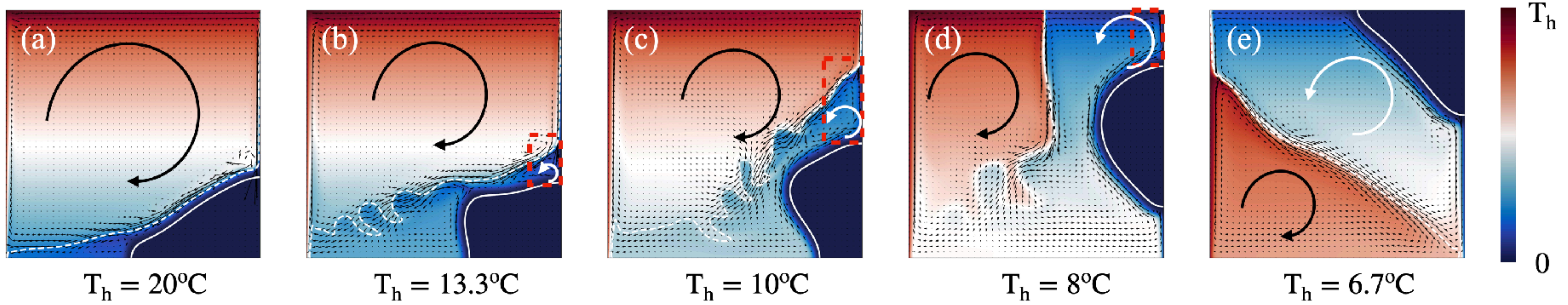

Explanation for the Nu trend - locally reversed flow

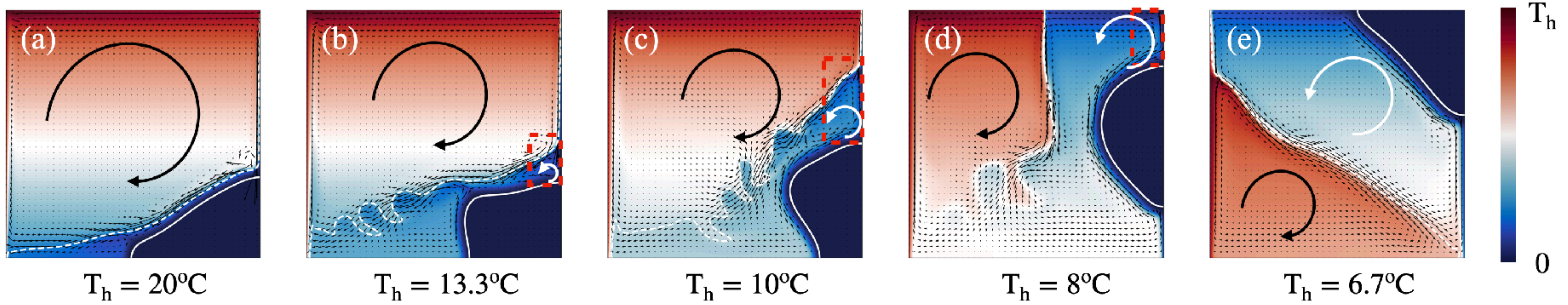

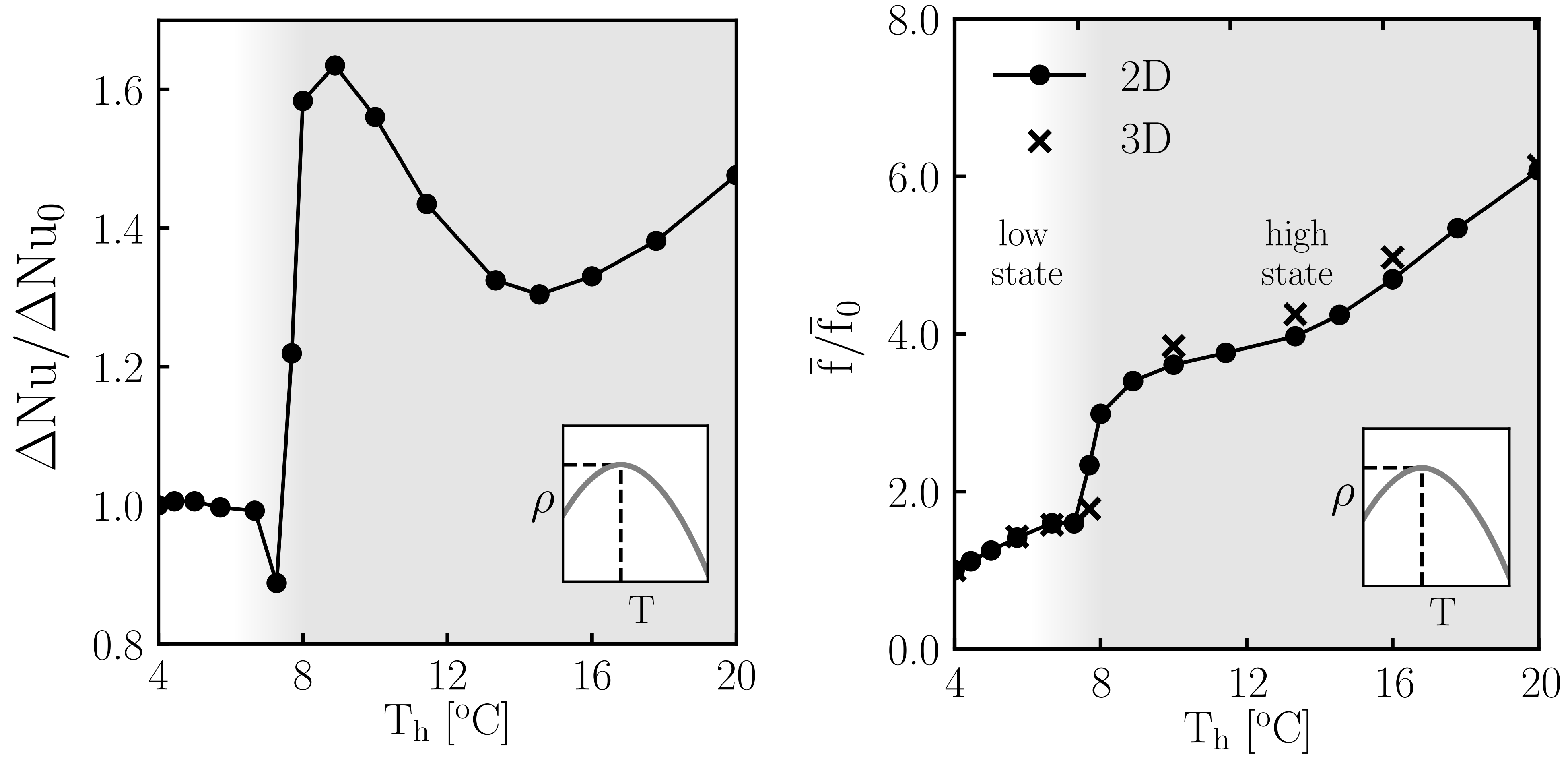

Appearance of reversal flow matches the fast melt regime

Quantify the melting rate - energy balance

Consider the temperature equation

$$\frac{\partial \theta}{\partial t} = -\mathbf{u} \cdot \nabla \theta + \sqrt{\frac{1}{RaPr}} \nabla^2 \theta - St^{-1} \frac{dQ(\phi)}{d\phi} \frac{\partial \phi}{\partial t}$$

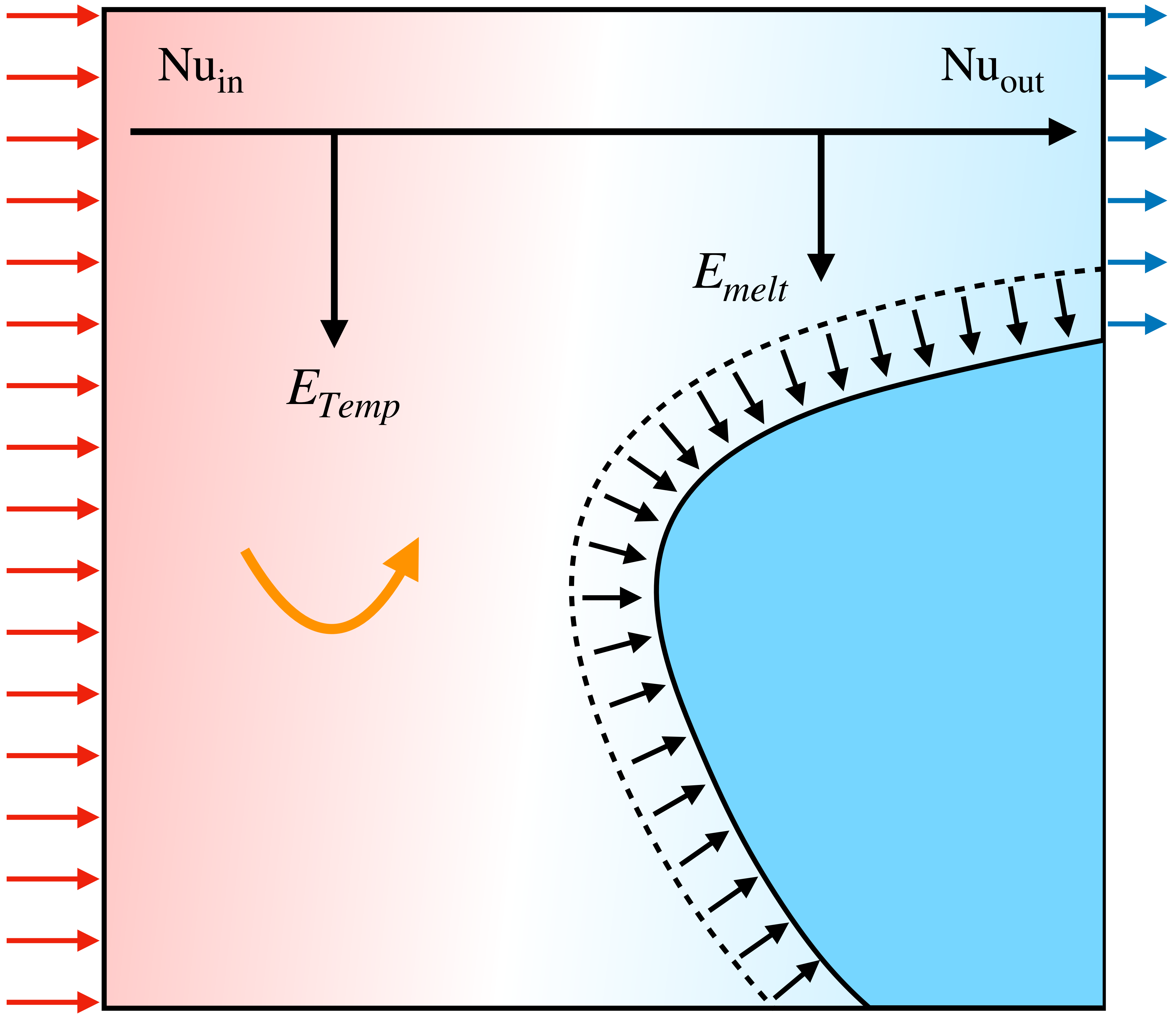

Quantify the melting rate - energy balance

Consider the temperature equation

$$\frac{\partial \theta}{\partial t} = -\mathbf{u} \cdot \nabla \theta + \sqrt{\frac{1}{RaPr}} \nabla^2 \theta - St^{-1} \frac{dQ(\phi)}{d\phi} \frac{\partial \phi}{\partial t}$$

$$\sqrt{\frac{1}{RaPr}} \left(\int_{left} \frac{\partial \theta}{\partial z} dA - \int_{right} \frac{\partial \theta}{\partial z} dA \right) = \frac{d}{dt} \int_V \theta dV + \frac{d}{dt} \int_V \left(St^{-1} \cdot Q(\phi) \right) dV$$

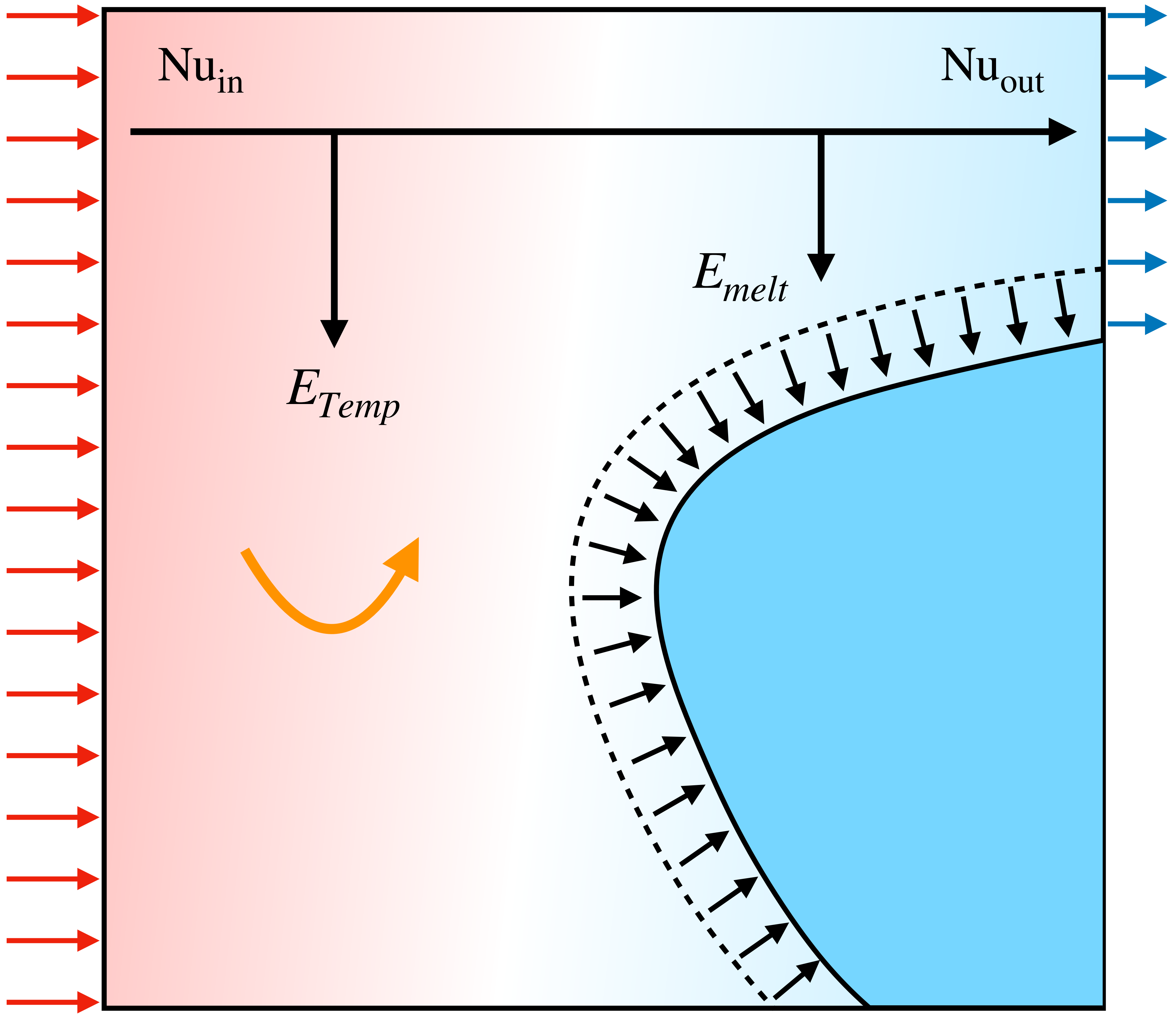

Quantify the melting rate - energy balance

Consider the temperature equation

$$\frac{\partial \theta}{\partial t} = -\mathbf{u} \cdot \nabla \theta + \sqrt{\frac{1}{RaPr}} \nabla^2 \theta - St^{-1} \frac{dQ(\phi)}{d\phi} \frac{\partial \phi}{\partial t}$$

$$\sqrt{\frac{1}{RaPr}} \left(\boxed{\int_{left} \frac{\partial \theta}{\partial z} dA - \int_{right} \frac{\partial \theta}{\partial z} dA} \right) = \boxed{\frac{d}{dt} \int_V \theta dV} + \boxed{\frac{d}{dt} \int_V \left(St^{-1} \cdot Q(\phi) \right) dV}$$

Heat net influx Bulk temperature Phase transition

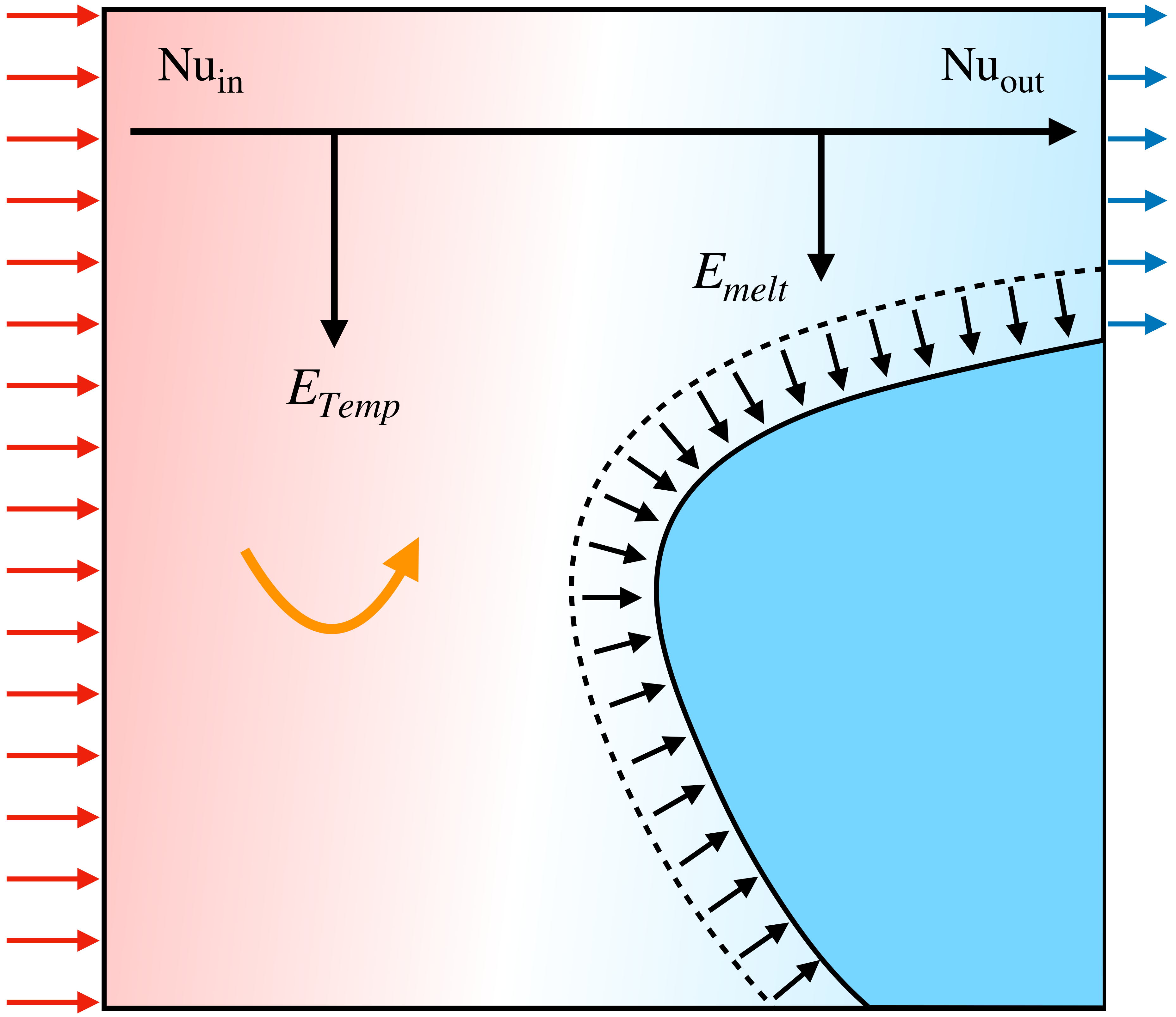

Quantify the melting rate - energy balance

Consider the temperature equation

$$\frac{\partial \theta}{\partial t} = -\mathbf{u}\cdot\nabla\theta + \sqrt{\frac{1}{RaPr}}\nabla^2\theta - St^{-1}\frac{dQ(\phi)}{d\phi}\frac{\partial \phi}{\partial t}$$

$$\sqrt{\frac{1}{RaPr}}\boxed{\left(\int_{left}\frac{\partial \theta}{\partial z}dA - \int_{right}\frac{\partial \theta}{\partial z}dA\right)} = \boxed{\frac{d}{dt}\int_V \theta dV} + \boxed{\frac{d}{dt}\int_V \left(St^{-1}\cdot Q(\phi)\right)dV}$$

Heat net influx   Bulk temperature   Phase transition

$$\sqrt{\frac{1}{RaPr}}\left(\int_{left}\frac{\partial \theta}{\partial z}dA - \int_{right}\frac{\partial \theta}{\partial z}dA\right) \approx \left(\bar{\theta} + St^{-1}\right)\frac{dV_{solid}}{dt}$$

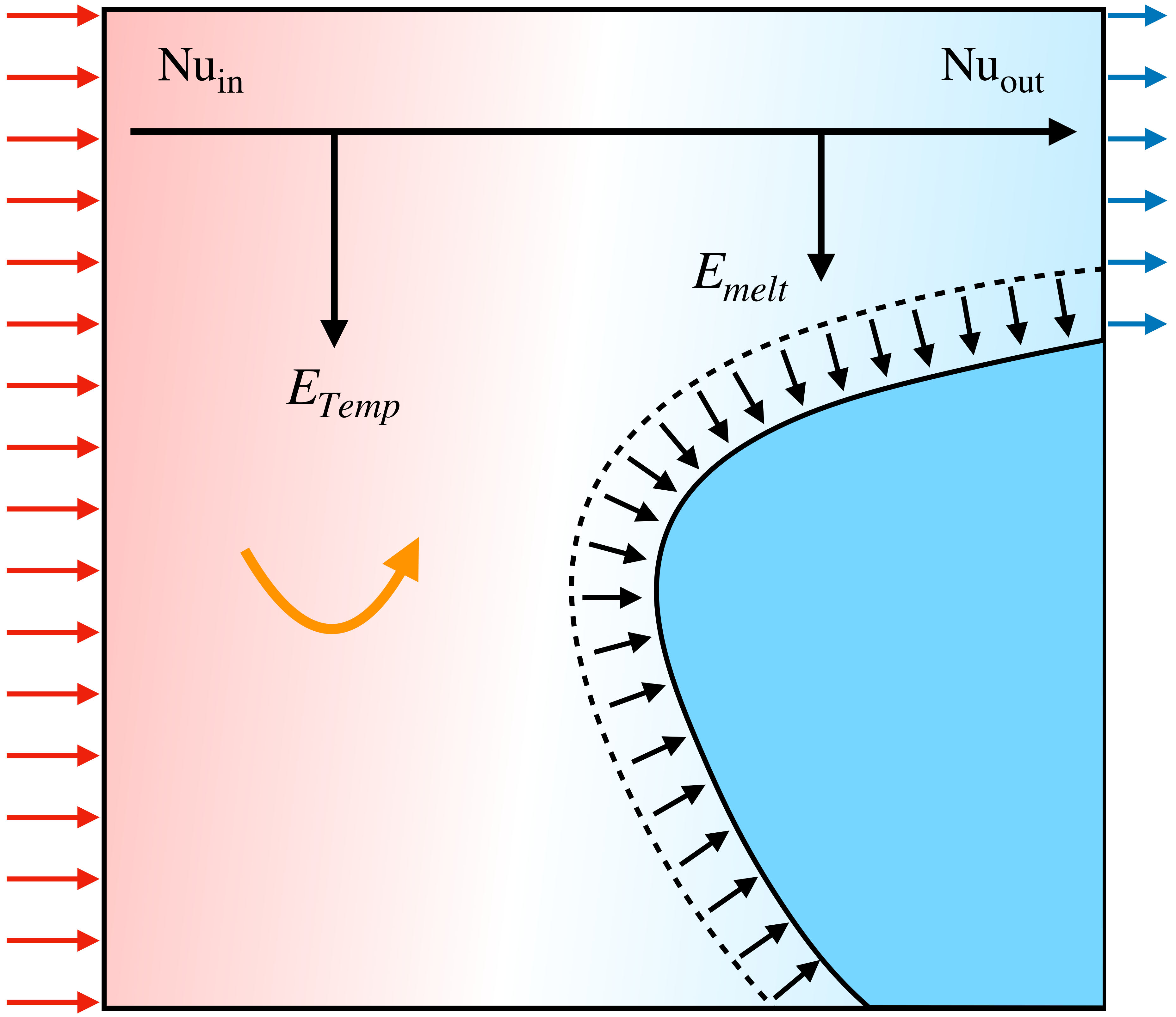

Quantify the melting rate - energy balance

Consider the temperature equation

$$\frac{\partial\theta}{\partial t} = -\mathbf{u}\cdot\nabla\theta + \sqrt{\frac{1}{RaPr}}\nabla^2\theta - St^{-1}\frac{dQ(\phi)}{d\phi}\frac{\partial\phi}{\partial t}$$

$$\sqrt{\frac{1}{RaPr}}\left(\boxed{\int_{left}\frac{\partial\theta}{\partial z}dA - \int_{right}\frac{\partial\theta}{\partial z}dA}\right) = \boxed{\frac{d}{dt}\int_V \theta dV} + \boxed{\frac{d}{dt}\int_V \left(St^{-1}\cdot Q(\phi)\right) dV}$$

Heat net influx Bulk temperature Phase transition

$$\sqrt{\frac{1}{RaPr}}\left(\int_{left}\frac{\partial\theta}{\partial z}dA - \int_{right}\frac{\partial\theta}{\partial z}dA\right) \approx \left(\bar{\theta} + St^{-1}\right)\frac{dV_{solid}}{dt}$$

$$\downarrow$$

$$\overline{\Delta\theta_z} \approx \sqrt{RaPr}\left(\bar{\theta} + St^{-1}\right)\bar{f}$$

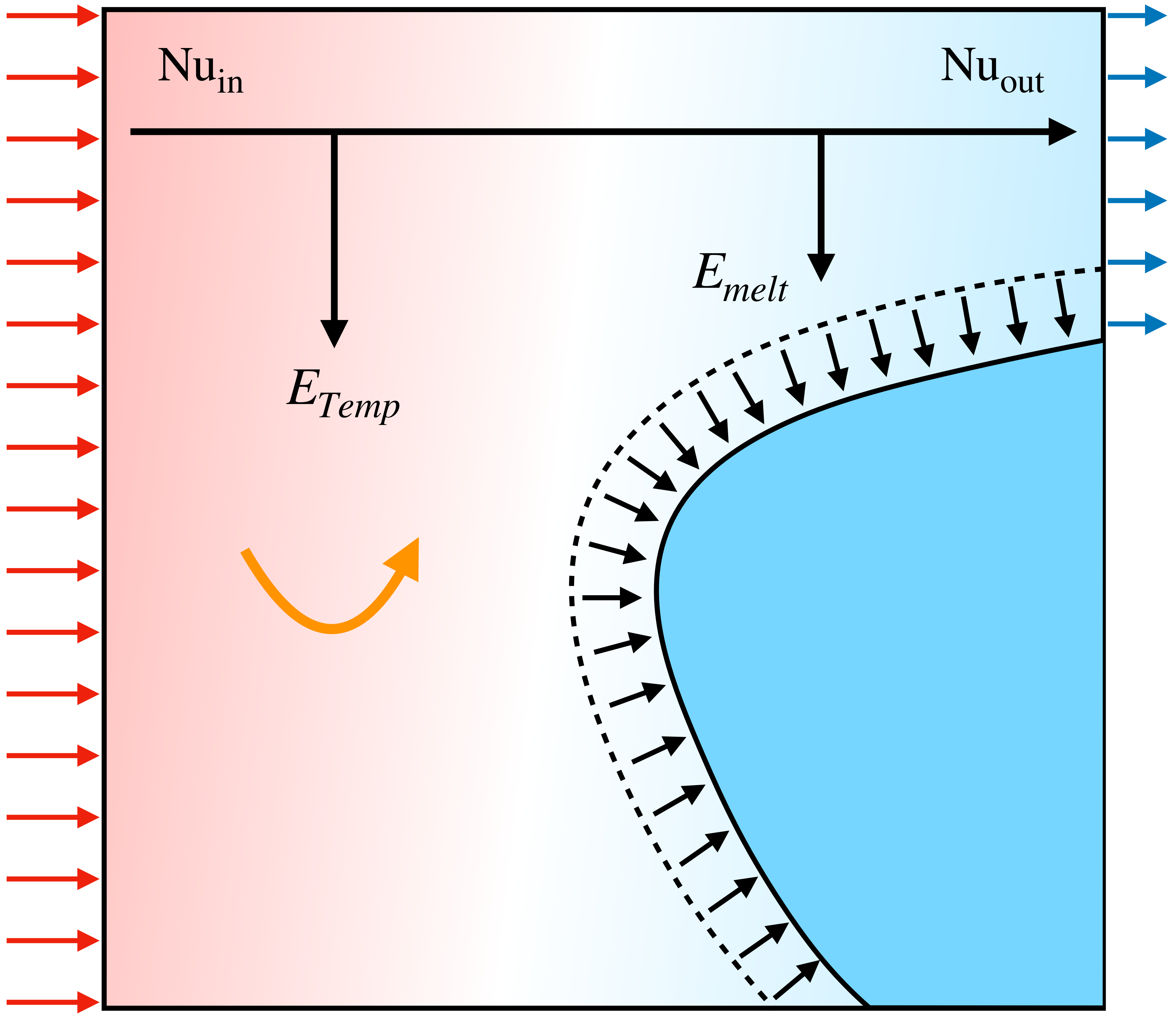

Quantify the melting rate - energy balance

Consider the temperature equation

$$\frac{\partial \theta}{\partial t} = -\mathbf{u}\cdot\nabla\theta + \sqrt{\frac{1}{RaPr}}\nabla^2\theta - St^{-1}\frac{dQ(\phi)}{d\phi}\frac{\partial \phi}{\partial t}$$

$$\sqrt{\frac{1}{RaPr}}\boxed{\left(\int_{left}\frac{\partial\theta}{\partial z}dA - \int_{right}\frac{\partial\theta}{\partial z}dA\right)} = \boxed{\frac{d}{dt}\int_V \theta dV} + \boxed{\frac{d}{dt}\int_V \left(St^{-1}\cdot Q(\phi)\right) dV}$$

Heat net influx   Bulk temperature   Phase transition

$$\sqrt{\frac{1}{RaPr}}\left(\int_{left}\frac{\partial\theta}{\partial z}dA - \int_{right}\frac{\partial\theta}{\partial z}dA\right) \approx \left(\bar{\theta} + St^{-1}\right)\frac{dV_{solid}}{dt}$$

$$\downarrow$$

$$\boxed{\overline{\Delta\theta_z} \approx \sqrt{RaPr}\left(\bar{\theta} + St^{-1}\right)\bar{f}}$$

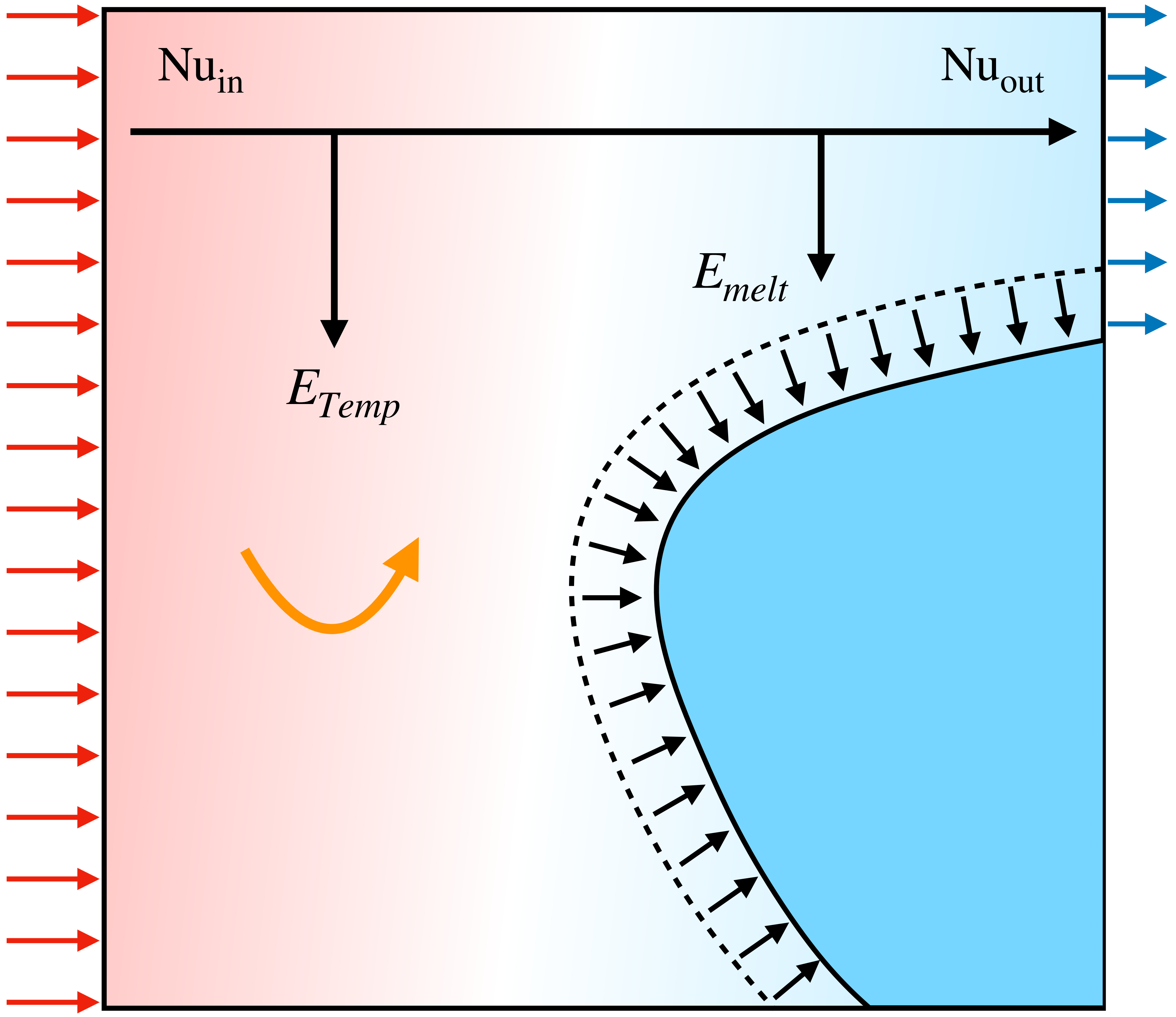

Quantify the melting rate - energy balance

Consider the temperature equation

$$\frac{\partial \theta}{\partial t} = -\mathbf{u}\cdot\nabla\theta + \sqrt{\frac{1}{RaPr}}\nabla^2\theta - St^{-1}\frac{dQ(\phi)}{d\phi}\frac{\partial \phi}{\partial t}$$

$$\sqrt{\frac{1}{RaPr}}\left(\int_{left}\frac{\partial \theta}{\partial z}dA - \int_{right}\frac{\partial \theta}{\partial z}dA\right) = \frac{d}{dt}\int_V \theta dV + \frac{d}{dt}\int_V \left(St^{-1}\cdot Q(\phi)\right)dV$$

Heat net influx Bulk temperature Phase transition

$$\sqrt{\frac{1}{RaPr}}\left(\int_{left}\frac{\partial \theta}{\partial z}dA - \int_{right}\frac{\partial \theta}{\partial z}dA\right) \approx \left(\bar{\theta} + St^{-1}\right)\frac{dV_{solid}}{dt}$$

$$\boxed{\overline{\Delta\theta_z} \approx \sqrt{RaPr}\left(\bar{\theta} + St^{-1}\right)\bar{f}}$$

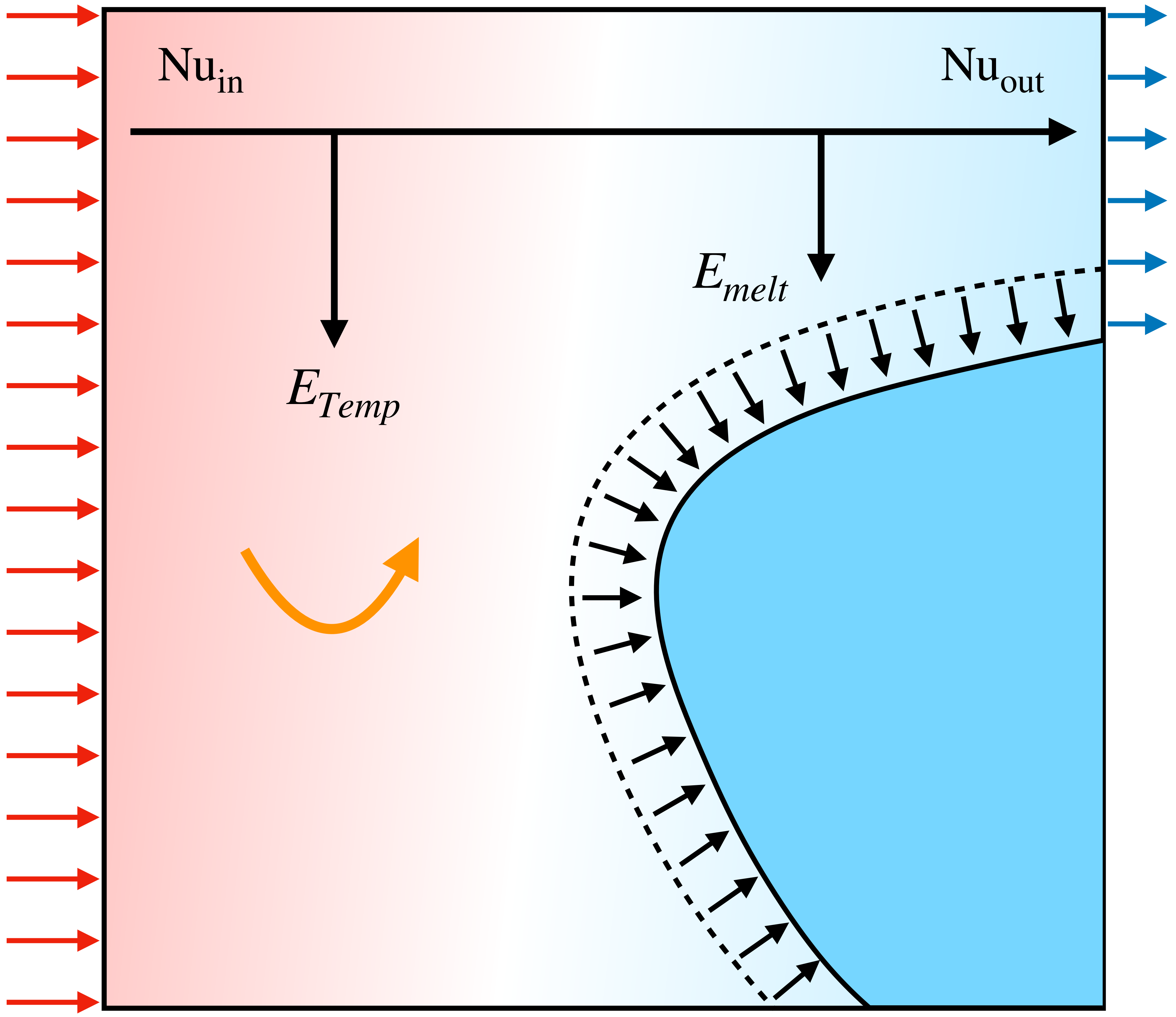

$\overline{\Delta\theta_z} = \Delta Nu/\bar{h}$ = effective net heat flux

$\bar{h}$ = average melt width (distance ice - hot plate)

Quantify the melting rate - energy balance

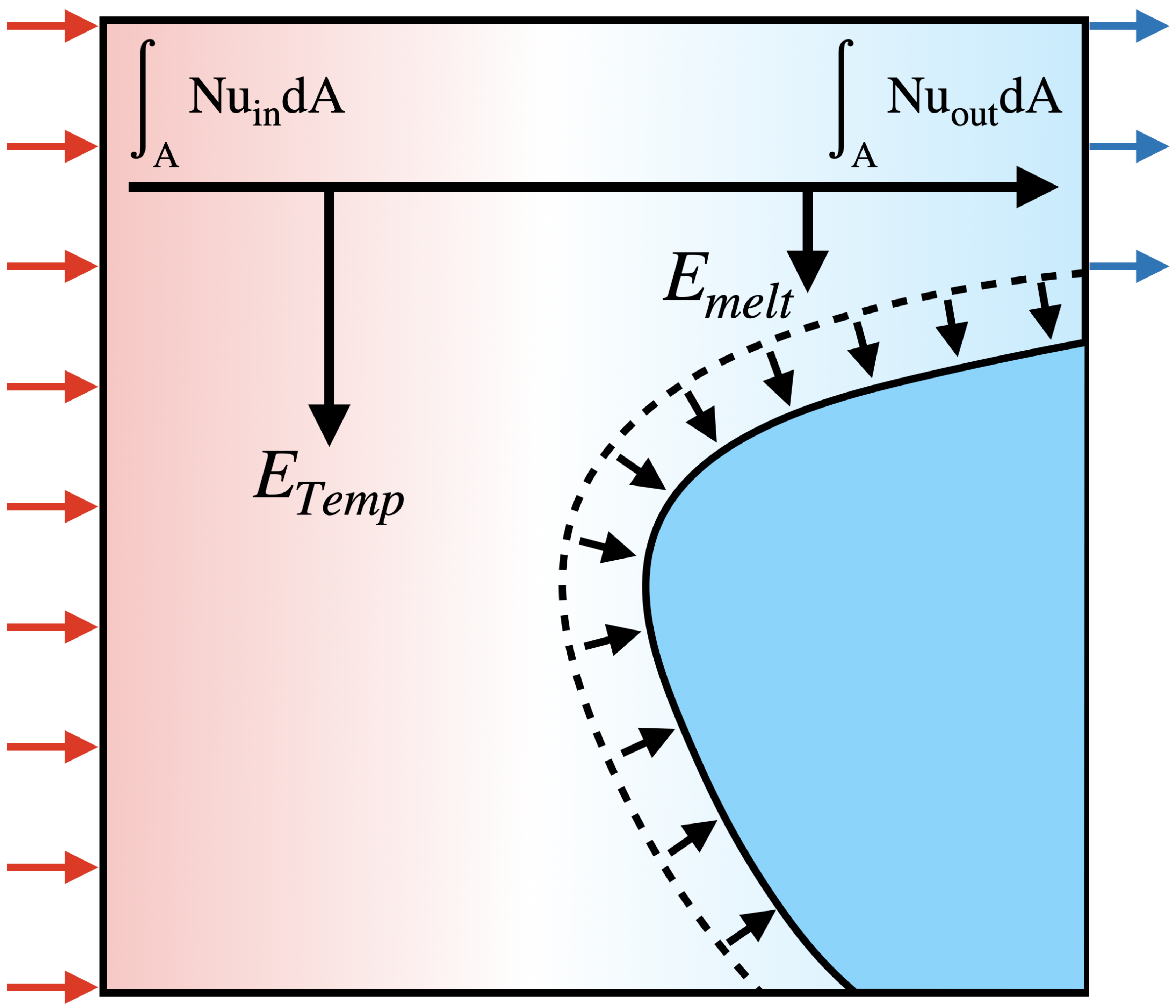

$$\overline{\Delta\theta_z} \approx \sqrt{RaPr}\,\left(\bar{\theta} + St^{-1}\right)\bar{f}$$

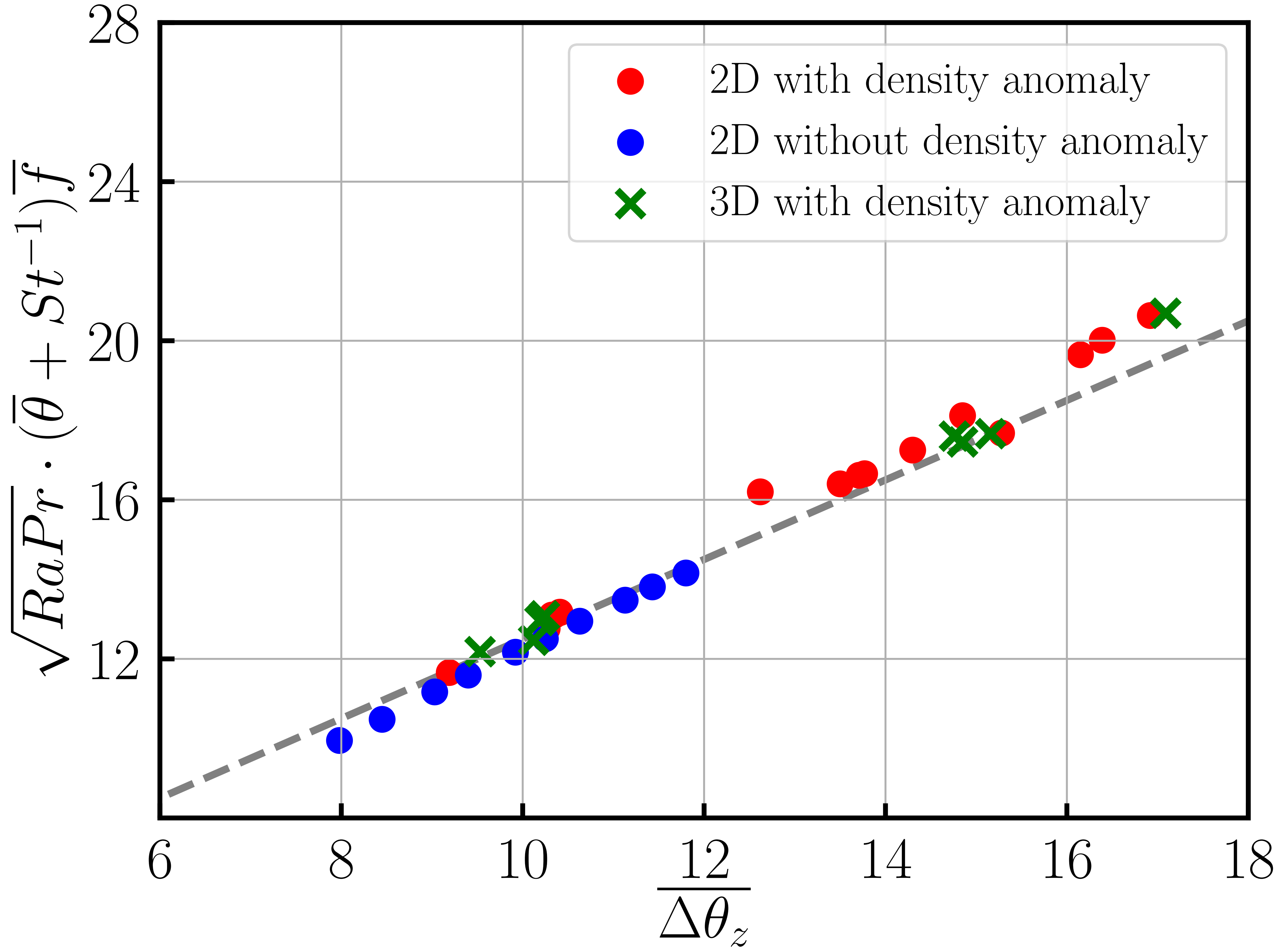

Quantify the melting rate - energy balance

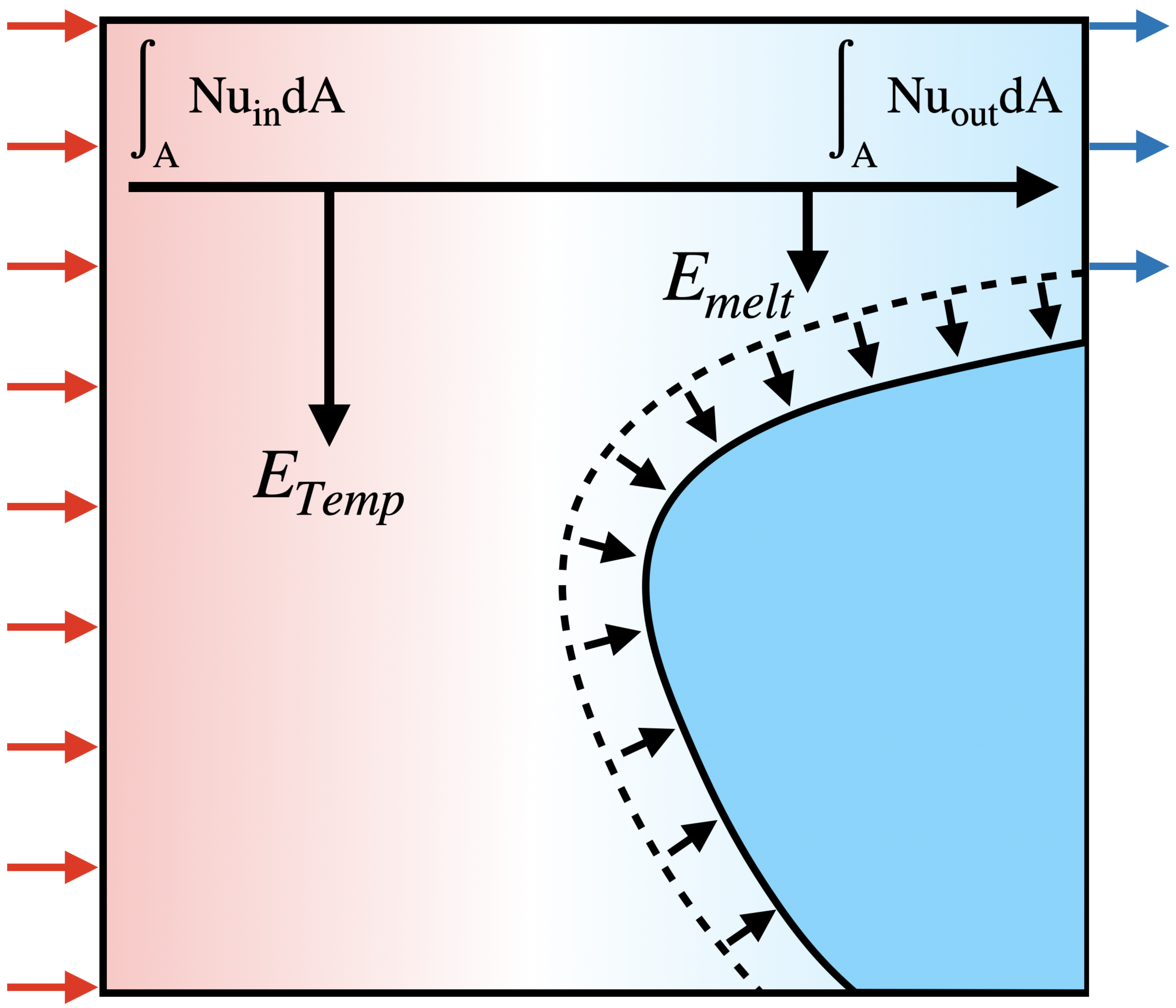

$$\overline{\Delta\theta_z} \approx \sqrt{RaPr}\,\left(\bar{\theta} + St^{-1}\right)\bar{f}$$

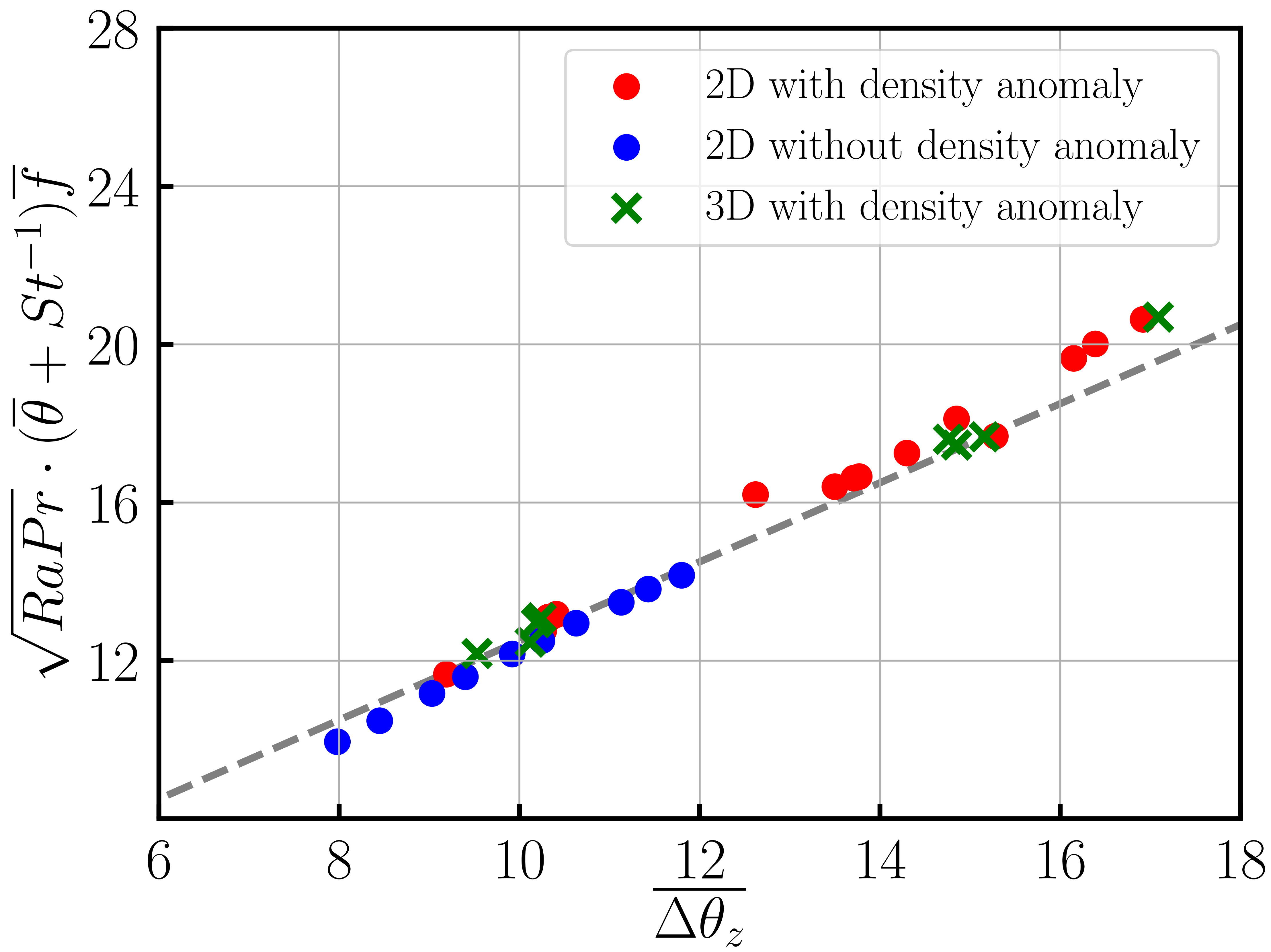

The relation successfully describes the melting rate for both with & without density anomaly

Unifying view

$$\overline{\Delta\theta_z} \approx \sqrt{RaPr}\,\left(\bar{\theta} + St^{-1}\right)\bar{f}$$

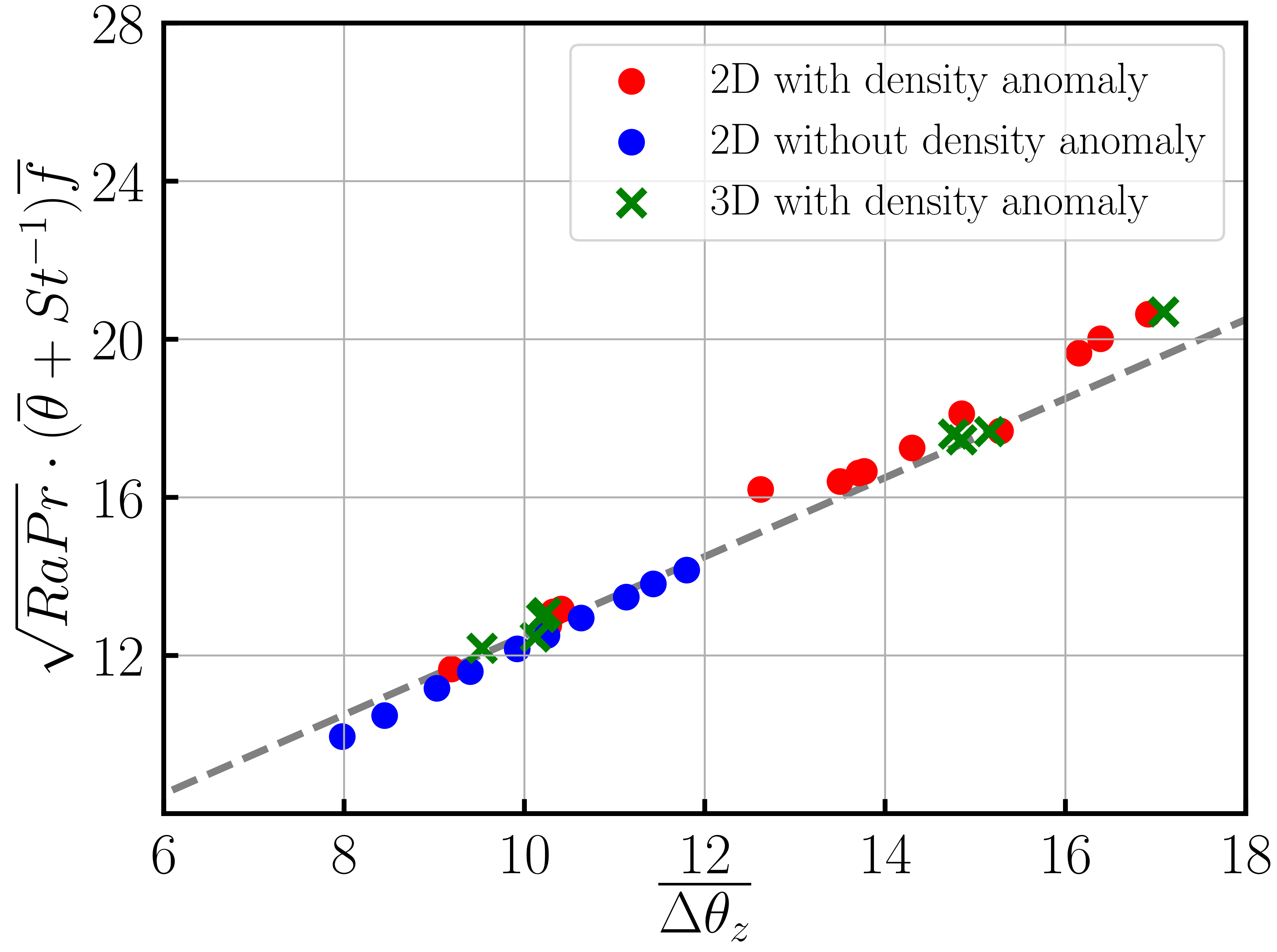

Unifying view

$$\overline{\Delta\theta_z} \approx \sqrt{RaPr}\,\left(\bar{\theta} + St^{-1}\right)\bar{f}$$

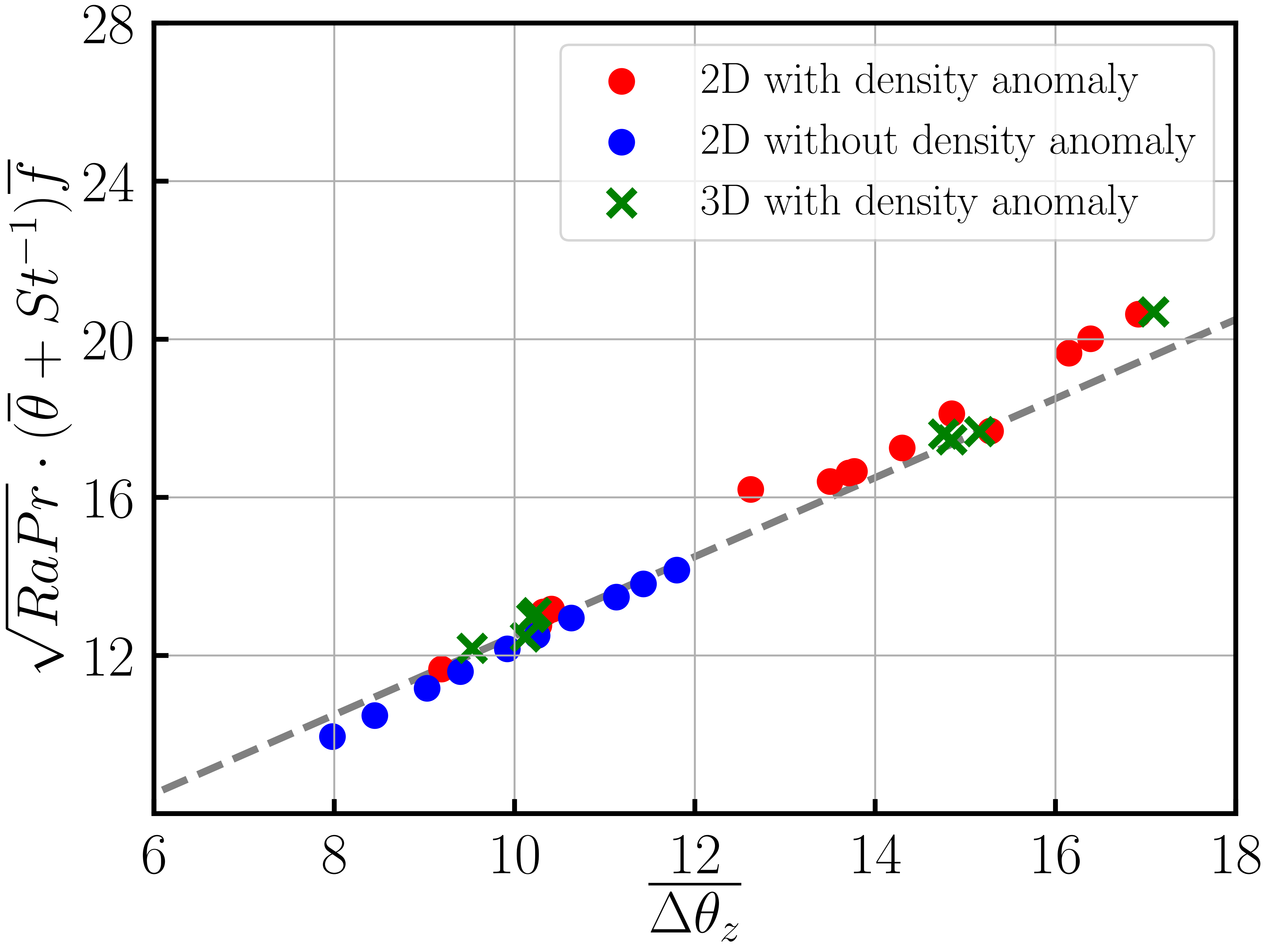

No density anomaly

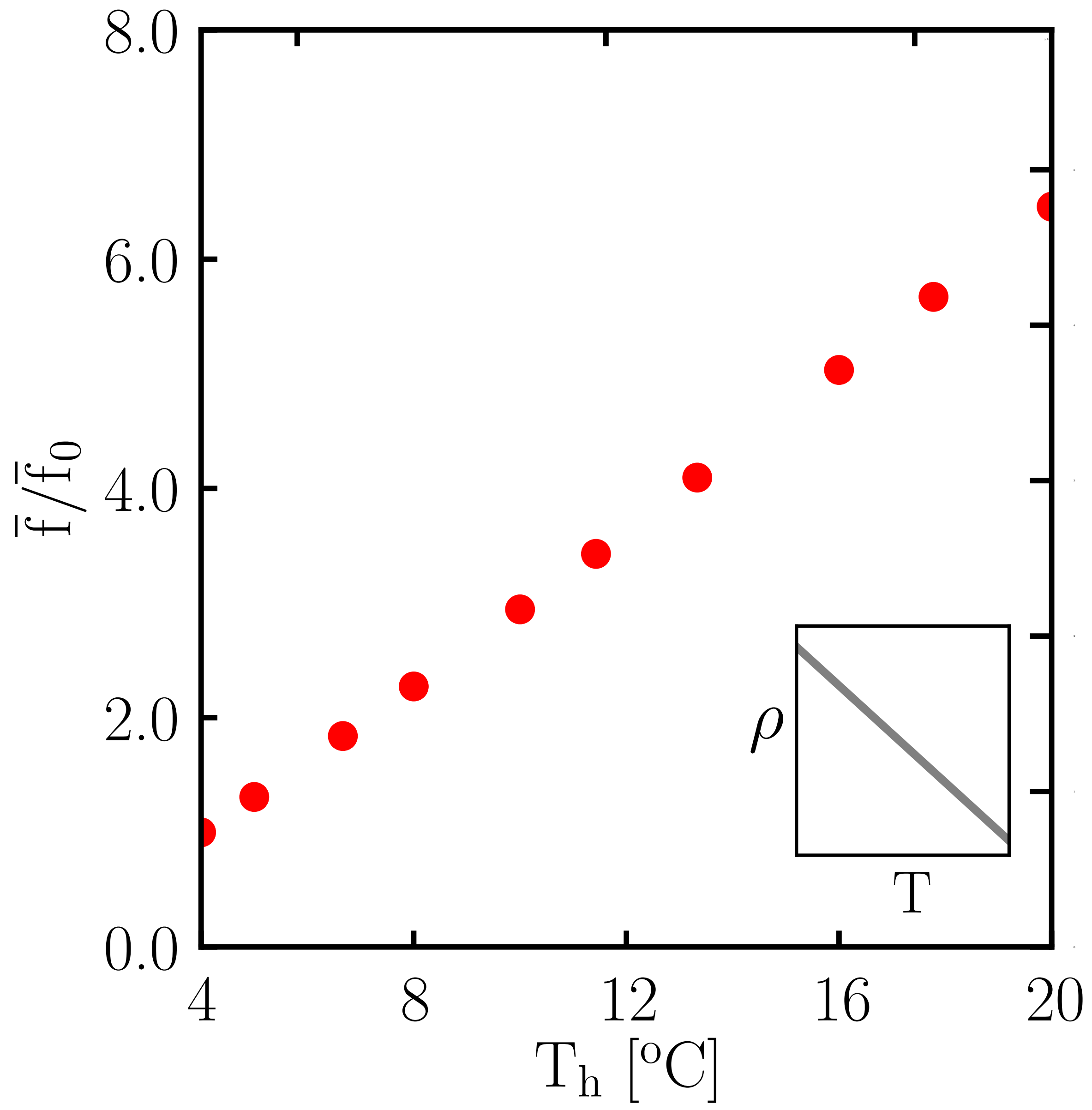

Unifying view

$$\overline{\Delta\theta_z} \approx \sqrt{RaPr}\left(\bar{\theta} + St^{-1}\right)\bar{f}$$

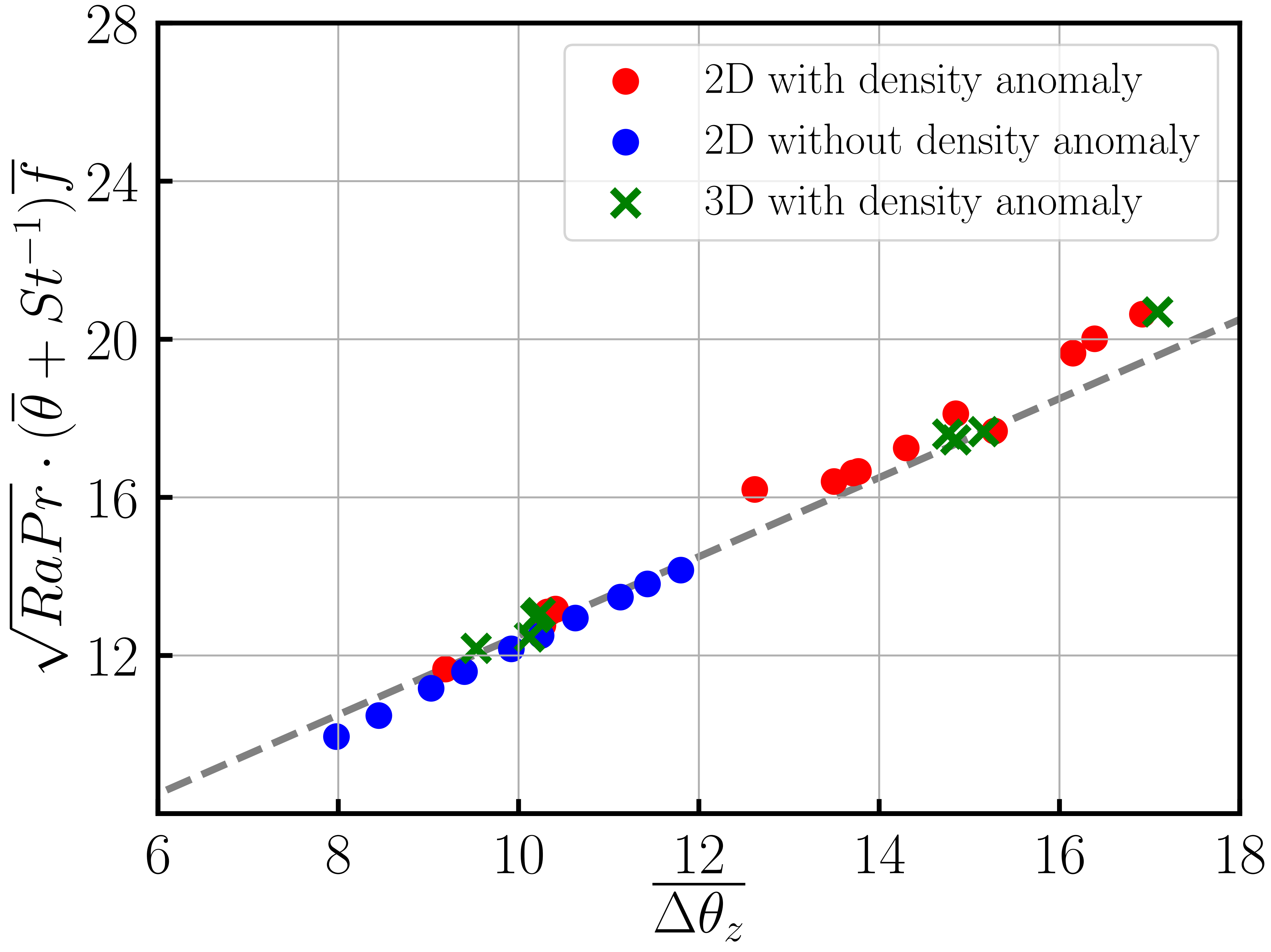

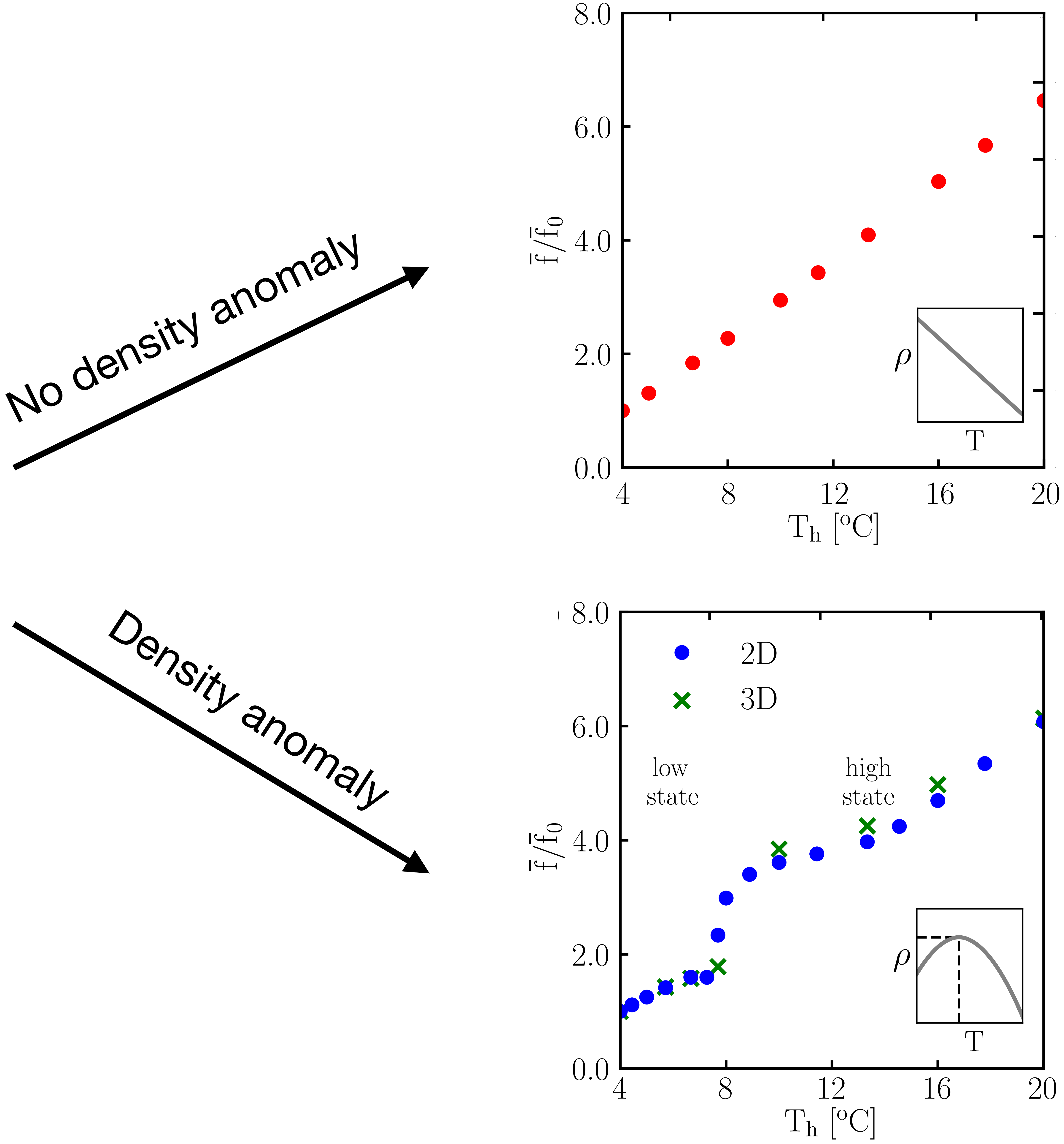

Conclusions on part III.

Rui Yang et al., Phys. Rev. Fluids 7, 083503 (2022)

- The **density anomaly** plays an important role in ice morphology and melt speed
- **Energy balance** successfully describes melting rate for both with & without density anomaly:

$$\overline{\Delta\theta_z} \approx \sqrt{RaPr}\left(\bar{\theta} + St^{-1}\right)\bar{f}$$

- Abrupt transition from slow to fast melting state due to **locally reversed flow: tipping point**

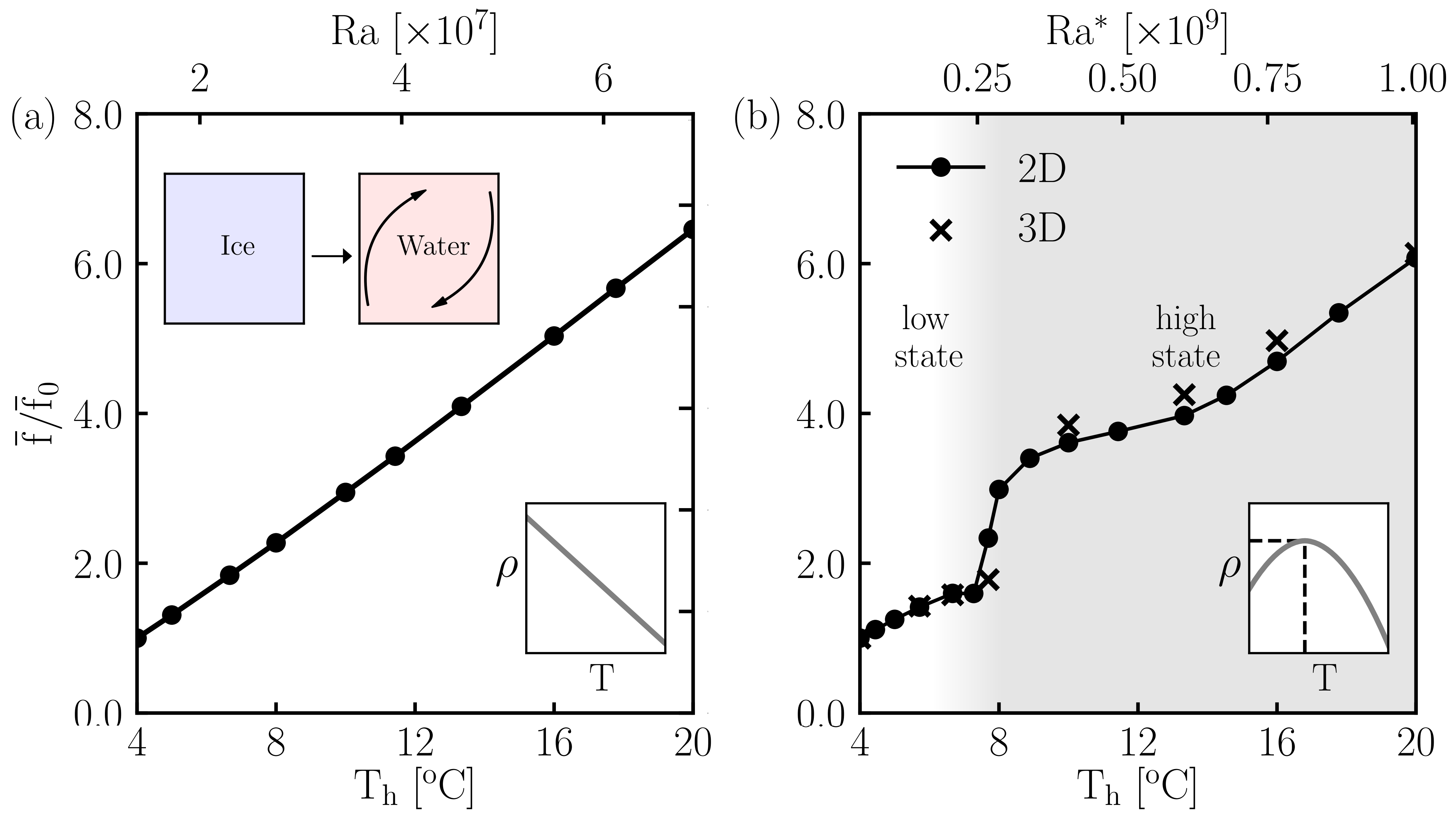

Conclusions on part III.

Rui Yang et al., Phys. Rev. Fluids 7, 083503 (2022)

- The **density anomaly** plays an important role in ice morphology and melt speed
- **Energy balance** successfully describes melting rate for both with & without density anomaly:

$$\overline{\Delta\theta_z} \approx \sqrt{RaPr}\,\left(\bar{\theta} + St^{-1}\right)\bar{f}$$

- Abrupt transition from slow to fast melting state due to **locally reversed flow: tipping point**

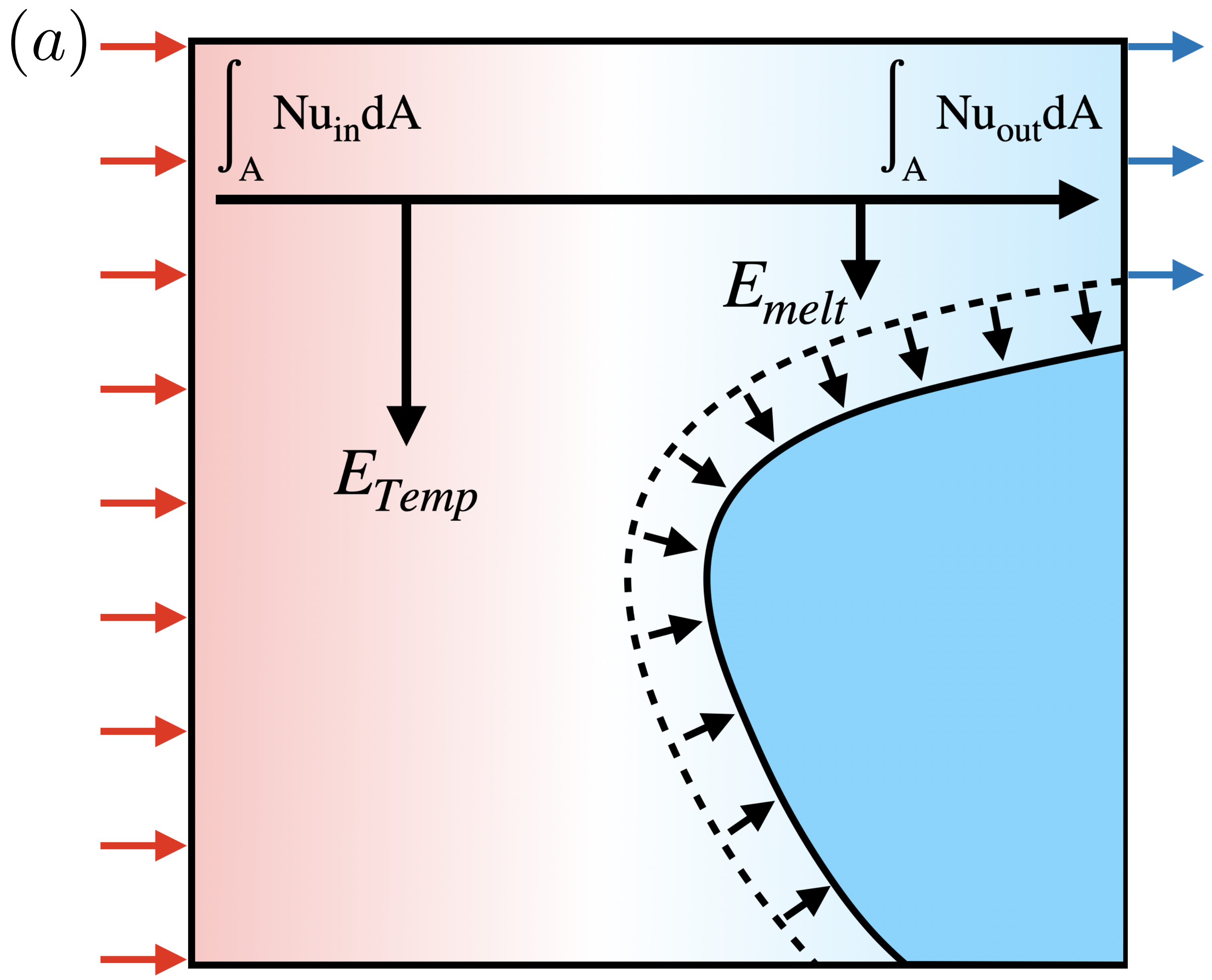

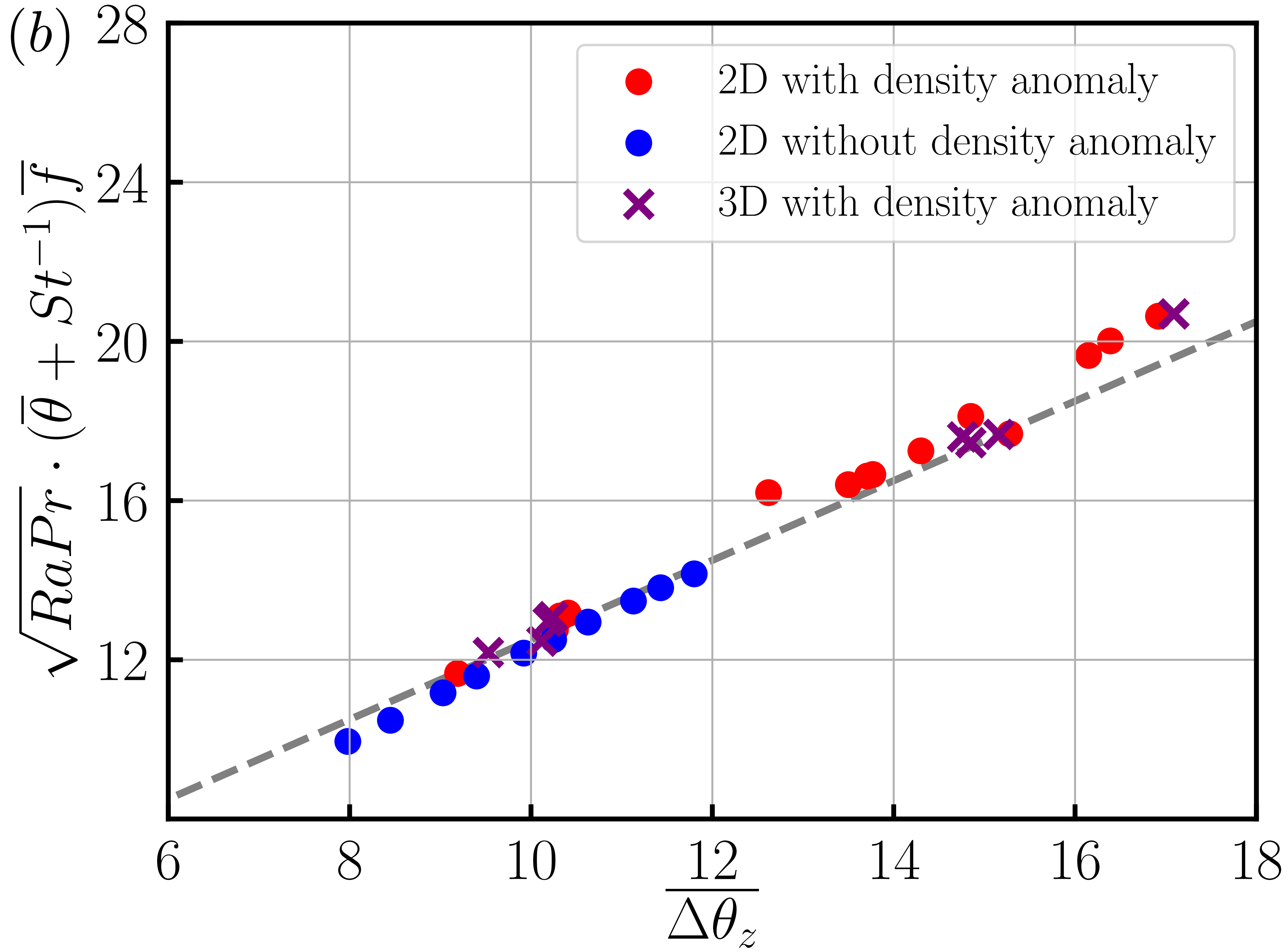

Conclusions on part III.

Rui Yang et al., Phys. Rev. Fluids 7, 083503 (2022)

- The **density anomaly** plays an important role in ice morphology and melt speed
- **Energy balance** successfully describes melting rate for both with & without density anomaly:

$$\overline{\Delta\theta_z} \approx \sqrt{RaPr}\left(\bar{\theta} + St^{-1}\right)\bar{f}$$

- Abrupt transition from slow to fast melting state due to **locally reversed flow: tipping point**

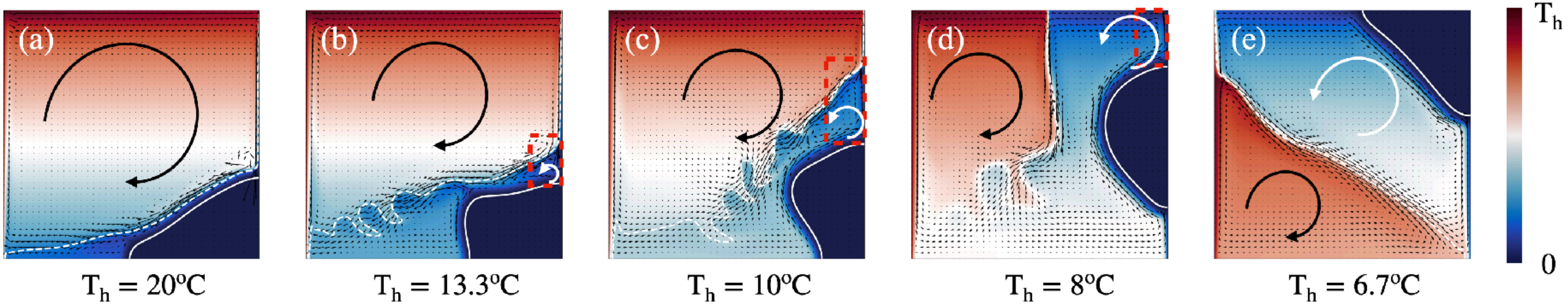

IV. Vertical convection with salty water

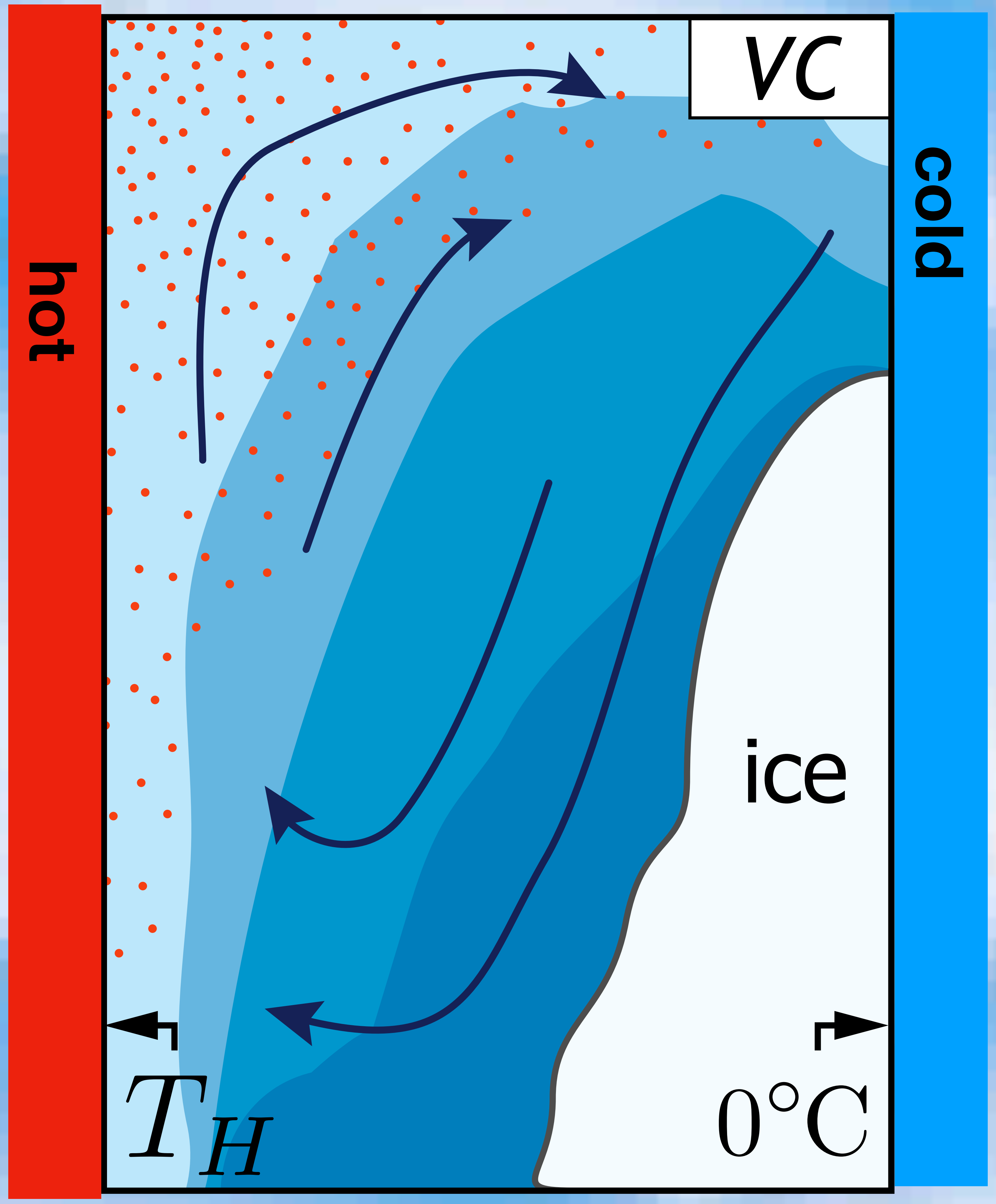

Ice melting in salty water

Yang, Howland, Liu, Verzicco, Lohse, JFM 969, R2 (2023)

Huge effect of salt on ice melting - huge relevance

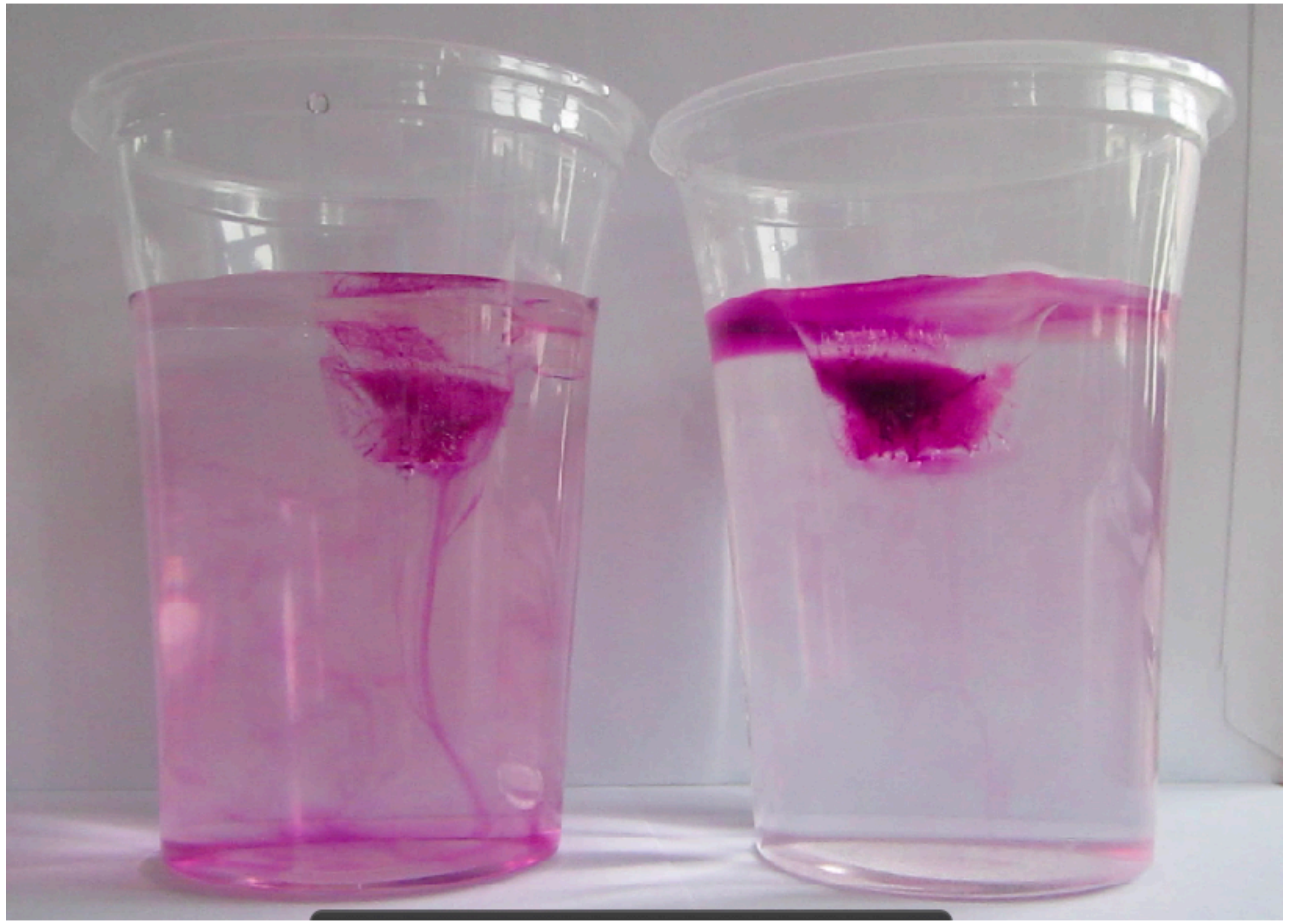

Try yourself at home:
Ice cube melting in fresh/salty water

Huge effect of salt on ice melting - huge relevance

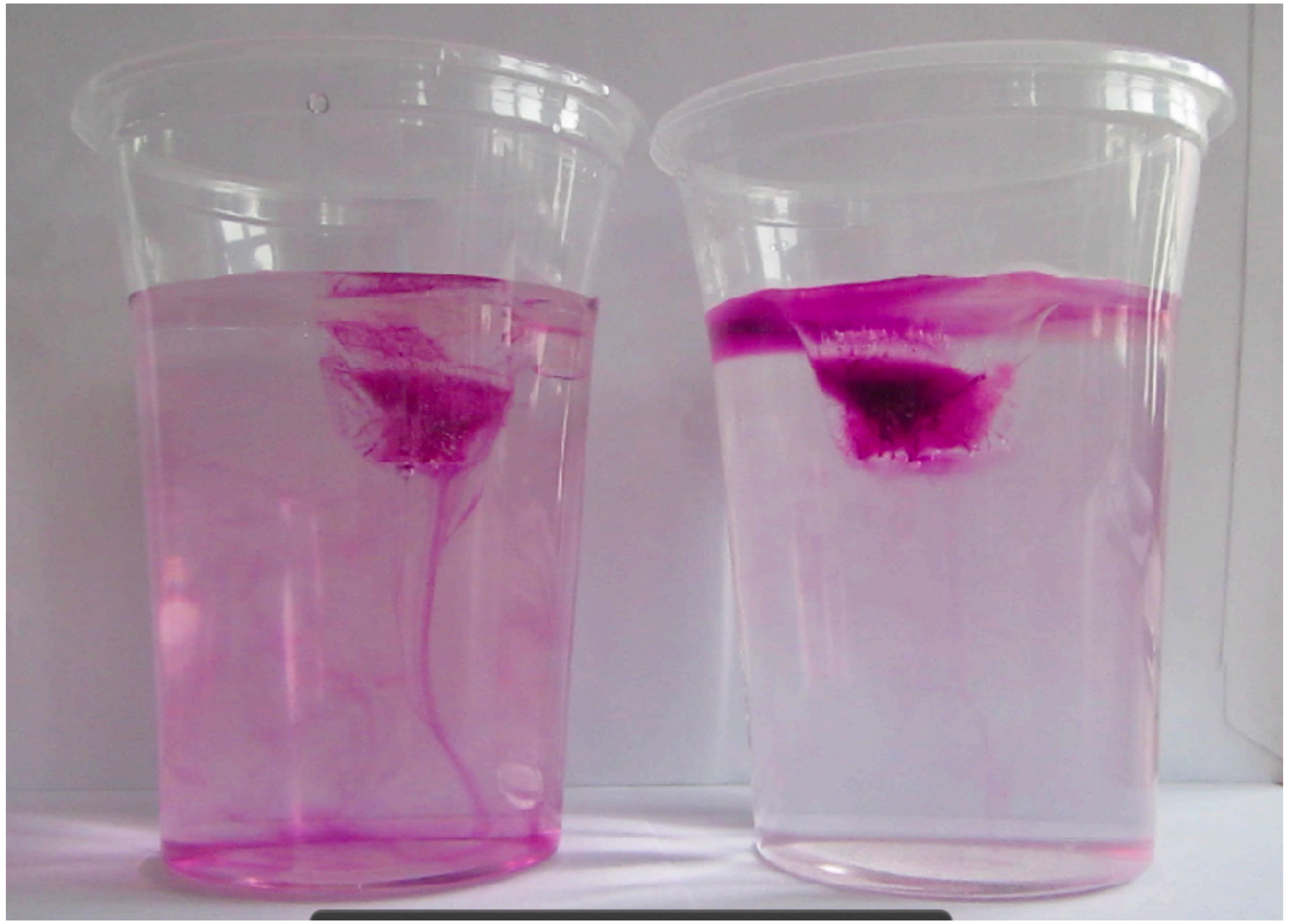

Try yourself at home:
Ice cube melting in fresh/salty water

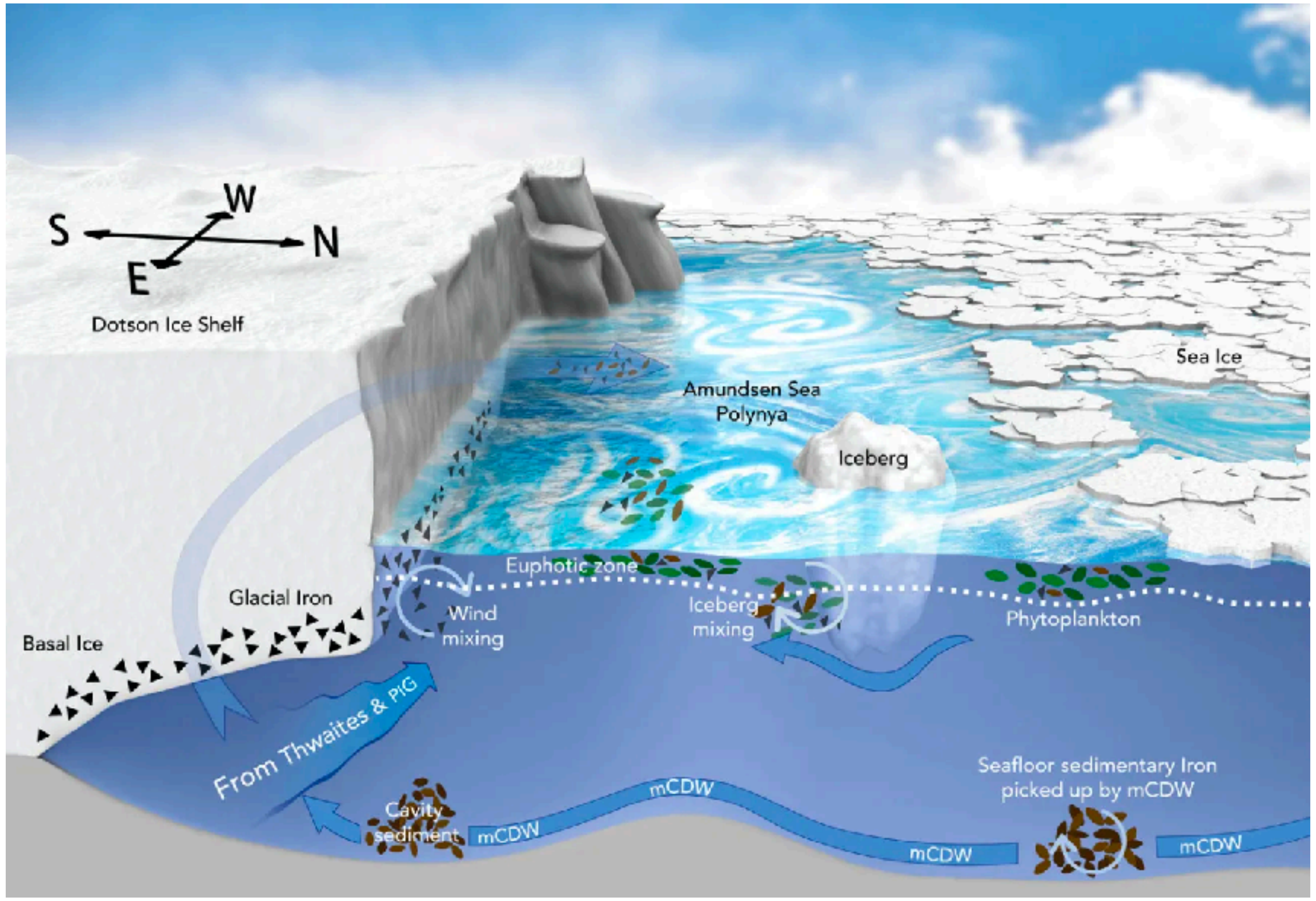

Ice melting in ocean

Questions to ask

- How fast does the ice melt (global melt rate)?
- How does the shape evolve (local melt rate)?
- Do scallop patterns emerge?
- Dependence on control parameters?
- How to upscale to glacier scale and beyond?

J. Fluid Mech. (1980), *vol.* 100, *part* 2, *pp.* 367–384
Printed in Great Britain

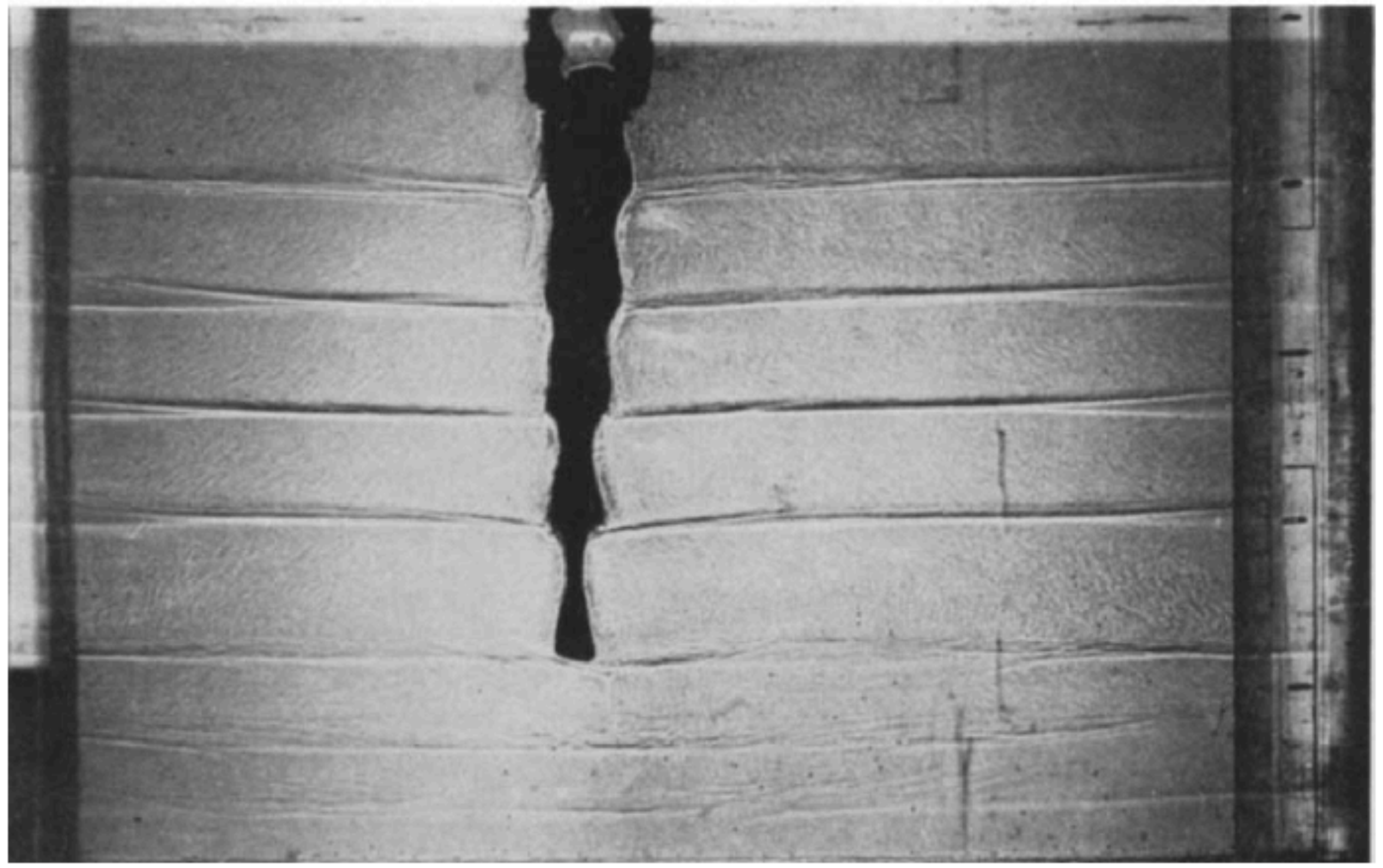

Ice blocks melting into a salinity gradient

By HERBERT E. HUPPERT

Department of Applied Mathematics and Theoretical Physics,
University of Cambridge

AND J. STEWART TURNER

Research School of Earth Sciences,
Australian National University, Canberra

(Received 21 June 1979 and in revised form 21 November 1979)

In our previous qualitative paper, it was shown that when a vertical ice surface melts into a stable salinity gradient, the melt water spreads out into the interior in a series of nearly horizontal layers. The experiments reported here are aimed at quantifying this effect, which could be of some importance in the application to melting icebergs. Experiments have also been carried out with heated and cooled vertical walls.

Parameter & phase space: when to expect layering in DDC-RB?

(for fixed Prandtl numbers (Pr_T, Pr_S) = fixed fluid)

Meling of ice in stratified flow

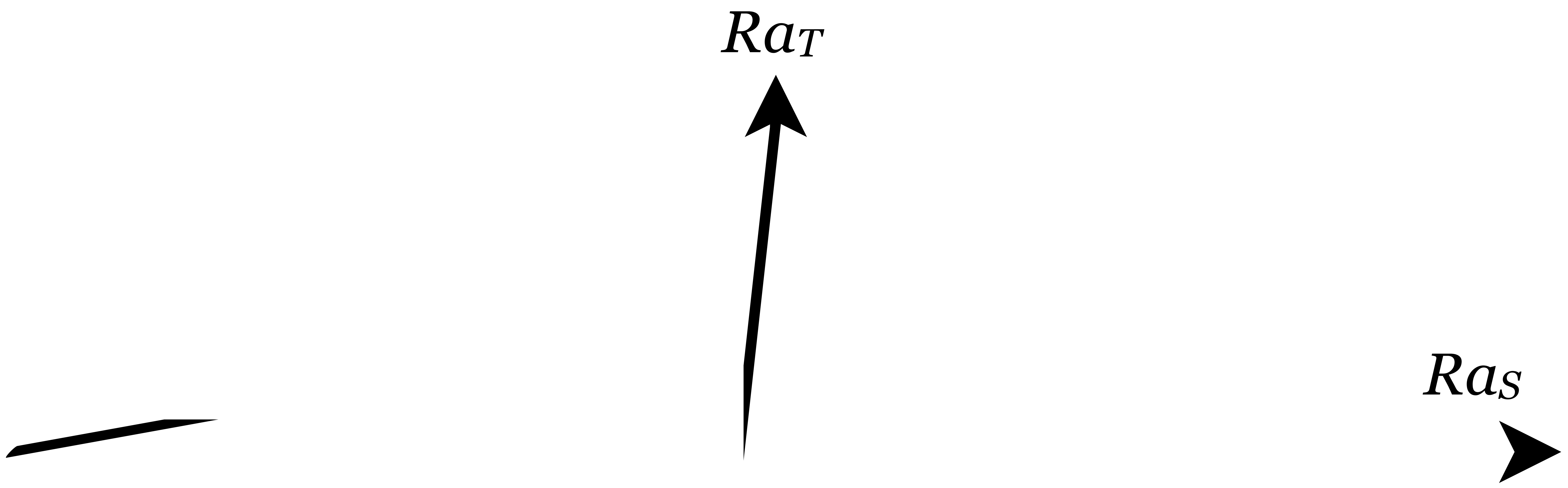

Parameter & phase space: when to expect layering in DDC-RB?

(for fixed Prandtl numbers (Pr_T, Pr_S) = fixed fluid)

Meling of ice in stratified flow

Ra_T

Two-Scalar RB

$T_{\text{top}} < T_{\text{bottom}}, \;\; S_{\text{top}} > S_{\text{bottom}}$

Both scalar fields destabilise the flow, statically unstable

Ra_S

Stable Layer

$T_{\text{top}} > T_{\text{bottom}}, \;\; S_{\text{top}} < S_{\text{bottom}}$

Both scalar fields stabilise the flow, statically stable

Parameter & phase space: when to expect layering in DDC-RB?

(for fixed Prandtl numbers (Pr_T, Pr_S) = fixed fluid)

Meling of ice in stratified flow

Ra_T

Ra_S

including Diffusive DDC

$$T_{\text{top}} < T_{\text{bottom}}, \;\; S_{\text{top}} < S_{\text{bottom}}$$

temperature field destabilises while salinity field stabilises the flow, statically stable or unstable

Two-Scalar RB

$$T_{\text{top}} < T_{\text{bottom}}, \;\; S_{\text{top}} > S_{\text{bottom}}$$

Both scalar fields destabilise the flow, statically unstable

Stable Layer

$$T_{\text{top}} > T_{\text{bottom}}, \;\; S_{\text{top}} < S_{\text{bottom}}$$

Both scalar fields stabilise the flow, statically stable

including Fingering DDC

$$T_{\text{top}} > T_{\text{bottom}}, \;\; S_{\text{top}} > S_{\text{bottom}}$$

salinity field destabilises while temperature field stabilises the flow, statically stable or unstable

Parameter & phase space: when to expect layering in DDC-RB?

(for fixed Prandtl numbers (Pr_T, Pr_S) = fixed fluid)

Meling of ice in stratified flow

Ra_T

including Diffusive DDC

$$T_{\mathrm{top}} < T_{\mathrm{bottom}}, \quad S_{\mathrm{top}} < S_{\mathrm{bottom}}$$

temperature field destabilises
while salinity field stabilises the flow,
statically stable or unstable

Two-Scalar RB

$$T_{\mathrm{top}} < T_{\mathrm{bottom}}, \quad S_{\mathrm{top}} > S_{\mathrm{bottom}}$$

Both scalar fields
destabilise the flow,
statically unstable

Ra_S

Stable Layer

$$T_{\mathrm{top}} > T_{\mathrm{bottom}}, \quad S_{\mathrm{top}} < S_{\mathrm{bottom}}$$

Both scalar fields
stabilise the flow,
statically stable

including Fingering DDC

$$T_{\mathrm{top}} > T_{\mathrm{bottom}}, \quad S_{\mathrm{top}} > S_{\mathrm{bottom}}$$

salinity field destabilises while
temperature field stabilises the flow,
statically stable or unstable

Thermohaline staircases

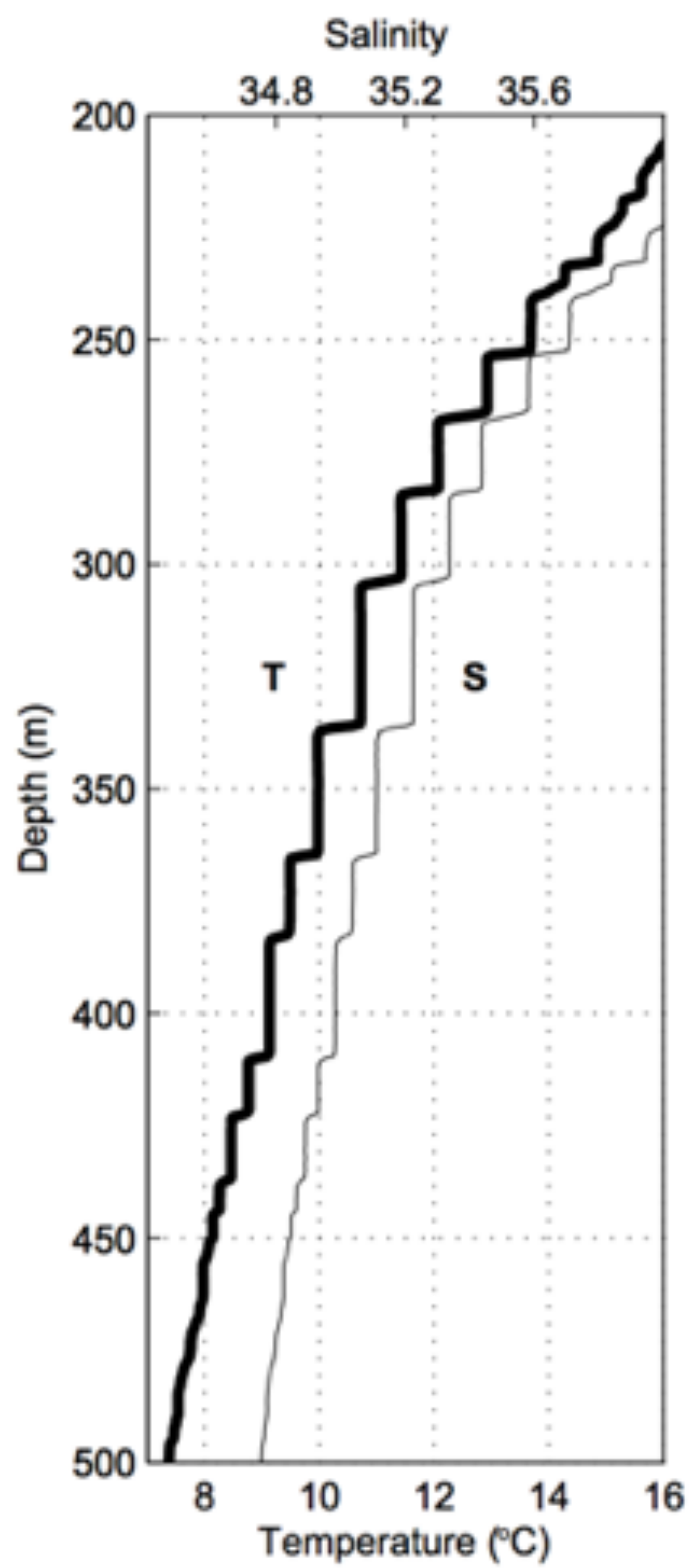

from Schmitt et al.,
Science 308, 685 (2005)

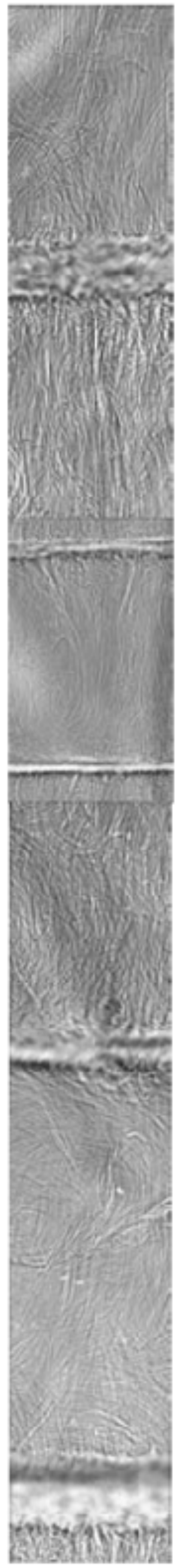

from Krishnamurti
JFM 483, 287 (2003)

Temperature field of fully periodic 3D simulation

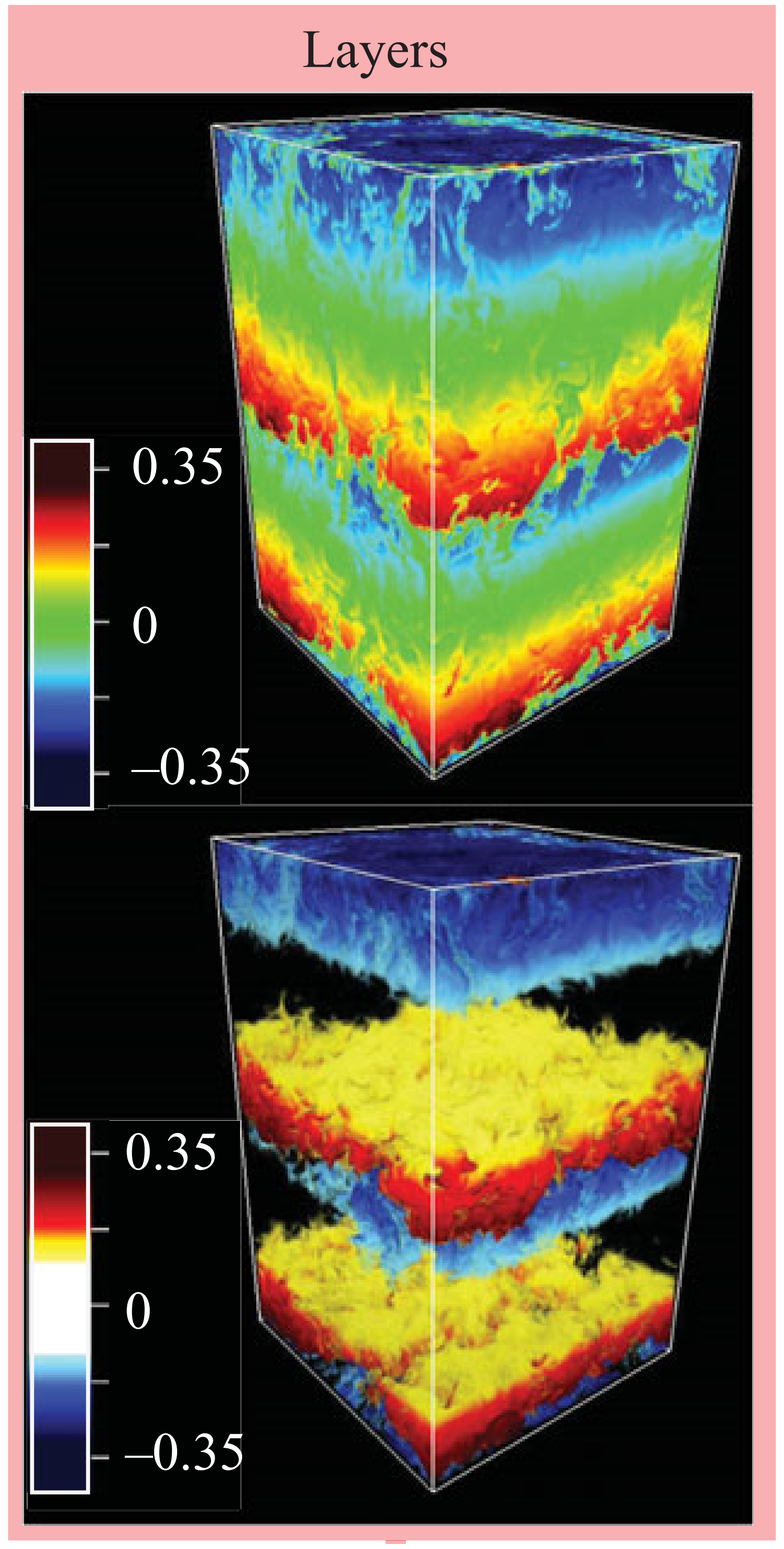

from Stellmach et al.
JFM 677, 554 (2013)

$Pr_T = 7$, $Pr_S = 21$, Λ=1.1

VC-DDC melting setup with control parameters

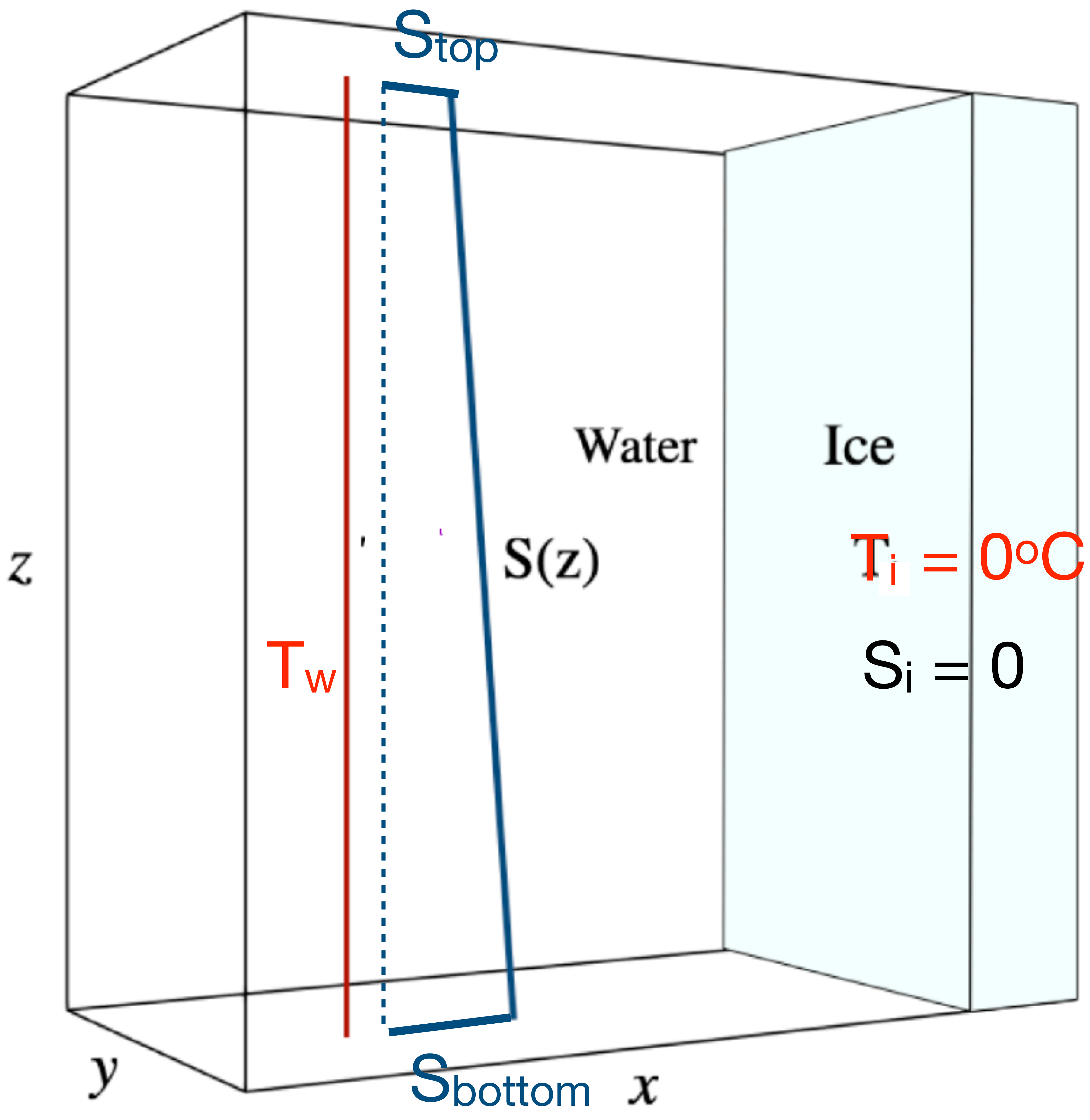

Horizontal temperature gradient:

$\Delta T = T_w - T_i$ T_w = initial water temp

VC-DDC melting setup with control parameters

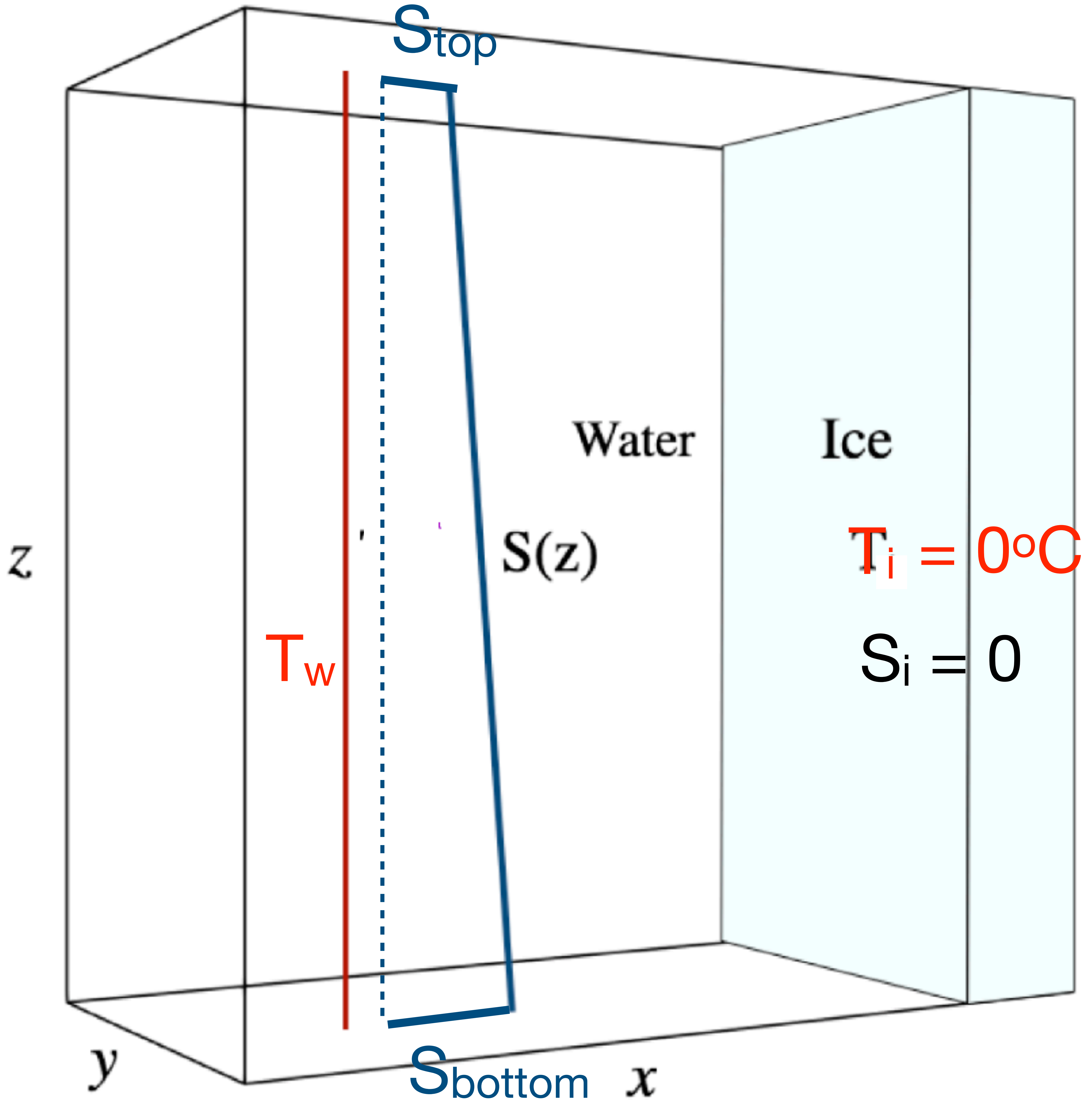

Horizontal temperature gradient:

$\Delta T = T_w - T_i$ $\quad$ T_w = initial water temp

Vertical salt stratification (stable):

$\Delta S_v = S_{bottom} - S_{top}$

VC-DDC melting setup with control parameters

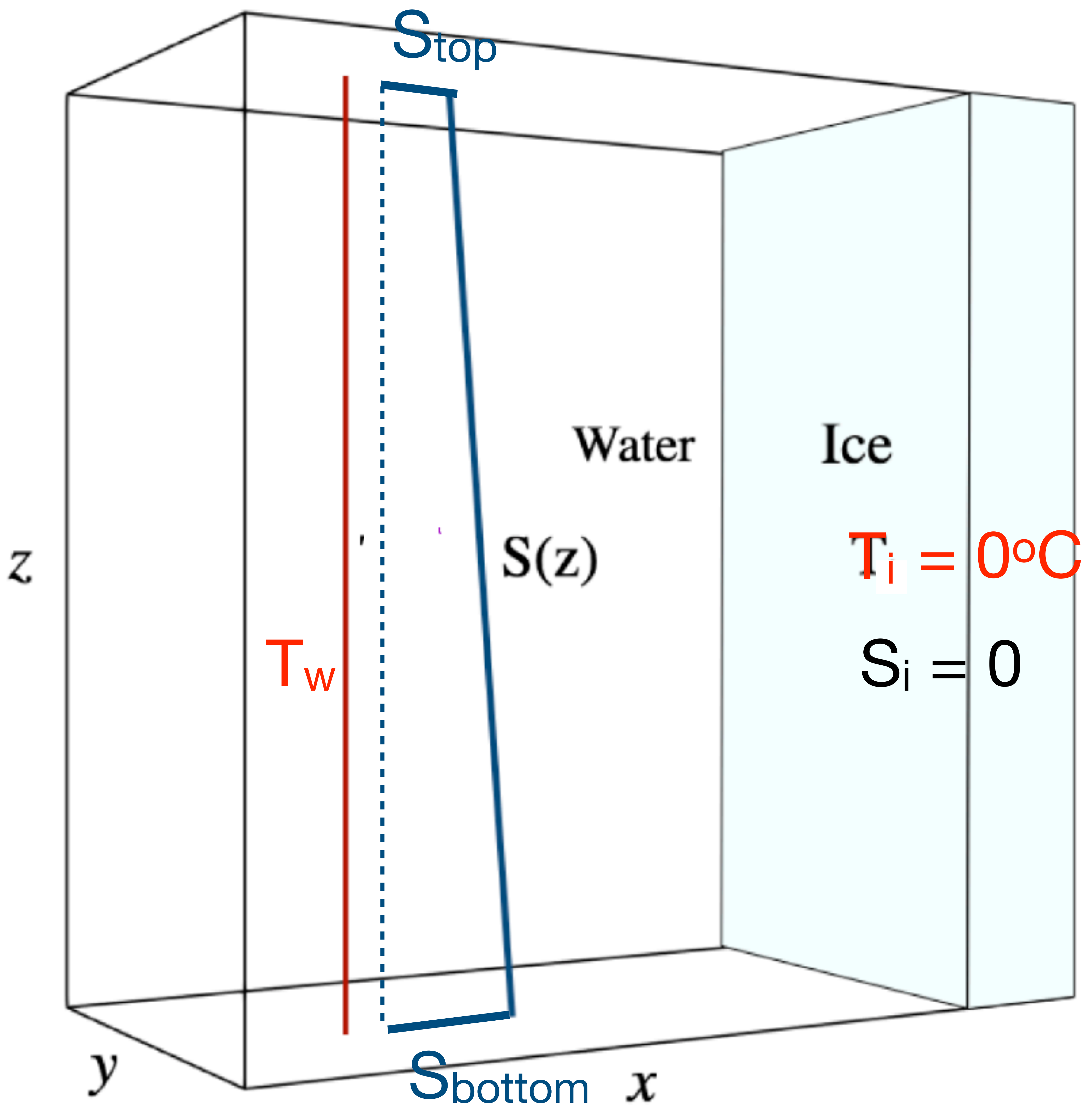

Horizontal temperature gradient:

$\Delta T = T_w - T_i$ $\quad T_w$ = initial water temp

Vertical salt stratification (stable):

$\Delta S_v = S_{bottom} - S_{top}$

Horizontal salt gradient = average salt conc.

$$\Delta S_h = \frac{1}{2}(S_{bottom} + S_{top}) - S_i$$

VC-DDC melting setup with control parameters

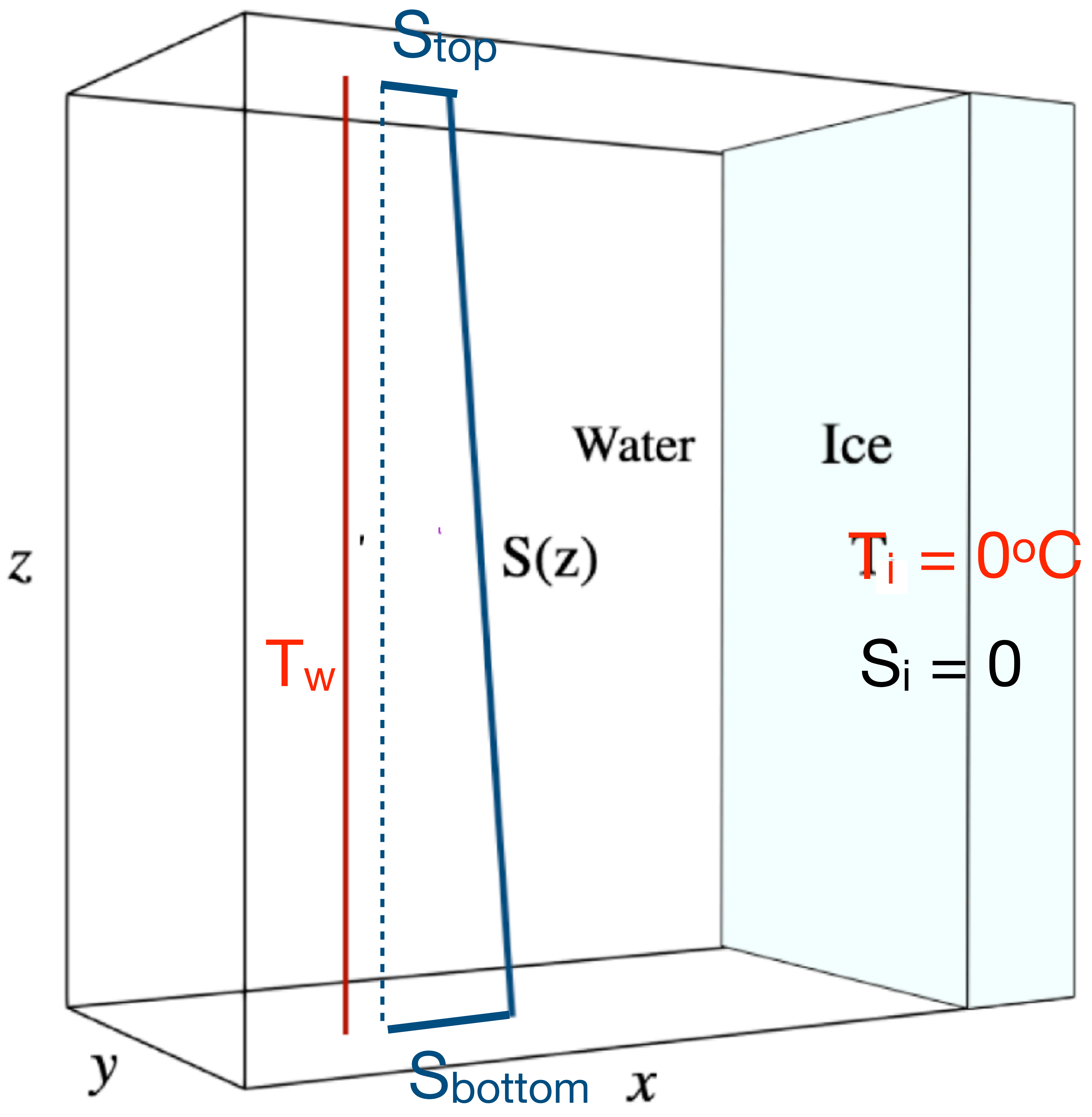

Horizontal temperature gradient:

$\Delta T = T_w - T_i$ $\quad T_w$ = initial water temp

Vertical salt stratification (stable):

$\Delta S_v = S_{bottom} - S_{top}$

Horizontal salt gradient = average salt conc.

$$\Delta S_h = \frac{1}{2}(S_{bottom} + S_{top}) - S_i$$

No flux BCs (for heat & salt)

Dimensional and dimensionless control parameters

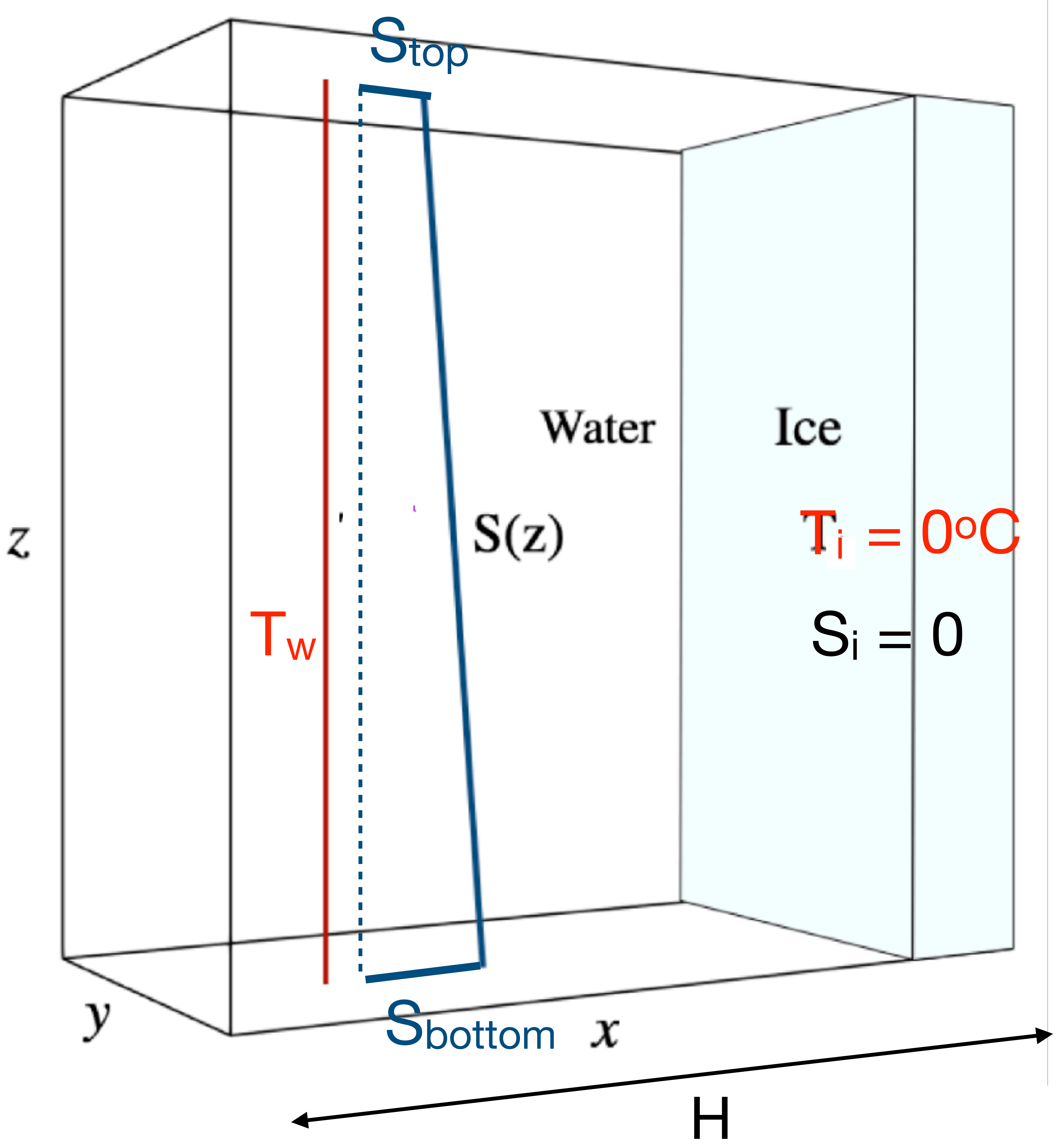

Dimensional:

Temperature difference: $\Delta T = T_0$ - 0K

Horizontal salinity difference: $\Delta S_h = (S_{top} + S_{bottom})/2$ - 0

Vertical salinity difference: $\Delta S_v = S_{bottom} - S_{top}$

Values taken:

$\Delta T = 10K,\ 15K,\ 20K$

$\Delta S_h = 0 - 20$ g/kg

$\Delta S_v = 0 - 10$ g/kg

$H = 2.5,\ 5,\ 10$ cm

Other parameters are kept at realistic values

Dimensional and dimensionless control parameters

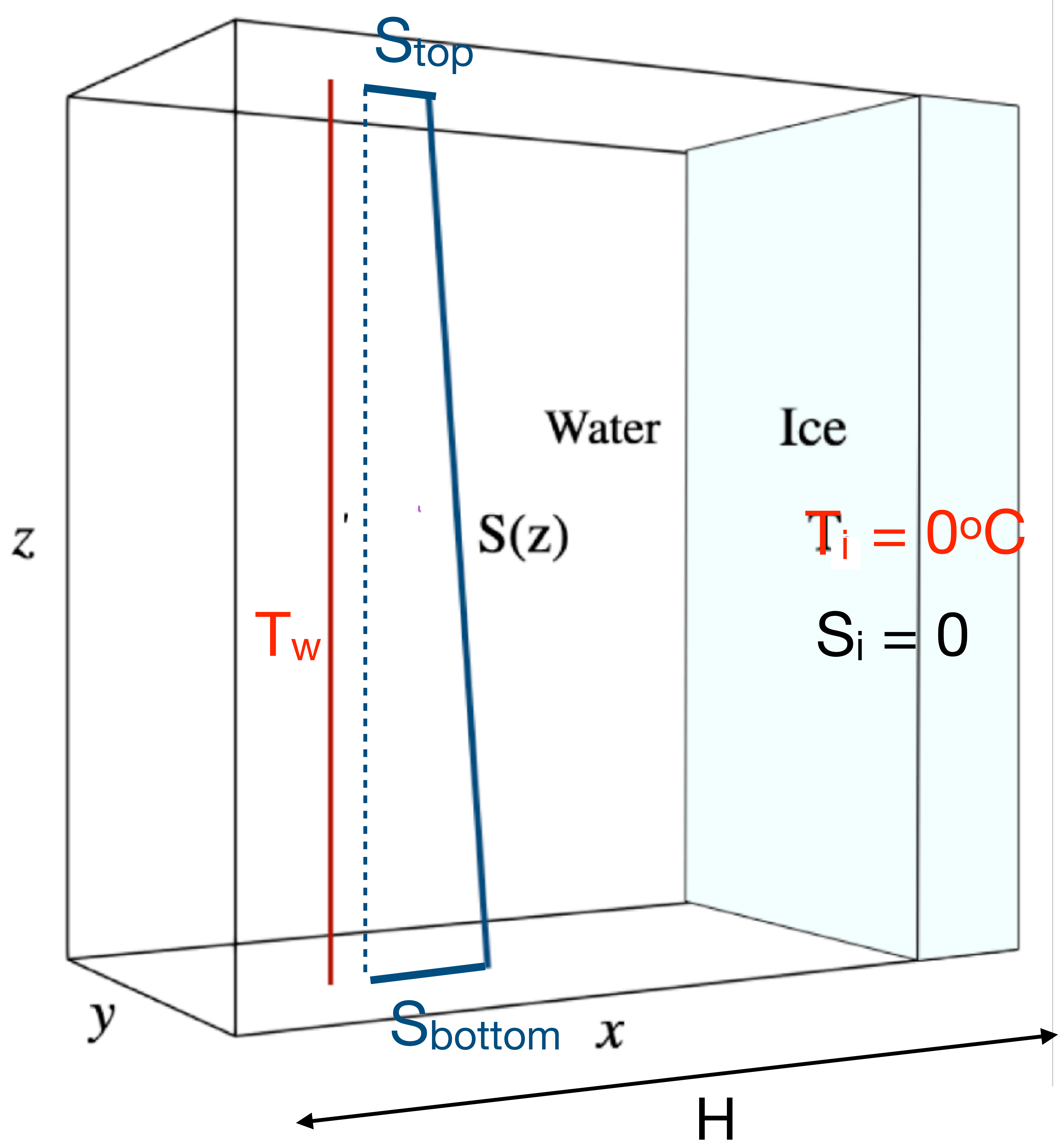

Dimensional:

Temperature difference: $\Delta T = T_0$ - 0K

Horizontal salinity difference: $\Delta S_h = (S_{top} + S_{bottom})/2$ - 0

Vertical salinity difference: $\Delta S_v = S_{bottom} - S_{top}$

Values taken:

$\Delta T = 10K,\ 15K,\ 20K$

$\Delta S_h = 0 - 20$ g/kg $\longrightarrow$

$\Delta S_v = 0 - 10$ g/kg

$H = 2.5,\ 5,\ 10$ cm

Other parameters are kept at realistic values

Dimensionless control parameters

$$Ra_T = \frac{C_b g \Delta T^2 H^3}{2\nu\kappa_T} = [1.8 \times 10^6 - 1.2 \times 10^9]$$

$$Ra_S = \frac{b_0 g \Delta S_h H^3}{\nu\kappa_S} = [0 - 2.5 \times 10^{10}]$$

$$Pr_T = \frac{\nu}{\kappa_T} = 10$$

$$Pr_S = \frac{\nu}{\kappa_S} = 1000$$

$$St = \frac{L}{c_p \Delta T}$$

Known density dependence on T & S: $\rho(T, S)$

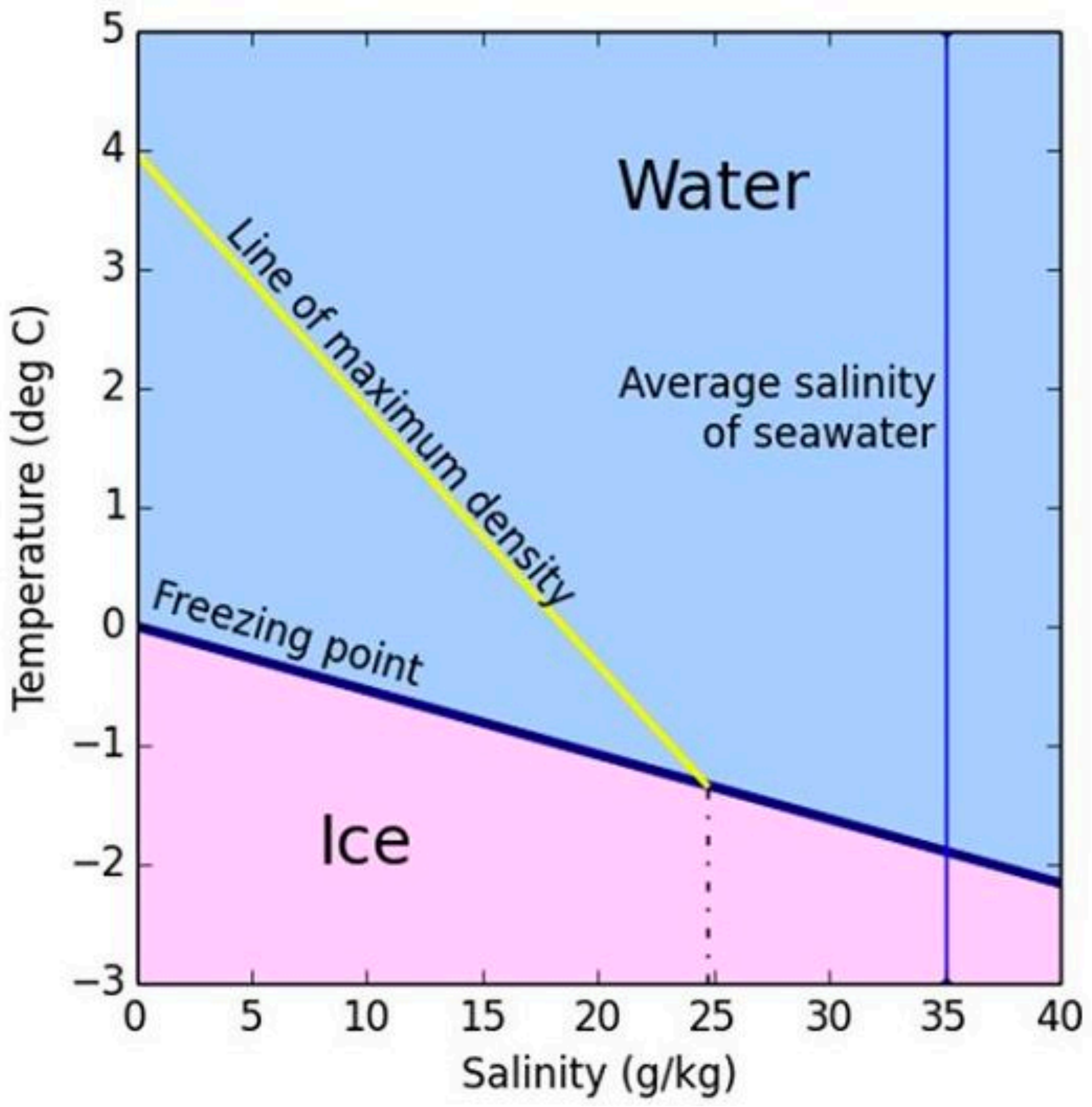

$$\rho' = -\frac{C_b}{2}(\Theta - \Theta_o - \varepsilon S_A)^2 - T_h Z\Theta + b_o S_A$$

Note:

- Freezing point goes down with increasing salt concentration
- Density maximum no issue at seawater any more

Effect of vertical stratification ΔS_v on ice melting

2D

$\Delta S_h = 5$ g/kg

$\Delta T = 20$ K

Effect of vertical stratification ΔS_v on ice melting

2D

$\Delta S_h = 5$ g/kg

$\Delta T = 20$ K

Effect of vertical stratification ΔS_v on ice melting

2D

$\Delta S_h = 5$ g/kg

$\Delta T = 20$ K

Effect of vertical stratification ΔS_v on ice melting

2D

$\Delta S_h = 5$ g/kg

$\Delta T = 20$ K

Effect of vertical stratification ΔS_v on ice melting

2D

$\Delta S_h = 5$ g/kg

$\Delta T = 20$ K

Ripples develop for medium vertical stratification!

Details of interplay between DDC layers & ice structure

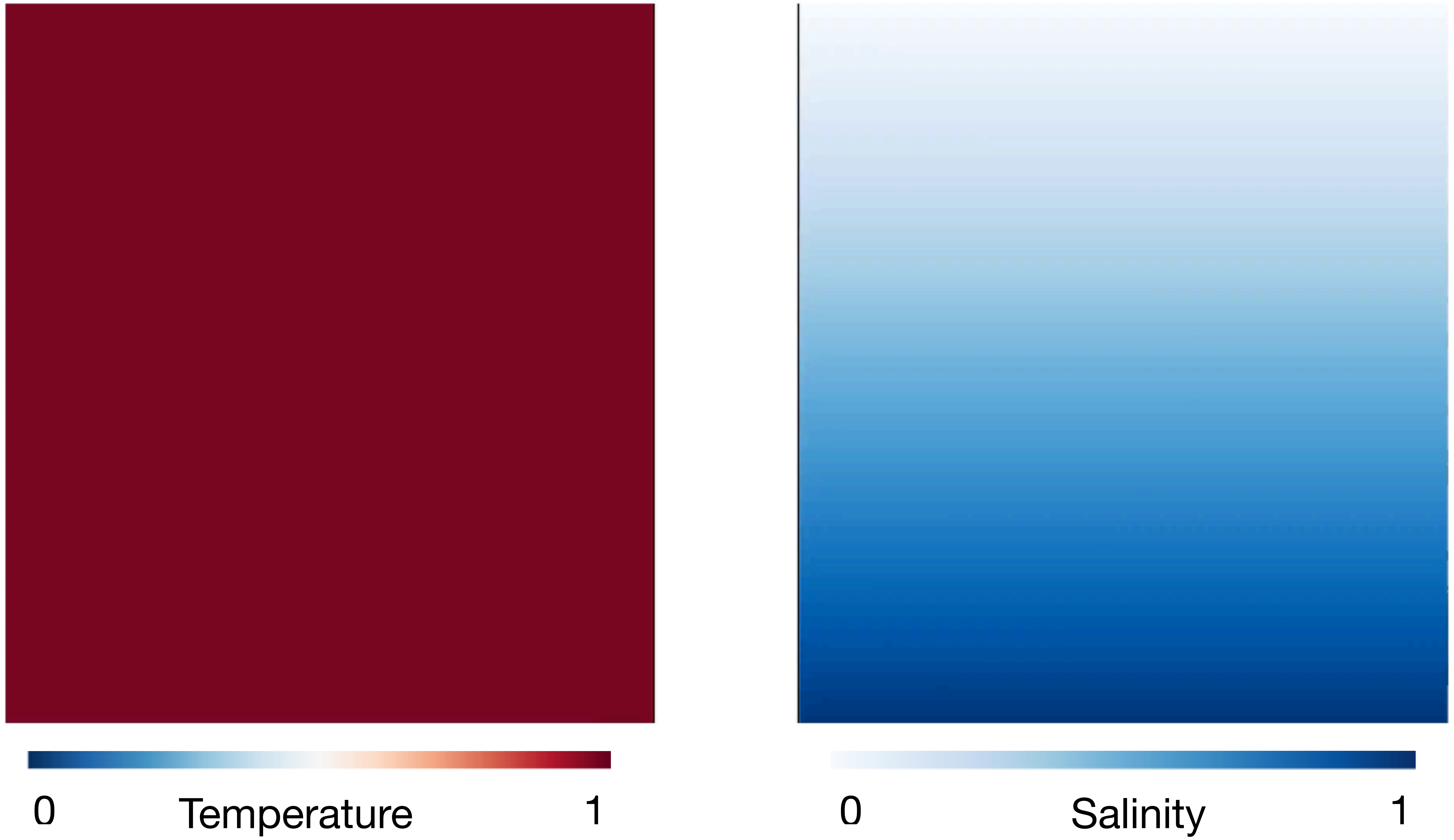

$$\Delta S_v = 5 \text{ g/kg}$$
$$\Delta S_h = 5 \text{ g/kg}$$
$$\Delta T = 20 \text{ K}$$

2D

Ripples develop for medium vertical stratification!

Details of interplay between DDC layers & ice structure

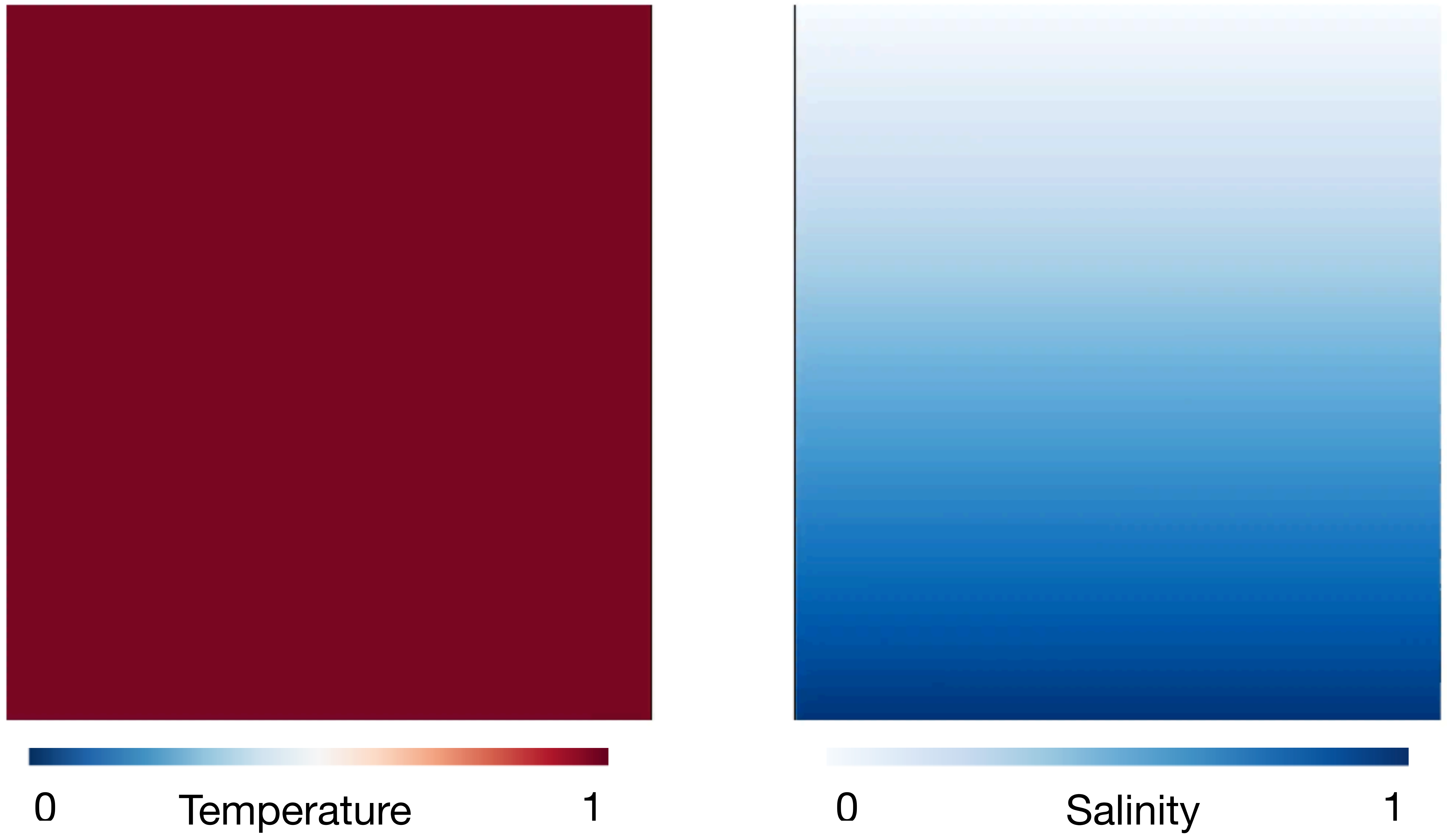

2D

$$\Delta S_v = 5 \ \mathrm{g/kg}$$
$$\Delta S_h = 5 \ \mathrm{g/kg}$$
$$\Delta T = 20 \ \mathrm{K}$$

Ripples develop for medium vertical stratification!

Effect of vertical stratification ΔS_v on ice melting

3D

$\Delta S_v = 0$ g/kg

$\Delta S_v = 5$ g/kg

$\Delta S_v = 10$ g/kg

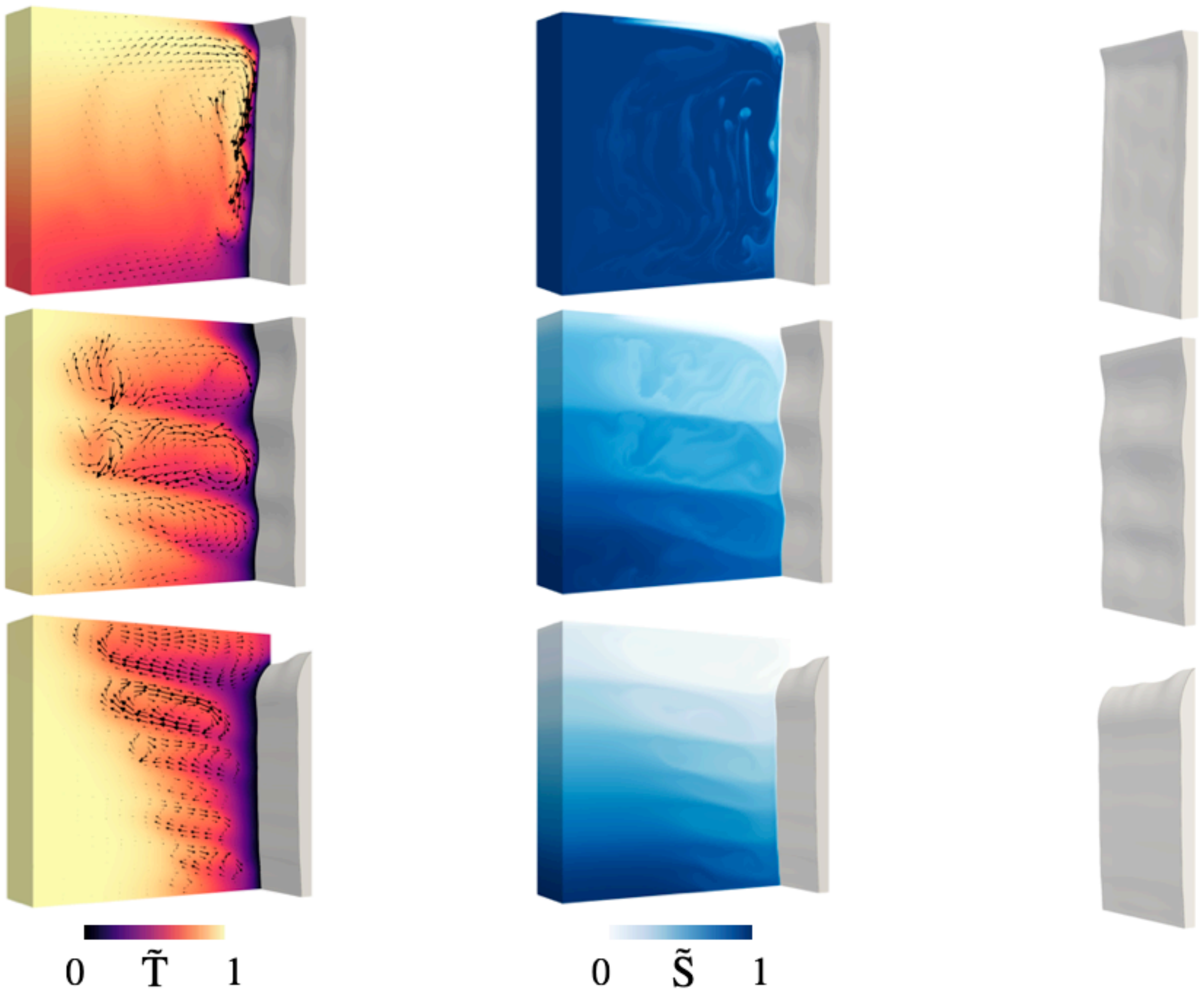

$\Delta S_h = 5$ g/kg

Ripples also develop in 3D simulations

Effect of vertical stratification ΔSᵥ on ice melting

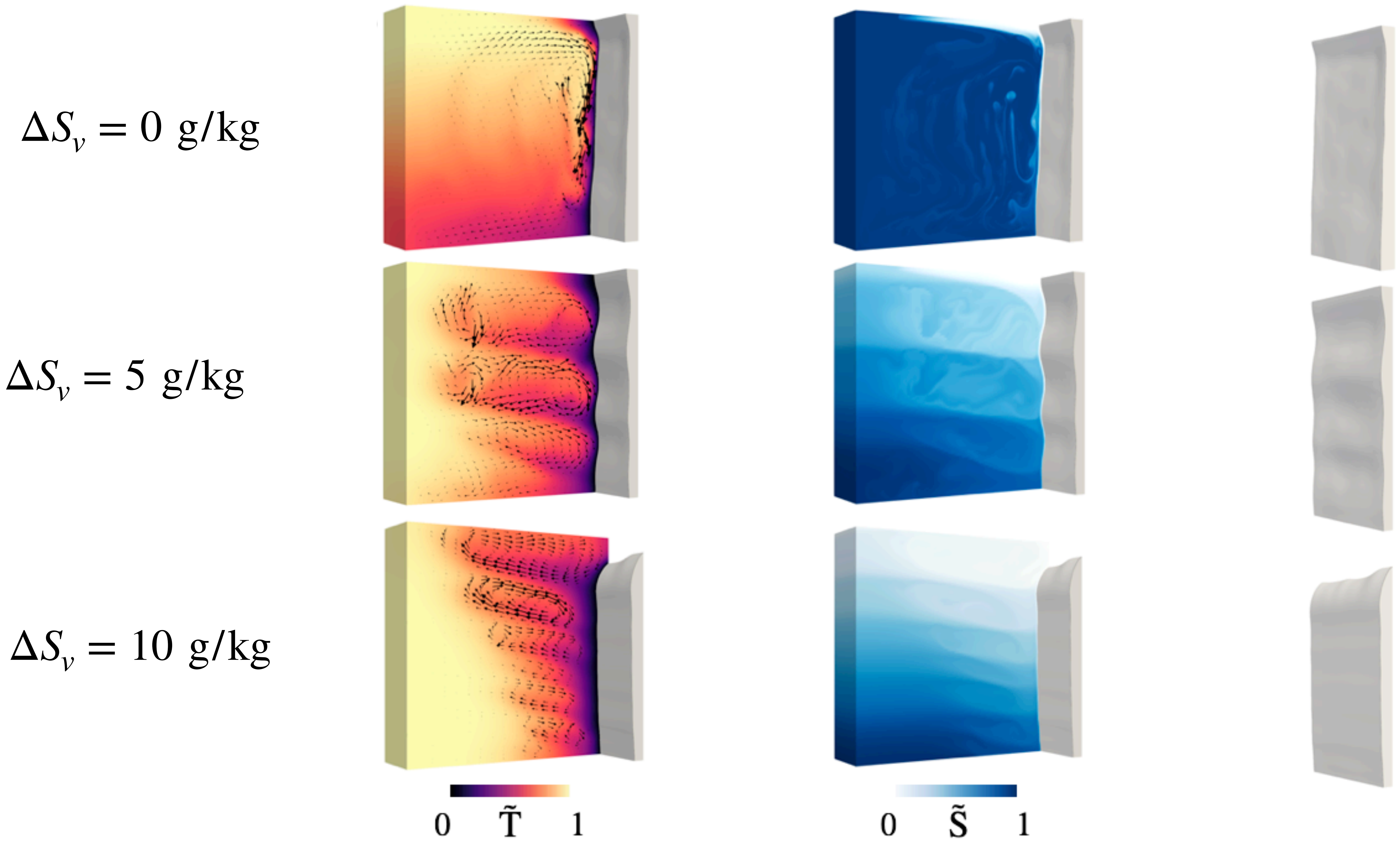

3D

Ripples also develop in 3D simulations

Note difference: Ripples vs scallops

$\Delta S_h = 5$ g/kg

Effect of vertical stratification ΔSᵥ on ice melting

$\Delta S_v = 0$ g/kg

$\Delta S_v = 5$ g/kg

$\Delta S_v = 10$ g/kg

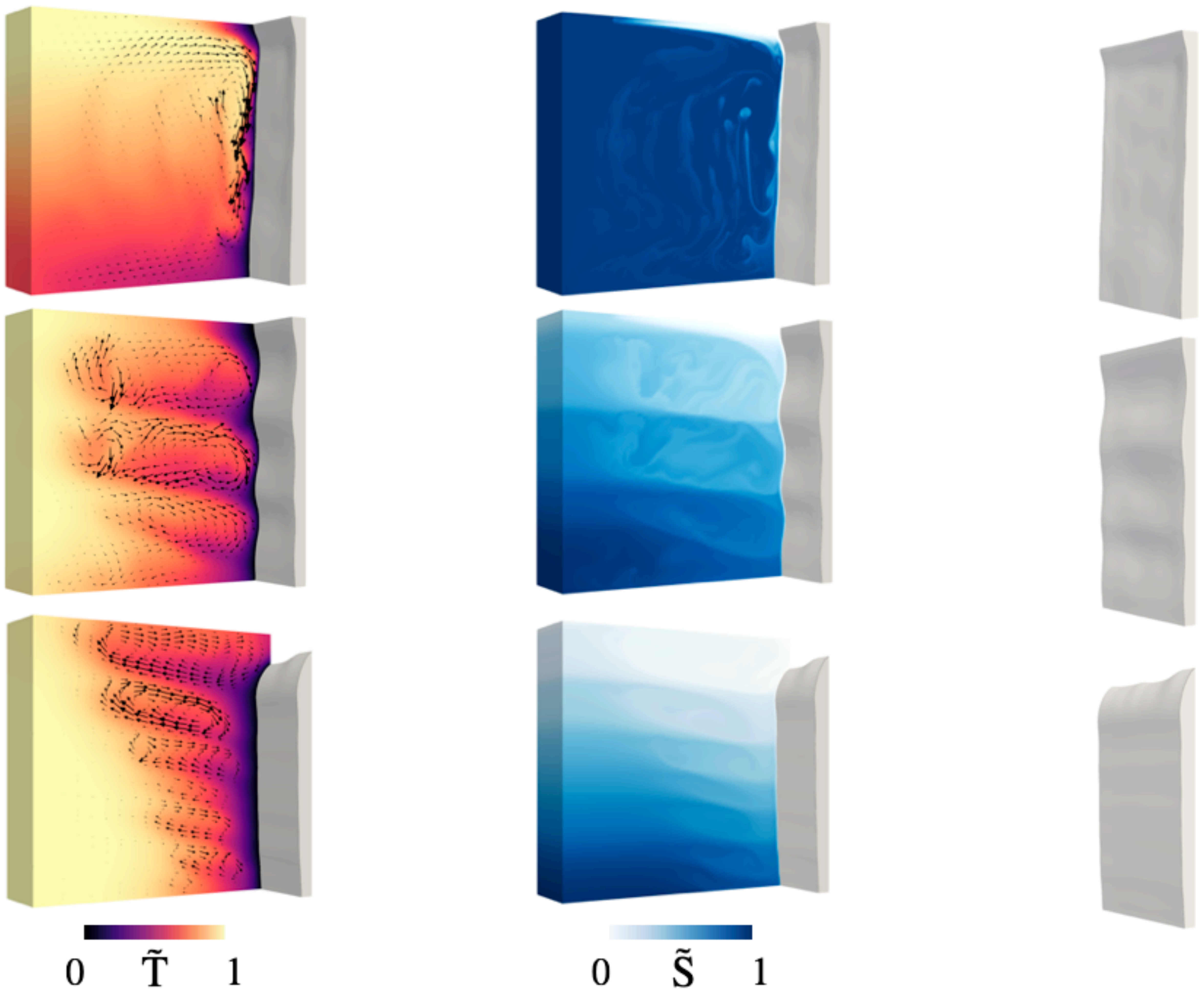

$\Delta S_h = 5$ g/kg

3D

Ripples also develop in 3D simulations

Note difference: Ripples vs scallops

Ripple length scale determined by staircase flow structure

Effect of average salt concentration ΔS_h on ice melting

$\Delta S_h = 5$ g/kg
($S_{top} = 2.5$ g/kg, $S_{bot} = 7.5$ g/kg)

$\Delta S_h = 7.5$ g/kg
($S_{top} = 5$ g/kg, $S_{bot} = 10$ g/kg)

$\Delta S_h = 10$ g/kg
($S_{top} = 7.5$ g/kg, $S_{bot} = 12.5$ g/kg)

$\Delta S_v = 5$ g/kg

$\Delta T = 20$ K

Effect of average salt concentration ΔS_h on ice melting

$\Delta S_v = 5$ g/kg

$\Delta T = 20$ K

Effect of average salt concentration ΔS_h on ice melting

$\Delta S_v = 5$ g/kg

$\Delta T = 20$ K

Effect of average salt concentration ΔS_h on ice melting

$\Delta S_v = 5$ g/kg

$\Delta T = 20$ K

Effect of average salt concentration ΔS_h on ice melting

$\Delta S_v = 5$ g/kg
$\Delta T = 20$ K

Ripple formation robust phenomenon

Synopsis: Flow & ice structures (2D)

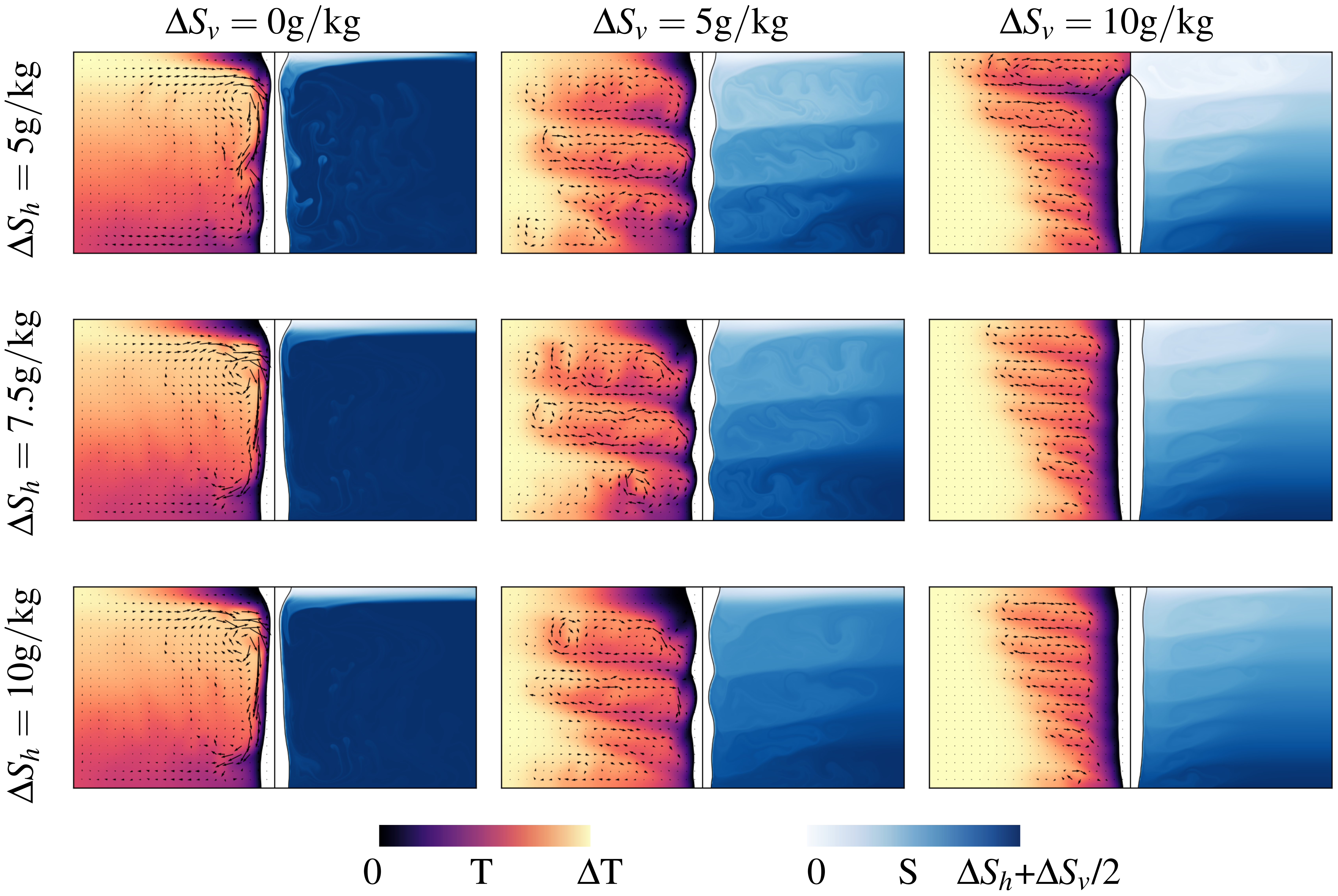

Synopsis: Flow & ice structures (2D)

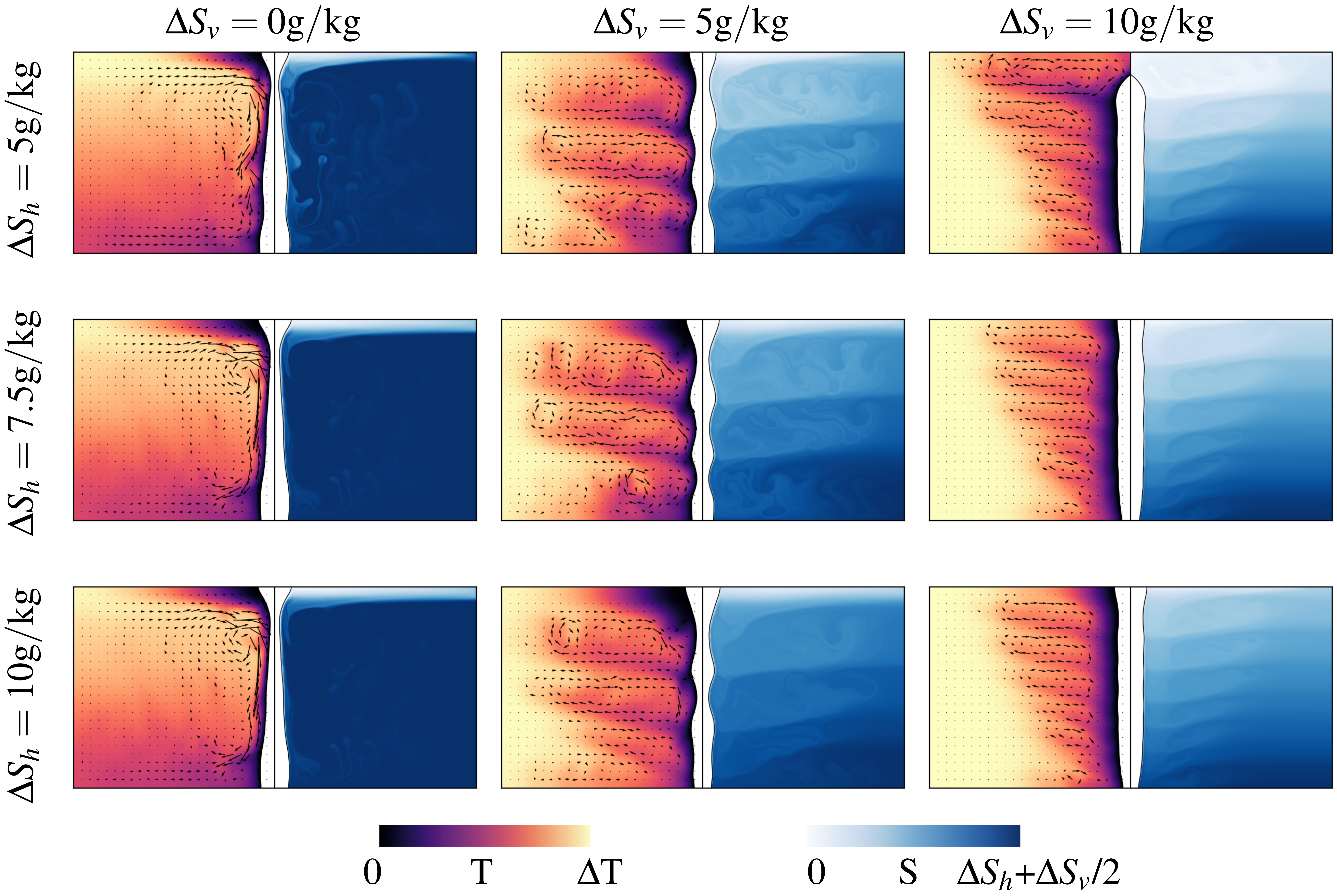

Do the developing wavelengths agree with the experimental ones?

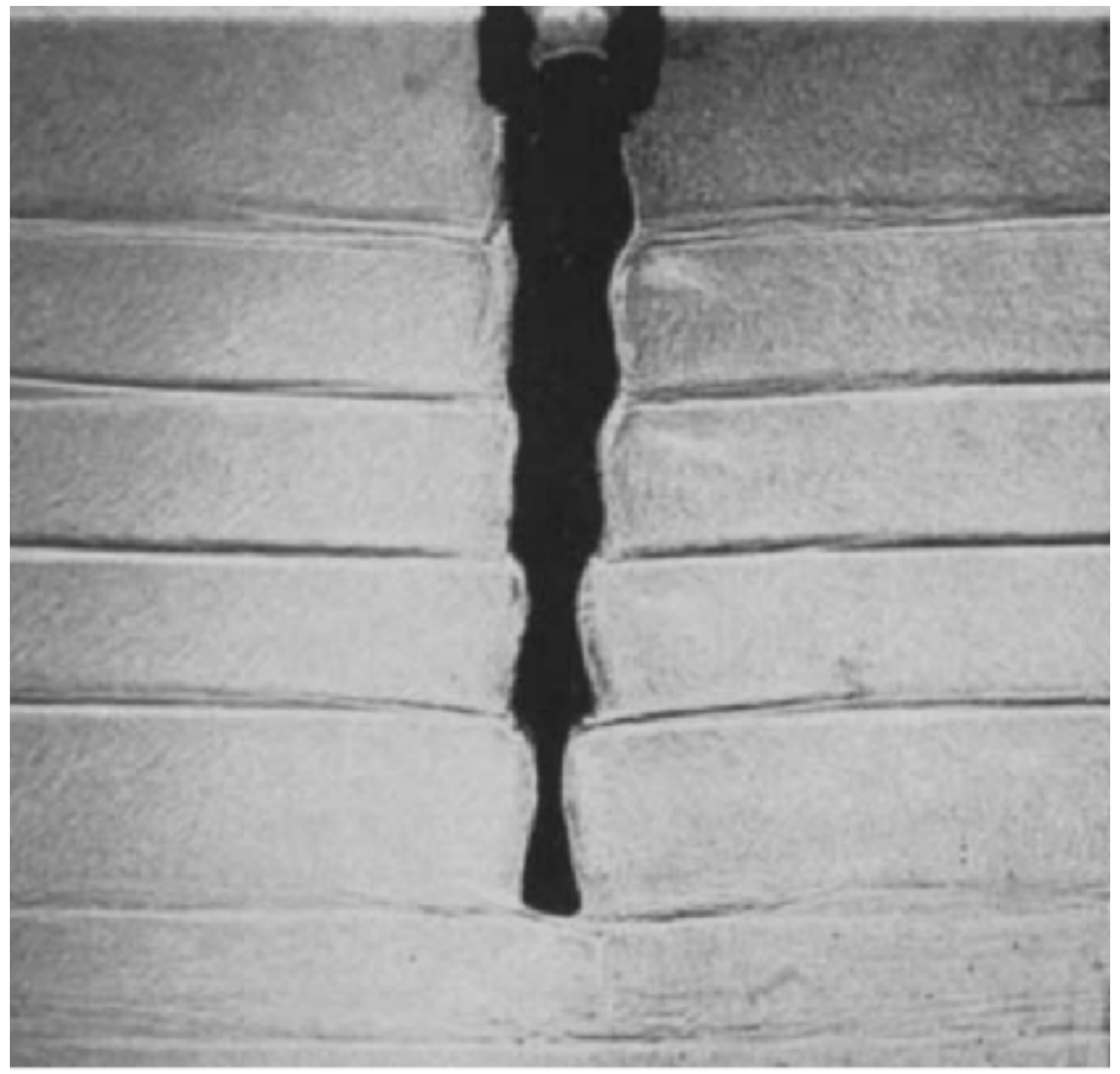

Huppert & Turner, JFM (1980)

Wavelength: Compare numerics & experiment & theory

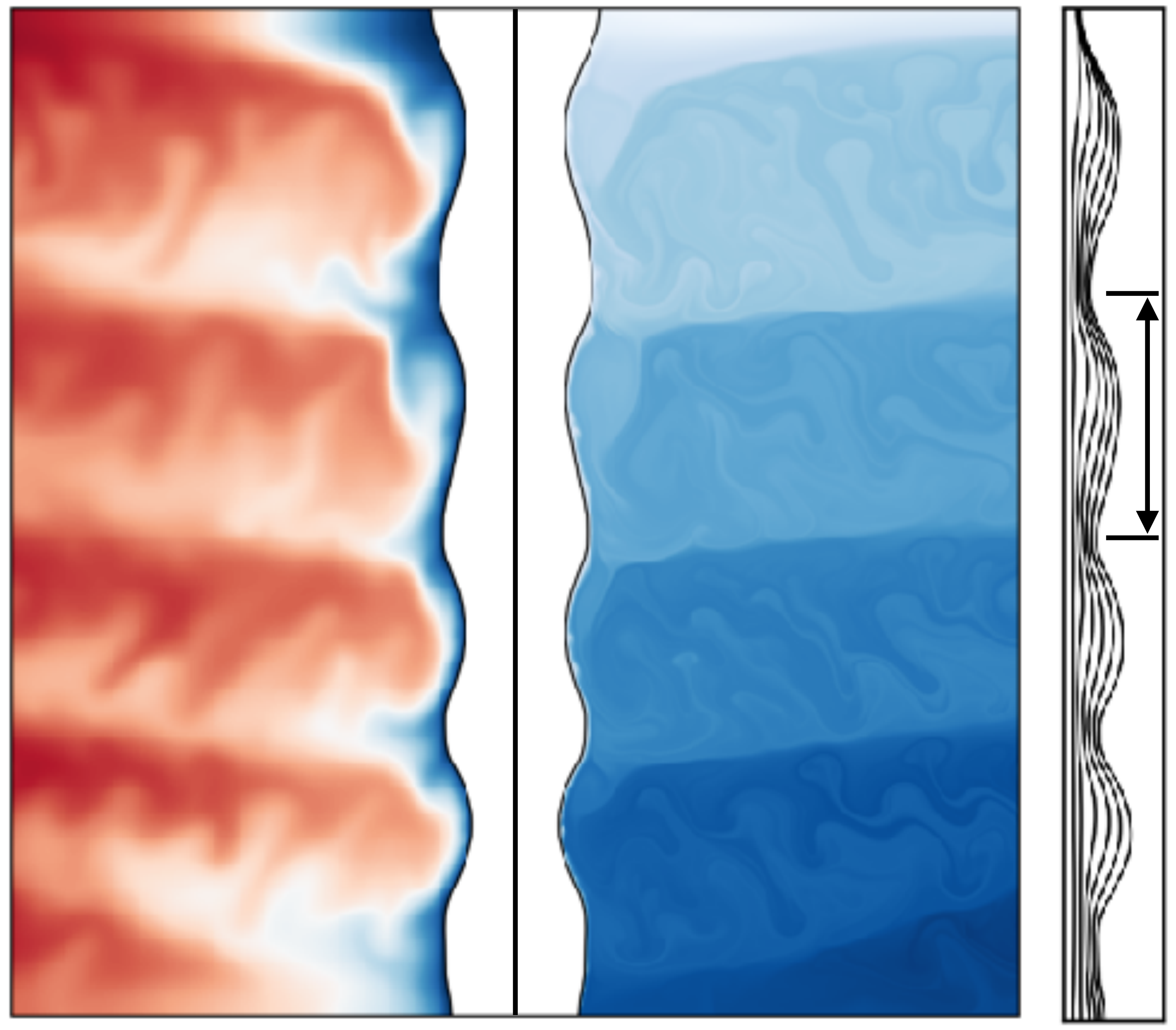

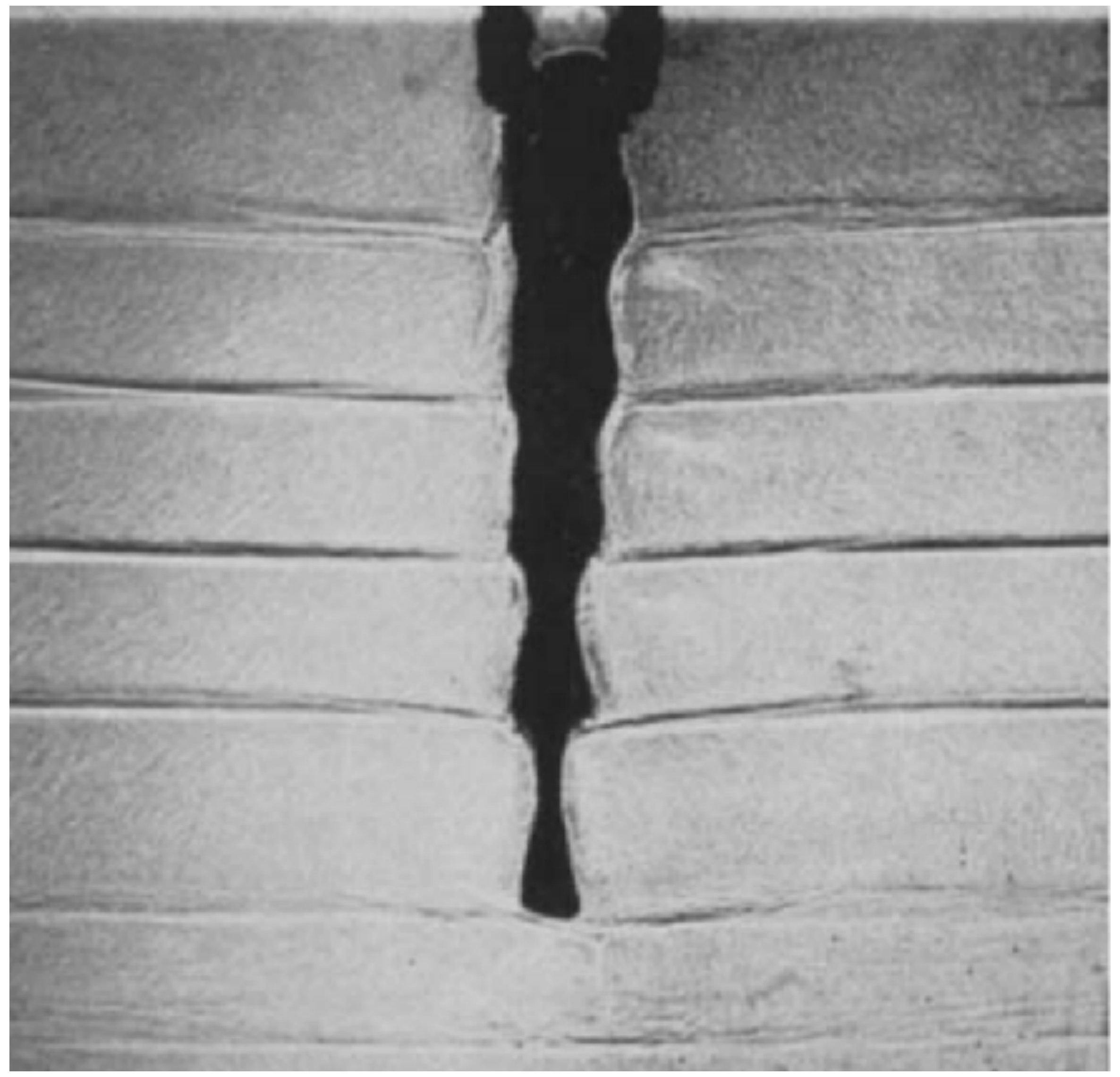

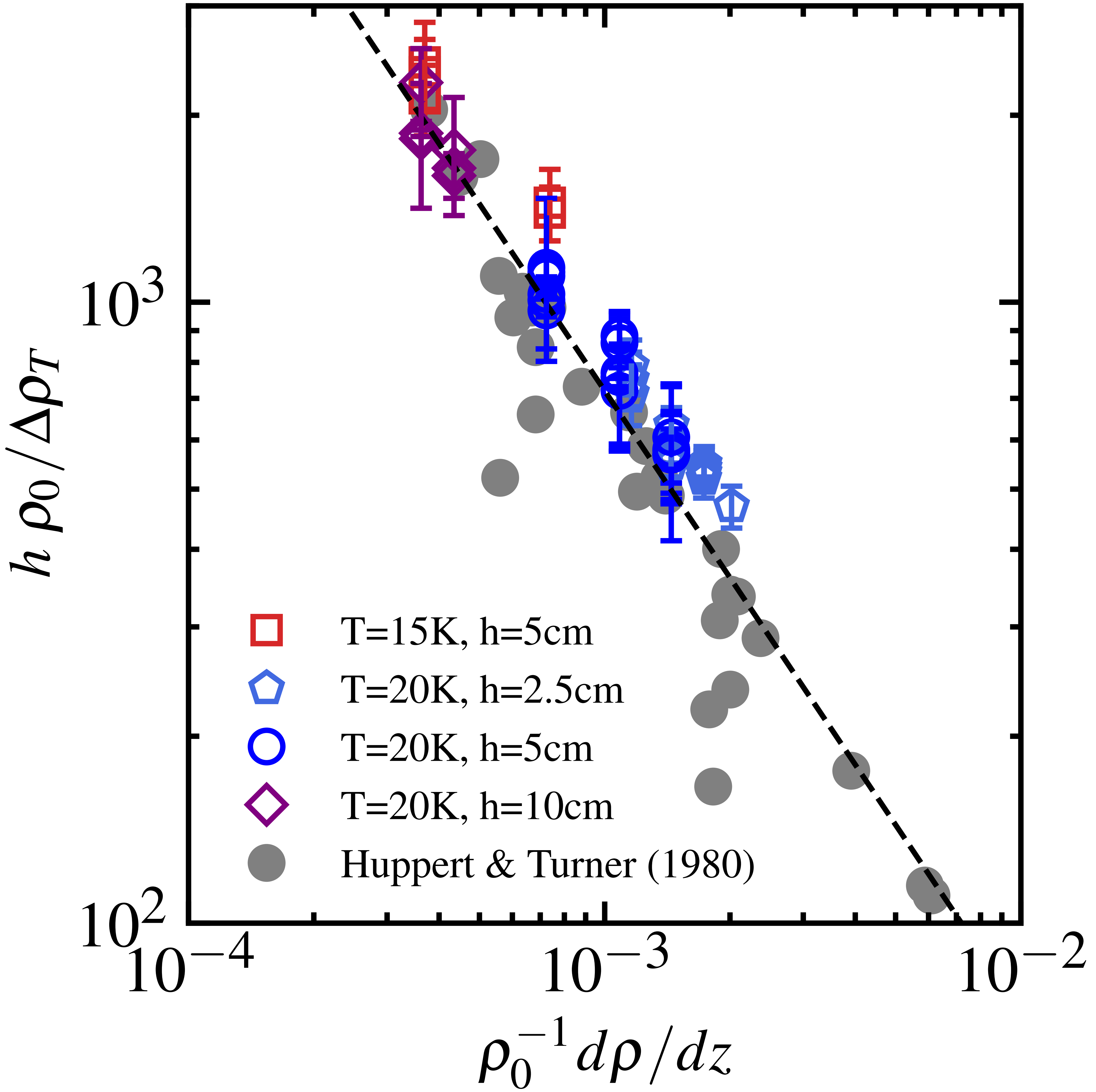

$$h = (0.65 \pm 0.06)\,[\rho(0,S_\infty) - \rho(T_\infty,S_\infty)]\left(\frac{\mathrm{d}\rho}{\mathrm{d}z}\right)^{-1}$$

Wavelengths from simulations nicely agree with the experimental ones!

Conclusions on part IV.

- DNS of ice melting in saline water
- Scallops/layered structures of melt front: quantitative agreement between experiments, DNS, and theory
- Non-monotonic dependence of melt rate on ambient salinity
- Origin thereof: competition between thermal-driven buoyancy, salinity-driven buoyancy, and salinity stable stratification

Yang, Howland, Liu, Verzicco, Lohse, JFM 969, R2 (2023)

What is the optimal shape for minimal melting?

Simplified shape: ellipse

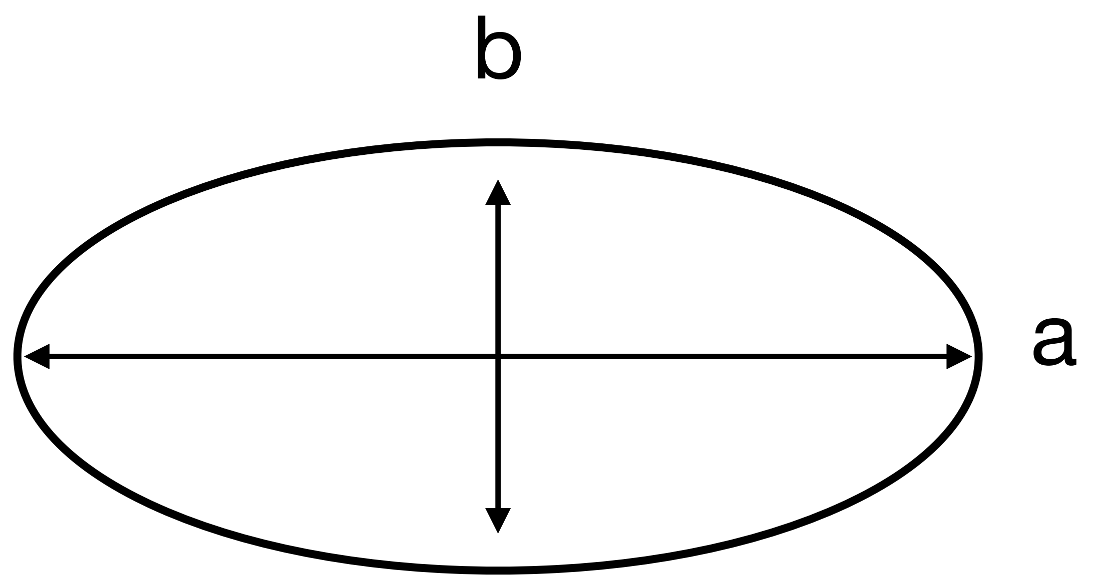

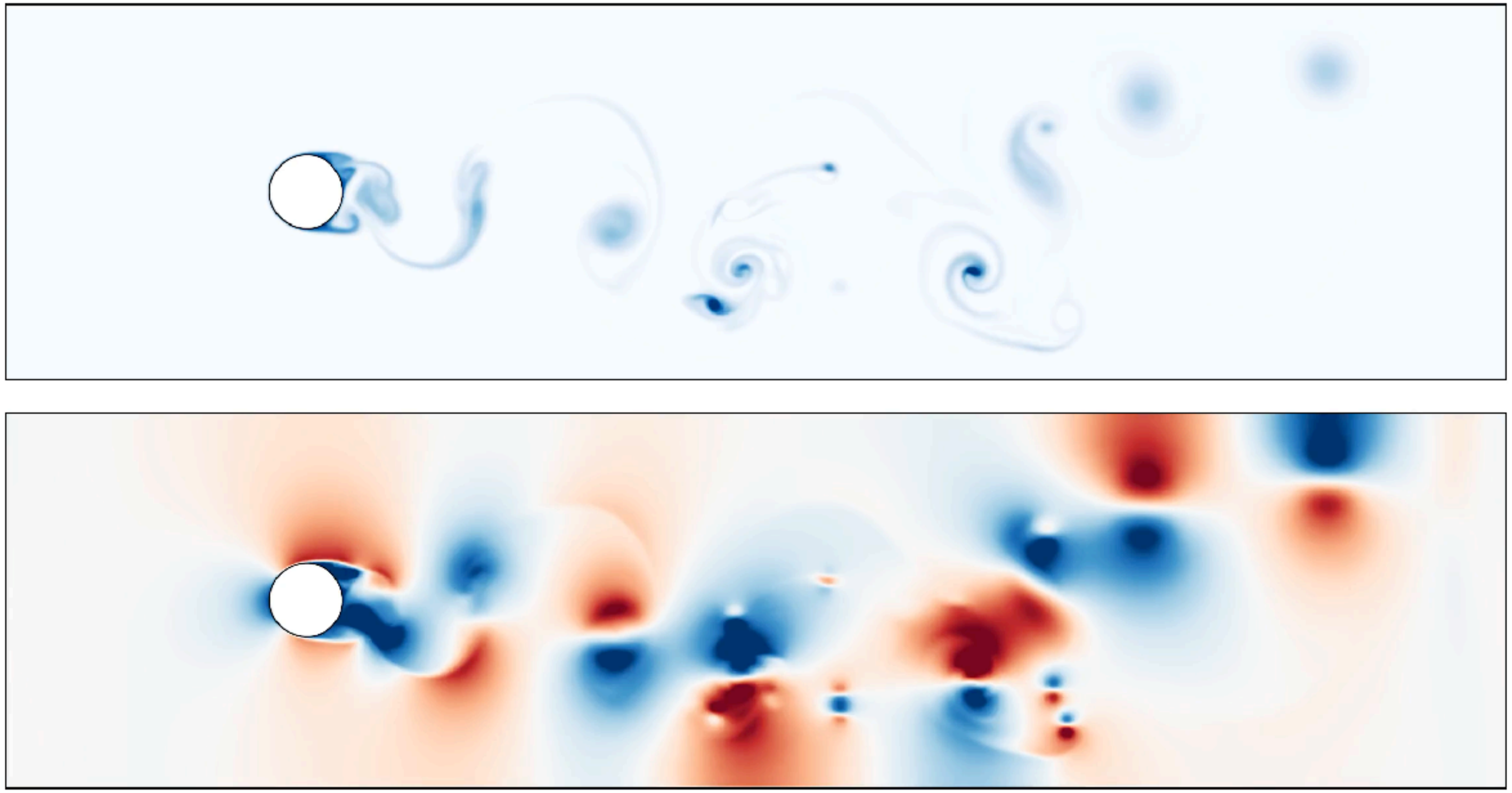

Control parameters:

$$Re_0 = \frac{U_0\sqrt{A_0}}{\nu}$$

Initial area

$$\varepsilon = \frac{b}{a}$$

What is the optimal shape for minimal melting?

Simplified shape: ellipse

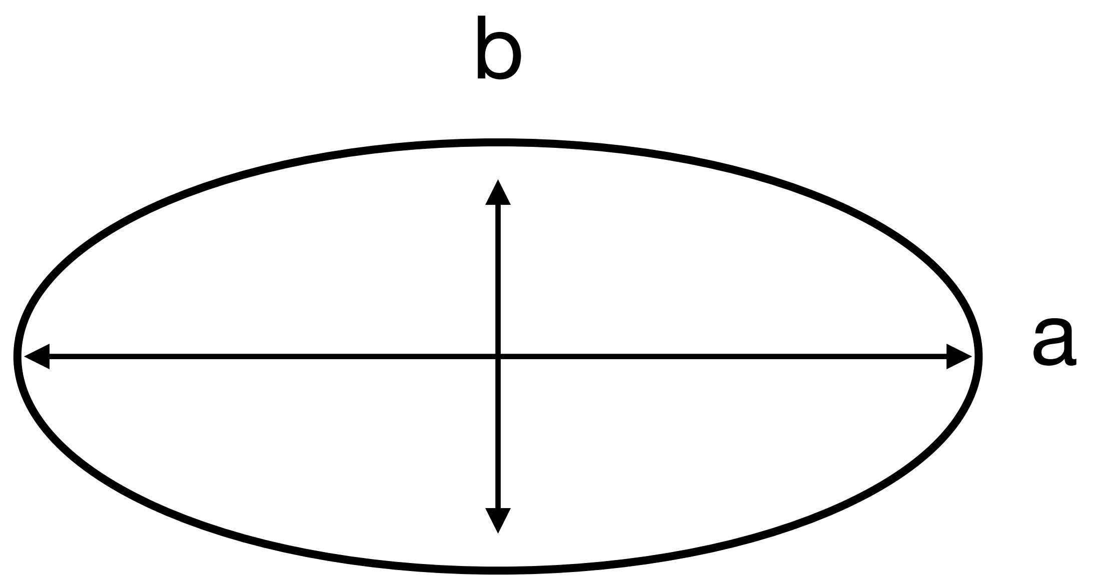

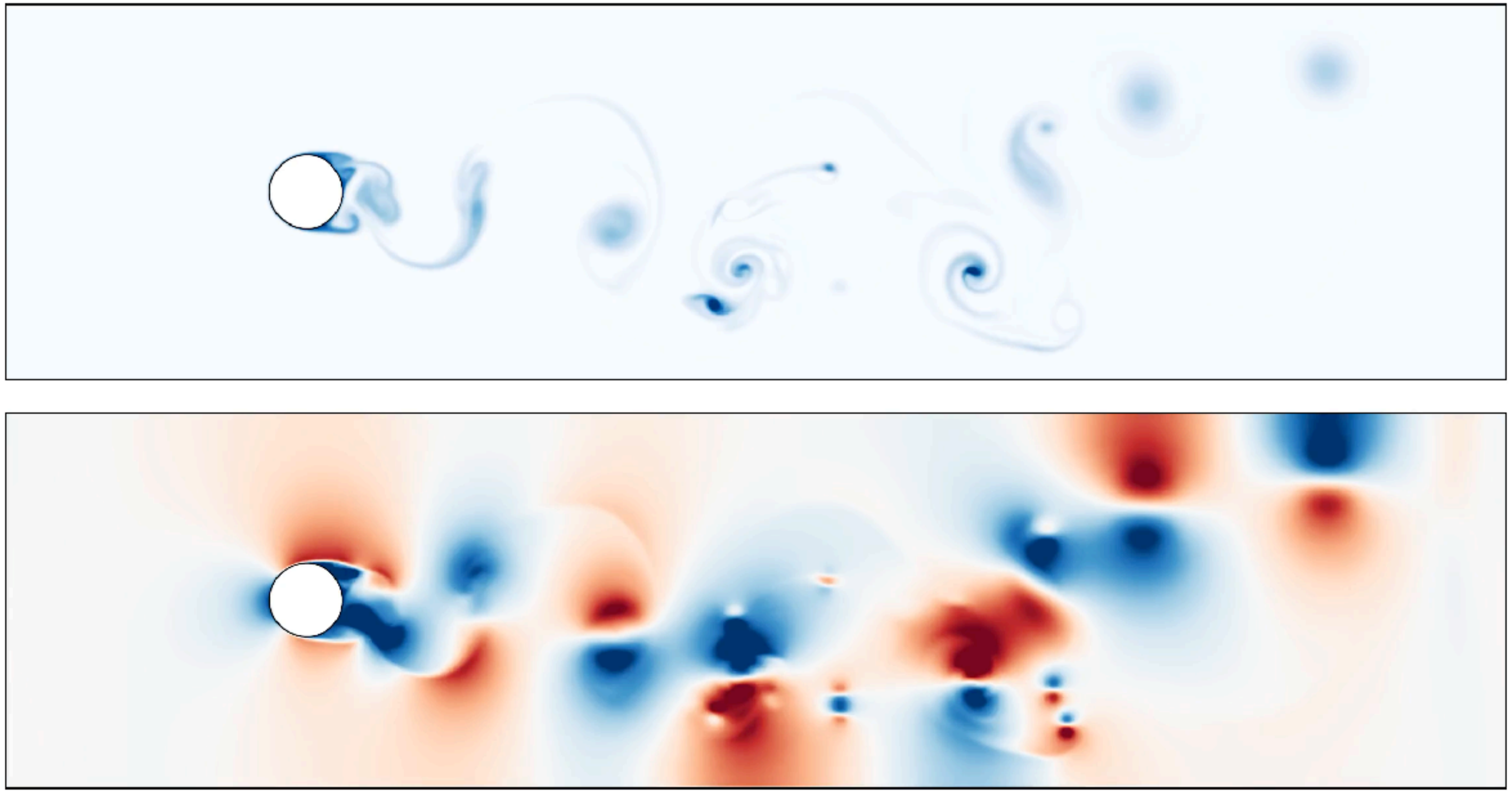

Control parameters:

$$Re_0 = \frac{U_0\sqrt{A_0}}{\nu}$$

Initial area

$$\varepsilon = \frac{b}{a}$$

Competition of three different shapes

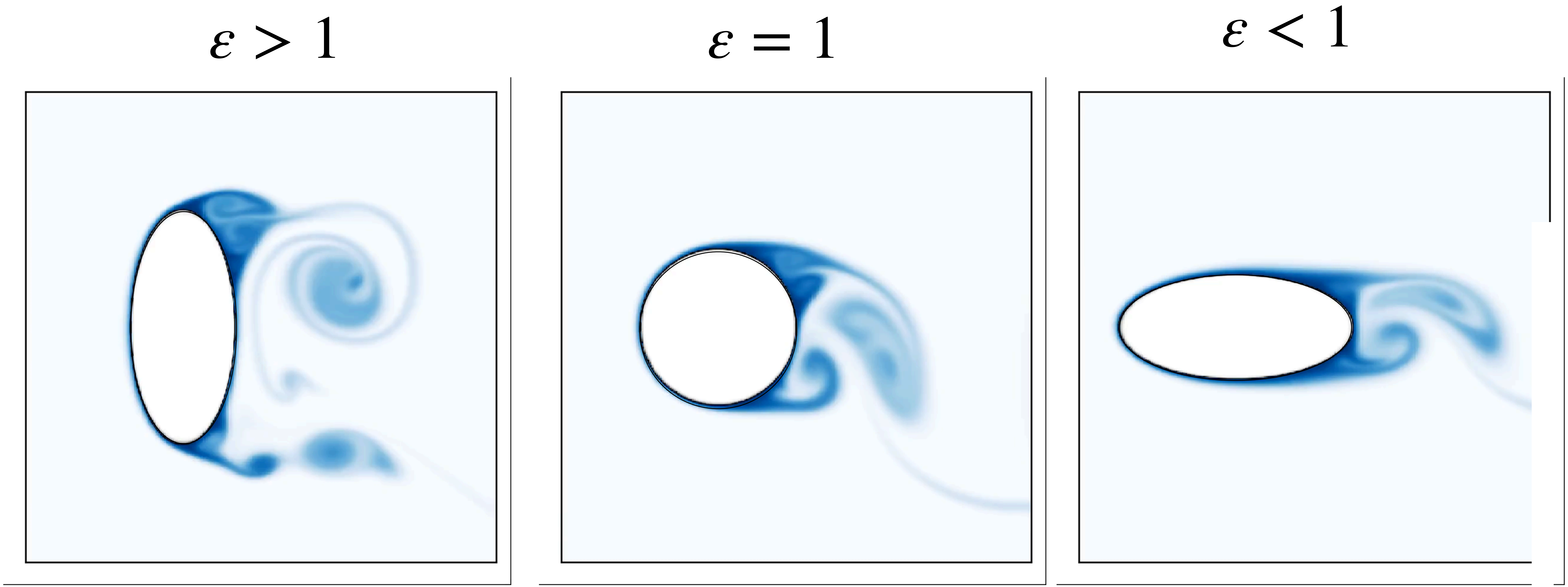

Re_0=2000

Which one will melt slowest?

Competition of three different shapes

$\varepsilon > 1$ $\varepsilon = 1$ $\varepsilon < 1$

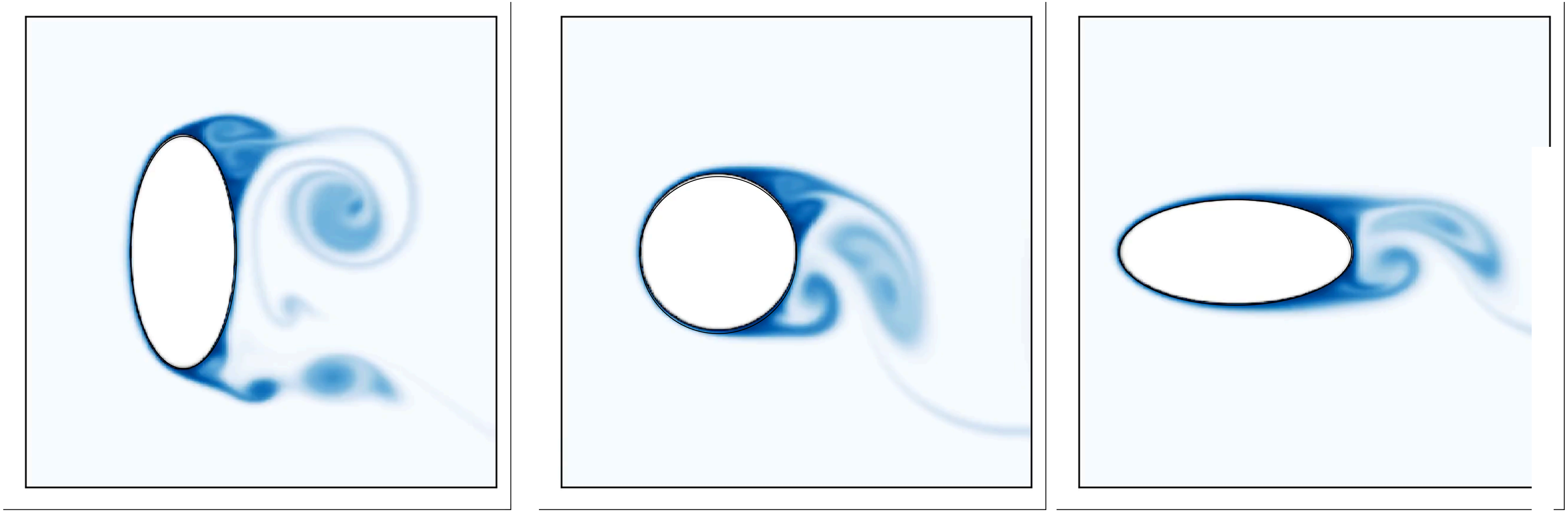

Re_0=2000

Which one will melt slowest?

J. Fluid Mech. (2024), *vol.* 980, R1, doi:10.1017/jfm.2023.1080

JFM RAPIDS

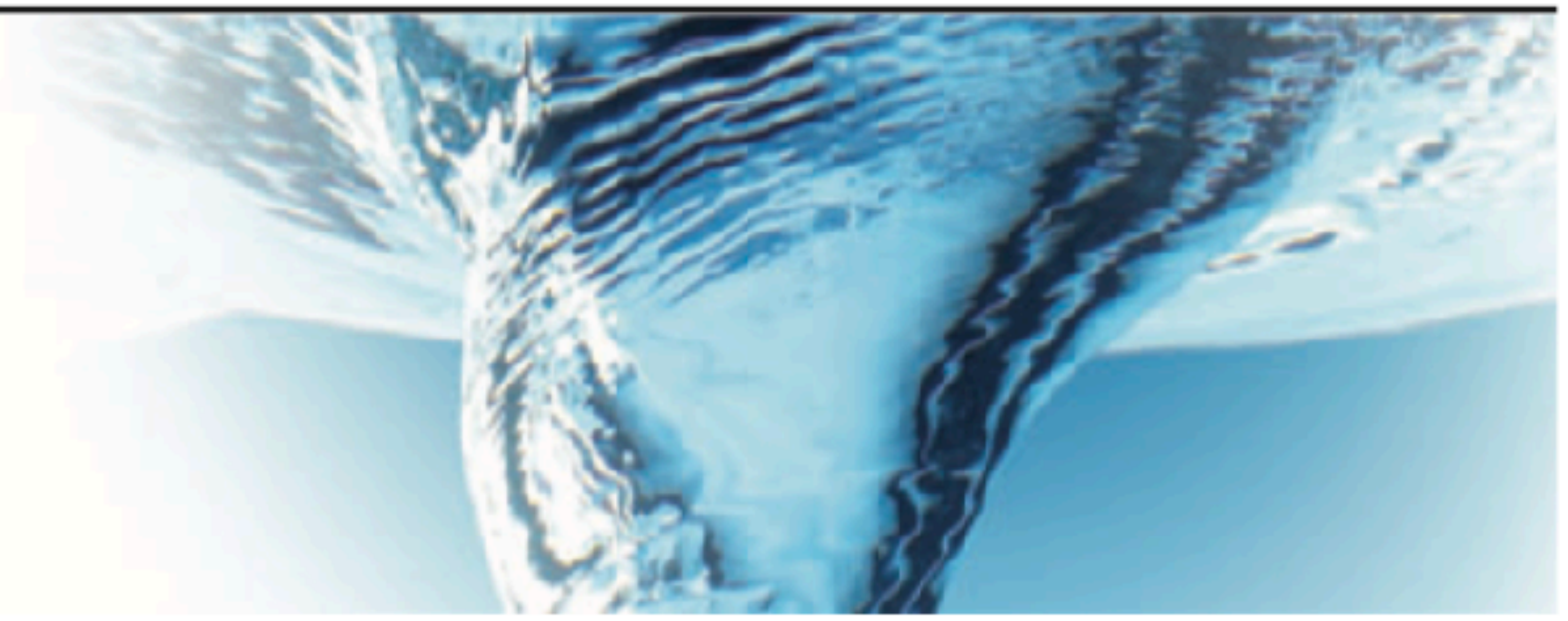

Shape effect on solid melting in flowing liquid

Rui Yang[1,†], Christopher J. Howland[1], Hao-Ran Liu[2], Roberto Verzicco[1,3,4] and Detlef Lohse[1,5]

Overall summary

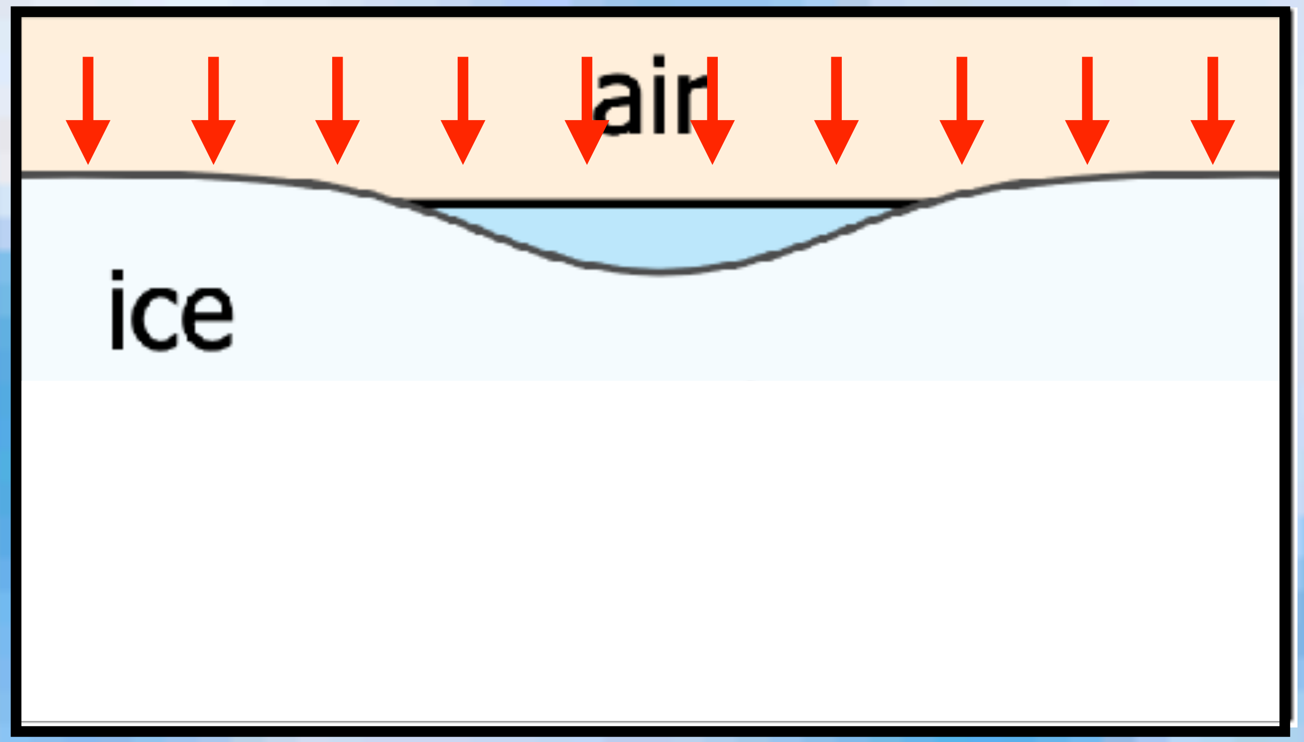

I. Bistability in radiatively heated melt ponds

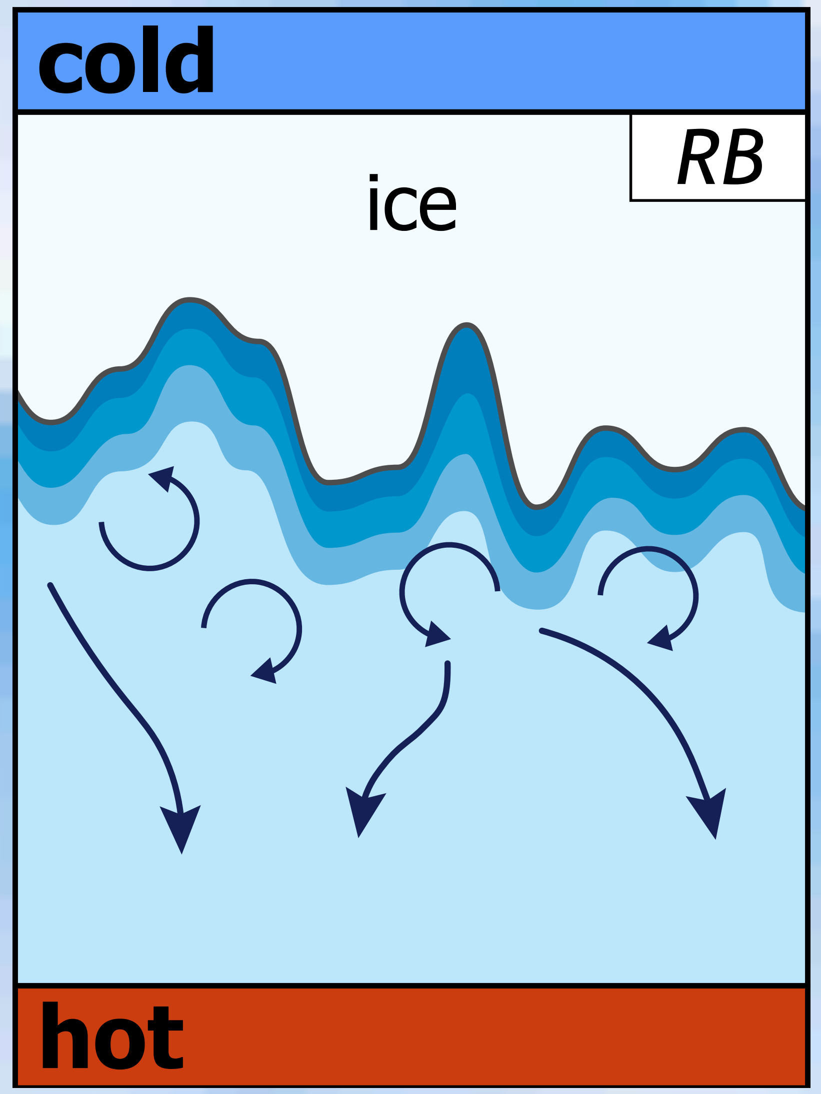

II. RB with fresh water at large Ra

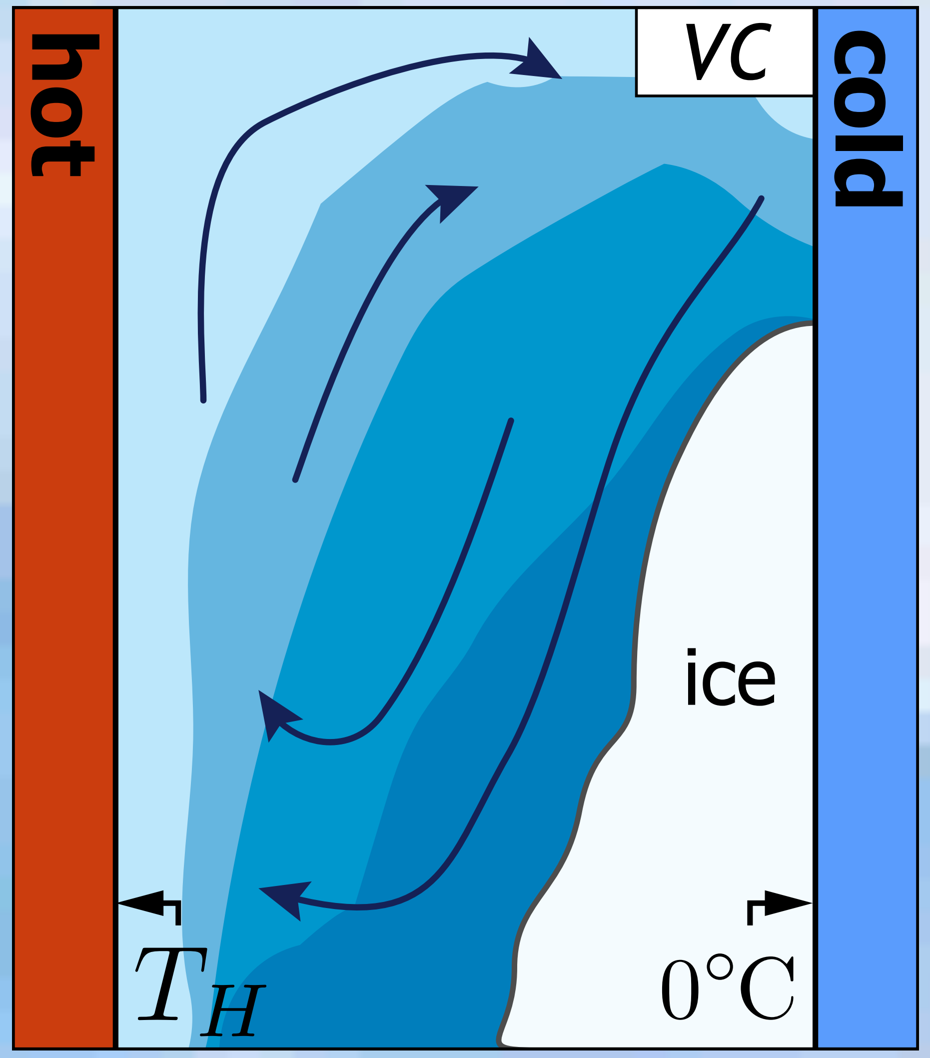

III. Vertical convection with fresh water

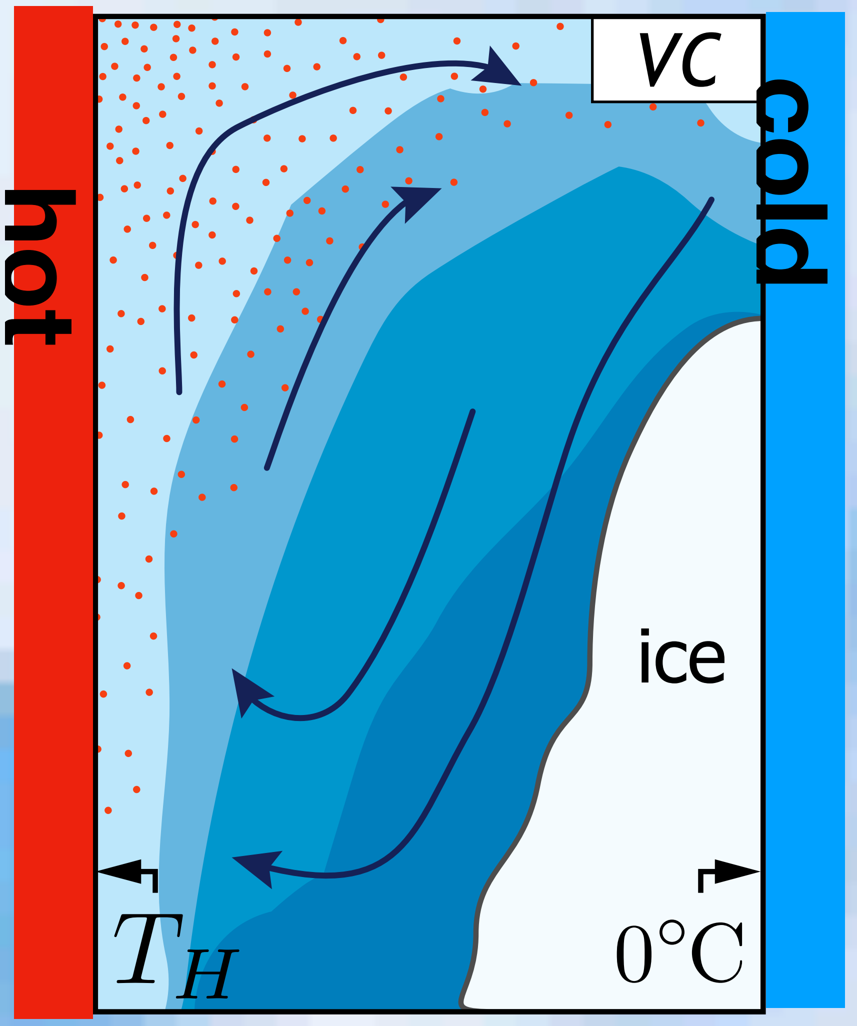

IV. Vertical convection with salty water

Overall summary

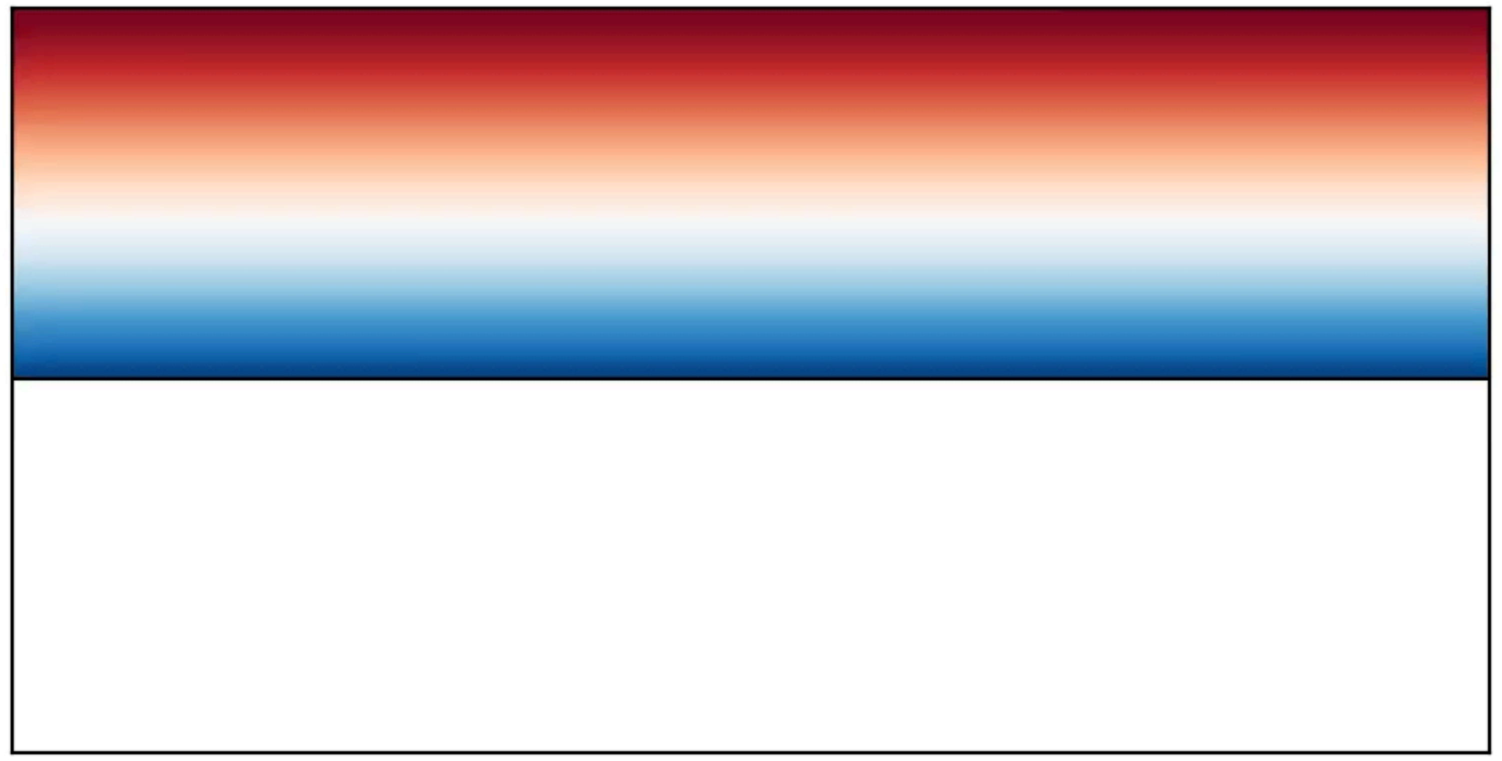

I. Bistability in radiatively heated melt ponds

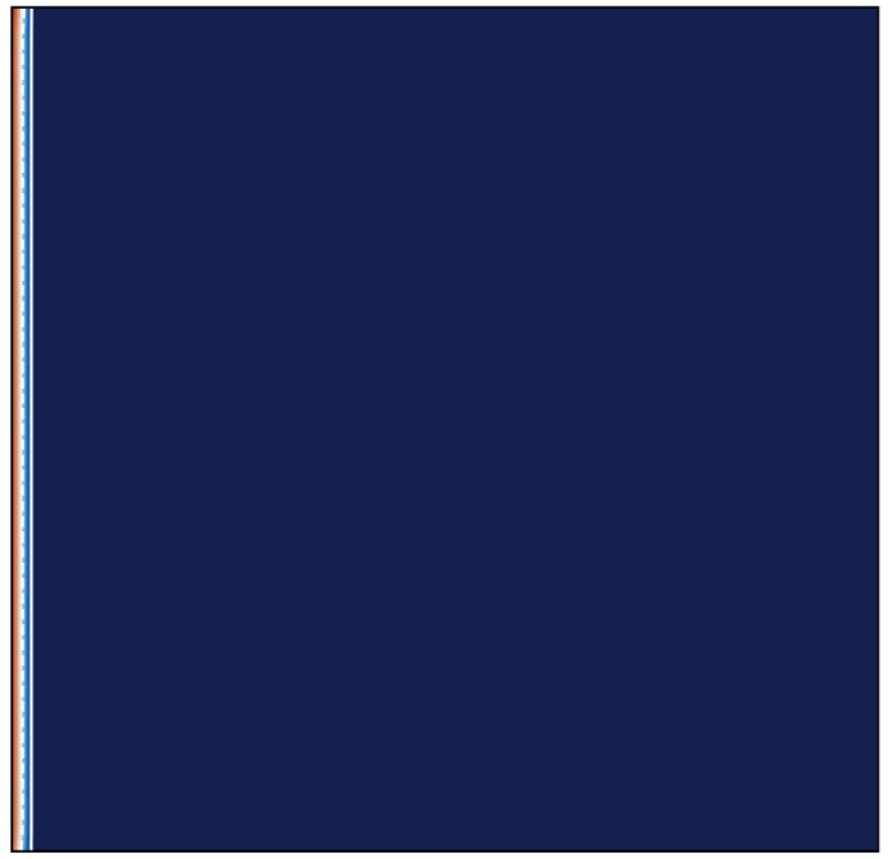

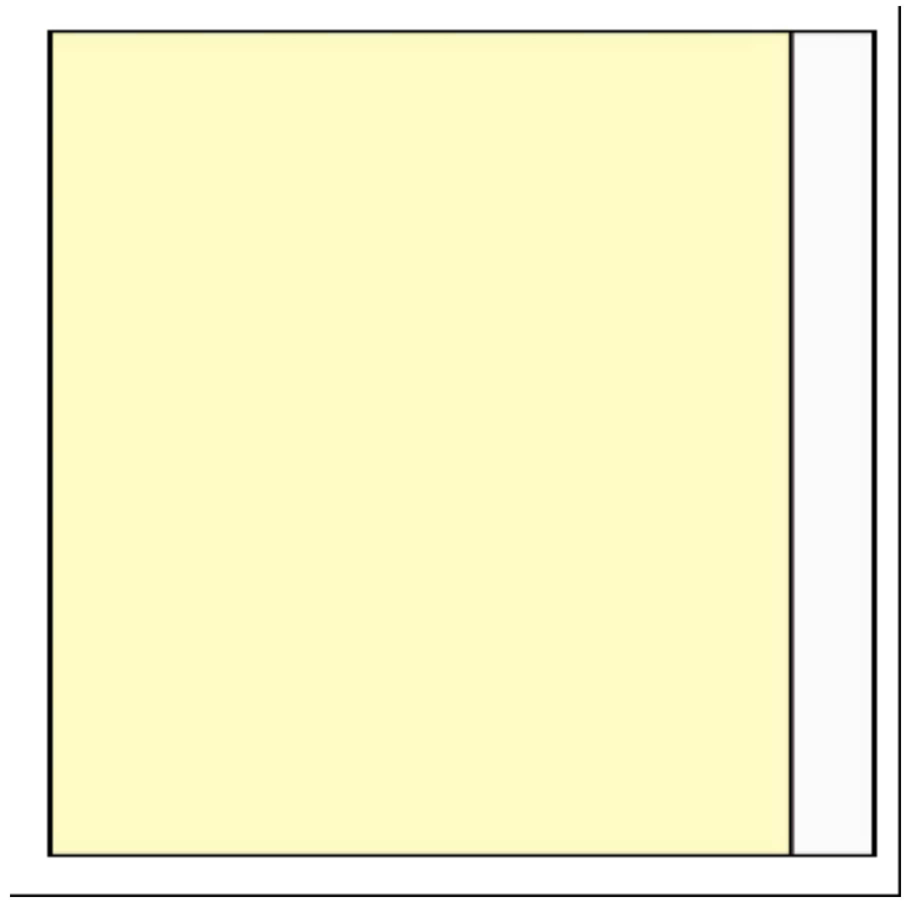

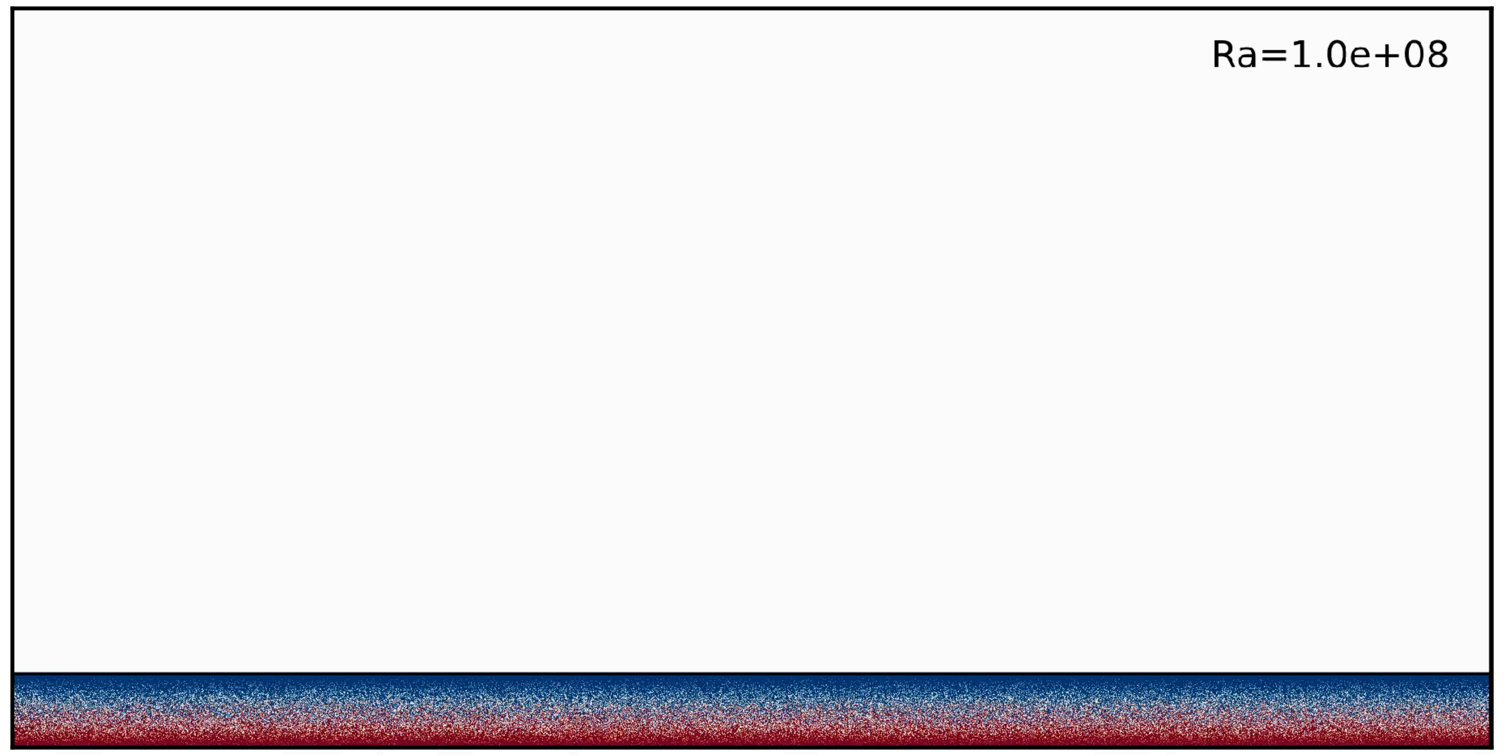

II. RB with fresh water at large Ra

III. Vertical convection with fresh water

IV. Vertical convection with salty water

Overall summary

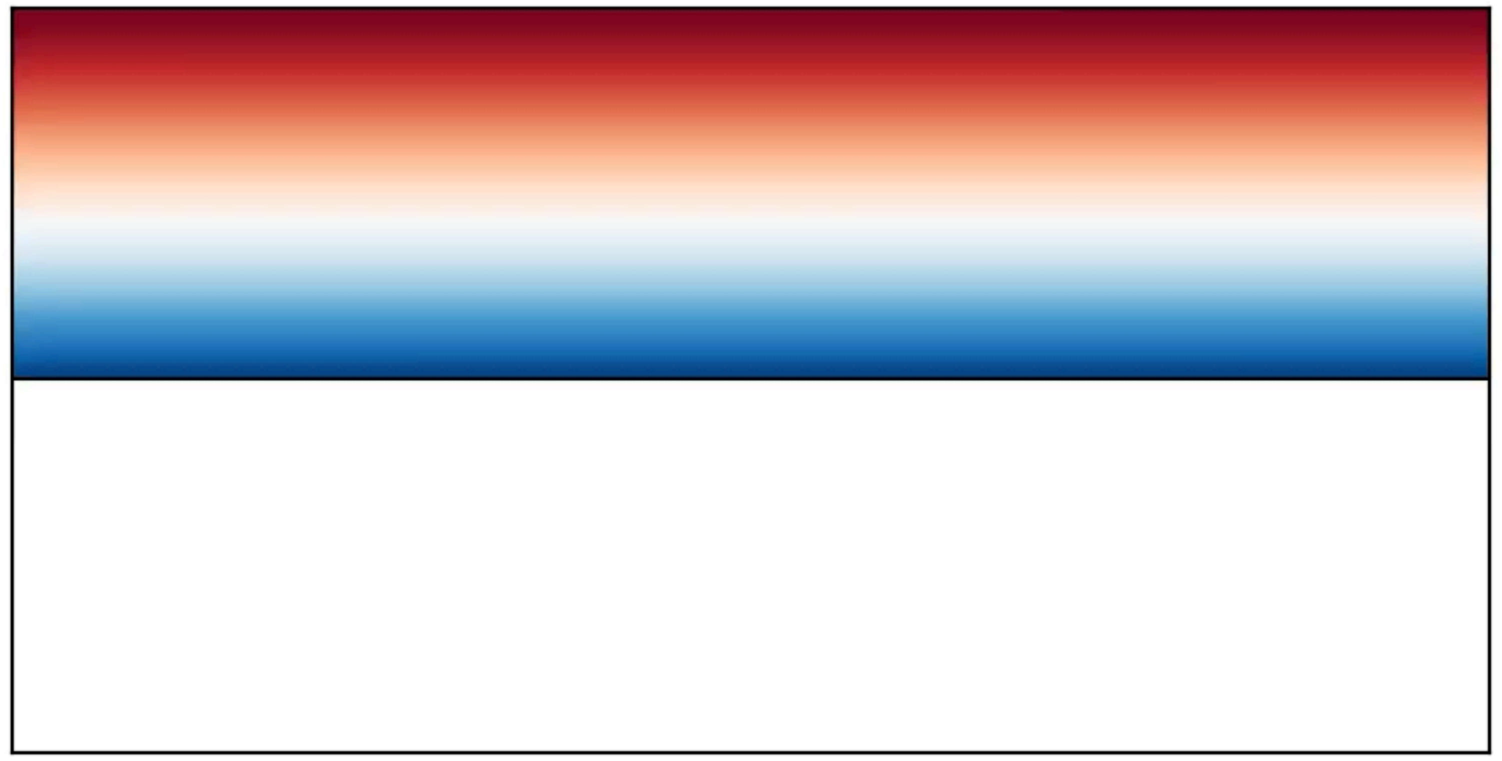

I. Bistability in radiatively heated melt ponds

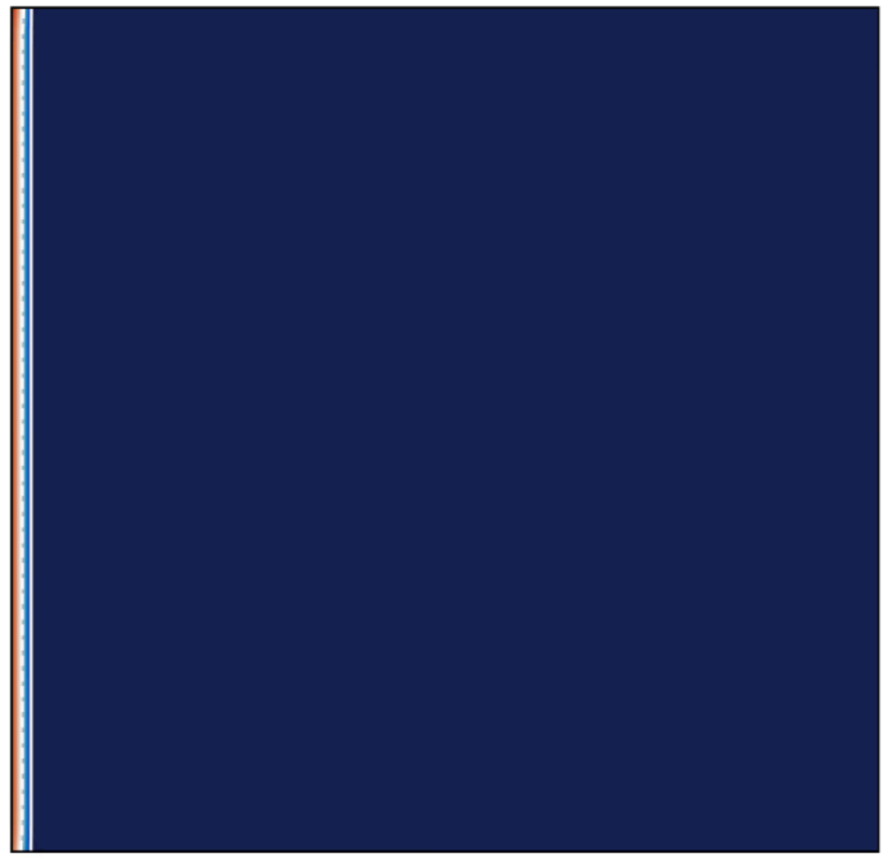

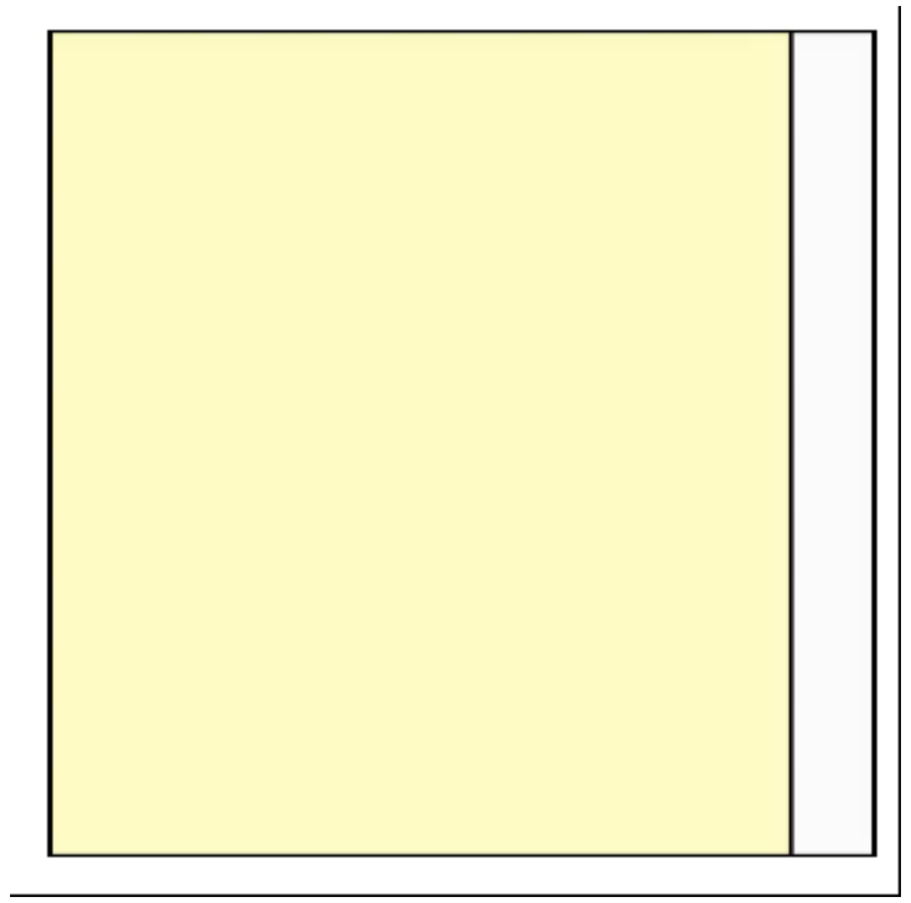

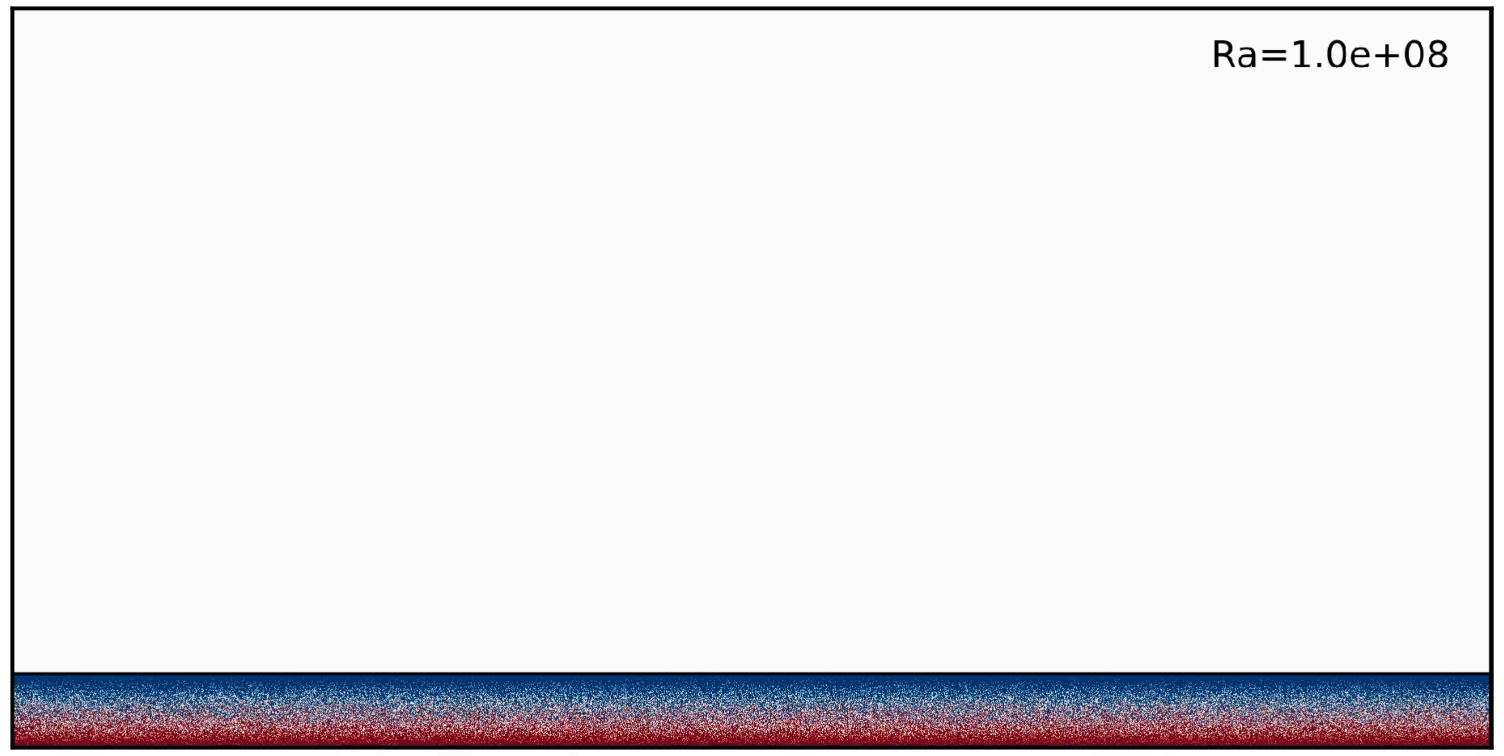

II. RB with fresh water at large Ra

III. Vertical convection with fresh water

IV. Vertical convection with salty water

More general lessons on melting

- Relevance huge in context of climate and energy transition
- Melting offers great problems to fluid dynamics
- Closing gap between what can be measured (a lot still to be done) and what can be simulated (also a lot to be done): One-to-one comparison seems achievable
- Closing gap between fluid dynamics in the field (ocean, lake), in the lab, and on the computer
- Extremely rich phenomenology and multi-dimensional parameter spaces
- Field offers excellent examples to learn how to decipher often surprising & counterintuitive phenomena: excellent training ground for young scientists

More general lessons on melt

- Relevance huge in context of climate and ene
- Melting offers great problems to fluid d
- Closing gap between what can b still to be done) and what can be simulated (also ne-to-one comparison seems achievable
- Closing gap betw in the field (ocean, lake), in the lab, and on the co
- Extrem ology and multi-dimensional parameter spaces
- Fiel t examples to learn how to decipher often surpri unterintuitive phenomena: excellent training ground for young s tists

Work in progress

My time has melted away! Thank you for your attention

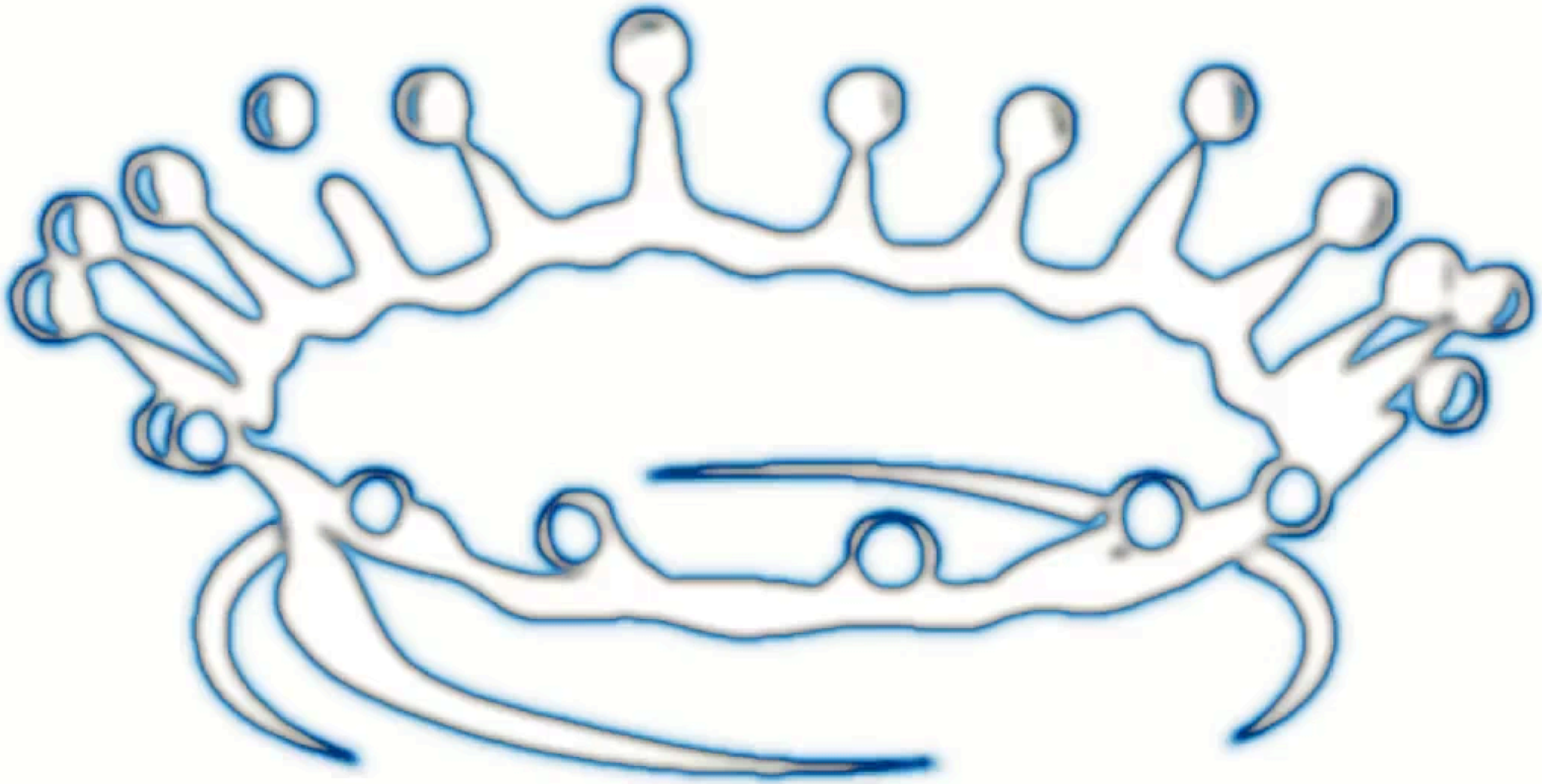

My time has melted away!

Thank you for your attention